EMERGING TRANSLATIONAL OPPORTUNITIES IN COMPARATIVE ONCOLOGY WITH COMPANION CANINE CANCERS

EDITED BY: Mark W. Dewhirst and Rodney L. Page

PUBLISHED IN: Frontiers in Oncology and Frontiers in Immunology

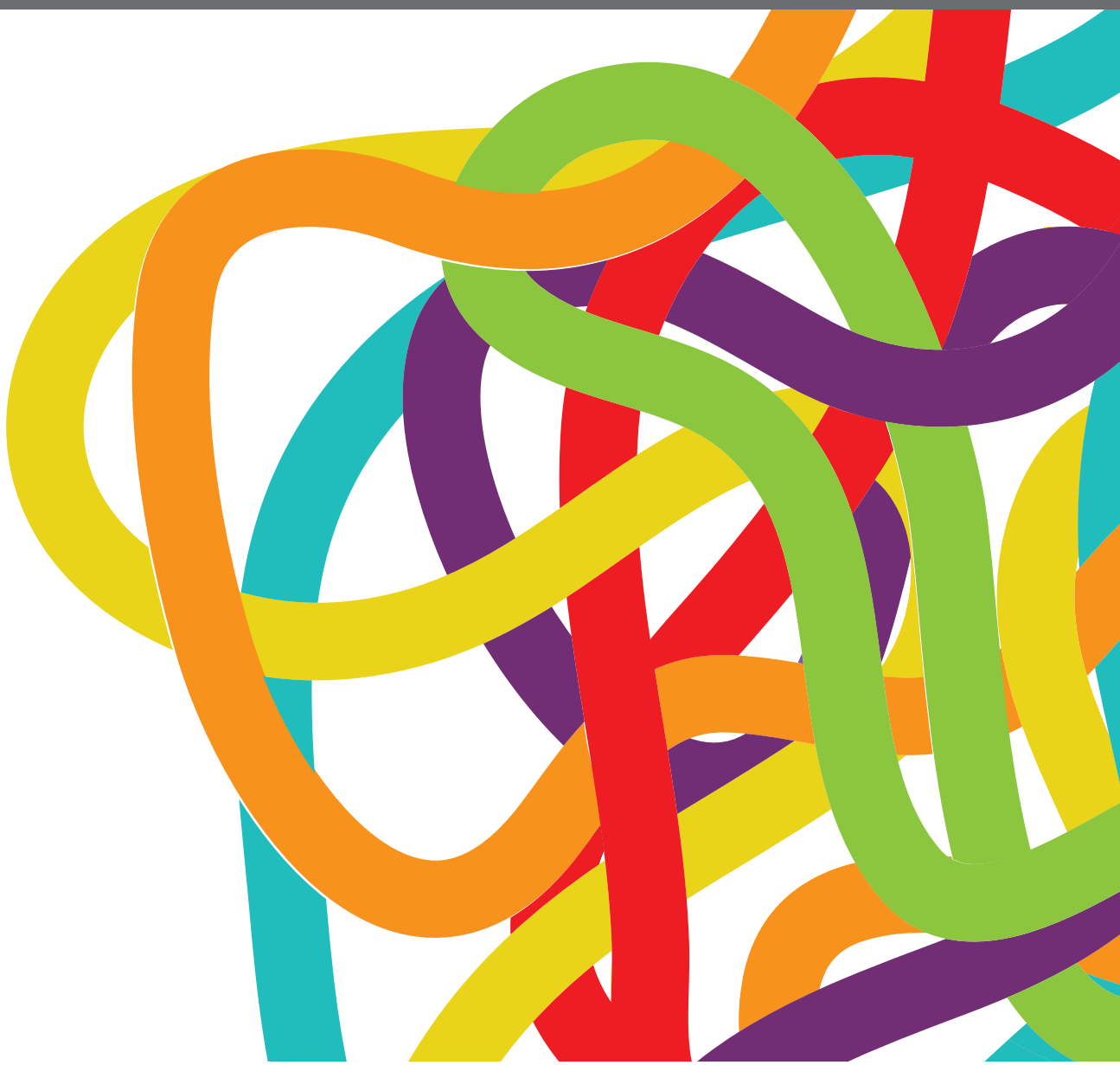

frontiers Research Topics

frontiers

Frontiers eBook Copyright Statement

The copyright in the text of individual articles in this eBook is the property of their respective authors or their respective institutions or funders. The copyright in graphics and images within each article may be subject to copyright of other parties. In both cases this is subject to a license granted to Frontiers.

The compilation of articles constituting this eBook is the property of Frontiers.

Each article within this eBook, and the eBook itself, are published under the most recent version of the Creative Commons CC-BY licence. The version current at the date of publication of this eBook is CC-BY 4.0. If the CC-BY licence is updated, the licence granted by Frontiers is automatically updated to the new version.

When exercising any right under the CC-BY licence, Frontiers must be attributed as the original publisher of the article or eBook, as applicable.

Authors have the responsibility of ensuring that any graphics or other materials which are the property of others may be included in the CC-BY licence, but this should be checked before relying on the CC-BY licence to reproduce those materials. Any copyright notices relating to those materials must be complied with.

Copyright and source acknowledgement notices may not be removed and must be displayed in any copy, derivative work or partial copy which includes the elements in question.

All copyright, and all rights therein, are protected by national and international copyright laws. The above represents a summary only. For further information please read Frontiers' Conditions for Website Use and Copyright Statement, and the applicable CC-BY licence.

ISSN 1664-8714
ISBN 978-2-88963-645-7
DOI 10.3389/978-2-88963-645-7

About Frontiers

Frontiers is more than just an open-access publisher of scholarly articles: it is a pioneering approach to the world of academia, radically improving the way scholarly research is managed. The grand vision of Frontiers is a world where all people have an equal opportunity to seek, share and generate knowledge. Frontiers provides immediate and permanent online open access to all its publications, but this alone is not enough to realize our grand goals.

Frontiers Journal Series

The Frontiers Journal Series is a multi-tier and interdisciplinary set of open-access, online journals, promising a paradigm shift from the current review, selection and dissemination processes in academic publishing. All Frontiers journals are driven by researchers for researchers; therefore, they constitute a service to the scholarly community. At the same time, the Frontiers Journal Series operates on a revolutionary invention, the tiered publishing system, initially addressing specific communities of scholars, and gradually climbing up to broader public understanding, thus serving the interests of the lay society, too.

Dedication to Quality

Each Frontiers article is a landmark of the highest quality, thanks to genuinely collaborative interactions between authors and review editors, who include some of the world's best academicians. Research must be certified by peers before entering a stream of knowledge that may eventually reach the public - and shape society; therefore, Frontiers only applies the most rigorous and unbiased reviews.
Frontiers revolutionizes research publishing by freely delivering the most outstanding research, evaluated with no bias from both the academic and social point of view. By applying the most advanced information technologies, Frontiers is catapulting scholarly publishing into a new generation.

What are Frontiers Research Topics?

Frontiers Research Topics are very popular trademarks of the Frontiers Journals Series: they are collections of at least ten articles, all centered on a particular subject. With their unique mix of varied contributions from Original Research to Review Articles, Frontiers Research Topics unify the most influential researchers, the latest key findings and historical advances in a hot research area! Find out more on how to host your own Frontiers Research Topic or contribute to one as an author by contacting the Frontiers Editorial Office: researchtopics@frontiersin.org

EMERGING TRANSLATIONAL OPPORTUNITIES IN COMPARATIVE ONCOLOGY WITH COMPANION CANINE CANCERS

Topic Editors:
Mark W. Dewhirst, Duke University, United States
Rodney L. Page, Colorado State University, United States

Citation: Dewhirst, M. W., Page, R. L., eds. (2020). Emerging Translational Opportunities in Comparative Oncology With Companion Canine Cancers. Lausanne: Frontiers Media SA. doi: 10.3389/978-2-88963-645-7

Table of Contents

frontiers in Oncology

EDITORIAL
published: 28 February 2020
doi: 10.3389/fonc.2020.00270

Editorial: Emerging Translational Opportunities in Comparative Oncology with Companion Canine Cancers

Mark W. Dewhirst[1] *and Rodney L. Page*[2]*

[1] Department of Radiation Oncology, Duke University, Durham, NC, United States, [2] Colorado State University, Fort Collins, CO, United States

Keywords: comparative oncology, canine, cancer biology, cancer therapy, cancer diagnostic

Editorial on the Research Topic

Emerging Translational Opportunities in Comparative Oncology with Companion Canine Cancers

The accelerated pace of discoveries in cancer biology is due, in large measure, to the engagement of an increasingly wide matrix of scientific disciplines focused on improved understanding and treatment of cancer. The intersection between physical sciences such as engineering, chemistry, biophysics, and mathematics with the traditional disciplines of biochemistry, cell biology, immunology, and genetics have created new opportunities to better define functional aberrations in the cancer process and explore novel concepts for prevention and management. This expanded understanding of the complexity inherent in cancer development and progression has occurred in parallel with the fundamental growth in technology that has accelerated resolution of the genetic, structural, and functional differences between normal, preneoplastic, and neoplastic conditions.

Vital to the application of new discoveries into clinical practice has been the vigorous development of preclinical systems for proof-of-concept studies, safety determination, and gauging potential efficacy. A vast number of genetically engineered laboratory animal models of human cancer are now available to resolve the importance of selective or aggregate alterations in the genetic code on critical biological functions. Although vital to preliminary confirmation of cancer discoveries, rodent models of cancer cannot fully recapitulate the complexity of driver mutations or tumor-host microenviroments seen in human cancer. Further, the presence of co-morbidities that occur in nearly all human patients contribute to tumor progression, treatment resistance, and normal tissue toxicities that cannot be readily modeled in rodents.

Unique similarities and differences in incidence, origin, development of cancer, and existence of co-morbidities between companion animals and humans makes studies in pet dogs directly applicable to people. To date, however, the value of canine cancer has been an underappreciated and incompletely developed scientific resource. In response to this gap, the veterinary profession established important components of a coordinated canine cancer research effort. Importantly, these efforts have been led by the Comparative Oncology Program at the National Cancer Institute (NCI Comparative Oncology Program). In 2015 the Institute of Medicine conducted a workshop to identify knowledge gaps and policy needs for integration of data obtained from clinical trials in companion animals for human drug development (Workshop Summary).

Substantial federal and non-profit research foundation resources have recently been committed to expand the scientific tools needed to better understand canine cancers and to coordinate multicenter clinical studies to expedite clinical cancer control strategies for humans and companion animals. Additional resources are needed to support identification of basic

OPEN ACCESS

Edited and reviewed by:
Giuseppe Giaccone,
Cornell University, United States

***Correspondence:**
Rodney L. Page
rodney.page@colostate.edu

Specialty section:
This article was submitted to Cancer Molecular Targets and Therapeutics, a section of the journal Frontiers in Oncology

Received: *11 February 2020*
Accepted: *17 February 2020*
Published: *28 February 2020*

Citation:
Dewhirst MW and Page RL (2020) Editorial: Emerging Translational Opportunities in Comparative Oncology with Companion Canine Cancers. Front. Oncol. 10:270. doi: 10.3389/fonc.2020.00270

biological, immunological, and genetic drivers of neoplasia in companion animals, enhancements infrastructure and core resources for clinical trial management as well as enabling opportunities for proof of concept studies for industry. Once accomplished, these investments will permit more robust integration of canine comparative oncology with other cancer research resources.

This collection of review articles describes the current status of information relevant to comparative oncology in a variety of basic, preclinical and clinical categories. The goals of this curated collection are:

- To elucidate basic and pre-clinical research which has described how spontaneously arising cancers in dogs parallel the biologic complexity of human disease. Collection citations include—Langsten et al., Hlavaty et al., and Brocca et al..
- Discuss similar, as well as different, mechanisms of cancer progression in naturally occurring cancers of humans and companion dogs which are common across relevant histologies. For example, Interspecies translation of therapeutic targets for invasion, metastasis and drug resistance may support broadly applicable strategies due to the authentic mechanisms which are operative in both species. Collection citations include—Avery, Rao et al., Knapp et al., Miller et al., and Fan et al..
- Create awareness of the existing resources and capabilities available to produce and access high-value information obtainable in companion animal clinical cancer research—potentially improving the predictability of translational research. Collection citations include—Vail et al., Thamm, Dow, Nolan et al., and Etienne et al..
- Promote an increased level of collaboration between human and veterinary oncologists from both industry and academia in particular to narrow the gaps in awareness, understanding, and utilization that exist regarding companion animal data.

We believe that this collection of reviews and scientific manuscripts creates a representative cross-section of the discipline of comparative oncology in 2020 and, in aggregate, builds a roadmap for implementation of comparative oncology. The ability to fully integrate the biologic, genetic, and immunologic determinants of canine cancers into the broad landscape of cancer research is dependent on generation of a thorough portfolio of technological tools, clinical infrastructure and data repositories. Access to novel drugs and devices is then needed to demonstrate the business value of comparative oncology. Drug discovery case studies that demonstrate such value are accumulating, albeit slowly. Proper stimulation will generate additional interest, growth, and progress in cancer research for the benefit of all species.

AUTHOR CONTRIBUTIONS

MD and RP contributed equally to the review and editorial process for this collection.

ACKNOWLEDGMENTS

The Cost of Publication was provided by the Flint Animal Cancer Center, Colorado State University.

Conflict of Interest: The authors declare that the research was conducted in the absence of any commercial or financial relationships that could be construed as a potential conflict of interest.

Copyright © 2020 Dewhirst and Page. This is an open-access article distributed under the terms of the Creative Commons Attribution License (CC BY). The use, distribution or reproduction in other forums is permitted, provided the original author(s) and the copyright owner(s) are credited and that the original publication in this journal is cited, in accordance with accepted academic practice. No use, distribution or reproduction is permitted which does not comply with these terms.

frontiers in Immunology

ORIGINAL RESEARCH
published: 10 October 2019
doi: 10.3389/fimmu.2019.02371

Bacterial Killing Activity of Polymorphonuclear Myeloid-Derived Suppressor Cells Isolated From Tumor-Bearing Dogs

*Sabina I. Hlavaty[1], Yu-Mei Chang[2], Rachel P. Orth[3], Mark Goulian[4], Paul J. Planet[5,6], Douglas H. Thamm[7], Jennifer A. Punt[8] and Oliver A. Garden[1]**

[1] Garden Immune Regulation Laboratory, Department of Clinical Sciences and Advanced Medicine, School of Veterinary Medicine, University of Pennsylvania, Philadelphia, PA, United States, [2] Research Support Office, Royal Veterinary College, London, United Kingdom, [3] School of Arts and Sciences, University of Pennsylvania, Philadelphia, PA, United States, [4] Department of Biology, School of Arts and Sciences, University of Pennsylvania, Philadelphia, PA, United States, [5] Department of Pediatrics, Perelman School of Medicine, University of Pennsylvania, Philadelphia, PA, United States, [6] Pediatric Infectious Disease Division, Children's Hospital of Philadelphia, Philadelphia, PA, United States, [7] Flint Animal Cancer Center, Department of Clinical Sciences, Colorado State University, Fort Collins, CO, United States, [8] Department of Pathobiology, School of Veterinary Medicine, University of Pennsylvania, Philadelphia, PA, United States

OPEN ACCESS

Edited by:
Mark W. Dewhirst, Duke University, United States

Reviewed by:
Sita Withers, Louisiana State University, United States
Bonnie L. Hylander, Roswell Park Comprehensive Cancer Center, University at Buffalo, United States

***Correspondence:**
Oliver A. Garden
ogarden@upenn.edu

Specialty section:
This article was submitted to Comparative Immunology, a section of the journal Frontiers in Immunology

Received: *31 July 2019*
Accepted: *20 September 2019*
Published: *10 October 2019*

Citation:
Hlavaty SI, Chang Y-M, Orth RP, Goulian M, Planet PJ, Thamm DH, Punt JA and Garden OA (2019) Bacterial Killing Activity of Polymorphonuclear Myeloid-Derived Suppressor Cells Isolated From Tumor-Bearing Dogs. Front. Immunol. 10:2371. doi: 10.3389/fimmu.2019.02371

Polymorphonuclear myeloid-derived suppressor cells (PMN-MDSCs) are implicated in the progression and outcome of a variety of pathological states, from cancer to infection. Our previous work has identified three antimicrobial peptides differentially expressed by PMN-MDSCs compared to conventional neutrophils isolated from dogs, mice, and human patients with cancer. We therefore hypothesized that PMN-MDSCs in dogs with cancer possess antimicrobial activity. In the current work, we observed that exposure of PMN-MDSCs to Gram-negative bacteria (*Escherichia coli*) increased the expression of reactive oxygen species by the PMN-MDSCs, indicating that they are capable of initiating an anti-microbial response. Electron microscopy revealed that the PMN-MDSCs phagocytosed Gram-negative and Gram-positive (*Staphylococcus aureus*) bacterial species. Lysis of bacteria within some of the PMN-MDSCs suggested bactericidal activity, which was confirmed by the recovery of significantly lower numbers of bacteria of both species following exposure to PMN-MDSCs isolated from tumor-bearing dogs. Our data therefore indicate that PMN-MDSCs isolated from dogs with cancer, in common with PMNs, have phagocytic and bactericidal activity. This nexus of immunosuppressive and antimicrobial activity reveals a hitherto unrecognized function of MDSCs.

Keywords: MDSC, PMN-MDSC, G-MDSC, canine, cancer, bactericidal, phagocytosis, reactive oxygen species

INTRODUCTION

Myeloid-derived suppressor cells (MDSCs) are a subset of immunosuppressive myeloid cells that expand under chronic inflammatory conditions. In cancer, MDSCs release reactive oxygen species (ROS) and cytokines such as IL-10, resulting in the suppression of cytotoxic T cells and attenuation of their antineoplastic activity (1, 2). In infections, the immunosuppressive activity of MDSCs may be beneficial or harmful to the host, depending on the context and bacterial targets.

In models of pneumonia and *Leishmania major* infection, for example, increased frequencies of MDSCs are associated with improved survival by preventing excessive inflammation (3–5). In contrast, increased frequencies of MDSCs in *Staphylococcus aureus* biofilm infections in a murine model are associated with enhanced T cell suppression and increased bacterial load, reducing survival (6, 7). Recent work has demonstrated the role of the microbiome in driving the expansion of MDSC populations in the context of cancer. A murine model of pancreatic cancer demonstrated an increased bacterial load in the neoplastic pancreas; ablation of the bacterial load by treating wild-type mice with an oral antibiotic regimen attenuated MDSC frequency and improved T cell activation and outcome (8). Such studies therefore suggest a relationship between the ability of MDSCs to respond to microbes and their immunosuppressive activities.

Dogs with naturally occurring cancer are gaining traction as a model to study a variety of biological processes in tumor development. Our work has demonstrated that the polymorphonuclear subset of MDSCs (PMN-MDSCs, also known as granulocytic (G)-MDSCs) isolated from dogs are functionally and phenotypically representative of human PMN-MDSCs, further supporting the dog as a model species. Murine PMN-MDSCs are defined as $CD11b^+Ly6G^+Ly6C^{lo}$ peripheral blood mononuclear cells (PBMCs), while human PMN-MDSCs are traditionally defined as $CD11b^+CD14^-CD15^+$ or $CD11b^+CD14^-CD66b^+$ PBMCs, with Ly6G, CD15 and CD66b acting as neutrophil (or polymorphonuclear cell; PMN) markers (2). In dogs, we used a parallel marker approach using CADO48A as our canine-specific PMN marker. We found that $CD11b^+CD14^-CADO48A^+$ PBMCs suppressed T cell function and therefore represented the canine equivalent of PMN-MDSCs (9). Our cross-species transcriptomic analysis revealed that three of the five commonly upregulated genes in PMN-MDSCs isolated from dogs, humans, and mice encode antimicrobial peptides (9). Furthermore, these cells synthesize a number of products attributed to conventional PMN killing of bacteria (2), prompting us to hypothesize that PMN-MDSCs may serve a bactericidal role in certain contexts, including cancer. We show for the first time that PMN-MDSCs isolated from canine cancer patients are able to phagocytose and kill bacteria. Our findings suggest a novel duality of function of MDSCs, raising the possibility that their immunosuppressive function can be modulated by interactions with microbes, which may enhance cancer progression.

MATERIALS AND METHODS

Isolation of Canine Cells

This study was approved by the Institutional Animal Care and Use Committee, and the Privately Owned Animal Protocol Committee (Protocol #500), of the School of Veterinary Medicine, University of Pennsylvania (Penn Vet). Written informed consent was obtained from all owners of dogs sampled in this study. These dogs were patients at the Matthew J Ryan Hospital of Penn Vet. Samples collected at the Flint Animal Cancer Center at Colorado State University were approved under the Clinical Review Board Protocol CS2019-208: Flint Animal Cancer Center Biobanking and Sample Collection. The signalments and clinical diagnoses of the dogs sampled for this study are listed in **Supplemental Table 1**.

Peripheral blood was aseptically collected from healthy and tumor-bearing dogs, stored at room temperature in the dark, and processed within 24 h. Briefly, blood was diluted 1:1 in sterile Dulbecco's phosphate buffered saline (DPBS) and layered gently over Histopaque-1077 (Sigma-Aldrich, St. Louis, MO, USA). Samples were centrifuged for 30 min at 400 g with acceleration and deceleration set to zero. The PBMC layer was removed using a transfer pipet and transferred to a fresh tube. The remaining serum and Histopaque layer was aspirated and discarded, leaving the red blood cell (RBC) layer. PMNs were isolated from the RBC layer after incubation with 10 times the volume of 1X RBC Lysis Buffer (Multi-Species; Thermo Fisher Scientific, San Diego, CA, USA) for 5 min at room temperature. PBMCs were incubated with RBC Lysis Buffer for 1 min to remove contaminating RBCs. PBMCs and PMNs were then washed with 10% v/v fetal bovine serum (FBS; Hyclone, Logan, UT, USA) in DPBS twice, prior to counting.

PBMCs from healthy control dogs were stained with PE-conjugated anti-dog-CD5 monoclonal antibody (1:200, clone YKIX322.3; Bio-Rad, Hercules, CA, USA). PBMCs from healthy dogs and PBMCs and PMNs from tumor-bearing dogs were stained with PE-Cy7-conjugated anti-dog PMN leukocyte antigen (1:1,600, clone CADO48A; University of Washington, Pullman, WA, USA, https://secure.vetmed.wsu.edu/moab/shop/item.aspx?itemid=246). All staining was performed for 30 min in the dark at 4°C. In our previous publication, we utilized a larger panel to identify canine PMN-MDSCs in a manner that paralleled the panel used to identify human PMN-MDSCs (2, 9). For this study, a simplified, single antigen panel was deployed for FACS™ to conserve reagents and minimize the preparation time of cells prior to setting up bacterial killing assays, following preliminary experiments that demonstrated equivalence of gated cells in the full and abbreviated panels (**Supplemental Figure 1**). Cells were then washed and resuspended in DPBS containing 2% v/v FBS and 2 mM ethylenediaminetetraacetic acid, and incubated with 4′,6-diamidino-2-phenylindole (DAPI; BioLegend, San Diego, CA, USA) at room temperature in the dark for 10 min, prior to sorting on a BD FACSAria II and analysis on FlowJo® software, version 10.3 (Tree Star, Ashland, OR, USA). PMN-MDSCs were sorted from PBMCs of tumor-bearing dogs, identified as live hypodense $CADO48A^+$ granulocytes, while PMNs were sorted from the lysed RBC fraction, identified as live hyperdense $CADO48A^+$ granulocytes (healthy control dog: H-PMN, tumor-bearing [cancer] dog: C-PMN). T cells were identified as live $CD5^+$ lymphocytes.

Reactive Oxygen Species Assay

To measure ROS using a modification of a published protocol (10), 5×10^5 cell aliquots of PBMCs and PMNs isolated from four healthy control dogs and six tumor-bearing dogs were loaded with dihydrorhodamine-123 (DHR, Sigma-Aldrich, St. Louis, MO, USA; final concentration = 40 μM) and incubated with or without stimulation at 37°C in a final volume of 200 μl. To

induce production of ROS, samples were incubated for 30 min with a 20:1 ratio of *E. coli* to cells. To inhibit ROS production, diphenyleneiodonium (DPI, Sigma-Aldrich) was added to a final concentration of 19.1 μM. After incubation, samples were immediately placed on ice and washed in 1 mL of cold PBS. PBMCs were subsequently resuspended in 100 μL of cold PBS, stained with 0.5 μg anti-CADO48A [conjugated with either APC (Bio-Rad) or PE-Cy7 (Bio-Rad)], incubated on ice in the dark for 30 min, then washed with 1 mL of cold PBS. Stained PMNs and PBMCs were resuspended in 350 μL of staining medium (PBS; 0.1%BSA; 0.1%NaN_3) for analysis via flow cytometry on a FACSCalibur™ and analyzed using FlowJo® software, version 10.6.

Bacterial Killing Assay

Our bacterial killing assay was modified from a published protocol (11). Single colonies of *E. coli* (strain MG1655) and *S. aureus* (RN6607; strain 502A) were grown as an overnight culture, diluted the next morning 1:10 in sterile Luria-Bertani (LB) broth, and grown at 250 rotations per minute (rpm) to an optical density at 600 nm of 1.0, before placing on ice. Prior to incubation with canine cells (*E. coli*: eleven healthy control dogs, six tumor-bearing dogs; *S. aureus*: eight healthy control dogs, five tumor-bearing dogs), bacteria were diluted 1:10 in DPBS and grown for 30 min at 80 rpm at 37°C, before resuspension in Roswell-Park Memorial Institute (RPMI)-1640 medium (Life Technologies, Carlsbad, CA, USA) containing 10 mM HEPES. Canine cells (2×10^5 cells in 50 μL) were incubated for 15 min alone at room temperature in a round bottom 96-well plate, after which the bacteria were added at a ratio of bacteria: cells of 10:1. The plate was centrifuged at 500 g for 5 min, before incubation at 37°C for 40 min at 80 rpm. Serial dilutions of each condition were prepared in 0.1% Triton-X in sterile water in order to release any viable, internalized bacteria by lysis, before the preparation of LB plates that were incubated overnight to count resulting colony-forming units (CFUs) the next day. Co-culture CFUs were normalized to CFUs for bacteria alone.

Electron Microscopy

Canine cells were isolated from one tumor-bearing dog and one healthy control dog, and incubated with *E. coli or S. aureus* as described above. After centrifugation at 500 g for 10 min, the cells were resuspended in 1 mL of fixative buffer (2.5% glutaraldehyde, 2.0% paraformaldehyde in 0.1 M sodium cacodylate buffer, pH 7.4) for 30 min at room temperature. After storage at 4°C for up to 16 h, the cells were washed with 0.1 M sodium cacodylate at pH 7 and post-fixed in 2.0% osmium tetroxide for 1 h at room temperature, before another wash in buffer and then distilled water. After dehydration through a graded ethanol series, the cells were embedded in Embed-812 (Electron Microscopy Sciences, Fort Washington, PA). Thin sections were stained with uranyl acetate and lead citrate, before examination with a JEOL 1010 electron microscope fitted with a Hamamatsu digital camera and AMT Advantage image capture software.

Approximately 100 images of each cell type were collected in a grid-like and unbiased manner for quantification. All images for quantification were collected at a magnification of 15,000×. The images were scrambled using random.org, before review of all images in a blinded manner to assess the number of bacteria internalized, and endoplasmic reticulum (ER) dilation score. At least half of the cross-sectional profile of a bacterium had to be internalized by the canine cell to be counted as internal. Endoplasmic reticulum dilation score was determined as previously published (12): dilated ER not observed in the cytoplasm (score 0), dilated ER present in up to one third of the cytoplasm (score 1), one third to two thirds of the cytoplasm (score 2), or more than two thirds of the cytoplasm (score 3).

Statistics

Linear mixed effects models were used to evaluate differences in normalized percentage DHR positivity and normalized median fluorescence intensity (MFI) between conditions, cell types and their interactions, in which subject dog identification was included as a random effect. Both DHR percentage and MFI were skewed, prompting log transformation prior to analysis. Poisson regression and ordinal logistic regression were used to compare bacterial count or dilated ER score between cell types. For *E. coli* and *S. aureus* killing assays, linear mixed effects models were adopted to compare cell types and bacteria; experimental date and dog were considered as random effects. Raw frequency was log-transformed prior to analysis. Fisher's Least Significant Difference was adopted for all *post-hoc* comparisons.Frequencies are displayed as mean ± standard deviation (SD) or median [inter-quartile range (IQR)], as appropriate. All analyses were carried out in R, version 3.5.1 (R Foundation for Statistical Computing; Vienna, Austria).

RESULTS

Bacteria Elicit the Synthesis of Reactive Oxygen Species by PMN-MDSCs

Given that PMN-MDSC suppressive activity is attributed partially to their production of ROS (1), and ROS mediate bacterial killing (13), we first set out to ask whether exposure of PMN-MDSCs to bacteria increased cellular ROS synthesis. We loaded canine cells with DHR and measured its oxidation by ROS, which results in a green fluorescent product that can be detected by flow cytometry (**Figure 1A**). Exposure of both C-PMNs ($p = 0.0012$) and PMN-MDSCs ($p = 0.0062$) to *E. coli* increased the percentage of DHR^+ $CADO48A^+$ cells when compared to canine cells alone, indicating an increase in ROS production. This phenomenon was extinguished when NADPH oxidase was inhibited with DPI (C-PMN: $p = 0.122$, PMN-MDSC: $p = 0.33$; **Figure 1B**). Comparison of the MFI for each condition yielded similar observations. *E. coli* once again elicited an increased DHR MFI (C-PMN: $p = 0.00012$, PMN-MDSC: $p = 0.0086$), which was inhibited by DPI (C-PMN: $p = 0.13$, PMN-MDSC: $p = 0.74$; **Figure 1C**). PMN-MDSCs therefore produce ROS in an NADPH-dependent manner in direct response to bacteria.

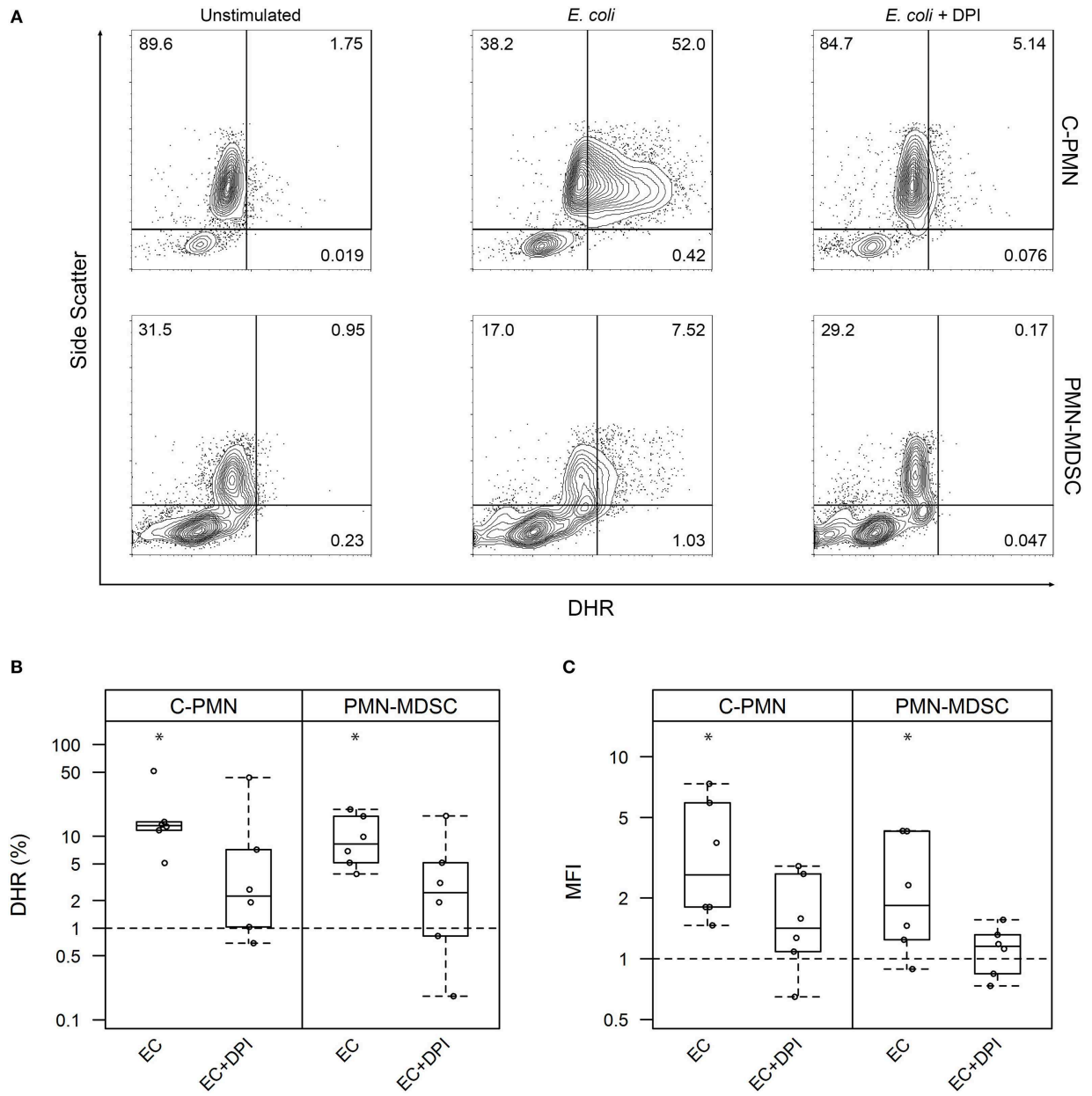

FIGURE 1 | Exposure of PMNs and PMN-MDSCs from tumor-bearing dogs to *E. coli* leads to production of reactive oxygen species. **(A)** Exemplar of flow cytometric data for C-PMNs and PMN-MDSCs isolated from the same tumor-bearing dog. Numbers indicate frequency of total cells that fall within each gate. **(B,C)** Summary of all experiments displaying results as a measure of **(B)** proportion of CADO48A$^+$ cells that are DHR$^+$ and **(C)** MFI of CADO48A$^+$ cells on the DHR channel. DPI was used to inhibit NADPH oxidase production of ROS. Percentage or MFI of DHR$^+$ cells following exposure to *E. coli* is normalized to the percentage or MFI of DHR$^+$ cells under the unstimulated condition. An asterisk denotes $p < 0.01$ and is based on a least square means analysis, comparing each condition to the normalized unstimulated condition ($y = 1$). Each dot represents a different dog. Box-and-whisker plots display the 25th and 75th percentile with median indicated by the center line, while the whiskers indicate the lowest and the highest data points still within 1.5 times the interquartile range of the respective lower and upper quartiles. C, cancer; PMN, polymorphonuclear cell; ROS, reactive oxygen species; MFI, mean fluorescence intensity; DPI, diphenyleneiodonium; DHR, dihydrorhodamine-123; EC, *E. coli*.

PMN-MDSCs Phagocytose *E. coli* and *S. aureus*

ROS production was enhanced in PMN-MDSCs exposed to bacteria in an NADPH-oxidase-dependent manner. This phenomenon is known to accompany phagocytosis (13), prompting us to ask whether PMN-MDSCs are phagocytic. While T cells did not phagocytose *E. coli* (a negative control in these assays; data not shown), PMN-MDSCs showed clear evidence of phagocytosis, in common with C-PMNs (**Figures 2A,B**). Identity of the PMN-MDSCs was verified by

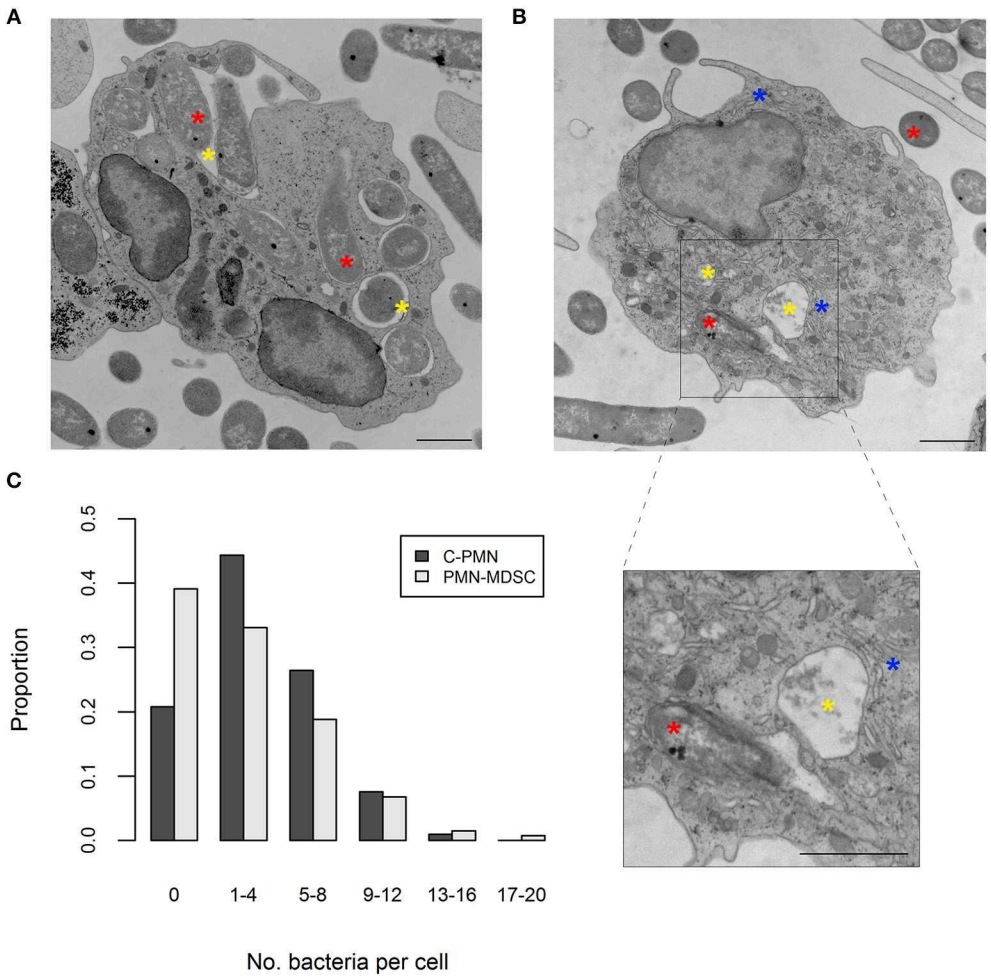

FIGURE 2 | PMN-MDSCs phagocytose bacteria. **(A,B)** EM images of **(A)** C-PMN and **(B)** PMN-MDSC isolated from tumor-bearing dogs. Blue asterisks indicate dilated endoplasmic reticulum, yellow asterisks indicate phagolysosomes, and red asterisks indicate *E. coli*. Scale bar = 1 μm. **(C)** Bar graph depicting the proportion of total cells of each cell type analyzed by EM that had the respective range of bacteria internalized. C, cancer; PMN, polymorphonuclear cell; EM, electron microscopy.

analysis of dilated ER (**Supplemental Figure 2A**) (9, 12). Both populations had a similar range of internalized *E. coli* present in the cytoplasm per cell (C-PMNs: 0–16, PMN-MDSCs: 0–19; **Figure 2C**, **Supplemental Figure 2B**), although median [IQR] numbers of bacteria per cell were marginally lower in PMN-MDSCs (1 [5]) compared to C-PMNs (3 [5]; $p = 0.0044$). PMN-MDSCs also showed evidence of phagocytosis of *S. aureus* (**Supplemental Figure 3**). PMN-MDSCs are therefore able to phagocytose both Gram-negative and Gram-positive bacteria.

PMN-MDSCs Exhibit Bactericidal Activity

Having confirmed that PMN-MDSCs are able to phagocytose *E. coli*, we next asked whether PMN-MDSCs kill bacteria. The growth of bacteria exposed to PMN-MDSCs was significantly lower, when normalized to bacteria alone, than a negative control population of T cells (PMN-MDSCs: 0.445 ± 0.278, T cells: 0.971 ± 0.340, $p = 2.6 \times 10^{-8}$; **Figure 3A**). Similarly, PMNs isolated from both healthy control dogs (0.282 ± 0.172; $p < 2 \times 10^{-16}$) and tumor-bearing dogs (0.268 ± 0.156; $p = 1.5 \times 10^{-13}$) inhibited bacterial growth. PMN-MDSCs (0.430 ± 0.291) also showed enhanced bactericidal activity against *S. aureus* compared to T cells (0.934 ± 0.128, $p = 1.5 \times 10^{-7}$; **Figure 3B**). Similar results were observed for PMNs isolated from healthy control (0.260 ± 0.231, $p = 6.7 \times 10^{-12}$) and tumor-bearing (0.376 ± 0.332, $p = 9.0 \times 10^{-9}$) dogs. PMN-MDSCs isolated from tumor-bearing dogs are therefore able to kill both Gram-negative and Gram-positive bacteria.

DISCUSSION

PMN-MDSCs promote an immunosuppressive microenvironment, which may be beneficial or harmful to the host depending on circumstances (14). In the context of cancer, they play an important role in suppressing T cell activity and promoting tumor development (1, 2). However, many questions about PMN-MDSC function remain unanswered, including the possibility that they serve roles other than suppression in certain contexts. Capitalizing on our former studies of canine MDSCs and previous work suggesting that

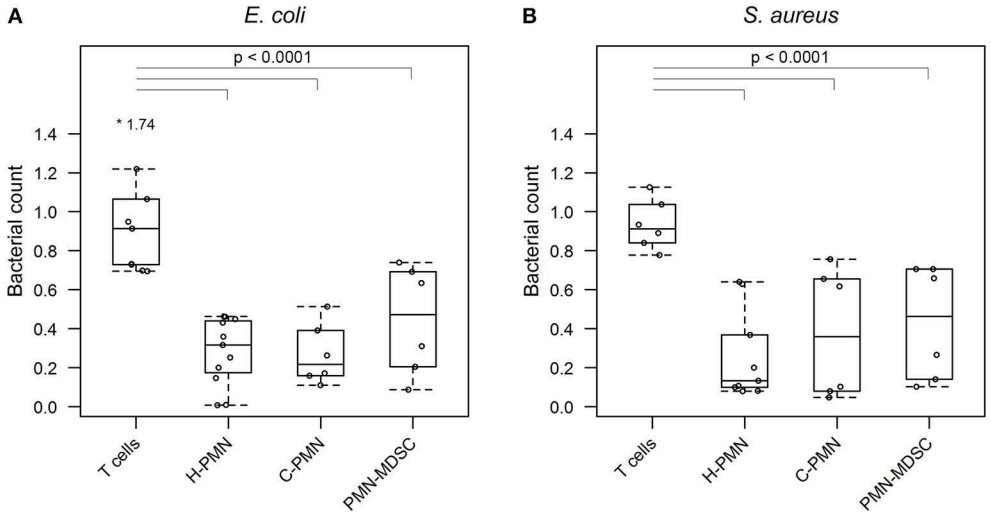

FIGURE 3 | PMN-MDSCs exhibit bactericidal activity. Summary data from bacterial killing assays co-incubating **(A)** *E. coli* or **(B)** *S. aureus* with T cells and PMNs isolated from healthy dogs, and PMNs and PMN-MDSCs isolated from tumor-bearing dogs. Bacterial growth with canine cells was normalized to growth of bacteria alone. A linear mixed effects approach was used for statistical analyses, with the statistically significant comparisons indicated by a solid black line. Each dot represents a different dog. Boxes indicate 25th and 75th percentile with median graphed in the center, while whiskers indicate the lowest and highest data points within 1.5 times the interquartile range of the upper and lower limits. Outlier results are indicated with an asterisk. H, healthy; C, cancer; PMN, polymorphonuclear cell.

MDSCs may be phagocytic in certain contexts (4, 9), we set out to address whether PMN-MDSCs isolated from tumor-bearing dogs have bacterial killing activity.

Since production of ROS as part of the oxidative burst has been linked to killing of bacteria by PMNs (13), and PMN-MDSCs utilize ROS as one of the mechanisms of suppression, we first asked whether exposure to bacteria elicited ROS production in canine PMN-MDSCs. We found that exposure to *E. coli* increased the concentration of ROS in PMN-MDSCs in an NADPH oxidase-dependent manner, suggesting that *E. coli* interactions with PMN-MDSCs stimulate downstream signaling pathways that culminate in ROS production.

We next wished to understand whether PMN-MDSCs from tumor-bearing dogs are able to phagocytose bacteria. This aspect of PMN-MDSC function has not been studied as extensively as it has in PMNs; however, a number of studies in a variety of contexts have found these cells to be capable of phagocytic activity. PMN-MDSCs isolated from tumor-bearing mice were able to phagocytose latex beads (15), while PMN-MDSCs isolated from infected mice phagocytosed Gram-negative bacteria, although not as proficiently as PMNs (16). Similarly, PMN-MDSCs isolated from human cord blood phagocytosed both Gram-positive and Gram-negative bacteria (4). However, to the best of our knowledge the phagocytosis of living Gram-positive and Gram-negative bacteria by PMN-MDSCs has not been investigated in the context of cancer. Confirming by electron microscopy that PMN-MDSCs isolated from dogs with cancer are able to phagocytose both *E. coli* and *S. aureus*, we extended these observations by demonstrating that PMN-MDSCs have a direct bactericidal function. This phenomenon was consistent with our observation of bacterial debris in phagolysosomes within some of the PMN-MDSCs we imaged. Interestingly, the median number of bacteria per cell was higher in C-PMNs than in PMN-MDSCs, but the difference was marginal and of questionable biological significance. While these results may indicate that PMN-MDSCs are intrinsically less phagocytic than PMNs, several variables—such as random plane of section, the limitations of static images, the limited number of dogs used for imaging, and our interrogation of only two bacterial species—precluded reliable quantitative comparisons of phagocytic efficiency in our experiments. Further work will be required to address the comparative phagocytic ability of PMN-MDSCs and PMNs.

In summary, our findings highlight a novel bacterial killing function of PMN-MDSCs isolated from tumor-bearing dogs. This adds another function to PMN-MDSCs' repertoire of activities and raises intriguing questions about how PMN-MDSCs might be involved in establishing a pre-neoplastic niche in tumors associated with certain bacteria (17–19). For example, we speculate that PMN-MDSCs function in regions of bacterial colonization or infection in order to target the bacteria, yet in doing so promote an immune suppressive microenvironment that drives aggressive expansion of neoplastic cells (20–22). We hypothesize that PMN-MDSCs promote a suppressive microenvironment early in certain bacterial infections, contributing to the development of a pre-neoplastic niche and tumor development. The nexus of suppressive and bactericidal MDSC function may therefore represent an important focus of future research into oncogenesis.

DATA AVAILABILITY STATEMENT

The datasets generated for this study are available on request to the corresponding author.

ETHICS STATEMENT

The animal study was reviewed and approved by University of Pennsylvania's Institutional Animal Care and Use Committee, the Privately Owned Animal Protocol Committee (Protocol #500) at the School of Veterinary Medicine, University of Pennsylvania, and the Clinical Review Board Protocol CS2019-208: Flint Animal Cancer Center Biobanking and Sample Collection at the Flint Animal Cancer Center at Colorado State University. Written informed consent was obtained from the owners for the participation of their animals in this study.

AUTHOR CONTRIBUTIONS

SH and OG conceived and planned the experiments. SH processed samples for EM, collected and analyzed EM images, performed bacterial killing assays, and wrote the first draft of the manuscript. Y-MC performed statistical analyses and created summary figures. RO performed the oxidative burst assays under the guidance of JP. DT provided samples from tumor-bearing dogs. PP and MG provided bacterial strains and advice on bacterial assays. OG funded the project, supervised SH, and edited all drafts of the manuscript. All authors read and approved the final draft of the manuscript.

FUNDING

SH was supported by the Howard Hughes Medical Institute-Burroughs Wellcome Fund Medical Research Fellowship. RO and JP were funded by UPenn's Center for Undergraduate Research Funds, with a Team Grant for Interdisciplinary Activities (TGIA). Work in the Garden Immune Regulation Laboratory was funded in part by an International Canine Health Award to OG from The Kennel Club (U.K.).

ACKNOWLEDGMENTS

The authors would like to thank the entire Garden Immune Regulation Laboratory for all their assistance with this project, especially Brandon Lawson, who scrambled the EM images for analysis. Thank you as well to Penn Vet's Veterinary Clinical Investigations Center, the Penn Vet Medical Oncology Service, and Lynelle Lopez at Colorado State University's Flint Animal Cancer Center for assistance with collecting blood samples. We would also like to thank Dr. Dieter Schifferli for sharing his expertise in bacterial killing assays. We are also grateful to the Electron Microscopy Resource Laboratory at the Perelman School of Medicine, University of Pennsylvania for processing cells for EM, as well as assisting with imaging.

SUPPLEMENTARY MATERIAL

The Supplementary Material for this article can be found online at: https://www.frontiersin.org/articles/10.3389/fimmu.2019.02371/full#supplementary-material

REFERENCES

1. Kumar V, Patel S, Tcyganov E, Gabrilovich DI. The nature of myeloid-derived suppressor cells in the tumor microenvironment. *Trends Immunol.* (2016) 37:208–20. doi: 10.1016/j.it.2016.01.004
2. Bronte V, Brandau S, Chen SH, Colombo MP, Frey AB, Greten TF, et al. Recommendations for myeloid-derived suppressor cell nomenclature and characterization standards. *Nat Commun.* (2016) 7:12150. doi: 10.1038/ncomms12150
3. Pereira WF, Ribeiro-Gomes FL, Guillermo LV, Vellozo NS, Montalvao F, Dosreis GA, et al. Myeloid-derived suppressor cells help protective immunity to Leishmania major infection despite suppressed T cell responses. *J Leukoc Biol.* (2011) 90:1191–7. doi: 10.1189/jlb.1110608
4. Leiber A, Schwarz J, Kostlin N, Spring B, Fehrenbach B, Katava N, et al. Neonatal myeloid derived suppressor cells show reduced apoptosis and immunosuppressive activity upon infection with *Escherichia coli*. *Eur J Immunol.* (2017) 47:1009–21. doi: 10.1002/eji.201646621
5. Poe SL, Arora M, Oriss TB, Yarlagadda M, Isse K, Khare A, et al. STAT1-regulated lung MDSC-like cells produce IL-10 and efferocytose apoptotic neutrophils with relevance in resolution of bacterial pneumonia. *Mucosal Immunol.* (2013) 6:189–99. doi: 10.1038/mi.2012.62
6. Heim CE, Vidlak D, Scherr TD, Kozel JA, Holzapfel M, Muirhead DE, et al. Myeloid-derived suppressor cells contribute to Staphylococcus aureus orthopedic biofilm infection. *J Immunol.* (2014) 192:3778–92. doi: 10.4049/jimmunol.1303408
7. Tebartz C, Horst SA, Sparwasser T, Huehn J, Beineke A, Peters G, et al. A major role for myeloid-derived suppressor cells and a minor role for regulatory T cells in immunosuppression during Staphylococcus aureus infection. *J Immunol.* (2015) 194:1100–11. doi: 10.4049/jimmunol.1400196
8. Pushalkar S, Hundeyin M, Daley D, Zambirinis CP, Kurz E, Mishra A, et al. The pancreatic cancer microbiome promotes oncogenesis by induction of innate and adaptive immune suppression. *Cancer Discov.* (2018) 8:403–16. doi: 10.1158/2159-8290.CD-17-1134
9. Goulart MR, Hlavaty SI, Chang Y-M, Polton G, Stell A, Perry J, et al. Phenotypic and transcriptomic characterization of canine myeloid-derived suppressor cells. *Sci Rep.* (2019) 9:3574. doi: 10.1038/s41598-019-40285-3
10. Chen Y, Junger WG. Measurement of oxidative burst in neutrophils. *Methods Mol Biol.* (2012) 844:115–24. doi: 10.1007/978-1-61779-527-5_8
11. Lu T, Porter AR, Kennedy AD, Kobayashi SD, DeLeo FR. Phagocytosis and killing of Staphylococcus aureus by human neutrophils. *J Innate Immun.* (2014) 6:639–49. doi: 10.1159/000360478
12. Condamine T, Kumar V, Ramachandran IR, Youn JI, Celis E, Finnberg N, et al. ER stress regulates myeloid-derived suppressor cell fate through TRAIL-R-mediated apoptosis. *J Clin Invest.* (2014) 124:2626–39. doi: 10.1172/JCI74056
13. Segal AW. How neutrophils kill microbes. *Annu Rev Immunol.* (2005) 23:197–223. doi: 10.1146/annurev.immunol.23.021704.115653
14. Pawelec G, Verschoor CP, Ostrand-Rosenberg S. Myeloid-derived suppressor cells: not only in tumor immunity. *Front Immunol.* (2019) 10:1099. doi: 10.3389/fimmu.2019.01099
15. Youn JI, Collazo M, Shalova IN, Biswas SK, Gabrilovich DI. Characterization of the nature of granulocytic myeloid-derived suppressor cells in tumor-bearing mice. *J Leukoc Biol.* (2012) 91:167–81. doi: 10.1189/jlb.0311177
16. Periasamy S, Avram D, McCabe A, MacNamara KC, Sellati TJ, Harton JA. An immature myeloid/myeloid-suppressor cell response associated with necrotizing inflammation mediates lethal pulmonary tularemia. *PLoS Pathog.* (2016) 12:e1005517. doi: 10.1371/journal.ppat.1005517
17. Irrazabal T, Belcheva A, Girardin SE, Martin A, Philpott DJ. The multifaceted role of the intestinal microbiota in colon cancer. *Mol Cell.* (2014) 54:309–20. doi: 10.1016/j.molcel.2014.03.039

18. Wang F, Meng W, Wang B, Qiao L. Helicobacter pylori-induced gastric inflammation and gastric cancer. *Cancer Lett.* (2014) 345:196–202. doi: 10.1016/j.canlet.2013.08.016
19. Zhou Z, Chen J, Yao H, Hu H. Fusobacterium and colorectal cancer. *Front Oncol.* (2018) 8:371. doi: 10.3389/fonc.2018.00371
20. Lu LC, Chang CJ, Hsu CH. Targeting myeloid-derived suppressor cells in the treatment of hepatocellular carcinoma: current state and future perspectives. *J Hepatocell Carcinoma.* (2019) 6:71–84. doi: 10.2147/JHC.S159693
21. Groth C, Hu X, Weber R, Fleming V, Altevogt P, Utikal J, et al. Immunosuppression mediated by myeloid-derived suppressor cells (MDSCs) during tumour progression. *Br J Cancer.* (2019) 120:16–25. doi: 10.1038/s41416-018-0333-1
22. Ma J, Xu H, Wang S. Immunosuppressive role of myeloid-derived suppressorcells and therapeutic targeting inlung cancer. *J Immunol Res.* (2018) 2018:6319649. doi: 10.1155/2018/6319649

Conflict of Interest: The authors declare that the research was conducted in the absence of any commercial or financial relationships that could be construed as a potential conflict of interest.

Copyright © 2019 Hlavaty, Chang, Orth, Goulian, Planet, Thamm, Punt and Garden. This is an open-access article distributed under the terms of the Creative Commons Attribution License (CC BY). The use, distribution or reproduction in other forums is permitted, provided the original author(s) and the copyright owner(s) are credited and that the original publication in this journal is cited, in accordance with accepted academic practice. No use, distribution or reproduction is permitted which does not comply with these terms.

frontiers in Oncology

REVIEW
published: 07 November 2019
doi: 10.3389/fonc.2019.01185

Comparative Approach to the Temporo-Spatial Organization of the Tumor Microenvironment

Kendall L. Langsten[1]*, *Jong Hyuk Kim*[2,3,4], *Aaron L. Sarver*[2,4,5], *Mark Dewhirst*[6] and *Jaime F. Modiano*[2,3,4,7,8,9,10]*

[1] Department of Veterinary Population Medicine, University of Minnesota, St. Paul, MN, United States, [2] Animal Cancer Care and Research Program, University of Minnesota, St. Paul, MN, United States, [3] Department of Veterinary Clinical Sciences, College of Veterinary Medicine, University of Minnesota, St. Paul, MN, United States, [4] Masonic Cancer Center, University of Minnesota, Minneapolis, MN, United States, [5] Institute for Health Informatics, University of Minnesota, Minneapolis, MN, United States, [6] Radiation Oncology Department, Duke University Medical School, Durham, NC, United States, [7] Department of Laboratory Medicine and Pathology, University of Minnesota Medical School, Minneapolis, MN, United States, [8] Center for Immunology, University of Minnesota, Minneapolis, MN, United States, [9] Stem Cell Institute, University of Minnesota, Minneapolis, MN, United States, [10] Institute for Engineering in Medicine, University of Minnesota, Minneapolis, MN, United States

OPEN ACCESS

Edited by:
Thomas Daubon,
Institut National de la Santé et de la Recherche Médicale (INSERM), France

Reviewed by:
Paolo Cirri,
University of Florence, Italy
Guanglin Cui,
Nord University, Norway

***Correspondence:**
Kendall L. Langsten
kannetti@umn.edu
Jaime F. Modiano
modiano@umn.edu

Specialty section:
This article was submitted to Cancer Molecular Targets and Therapeutics, a section of the journal Frontiers in Oncology

Received: 04 September 2019
Accepted: 21 October 2019
Published: 07 November 2019

Citation:
Langsten KL, Kim JH, Sarver AL, Dewhirst M and Modiano JF (2019) Comparative Approach to the Temporo-Spatial Organization of the Tumor Microenvironment. Front. Oncol. 9:1185. doi: 10.3389/fonc.2019.01185

The complex ecosystem in which tumor cells reside and interact, termed the tumor microenvironment (TME), encompasses all cells and components associated with a neoplasm that are not transformed cells. Interactions between tumor cells and the TME are complex and fluid, with each facet coercing the other, largely, into promoting tumor progression. While the TME in humans is relatively well-described, a compilation and comparison of the TME in our canine counterparts has not yet been described. As is the case in humans, dog tumors exhibit greater heterogeneity than what is appreciated in laboratory animal models, although the current level of knowledge on similarities and differences in the TME between dogs and humans, and the practical implications of that information, require further investigation. This review summarizes some of the complexities of the human and mouse TME and interjects with what is known in the dog, relaying the information in the context of the temporo-spatial organization of the TME. To the authors' knowledge, the development of the TME over space and time has not been widely discussed, and a comprehensive review of the canine TME has not been done. The specific topics covered in this review include cellular invasion and interactions within the TME, metabolic derangements in the TME and vascular invasion, and the involvement of the TME in tumor spread and metastasis.

Keywords: tumor microenvironment, temporo-spatial organization, dog, canine, human

INTRODUCTION

Cancer, the uncontrolled proliferation of cells, is a significant cause of morbidity and mortality in humans and their canine companions worldwide (1, 2). The process of neoplastic transformation is similar amongst species and can most easily be conceptualized in the three steps of initiation, promotion, and progression toward malignancy (3), although it is now apparent that these steps are neither sequential nor obligate. In the seminal work by Hanahan and Weinberg (4), tumors were introduced as complex heterotypic tissues where a non-transformed milieu influences the

progression of transformed cells with which it co-exists in the same space and time. This milieu, the tumor microenvironment (TME), may be thought of as the ecosystem or community within which neoplastic cells survive and reside. The genomic landscape of the malignant cells and the composition and behavior of the TME are shaped by intense selection that can be described as prototypical Darwinian evolution in a microscopic scale. All non-transformed cells that interact with tumor cells, including inflammatory cells, endothelium, adipocytes, and fibroblasts, among others, as well as the non-cellular components, including structural scaffold surrounding the cells and the soluble factors secreted by the tumor and non-tumor components, compose the TME [**Figure 1**; (5)]. In a non-neoplastic environment, these components have a vast range of functions, including forming the interstitium that creates a scaffold for parenchyma to organize, sequestering growth factors, supplying nutrients, draining waste from tissue, and creating a competent immune system to protect the body against invaders.

The interplay between the TME and tumor cells is paramount in the progression and response to neoplastic growth. While our understanding of the TME in dogs is rudimentary, there are the similarities in tumor heterogeneity between dogs and humans (**Table 1**), which are often not appreciated in laboratory animal models. Although the current level of knowledge on similarities and differences in the TME between dogs and humans, and the practical implications of that information require further investigation. This review provides an overview of the complexity observed in the human and mouse TME, interjects known similarities and differences in the dog, and relays them in the context of the temporo-spatial organization of the TME. In short, the proposed temporo-spatial organization of the TME involves neoplastic tells transforming, the transformation of adjacent TME into a cancer associated phenotype, and vascular invasion, potentially culminating in tumor cell spread and metastasis (**Figure 2**). To the authors' knowledge, this approach to the organization and conceptualization of the TME, as well as a review of the TME in the dog, have not been described before. Discussions include cellular invasion and interactions within the TME, metabolic derangements in the TME and vascular invasion, and the involvement of the TME in tumor spread and metastasis.

CELLULAR INVASION AND INTERACTIONS WITHIN THE TME

While the definition of "cancer stem cells" (CSCs; also called tumor-initiating cells or tumor-propagating cells) is mostly

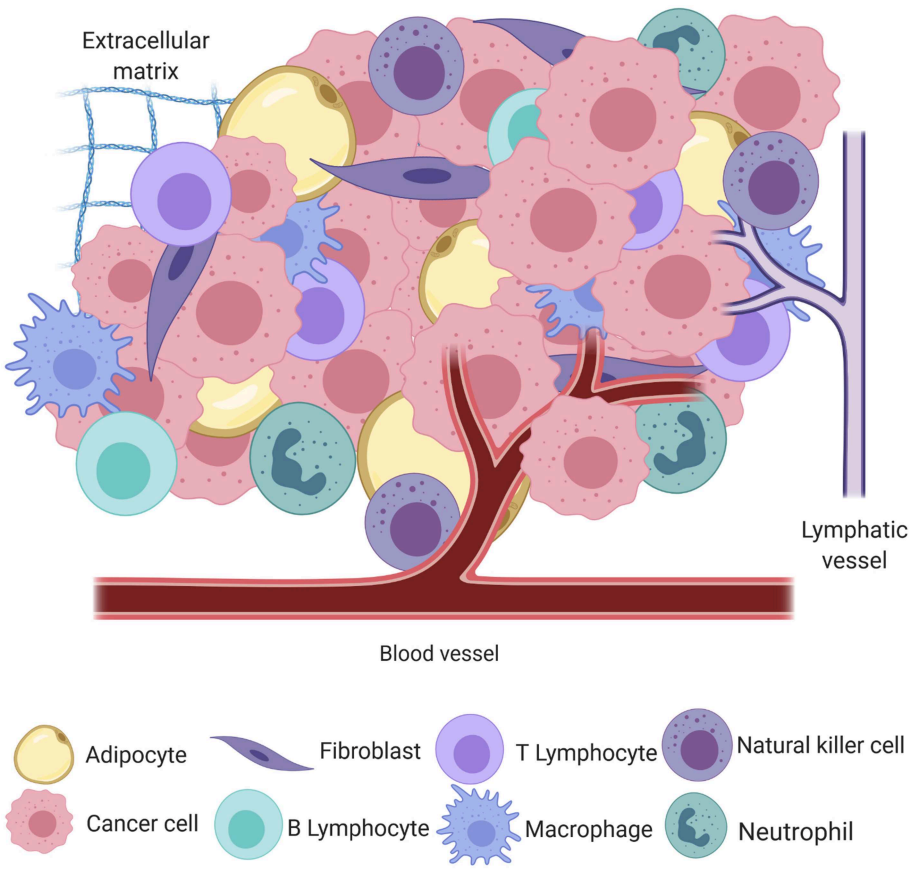

FIGURE 1 | A simplified schematic of the cellular and structural component of the tumor microenvironment, including adipocytes, fibroblasts, B and T lymphocytes, macrophages, natural killer cells, neutrophils, blood and lymphatic vessels, and the extracellular matrix, all intermingled with transformed cancer cells (created with Biorender.com).

TABLE 1 | Comparative features of the TME between dogs and humans.

Components of the TME	Dog	Human
Adipocytes	Produce aromatase cytochrome P450, estrogen, and progesterone which stimulates tumor development	
Adipose-derived mesenchymal stem cells	Suppress T cells through TGFβ and adenosine pathways	Suppress T cells through indoleamine 2,3-dioxygenase (IDO) pathway
Fibroblasts	Unknown	Matrix is capable of inhibiting tumor cell spread
Cancer-associated fibroblasts	Modulate gene expression of cancer cells	
Soluble factors	IL-8 receptors are upregulated on cancer cells, leads to increase in angiogenesis and inflammation	
	Elevated Cox-2 levels in certain tumor types; Cox-inhibitors utilized for anti-tumor effects	
Lymphatics	Density of lymphatic vessel is correlated with tumor growth and metastasis	
Immune cells	Osteosarcoma can be separated into "hot" (active) and "cold" (barren) tumors, in regards to inflammatory response	
	Increased presence of immune transcripts in osteosarcoma is not prognostically significant	Increased presence of immune transcripts in osteosarcoma is associated with better prognosis

semantic, the importance of cells that retain or acquire stem-like features in the tumor cannot be underestimated. Whether they be few, as in traditional hierarchically-organized tumors, or many, as in stochastically organized tumors, these cells contribute to remodeling the TME (6).

Recent work characterized genome-wide gene expression signatures in canine tumor models (hemangiosarcoma, osteosarcoma, and glioblastoma) that were grouped according to their hierarchical organization (7). Cell lines derived from these three tumor types were cultured under non-adherent low serum conditions that promote sphere formation and enrich CSCs. The steady state gene expression associated with CSC maintenance in tumors with high sphere-forming efficiency (i.e., hierarchically organized with relatively few CSCs) showed metabolic skewing toward fatty acid synthesis and secretion of immunosuppressive cytokines. On the other hand, tumors with low sphere-forming efficiency (i.e., stochastically organized with many or most cells having CSC potential) showed metabolic skewing toward fatty acid oxidation and potential immunoevasion through upregulation of CD40. In the incipient tumor, CSCs create reactive microenvironments that support tumor growth (8), importantly, by producing cytokines that leverage the innate properties of resident macrophages to remodel the microenvironment. CSCs also interact bidirectionally with myeloid cells, which can remain in an incompletely differentiated state and become myeloid-derived suppressor cells (MDSCs, a highly heterogeneous population of cells that contributes to cancer stemness as well as to the functional immunosuppressive barrier (9, 10).

Intriguingly, the CSC condition appears to be at least partly under extrinsic control. Depletion of CSCs in cultured canine and human cell lines leads to reprogramming of differentiated cells to become CSCs, maintaining the population in a steady state (11). The signals that regulate this process are poorly understood, but they might involve dysregulated expression of Snail family transcription factors Snail (SNAI1), Slug (SNAI2), as well as TWIST1 and Zeb1 (12–14), perhaps through epigenetic modification of their respective promoters (15). These responses are tightly regulated by environmental cues. For example, expression of SNAI2 and its targets, CDH1, VIM, and JUP in hemangiosarcoma cells showed a biphasic response to interkeukin-8 (IL-8), with small amounts of IL-8 favoring self-renewal and abundant IL-8 favoring expansion of bulk (differentiated) tumor cells (8, 16).

The role of adipocytes in the TME has received more attention as evidence mounts for a link between obesity and cancer risk in dogs and humans (17, 18). Adipocytes adjacent to tumor cells, known as cancer-associated adipocytes (CAAs), are recruited to be actively involved in tumor initiation, promotion, and progression. The mechanism of CAA development is unclear, but likely involves a bidirectional communication stream that includes adipokines and extracellular vesicles, among other factors. Adipokines, metabolically active substances secreted by adipocytes to create a permissive TME, include substances such as leptin, tumor necrosis factor-α (TNFα), C-C Motif Chemokine Ligand 2 (CCL2), and adiponectin. A concise review of adipokines in domestic animals was recently published (19).

Adipocytes promote neoplastic development through a variety of mechanisms, including supporting angiogenesis (described later in this review), manipulating tumor cell metabolism, and encouraging a pro-inflammatory state, leading to the recruitment of macrophages. Adipocytes play an important role in reprogramming tumor cell metabolism. For example, ovarian cancer cells co-cultured with abdominal adipose cells were shown to coerce neighboring adipocytes into supplying free fatty acids, thereby providing substrates for sustained tumor cell replication (20). The role of adipocytes in promoting chronic inflammation has been the subject of numerous studies. Adipocytes produce pro-inflammatory adipokines and cytokines [including CCL2, interleukin-6 (IL-6), and TNFα], which increase inflammation and metastatic risk, supporting tumor survival (20, 21). In the case of mammary and breast carcinomas in dogs and humans, respectively, adipocyte-derived aromatase cytochrome P450, estrogen, and progesterone have been reported to stimulate tumor development and enhance invasive potential [**Table 1**; (22, 23)]. Finally, extracellular remodeling in tumors, including increased collagen deposition by adipocytes, can lead to adipocyte apoptosis and necrosis. Macrophages are then recruited into the tumor due to the release of pro-inflammatory damage-associated molecular patterns (DAMPs) from the dying adipocytes (17).

Recently, attention has been given to the influence of adipose-derived mesenchymal stem cells (ad-MSCs) in tumor progression. The secretome of ad-MSCs is incompletely understood but is thought to have overarching

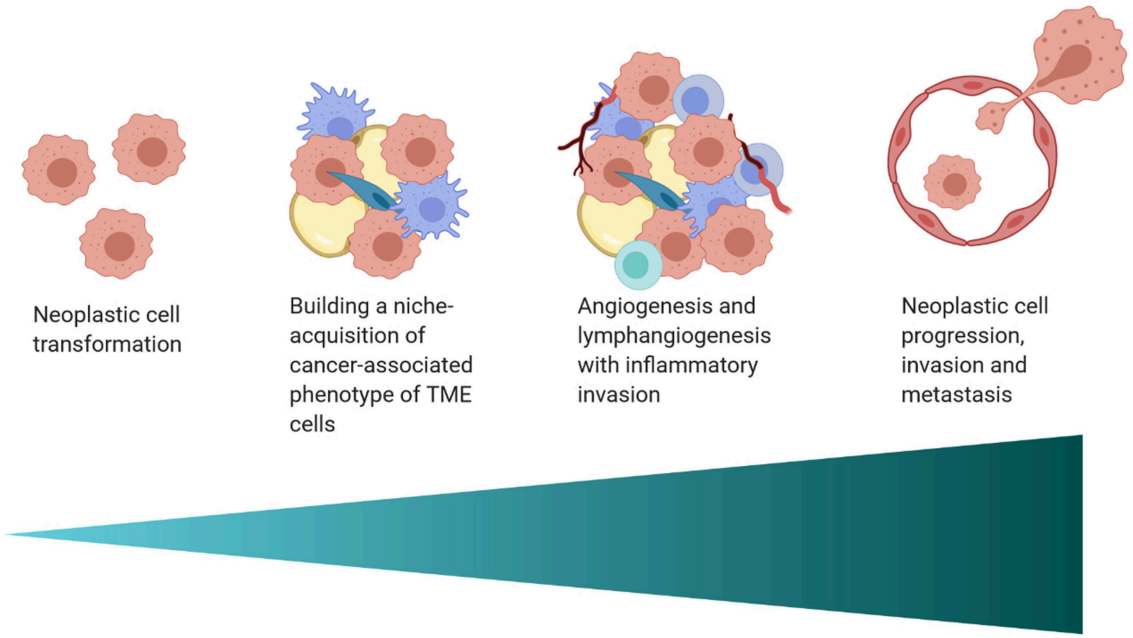

FIGURE 2 | A schematic of the proposed temporo-spatial organization of the TME. Cells must first undergo neoplastic transformation, allowing for the creation of a permissive micro-ecological niche. Neighboring cells, including adipocytes, fibroblasts, and macrophages, among others, can adopt a cancer-associated phenotype, with complex, pro-tumorigenic effects. Hypoxia induced by cell proliferation and metabolic changes encourage lymph and blood vessel invasion, increasing infiltration by inflammatory cells. Furthermore, angiogenesis and lymphangiogenesis create increased opportunity for neoplastic cell spread and metastasis (created with Biorender.com).

immunomodulatory and pro-angiogenic properties (24). The immunomodulatory properties of these cells are dependent on the inflammatory milieu in which the cells reside. Some of the anti-inflammatory properties of human and dog MSCs seem to differ mechanistically. Ad-MSC dependent T cell suppression in humans is through the indoleamine 2,3-dioxygenase (IDO) pathway, resulting in decreased T cell function through tryptophan depletion (25). Alternatively, in dogs ad-MSCs most likely decrease T cell activity through TGFβ and adenosine pathways [**Table 1**; (26)]. While a solid body of knowledge about the influence of adipocytes and ad-MSCs in human tumor growth and progression has been developed in recent years, the influence of these cells on the TME in dogs remains to be elucidated.

In a non-cancer associated microenvironment, fibroblasts play a major role in producing components of the extracellular matrix (ECM) including fibrillar collagen, elastin, laminin, fibronectin, and glycosaminoglycans (27). Fibroblasts are critical in wound healing, inflammatory reactions, fibrosis, promoting angiogenesis, and cancer progression. Tumors are often conceptualized as a "wound that will not heal" with abundant collagen deposition (28). *In vitro* studies using cell lines from various species, although to the authors' knowledge not from dogs, have demonstrated that normal, non-cancer associated fibroblasts and the matrix they produce are capable of inhibiting the spread of tumor cells, a phenomenon termed neighbor suppression (29–31). Since neighbor suppression was first recognized by Stoker et al. (29), many theories have developed around the molecular mechanisms influencing this finding, including heterologous communication between transformed and non-transformed cells through junctional complexes and through soluble factors within the ECM (32, 33). Neighbor suppression has not yet been recognized in canine tumors (**Table 1**).

Cancer-associated fibroblasts (CAFs) are corrupted by the neoplastic cells in their proximity and have drastically different functions than their non-transformed counterparts. The origin of CAFs is not entirely clear; many theories on their origin claim CAFs originate from resident mesodermal precursors (34–38). An influential paper by Erez et al. (39) demonstrated that the transcription factor NFκB induces the CAF phenotype through upregulation of pro-inflammatory genes. These findings suggest a necessity for innate immune involvement in the education of CAFs. Furthermore, epigenetic changes also play a role in the development of CAFs. Albrengues et al. (36) demonstrated that CAFs have constitutively activated JAK1/STAT3 signaling pathways secondary to epigenetic changes. Histone acetylation of STAT3 in CAFs by leukemia inhibitory factor (LIF) caused subsequent activation of DNMT3b (a DNA methyltransferase). This in turn led to decreased SHP-1 expression with subsequent sustained activation of JAK1. Interestingly, inhibition of DNMTs caused CAFs to convert to a non-cancer associated fibroblast phenotype (36). CAFs have diverse phenotypes without unique markers, although phenotypic similarities to myofibroblasts,

including reduced caveolin-1 (CAV-1) expression and increased expression of α-SMA, vimentin, fibroblast-activating protein, and MCT-4 (40, 41) have been described. Additionally, CAFs have been shown to increase tumor cell growth, motility, and local invasion through ECM remodeling and cytokine release (37, 42, 43). In both humans and dogs, CAFs modulate gene expression of cancer cells (44, 45). However, it is difficult to compare their transcriptional programs across species, as experimental protocols and genes of interest differ between published studies. Functionally, CAFs differ from normal fibroblasts in the products and quantities of enzymes that they produce. For example, in both canine mammary carcinoma and human breast carcinoma CAFs exhibit increased aromatase activity, which is associated with hormone-driven tumor progression (46, 47).

Mesenchymal stem cells (MSCs), also known as undifferentiated fibroblasts or mesenchymal stromal cells, are another important component of the TME. These cells are phenotypically plastic cells that originate from the mesoderm (48). MSCs home from bone marrow, spleen and other locations to sites of injury and inflammation, including tumors (49). The role of MSCs in the TME are numerous; one of the better-studied functions is their influence in changing the immune landscape (for more information, see the section on metabolism, vascular invasion, and immune cells within the TME).

Tumor-associated ECM is markedly different from ECM in a non-pathologic milieu. As an active driver of tumor progression, tumor-associated ECM is reorganized, directing tumor cell migration and promoting local invasion along collagen fibers (50, 51). Furthermore, tumor-associated ECM is associated with increased pro-inflammatory cytokines, promotes angiogenesis, and factors that increase fibroblast proliferation (52). As all components of the TME are simultaneously interacting with one another and tumor cells, it stands to reason that by encouraging inflammation, tumor-associated ECM likely contributes to the production of CAFs. Collagen is one of the most abundant components of the ECM and is known to exhibit tumor-associated collagen signatures. Differences in collagen density, width, length, and straightness, as well as reorganization of the boundary between tumor and stroma, are some of the collagen signatures appreciated (53, 54). In dogs and humans, collagen signatures are important prognostic indicators in mammary and breast carcinoma (53, 54). For example, in a study analyzing characteristics of mammary carcinoma in dogs, tumor-associated ECM had upregulated collagen1α1, α-SMA, fibroblast activation protein (FAP), platelet-derived growth factor (PDGF)-β, and paradoxically, CAV-1 (55).

Interactions between tumor cells, stromal cells, and the ECM are heterogeneous and tumor-specific. However, fragmentation of hyaluronic acid, which is pro-inflammatory, and deposition of tenascin-C seem to occur in most tumor types (56–58). The hyaluronic acid receptor, CD44, is expressed by most tumor and stromal cells, but the highest levels are seen in CSCs (6). In addition to HA, the ECM is composed of collagens, elastins, laminins, fibrinogen, and tissue-specific proteoglycans. The stoichiometry and topology of these components regulates adhesion (for example, by interaction with cell surface integrins) and stiffness of the ECM. Tumor cells and inflammatory cells secrete proteases that degrade the ECM, and proteins and proteoglycans to remodel it. The interactions of the ECM with integrins, mechanoreceptors, and signaling proteins that activate contractility, such as focal adhesion kinase, modulate cellular motility, proliferation and survival (59–61). The interactions are bidirectional, as the cytoskeleton "pushes back" into the ECM, maintaining integrins and focal adhesions in a state of isometric tension. Increased tension also activates the small G protein Rho and its target Rho-associated kinase (ROCK), which controls myosin light chain phosphorylation. The ECM in most tumors is several orders of magnitude stiffer than their normal tissue counterparts, making it permissive for cell migration and ultimately, metastasis (59). There are myriad studies documenting the importance of ROCKs in tumor progression, but a noteworthy study showed that ROCK inhibitors were able to push chemoresistant mouse osteosarcoma cells away from a malignant phenotype and into terminal adipocyte differentiation (62). Perhaps more interestingly, cells that escaped terminal differentiation in the presence of ROCK inhibitors regained sensitivity to chemotherapy and could be eliminated by treatment with doxorubicin (62).

The extensive heterogeneity and adaptation of the tumor niche is partly dependent on intercellular communication. Malignant cells co-opt developmental programs of intercellular communication to create and maintain a niche with unique properties that promote growth and survival (6). Intercellular communication involves a multitude of interactions mediated by cell-to-cell contacts and soluble mediators. Cell-to-cell contacts include adhesion molecules, stable ligand-receptor interactions, and promiscuous, transient to stable interactions between cell surface proteins, glycans, and lipids (63, 64). Emerging evidence also suggests that cells can communicate in the local environment by exchanging genetic and biochemical mediators through tunneling nanotubes (65, 66). Soluble mediators of communication include hormones, cytokines, chemokines, lipids, and microvesicles (67–70). Cells also interact with their external environment through pressure receptors and by molding the ECM (59, 71–73).

Soluble mediators of communication have been relatively well-described in humans, although there is little information available as to the impact of the stroma and soluble factors in dogs. Kim et al. (8) showed that IL-8, a cytokine produced by fibroblasts, neoplastic cells, and other cell types, supports tumor progression by modulating the TME in canine hemangiosarcoma into a more "reactive" state; increasing the propensity toward inflammation, fibrosis, and coagulation. Intriguingly, IL-8 blockade reduced tumor cell survival and engraftment in a xenograft model of canine hemangiosarcoma, indicating this cytokine may be necessary to establish the initial niche for this disease (8). Similar findings have been reported in humans, with tumor cells of various tumor types upregulating IL-8 production and IL-8 receptors on cancer cells as well as other cells types with increases in angiogenesis and inflammation within those tissues [**Table 1**; (74, 75)]. The implications and utilization of soluble factors in cancer treatment is a topic that in recent years has begun to gain traction as an important area for investigation.

Intercellular interactions are also critical to establish and maintain the tumor immunosuppressive barrier, by excluding or incapacitating host immune cells. For example, expression of pro-apoptotic molecules, such as FasL can target infiltrating effector T cells in the tumor environment, while sparing apoptosis resistant tumor cells, CAFs, and cancer-associated endothelial cells. For more information on immune cells within the TME, please see the next section on metabolism, vascular invasion, and immune cells within the TME.

METABOLISM, VASCULAR INVASION, AND IMMUNE CELLS WITHIN THE TME

Formation of blood vessels is an absolute requirement for tumor growth, survival, and progression. Without access to oxygen and nutrients supplied by the blood, tumor growth is restricted to an ∼1–3 mm diameter mass *ex vivo* and ∼100–500 microns *in vivo* (76–78). It stands to reason that the aspects of the TME reviewed might precede angiogenesis, lymphangiogenesis, and immune invasion due to the size of the tumor where these processes occur. Tumor neovascularization is a complex and multifaceted process driven by tissue hypoxia, defined as tissue with oxygen concentrations below 10 mmHg, which is a common feature of solid tumors (79, 80). Below this threshold, cells upregulate a host of adaptive proteins; a response mostly driven by the heterodimeric transcription factor, hypoxia-inducible factor (HIF-1) (81). In normoxic conditions, prolyl hydroxylases (which have oxygen dependent enzymatic activity), hydroxylate proline residues in the oxygen degradation domain of HIF-1α. The von Hippel-Lindau (VHL) complex is then able to recognize HIF-1α for subsequent proteasomal degradation (81). Under hypoxic conditions, VHL itself undergoes proteasomal degradation, leading to stabilization of HIF-1α and subsequent binding to its constitutively regulated partner, HIF-1β (82). Once this occurs, the HIF-1α/HIF-1β heterodimer enters the nucleus and binds to hypoxia-regulated-elements (HREs) of hundreds of genes (83). Binding targets of HIF-1 are in part controlled by epigenetic changes that promote active chromatin states at HIF binding sites (84). The impacts of HIF-1 binding are numerous, from reducing oxygen consumption to increasing angiogenesis through regulation of vascular endothelial growth factor (VEGF), the angiopoietin-1 regulated tyrosine kinase receptor TIE2 (also known as TEK), and angiopoietin, among others (83, 85).

VEGF is a potent growth factor influencing vascular permeability and angiogenesis (86). VEGF-A is one of the best-characterized forces in the development of new vessels and binds to VEGF receptors-1 and -2 (VEGFR-1 and VEGFR-2). VEGF-A can be secreted along with other pro-angiogenic factors by numerous cell types, including adipocytes, within the TME (87). VEGFR-1 and VEGFR-2 are both receptor tyrosine kinases that contain a split tyrosine-kinase domain, although they function differently within the TME (88). VEGFR-2 is upregulated in endothelial cells of newly forming blood vessels within tumors and is commonly implicated in neovascularization. A recent study demonstrated that the α4β1-integrin is capable of VEGFR2 binding and activation, presenting a novel potential target for therapy (89). Alternatively, VEGFR-1 has relatively weak pro-angiogenic properties and can recruit and activate tumor-associated macrophages (TAMs) and myeloid cells, promoting tumor cell metastasis and proliferation [**Figure 3**; (90)]. Little is known about the dynamic balance between VEGFR-2 and VEGFR-1 in tumors of dogs, but there is one report suggesting that heritable traits or the breed background might influence the expression and function of these receptors in vascular sarcomas (91). A second major regulator of angiogenesis is Tie-2. In the presence of active Tie-2 signaling, the vasculature remains in a mature state surrounded by pericytes (92). Angiopoietin 2 (ANGPT2), an angiopoietin 1 competitive antagonist and HIF-1 target gene, binds to endothelial cells, preventing Tie-2 signaling. This causes the vasculature to become less mature with fewer pericytes (93). This microvasculature is then primed for maximum response to VEGF.

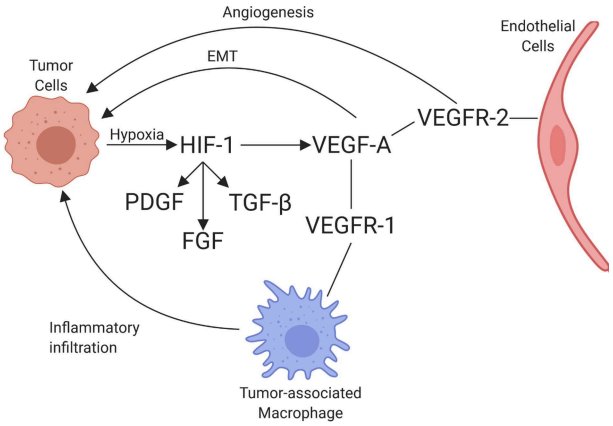

FIGURE 3 | Schematic of the interaction between tumor cells and endothelial cells, including the associated recruitment of inflammatory cells by endothelium. Through hypoxia, HIF-1 is upregulated, increasing PDGF, FGF, TGFβ, and VEGF-A expression. VEGF-A binds to its receptors, VEGFR-1 and VEGFR-2, leading to angiogenesis (through VEGFR-2 signaling), immune cell invasion (through VEGFR-1 signaling), and promotion of epithelial-mesenchymal transition (EMT) in tumor cells (created with Biorender.com).

Cyclo-oxygenase 2 (Cox-2), which is involved in the formation of some types of prostaglandin production, has been shown to increase expression of VEGF-A mRNA in tumors, thus having pro-angiogenic properties (94). The mechanism by which Cox-2 increases VEGF-A expression in tumors likely involves p38 mitogen activated protein kinase (MAPK) and Janus kinase (JNK) pathways. These pathways are integral in the transcriptional and post-transcriptional regulation of VEGF-A (95, 96). Elevated Cox-2 levels have been reported in canine and human prostatic carcinoma, transitional cell carcinoma, and squamous cell carcinoma, among others [**Table 1**; (97–102)]. As such, anti-Cox-2 therapies, including non-steroidal anti-inflammatory drugs (NSAIDs) which inhibit the production of Cox-2, have been the subject of anti-cancer initiatives.

In dogs with urothelial cell carcinoma, treatment with the NSAIDs piroxicam and deracoxib have shown promising clinical results, including decreasing tumor volume and increasing apoptosis of neoplastic cells (103, 104). Similarly, NSAIDs have been used for their anti-tumor effects in humans, such as a chemopreventative agent for colorectal cancer and certain subtypes of breast cancer (105, 106). Another promising anti-tumor therapy that leverages increased Cox-2 expression in tumors utilizes conditionally replicative oncolytic adenoviruses. To overcome the traditionally poor infectivity of these viruses, an oncolytic adenovirus with Cox-2 promoter-based targeting control mechanisms was designed. This viral therapy is specific to Cox-2 positive cells with the potential to specifically target a variety of Cox-2 positive tumors, thereby increasing efficacy and safety of this potential therapy (107, 108).

The clinical implications of HIF-1 and VEGF expression and regulation have been the subjects of recent investigation. Moeller et al. (109) were the first to demonstrate that radiotherapy upregulates HIF-1 protein levels, even at a time when the tumor is re-oxygenated. The mechanism for this effect was shown to be related to two factors: (1) release of HIF-1 mediated transcripts of HIF-1 stored in stress granules during hypoxia, and (2) an increase in oxidative stress after radiotherapy, preventing the activity of prolyl hydroxylases to prime HIF-1α for degradation. As a follow on, Li et al. (110) demonstrated that infiltration of macrophages into irradiated tumors stabilized HIF-1 via a nitric oxide mediated mechanism. Other cytotoxic treatments have been shown to increase HIF-1α levels via mechanisms involving oxidative stress. Doxorubicin can upregulate HIF-1α levels in aerobic tumor cells by stimulating inducible nitric oxide synthase (iNOS) activity (111). Hyperthermia increases the activity of NADPH-oxidase in tumor cells, thereby stabilizing HIF-1α. There are multiple potential consequences of chronic HIF-1 transcriptional upregulation, but of central importance is the upregulation of VEGF. As part of a clinical trial conducted in dogs with soft tissue sarcomas, treated with fractionated hyperthermia and radiotherapy, Chi et al. (112) examined the hypothesis that there would be an increase in HIF-1 mediated transcripts and associated physiologic modification early in the course of treatment. Tumor tissues were removed prior to, and 24 h after, radiotherapy and the first hyperthermia treatment. Tissues were examined for changes in gene expression and, concomitantly, the apparent diffusion constant of water of these tumors was measured using magnetic resonance imaging (ADC-MRI; a biomarker of hyperpermeability). Unsupervised gene expression analysis showed two main groupings, distinguished by whether ADC-MRI increased (indicating increased water content) or remained unchanged. Among several HIF-1 regulated genes observed in the subgroup that showed increased ADC, VEGF upregulation was one of the most predominant (113). Thus, this canine clinical study supported pre-clinical results; that the combination of hyperthermia and radiotherapy increases HIF-1 transcriptional activity. The fact that ADC only increased in a fraction of tumors, suggests that ADC may be a viable biomarker for understanding how the physiologic microenvironment responds to cytotoxic therapy. An important future direction of these observations includes ascertaining whether changes in ADC are associated with treatment outcome.

Hypoxia affects innate and adaptive immune function in multiple and complex ways (114). Macrophage response to hypoxia is multifaceted and relies on the presence and concentration of cytokines and other immune cells. TAMs, which are believed to arise from the resident macrophage pool, have been categorized as "M0" (uncommitted), "M1" (pro-immune), and "M2" (pro-angiogenic and immunosuppressive) (115–117). However, both resident and recruited macrophages are remarkably plastic and can revert among these phenotypes, with all three co-existing in different stages of tumor development and progression. M2 TAMs tend to accumulate in hypoxic regions due to hypoxia-mediated chemokine expression by both tumor and stromal cells (116, 118). The presence of macrophages in hypoxic regions promotes immunosuppressive functions, including release of immunosuppressive cytokines such as TGFβ, recruitment of regulatory T cells (Tregs), and binding of programmed death-1 (PD-1) receptor on cytotoxic T-cells by the HIF-1 target, programmed death ligand-1 (PD-L1) (118, 119). Additionally, hypoxia inhibits the adaptive immune system by downregulating T-cell motility and upregulating the HIF-1 targets SDF-1 and its ligand CXCR4, thereby stimulating intratumoral recruitment of immunosuppressive MDSCs (120–122). Hypoxia disturbs the balance between effector T cells and Tregs, tipping the balance toward the latter (123).

In the absence of oxygen, cells are obligated to use glycolysis to produce ATP. Reprogramming energy metabolism is regarded as a hallmark of cancer, as described by Hananhan and Weinberg (124). The "Warburg Effect," the unique process of tumor cells utilizing aerobic glycolysis, was first described by Warburg (125). Lactate is the product of both aerobic and anaerobic glycolysis (126). The relative predominance of hypoxia in tumors, therefore, is a major contributor to the production of lactate. In addition, the relative inefficiency in solute transport by tumor vasculature leads to accumulation of lactate to substantially elevated levels. Concentrations of lactate can range from normal levels of 1–2 mM to as high as 15–40 mM in both pre-clinical and human clinical samples (127, 128).

Lactic acid is a major component that fuels metabolic symbiosis between the aerobic and hypoxic tumor compartments (129). Lactate produced by hypoxic tumor cells is transported by passive monocarboxylic acid transporters (MCTs), which enable lactate to be excreted by cells that produce it and to be taken up by aerobic cells where in high concentrations, is back converted to pyruvate, where it enters the tricarboxylic acid (TCA) cycle to produce alanine and glutamate (126, 130). The affinity of aerobic tumor cells for lactate is 10 times higher than glucose, indicating that aerobic tumor cells preferentially use lactate (130). If the ability of aerobic tumor cells to use lactate is blocked, the cells will switch to utilizing glucose, thereby depleting local glucose concentrations. Excess glucose present in aerobic tumor regions can diffuse to hypoxic regions, where the glucose is catabolized to lactate (129). Since hypoxic tumor cells are reliant on glucose, even though some can use glutamine in its stead, this can lead to death of the cell (129, 131).

Utilization of lactate has also been described in tumor-associated fibroblasts, which have low expression of CAV-1, an inhibitor of myofibroblast differentiation (132). An informative study showed that tumor-associated myofibroblasts could use aerobic glycolysis to produce lactate. Lactate was then used by aerobic tumor cells to fuel the TCA cycle through its conversion to pyruvate. The authors termed this symbiosis the "Reverse Warburg Effect" because the myofibroblasts were responsible for aerobic glycolysis instead of the tumor cells (132). Lactate can also stimulate the stabilization of HIF-1α in aerobic tumor and endothelial cells (133). Like aerobic tumor cells, endothelial cells uptake lactate (133). The conversion of lactate to pyruvate interferes with the activity of the prolyl hydroxylases responsible for HIF-1α degradation. In the presence of elevated pyruvate, HIF-1α levels, and consequently VEGF levels increase, which promotes angiogenesis. The negative influence of lactate on cancer prognosis in humans is most likely attributed to downstream stabilization of HIF-1α in tumor and stromal cells (134). Lora-Michiels et al. (135) demonstrated that in 39 dogs with soft tissue sarcoma, those with relatively low pH tumors were associated with shorter progression free interval and overall survival than dogs with higher tumor pH. Extracellular pH, which is simpler to measure, can be used as a surrogate of lactate, since transport of lactate across a cell membrane via the MCT transporters includes a hydrogen ion (135). High lactate levels and associated extracellular acidosis also contribute to immune suppression (136).

Once tumor-associated blood vessels are formed, they are structurally and epigenetically abnormal, which facilitates metastatic spread. These vessels tend to be irregularly dilated and tortuous with increased permeability, decreased pericyte numbers, and abnormal deposition of collagen type IV in the basement membrane. Endothelial cell adhesion molecules, such as selectins and integrins are required for leukocyte transmigration into tissues (137, 138). It has been reported that these adhesion molecules are often absent in tumor microvessels, thereby reducing the ability of immune cells to gain access into tumors (137, 139). The downregulation of adhesion molecules is regulated by VEGF (139) and can be reversed by blocking VEGF or by altering IL-6 trans-signaling (138). Thus, the first line of defense that tumors use to inhibit immune surveillance is the blockade of transmigration of immune cells. Furthermore, there is substantial signaling between endothelial cells and tumor cells, especially CSCs, which have a tendency to seek out or create vascular niches (140). Several signaling pathways, including Sonic Hedgehog, and Notch, to name a few, emanate from endothelial cells and promote acquisition of CSC properties and proliferation within vascular niches (141). In the tumor microenvironment, it is likely that the balance between these pro and anti-inflammatory mediators dictates the extent of leukocyte-endothelial cell interactions that occur naturally and in response to therapy. Modulation of these interactions is likely essential for optimization of immunotherapy.

Like neoangiogenesis, lymphangiogenesis can act as an important gateway to tumor metastasis. The density of lymphatic vessels within a tumor has been correlated with tumor growth and metastasis in both dogs and humans [**Table 1**; (142–145)]. Mechanistic control of lymphangiogenesis is complex, involving a multitude of factors including many of the same factors described in tumor-associated neovascularization. Two of the major mechanisms controlling lymphangiogenesis are well-described. One is dependent on VEGF-C and VEGF-D produced by both tumor cells and TAMs, which bind VEGFR-3 on lymphatic endothelial cells (LECs) (146). The other is the SRY-related HMG-box (SOX18) pathway through prospero homeobox-1 activation (147, 148). Lymphangiogenic factors not only increase the number of lymphatic vessels within solid tumors, but also are capable of enlarging the diameter of the lymphatic vessels, increasing tumor cell metastasis to local lymph nodes (149). Furthermore, VEGF-C secreted by tumor cells can promote lymphangiogenesis within draining lymph nodes, increasing the number and diameter of lymphatic vessels thereby increasing the overall metastatic potential of the tumor (150). Although little is known about tumor cell entry into lymphatic vessels, multiple studies have demonstrated that cancer cells can express CC-chemokine receptor 7 (CCR7), which lymphocytes use to home to lymph nodes via CCL21 binding, in a sense, hijacking the lymphatic system to gain entry to lymphatic vessels and lymph nodes (151). LECs have additionally been implicated in immunomodulation within the TME, including multifaceted mechanisms to promote immune evasion. These include local deletional tolerance of CD8+ T cells, inhibition of dendritic cell maturation leading to decreased effector T cell activity, and tumor antigen trapping and retainment to archive for antigen-presenting cells (152–154).

In their landmark update of the Hallmarks of Cancer in 2011 (124), Hanahan and Weinberg called tumor-promoting inflammation an enabling characteristic of cancer. Inflammation is critical for the formation and maintenance of the tumor niche. It persists throughout the existence of the tumor, through therapy, remission, stabilization of disease, and relapse, and it is foundational in creating the metastatic niche. In its steady state, inflammation in the TME can promote or inhibit the capacity of innate and adaptive immune cells to infiltrate the tumor stroma and eliminate the tumor cells. However, the inflammatory TME is highly dynamic (155), characterized by a recurring cycle that established an evolutionary arms race at microscopic scale. Whether the balance tips toward immunosuppression or toward productive anti-tumor immunity is a critical determinant in the ultimate rate of tumor progression and patient outcomes.

Thousands of studies have examined the composition of the TME in humans and animals. Most studies focused on one or a few features in isolation, such as infiltration by immunosuppressive elements like Tregs or by tumoricidal NK cells or cytolytic T cells. For example, increased CD4+:CD8+ T cell ratios were correlated with decreased survival in dogs with mammary carcinomas (156), and enrichment of Foxp3+ regulatory T cells within tumors was associated with tumor progression in mammary and testicular cancers (157, 158). As another example, the immunomodulatory properties of MSCs follow licensing by inflammatory cytokines such as interferon-γ (IFNγ) and TNFα (159, 160). Licensed MSCs are resistant to apoptosis, and thus impervious to immune attack. In both syngeneic and xenograft models, MSCs reorganize the TME,

excluding T cells, macrophages, and other host effector cells, tilting the balance away from tumor host control and toward tumor progression (161, 162). MSCs are also able to inhibit T cell proliferation and inhibit natural killer (NK) cell function through soluble factors, and cell-cell communication (163–165). Paradoxically, these cells can inhibit TNFα and IFNγ which are initially necessary for licensing or "tumor-mediated education," while also increasing IL-10, an immunosuppressive cytokine (164). In dogs, MSCs induced from skin fibroblasts have shown similar immunomodulatory effects to naturally sourced MSCs (166).

Recent advances in next generation sequencing and bioinformatics, as well as the availability of high-quality samples that comprise The Cancer Genome Atlas (TCGA), made it possible to divide the immune landscape of human tumors into six distinct steady states or subtypes (167). Thorsson et al. based these subtypes on their respective transcriptional programs (**Table 2**), which in turn allowed them to establish the predicted cellular composition for each tumor (167). While these subtypes are probably not static, their dominance at any given type in any given tumor is prognostically significant. It should be noted that there was extensive overlap among genes, and therefore among predicted cell types comprising these subtypes, underscoring the futility of trying to understand the relationship between cancer and the immune system without the benefit of comprehensive information. For this reason, the extensive literature describing unique components of the immune TME will not be further summarized in this review. Emerging technologies such as single cell sequencing (168, 169) and highly multiplexed 3-dimensional optical imaging (170, 171), individually and combined, will bring about the next transformation in the understanding of the immune landscape of cancer.

Recent advances in sequencing technology and bioinformatics (172) are being applied to studies of canine immuno-oncology. Specifically, genome-wide gene expression profiles using RNA-Seq transcriptomic data can be utilized to estimate the abundance of distinct subsets of immune infiltrate in the tumor tissues and to examine the features of the inflammatory response (167, 173, 174). Scott et al. (175) showed that, even though osteosarcomas are immunologically "cold" (barren) tumors, RNA sequencing was sufficiently sensitive to detect transcripts (**Table 1**). This points to the presence of immune cellular infiltrates that allow stratification of spontaneous osteosarcomas of humans and dogs into immunologically "hot" and "cold" tumors. The transcriptional programs associated with immune cells were remarkably well-conserved across tumors from both species and did not show specificity regarding cell type or upregulation of specific molecules, such as those associated with immune checkpoints. While the increased presence of immune transcripts in tumors was associated with significantly better prognosis in human patients, such relationship was absent in dogs (**Table 1**). This observation is especially paradoxical when considering the reproducible success of experimental immunotherapies in canine osteosarcoma models (176), and even though the basis for it is not yet understood, it raises an important cautionary note in the application of canine osteosarcoma as a model for immunotherapy of human osteosarcoma.

Gorden et al. (177) showed that spontaneous canine hemangiosarcomas can be classified into three distinct molecular subtypes. Preliminary data suggest that these tumors in virtually all dogs that achieved durable remissions after conventional therapy show enrichment of immune gene signatures. Other groups have reported the immune characteristics of canine gliomas (178) and canine malignant melanoma (179), both showing similar patterns of immune infiltration to those reported for bone and vascular sarcomas.

It is widely accepted that macrophages play a major role in molding the TME, making them attractive targets for tumor therapy. Myeloid antigen presenting cells (APCs), and especially dendritic cells, control the initial steps in the cancer-immunity cycle, engulfing tumor cells and tumor debris and presenting it to T cells in the draining lymph nodes (155). Since tumors are derived from "self," immune recognition can be compromised, and this process can lead to tolerance (155, 180). Immune recognition and activation, however, is aided by genomic instability. Tumors show a direct relationship between mutational burden and immune infiltration, and this relationship extends to the observed response to immunotherapies (167, 181, 182). After immune recognition, T cells must traffic to the tumor, extravasate and infiltrate the tumor stroma, recognize the cancer cells, and selectively kill them (155). Each of these steps creates opportunities for the tumor to inhibit or evade the immune response—and concomitantly, a potential step for therapeutic intervention.

Immune recognition of the tumor intensifies the selective pressures that drive tumor evolution through the process of immunoediting (183). T cells can potentially eliminate the majority of cells in a tumor that display particular mutations. The T cell receptor repertoire in tumors is becoming increasingly well-understood, following conventional roles of clonal evolution. In virally induced tumors, such as those associated with Epstein Barr virus, narrowing of the repertoire through strong selection for foreign viral epitopes is associated

TABLE 2 | Immune subtypes of cancer.

	Mϕ:Lymph ratio*	TH1:Th2 ratio	Proliferation	Intratumoral heterogeneity	Other
Wound healing	Balanced	Low	High	High	
IFNγ dominant	Lowest	Lowest	High	Highest	Highest M1 and highest CD8 T cells
Inflammatory	Balanced	High	Low	Lowest	Highest Th17
Lymphocyte depleted	High	Minimal Th	Moderate	Moderate	
Immunologically quiet	Highest	Minimal Th	Low	Low	Highest M2
TGFβ dominant	High	Balanced	Moderate	Moderate	Highest TGFβ signature

Mϕ:Lymph ratio, macrophage to lymphocyte ratio.

with worse prognosis (184). This observation extends to tumors without viral etiologies, where tumor epitopes promote selection of a narrow diversity of clones. Greater clonal heterogeneity is associated with a more favorable prognosis in multiple tumor types (185–187). Lymphocyte clonal diversity and the potential to modulate it therapeutically in canine osteosarcoma has been examined. Preliminary results document feasibility and show variation in the diversity of the T cell repertoire across different tumors (188). However, the influence of clonal diversity on outcomes for dogs with cancer remains to be determined.

The elimination phase of immunoediting gives way to an equilibrium phase where the immune system appears to control the tumor. However, editing is not static, and the process eventually favors outgrowth of resistant tumor cells that "edit" the epitopes recognized by the immune system. Editing can occur through downregulation of major histocompatibility complex (MHC) proteins, upregulation of proteins that resist T cell activation and killing, acquisition of the ability to kill activated T cells or resist T-cell induced apoptosis, or alteration of target epitopes by further mutation or epigenetic regulation (183). The host is able to respond to these immune evasive mechanisms, for example by deploying NK cells that recognize tumor (and other) cells that downregulate MHC (180, 189). However, most cases progress to the third phase of escape (183). The immune system has evolved over millions of years to defend hosts against lethal pathogens, with the function of cancer immunosurveillance probably arising as a secondary benefit (190). Cancer is rare before reproductive age and even into young adulthood, and so robust anti-tumor immunity is unlikely to create sufficiently large selective pressure to favor individual survival.

Some common steps in the evolution of the immune microenvironment of cancer has led to the development of highly effective immunotherapies. Immune checkpoint blockade using antibodies that interfere with binding of cytotoxic T-lymphocyte-associated protein 4 (CTLA-4) to CD80 and CD86, or with binding of PD-1 to PD-L1 and PD-L2, are the first therapies directed against the TME that have been effective at achieving meaningful cancer control. Durable remissions in as many as 50% of patients with advanced cutaneous melanoma, various types of tobacco-related malignancies, gastrointestinal tumors, and certain blood cancers have been achieved via these therapies (182, 191–193). The best responses cluster in tumors (or tumor types) with high mutational burden and robust immune infiltration (182). Multitudes of other immune-enhancing therapies that can modulate the TME, and especially that can shift the inflammatory response toward T helper-1 (Th1) programs are under development, alone or in combination with immune checkpoint blockade. These include Toll-like receptor (TLR) agonists, oncolytic viruses, VEGF inhibitors that promote blood vessel normalization and improve T cell trafficking to tumors, among others (194). Indeed, the first chimeric antigen receptor redirected T cells (CAR T cells) directed against mesothelin, a protein expressed exclusively in the TME, have completed early phase clinical trials (ClinicalTrials.gov Identifier: NCT01583686).

Spontaneous canine cancers provide a rich resource to understand both conserved and species-specific mechanisms that create and maintain the tumor immune landscape. Dogs can teach us much about therapeutic immune system manipulation in the context of cancer, including the potential to alter the TME to enhance immune responses. There are numerous published studies on the subject, including using pharmacologic intratumoral delivery of vectors encoding FasL (195), a variety of tumor vaccine approaches that activate molecular pattern receptors (196–198), applications of CAR-T cell immunotherapies (199), and others (200, 201). That being said, these data must be interpreted with due caution. It should be recognized that the canine and human immune systems are separated by millions of years of evolution and were adapted to distinct pathogens in distinct environments until both species collided into shared social structures about 20,000 years ago (202), that became more intimate over the past three to five decades (203). The timeline of the canine-human relationship is rather short, and the strong influence of artificial selection will inevitably diminish the role of immunosurveillance in adaptive evolution for both species.

INVOLVEMENT OF THE TME IN TUMOR INVASION AND METASTASIS

The components of the TME work in concert through epigenetic and functional means to promote tumor cell invasion and metastasis. Although metastasis can occur at any point in space and time during the course of tumor evolution, the cellular, structural, and molecular components of the TME are able to enhance numerous pro-tumorigenic activities, which in turn facilitate invasion and enhance the metastatic potential of tumor cells. The organization of the primary tumor niche requires significant alterations to the normal extracellular environment. Molecular interactions are highly specific to different tumors and can vary substantially even within tumor types; but the general features include "loosening" of stable cell-cell adhesion, loss of cell polarity, and reorganization of the cytoskeleton, as well as stiffening of the extracellular matrix, which enhances motility, facilitates invasion, and enables the metastatic phenotype (59, 71, 73). Collectively, these alterations are linked to the "epithelial to mesenchymal transition" (EMT). EMT is characterized by genetic and epigenetic changes that alter expression of genes encoding cadherins, occludins, claudins, integrins, and a multitude of other adhesion and cell surface proteins, as well as cytokines, extracellular proteases, and many others. Reduced expression of epithelial (E) cadherin (CDH1) with a concomitant increase in neuronal (N) cadherin (CDH2) is among the most well-studied features of EMT (12, 15, 64). Loss of E-cadherin, which is widely conserved in epithelial tumors across species, is an indicator of more aggressive behavior and poor prognosis for a multitude of human as well as canine (204, 205) tumors. Tumor cells themselves can enhance EMT potential; for example VEGF-A produced by tumor cells, in contrast to VEGF-A produced by the TME, has been shown to promote EMT (206). Regardless,

the influence of the TME on EMT should not be overlooked. For example, collagen type I in the adjacent ECM has been implicated in promoting EMT through numerous mechanisms, including upregulation of NFκB, Snail, and lymphoid enhancer-binding factor-1 (LEF-1) in tumor cells. These factors promote a mesenchymal phenotype with subsequent cell migration [**Figure 4**; (207)]. Other pro-EMT transcripts, such as TWIST1, are expressed in higher concentration in tumor cells adjacent to collagen dense stroma (208). Additionally, intercellular interactions establish a pro-inflammatory environment where autocrine and paracrine loops, such as those mediated by interactions between colony-stimulating factor-1 (CSF-1) and its receptor in CSCs and TAMs, support the EMT transcriptional programs (209).

Changes in cell-to-cell contacts in sarcomas have been less well-studied, almost certainly due to the rarity of these tumors in humans. The concept of EMT in sarcomas presents a paradox: some, but not all sarcomas exhibit aggressive, rapidly metastatic phenotypes, and cells in these tumors undergo phenotypic changes that resemble EMT. Yet, all sarcoma cells possess a mesenchymal phenotype. This has given rise to a more nuanced vision of EMT, and the reverse process called mesenchymal to epithelial transition (MET), where the transcriptional and epigenetic mechanisms that regulate these transitions give rise to metastable phenotypes that are adaptive (12). In other words, cells acquire these phenotypes in response to environmental cues, as well as to natural selection on a microscopic scale.

Emerging evidence suggests that exosomes are critically important mediators that mold the distant or metastatic tumor niche in blood-derived and solid tumors. Exosomes are formed by inward budding of early endosome membranes by the endosomal sorting complex required for the transport (ESCRT) complex. Mature endosomes, also known as multi-vesicular bodies (MVBs) fuse with plasma membranes releasing exosomes vesicles to the extracellular space. Exosomes circulate systemically and can bind to and merge with other cells, creating a mechanism for horizontal transfer of activated oncoproteins, oncogenic DNA, and oncogenic and regulatory microRNAs (210). For example, CAAs and ad-MSCs, a developmentally plastic cell type that can be derived from, or differentiate to adipocytes within the TME, can produce extracellular vesicles (211, 212). To the authors' knowledge, there are no reports characterizing the role of CAAs in dogs; however, extracellular vesicles from human adipocytes have been shown to enhance tumor cell invasiveness by providing substrates for increased fatty acid oxidation in the tumor cells (211). Tumor exosomes carry biologically active molecules; thus, they can reprogram the activity of cells locally, as well as at distant sites, in essence "conditioning" these sites for metastatic tumor growth. Exosomes contribute to the formation of each component of the primary tumor niche, including the metabolic, immune, hypoxic, and infiltrating regions (68, 213). However, their role in metastatic conditioning makes them attractive targets for diagnosis and therapy. Early data in the field of exosome biology and metastasis showed that secreted exosomes could condition regional lymph nodes to create a favorable metastatic niche for melanoma cells (214). These results have been extensively reproduced in multiple experimental tumor systems, extending to other niches such as liver and lungs (213). Strategies to

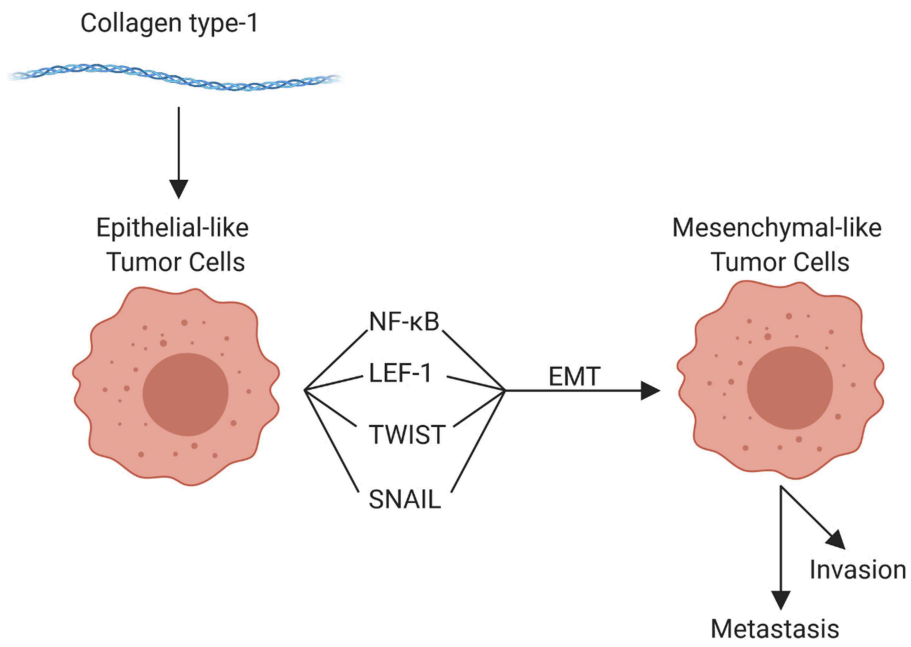

FIGURE 4 | Role of collagen type 1 in the tumor microenvironment and in epithelial-mesenchymal transition (EMT). Collagen type 1 leads to the upregulation of numerous factors that promote EMT, promoting invasion, and metastasis (created with Biorender.com).

leverage the capacity and specificity of exosomes to home to the metastatic niche are under development as means to improve delivery and activity of drugs that can delay or arrest metastasis. Perhaps most promising is the use of exosomes in early detection and targeted chemoprevention. Canine osteosarcoma was instrumental in the development of an innovative discovery platform to distinguish RNA signatures in serum exosomes originating, respectively from tumor and host cells (215, 216). While this work is still in the early stages, there is potential that these signatures can be used in rationally designed screening programs aimed at detecting changes in the TME in the earliest stages of tumor formation. Novel therapies may be developed that are able to arrest the development of tumors before they form, creating a completely new outlook on cancer prevention.

SUMMARY

Cancers are complex and dynamic multicellular tissues; multiple distinct events contribute to initiation, promotion, and progression. Ultimately, these events converge into more rigid molecular programs and create recognizable histological tumor phenotypes that are widely conserved across species. Tumor formation is a tightly orchestrated process, molded by selection to support growth and survival of a clonal population of immortalized cells. This review has demonstrated the complexity and intricacies of the TME in the human and mouse, and established, to the best of the author's abilities, the same complexities within the dog. While there is much room for growth in the understanding of the TME in the dog, the current knowledge base in conjunction with the information known about the TME in humans and mice, provides a solid foothold for the development of further basic and clinical endeavors.

AUTHOR CONTRIBUTIONS

KL, JK, MD, and JM contributed to the writing of this manuscript. Figures were rendered by KL and AS. Editing was performed by all authors of this paper.

FUNDING

The authors wish to acknowledge support from grants R21CA208529 (JM) and R50CA211249 (AS) from the National Cancer Institute of the National Institutes of Health, grant CA170218 (JM) from the United States Department of Defense, grant T2018-018 (JM) from the V Foundation for Cancer Research, and by the Zach Sobiech Osteosarcoma Fund of the Children's Cancer Research Fund. JK receives support from the Animal Cancer Care and Research Program of the University of Minnesota. AS receives support from the Masonic Cancer Center Comprehensive Cancer Center Support Grant (P30CA077598; bioinformatics core) from the National Cancer Institute of the National Institutes of Health. JM was supported by the Alvin and June Perlman Endowed Chair in Animal Oncology. The content is solely the responsibility of the authors and does not necessarily represent the official views of the National Institutes of Health, U.S. Department of Defense, the V Foundation for Cancer Research, or the Children's Cancer Research Fund.

ACKNOWLEDGMENTS

The authors would like to acknowledge Erin Dickerson, Doug Fearon, Derek Korpela, Ben Langsten, and Ashleigh McKinnon for their invaluable editorial suggestions and advice on this manuscript. We extend our deepest appreciation to Jim McCarthy for his insightful and constructive editing during the writing process.

REFERENCES

1. Albuquerque TAF, Drummond do Val L, Doherty A, de Magalhães JP. From humans to hydra: patterns of cancer across the tree of life. *Biol Rev Camb Philos Soc.* (2018) 93:1715–34. doi: 10.1111/brv.12415
2. Schiffman JD, Breen M. Comparative oncology: what dogs and other species can teach us about humans with cancer. *Philos Trans R Soc Lond B Biol Sci.* (2015) 370:20140231. doi: 10.1098/rstb.2014.0231
3. Pitot HC. The molecular biology of carcinogenesis. *Cancer.* (1993) 72:962–70. doi: 10.1002/1097-0142(19930801)72:3+<962::aid-cncr2820721303>3.0.co;2-h
4. Hanahan D, Weinberg RA. The hallmarks of cancer. *Cell.* (2000) 100:57–70. doi: 10.1016/S0092-8674(00)81683-9
5. Balkwill FR, Capasso M, Hagemann T. The tumor microenvironment at a glance. *J Cell Sci.* (2012) 125(Pt 23):5591–6. doi: 10.1242/jcs.116392
6. Prager BC, Xie Q, Bao S, Rich JN. Cancer stem cells: the architects of the tumor ecosystem. *Cell Stem Cell.* (2019) 24:41–53. doi: 10.1016/j.stem.2018.12.009
7. Kim JH, Frantz AM, Sarver AL, Gorden Klukas BH, Lewellen M, O'Brien TD, et al. Modulation of fatty acid metabolism and immune suppression are features of in vitro tumour sphere formation in ontogenetically distinct dog cancers. *Vet Comp Oncol.* (2018) 16:E176–84. doi: 10.1111/vco.12368
8. Kim JH, Frantz AM, Anderson KL, Graef AJ, Scott MC, Robinson S, et al. Interleukin-8 promotes canine hemangiosarcoma growth by regulating the tumor microenvironment. *Exp Cell Res.* (2014) 323:155–64. doi: 10.1016/j.yexcr.2014.02.020
9. Cui TX, Kryczek I, Zhao L, Zhao E, Kuick R, Roh MH, et al. Myeloid-derived suppressor cells enhance stemness of cancer cells by inducing microRNA101 and suppressing the corepressor CtBP2. *Immunity.* (2013) 39:611–21. doi: 10.1016/j.immuni.2013.08.025
10. Maccalli C, Parmiani G, Ferrone S. Immunomodulating and immunoresistance properties of cancer-initiating cells: implications for the clinical success of immunotherapy. *Immunol Invest.* (2017) 46:221–38. doi: 10.1080/08820139.2017.1280051
11. Lin W, Modiano JF, Ito D. Stage-specific embryonic antigen: determining expression in canine glioblastoma, melanoma, and mammary cancer cells. *J Vet Sci.* (2017) 18:101–4. doi: 10.4142/jvs.2017.18.1.101
12. Sannino G, Marchetto A, Kirchner T, Grunewald TGP. Epithelial-to-mesenchymal and mesenchymal-to-epithelial transition in mesenchymal tumors: a paradox in sarcomas? *Cancer Res.* (2017) 77:4556–61. doi: 10.1158/0008-5472.CAN-17-0032
13. Li Y, Laterra J. Cancer stem cells: distinct entities or dynamically regulated phenotypes? *Cancer Res.* (2012) 72:576–80. doi: 10.1158/0008-5472.CAN-11-3070

14. Zhou H, Neelakantan D, Ford HL. Clonal cooperativity in heterogenous cancers. *Semin Cell Dev Biol*. (2017) 64:79–89. doi: 10.1016/j.semcdb.2016.08.028
15. Tam WL, Weinberg RA. The epigenetics of epithelial-mesenchymal plasticity in cancer. *Nat Med*. (2013) 19:1438–49. doi: 10.1038/nm.3336
16. Kim JH, Anderson KL, Frantz AM, Graef AJ, Dickerson EB, Modiano JF. IL-8 and Slug regulate cancer cell self-renewal and microenvironment interactions in hemangiosarcoma. In: *Proceedings of the Annual Meeting of the Veterinary Cancer Society VCS*. Minneapolis, MI (2013).
17. Cozzo AJ, Fuller AM, Makowski L. Contribution of adipose tissue to development of cancer. *Compr Physiol*. (2017) 8:237–82. doi: 10.1002/cphy.c170008
18. Perez Alenza MD, Peña L, del Castillo N, Nieto AI. Factors influencing the incidence and prognosis of canine mammary tumours. *J Small Anim Pract*. (2000) 41:287–91. doi: 10.1111/j.1748-5827.2000.tb03203.x
19. Radin MJ, Sharkey LC, Holycross BJ. Adipokines: a review of biological and analytical principles and an update in dogs, cats, and horses. *Vet Clin Pathol*. (2009) 38:136–56. doi: 10.1111/j.1939-165X.2009.00133.x
20. Nieman KM, Kenny HA, Penicka CV, Ladanyi A, Buell-Gutbrod R, Zillhardt MR, et al. Adipocytes promote ovarian cancer metastasis and provide energy for rapid tumor growth. *Nat Med*. (2011) 17:1498–503. doi: 10.1038/nm.2492
21. Himbert C, Delphan M, Scherer D, Bowers LW, Hursting S, Ulrich CM. Signals from the adipose microenvironment and the obesity-cancer link-a systematic review. *Cancer Prev Res*. (2017) 10:494–506. doi: 10.1158/1940-6207.CAPR-16-0322
22. Lim HY, Im KS, Kim NH, Kim HW, Shin JI, Yhee JY, et al. Effects of obesity and obesity-related molecules on canine mammary gland tumors. *Vet Pathol*. (2015) 52:1045–51. doi: 10.1177/0300985815579994
23. Bulun SE, Price TM, Aitken J, Mahendroo MS, Simpson ER. A link between breast cancer and local estrogen biosynthesis suggested by quantification of breast adipose tissue aromatase cytochrome P450 transcripts using competitive polymerase chain reaction after reverse transcription. *J Clin Endocrinol Metab*. (1993) 77:1622–8. doi: 10.1210/jcem.77.6.8117355
24. Kapur SK, Katz AJ. Review of the adipose derived stem cell secretome. *Biochimie*. (2013) 95:2222–8. doi: 10.1016/j.biochi.2013.06.001
25. Rivera-Cruz CM, Shearer JJ, Figueiredo Neto M, Figueiredo ML. The immunomodulatory effects of mesenchymal stem cell polarization within the tumor microenvironment niche. *Stem Cells Int*. (2017) 2017:4015039. doi: 10.1155/2017/4015039
26. Chow L, Johnson V, Coy J, Regan D, Dow S. Mechanisms of immune suppression utilized by canine adipose and bone marrow-derived mesenchymal stem cells. *Stem Cells Dev*. (2017) 26:374–89. doi: 10.1089/scd.2016.0207
27. Zachary JF, McGavin MD. *Pathologic Basis of Veterinary Disease*. St. Louis, MO: Elsevier (2012).
28. Dvorak HF. Tumors: wounds that do not heal-A historical perspective with a focus on the fundamental roles of increased vascular permeability and clotting. *Semin Thromb Hemost*. (2019) 45:576–92. doi: 10.1055/s-0039-1687908
29. Stoker MG, Shearer M, O'Neill C. Growth inhibition of polyoma-transformed cells by contact with static normal fibroblasts. *J Cell Sci*. (1966) 1:297–310.
30. Kirk D, Kaighn ME. Non-reciprocal interactions in normal-neoplastic human cells. A quantitative, kinetic approach to cell interactions *in vitro*. *Cell Biol Int Rep*. (1980) 4:599–608. doi: 10.1016/0309-1651(80)90027-2
31. Flaberg E, Markasz L, Petranyi G, Stuber G, Dicso F, Alchihabi N, et al. High-throughput live-cell imaging reveals differential inhibition of tumor cell proliferation by human fibroblasts. *Int J Cancer*. (2011) 128:2793–802. doi: 10.1002/ijc.25612
32. Mehta PP, Bertram JS, Loewenstein WR. Growth inhibition of transformed cells correlates with their junctional communication with normal cells. *Cell*. (1986) 44:187–96. doi: 10.1016/0092-8674(86)90497-6
33. Rhim AD, Oberstein PE, Thomas DH, Mirek ET, Palermo CF, Sastra SA, et al. Stromal elements act to restrain, rather than support, pancreatic ductal adenocarcinoma. *Cancer Cell*. (2014) 25:735–47. doi: 10.1016/j.ccr.2014.04.021
34. Madar S, Goldstein I, Rotter V. 'Cancer associated fibroblasts'–more than meets the eye. *Trends Mol Med*. (2013) 19:447–53. doi: 10.1016/j.molmed.2013.05.004
35. Kalluri R. The biology and function of fibroblasts in cancer. *Nat Rev Cancer*. (2016) 16:582–98. doi: 10.1038/nrc.2016.73
36. Albrengues J, Bertero T, Grasset E, Bonan S, Maiel M, Bourget I, et al. Epigenetic switch drives the conversion of fibroblasts into proinvasive cancer-associated fibroblasts. *Nat Commun*. (2015) 6:10204. doi: 10.1038/ncomms10204
37. Klymenko Y, Nephew KP. Epigenetic crosstalk between the tumor microenvironment and ovarian cancer cells: a therapeutic road less traveled. *Cancers*. (2018) 10:E295. doi: 10.3390/cancers10090295
38. Bu L, Baba H, Yoshida N, Miyake K, Yasuda T, Uchihara T, et al. Biological heterogeneity and versatility of cancer-associated fibroblasts in the tumor microenvironment. *Oncogene*. (2019) 38:4887–901. doi: 10.1038/s41388-019-0765-y
39. Erez N, Truitt M, Olson P, Arron ST, Hanahan D. Cancer-associated fibroblasts are activated in incipient neoplasia to orchestrate tumor-promoting inflammation in an NF-kappaB-dependent manner. *Cancer Cell*. (2010) 17:135–47. doi: 10.1016/j.ccr.2009.12.041
40. Sappino AP, Skalli O, Jackson B, Schürch W, Gabbiani G. Smooth-muscle differentiation in stromal cells of malignant and non-malignant breast tissues. *Int J Cancer*. (1988) 41:707–12. doi: 10.1002/ijc.2910410512
41. Yoshimoto S, Hoshino Y, Izumi Y, Takagi S. α-smooth muscle actin expression in cancerassociated fibroblasts in canine epithelial tumors. *Japanese J Vet Res*. (2017) 65:135–44. doi: 10.14943/jjvr.65.3.135
42. Buganim Y, Madar S, Rais Y, Pomeraniec L, Harel E, Solomon H, et al. Transcriptional activity of ATF3 in the stromal compartment of tumors promotes cancer progression. *Carcinogenesis*. (2011) 32:1749–57. doi: 10.1093/carcin/bgr203
43. Goetz JG, Minguet S, Navarro-Lérida I, Lazcano JJ, Samaniego R, Calvo E, et al. Biomechanical remodeling of the microenvironment by stromal caveolin-1 favors tumor invasion and metastasis. *Cell*. (2011) 146:148–63. doi: 10.1016/j.cell.2011.05.040
44. Król M, Pawłowski KM, Szyszko K, Maciejewski H, Dolka I, Manuali E, et al. The gene expression profiles of canine mammary cancer cells grown with carcinoma-associated fibroblasts (CAFs) as a co-culture *in vitro*. *BMC Vet Res*. (2012) 8:35. doi: 10.1186/1746-6148-8-35
45. Rozenchan PB, Carraro DM, Brentani HLD, de Carvalho Mota LD, Bastos EP, e Ferreira EN, et al. Reciprocal changes in gene expression profiles of cocultured breast epithelial cells and primary fibroblasts. *Int J Cancer*. (2009) 125:2767–77. doi: 10.1002/ijc.24646
46. van Duursen MB, Nijmeijer SM, de Morree ES, de Jong PC, van den Berg M. Genistein induces breast cancer-associated aromatase and stimulates estrogen-dependent tumor cell growth in in vitro breast cancer model. *Toxicology*. (2011) 289:67–73. doi: 10.1016/j.tox.2011.07.005
47. Purohit A, Ghilchik MW, Duncan L, Wang DY, Singh A, Walker MM, et al. Aromatase activity and interleukin-6 production by normal and malignant breast tissues. *J Clin Endocrinol Metab*. (1995) 80:3052–8. doi: 10.1210/jcem.80.10.7559896
48. Salem HK, Thiemermann C. Mesenchymal stromal cells: current understanding and clinical status. *Stem Cells*. (2010) 28:585–96. doi: 10.1002/stem.269
49. Lin W, Huang L, Li Y, Fang B, Li G, Chen L, et al. Mesenchymal stem cells and cancer: clinical challenges and opportunities. *Biomed Res Int*. (2019) 2019:2820853. doi: 10.1155/2019/2820853
50. Fang M, Yuan J, Peng C, Li Y. Collagen as a double-edged sword in tumor progression. *Tumour Biol*. (2014) 35:2871–82. doi: 10.1007/s13277-013-1511-7
51. Provenzano PP, Eliceiri KW, Campbell JM, Inman DR, White JG, Keely PJ. Collagen reorganization at the tumor-stromal interface facilitates local invasion. *BMC Med*. (2006) 4:38. doi: 10.1186/1741-7015-4-38
52. Yamauchi M, Barker TH, Gibbons DL, Kurie JM. The fibrotic tumor stroma. *J Clin Invest*. (2018) 128:16–25. doi: 10.1172/JCI93554
53. Case A, Brisson BK, Durham AC, Rosen S, Monslow J, Buza E, et al. Identification of prognostic collagen signatures and potential therapeutic stromal targets in canine mammary gland carcinoma. *PLoS ONE*. (2017) 12:e0180448. doi: 10.1371/journal.pone.0180448

54. Conklin MW, Eickhoff JC, Riching KM, Pehlke CA, Eliceiri KW, Provenzano PP, et al. Aligned collagen is a prognostic signature for survival in human breast carcinoma. *Am J Pathol.* (2011) 178:1221–32. doi: 10.1016/j.ajpath.2010.11.076
55. Ettlin J, Clementi E, Amini P, Malbon A, Markkanen E. Analysis of gene expression signatures in cancer-associated stroma from canine mammary tumours reveals molecular homology to human breast carcinomas. *Int J Mol Sci.* (2017) 18:E1101. doi: 10.3390/ijms18051101
56. Jia D, Liu Z, Deng N, Tan TZ, Huang RY, Taylor-Harding B, et al. A COL11A1-correlated pan-cancer gene signature of activated fibroblasts for the prioritization of therapeutic targets. *Cancer Lett.* (2016) 382:203–14. doi: 10.1016/j.canlet.2016.09.001
57. Mueller MM, Fusenig NE. Friends or foes - bipolar effects of the tumour stroma in cancer. *Nat Rev Cancer*. (2004) 4:839–49. doi: 10.1038/nrc1477
58. Trembley JH, Unger GM, Korman VL, Abedin MJ, Nacusi LP, Vogel RI, et al. Tenfibgen ligand nanoencapsulation delivers bi-functional anti-CK2 RNAi oligomer to key sites for prostate cancer targeting using human xenograft tumors in mice. *PLoS ONE.* (2014) 9:e109970. doi: 10.1371/journal.pone.0109970
59. Poltavets V, Kochetkova M, Pitson SM, Samuel MS. The role of the extracellular matrix and its molecular and cellular regulators in cancer cell plasticity. *Front Oncol.* (2018) 8:431. doi: 10.3389/fonc.2018.00431
60. Jang I, Beningo KA. Integrins, CAFs and mechanical forces in the progression of cancer. *Cancers.* (2019) 11:E721. doi: 10.3390/cancers11050721
61. Stupack DG. Integrins as a distinct subtype of dependence receptors. *Cell Death Differ*. (2005) 12:1021–30. doi: 10.1038/sj.cdd.4401658
62. Takahashi N, Nobusue H, Shimizu T, Sugihara E, Yamaguchi-Iwai S, Onishi N, et al. ROCK inhibition induces terminal adipocyte differentiation and suppresses tumorigenesis in chemoresistant osteosarcoma cells. *Cancer Res.* (2019) 79:3088–99. doi: 10.1158/0008-5472.CAN-18-2693
63. Cohen DJ, Nelson WJ. Secret handshakes: cell-cell interactions and cellular mimics. *Curr Opin Cell Biol.* (2018) 50:14–9. doi: 10.1016/j.ceb.2018.01.001
64. Gloushankova NA, Zhitnyak IY, Rubtsova SN. Role of epithelial-mesenchymal transition in tumor progression. *Biochemistry.* (2018) 83:1469–76. doi: 10.1134/S0006297918120052
65. Lou E, Zhai E, Sarkari A, Desir S, Wong P, Iizuka Y, et al. Cellular and molecular networking within the ecosystem of cancer cell communication via tunneling nanotubes. *Front Cell Dev Biol.* (2018) 6:95. doi: 10.3389/fcell.2018.00095
66. Yamashita YM, Inaba M, Buszczak M. Specialized intercellular communications via cytonemes and nanotubes. *Annu Rev Cell Dev Biol.* (2018) 34:59–84. doi: 10.1146/annurev-cellbio-100617-062932
67. Becker A, Thakur BK, Weiss JM, Kim HS, Peinado H, Lyden D. Extracellular vesicles in cancer: cell-to-cell mediators of metastasis. *Cancer Cell.* (2016) 30:836–48. doi: 10.1016/j.ccell.2016.10.009
68. Maia J, Caja S, Strano Moraes MC, Couto N, Costa-Silva B. Exosome-based cell-cell communication in the tumor microenvironment. *Front Cell Dev Biol.* (2018) 6:18. doi: 10.3389/fcell.2018.00018
69. Robinson SC, Coussens LM. Soluble mediators of inflammation during tumor development. *Adv Cancer Res.* (2005) 93:159–87. doi: 10.1016/S0065-230X(05)93005-4
70. Rodriguez AM, Graef AJ, LeVine DN, Cohen IR, Modiano JF, Kim JH. Association of sphingosine-1-phosphate (S1P)/S1P receptor-1 pathway with cell proliferation and survival in canine hemangiosarcoma. *J Vet Intern Med.* (2015) 29:1088–97. doi: 10.1111/jvim.13570
71. Huang S, Ingber DE. Cell tension, matrix mechanics, and cancer development. *Cancer Cell.* (2005) 8:175–6. doi: 10.1016/j.ccr.2005.08.009
72. Wei L, Surma M, Shi S, Lambert-Cheatham N, Shi J. Novel insights into the roles of rho kinase in cancer. *Arch Immunol Ther Exp.* (2016) 64:259–78. doi: 10.1007/s00005-015-0382-6
73. Holle AW, Young JL, Spatz JP. *In vitro* cancer cell-ECM interactions inform *in vivo* cancer treatment. *Adv Drug Deliv Rev.* (2016) 97:270–9. doi: 10.1016/j.addr.2015.10.007
74. Waugh DJ, Wilson C. The interleukin-8 pathway in cancer. *Clin Cancer Res.* (2008) 14:6735–41. doi: 10.1158/1078-0432.CCR-07-4843
75. De Larco JE, Wuertz BR, Furcht LT. The potential role of neutrophils in promoting the metastatic phenotype of tumors releasing interleukin-8. *Clin Cancer Res.* (2004) 10:4895–900. doi: 10.1158/1078-0432.CCR-03-0760
76. Gimbrone MA, Leapman SB, Cotran RS, Folkman J. Tumor dormancy *in vivo* by prevention of neovascularization. *J Exp Med.* (1972) 136:261–76. doi: 10.1084/jem.136.2.261
77. Folkman J. Tumor angiogenesis: therapeutic implications. *N Engl J Med.* (1971) 285:1182–6. doi: 10.1056/NEJM197111182852108
78. Bielenberg DR, Zetter BR. The contribution of angiogenesis to the process of metastasis. *Cancer J.* (2015) 21:267–73. doi: 10.1097/PPO.0000000000000138
79. Vaupel P, Mayer A. Hypoxia in cancer: significance and impact on clinical outcome. *Cancer Metastasis Rev.* (2007) 26:225–39. doi: 10.1007/s10555-007-9055-1
80. Snyder SA, Dewhirst MW, Hauck ML. The role of hypoxia in canine cancer. *Vet Comp Oncol.* (2008) 6:213–23. doi: 10.1111/j.1476-5829.2008.00163.x
81. Samanta D, Semenza GL. Metabolic adaptation of cancer and immune cells mediated by hypoxia-inducible factors. *Biochim Biophys Acta Rev Cancer.* (2018) 1870:15–22. doi: 10.1016/j.bbcan.2018.07.002
82. Liu W, Xin H, Eckert DT, Brown JA, Gnarra JR. Hypoxia and cell cycle regulation of the von Hippel-Lindau tumor suppressor. *Oncogene.* (2011) 30:21–31. doi: 10.1038/onc.2010.395
83. Pugh CW, Ratcliffe PJ. Regulation of angiogenesis by hypoxia: role of the HIF system. *Nat Med.* (2003) 9:677–84. doi: 10.1038/nm0603-677
84. Watson JA, Watson CJ, McCann A, Baugh J. Epigenetics, the epicenter of the hypoxic response. *Epigenetics.* (2010) 5:293–96. doi: 10.4161/epi.5.4.11684
85. Majmundar AJ, Wong WJ, Simon MC. Hypoxia-inducible factors and the response to hypoxic stress. *Mol Cell.* (2010) 40:294–309. doi: 10.1016/j.molcel.2010.09.022
86. Carmeliet P. Mechanisms of angiogenesis and arteriogenesis. *Nat Med.* (2000) 6:389–95. doi: 10.1038/74651
87. Corvera S, Gealekman O. Adipose tissue angiogenesis: impact on obesity and type-2 diabetes. *Biochim Biophys Acta.* (2014) 1842:463–72. doi: 10.1016/j.bbadis.2013.06.003
88. Rahimi N. Vascular endothelial growth factor receptors: molecular mechanisms of activation and therapeutic potentials. *Exp Eye Res.* (2006) 83:1005–16. doi: 10.1016/j.exer.2006.03.019
89. Gutiérrez-González A, Aguilera-Montilla N, Ugarte-Berzal E, Bailón E, Cerro-Pardo I, Sánchez-Maroto C, et al. α4β1 integrin associates with VEGFR2 in CLL cells and contributes to VEGF binding and intracellular signaling. *Blood Adv.* (2019) 3:2144–8. doi: 10.1182/bloodadvances.2019000019
90. Shibuya M, Claesson-Welsh L. Signal transduction by VEGF receptors in regulation of angiogenesis and lymphangiogenesis. *Exp Cell Res.* (2006) 312:549–60. doi: 10.1016/j.yexcr.2005.11.012
91. Tamburini BA, Trapp S, Phang TL, Schappa JT, Hunter LE, Modiano JF. Gene expression profiles of sporadic canine hemangiosarcoma are uniquely associated with breed. *PLoS ONE.* (2009) 4:e5549. doi: 10.1371/journal.pone.0005549
92. Peters KG, Kontos CD, Lin PC, Wong AL, Rao P, Huang L, et al. Functional significance of Tie2 signaling in the adult vasculature. *Recent Prog Horm Res.* (2004) 59:51–71. doi: 10.1210/rp.59.1.51
93. Pichiule P, Chavez JC, LaManna JC. Hypoxic regulation of angiopoietin-2 expression in endothelial cells. *J Biol Chem.* (2004) 279:12171–80. doi: 10.1074/jbc.M305146200
94. Harada S, Nagy JA, Sullivan KA, Thomas KA, Endo N, Rodan GA, et al. Induction of vascular endothelial growth factor expression by prostaglandin E2 and E1 in osteoblasts. *J Clin Invest.* (1994) 93:2490–6. doi: 10.1172/JCI117258
95. Wu G., Luo, J., Rana, J. S., Laham, R., Sellke, F. W., and Li, J.. (2006). Involvement of COX-2 in VEGF-induced angiogenesis via P38 and JNK pathways in vascular endothelial cells. *Cardiovasc Res* 69, 512–519. doi: 10.1016/j.cardiores.2005.09.019
96. Yoshino Y, Aoyagi M, Tamaki M, Duan L, Morimoto T, Ohno K. Activation of p38 MAPK and/or JNK contributes to increased levels of VEGF secretion in human malignant glioma cells. *Int J Oncol.* (2006) 29:981–7. doi: 10.3892/ijo.29.4.981

97. Tremblay C, Doré M, Bochsler PN, Sirois J. Induction of prostaglandin G/H synthase-2 in a canine model of spontaneous prostatic adenocarcinoma. *J Natl Cancer Inst*. (1999) 91:1398–403. doi: 10.1093/jnci/91.16.1398
98. Madaan S, Abel PD, Chaudhary KS, Hewitt R, Stott MA, Stamp GW, et al. Cytoplasmic induction and over-expression of cyclooxygenase-2 in human prostate cancer: implications for prevention and treatment. *BJU Int.* (2000) 86:736–41. doi: 10.1046/j.1464-410x.2000.00867.x
99. Khan KN, Knapp DW, Denicola DB, Harris RK. Expression of cyclooxygenase-2 in transitional cell carcinoma of the urinary bladder in dogs. *Am J Vet Res.* (2000) 61:478–81. doi: 10.2460/ajvr.2000.61.478
100. Mohammed SI, Knapp DW, Bostwick DG, Foster RS, Khan KN, Masferrer JL, et al. Expression of cyclooxygenase-2 (COX-2) in human invasive transitional cell carcinoma (TCC) of the urinary bladder. *Cancer Res.* (1999) 59:5647–50. doi: 10.1097/00005392-199904020-00268
101. Zhi H, Wang L, Zhang J, Zhou C, Ding F, Luo A, et al. Significance of COX-2 expression in human esophageal squamous cell carcinoma. *Carcinogenesis*. (2006) 27:1214–21. doi: 10.1093/carcin/bgi304
102. Pestili de Almeida EM, Piché C, Sirois J, Doré M. Expression of cyclo-oxygenase-, in naturally occurring squamous cell carcinomas in dogs. *J Histochem Cytochem*. (2001) 49:867–75. doi: 10.1177/002215540104900707
103. Mohammed SI, Bennett PF, Craig BA, Glickman NW, Mutsaers AJ, et al. Effects of the cyclooxygenase inhibitor, piroxicam, on tumor response, apoptosis, and angiogenesis in a canine model of human invasive urinary bladder cancer. *Cancer Res.* (2002) 62:356–8.
104. McMillan SK, Boria P, Moore GE, Widmer WR, Bonney PL, Knapp DW. Antitumor effects of deracoxib treatment in 26 dogs with transitional cell carcinoma of the urinary bladder. *J Am Vet Med Assoc.* (2011) 239:1084–9. doi: 10.2460/javma.239.8.1084
105. Jolly K, Cheng KK, Langman MJ. NSAIDs and gastrointestinal cancer prevention. *Drugs*. (2002) 62:945–56. doi: 10.2165/00003495-200262060-00006
106. Brasky TM, Bonner MR, Moysich KB, Ambrosone CB, Nie J, Tao MH, et al. Non-steroidal anti-inflammatory drugs (NSAIDs) and breast cancer risk: differences by molecular subtype. *Cancer Causes Control.* (2011) 22:965–75. doi: 10.1007/s10552-011-9769-9
107. Sato-Dahlman M, Yamamoto M. The development of oncoltyic adenovirus therapy in the past and future - for the case of pancreatic cancer. *Curr Cancer Drug Targets*. (2018) 18:153–61. doi: 10.2174/1568009617666170222123925
108. Yamamoto M, Davydova J, Wang M, Siegal GP, Krasnykh V, Vickers SM, et al. Infectivity enhanced, cyclooxygenase-2 promoter-based conditionally replicative adenovirus for pancreatic cancer. *Gastroenterology.* (2003) 125:1203–18. doi: 10.1016/S0016-5085(03)01196-X
109. Moeller BJ, Cao Y, Li CY, Dewhirst MW. Radiation activates HIF-1 to regulate vascular radiosensitivity in tumors: role of reoxygenation, free radicals, and stress granules. *Cancer Cell.* (2004) 5:429–41. doi: 10.1016/S1535-6108(04)00115-1
110. Li F, Sonveaux P, Rabbani ZN, Liu S, Yan B, Huang Q, et al. Regulation of HIF-1alpha stability through S-nitrosylation. *Mol Cell.* (2007) 26:63–74. doi: 10.1016/j.molcel.2007.02.024
111. Cao Y, Eble JM, Moon E, Yuan H, Weitzel DH, Landon CD, et al. Tumor cells upregulate normoxic HIF-1α in response to doxorubicin. *Cancer Res.* (2013) 73:6230–42. doi: 10.1158/0008-5472.CAN-12-1345
112. Chi JT, Thrall DE, Jiang C, Snyder S, Fels D, Landon C, et al. Comparison of genomics and functional imaging from canine sarcomas treated with thermoradiotherapy predicts therapeutic response and identifies combination therapeutics. *Clin Cancer Res.* (2011) 17:2549–60. doi: 10.1158/1078-0432.CCR-10-2583
113. Thrall DE, Maccarini P, Stauffer P, Macfall J, Hauck M, Snyder S, et al. Thermal dose fractionation affects tumour physiological response. *Int J Hyperthermia*. (2012) 28:431–40. doi: 10.3109/02656736.2012.689087
114. Zhang X, Ashcraft KA, Betof Warner A, Nair SK, Dewhirst MW. Can exercise-induced modulation of the tumor physiologic microenvironment improve antitumor immunity? *Cancer Res.* (2019) 79:2447–56. doi: 10.1158/0008-5472.CAN-18-2468
115. Italiani P, Boraschi D. From monocytes to M1/M2 macrophages: phenotypical vs. functional differentiation. *Front Immunol*. (2014) 5:514. doi: 10.3389/fimmu.2014.00514
116. Leblond MM, Gerault AN, Corroyer-Dulmont A, MacKenzie ET, Petit E, Bernaudin M, et al. Hypoxia induces macrophage polarization and re-education toward an M2 phenotype in U87 and U251 glioblastoma models. *Oncoimmunology*. (2016) 5:e1056442. doi: 10.1080/2162402X.2015.1056442
117. Tarique AA, Logan J, Thomas E, Holt PG, Sly PD, Fantino E. Phenotypic, functional, and plasticity features of classical and alternatively activated human macrophages. *Am J Respir Cell Mol Biol.* (2015) 53:676–88. doi: 10.1165/rcmb.2015-0012OC
118. DeNardo DG, Ruffell B. Macrophages as regulators of tumour immunity and immunotherapy. *Nat Rev Immunol*. (2019) 19:369–82. doi: 10.1038/s41577-019-0127-6
119. Noman MZ, Desantis G, Janji B, Hasmim M, Karray S, Dessen P, et al. PD-L1 is a novel direct target of HIF-1α, and its blockade under hypoxia enhanced MDSC-mediated T cell activation. *J Exp Med.* (2014) 211:781–90. doi: 10.1084/jem.20131916
120. Huang JH, Cárdenas-Navia LI, Caldwell CC, Plumb TJ, Radu CG, Rocha PN, et al. Requirements for T lymphocyte migration in explanted lymph nodes. *J Immunol.* (2007) 178:7747–55. doi: 10.4049/jimmunol.178.12.7747
121. Ceradini DJ, Kulkarni AR, Callaghan MJ, Tepper OM, Bastidas N, Kleinman ME, et al. Progenitor cell trafficking is regulated by hypoxic gradients through HIF-1 induction of SDF-1. *Nat Med.* (2004) 10:858–64. doi: 10.1038/nm1075
122. Schioppa T, Uranchimeg B, Saccani A, Biswas SK, Doni A, Rapisarda A, et al. Regulation of the chemokine receptor CXCR4 by hypoxia. *J Exp Med.* (2003) 198:1391–402. doi: 10.1084/jem.20030267
123. Westendorf AM, Skibbe K, Adamczyk A, Buer J, Geffers R, Hansen W, et al. Hypoxia enhances immunosuppression by inhibiting CD4+ effector T cell function and promoting treg activity. *Cell Physiol Biochem.* (2017) 41:1271–84. doi: 10.1159/000464429
124. Hanahan D, Weinberg RA. Hallmarks of cancer: the next generation. *Cell*. (2011) 144:646–74. doi: 10.1016/j.cell.2011.02.013
125. Warburg O. On the origin of cancer cells. *Science*. (1956) 123:309–14. doi: 10.1126/science.123.3191.309
126. Kennedy KM, Dewhirst MW. Tumor metabolism of lactate: the influence and therapeutic potential for MCT and CD147 regulation. *Future Oncol*. (2010) 6:127–48. doi: 10.2217/fon.09.145
127. Schroeder T, Yuan H, Viglianti BL, Peltz C, Asopa S, Vujaskovic Z, et al. Spatial heterogeneity and oxygen dependence of glucose consumption in R3230Ac and fibrosarcomas of the Fischer 344 rat. *Cancer Res.* (2005) 65:5163–71. doi: 10.1158/0008-5472.CAN-04-3900
128. Walenta S, Wetterling M, Lehrke M, Schwickert G, Sundfør K, Rofstad EK, et al. High lactate levels predict likelihood of metastases, tumor recurrence, and restricted patient survival in human cervical cancers. *Cancer Res.* (2000) 60:916–21.
129. Sonveaux P, Végran F, Schroeder T, Wergin MC, Verrax J, Rabbani ZN, et al. Targeting lactate-fueled respiration selectively kills hypoxic tumor cells in mice. *J Clin Invest.* (2008) 118:3930–42. doi: 10.1172/JCI36843
130. Kennedy KM, Scarbrough PM, Ribeiro A, Richardson R, Yuan H, Sonveaux P, et al. Catabolism of exogenous lactate reveals it as a legitimate metabolic substrate in breast cancer. *PLoS ONE.* (2013) 8:e75154. doi: 10.1371/journal.pone.0075154
131. Cluntun AA, Lukey MJ, Cerione RA, Locasale JW. Glutamine metabolism in cancer: understanding the heterogeneity. *Trends Cancer.* (2017) 3:169–80. doi: 10.1016/j.trecan.2017.01.005
132. Pavlides S, Whitaker-Menezes D, Castello-Cros R, Flomenberg N, Witkiewicz AK, Frank PG, et al. The reverse Warburg effect: aerobic glycolysis in cancer associated fibroblasts and the tumor stroma. *Cell Cycle.* (2009) 8:3984–4001. doi: 10.4161/cc.8.23.10238
133. Sonveaux P, Copetti T, De Saedeleer CJ, Végran F, Verrax J, Kennedy KM, et al. Targeting the lactate transporter MCT1 in endothelial cells inhibits lactate-induced HIF-1 activation and tumor angiogenesis. *PLoS ONE.* (2012) 7:e33418. doi: 10.1371/journal.pone.0033418
134. Brizel DM, Schroeder T, Scher RL, Walenta S, Clough RW, Dewhirst MW, et al. Elevated tumor lactate concentrations predict for an increased risk of metastases in head-and-neck cancer. *Int J Radiat Oncol Biol Phys.* (2001) 51:349–53. doi: 10.1016/S0360-3016(01)01630-3
135. Lora-Michiels M, Yu D, Sanders L, Poulson JM, Azuma C, Case B, et al. Extracellular pH and P-31 magnetic resonance spectroscopic

variables are related to outcome in canine soft tissue sarcomas treated with thermoradiotherapy. *Clin Cancer Res.* (2006) 12:5733–40. doi: 10.1158/1078-0432.CCR-05-2669
136. Lardner A. The effects of extracellular pH on immune function. *J Leukoc Biol.* (2001) 69:522–30.
137. Wu NZ, Klitzman B, Dodge R, and Dewhirst, M. W.. (1992). Diminished leukocyte-endothelium interaction in tumor microvessels. *Cancer Res* 52, 4265–4268.
138. Fisher DT, Chen Q, Skitzki JJ, Muhitch JB, Zhou L, Appenheimer MM, et al. IL-6 trans-signaling licenses mouse and human tumor microvascular gateways for trafficking of cytotoxic T cells. *J Clin Invest.* (2011) 121:3846–59. doi: 10.1172/JCI44952
139. Bessa X, Elizalde JI, Mitjans F, Piñol V, Miquel R, Panés J, et al. Leukocyte recruitment in colon cancer: role of cell adhesion molecules, nitric oxide, and transforming growth factor beta1. *Gastroenterology.* (2002) 122:1122–32. doi: 10.1053/gast.2002.32369
140. Ping YF, Zhang X, Bian XW. Cancer stem cells and their vascular niche: do they benefit from each other? *Cancer Lett.* (2016) 380:561–7. doi: 10.1016/j.canlet.2015.05.010
141. Cao X, Geradts J, Dewhirst MW, Lo HW. Upregulation of VEGF-A and CD24 gene expression by the tGLI1 transcription factor contributes to the aggressive behavior of breast cancer cells. *Oncogene*. (2012) 31:104–15. doi: 10.1038/onc.2011.219
142. Al-Rawi MA, Mansel RE, Jiang WG. Lymphangiogenesis and its role in cancer. *Histol Histopathol.* (2005) 20:283–98. doi: 10.1177/1947601911423028
143. Sleeckx N, Van Brantegem L, Fransen EG, Van den Eynden Casteleyn C, Veldhuis Kroeze E, Van Ginneken C. Evaluation of immunohistochemical markers of lymphatic and blood vessels in canine mammary tumours. *J Comp Pathol.* (2013) 148:307–17. doi: 10.1016/j.jcpa.2012.09.007
144. Tammela T, Alitalo K. Lymphangiogenesis: Molecular mechanisms and future promise. *Cell*. (2010) 140:460–76. doi: 10.1016/j.cell.2010.01.045
145. Stacker SA, Baldwin ME, Achen MG. The role of tumor lymphangiogenesis in metastatic spread. *FASEB J.* (2002) 16:922–34. doi: 10.1096/fj.01-0945rev
146. Schoppmann SF, Fenzl A, Nagy K, Unger S, Bayer G, Geleff S, et al. VEGF-C expressing tumor-associated macrophages in lymph node positive breast cancer: impact on lymphangiogenesis and survival. *Surgery.* (2006) 139:839–46. doi: 10.1016/j.surg.2005.12.008
147. Karpanen T, Alitalo K. Molecular biology and pathology of lymphangiogenesis. *Annu Rev Pathol.* (2008) 3:367–97. doi: 10.1146/annurev.pathmechdis.3.121806.151515
148. François M, Caprini A, Hosking B, Orsenigo F, Wilhelm D, Browne C, et al. Sox18 induces development of the lymphatic vasculature in mice. *Nature*. (2008) 456:643–7. doi: 10.1038/nature07391
149. Kim HS, Park YW. Metastasis via peritumoral lymphatic dilation in oral squamous cell carcinoma. *Maxillofac Plast Reconstr Surg.* (2014) 36:85–93. doi: 10.14402/jkamprs.2014.36.3.85
150. Hirakawa S, Brown LF, Kodama S, Paavonen K, Alitalo K, Detmar M. VEGF-C-induced lymphangiogenesis in sentinel lymph nodes promotes tumor metastasis to distant sites. *Blood.* (2007) 109:1010–7. doi: 10.1182/blood-2006-05-021758
151. Legler DF, Uetz-von Allmen E, Hauser MA. CCR7: roles in cancer cell dissemination, migration and metastasis formation. *Int J Biochem Cell Biol.* (2014) 54:78–82. doi: 10.1016/j.biocel.2014.07.002
152. Lund AW, Duraes FV, Hirosue S, Raghavan VR, Nembrini C, Thomas SN, et al. VEGF-C promotes immune tolerance in B16 melanomas and cross-presentation of tumor antigen by lymph node lymphatics. *Cell Rep.* (2012) 1:191–9. doi: 10.1016/j.celrep.2012.01.005
153. Kedl RM, Tamburini BA. Antigen archiving by lymph node stroma: a novel function for the lymphatic endothelium. *Eur J Immunol.* (2015) 45:2721–9. doi: 10.1002/eji.201545739
154. Swartz MA. Immunomodulatory roles of lymphatic vessels in cancer progression. *Cancer Immunol Res.* (2014) 2:701–7. doi: 10.1158/2326-6066.CIR-14-0115
155. Chen DS, Mellman I. Oncology meets immunology: the cancer-immunity cycle. *Immunity*. (2013) 39:1–10. doi: 10.1016/j.immuni.2013.07.012
156. Estrela-Lima A, Araujo MS, Costa-Neto JM, Teixeira-Carvalho A, Barrouin-Melo SM, Cardoso SV, et al. Immunophenotypic features of tumor infiltrating lymphocytes from mammary carcinomas in female dogs associated with prognostic factors and survival rates. *BMC Cancer.* (2010) 10:256. doi: 10.1186/1471-2407-10-256
157. Kim JH, Hur JH, Lee SM, Im KS, Kim NH, Sur JH. Correlation of Foxp3 positive regulatory T cells with prognostic factors in canine mammary carcinomas. *Vet J.* (2012) 193:222–7. doi: 10.1016/j.tvjl.2011.10.022
158. Kim JH, Chon SK, Im KS, Kim NH, Cho KW, Sur JH. Infiltrating Foxp3+ regulatory T cells and histopathological features in canine classical and spermatocytic seminomas. *Reprod Domest Anim.* (2013) 48:218–22. doi: 10.1111/j.1439-0531.2012.02135.x
159. Chinnadurai R, Copland IB, Patel SR, Galipeau J. IDO-independent suppression of T cell effector function by IFN-γ-licensed human mesenchymal stromal cells. *J Immunol.* (2014) 192:1491–501. doi: 10.4049/jimmunol.1301828
160. Dorronsoro A, Ferrin I, Salcedo JM, Jakobsson E, Fernández-Rueda J, Lang V, et al. Human mesenchymal stromal cells modulate T-cell responses through TNF-α-mediated activation of NF-κB. *Eur J Immunol.* (2014) 44:480–8. doi: 10.1002/eji.201343668
161. Modiano JF, Lindborg BA, McElmurry RT, Lewellen M, Forster CL, Zamora EA, et al. Mesenchymal stromal cells inhibit murine syngeneic anti-tumor immune responses by attenuating inflammation and reorganizing the tumor microenvironment. *Cancer Immunol Immunother.* (2015) 64:1449–60. doi: 10.1007/s00262-015-1749-6
162. Joyce JA, Fearon DT. T cell exclusion, immune privilege, and the tumor microenvironment. *Science.* (2015) 348:74–80. doi: 10.1126/science.aaa6204
163. Krampera M, Cosmi L, Angeli R, Pasini A, Liotta F, Andreini A, et al. Role for interferon-gamma in the immunomodulatory activity of human bone marrow mesenchymal stem cells. *Stem Cells*. (2006) 24:386–98. doi: 10.1634/stemcells.2005-0008
164. Aggarwal S, Pittenger MF. Human mesenchymal stem cells modulate allogeneic immune cell responses. *Blood.* (2005) 105:1815–22. doi: 10.1182/blood-2004-04-1559
165. Di Nicola M, Carlo-Stella C, Magni M, Milanesi M, Longoni PD, Matteucci P, et al. Human bone marrow stromal cells suppress T-lymphocyte proliferation induced by cellular or nonspecific mitogenic stimuli. *Blood.* (2002) 99:3838–43. doi: 10.1182/blood.V99.10.3838
166. Chow L, Johnson V, Regan D, Wheat W, Webb S, Koch P, et al. Safety and immune regulatory properties of canine induced pluripotent stem cell-derived mesenchymal stem cells. *Stem Cell Res.* (2017) 25:221–32. doi: 10.1016/j.scr.2017.11.010
167. Thorsson V, Gibbs DL, Brown SD, Wolf D, Bortone DS, Ou Yang TH, et al. The immune landscape of cancer. *Immunity.* (2018) 48:812–30.e14. doi: 10.1016/j.immuni.2018.03.023
168. Chung W, Eum HH, Lee HO, Lee KM, Lee HB, Kim KT, et al. Single-cell RNA-seq enables comprehensive tumour and immune cell profiling in primary breast cancer. *Nat Commun.* (2017) 8:15081. doi: 10.1038/ncomms15081
169. Tirosh I, Izar B, Prakadan SM, Wadsworth MH, Treacy D II, Trombetta JJ, et al. Dissecting the multicellular ecosystem of metastatic melanoma by single-cell RNA-seq. *Science.* (2016) 352:189–96. doi: 10.1126/science.aad0501
170. Angelo M, Bendall SC, Finck R, Hale MB, Hitzman C, Borowsky AD, et al. Multiplexed ion beam imaging of human breast tumors. *Nat Med.* (2014) 20:436–42. doi: 10.1038/nm.3488
171. Li W, Germain RN, Gerner MY. High-dimensional cell-level analysis of tissues with Ce3D multiplex volume imaging. *Nat Protoc.* (2019) 14:1708–33. doi: 10.1038/s41596-019-0156-4
172. Binnewies M, Roberts EW, Kersten K, Chan V, Fearon DF, Merad M, et al. Understanding the tumor immune microenvironment (TIME) for effective therapy. *Nat Med.* (2018) 24:541–50. doi: 10.1038/s41591-018-0014-x
173. Newman AM, Liu CL, Green MR, Gentles AJ, Feng W, Xu Y, et al. Robust enumeration of cell subsets from tissue expression profiles. *Nat Methods.* (2015) 12:453–7. doi: 10.1038/nmeth.3337

174. Aran D, Hu Z, Butte AJ. xCell: digitally portraying the tissue cellular heterogeneity landscape. *Genome Biol.* (2017) 18:220. doi: 10.1186/s13059-017-1349-1
175. Scott MC, Temiz NA, Sarver AE, LaRue RS, Rathe SK, Varshney J, et al. Comparative transcriptome analysis quantifies immune cell transcript levels, metastatic progression, and survival in osteosarcoma. *Cancer Res.* (2018) 78:326–37. doi: 10.1158/0008-5472.CAN-17-0576
176. Wycislo KL, Fan TM. The immunotherapy of canine osteosarcoma: a historical and systematic review. *J Vet Intern Med.* (2015) 29:759–69. doi: 10.1111/jvim.12603
177. Gorden BH, Kim JH, Sarver AL, Frantz AM, Breen M, Lindblad-Toh K, et al. Identification of three molecular and functional subtypes in canine hemangiosarcoma through gene expression profiling and progenitor cell characterization. *Am J Pathol.* (2014) 184:985–95. doi: 10.1016/j.ajpath.2013.12.025
178. Filley A, Henriquez M, Bhowmik T, Tewari BN, Rao X, Wan J, et al. Immunologic and gene expression profiles of spontaneous canine oligodendrogliomas. *J Neurooncol.* (2018) 137:469–79. doi: 10.1007/s11060-018-2753-4
179. Giannuzzi D, Marconato L, Elgendy R, Ferraresso S, Scarselli E, Fariselli P, et al. Longitudinal transcriptomic and genetic landscape of radiotherapy response in canine melanoma. *Vet Comp Oncol.* (2019) 17:308–16. doi: 10.1111/vco.12473
180. Garrido F, Aptsiauri N, Doorduijn EM, Garcia Lora AM, van Hall T. The urgent need to recover MHC class I in cancers for effective immunotherapy. *Curr Opin Immunol.* (2016) 39:44–51. doi: 10.1016/j.coi.2015.12.007
181. Alexandrov LB, Nik-Zainal S, Wedge DC, Aparicio SA, Behjati S, Biankin AV, et al. Signatures of mutational processes in human cancer. *Nature.* (2013) 500:415–21. doi: 10.1038/nature12477
182. Samstein RM, Lee CH, Shoushtari AN, Hellmann MD, Shen R, Janjigian YY, et al. Tumor mutational load predicts survival after immunotherapy across multiple cancer types. *Nat Genet.* (2019) 51:202–6. doi: 10.1038/s41588-018-0312-8
183. O'Donnell JS, Teng MW, Teng MWL, Smyth MJ. Cancer immunoediting and resistance to T cell-based immunotherapy. *Nat Rev Clin Oncol.* (2019) 16:151–67. doi: 10.1038/s41571-018-0142-8
184. Varn FS, Schaafsma E, Wang Y, Cheng C. Genomic characterization of six virus-associated cancers identifies changes in the tumor immune microenvironment and altered genetic programs. *Cancer Res.* (2018) 78:6413–23. doi: 10.1158/0008-5472.CAN-18-1342
185. Iglesia MD, Parker JS, Hoadley KA, Serody JS, Perou CM, Vincent BG. Genomic analysis of immune cell infiltrates across 11 tumor types. *J Natl Cancer Inst.* (2016) 108:djw144. doi: 10.1093/jnci/djw144
186. Keane C, Gould C, Jones K, Hamm D, Talaulikar D, Ellis J, et al. The T-cell receptor repertoire influences the tumor microenvironment and is associated with survival in aggressive B-cell lymphoma. *Clin Cancer Res.* (2017) 23:1820–8. doi: 10.1158/1078-0432.CCR-16-1576
187. Kikutake C, Yoshihara M, Sato T, Saito D, Suyama M. Pan-cancer analysis of intratumor heterogeneity associated with patient prognosis using multidimensional measures. *Oncotarget.* (2018) 9:37689–99. doi: 10.18632/oncotarget.26485
188. Naik S, Makielsi KM, Henson MS, Stuebner KM, Tabaran AF, Cornax IOSMG, et al. Characterization of anti-tumor immune responses and effects on survival of neoadjuvant oncolytic virotherapy in spontaneous osteosarcoma. Abstract O43. In: *Society for Immunotherapy of Cancer 2018.* Washington, DC: SITC (2018).
189. Miller JS, Lewis LL. Natural killer cells in cancer immunotherapy. *Ann Rev Cancer Biol.* (2019) 3:77–103. doi: 10.1146/annurev-cancerbio-030518-055653
190. Cooper EL. Evolution of immune systems from self/not self to danger to artificial immune systems (AIS). *Phys Life Rev.* (2010) 7:55–78. doi: 10.1016/j.plrev.2009.12.001
191. Postow MA, Callahan MK, Wolchok JD. Immune checkpoint blockade in cancer therapy. *J Clin Oncol.* (2015) 33:1974–82. doi: 10.1200/JCO.2014.59.4358
192. Helmink BA, Gaudreau PO, Wargo JA. Immune checkpoint blockade across the cancer care continuum. *Immunity.* (2018) 48:1077–80. doi: 10.1016/j.immuni.2018.06.003
193. Goodman A, Patel SP, Kurzrock R. PD-1-PD-L1 immune-checkpoint blockade in B-cell lymphomas. *Nat Rev Clin Oncol.* (2017) 14:203–20. doi: 10.1038/nrclinonc.2016.168
194. Gajewski TF. The next hurdle in cancer immunotherapy: overcoming the non-T-cell-inflamed tumor microenvironment. *Semin Oncol.* (2015) 42:663–71. doi: 10.1053/j.seminoncol.2015.05.011
195. Modiano JF, Bellgrau D, Cutter GR, Lana SE, Ehrhart NP, Ehrhart E, et al. Inflammation, apoptosis, and necrosis induced by neoadjuvant fas ligand gene therapy improves survival of dogs with spontaneous bone cancer. *Mol Ther.* (2012) 20:2234–43. doi: 10.1038/mt.2012.149
196. Sorenmo KU, Krick E, Coughlin CM, Overley B, Gregor TP, Vonderheide RH, et al. CD40-activated B cell cancer vaccine improves second clinical remission and survival in privately owned dogs with non-Hodgkin's lymphoma. *PLoS ONE.* (2011) 6:e24167. doi: 10.1371/journal.pone.0024167
197. Mason NJ, Gnanandarajah JS, Engiles JB, Gray F, Laughlin D, Gaurnier-Hausser A, et al. Immunotherapy with a HER2-targeting listeria induces HER2-specific immunity and demonstrates potential therapeutic effects in a phase I trial in canine osteosarcoma. *Clin Cancer Res.* (2016) 22:4380–90. doi: 10.1158/1078-0432.CCR-16-0088
198. Andersen BM, Pluhar GE, Seiler CE, Goulart MR, SantaCruz KS, Schutten MM, et al. Vaccination for invasive canine meningioma induces in situ production of antibodies capable of antibody-dependent cell-mediated cytotoxicity. *Cancer Res.* (2013) 73:2987–97. doi: 10.1158/0008-5472.CAN-12-3366
199. Panjwani MK, Smith JB, Schutsky K, Gnanandarajah J, O'Connor CM, Powell DJ, et al. Feasibility and safety of RNA-transfected CD20-specific chimeric antigen receptor T cells in dogs with spontaneous B cell lymphoma. *Mol Ther.* (2016) 24:1602–14. doi: 10.1038/mt.2016.146
200. Regan D, Dow S. Manipulation of innate immunity for cancer therapy in dogs. *Vet Sci.* (2015) 2:423–39. doi: 10.3390/vetsci2040423
201. Anderson KL, Modiano JF. Progress in adaptive immunotherapy for cancer in companion animals: success on the path to a cure. *Vet Sci.* (2015) 2:363–87. doi: 10.3390/vetsci2040363
202. Larson G, Karlsson EK, Perri A, Webster MT, Ho SY, Peters J, et al. Rethinking dog domestication by integrating genetics, archeology, and biogeography. *Proc Natl Acad Sci USA.* (2012) 109:8878–83. doi: 10.1073/pnas.1203005109
203. Song SJ, Lauber C, Costello EK, Lozupone CA, Humphrey G, Berg-Lyons D, et al. Cohabiting family members share microbiota with one another and with their dogs. *Elife.* (2013) 2:e00458. doi: 10.7554/eLife.00458
204. Raposo-Ferreira TMM, Brisson BK, Durham AC, Laufer-Amorim R, Kristiansen V, Pure E, et al. Characteristics of the epithelial-mesenchymal transition in primary and paired metastatic canine mammary carcinomas. *Vet Pathol.* (2018) 55:622–33. doi: 10.1177/0300985818776054
205. Im KS, Kim JH, Kim NH, Yu CH, Hur TY, Sur JH. Possible role of Snail expression as a prognostic factor in canine mammary neoplasia. *J Comp Pathol.* (2012) 147:121–8. doi: 10.1016/j.jcpa.2011.12.002
206. Fantozzi A, Gruber DC, Pisarsky L, Heck C, Kunita A, Yilmaz M, et al. VEGF-mediated angiogenesis links EMT-induced cancer stemness to tumor initiation. *Cancer Res.* (2014) 74:1566–75. doi: 10.1158/0008-5472.CAN-13-1641
207. Medici D, Nawshad A. Type I collagen promotes epithelial-mesenchymal transition through ILK-dependent activation of NF-kappaB and LEF-1. *Matrix Biol.* (2010) 29:161–5. doi: 10.1016/j.matbio.2009.12.003
208. Vellinga TT, den Uil S, Rinkes IH, Marvin D, Ponsioen B, Alvarez-Varela A, et al. Collagen-rich stroma in aggressive colon tumors induces mesenchymal gene expression and tumor cell invasion. *Oncogene.* (2016) 35:5263–71. doi: 10.1038/onc.2016.60
209. Sainz B Jr, Carron E, Vallespinos M, Machado HL. Cancer stem cells and macrophages: implications in tumor biology and therapeutic strategies. *Mediators Inflamm.* (2016) 2016:9012369. doi: 10.1155/2016/9012369
210. Rak J, Guha A. Extracellular vesicles–vehicles that spread cancer genes. *Bioessays.* (2012) 34:489–97. doi: 10.1002/bies.201100169

211. Lazar I, Clement E, Dauvillier S, Milhas D, Ducoux-Petit M, LeGonidec S, et al. Adipocyte exosomes promote melanoma aggressiveness through fatty acid oxidation: a novel mechanism linking obesity and cancer. *Cancer Res*. (2016) 76:4051–7. doi: 10.1158/0008-5472.CAN-16-0651
212. Robado de Lope L, Alcíbar OL, Amor López A, Hergueta-Redondo M, Peinado H. Tumour-adipose tissue crosstalk: fuelling tumour metastasis by extracellular vesicles. *Philos Trans R Soc Lond B Biol Sci*. (2018) 373:20160485. doi: 10.1098/rstb.2016.0485
213. Ruivo CF, Adem B, Silva M, Melo SA. The biology of cancer exosomes: insights and new perspectives. *Cancer Res*. (2017) 77:6480–8. doi: 10.1158/0008-5472.CAN-17-0994
214. Hood JL, San RS, Wickline SA. Exosomes released by melanoma cells prepare sentinel lymph nodes for tumor metastasis. *Cancer Res*. (2011) 71:3792–801. doi: 10.1158/0008-5472.CAN-10-4455
215. Scott MC, Garbe JR, Tomiyasu H, Donnelly A, Bryan BA, Subramanian S, et al. Unbiased discovery of exosome-associated biomarkers using xenograft models. In: *Proceedings of the American Association for Cancer Research Annual Meeting 2017*. Washington, DC; Philadelphia, PA: AACR. doi: 10.1158/1538-7445.AM2017-817
216. Scott MC, Tomiyasu H, Garbe JR, Cornax I, Amaya C, O'Sullivan MG, et al. Heterotypic mouse models of canine osteosarcoma recapitulate tumor heterogeneity and biological behavior. *Dis Model Mech*. (2016) 9:1435–44. doi: 10.1242/dmm.026849

Conflict of Interest: The authors declare that the research was conducted in the absence of any commercial or financial relationships that could be construed as a potential conflict of interest.

Copyright © 2019 Langsten, Kim, Sarver, Dewhirst and Modiano. This is an open-access article distributed under the terms of the Creative Commons Attribution License (CC BY). The use, distribution or reproduction in other forums is permitted, provided the original author(s) and the copyright owner(s) are credited and that the original publication in this journal is cited, in accordance with accepted academic practice. No use, distribution or reproduction is permitted which does not comply with these terms.

frontiers in Oncology

REVIEW
published: 08 November 2019
doi: 10.3389/fonc.2019.01151

Canine Primary Intracranial Cancer: A Clinicopathologic and Comparative Review of Glioma, Meningioma, and Choroid Plexus Tumors

Andrew D. Miller[1], C. Ryan Miller[2] and John H. Rossmeisl[3]*

[1] Section of Anatomic Pathology, Department of Biomedical Sciences, Cornell University College of Veterinary Medicine, Ithaca, NY, United States, [2] Division of Neuropathology, Department of Pathology, O'Neal Comprehensive Cancer Center and Comprehensive Neuroscience Center, University of Alabama School of Medicine, Birmingham, AL, United States, [3] Section of Neurology and Neurosurgery, Veterinary and Comparative Neuro-Oncology Laboratory, Department of Clinical Sciences, Virginia-Maryland College of Veterinary Medicine, Blacksburg, VA, United States

In the dog, primary intracranial neoplasia represents ∼2–5% of all cancers and is especially common in certain breeds including English and French bulldogs and Boxers. The most common types of primary intracranial cancer in the dog are meningioma, glioma, and choroid plexus tumors, generally occurring in middle aged to older dogs. Much work has recently been done to understand the characteristic imaging and clinicopathologic features of these tumors. The gross and histologic landscape of these tumors in the dog compare favorably to their human counterparts with many similarities noted in histologic patterns, subtype, and grades. Data informing the underlying molecular abnormalities in the canine tumors have only begun to be unraveled, but reveal similar pathways are mutated between canine and human primary intracranial neoplasia. This review will provide an overview of the clinicopathologic features of the three most common forms of primary intracranial cancer in the dog, delve into the comparative aspects between the dog and human neoplasms, and provide an introduction to current standard of care while also highlighting novel, experimental treatments that may help bridge the gap between canine and human cancer therapies.

Keywords: canine, glioma, meningioma, choroid plexus tumor, pathology, immunohistochemistry

OPEN ACCESS

Edited by:
Rodney L. Page, Colorado State University, United States

Reviewed by:
Justin Vareecal Joseph, Aarhus University, Denmark
M. Renee Chambers, University of Alabama at Birmingham, United States

****Correspondence:***
Andrew D. Miller
adm10@cornell.edu

Specialty section:
This article was submitted to Cancer Molecular Targets and Therapeutics, a section of the journal Frontiers in Oncology

Received: *09 August 2019*
Accepted: *16 October 2019*
Published: *08 November 2019*

Citation:
Miller AD, Miller CR and Rossmeisl JH (2019) Canine Primary Intracranial Cancer: A Clinicopathologic and Comparative Review of Glioma, Meningioma, and Choroid Plexus Tumors. Front. Oncol. 9:1151. doi: 10.3389/fonc.2019.01151

INTRODUCTION

Dogs are the only mammalian species besides humans in which spontaneous brain tumors arise frequently (1–4). The estimated incidence of canine nervous system tumors is reported as 14.5 cases per 100,000 (5). Other studies indicate that intracranial neoplasms are observed in 2–4.5% of dogs that are subjected to post-mortem examinations (2, 4, 5).

In dogs, ∼90% of primary brain tumors (PBT) encountered in clinical practice are represented by meningiomas (∼50%), gliomas (∼35%), and choroid plexus tumors (CPT; ∼7%), although the distribution of specific PBT in individual studies varies considerably (1–5). Other PBT, including ependymoma, germinoma, and embryonal tumors are all extremely rare, poorly defined outside of scattered case reports and series, and will not be considered in this review. Secondary brain tumors (SBT) comprise approximately one-half of all canine intracranial tumors, with hemangiosarcoma (29–35%), lymphoma (12–20%), and metastatic carcinomas (11–20%) accounting for 77–86% of all SBT (4, 6).

Brain tumors in dogs occur at any age and in any breed, and there are no reported sex predispositions. However, most PBT and SBT occur in middle-aged to older dogs, with the majority of cases described being > 5 years of age (3, 4, 7, 8). Median ages at diagnosis for dogs with gliomas, meningiomas, and CPT are 8 years, 10.5 years, and 5.5 years, respectively (3, 4, 7, 8). There is a propensity for intracranial tumors identified in juvenile animals to be neuroepithelial tumors of glial, neuronal, or embryonal origin (4, 9). One study identified a statistically significant linear relationship between age and body weight and the occurrence of PBT, and large breed dogs were at significantly increased risk for developing meningiomas and CPT (4). Golden retrievers, boxers, miniature schnauzers, and rat terriers have been identified as breeds in which intracranial meningiomas are overrepresented (3, 4).

Although CPT were also overrepresented in Golden Retrievers in one study (8), this breed predisposition was not substantiated in a subsequent investigation (4). Gliomas (astrocytomas, oligodendrogliomas, and undefined gliomas) are highly overrepresented in several brachycephalic breeds including boxers, Boston terrier, bullmastiffs, and English and French bulldogs (2–4). A locus on canine chromosome (CFA) 26 has been strongly associated with glioma risk across multiple dog breeds, with regional mapping revealing single nucleotide variants in three neighboring genes *DENR*, *CAMKK2*, and *P2RX7* that are highly associated with glioma susceptibility (10). The *CAMKK2* and *P2RX7* genes are relevant to the development or progression of human cancers (10). Further characterization of these genetic associations may provide insight into the drivers of gliomas in dogs and humans, identify new therapeutic targets, or decrease the incidence of gliomas in dogs through selective breeding strategies.

PATHOPHYSIOLOGY AND CLINICAL SIGNS

PBT are intracranial mass lesions that cause clinical signs of brain dysfunction by directly invading or compressing brain tissue and secondarily by causing peritumoral edema, neuroinflammation, obstructive hydrocephalus, and intracranial hemorrhage (11). Compensatory autoregulatory mechanisms, such as decreased cerebrospinal fluid (CSF) production and shifting of CSF into the spinal subarachnoid space, are effective at maintaining the intracranial pressure within physiologic ranges in the early phases of tumor growth. For slow-growing tumor types, such as meningiomas, intracranial pressure-volume homeostatic regulatory mechanisms can often remain intact despite large tumor volumes associated with significant mass effect. However, with progressive increases in tumor volume, autoregulatory mechanisms are eventually overwhelmed and intracranial hypertension (ICH) develops. ICH and the resulting cerebral hypoperfusion is the common pathophysiologic denominator underlying many of the mechanisms of tumor-associated brain injury. Acute clinical deterioration observed in animals with brain tumors and ICH is often the result of vasogenic edema, obstructive hydrocephalus, brain ischemia or hemorrhage, brain herniation, or combinations of these mechanisms (11).

A brain tumor should be considered a differential diagnosis in any middle-aged or older dog with a clinical history consistent with brain dysfunction, especially when clinical signs are progressive. Seizures are the most common clinical manifestation of intracranial neoplasia, and are observed in ∼50% of dogs with prosencephalic tumors (3, 12–17). Structural causes of epilepsy, such as brain tumors, should also be suspected in dogs that experience a new onset of seizure activity after 5 years of age, particularly in predisposed breeds (14). Risk factors for tumor-associated structural epilepsy identified on MRI scans in dogs include the presence of tumor involving the frontal lobe, falcine or subtentorial brain herniations, and marked contrast enhancement of the tumor (16). The pathophysiology of tumor-related epilepsy is currently poorly understood, but both the tumoral and peritumoral microenvironments may contribute to epileptogenic phenotypes owing to disordered neuronal connectivity and regulation, impaired glial cell function, and the presence of altered vascular supply and permeability (18–20). Central vestibular dysfunction is the most common clinical sign associated with brain tumors originating in the caudal brainstem (14, 21). Dogs with brain tumors may also present with non-specific clinical signs, such as lethargy, inappetence, and weight loss (22). Tumors in the fronto-olfactory region are often associated with only historical evidence of brain disease such as seizures or behavioral changes and a normal interictal neurological examination.

Most PBT in dogs occur as solitary mass lesions, and tumors involving forebrain structures are more common than those in the brainstem (3, 4, 21). In many cases with solitary masses, the neurological deficits observed reflect the focal neuroanatomic area of the brain containing the tumor. However, dogs with PBT or SBT may also present with neurological deficits indicative of multifocal intracranial disease.

Multifocal clinical signs may result from several phenomena. The tumor or its secondary effects (vasogenic edema, brain herniation, or hemorrhage) may involve more than one region of the brain, which has been reported in up to 50% of dogs with solitary PBT (3). The phenotypes of some PBT, such as butterfly glioblastomas, diffuse glioma, or leptomeningeal oligodendrogliomatosis, are characterized by invasion of both cerebral hemispheres or diffuse brain or meningeal involvement (23–26). Multiple discrete tumor foci may also be present, which occurs occasionally in canine meningiomas and histiocytic sarcomas (1, 27). Rare reports describing synchronous PBT of different histologies, and concurrent PBT and SBT also exist (28, 29). PBT, and particularly choroid plexus carcinomas, may metastasize within the CNS by a unique mechanism termed drop metastases (8, 11, 30). This involves exfoliation of cancer cells into and circulation within the CSF, with implantation of tumor foci distant from the site of the primary tumor in the ventricular system or subarachnoid space.

DIAGNOSIS OF INTRACRANIAL TUMORS

As brain tumors typically affect middle-aged to older dogs that may have significant concurrent disease, performance of a complete blood count, chemistry profile, and urinalysis is generally indicated in dogs with suspected brain tumors to

evaluate the animal's systemic health status (3). These diagnostics also allow for rational formulation of an anesthetic protocol, as anesthesia is required for the performance of ancillary diagnostics that provide the highest diagnostic yield in dogs with structural brain disease, such as brain biopsy, magnetic resonance [MRI] imaging, and CSF analysis. Other diagnostics indicated prior to anesthesia are dictated by the individual dog's history and physical examination findings.

Radiographs of the thorax and abdominal ultrasound (AUS) should be considered in an attempt to identify concurrent unrelated neoplasia or other significant comorbidities. Studies in dogs with intracranial tumors report finding contemporaneous and unrelated neoplasms in 3–23% of dogs with PBT, most of which involve either the thoracic or abdominal cavity (3, 31). Additional studies investigating the clinical utility of screening thoracic radiography and AUS in dogs with intracranial tumors have indicated that abnormalities are frequently identified on these imaging examinations, the results of these procedures rarely negatively affect the decision to perform neurodiagnostic procedures indicated for the patient's neurological presentation, and significantly alter therapeutic recommendations for the brain tumor in <10% of cases (31, 32).

Cross-sectional diagnostic imaging techniques, such as computed tomography (CT) and MRI have revolutionized the clinical diagnosis and management of brain tumors in veterinary medicine, although MRI is the preferred modality for the assessment of animals with intracranial disease (33–53). Data obtained from MR imaging such as mass number (solitary vs. multiple), origin within the neuraxis (meningeal [extra-axial], parenchymal [intra-axial], or intraventricular) and intrinsic signal appearances, collectively provides characteristic patterns that allow for the presumptive diagnosis of most frequently encountered PBT and SBT in veterinary medicine or refinement of the list of differential diagnoses. The diagnostic imaging features of each of the common types of PBT are reviewed with their comparative neuropathologic features below. In one investigation of 40 dogs, the accuracy of predicting the type of PBT based on MR images was 70% (44). It remains common in veterinary practice to make clinical decisions in patients with presumptively diagnosed tumors based on imaging derived data, despite the potential consequences this has on management of individual patients. There are also significant implications associated with the strength of evidence provided by studies that include cohorts of dogs without histopathologic tumor diagnoses.

Cerebrospinal fluid (CSF) analysis generally provides data that is complementary to the clinical examination and diagnostic imaging results and may assist in the prioritization of differential diagnosis. Obtaining CSF in dogs with brain tumors and intracranial hypertension carries a risk of causing clinical deterioration. Although this risk is low, it should be critically assessed in each patient and evaluated in context of the likelihood of obtaining a non-specific test result. Advanced imaging of the brain should always precede CSF collection to best evaluate individual patient risk.

While CSF is a sensitive indicator of intracranial disease and is frequently abnormal in patients with brain tumors, white blood cell (WBC) counts, WBC differentials, and total protein concentrations are highly variable and are often non-specific for neoplasia. There are conflicting data in the literature about the cytological characteristics of CSF in dogs with meningiomas, with one study reporting that meningiomas were commonly associated with a modest neutrophilic pleocytosis, and a later investigation concluding that the majority of meningiomas have WBC counts <5 cells, and a neutrophilic pleocytosis was an atypical finding for canine meningiomas located in the rostral or middle fossas (54, 55). In one study of CPT, CSF analysis was helpful for the differentiation of CPC from CPP, as observation of a CSF total protein concentration >80 mg/dL was exclusively associated with a diagnosis of CPC (8). Exfoliated neoplastic cells may be observed in the CSF cytology of dogs with any type of brain tumor, but CPT, lymphoma, and histiocytic sarcoma are the tumors most commonly reported to be detected with CSF analysis (3, 8, 56–58).

An evolving field in comparative medicine is the identification of circulating biomarkers in blood or CSF that correlate with brain tumor load, biological behavior, or treatment response. Liquid biopsy is a technique for sampling and analyzing non-solid biological tissues, and is mainly used to diagnose disease or monitor therapy. Serum or plasma compounds such as VEGF, glial fibrillary acidic protein, plasma free amino acid profiles, and CSF concentrations of uric acid, D-dimers, and MMP-2 and MMP-9 have been quantified in dogs with brain tumors, but results to date suggest that these compounds will not fulfill ideal biomarker criteria due to limitations associated with sensitivity and specificity (59–65).

Circulating tumor DNA (ctDNA), circulating cell-free RNA, serum proteomic profiling, and exosomes are also currently being explored as liquid biopsy biomarkers in veterinary neurooncology (66, 67). Serum proteomic microarray profiles classified dogs as having intracranial neoplasia, meningoencephalitis of unknown etiology, or being healthy with 100% accuracy and preliminary data suggests that proteomic immunosignatures may also have utility in distinguishing tumor types (67). A feasibility study in canine glioma has demonstrated that expression of cell surface integrins αvβ3 and α3β can be detected in canine glioma cell lines, as well as exosomes derived from these lines using integrin specific peptide targeting methods (66). This investigation provides the foundation for further exploration of serum and CSF exosomes as potential *in vivo* biomarkers of canine glioma.

Given the limitations of imaging, CSF analyses, and liquid biopsy techniques, histopathologic examination of representative tissue is required for the definitive diagnosis and grading of nervous system tumors. Excisional biopsy performed during curative intent surgery remains the most frequently employed biopsy technique for PBT in veterinary practice, but these procedures have been historically limited to patients with superficially located, extra-axial forebrain tumors. In cases where surgical resection may not be a possible or optimal approach to management, stereotactic brain biopsy (SBB) techniques are often a viable alternative method for establishing a histopathologic diagnosis.

Several SBB techniques have been utilized in dogs with brain tumors including endoscopic assisted, free-hand, and image-guided procedures. SBB associated diagnostic yields, morbidity, and mortality are variable and dependent on the technique used, the neurologic status of the patient, experience of the surgeon, and the neuroanatomic location of the lesion (68–74). However, similar to the human experience, when SBB is performed in dogs with brain tumors by an experienced veterinary neurosurgeons, diagnostic yields are 95%, and serious adverse events occur in <5% of cases (72, 74). The histological classification and grading of CNS tumors can be challenging, especially when evaluating the limited sample sizes associated with SBB, but accurate diagnoses can be facilitated by taking multiple biopsy specimens (72, 74).

GLIOMA

Diagnostic Imaging Features

Gliomas originate within the brain parenchyma (intra-axial). As gliomas may infiltrate or displace the neuroparenchyma, they may appear poorly or well marginated and may or may not demonstrate contrast enhancement (**Table 1**) (33, 44, 46, 51, 75). Among contrast enhancing gliomas, the patterns and degree of enhancement seen can be highly variable. A "ring enhancing" pattern, in which a circular ring of contrast enhancement surrounds non-enhancing abnormal tissue, is often associated with gliomas (**Figure 1A**). However, ring enhancement is a non-specific finding that has been associated with several neoplastic, vascular, and inflammatory brain diseases (35, 49). Using conventional MRI sequences, it is not currently possible to reliably differentiate types of gliomas (astrocytomas from oligodendrogliomas) or accurately predict the grade of gliomas. However, contrast enhancement is more commonly observed in high-grade compared to low-grade gliomas, and oligodendrogliomas are more likely to distort the ventricles and have contact with the brain surface than astrocytomas (47, 50, 75). The significant overlap that exists in the imaging features of gliomas, cerebrovascular accidents, and inflammatory lesions results in frequent misdiagnosis of these categories of intra-axial lesions (40, 49). The addition of diffusion weighted (DWI), spectroscopic, and perfusion weighted imaging sequences to conventional MRI sequences improves the ability of MRI to discriminate between neoplastic and non-neoplastic lesions, and prediction of tumor grades. However, the utility of this suite of imaging techniques has not yet been evaluated in large populations of dogs with histologically confirmed lesions (34, 41–43, 45, 48, 53, 76).

Pathologic and Comparative Features

The pathology underpinnings of canine glioma have undergone much development in the last several decades with advances in histologic interpretation, immunohistochemical profiling, and molecular diagnostics. Of the total glioma number, oligodendrogliomas have an incidence close to 70% with astrocytomas ∼20%, and undefined 10%. Grossly, oligodendrogliomas vary from well-demarcated white to tan, fleshy, soft masses (**Figure 1B**) to those that are more infiltrative in the neuroparenchyma. They are commonly gelatinous owing to a high level of mucin production. They can be found intraventricularly, multifocally within the central nervous system, or diffusely in the leptomeninges as either a primary mass or metastatic spread (77–79). Astrocytomas tend to be similar in color to the adjacent neuroparenchyma and often blend with the adjacent parenchyma without obvious mass formation (78). Undefined gliomas have a population of astrocytic and oligodendroglial differentiation that are roughly equivalent and therefore the gross features can include any or all of those noted above. For all of the three glioma subtypes in the dog, higher grade tumors are more likely to have associated hemorrhage. In some instances, calvarial bone erosion can be associated with glioma; however, this is not specific to glioma (80).

Historically, canine gliomas were defined based on the original World Health Organization criteria; however, this outdated classification scheme has been replaced by a more comprehensive grading system (78, 81). Based on the new histologic grading scheme, gliomas are divided into oligodendroglioma, astrocytoma, and undefined glioma based on their histomorphology (**Figure 1C**). Neoplasms are further divided into low- or high-grade. High-grade tumors are diagnosed based on any one of the following being present in the tumor sections examined: microvascular proliferation (**Figure 1C**, inset), intratumoral, geographic necrosis, pseudopalisading around the regions of necrosis (**Figure 1D**), increased mitotic activity, or overt features of malignancy (78). The degree of infiltration is not a criterion for differentiating low- vs. high-grade; however, the pattern (non-infiltrative, focally infiltrative, or diffusely infiltrative) should be noted when making the diagnosis (78). Readers are urged to review the updated histologic characterization criteria as an in depth discussion of histologic features are outside the scope of this review paper (78). However, generally speaking, oligodendrogliomas are composed of sheets and linear cords of round to polygonal cells with variable amounts of cytoplasm, round nuclei, and a finely stippled chromatin pattern (82). Especially in necropsy or poorly fixed samples, neoplastic cells often have abundant clear cytoplasm leading to a fried-egg appearance. This is a feature absent in biopsy samples due to timely and appropriate fixation. The formation of secondary structures (neuronal satellitosis, leptomeningeal spread, and perivascular proliferation) are commonly noted in canine oligodendroglioma (**Figure 1E**). Low-grade tumors often have a delicate meshwork of branching vasculature whereas high-grade tumors have marked vascular proliferation with a glomeruloid appearance (78). Other features that can be observed in canine oligodendroglioma nuclear molding, pseudorosettes, mineralization, and microcysts, which all occur regardless of grade (78).

Astrocytomas have distinct histologic features compared to oligodendrogliomas. High-grade astrocytomas are more frequently invasive than low-grade astrocytomas (78). Neoplastic astrocytes generally have variable amounts of eosinophilic cytoplasm, elongate to ovoid nuclei, with an open chromatin pattern. Various phenotypic features that can be observed histologically in canine astrocytomas include gemistocytic and pilocytic patterns (83). Similar to oligodendrogliomas,

TABLE 1 | Magnetic resonance imaging features of common canine primary brain tumors.

	Meningioma (3, 7, 36–40, 44, 46, 51)	**Glioma (35, 37, 39, 40, 43, 44, 46, 47, 49–51, 75)**	**Choroid plexus tumor (3, 8, 44, 46, 51)**
Imaging feature			
Mass origin	Extra-axial	Intra-axial	Intraventricular; lateral aperture of 4th ventricle
Margination			
• Well-defined/regular	85%	55%	85%
• Poorly-defined/irregular	15%	45%	15%
T1W signal			
• Isointense	70%	80%	35%
• Hypointense	10%		20%
• Hyperintense	20%	50%	45%
• Heterogeneous			
T2W signal			
• Isointense	24%		10%
• Hypointense	1%		
• Hyperintense	75%	90%	90%
• Heterogeneous		60%	
Contrast enhancement pattern			
• None	10%	25% (more likely with LGG)	<5%
• Partial or complete ring	55%-homogeneous	45% (more likely with HGG)	
• Moderate/severe	35%-heterogeneous	35%	95+%
Peritumoral edema			
• Present	90%	60%	55%
• Absent	10%	40%	45%
Mass effect			
• Present	90%	85%	65%
• Absent	10%	15%	35%
Other features	Dural tail (35%) Cysts/ITF (20%)	Ventricular distortion (Oligo) No Cysts/ITF (more likely with LGG)	Ventriculomegaly (75%) Drop metastases (33% CPC)

CPC, Choroid plexus carcinoma; HGG, high-grade glioma; ITF, intratumoral fluid; LGG, low-grade glioma; Oligo, Oligodendroglioma.

microcysts and mineralization can be observed and while rare deposits of mucin can be noted, they are never as abundant as they are in oligodendrogliomas (78, 82). A seemingly unique astrocytoma phenotypic variant has been observed in the cerebellum/caudal fossa in which tumors are well-demarcated and formed by sheets of gemistocyte-like cells (78). High-grade features are the same as those defined for oligodendroglioma and while the highest grade astrocytoma has traditionally been referred to as a glioblastoma, that term was replaced with the more encompassing high-grade astrocytoma in the most recent classification (78, 84). Undefined gliomas have any of the histologic features described above for oligodendroglioma and astrocytoma; however, the proportions of each are relatively equal thereby preventing classification into one group or the other.

Immunohistochemistry has been widely studied in canine glioma. For basic diagnostic purposes, immunolabeling for the glial cell transcription factor, Olig2, stains canine glioma effectively (**Figure 1F**). Its pattern of immunolabeling is most robust in oligodendrogliomas as opposed to astrocytic tumors where the staining intensity and percent of positive cells is decreased (78). Immunolabeling for glial fibrillary acidic protein (GFAP) is considered supportive of the diagnosis of astrocytoma whereas immunolabeling for CNPase is considered supportive of the diagnosis of oligodendroglioma (78). While Ki67 has been utilized in canine glioma, its widely variable expression patterns in the face of expected staining patterns (i.e., in a tumor with markedly increased mitotic activity) questions its utility in these tumors. Importantly, all of the markers noted above are known to have marked variation in labeling patterns in necropsy samples (owing to variations in fixation time, autolysis, amount of formalin used, and other factors) and use of these markers in necropsy samples should be interpreted with caution (78). Immunohistochemical studies in canine oligodendrogliomas support that these tumors have a dedifferentiated phenotype, one that may arise from an oligodendrocyte precursor cell, perhaps specific to the subventricular zone (85). Some of the markers used to support the origin from oligodendrocyte precursor cells include SOX10, nestin, NG2, and doublecortin (85). In addition, canine gliomas express several neuronal markers including synaptophysin supporting an origin from a multipotential cell type (82). Utilization of tissue microarrays of canine glioma for immunohistochemistry has revealed overexpression of EGFR, PDGFRα, IGFBP2 with EGFR expression moderately correlated to Ki67 immunoreactivity (86, 87). Neither COX-2 nor c-kit have been shown to be expressed in canine glioma (88). While isocitrate dehydrogenase 1 (IDH1) expression has been confirmed in canine glioma via immunohistochemistry,

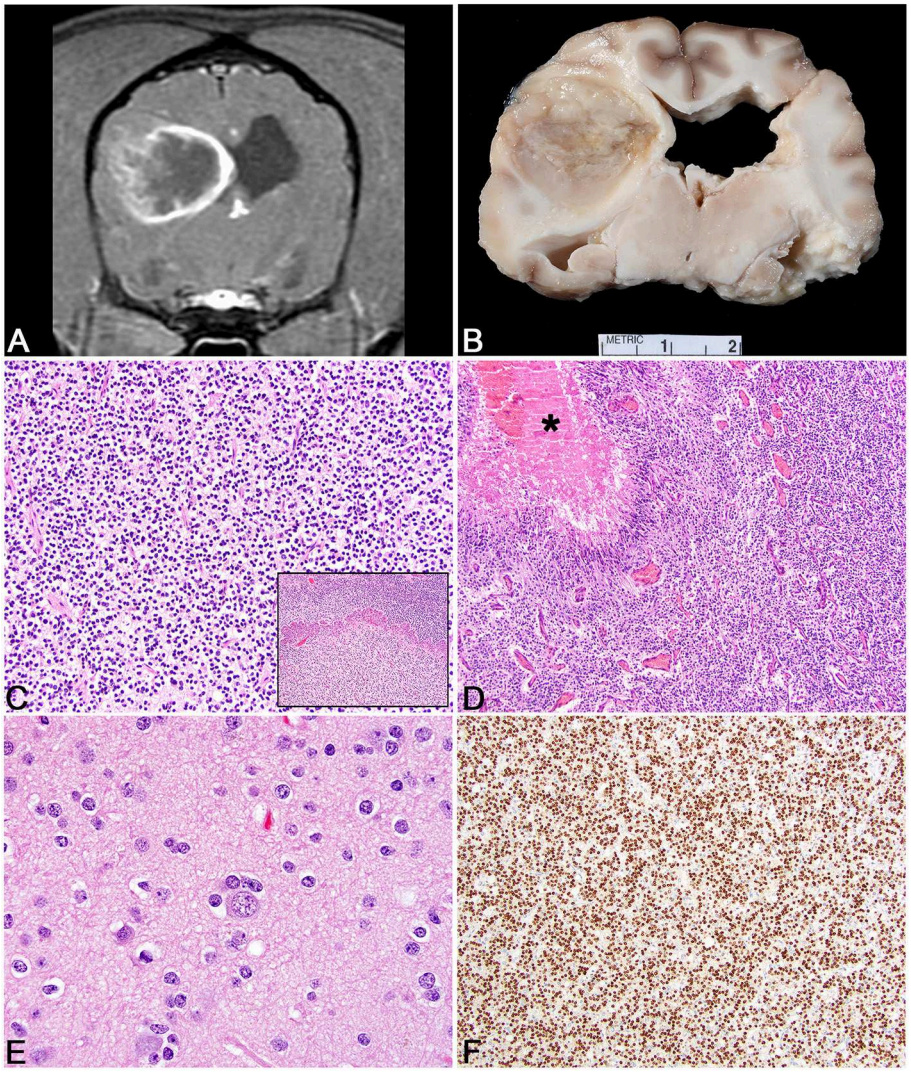

FIGURE 1 | Glioma. **(A)** Canine; MRI-High-Grade Oligodendroglioma. Transverse, post-contrast T1W image illustrating heterogeneously hypointense and ring-enhancing intra-axial mass in the right parieto-temporal lobes. The mass is markedly attenuating the right lateral ventricle. **(B)** Canine, High-Grade Oligodendroglioma. Corresponding necropsy specimen of **(A)** illustrating a well-demarcated mass is present in cerebral cortex causing compression of the thalamus and dilation of the lateral ventricles. **(C)** Canine, High-Grade Oligodendroglioma. Sheets of neoplastic oligodendrocytes embedded in a loose matrix. Hematoxylin and eosin (HE). Inset: Areas of microvascular proliferation. HE. **(D)** Canine, High-Grade Astrocytoma. Discrete areas of necrosis (asterisk) with pseuopalisading by neoplastic cells. HE. **(E)** Human, Grade II Oligodendroglioma. Abundant peri-neuronal satellitosis (secondary structure) is present in this neoplasm. HE. **(F)** Canine, High-Grade Oligodendroglioma. Diffuse intranuclear immunolabeling for Olig2 immunohistochemistry (IHC).

further genome analysis has failed to reveal consistent mutations within the gene as opposed to human gliomas where IDH1 mutation is a common finding (89). Lastly, the inflammatory microenvironment has begun to be explored in canine oligodendroglioma with neoplasms having a robust population of infiltrating T lymphocytes and macrophages (typically with a dendritic cell morphology) with far fewer B lymphocytes (90). Increased numbers of regulatory T cells and dendritic cells have also been recorded in the peripheral blood of canine glioma patients (91). Canine gliomas express PD-L1 which may directly relate to the inflammatory milieu present in these patients (91).

Our understanding of the molecular pathogenesis of canine glioma has also greatly expanded in the last few years. Cell lines generated from canine glioma support multipotentiality in these tumors (92). A wide-ranging genomic profiling of canine glioma has been occurring in parallel with the histologic reclassification of canine glioma. This molecular analysis has confirmed some previous reports in the literature and revealed frequently occurring mutations in the p53 pathway, CDK4, CDKN2A, EGFR, and PDGFRA (93–95). PDGFRA is an especially attractive driver mutation as it is expressed in neural stem cells and known to be critical to gliomagenesis; however, it remains to be determined how it exactly exerts its effects in

the development of glioma. Specific to the p53 pathway, TP53 protein is commonly recognized in canine astrocytic tumors compared to oligodendrogliomas with more variable expression of MDM2 and p21 noted across the other glioma tumor types (93). Phosphorylated members of the PI3K/AKT/MTOR and RAS/MAPK-pathways are seen more commonly in astrocytic tumors than oligodendrogliomas or undefined gliomas (93, 96). When canine and human glioma molecular signatures are compared, it is clear that there is an abundance of heterogeneity amongst these two species as it relates to gliomagenesis (97). 1p/19q co-deletion, which is common in human gliomas, is absent in the dog (94, 95). Similarly *Tert* promotor mutations are lacking and while R132 mutations of IDH1 have been noted rarely in canine glioma, they do not appear to have a cancer-promoting effect like they do in human glioma (94, 95). Much work remains in determining the molecular pathogenesis of canine glioma and its application to glioma prognosis in the dog.

Histological classification of human gliomas has had a long history (98). Yet each iteration that was based solely on microscopic morphology suffered from intra- and interobserver variability that contributed to prognostic imprecision and negatively impacted treatment decision-making (99, 100). Indeed, microscopic discrimination of astrocytomas from oligodendrogliomas has long proven difficult, even for experienced neuropathologists (101, 102).

The 2007 World Health Organization (WHO) classification was the last to rely solely on microscopy to subdivide tumors into astrocytomas, oligodendrogliomas, or (mixed) oligoastrocytomas. Grading was based on morphological features such as mitoses, microvascular proliferation, and necrosis. Their presence correlated strongly with aggressive biology and permitted diagnostic refinement into seven distinct prognostic entities (98). Comprehensive molecular analyses have transformed contemporary tumor classification schemes. Studies have clearly established that significant intertumoral molecular heterogeneity exists among each of the morphologically-defined diffuse gliomas (103, 104).

Discovery of mutations in isocitrate dehydrogenase 1 (*IDH1*), which encodes a metabolic enzyme involved in the tricarboxylic acid cycle, significantly altered the trajectory of diagnostic neuropathology and laid the groundwork for the 2016 WHO classification update, particularly for lower-grade (WHO grades II and III) gliomas (105). Subsequent studies identified mutations in either *IDH1* or *IDH2* in over 70% of lower-grade gliomas, as well as a small subset (∼5%) of secondary glioblastomas that evolved from lower-grade precursors (106). IDH1/2 mutations were found in both astrocytomas and oligodendrogliomas and portended a better outcome that IDH1/2-wild-type (wt) tumors.

Oligodendrogliomas have been known for several decades to feature a recurrent genetic mutation, loss of chromosomes 1p and 19q, which correlates with improved prognosis and response to therapy (107, 108). Comprehensive genomics and integrative bioinformatics studies solidified its role in contemporary human glioma classification. A population-based study that analyzed 3 molecular markers (1p/19q, IDH1/2, and TERT promoter) stratified grade II and III gliomas into five molecular subgroups independently associated with clinical outcomes (109). A TCGA lower-grade glioma study used comprehensive multiple omics data and unbiased integrative bioinformatics analyses to define three molecular subtypes based on two molecular markers, 1p/19q codeletion and IDH1/2 mutations (110). Importantly, each subtype—IDHmt lacking 1p/19q codeletion, IDHmt with1p/19q codeletion, and IDHwt—were prognostically significant and non-overlapping. Half of patients with 1p/19q-codeleted tumors survived 8.0 years, IDHmt, non-codeleted tumors 6.3 years and IDHwt tumors 1.7 years. Most IDH-mt tumors without codeletion were histological astrocytomas, and nearly all featured mutations in TP53 and ATRX. Most IDH-mt tumors with codeletion were histological oligodendrogliomas and harbored CIC, FUBP1, NOTCH1, and TERT promoter (TERTp) mutations. These data confirmed previous reports identifying CIC and FUBP1 as candidate oligodendroglioma tumor suppressor genes lost on chromosomes 1p and 19q respectively (111). Other large studies have reported similar findings (112, 113).

A significant fraction of WHO grade II/III gliomas lack IDH mutations, especially grade III tumors with astrocytic histology (114). These tumors frequently harbor molecular alterations typically seen in WHO grade IV glioblastomas, including chromosome 7 gains, chromosome 10 deletions, *EGFR* amplification, TERTp mutations, and deletions of *CDKN2A*. The prognosis of these IDHwt tumors is worse than their corresponding IDHmt counterparts. The unfavorable prognosis is particularly strong for IDHwt anaplastic gliomas (114). In this study, IDHwt tumors were further divided into a molecularly unfavorable group (those having either EGFR amplification, H3F3A mutation, or TERTp mutation) and a favorable group lacking those alterations. A subsequent TCGA analysis of both lower-grade glioma and glioblastoma datasets showed that IDHwt lower-grade gliomas segregated into three DNA methylation subtypes (115). Two harbored glioblastoma-like mutations, including EGFR, PTEN, and NF1. The third methylation subtype shared mutational similarities to the non-diffuse glioma, pilocytic astrocytoma (WHO grade I), and portended a similarly favorable prognosis.

Based largely on these studies, the 2016 WHO classification of human gliomas represented a nosological shift in focus away from diagnoses based solely on morphological criteria to one of integrative diagnoses based on both phenotype and genotype (116). Six diagnostic entities were established, each with a required molecular marker (**Table 2**). With increased interest in canine glioma and larger molecular studies being performed in these tumors, it is logical that molecular classification will be layered onto the newly revised histologic classification to create a more detailed stratification of canine glial tumors.

MENINGIOMA

Diagnostic Imaging Features

Meningiomas are the most common extra-axial meningeal origin tumors in dogs (**Table 1**). Although most meningiomas occur as solitary masses, multiple tumors can be seen (27). Meningiomas usually have a broad-based attachment where they interface with the skull, have distinct tumor margins, and demonstrate marked

TABLE 2 | Current classification scheme of human glioma.

WHO grade	2007 WHO	2016 WHO
II	Diffuse astrocytoma Oligoastrocytoma Oligodendroglioma	Diffuse astrocytoma, IDH-mutant Oligodendroglioma, IDH-mutant and 1p/19q codeleted
III	Anaplastic astrocytoma Anaplastic oligoastrocytoma Anaplastic oligodendrogliomas	Anaplastic astrocytoma, IDH-mutant Anaplastic oligodendroglioma, IDH-mutant and 1p/19q codeleted
IV	Glioblastoma	Glioblastoma, IDH-wildtype Glioblastoma, IDH-mutant

and often uniform contrast enhancement (**Figure 2A**). Some meningiomas will also contain intratumoral fluid, large cystic regions, intratumoral mineralization, calvarial hyperostosis, or demonstrate a dural tail sign (36, 38, 46, 51). Although the dural tail feature is commonly associated with meningiomas, it is not specific for this tumor type, or for neoplastic diseases in general (38, 40). Peritumoral edema is present in >90% of canine meningiomas, and is extensive and diffuse in many cases (7, 44, 46). In dogs, reported sensitivities of MRI to correctly identify intracranial meningiomas range between 60 and 100% (3, 35, 37, 39, 44). Histiocytic sarcomas and granular cell tumors share many overlapping imaging features significant with those of meningiomas (46, 51). Specific subtypes of meningiomas cannot be distinguished using conventional MRI sequences (7), although quantitative radiomic analyses has shown some promise in discriminating grades of meningiomas (52).

Pathologic and Comparative Features

As noted, meningiomas are the most common primary brain and spinal cord neoplasm in the dog. These tumors arise from the arachnoid cap cells that line the middle layer of meninges. They are an intradural, but extraparenchymal solitary neoplasm of which their incidence decreases caudally through the central nervous system, perhaps due to a decreased density of arachnoid cells. Grossly, they tend to be firm, multilobulated, gray to white masses that are compressive and variably infiltrative (**Figure 2B**). Less common manifestations include a broad, *en plaque* presentation, in which the meningioma spreads over a large area of the brain and is commonly infiltrative into the adjacent neuroparenchyma. This less common pattern most often presents around the ventral portion of the brainstem, especially along the skull base (117). While they can often be locally infiltrative, spread within the central nervous system is not well recorded in the literature and metastatic spread to extra-CNS organs is an exceedingly rare event (118).

Based on their location, they are one of the few primary brain tumors that can be amenable to surgical excision and owing to their complex origin from neural crest cells and mesoderm, they exhibit a vast array of histologic patterns that correlate well to similar patterns seen in human meningioma. The World Health Organization (WHO) histologic classification scheme of canine meningioma recognizes two broad categories: slow-growing, generally benign neoplasms (which represents a number of subtypes: meningothelial, fibrous, transitional, psammomatous, angiomatous, myxoid, granular, and papillary) and more anaplastic tumors which generally don't have as much benign behavior (81). However, it must be stressed that the canine classification scheme is greatly outdated, and much work remains to be done to develop a canine classification scheme that can be correlated with and predict biologic behavior. In comparison, the human classification scheme is vastly more advanced (116). Indeed, many veterinary pathologists have resorted to using the human criteria for grading canine meningiomas due to a lack of adequate canine grading criteria (7). While the 2016 WHO classification of human meningiomas continues to rely solely on microscopic morphology, molecular analyses coupled with detailed histologic analysis are poised to revolutionize classification of these neoplasms. Such advances promise better determination of tumor behavior and patient outcome.

The most common histologic subtypes of canine meningioma are meningothelial, fibroblastic, transitional, and atypical. Meningothelial meningiomas are formed by sheets of meningothelial cells often with vague whorling (**Figures 2C,D**). Cells typically have abundant cytoplasm, large round to ovoid nuclei with an open chromatin pattern and a single, often prominent nucleolus. The nuclear features are especially well conserved across different subtypes and can be helpful in guiding the diagnosis on less common subtypes. Fibroblastic meningiomas consist of streams of spindle cells with abundant collagen deposition. The transitional subtype combines the feature of the meningothelial and fibrous subtypes such that both patterns are a significant portion of the neoplasm (**Figure 2E**). A further subtype of the transitional meningioma is the psammomatous meningioma, so named based on the abundant mineralized concretions that are present in the center of meningothelial whorls. This subtype should only be diagnosed if the psammoma bodies are the predominant histologic pattern as small numbers of psammoma bodies can be found in many subtypes of canine meningioma. Meningothelial and transitional subtypes represent anywhere from 20 to 30% or higher of meningioma incidence (119). Microcystic meningiomas are also a relatively common subtype in the dog and have large, variably sized vacuoles that develop in the neoplastic cells that can often coalesce to form large cysts within the tumor (120). In this rare instance, the gross texture of a microcystic meningioma is more fluctuant than the more common firm texture. Importantly, the microcystic subtype should only be designated if this is the predominant pattern as focal to multifocal microcystic change is common in many subtypes of canine meningioma. The granular cell subtype of meningioma consists of large meningothelial cells with abundant periodic acid-Schiff positive granules within the cytoplasm. It remains to be determined if the granular cell variant of canine meningioma is distinct from the intracranial granular cell tumor in the dog; however, it is likely that they represent the same entity as meningothelial whorls can be found in granular cell tumors of the canine CNS with methodical histologic analysis (121).

Other histologic subtypes include rhabdoid meningioma, which has meningothelial cells with abundant eosinophilic

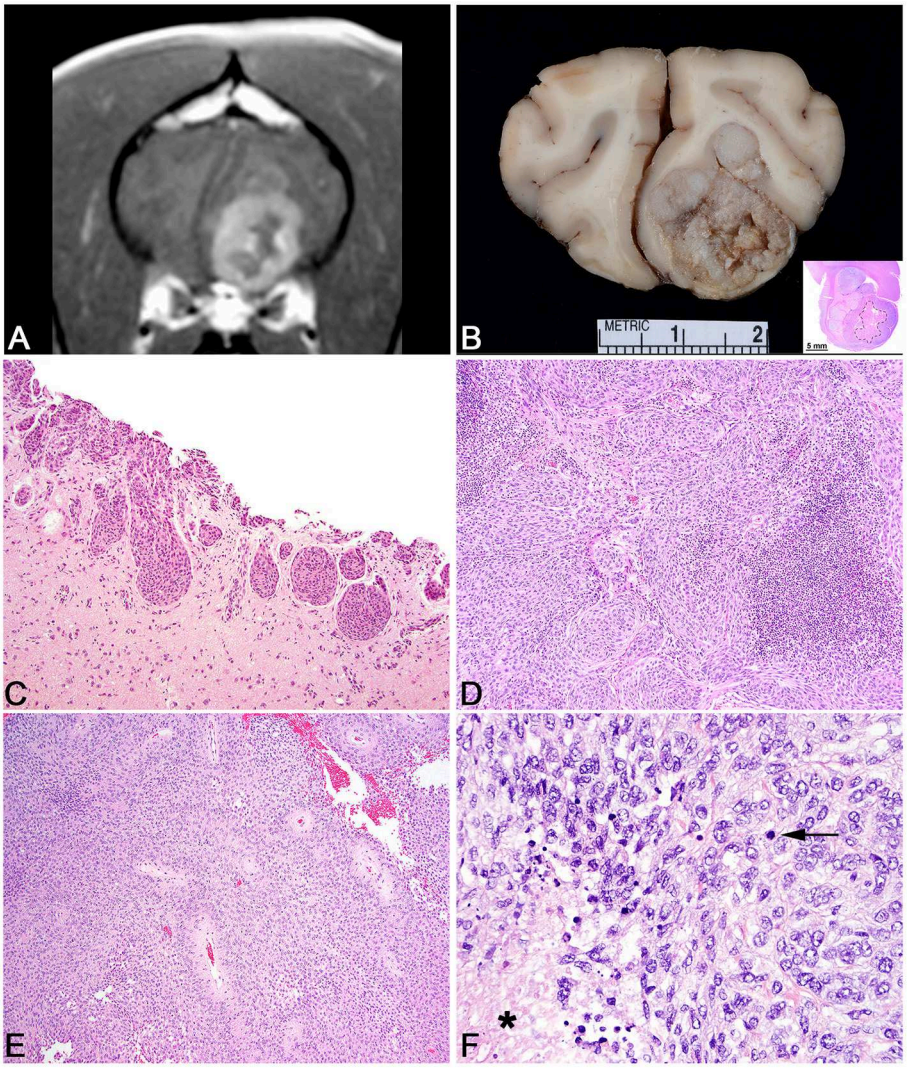

FIGURE 2 | Meningioma. **(A)** Canine; MRI. Transverse, post-contrast T1W image of a well-demarcated, ring-enhancing extra-axial mass in the ventral aspect of the left frontal lobe. Mass effect is present as manifested by the falx shift to the right. **(B)** Canine, Meningioma. Corresponding necropsy specimen of **(A)** illustrating a large, multilobular, white to tan mass that invades the neuroparenchyma. Inset: subgross histologic representation of the meningioma characterized by peripheral sheets of meningothelial cells centered on a core of necrosis. Hematoxylin and eosin (HE). **(C)** Canine, Transitional Meningioma, Invasive. Markedly invasive whorls and clusters of neoplastic meningothelial cells. HE. **(D)** Canine, Transitional Meningioma. Tightly packed whorls and clusters with an associated focus of neutrophils. HE. **(E)** Canine, Meningothelial Meningioma. Sheets of meningothelial cells that surround blood vessels with an acellular perivascular halo. HE. **(F)** Human, Anaplastic Meningioma. Large area of necrosis (asterisk) with sheets of meningothelial cells with increased mitotic figures (arrows). HE.

cytoplasm and small, peripheralized nuclei. Papillary subtypes are defined by an abundance of pseudorosettes (122). While this can be the predominant histologic pattern, papillary change can also be a focal change within a meningioma. Although suggested by the WHO canine criteria as being a more benign variant, data supports that these are often aggressive subtypes of canine meningioma with a high degree of recurrence (122). This suggests a more malignant behavior for these tumors in the dog, which would be analogous to the human papillary subtype (122). Angiomatous meningiomas are uncommon and represent a meningioma that is highly vascularized. Atypical meningiomas have any of the features noted above, but also have increased mitotic activity (>4 mitoses per ten 400x fields) or have three or more of the following: increased cellularity, increased anisocytosis and anisokaryosis, patterned necrosis, or patternless growth patterns (7). It must be noted, that in canine meningioma, regions of necrosis are common and should not be over interpreted as always indicating an atypical subtype. While the cut off for mitotic count at 4 in ten 400x fields is based on the human WHO meningioma criteria, it remains to be determined if this is an appropriate cut off for canine meningioma or if a better determination of mitotic activity (i.e., Ki67 or AgNOR) is more predictive. Based on some canine studies, the incidence of atypical meningiomas reaches ∼40%, a percentage that far

outpaces the incidence of human atypical meningiomas (7). Lastly anaplastic meningiomas represent a very uncommon diagnosis in the dog and have greatly exaggerated features of malignancy compared to the atypical variant (**Figure 2F**).

Other histologic features of importance in the dog include rare deposition of amyloid and exceedingly rare formations of amianthoid fibers (123). Canine meningiomas are widely infiltrated by inflammatory cells including an abundance of neutrophils, either associated with or unassociated with areas of necrosis, large numbers of macrophages and an abundance of lymphocyte subtypes (124). Initial immunohistochemical analysis for interleukin 6 and 8 expression failed to yield significant expression levels; however, RNA transcriptome analysis of canine meningioma revealed overexpression in a number of immunomodulatory genes (125, 126). Chondroid and osseous metaplasia are sporadically seen in various subtypes, although they are most commonly seen in the optic nerve-associated meningiomas.

Owing to their diverse embryologic origin, it is not surprising that canine meningiomas have recorded immunoreactivity to a wide number of antibodies, none of which are specific to the diagnosis of a meningioma. Diagnosis of a meningioma still relies predominately on histologic analysis even though it can be augmented by specific immunohistochemical assays. Canine meningiomas are almost always positive for vimentin and also commonly express laminin, NSE, E-cadherin, CD34, GLUT-1, claudin-1, PGP9.5, pancytokeratin, and S100 (127, 128). The combination of immunolabeling for vimentin, CD34, and E-cadherin has been proposed as being supportive of the diagnosis of meningioma (127). Additional studies on cell adhesion molecules in canine meningioma has revealed that N-cadherin expression is directly correlated with an invasive phenotype (129). This N-cadherin expression is joined by expression of doublecortin at the invading line of the meningioma as well as increased nuclear β-catenin, all three of which may hold prognostic value for more aggressive meningiomas (129). Progesterone receptor expression has been noted in canine meningiomas, where it is inversely related to Ki67 and a better response to radiation therapy (130, 131). Estrogen receptors are less commonly expressed in canine meningiomas (131).

Vascular endothelial growth factor (VEGF) expression has been studied to some detail in the dog. Various isoforms have been identified in the dog and expression of VEGF in both the meningiomas and plasma from affected patients is related to increased tumor malignancy and a poorer prognosis (60, 132, 133). VEGF expression has not been correlated to proliferation indices nor has it been correlated to peritumoral edema (133, 134). Matrix metalloproteinases have also been a common avenue of exploration in the dog. MMP-2 and - 9 are widely expressed in canine meningioma; however, expression is not correlated with peritumoral edema (135, 136). Additionally, tissue inhibitors of metalloproteinases are also expressed in canine meningioma and is highest in papillary subtypes where it and a similar increase in MMP-2 expression may be associated with the more aggressive phenotype seen in this subtype (137). Human-telomerase reverse transcriptase expression has been described in a number of canine meningioma subtypes; however, has not been evaluated in a prognostic setting (138). Somatostatin receptor-2 expression has recently been described in a variety of canine meningioma subtypes, a finding that is supported by RNAseq data analysis of canine meningioma that revealed increased expression of somatostatin receptors (126, 139). The significance of this finding is unclear; however, similar findings have been noted in a number of human tumors, including meningioma. Folate receptor-α is also overexpressed in canine meningioma, as it is in human meningioma (140).

In depth transcriptome-level analysis of canine meningioma remains in its infancy. Analysis of formalin-fixed, paraffin embedded canine meningioma tissue has proven feasible and yielded significant data to suggest a wide variety of intratumoral abnormalities (126). Underexpressed genes included those associated with tumor suppression and cell adhesion among others (126). Real-time reverse-transcription polymerase chain reaction (RT-PCR) studies do not support significant alterations in *NF2* in the dog compared to human cases (141). Western blot analysis has revealed that dogs have decreased expression of tumor suppressor genes *4.1B* and *TSLC1*; however, additional studies are needed to determine the functional significance of these abnormalities (141). Owing to the relative ease of biopsy sampling for many canine meningiomas, the field is primed to better define the molecular pathogenesis of this common canine tumor.

Like gliomas, histological classification of human meningiomas has had a long history (116). However, microscopic morphology remains the foundation of diagnosis and prognostication of these tumors. Indeed, the 2016 WHO classification included only one addition to its 2007 predecessor: the introduction of brain invasion as an independent diagnostic criterion for atypical (WHO grade II) meningiomas (116). This inclusion has significant implications for its usage in canine meningioma as a significant number of canine meningiomas are invasive even without other atypical features. These tumors continue to be stratified into three histological grades (WHO grade I-III) with increased biological aggressiveness and worse prognosis.

The majority of human meningiomas are benign, slow growing, low grade (WHO grade I) lesions. Nine distinct variants of grade I tumors are recognized histologically: meningothelial, fibrous, transitional, psammomatous, angiomatous, microcystic, secretory, lymphoplasmacyte-rich, and metaplastic meningiomas. All have similar prognosis. WHO grade I meningiomas are distinguished from their benign counterparts on the basis of morphological features or patterns. Atypical meningiomas (WHO grade II) feature one of the nine histological patterns listed above, but also harbor increased mitotic activity (>4 mitoses per 10 high-powered fields), brain invasion, or at least three of the following "soft criteria:" increased cellularity, small cell change, prominent nucleoli, sheeting architecture, or necrotic foci. Two histological variants are also considered WHO grade II: clear cell and chordoid meningiomas. Each of these intermediate grade meningiomas portends an increased risk of recurrence (116). The most malignant meningiomas correspond to WHO grade III. These include anaplastic (malignant) meningiomas, which feature

overtly malignant cytology (resembling carcinoma, melanoma, or sarcoma) or histological patterns of their lower-grade counterparts with significantly increased mitotic activity (>20 mitoses per 10 high-powered fields). Two histological variants are also considered WHO grade III: papillary and rhabdoid meningiomas. Taken together, these tumors constitute 1–3% of all meningiomas and can be rapidly fatal. Extent of surgical resection is the most significant prognostic factor.

The molecular pathogenesis of meningioma in humans is better understood than in the dog. There is an association between patients that have neurofibromatosis type 2 and the development of meningioma due to variable mutations in the *NF2* gene and the subsequent production of a non-functional protein known as merlin (142). Although NF2 clearly illustrates that there are familial inheritance tendencies for meningioma, the majority of meningiomas in humans occur as sporadic tumors. Non-NF2 associated meningiomas are prone to a wide variety of mutations, many of which remain to be discovered. Known mutations in genes including *AKT1, TRRAF7, KLF4*, and *CDKN2A* predispose to meningioma, including high grade meningiomas in the human WHO grading scheme (143).

CHOROID PLEXUS TUMORS

Diagnostic Imaging Features

Choroid plexus tumors are the most common tumors found in an intraventricular location and these tumors types often demonstrate marked contrast enhancement following gadolinium administration (**Figure 3A**) (**Table 1**) (8, 46). Other intraventricular tumors that are occasionally or rarely seen include ependymomas, oligodendrogliomas, primitive neuroectodermal tumors, and central neurocytoma (3, 46, 51). The identification of intraventricular or subarachnoid metastatic tumor implants on MRI studies is a reliable means to clinically discriminate Grade III choroid plexus carcinomas (CPC) from Grade I papillomas (CPP) (8). While MRI is sensitive for the detection of intracranial neoplasms, a normal MRI does not rule out a brain tumor. Lymphomatosis and diffuse glioma (gliomatosis cerebri) are notable for their propensity to be occult on imaging studies of the brain.

Pathologic and Comparative Features

Choroid plexus tumors are intraventricular neoplasms that occur most commonly in the lateral and 4th ventricles, with a decreased incidence in the rest of the ventricular system. Grossly, the tumors are fleshy with a characteristic finely cobblestoned appearance that is gray to tan on section and variably invades the adjacent parenchyma (**Figure 3B**). Secondary hydrocephalus is a common accompanying feature due to obstruction of the ventricular system. Tumors are divided into papilloma, atypical papilloma, and carcinoma; however, the determination between the two can be difficult depending on the section examined and neoplasms with a benign histologic characteristics can nevertheless have parenchymal and distant spread. No accepted canine grading scheme is currently used and therefore tumors are commonly graded by the WHO human choroid plexus tumor criteria. The diagnosis of carcinoma is best based on the presence of desmoplasia, microvascular proliferation (which is rare in choroid plexus carcinomas compared to gliomas), and other overt malignant features like high mitotic rate, marked atypia, and patterned regions of necrosis (144). While vascular invasion and extra-neural spread are not a feature of choroid plexus carcinoma, they will seed throughout the ventricular system where they are associated with carcinomatosis in the cerebral spinal fluid and can cause a mass effect at sites distant from the primary location (145).

Histologically, tumors typically form papillary and frond-like arborizing cords and trabeculae supported by a variably dense fibrovascular stroma (**Figures 3C–E**). Less commonly, areas of more sheet-like growth admixed with pseudorosettes can be found in these tumors (146). Unless invasion into the adjacent parenchyma is present, there are generally few changes in the adjacent tissue and often limited to mild gliosis and edema. Hemorrhage is not typically a feature of this neoplasm. Cells are arranged in simple to multilayered trabeculae with a variable chromatin pattern and typically a single, often inapparent, nucleolus. The mitotic count as determined by histologic examination as well as immunolabeling with Ki67 is highest in carcinomas (144).

While the histologic appearance of these tumors is generally characteristic, they can be mistaken for a metastatic carcinoma on biopsy. Immunohistochemical detection of Kir7.1, an inwardly rectifying potassium channel that has been shown to be a marker for human choroid plexus tumors, will stain the apical portion of neoplastic choroid plexus cells in the dog and can be used as a specific marker to differentiation choroid plexus tumor origin from other carcinomas that may have metastasized to the central nervous system (**Figure 3F**) (147). Pan-cytokeratin (CKAE1/3) expression is diffuse in choroid plexus tumors (148). E-cadherin and β-catenin labeling are commonly observed in canine choroid plexus tumors and can be associated with aberrant cytoplasmic or nuclear localization (149). While E-cadherin labeling does not vary between benign and malignant CPTs, the related protein N-cadherin has been shown to be localized more commonly to choroid plexus papillomas than carcinomas (150). Immunolabeling for glial fibrillary acidic protein (GFAP) has also been recorded in canine CPTs; however, this is not a specific marker of choroid plexus cells (149). Vascular endothelial growth factor (VEGF), platelet-derived growth factor and it associated receptors, PDGFRα, and PDGFRβ exhibit labeling commonly in CPTs regardless of the designation of papilloma or carcinoma (144). Doublecortin labeling has not been recorded in these tumors (150).

The underlying molecular pathology of canine choroid plexus tumors remains poorly understood and an area ripe for further study. In the largest study to date, comparative cytogenic analysis of human and canine choroid plexus tumors revealed chromosomal losses in a number of chromosomes, including regions that included genes for TP53 and (151). Additional studies including regions that encode for tumor suppression and chromosomal instability genes transcriptome analysis of CPTs to normal canine choroid plexus are needed to better elucidate the underlying molecular mechanisms

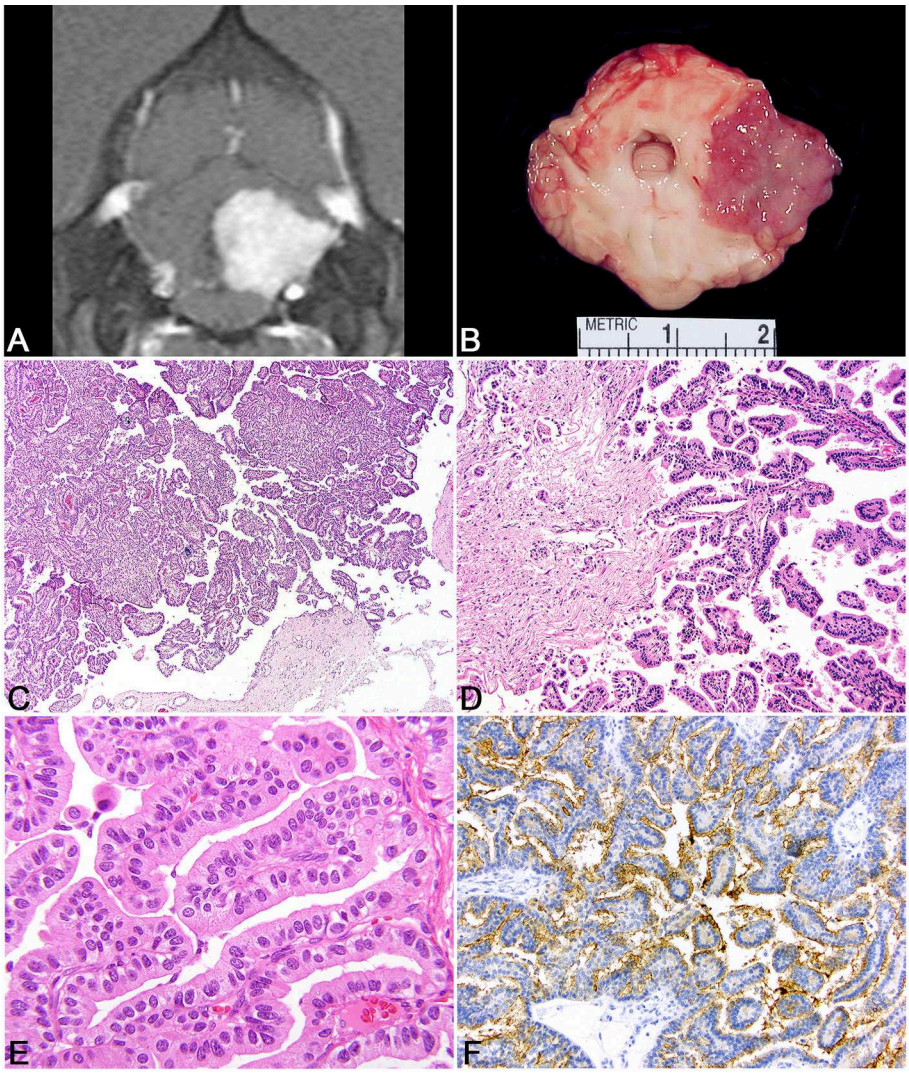

FIGURE 3 | Choroid plexus tumor. **(A)** Canine; MRI. Transverse, post-contrast T1W image demonstrating a uniformly and markedly enhancing, sharply defined mass lesion in the lateral aperture of the 4th ventricle causing compression of the overlying cerebellum. **(B)** Canine, choroid plexus tumor. Corresponding necropsy specimen of **(A)** illustrating a tan, fleshy, slightly granular neoplasm arising at the level of the lateral aperture. **(C)** Canine, choroid plexus tumor. Arborizing trabecular and papillary fronds lined by a single layer of choroid plexus epithelium. Hematoxylin and eosin (HE). **(D)** Canine, Choroid Plexus Carcinoma. Marked invasion into the underlying neuroparenchyma by tubular-like structure of choroid plexus epithelium. HE. **(E)** Human, Choroid Plexus Papilloma. Ribbons, cords, and papillary fronds of choroid plexus epithelium. HE. **(F)** Canine, Choroid Plexus Papilloma. Robust surface immunoreactivity for Kir7.1. Immunohistochemistry (IHC).

of these tumors and their potential as a comparative oncology model.

Choroid plexus tumors are uncommon in humans, although they are most commonly observed in children. As noted above, the histologic criteria are defined based on the WHO classification scheme which divides these tumors into three variants: papilloma, atypical papilloma, and carcinoma. Due to the uncommon nature of these tumors, most human studies concentrate on the histologic and immunohistochemical features of these tumors and genomic analysis is less well characterized although a significant number of choroid plexus carcinomas harbor *TP53* mutations (116).

CONTEMPORARY TREATMENT OF PBT IN VETERINARY MEDICINE

Studies regarding the treatment of canine brain tumors are frequently limited by the inclusion of presumptively diagnosed cases, variable survival definitions and end-points, lack of inclusion of control groups, no reporting of objective imaging-based criteria of therapeutic response or other quantitative follow-up metrics, retrospective study designs, and small case numbers (152–154). Thus, there currently exists a considerable void in the literature with respect to clinically relevant data regarding tumor type-specific therapeutic outcomes for canine

PBT, as well as a lack of adequately powered and rigorously designed trials comparing treatment modalities.

Palliative Care and Watchful Monitoring

The goal of palliative care is to improve the quality of life of patients and their caregivers through the identification, assessment, and treatment of pain and other physical or behavioral manifestations of the brain tumor. The primary pharmacologic palliative therapies administered to brain tumor patients are anticonvulsant drugs (ACD) for tumor-associated structural epilepsy, corticosteroids targeting peritumoral vasogenic edema, and analgesics for signs consistent with somatic, visceral, or neuropathic cancer pain (21, 152, 153). Although seizures are one of the most common clinical signs associated with brain tumors, ideal ACD protocols for the treatment of tumor-associated epilepsy are currently unknown (3, 21). Phenobarbital, levetiracetam, and zonisamide are popular clinical ACD monotherapy choices. Multidrug ACD protocols are frequently needed to control refractory seizures in dogs with PBT, and the aggressiveness and diligence of the clinician's approach to seizure management is often as important to the therapeutic outcome as the patient's tumor response to other treatment modalities.

Animals that have peritumoral vasogenic edema on MRI are more likely to respond favorably to corticosteroid treatment. However, animals without significant edema may benefit also from the anti-inflammatory and euphoric effects of corticosteroids, and corticosteroid therapy alone may also transiently reduce the tumor volume in some cases (21, 152). Corticosteroids may also provide benefit to animals with tumors causing secondary obstructive hydrocephalus, although surgical CSF diversion via placement of an intraventricular shunt is a more effective method of alleviating clinical signs of intracranial hypertension from obstructive hydrocephalus (155). Polyuria, polydipsia, polyphagia, and sedation are commonly anticipated and reported adverse effects of palliative treatment, but palliative therapies are rarely associated with significant morbidity that necessitates discontinuation of therapy (21, 154).

Pain arising from nervous system tumors can arise from compression or stretching of the meninges, nerve roots, or vasculature, tumor-associated meningitis, neuritis, or radiculitis, and tumor infiltration of the periosteum or musculature. Hyperesthesia of the head or neck is occasionally observed in dogs with brain tumors, being reported in 12% of dogs with PBT in one study (3). Clinical signs consistent with pain often respond to corticosteroid treatment, and additional narcotic or neuropathic pain agents can be added as indicated (156).

Up of 6% canine intracranial meningiomas are identified incidentally (3). Given the increasing clinical usage of serial cross-sectional imaging techniques to manage numerous diseases in veterinary medicine, it is likely that the frequency of identification of incidental brain tumors will increase. Objective observation (e.g., watchful monitoring) represents another reasonable approach to the management of some small and asymptomatic brain tumors. Further characterization of the natural disease history for specific brain tumors will be paramount to identifying optimal indications for watchful monitoring, as well as recommended observation intervals and protocols.

Currently, there is no robust data regarding survival associated with palliative care of specific PBT types or grades. When data for all PBT is pooled, the median survival time (MST) following palliative care is ∼9 weeks, with a range of 1–13 weeks (3, 13, 21, 154, 157–159). However, published data does indicate that some dogs with rostrotentorial tumors can experience survivals in excess of 6 months with palliative management (21).

Chemotherapy

Data evaluating the efficacy of systemically administered chemotherapies for the management of brain tumors in dogs is significantly limited by the lack of definitive tumor diagnoses in the vast majority of reported cases, variable dosing regimens, and a preponderance of small case series examining specific drugs (158, 159). The most commonly used chemotherapeutics for brain tumors are the alkylating agents lomustine (CCNU), carmustine (BCNU) and temozolomide (TMZ), or the antimetabolite hydroxyurea, all of which penetrate the blood-brain-barrier (BBB) (158–160). One retrospective study in 71 dogs with presumptively diagnosed brain tumors reported that lomustine treated dogs ($n = 56$, MST 3 months) experienced no survival benefit compared to dogs receiving palliative therapy ($n = 15$, MST 2 months) (158). In another study conducted in dogs with intra-axial mass lesions (presumptively diagnosed gliomas), dogs treated with lomustine ($n = 17$, MST 4.5 months) survived significantly longer than dogs receiving palliative care only ($n = 23$; MST 1 month) (159). In general, the prognosis is poor for dogs with PBT treated with chemotherapy when used as a monotherapy in the setting of gross disease. No difference in survival was also reported between groups of dogs with presumptively diagnosed gliomas treated with stereotactic radiotherapy with ($n = 20$, MST 13.5 months) or without ($n = 22$, MST 12.4 months) TMZ (160).

At the dose intensities reported in the literature, toxicities associated with CCNU, TMZ and hydroxyurea occur commonly but are rarely life-threatening or require discontinuation of therapy in dogs with brain tumors (158–160).

There is mechanistic justification for the investigation of the utility of existing and new classes of drugs for targeted use in canine brain tumors. Non-steroidal anti-inflammatory drugs (NSAIDs), particularly COX-2 selective inhibitors, have numerous potential, but largely unexplored uses for the management of brain tumors. In addition to their use for analgesia, NSAIDs can have antitumor, anti-edema, and immunomodulatory effects in humans and dogs (161, 162). Overexpression of COX-2 has been demonstrated in canine meningiomas, and this overexpression can promote cancer cell proliferation, angiogenesis, and peritumoral edema, reduce apoptosis of neoplastic cells, and decrease antitumor immunity (161–163). As VEGF/VEGFR1/2 and PDGFRa are also overexpressed in a variety of canine PBT, administration of VEGF-targeted antiangiogenic agents, such as bevacizumab, or the receptor tyrosine kinase inhibitors masitinib or toceranib phosphate have potential for therapeutic use in brain tumors (60, 86, 133, 134, 164).

In vitro investigations have demonstrated that responses to chemotherapeutic agents such as bleomycin, carboplatin, CCNU, irinotecan, and TMZ, as well as mechanisms of chemoresistance observed in canine glioma cell lines parallel those seen in human glioma cell lines (93, 165). Thus, it is reasonable to expect that the inclusion of adjuvant chemotherapy in multimodality canine brain tumor treatment protocols could result in modest clinical benefits, as is generally seen in humans. Metronomic chemotherapy with chlorambucil in conjunction with surgical resection is currently being evaluated in an early phase trial in dogs with gliomas (166). The histopathologic and molecular characterization of canine brain tumors and creation of additional of canine patient-derived tumor cell lines will be paramount to efforts necessary to develop and evaluate brain tumor-specific drug protocols, such as high-throughput drug library screening and the identification of biomarkers that predict chemoresponsiveness.

Surgery

Benefits associated with surgical resection of brain tumors include the rapid reduction or elimination of the tumor burden, the secondary beneficial effect this has on reducing ICP, and allowing for definitive histopathological diagnosis of the tumor. Numerous variables complicate critical comparisons of studies evaluating the efficacy surgical treatment of specific tumor types including the experience of the surgeon, availability, or standardized protocols for usage of a growing number of operating room technologies that may facilitate resection, and a nearly universal lack of inclusion of quantifiable surrogates of surgical success, such as surgeon- or imaging-based extent of resection (EOR) assessments (167, 168). Given that attainment of wide excisions of brain tumors are generally not possible for margin evaluation, objective evaluation of EOR is currently dependent on MRI-based assessments, which are associated with practical limitations including the need for anesthesia, expense and difficulties distinguishing residual tumor from surgically induced reactive changes in the acute postoperative period (167, 169).

Outcomes associated with surgical management of canine meningiomas are highly variable, reflective of the previously identified operator and technical factors, in addition to the propensity for all grades of canine meningiomas to locally invade brain tissue (7). Most surgical studies of canine meningiomas have included predominantly superficially located rostrotentorial tumors (170–174). Surgical treatment of basilar, cerebellopontomedulary angle, foramen magnum, parasellar, and tentorial meningiomas is technically challenging and has not been frequently reported (173). When standard cytoreductive surgical techniques are used, the average MST for canine meningiomas is ∼10 months (170–172, 174, 175). Studies describing the use of techniques or technologies that facilitate removal of infiltrative tumor or intraoperative visualization such as cortical resection, usage of an ultrasonic aspirator, or endoscopic assisted resection in canine meningiomas report superior MST (16–70 months) compared to conventional surgical methods (172, 173, 176). Dogs with meningiomas treated surgically also benefit from the addition of adjunctive radiation therapy (RT), as MST associated with multimodal surgery and RT protocols range from 16 and 30 months (130, 171, 177).

There is relatively little data regarding the surgical treatment of other PBT such gliomas and choroid plexus tumors, although a few individual animals with these tumor types experienced prolonged survivals after surgery (8, 152, 157, 178, 179). Surgical treatment of these tumors is infrequently attempted as approaching and removing them is technically demanding due to their intra-axial or intraventricular locations. In addition, as these tumors are poorly delineated and locally invasive, it is inherently more difficult to discriminate the margins of tumor from the neighboring neural tissue. Outcomes in the current literature suggests that surgery should probably not be used as a sole treatment modality for canine gliomas, as MST for rostrotentorial gliomas treated surgically was 2 months (174). MST of ∼6 months have been reported in dogs with gliomas treated surgically in combination with metronomic chemotherapy or immunotherapy (166, 180). Resection of these tumors types is likely to become more common and efficacious with the evolution of brain imaging techniques, intraoperative stereotactic and neuronavigational systems, minimally invasive automated tissue resection devices, and "tumor painting" with fluorophores to assist with intraoperative visualization of tumors (152, 153, 181, 182).

The frequency of significant adverse events associated with surgical treatment of PBT varies widely between individual studies, ranging from 6 and 100% (157, 166, 170–176, 178, 179, 183). Removing the outlier study with 100% perioperative mortality results in an average rate of acute perioperative mortality of ∼11%, although nearly 50% of dogs experience acute adverse effects associated with intracranial surgery in studies that focus on adverse event reporting (154, 179, 183). Common causes of morbidity and early perioperative mortality include aspiration pneumonia, intracranial hemorrhage or infarction, pneumocephalus, medically refractory provoked seizures, transient or permanent neurological disability, electrolyte and osmotic disturbances, and thermoregulatory dysfunction (154, 183).

Radiation Therapy (RT)

RT is beneficial for the treatment of PBT when used as a monotherapy or adjunctive modality. Extrapolating meaningful outcome data from the veterinary brain tumor RT literature associated with specific tumor types in confounded by a general lack of histologically diagnosed tumors included in RT studies, grouping of highly heterogeneous intracranial masses, which sometimes include PBT and SBT in data analyses, and considerable variability in the RT types and dose prescriptions used. RT equipment and techniques have advanced from the early use of orthovoltage RT to current predominantly linear accelerator based options, including advanced forms of intensity-modulated RT (IMRT) such as VMAT and tomotherapy, as well as stereotactic RT (SRT) and stereotactic radiosurgery (SRS) (160, 184).

Cohorts of dogs treated with RT as a sole treatment modality for presumptively diagnosed brain tumors indicate an average survival of ∼16 months, with reported overall MST ranging

from 7 and 24 months when all treated intracranial masses are analyzed (157, 160, 171, 177, 184–191). Some RT studies reported that extra-axial tumors (meningiomas) have a more favorable prognosis than intra-axial (glial) tumors (157, 187, 191). MST associated with RT treatment of extra-axial masses, the majority of which were presumptively diagnosed meningiomas, range from 9 and 30 months, and MST reported for intra-axial masses range from 7.5 and 13 months (33, 157, 160, 171, 177, 184, 186–191). Given the variable outcomes associated with both RT and surgery, there is currently no clearly superior choice between these two modalities when either is used a sole treatment for canine meningiomas (154).

RT also has utility in the adjunctive therapy of canine meningiomas, with combined surgical and RT therapy producing MST of 16–30 months (130, 171, 177). A select number of molecular biomarkers have been evaluated for their prognostic value in dogs with meningiomas treated with surgery and RT. In one study of 17 dogs treated with surgery and adjunctive hypofractionated RT, survival was negatively correlated with VEGF expression (132). The MST was 25 months for dogs with tumors with $\leq$75% cells demonstrating immunoreactivity to VEGF compared with 15 months for dogs with tumors with >75% of cell staining for VEGF, and dogs with tumors demonstrating more intense VEGF immunoreactivity also had a significantly shorter survival time (132). In a study that included 70 dogs with meningiomas treated with surgery and hypofractionated RT, tumor proliferative indices were assessed via MIB-1/Ki67 IHC, and were not associated with survival (134). There was also no association between VEGF and MIB-1/Ki67 expression (134). Progesterone receptor expression has also been shown to be inversely related to the tumor proliferative index (PF_{PCNA} index), which was predictive of survival in dogs with meningiomas after surgery and postoperative RT. The 2-year progression-free survival was 42% for tumors with a PF_{PCNA} index $\geq$24 and 91% for tumors with a PF_{PCNA} index <24% (130).

Approximately 10% of brain tumor cases treated with RT will experience treatment-related mortality or adverse effects (154). Frequently reported adverse effects include aspiration pneumonia, pulmonary thromboembolism, acute CNS toxicity which often manifests as a decreased level of consciousness, damage to at risk organs in the treatment field including deafness, cataract formation, and keratitis, and late-onset radiation necrosis (154). Although significant adverse events associated with SRT and SRS have been uncommonly reported in animals to date, the more frequent use of high-dose per fraction prescriptions may eventually influence the incidence of observed toxicity.

NOVEL THERAPEUTIC APPROACHES

The potential of pet dog dogs with naturally occurring cancers to provide answers to fundamental cancer drug and device development questions that meet a critical and shared need among stakeholders in the cancer research and global healthcare communities is being increasingly realized (192, 193). Translational studies in brain tumor-bearing dogs can provide a variety of safety, pharmacokinetic, mechanistic, toxicity and anti-tumor activity data in an immunocompetent host, and thus offer numerous opportunities to guide the therapeutic development process. The current landscape of comparative veterinary neuro-oncologic research encompasses four primary focus areas: (1) novel, macroscopic tumor targeting, imaging, or CNS delivery techniques, (2) therapeutics molecularly targeting tumor-specific markers or aberrant cellular pathways, (3) immunotherapy, and (4) modifications of the dosing or chemistry of existing or repurposing of therapeutics based on new mechanistic discoveries. Several of these therapeutic approaches have been evaluated in early phase clinical trials in dogs with brain tumors, and numerous others are in the pre-clinical developmental stages.

Macroscopic tumor targeting techniques seek to eliminate of the tumor burden by facilitating gross surgical resection or delivery of ablative energy doses by improving visualization of or sensitizing cancerous tissue, or to overcome therapeutic the drug delivery limitations imposed by the BBB in brain tissue within and surrounding the tumor mass that is visible on imaging studies. The use of intraoperative stereotactic equipment and neuronavigational systems with various tissue resection devices and techniques are being actively investigated for the surgical biopsy and treatment of canine brain tumors (152, 154, 181). The safety and feasibility of stereotactic tumor ablation using lasers and pulsed electrical fields have also been demonstrated in canine brain tumors (194–196). BBB disruptive technologies that allow for CNS drug delivery such as transcranial focused ultrasound and irreversible electroporation are also being used to treat canine brain tumors (195, 197). Convection-enhanced delivery (CED), an approach that bypasses the BBB and allows for direct intratumoral delivery of macromolecular drugs, has been used to evaluate the toxicity and preliminary efficacy of a variety of non-selective and targeted chemotherapeutics, gene therapy, and biodegradable nanomaterial drug carriers in several early phase trials in dogs with brain tumors (152, 153, 197–202). In dogs with intracranial gliomas, studies investigating intratumoral CED of non-selective chemotherapeutics, such as irinotecan (198), and molecularly targeted agents, including EGFRvIII- antibody conjugated magnetic iron oxide nanoparticles (201) and modified bacterial cytotoxins conjugated to IL-13RA2 and EphA2 receptor ligands (197), all have been shown to be capable of inducing significant antitumor effects without major adverse effects.

There is an expanding library of targeted agents being developed for and tested in canine brain tumors, and these agents represent a wide variety of mechanistic approaches including protease-conjugated oncolytic viruses, immunomodulatory microRNAs or small interfering RNAs, immune-checkpoint inhibitors, apoptosis promoters, radiosensitizing agents, and nanoparticular cytotoxic drugs. These compounds have shown promising anti-tumor effects *in vitro* or *in vivo* against non-CNS tumors, the ability to penetrate the BBB when administered systemically, or favorable safety and pharmacokinetic profiles in healthy dogs, and are currently in early phase trials in dogs with tumors (197, 203–206). Proof-of principle studies have demonstrated that both EGFR targeted, doxorubicin loaded minicells (204) and PAC-1, a pro-apoptotic, BBB-penetrant small molecule activator of procaspase-3 are capable of

achieving clinically relevant intratumoral concentrations when administered systemically to dogs with naturally brain tumors (205). The promising pre-clinical safety, pharmacokinetic, and antitumor results from the canine EGFR targeted, doxorubicin minicells study subsequently informed the design of a Phase I clinical trial applying this approach in human recurrent glioblastoma patients (204).

Numerous immunotherapy strategies whose unifying goal is to augment the patient's T-cell mediated immune response against cancer cells are being explored for use in companion animal brain tumors (152, 153). IT approaches that involve tumor vaccinations with stimulated patient-derived dendritic cells and autologous tumor lysates combined with toll-like receptor ligand adjuvants or immune-checkpoint inhibitors have demonstrated the safety, feasibility and potential efficacy of IT for use in canine glioma and meningioma (175, 207–209). In dogs with meningiomas, vaccination with an autologous tumor cell lysate combined with synthetic toll-like receptor ligands after cytoreductive surgery increased survival (median 645 days) compared with surgically treated historic controls (median 222 days), and the vaccine was demonstrated to induce tumor reactive antibodies (175). Extending findings observed in rodent models which demonstrated that administration of a CD200 peptide inhibitor overcomes immune tolerance induced by tumor vaccination by increasing leukocyte infiltration into the vaccine site, bolstering cytokine and chemokine production, and enhancing tumor cytolytic activity, this approach was recently evaluted in dogs with high-grade gliomas (209). In this study, gliomas were treated with cytoreductive surgery followed by intradermal injection of a CD200-directed peptide prior to delivery of an autologous tumor lysate vaccine. Dogs receiving the canine-specific CD200-directed inhibitor and the autologous tumor lysate had significanlty longer survivals (median 12.7 months) compared to a historical control group of dogs treated with surgery and autologous tumor lysate (median 6.4 months).

There are currently two studies that have evaluated modified dosing regimens of existing chemotherapeutics or repurposing of drugs specifically using canine models of brain cancer. One *in vivo* study demonstrated that metronomic chemotherapy with chlorambucil and lomustine in combination of surgical resection of canine gliomas was well tolerated and capable of achieving potentially therapeutic intratumoral drug concentrations (166). An additional *in vitro* study using canine glioma cell lines reported that benzimidazole anthelmintic treatment increased depolymerization of tubulin and glioma cell cytotoxicity compared to the controls (210), suggesting that both mebendazole and fenbendazole may be reasonable drug candidates for the treatment of canine glioma especially given their established safety profiles.

Advancements in the fields of veterinary and comparative neurooncology will require a change in current daily practice paradigms in which the biopsy of individual animal tumors prior to treatment becomes the new standard of care. This will facilitate the routine and systematic characterization of the histomorphologic and molecular features of canine brain cancers, the continuing global comparative genomic analyses of human and veterinary nervous system neoplasms, and the hosting of comprehensively annotated clinicopathological and neuroradiological data registries. These needs have been further recognized by the neurooncology community, and have begun to be addressed by several projects being conducted by the NCI Comparative Brain Tumor Consortium (193, 211). The NCI Comparative Brain Tumor Consortium was the driving force behind the categorization of canine glioma and has recently embarked on a similar goal of redefining the pathologic features of canine meningioma (78). These coordinated efforts are crucial to determining any prognostic relevance of tumor grading, objectively defining the impacts of treatment modalities on clinical outcomes associated with specific tumors, and the rigorous design of clinical trials, especially considering the expanding repertoire of targeted agents available for cancer diagnostics and treatment.

AUTHOR CONTRIBUTIONS

All authors listed have made a substantial, direct and intellectual contribution to the work, and approved it for publication.

REFERENCES

1. Priester WA, Mantel N. Occurrence of tumors in domestic animals. Data from 12 United States and Canadian colleges of veterinary medicine. *J Natl Cancer Inst*. (1971) 47:1333–44.
2. Hayes HM, Priester WA Jr, Pendergrass TW. Occurrence of nervous-tissue tumors in cattle, horses, cats and dogs. *Int J Cancer*. (1975) 15:39–47. doi: 10.1002/ijc.2910150106
3. Snyder JM, Shofer FS, Van Winkle TJ, Massicotte C. Canine intracranial primary neoplasia: 173 cases (1986-2003). *J Vet Intern Med*. (2006) 20:669–75. doi: 10.1111/j.1939-1676.2006.tb02913.x
4. Song RB, Vite CH, Bradley CW, Cross JR. Postmortem evaluation of 435 cases of intracranial neoplasia in dogs and relationship of neoplasm with breed, age, and body weight. *J Vet Intern Med*. (2013) 27:1143–52. doi: 10.1111/jvim.12136
5. Dorn CR, Taylor DO, Frye FL, Hibbard HH. Survey of animal neoplasms in Alameda and Contra Costa Counties, California. I Methodology and description of cases. *J Natl Cancer Inst*. (1968) 40:295–305.
6. Snyder JM, Lipitz L, Skorupski KA, Shofer FS, Van Winkle TJ. Secondary intracranial neoplasia in the dog: 177 cases (1986-2003). *J Vet Intern Med*. (2008) 22:172–7. doi: 10.1111/j.1939-1676.2007.0002.x
7. Sturges BK, Dickinson PJ, Bollen AW, Koblik PD, Kass PH, Kortz GD, et al. Magnetic resonance imaging and histological classification of intracranial meningiomas in 112 dogs. *J Vet Intern Med*. (2008) 22:586–95. doi: 10.1111/j.1939-1676.2008.00042.x
8. Westworth DR, Dickinson PJ, Vernau W, Johnson EG, Bollen AW, Kass PH, et al. Choroid plexus tumors in 56 dogs (1985-2007). *J Vet Intern Med*. (2008) 22:1157–65. doi: 10.1111/j.1939-1676.2008.0170.x
9. Kube SA, Bruyette DS, Hanson SM. Astrocytomas in young dogs. *J Am Anim Hosp Assoc*. (2003) 39:288–93. doi: 10.5326/0390288
10. Truve K, Dickinson P, Xiong A, York D, Jayashankar K, Pielberg G, et al. Utilizing the dog genome in the search for novel candidate genes involved in glioma development-genome wide association mapping followed by targeted massive parallel sequencing identifies a strongly associated locus. *PLoS Genet*. (2016) 12:e1006000. doi: 10.1371/journal.pgen.1006000

11. Rossmeisl JH, Pancotto TE. Intracranial neoplasia and secondary pathological effects. In: Platt S, Garosi L, editors. *Small Animal Neurological Emergencies*. London: Manson Publishing Ltd. (2012). p. 461–78. doi: 10.1201/b15214-30
12. Palmer AC, Malinowski W, Barnett KC. Clinical signs including papilloedema associated with brain tumours in twenty-one dogs. *J Small Anim Pract*. (1974) 15:359–86. doi: 10.1111/j.1748-5827.1974.tb06512.x
13. Foster ES, Carrillo JM, Patnaik AK. Clinical signs of tumors affecting the rostral cerebrum in 43 dogs. *J Vet Intern Med*. (1988) 2:71–4. doi: 10.1111/j.1939-1676.1988.tb02796.x
14. Bagley RS, Gavin PR. Seizures as a complication of brain tumors in dogs. *Clin Tech Small Anim Pract*. (1998) 13:179–84. doi: 10.1016/S1096-2867(98)80039-X
15. Bagley RS, Gavin PR, Moore MP, Silver GM, Harrington ML, Connors RL. Clinical signs associated with brain tumors in dogs: 97 cases (1992-1997). *J Am Vet Med Assoc*. (1999) 215:818–9.
16. Schwartz M, Lamb CR, Brodbelt DC, Volk HA. Canine intracranial neoplasia: clinical risk factors for development of epileptic seizures. *J Small Anim Pract*. (2011) 52:632–7. doi: 10.1111/j.1748-5827.2011.01131.x
17. Menchetti M, De Risio L, Galli G, Bruto Cherubini G, Corlazzoli D, Baroni M, et al. Neurological abnormalities in 97 dogs with detectable pituitary masses. *Vet Q*. (2019) 39:57–64. doi: 10.1080/01652176.2019.1622819
18. Beaumont A, Whittle IR. The pathogenesis of tumour associated epilepsy. *Acta Neurochir*. (2000) 142:1–15. doi: 10.1007/s007010050001
19. Aronica E, Gorter JA, Jansen GH, Leenstra S, Yankaya B, Troost D. Expression of connexin 43 and connexin 32 gap-junction proteins in epilepsy-associated brain tumors and in the perilesional epileptic cortex. *Acta Neuropathol*. (2001) 101:449–59. doi: 10.1007/s004010000305
20. Bartolomei F, Bosma I, Klein M, Baayen JC, Reijneveld JC, Postma TJ, et al. How do brain tumors alter functional connectivity? A magnetoencephalography study. *Ann Neurol*. (2006) 59:128–38. doi: 10.1002/ana.20710
21. Rossmeisl JHJr, Jones JC, Zimmerman KL, Robertson JL. Survival time following hospital discharge in dogs with palliatively treated primary brain tumors. *J Am Vet Med Assoc*. (2013) 242:193–8. doi: 10.2460/javma.242.2.193
22. Wood FD, Pollard RE, Uerling MR, Feldman EC. Diagnostic imaging findings and endocrine test results in dogs with pituitary-dependent hyperadrenocorticism that did or did not have neurologic abnormalities: 157 cases (1989-2005). *J Am Vet Med Assoc*. (2007) 231:1081–5. doi: 10.2460/javma.231.7.1081
23. Koch MW, Sanchez MD, Long S. Multifocal oligodendroglioma in three dogs. *J Am Anim Hosp Assoc*. (2011) 47:e77–85. doi: 10.5326/JAAHA-MS-5551
24. Bentley RT, Burcham GN, Heng HG, Levine JM, Longshore R, Carrera-Justiz S, et al. A comparison of clinical, magnetic resonance imaging and pathological findings in dogs with gliomatosis cerebri, focusing on cases with minimal magnetic resonance imaging changes(double dagger). *Vet Comp Oncol*. (2016) 14:318–30. doi: 10.1111/vco.12106
25. Rossmeisl JH, Clapp K, Pancotto TE, Emch S, Robertson JL, Debinski W. Canine butterfly glioblastomas: a neuroradiological review. *Front Vet Sci*. (2016) 3:40. doi: 10.3389/fvets.2016.00040
26. Lobacz MA, Serra F, Hammond G, Oevermann A, Haley AC. Imaging diagnosis-magnetic resonance imaging of diffuse leptomeningeal oligodendrogliomatosis in a dog with "Dural Tail Sign". *Vet Radiol Ultrasound*. (2018) 59:E1–E6. doi: 10.1111/vru.12441
27. Mcdonnell JJ, Kalbko K, Keating JH, Sato AF, Faissler D. Multiple meningiomas in three dogs. *J Am Anim Hosp Assoc*. (2007) 43:201–8. doi: 10.5326/0430201
28. Stacy BA, Stevenson TL, Lipsitz D, Higgins RJ. Simultaneously occurring oligodendroglioma and meningioma in a dog. *J Vet Intern Med*. (2003) 17:357–9. doi: 10.1111/j.1939-1676.2003.tb02462.x
29. Alves A, Prada J, Almeida JM, Pires I, Queiroga F, Platt SR, et al. Primary and secondary tumours occurring simultaneously in the brain of a dog. *J Small Anim Pract*. (2006) 47:607–10. doi: 10.1111/j.1748-5827.2006.00066.x
30. Patnaik AK, Erlandson RA, Lieberman PH, Fenner WR, Prata RG. Choroid plexus carcinoma with meningeal carcinomatosis in a dog. *Vet Pathol*. (1980) 17:381–5. doi: 10.1177/030098588001700312
31. Bigio Marcello A, Gieger TL, Jimenez DA, Granger LA. Detection of comorbidities and synchronous primary tumours via thoracic radiography and abdominal ultrasonography and their influence on treatment outcome in dogs with soft tissue sarcomas, primary brain tumours and intranasal tumours. *Vet Comp Oncol*. (2015) 13:433–42. doi: 10.1111/vco.12063
32. Tong NM, Zwingenberger AL, Blair WH, Taylor SL, Chen RX, Sturges BK. Effect of screening abdominal ultrasound examination on the decision to pursue advanced diagnostic tests and treatment in dogs with neurologic disease. *J Vet Intern Med*. (2015) 29:893–9. doi: 10.1111/jvim.12602
33. Turrel JM, Fike JR, Lecouteur RA, Higgins RJ. Computed tomographic characteristics of primary brain tumors in 50 dogs. *J Am Vet Med Assoc*. (1986) 188:851–6.
34. Shores A, Warber-Matich S, Cooper TG. The role of magnetic resonance spectroscopy in neuro-oncology. *Semin Vet Med Surg*. (1990) 5:237–40.
35. Wolf M, PedroiaV, Higgins RJ, Koblik PD, Turrel JM, Owens JM. Intracranial ring enhancing lesions in dogs: a correlative CT scanning and neuropathologic study. *Vet Radiol Ultrasound*. (1995) 36:16–20. doi: 10.1111/j.1740-8261.1995.tb00206.x
36. Hathcock J. Low field magnetic resonace imaging characteristics of cranial vault meningiomas in 13 dogs. *Vet Radiol Ultrasound*. (1996) 37:257–63. doi: 10.1111/j.1740-8261.1996.tb01227.x
37. Thomas WB, Wheeler SJ, Kramer R, Kornegay JN. Magnetic resonace imaging features of primary brain tumors in dogs. *Vet Radiol Ultrasound*. (1996) 37:20–7. doi: 10.1111/j.1740-8261.1996.tb00807.x
38. Graham JP, Newell SM, Voges AK, Roberts GD, Harrison JM. The dural tail sign in the diagnosis of meningiomas. *Vet Radiol Ultrasound*. (1998) 39:297–302. doi: 10.1111/j.1740-8261.1998.tb01609.x
39. Polizopoulou ZS, Koutinas AF, Souftas VD, Kaldrymidou E, Kazakos G, Papadopoulos G. Diagnostic correlation of CT-MRI and histopathology in 10 dogs with brain neoplasms. *J Vet Med A Physiol Pathol Clin Med*. (2004) 51:226–31. doi: 10.1111/j.1439-0442.2004.00633.x
40. Cherubini GB, Mantis P, Martinez TA, Lamb CR, Cappello R. Utility of magnetic resonance imaging for distinguishing neoplastic from non-neoplastic brain lesions in dogs and cats. *Vet Radiol Ultrasound*. (2005) 46:384–7. doi: 10.1111/j.1740-8261.2005.00069.x
41. Macleod AG, Dickinson PJ, Lecouteur RA, Higgins RJ, Pollard RE. Quantitative assessment of blood volume and permeability in cerebral mass lesions using dynamic contrast-enhanced computed tomography in the dog. *Acad Radiol*. (2009) 16:1187–95. doi: 10.1016/j.acra.2009.03.015
42. Zhao Q, Lee S, Kent M, Schatzberg S, Platt S. Dynamic contrast-enhanced magnetic resonance imaging of canine brain tumors. *Vet Radiol Ultrasound*. (2010) 51:122–9. doi: 10.1111/j.1740-8261.2009.01635.x
43. Cervera V, Mai W, Vite CH, Johnson V, Dayrell-Hart B, Seiler GS. Comparative magnetic resonance imaging findings between gliomas and presumed cerebrovascular accidents in dogs. *Vet Radiol Ultrasound*. (2011) 52:33–40. doi: 10.1111/j.1740-8261.2010.01749.x
44. Rodenas S, Pumarola M, Gaitero L, Zamora A, Anor S. Magnetic resonance imaging findings in 40 dogs with histologically confirmed intracranial tumours. *Vet J*. (2011) 187:85–91. doi: 10.1016/j.tvjl.2009.10.011
45. Sutherland-Smith J, King R, Faissler D, Ruthazer R, Sato A. Magnetic resonance imaging apparent diffusion coefficients for histologically confirmed intracranial lesions in dogs. *Vet Radiol Ultrasound*. (2011) 52:142–8. doi: 10.1111/j.1740-8261.2010.01764.x
46. Wisner ER, Dickinson PJ, Higgins RJ. Magnetic resonance imaging features of canine intracranial neoplasia. *Vet Radiol Ultrasound*. (2011) 52:S52–61. doi: 10.1111/j.1740-8261.2010.01785.x
47. Young BD, Levine JM, Porter BF, Chen-Allen AV, Rossmeisl JH, Platt SR, et al. Magnetic resonance imaging features of intracranial astrocytomas and oligodendrogliomas in dogs. *Vet Radiol Ultrasound*. (2011) 52:132–41. doi: 10.1111/j.1740-8261.2010.01758.x
48. Martin-Vaquero P, Da Costa RC, Echandi RL, Sammet CL, Knopp MV, Sammet S. Magnetic resonance spectroscopy of the canine brain at 3.0 T and 7.0 T. *Res Vet Sci*. (2012) 93:427–9. doi: 10.1016/j.rvsc.2011.07.025
49. Wolff CA, Holmes SP, Young BD, Chen AV, Kent M, Platt SR, et al. Magnetic resonance imaging for the differentiation of neoplastic, inflammatory, and cerebrovascular brain disease in dogs. *J Vet Intern Med*. (2012) 26:589–97. doi: 10.1111/j.1939-1676.2012.00899.x

50. Bentley RT, Ober CP, Anderson KL, Feeney DA, Naughton JF, Ohlfest JR, et al. Canine intracranial gliomas: relationship between magnetic resonance imaging criteria and tumor type and grade. *Vet J*. (2013) 198:463–71. doi: 10.1016/j.tvjl.2013.08.015
51. Bentley RT. Magnetic resonance imaging diagnosis of brain tumors in dogs. *Vet J*. (2015) 205:204–16. doi: 10.1016/j.tvjl.2015.01.025
52. Banzato T, Bernardini M, Cherubini GB, Zotti A. Texture analysis of magnetic resonance images to predict histologic grade of meningiomas in dogs. *Am J Vet Res*. (2017) 78:1156–62. doi: 10.2460/ajvr.78.10.1156
53. Stadler KL, Pease AP, Ballegeer EA. Dynamic susceptibility contrast magnetic resonance imaging protocol of the normal canine brain. *Front Vet Sci*. (2017) 4:41. doi: 10.3389/fvets.2017.00041
54. Bailey CS, Higgins RJ. Characteristics of cisternal cerebrospinal fluid associated with primary brain tumors in the dog: a retrospective study. *J Am Vet Med Assoc*. (1986) 188:414–7.
55. Dickinson PJ, Sturges BK, Kass PH, Lecouteur RA. Characteristics of cisternal cerebrospinal fluid associated with intracranial meningiomas in dogs: 56 cases (1985-2004). *J Am Vet Med Assoc*. (2006) 228:564–7. doi: 10.2460/javma.228.4.564
56. Bohn AA, Wills TB, West CL, Tucker RL, Bagley RS. Cerebrospinal fluid analysis and magnetic resonance imaging in the diagnosis of neurologic disease in dogs: a retrospective study. *Vet Clin Pathol*. (2006) 35:315–20. doi: 10.1111/j.1939-165X.2006.tb00138.x
57. Tzipory L, Vernau KM, Sturges BK, Zabka TS, Highland MA, Petersen SA, et al. Antemortem diagnosis of localized central nervous system histiocytic sarcoma in 2 dogs. *J Vet Intern Med*. (2009) 23:369–74. doi: 10.1111/j.1939-1676.2008.0264.x
58. Palus V, Volk HA, Lamb CR, Targett MP, Cherubini GB. MRI features of CNS lymphoma in dogs and cats. *Vet Radiol Ultrasound*. (2012) 53:44–9. doi: 10.1111/j.1740-8261.2011.01872.x
59. Platt SR, Marlin D, Smith N, Adams V. Increased cerebrospinal fluid uric acid concentrations in dogs with intracranial meningioma. *Vet Rec*. (2006) 158:830. doi: 10.1136/vr.158.24.830
60. Rossmeisl JH, Duncan RB, Huckle WR, Troy GC. Expression of vascular endothelial growth factor in tumors and plasma from dogs with primary intracranial neoplasms. *Am J Vet Res*. (2007) 68:1239–45. doi: 10.2460/ajvr.68.11.1239
61. Turba ME, Forni M, Gandini G, Gentilini F. Recruited leukocytes and local synthesis account for increased matrix metalloproteinase-9 activity in cerebrospinal fluid of dogs with central nervous system neoplasm. *J Neurooncol*. (2007) 81:123–9. doi: 10.1007/s11060-006-9213-2
62. De La Fuente C, Monreal L, Ceron J, Pastor J, Viu J, Anor S. Fibrinolytic activity in cerebrospinal fluid of dogs with different neurological disorders. *J Vet Intern Med*. (2012) 26:1365–73. doi: 10.1111/j.1939-1676.2012.00991.x
63. Mariani CL, Boozer LB, Braxton AM, Platt SR, Vernau KM, Mcdonnell JJ, et al. Evaluation of matrix metalloproteinase-2 and−9 in the cerebrospinal fluid of dogs with intracranial tumors. *Am J Vet Res*. (2013) 74:122–9. doi: 10.2460/ajvr.74.1.122
64. Miyake H, Inoue A, Tanaka M, Matsuki N. Serum glial fibrillary acidic protein as a specific marker for necrotizing meningoencephalitis in Pug dogs. *J Vet Med Sci*. (2013) 75:1543–5. doi: 10.1292/jvms.13-0252
65. Utsugi S, Azuma K, Osaki T, Murahata Y, Tsuka T, Ito N, et al. Analysis of plasma free amino acid profiles in canine brain tumors. *Biomed Rep*. (2017) 6:195–200. doi: 10.3892/br.2016.825
66. Li C-F, Mellema M, Carney R, Sturges B, York D, Liu R, et al. Exosome-associated integrins as liquid biopsy biomarkers for canine glioma. *J Vet Intern Med*. (2017) 31:1261.
67. Lake BB, Rossmeisl JH, Cecere J, Stafford P, Zimmerman KL. Immunosignature differentiation of non-infectious meningoencephalomyelitis and intracranial neoplasia in dogs. *Front Vet Sci*. (2018) 5:97. doi: 10.3389/fvets.2018.00097
68. Harari JM, Leathers MM, Roberts CW, Gavin PR. Computed tomographic-guided, free-hand needle biopsy of brain tumors in dogs. *Prog Vet Neurol*. (1993) 4:41–44.
69. Koblik PD, Lecouteur RA, Higgins RJ, Bollen AW, Vernau KM, Kortz GD, et al. CT-guided brain biopsy using a modified Pelorus Mark III stereotactic system: experience with 50 dogs. *Vet Radiol Ultrasound*. (1999) 40:434–40. doi: 10.1111/j.1740-8261.1999.tb00371.x
70. Moissonnier P, Blot S, Devauchelle P, Delisle F, Beuvon F, Boulha L, et al. Stereotactic CT-guided brain biopsy in the dog. *J Small Anim Pract*. (2002) 43:115–23. doi: 10.1111/j.1748-5827.2002.tb00041.x
71. Klopp LS, Ridgway M. Use of an endoscope in minimally invasive lesion biopsy and removal within the skull and cranial vault in two dogs and one cat. *J Am Vet Med Assoc*. (2009) 234:1573–7. doi: 10.2460/javma.234.12.1573
72. Rossmeisl JH, Andriani RT, Cecere TE, Lahmers K, Leroith T, Zimmerman KL, et al. Frame-based stereotactic biopsy of canine brain masses: technique and clinical results in 26 cases. *Front Vet Sci*. (2015) 2:20. doi: 10.3389/fvets.2015.00020
73. Sidhu DS, Ruth JD, Lambert G, Rossmeisl JH. An easy to produce and economical three-dimensional brain phantom for stereotactic computed tomographic-guided brain biopsy training in the dog. *Vet Surg*. (2017) 46:621–30. doi: 10.1111/vsu.12657
74. Kani Y, Cecere TE, Lahmers K, Leroith T, Zimmerman KL, Isom S, et al. Diagnostic accuracy of stereotactic brain biopsy for intracranial neoplasia in dogs: comparison of biopsy, surgical resection, and necropsy specimens. *J Vet Intern Med*. (2019) 33:1384–91. doi: 10.1111/jvim.15500
75. Stadler KL, Ruth JD, Pancotto TE, Werre SR, Rossmeisl JH. Computed tomography and magnetic resonance imaging are equivalent in mensuration and similarly inaccurate in grade and type predictability of canine intracranial gliomas. *Front Vet Sci*. (2017) 4:157. doi: 10.3389/fvets.2017.00157
76. Stadler KL, Ober CP, Feeney DA, Jessen CR. Multivoxel proton magnetic resonance spectroscopy of inflammatory and neoplastic lesions of the canine brain at 3.0 T. *Am J Vet Res*. (2014) 75:982–9. doi: 10.2460/ajvr.75.11.982
77. Rissi DR, Levine JM, Eden KB, Watson VE, Griffin JFT, Edwards JF, et al. Cerebral oligodendroglioma mimicking intraventricular neoplasia in three dogs. *J Vet Diagn Invest*. (2015) 27:396–400. doi: 10.1177/1040638715584619
78. Koehler JW, Miller AD, Miller CR, Porter B, Aldape K, Beck J, et al. A revised diagnostic classification of canine glioma: towards validation of the canine glioma patient as a naturally occurring preclinical model for human glioma. *J Neuropathol Exp Neurol*. (2018) 77:1039–54. doi: 10.1093/jnen/nly085
79. Nakamoto Y, Fukunaga D, Uchida K, Mori T, Kishimoto T, Ozawa T. Anaplastic oligodendroglioma with leptomeningeal dissemination in a french bulldog. *J Vet Med Sci*. (2018) 80:1590–5. doi: 10.1292/jvms.17-0652
80. Recio A, De La Fuente C, Pumarola M, Espada Y, Anor S. Magnetic resonance imaging and computed tomographic characteristics of a glioma causing calvarial erosion in a dog. *Vet Radiol Ultrasound*. (2019) 60:E1–5. doi: 10.1111/vru.12506
81. Koestner A, Bilzer T, Fatzer R, Schulman FY, Summers BA, Van Winkle TJ. *Histological Classification of Tumors of the Nervous System of Domestic Animals*. Washington, DC: Armed Forces Institute of Pathology (1999).
82. Rissi DR, Barber R, Burnum A, Miller AD. Canine spinal cord glioma. *J Vet Diagn Invest*. (2017) 29:126–32. doi: 10.1177/1040638716673127
83. Stoica G, Kim HT, Hall DG, Coates JR. Morphology, immunohistochemistry, and genetic alterations in dog astrocytomas. *Vet Pathol*. (2004) 41:10–9. doi: 10.1354/vp.41-1-10
84. Lipsitz D, Higgins RJ, Kortz GD, Dickinson PJ, Bollen AW, Naydan DK, et al. Glioblastoma multiforme: clinical findings, magnetic resonance imaging, and pathology in five dogs. *Vet Pathol*. (2003) 40:659–69. doi: 10.1354/vp.40-6-659
85. Kishimoto TE, Uchida K, Thongtharb A, Shibato T, Chambers JK, Nibe K, et al. Expression of oligodendrocyte precursor cell markers in canine oligodendrogliomas. *Vet Pathol*. (2018) 55:634–44. doi: 10.1177/0300985818777794
86. Higgins RJ, Dickinson PJ, Lecouteur RA, Bollen AW, Wang H, Wang H, et al. Spontaneous canine gliomas: overexpression of EGFR, PDGFRalpha and IGFBP2 demonstrated by tissue microarray immunophenotyping. *J Neurooncol*. (2010) 98:49–55. doi: 10.1007/s11060-009-0072-5
87. Fraser AR, Bacci B, Le Chevoir MA, Long SN. Epidermal growth factor receptor and Ki-67 expression in canine gliomas. *Vet Pathol*. (2016) 53:1131–7. doi: 10.1177/0300985816644301
88. Jankovsky JM, Newkirk KM, Ilha MR, Newman SJ. COX-2 and c-kit expression in canine gliomas. *Vet Comp Oncol*. (2013) 11:63–9. doi: 10.1111/j.1476-5829.2011.00302.x

89. Fraser AR, Bacci B, Le Chevoir MA, Long SN. Isocitrate dehydrogenase 1 expression in canine gliomas. *J Comp Pathol*. (2018) 165:33–9. doi: 10.1016/j.jcpa.2018.09.005
90. Sloma EA, Creneti CT, Erb HN, Miller AD. Characterization of inflammatory changes associated with canine oligodendroglioma. *J Comp Pathol*. (2015) 153:92–100. doi: 10.1016/j.jcpa.2015.05.003
91. Filley A, Henriquez M, Bhowmik T, Tewari BN, Rao X, Wan J, et al. Immunologic and gene expression profiles of spontaneous canine oligodendrogliomas. *J Neurooncol*. (2018) 137:469–79. doi: 10.1007/s11060-018-2753-4
92. Herranz C, Fernandez F, Martin-Ibanez R, Blasco E, Crespo E, De La Fuente C, et al. Spontaneously arising canine glioma as a potential model for human glioma. *J Comp Pathol*. (2016) 154:169–79. doi: 10.1016/j.jcpa.2015.12.001
93. Boudreau CE, York D, Higgins RJ, Lecouteur RA, Dickinson PJ. Molecular signalling pathways in canine gliomas. *Vet Comp Oncol*. (2017) 15:133–50. doi: 10.1111/vco.12147
94. Amin S, Boudreau B, Martinez-Ledesma JE, Anderson K, Kim H, Johnson K, et al. Comparative molecular life history of spontaneous canine and human glioma. *Neuro Oncol*. (2018) 20:vi64–65. doi: 10.1093/neuonc/noy148.262
95. Amin S, Martinez-Ledesma JE, Boudreau B, Kim H, Johnson KC, Dickinson PV, et al. Genomic profiling of canine glioma: comparative analyses with respect to drivers of human glioma. *Cancer Res*. (2018) 78:1176. doi: 10.1158/1538-7445.AM2018-1176
96. Dickinson PJ, York D, Higgins RJ, Lecouteur RA, Joshi N, Bannasch D. Chromosomal aberrations in canine gliomas define candidate genes and common pathways in dogs and humans. *J Neuropathol Exp Neurol*. (2016) 75:700–10. doi: 10.1093/jnen/nlw042
97. Connolly NP, Shetty AC, Stokum JA, Hoeschele I, Siegel MB, Miller CR, et al. Cross-species transcriptional analysis reveals conserved and host-specific neoplastic processes in mammalian glioma. *Sci Rep*. (2018) 8:1180. doi: 10.1038/s41598-018-19451-6
98. Miller CR, Perry A. Glioblastoma. *Arch Pathol Lab Med*. (2007) 131:397–406. doi: 10.1043/1543-2165(2007)131[397:G]2.0.CO;2
99. Coons SW, Johnson PC, Scheithauer BW, Yates AJ, Pearl DK. Improving diagnostic accuracy and interobserver concordance in the classification and grading of primary gliomas. *Cancer*. (1997) 79:1381–93.
100. Van Den Bent MJ. Interobserver variation of the histopathological diagnosis in clinical trials on glioma: a clinician's perspective. *Acta Neuropathol*. (2010) 120:297–304. doi: 10.1007/s00401-010-0725-7
101. Burger PC. What is an oligodendroglioma? *Brain Pathol*. (2002) 12:257–9. doi: 10.1111/j.1750-3639.2002.tb00440.x
102. Sahm F, Reuss D, Koelsche C, Capper D, Schittenhelm J, Heim S, et al. Farewell to oligoastrocytoma: in situ molecular genetics favor classification as either oligodendroglioma or astrocytoma. *Acta Neuropathol*. (2014) 128:551–9. doi: 10.1007/s00401-014-1326-7
103. Phillips HS, Kharbanda S, Chen R, Forrest WF, Soriano RH, Wu TD, et al. Molecular subclasses of high-grade glioma predict prognosis, delineate a pattern of disease progression, and resemble stages in neurogenesis. *Cancer Cell*. (2006) 9:157–73. doi: 10.1016/j.ccr.2006.02.019
104. Vitucci M, Hayes DN, Miller CR. Gene expression profiling of gliomas: merging genomic and histopathological classification for personalised therapy. *Br J Cancer*. (2011) 104:545–53. doi: 10.1038/sj.bjc.6606031
105. Parsons DW, Jones S, Zhang X, Lin JC, Leary RJ, Angenendt P, et al. An integrated genomic analysis of human glioblastoma multiforme. *Science*. (2008) 321:1807–12. doi: 10.1126/science.1164382
106. Yan H, Parsons DW, Jin G, Mclendon R, Rasheed BA, Yuan W, et al. IDH1 and IDH2 mutations in gliomas. *N Engl J Med*. (2009) 360:765–73. doi: 10.1056/NEJMoa0808710
107. Smith JS, Alderete B, Minn Y, Borell TJ, Perry A, Mohapatra G, et al. Localization of common deletion regions on 1p and 19q in human gliomas and their association with histological subtype. *Oncogene*. (1999) 18:4144–52. 10.1038/sj.onc.1202759 doi: 10.1038/sj.onc.1202759
108. Jenkins RB, Blair H, Ballman KV, Giannini C, Arusell RM, Law M, et al. A t(1;19)(q10;p10) mediates the combined deletions of 1p and 19q and predicts a better prognosis of patients with oligodendroglioma. *Cancer Res*. (2006) 66:9852–61. doi: 10.1158/0008-5472.CAN-06-1796
109. Eckel-Passow JE, Lachance DH, Molinaro AM, Walsh KM, Decker PA, Sicotte H, et al. Glioma groups based on 1p/19q, IDH, and TERT promoter mutations in tumors. *N Engl J Med*. (2015) 372:2499–508. doi: 10.1056/NEJMoa1407279
110. Cancer Genome Atlas Research N, Brat DJ, Verhaak RG, Aldape KD, Yung WK, Salama SR, et al. Comprehensive, integrative genomic analysis of diffuse lower-grade gliomas. *N Engl J Med*. (2015) 372:2481–98. doi: 10.1056/NEJMoa1402121
111. Bettegowda C, Agrawal N, Jiao Y, Sausen M, Wood LD, Hruban RH, et al. Mutations in CIC and FUBP1 contribute to human oligodendroglioma. *Science*. (2011) 333:1453–5. doi: 10.1126/science.1210557
112. Wiestler B, Capper D, Sill M, Jones DT, Hovestadt V, Sturm D, et al. Integrated DNA methylation and copy-number profiling identify three clinically and biologically relevant groups of anaplastic glioma. *Acta Neuropathol*. (2014) 128:561–71. doi: 10.1007/s00401-014-1315-x
113. Suzuki H, Aoki K, Chiba K, Sato Y, Shiozawa Y, Shiraishi Y, et al. Mutational landscape and clonal architecture in grade II and III gliomas. *Nat Genet*. (2015) 47:458–68. doi: 10.1038/ng.3273
114. Aibaidula A, Chan AK, Shi Z, Li Y, Zhang R, Yang R, et al. Adult IDH wild-type lower-grade gliomas should be further stratified. *Neuro Oncol*. (2017) 19:1327–37. doi: 10.1093/neuonc/nox078
115. Ceccarelli M, Barthel FP, Malta TM, Sabedot TS, Salama SR, Murray BA, et al. Molecular profiling reveals biologically discrete subsets and pathways of progression in diffuse glioma. *Cell*. (2016) 164:550–63. doi: 10.1016/j.cell.2015.12.028
116. Louis DN, Perry A, Reifenberger G, Von Deimling A, Figarella-Branger D, Cavenee WK, et al. The 2016 world health organization classification of tumors of the central nervous system: a summary. *Acta Neuropathol*. (2016) 131:803–20. doi: 10.1007/s00401-016-1545-1
117. Rissi DR. A retrospective study of skull base neoplasia in 42 dogs. *J Vet Diagn Invest*. (2015) 27:743–8. doi: 10.1177/1040638715611706
118. Schulman FY, Ribas JL, Carpenter JL, Sisson AF, Lecouteur RA. Intracranial meningioma with pulmonary metastasis in three dogs. *Vet Pathol*. (1992) 29:196–202. doi: 10.1177/030098589202900302
119. Montoliu P, Anor S, Vidal E, Pumarola M. Histological and immunohistochemical study of 30 cases of canine meningioma. *J Comp Pathol*. (2006) 135:200–7. doi: 10.1016/j.jcpa.2006.06.006
120. Salvadori C, Pintore MD, Ricci E, Konar M, Tartarelli CL, Gasparinetti N, et al. Microcystic meningioma of the fourth ventricle in a dog. *J Vet Med Sci*. (2011) 73:367–70. doi: 10.1292/jvms.10-0337
121. Takeuchi Y, Ohnishi Y, Matsunaga S, Nakayama H, Uetsuka K. Intracranial meningioma with polygonal granular cell appearance in a Chihuahua. *J Vet Med Sci*. (2008) 70:529–32. 10.1292/jvms.70.529
122. Mandara MT, Reginato A, Foiani G, Baroni M, Poli F, Gasparinetti N, et al. Papillary meningioma in the dog: a clinicopathological case series study. *Res Vet Sci*. (2015) 100:213–9. doi: 10.1016/j.rvsc.2015.03.029
123. Schoniger S, Woolford L, Jutras L, Head E, De Lahunta A, Summers BA. Unusual features in four canine meningiomas. *J Comp Pathol*. (2013) 149:237–41. doi: 10.1016/j.jcpa.2013.03.003
124. Boozer LB, Davis TW, Borst LB, Zseltvay KM, Olby NJ, Mariani CL. Characterization of immune cell infiltration into canine intracranial meningiomas. *Vet Pathol*. (2012) 49:784–95. doi: 10.1177/0300985811417249
125. Al-Nadaf S, Platt SR, Kent M, Northrup N, Howerth EW. Minimal interleukin expression in canine intracranial meningiomas. *Vet Rec*. (2015) 177:75. doi: 10.1136/vr.103135
126. Grenier JK, Foureman PA, Sloma EA, Miller AD. RNA-seq transcriptome analysis of formalin fixed, paraffin-embedded canine meningioma. *PLoS ONE*. (2017) 12:e0187150. doi: 10.1371/journal.pone.0187150
127. Ramos-Vara JA, Miller MA, Gilbreath E, Patterson JS. Immunohistochemical detection of CD34, E-cadherin, claudin-1, glucose transporter 1, laminin, and protein gene product 9.5 in 28 canine and 8 feline meningiomas. *Vet Pathol*. (2010) 47:725–37. doi: 10.1177/0300985810364528
128. Johnson GC, Coates JR, Wininger F. Diagnostic immunohistochemistry of canine and feline intracalvarial tumors in the age of brain biopsies. *Vet Pathol*. (2014) 51:146–60. doi: 10.1177/0300985813509387
129. Ide T, Uchida K, Suzuki K, Kagawa Y, Nakayama H. Expression of cell adhesion molecules and doublecortin in canine anaplastic meningiomas. *Vet Pathol*. (2011) 48:292–301. doi: 10.1177/0300985810389312
130. Theon AP, Lecouteur RA, Carr EA, Griffey SM. Influence of tumor cell proliferation and sex-hormone receptors on effectiveness of radiation

therapy for dogs with incompletely resected meningiomas. *J Am Vet Med Assoc*. (2000) 216:701–707:684–705. doi: 10.2460/javma.2000.216.701
131. Mandara MT, Ricci G, Rinaldi L, Sarli G, Vitellozzi G. Immunohistochemical identification and image analysis quantification of oestrogen and progesterone receptors in canine and feline meningioma. *J Comp Pathol*. (2002) 127:214–8. doi: 10.1053/jcpa.2002.0572
132. Platt SR, Scase TJ, Adams V, Wieczorek L, Miller J, Adamo F, et al. Vascular endothelial growth factor expression in canine intracranial meningiomas and association with patient survival. *J Vet Intern Med*. (2006) 20:663–8. doi: 10.1111/j.1939-1676.2006.tb02912.x
133. Dickinson PJ, Sturges BK, Higgins RJ, Roberts BN, Leutenegger CM, Bollen AW, et al. Vascular endothelial growth factor mRNA expression and peritumoral edema in canine primary central nervous system tumors. *Vet Pathol*. (2008) 45:131–9. doi: 10.1354/vp.45-2-131
134. Matiasek LA, Platt SR, Adams V, Scase TJ, Keys D, Miller J, et al. Ki-67 and vascular endothelial growth factor expression in intracranial meningiomas in dogs. *J Vet Intern Med*. (2009) 23:146–51. doi: 10.1111/j.1939-1676.2008.0235.x
135. Mandara MT, Pavone S, Mandrioli L, Bettini G, Falzone C, Baroni M. Matrix metalloproteinase-2 and matrix metalloproteinase-9 expression in canine and feline meningioma. *Vet Pathol*. (2009) 46:836–45. doi: 10.1354/vp.08-VP-0185-M-FL
136. Beltran E, Matiasek K, De Risio L, De Stefani A, Feliu-Pascual AL, Matiasek LA. Expression of MMP-2 and MMP-9 in benign canine rostrotentorial meningiomas is not correlated to the extent of peritumoral edema. *Vet Pathol*. (2013) 50:1091–8. doi: 10.1177/0300985813481610
137. Mandara MT, Reginato A, Foiani G, De Luca S, Guelfi G. Gene expression of matrix metalloproteinases and their inhibitors (TIMPs) in meningiomas of dogs. *J Vet Intern Med*. (2017) 31:1816–21. doi: 10.1111/jvim.14809
138. Mandrioli L, Panarese S, Cesari A, Mandara MT, Marcato PS, Bettini G. Immunohistochemical expression of h-telomerase reverse transcriptase in canine and feline meningiomas. *J Vet Sci*. (2007) 8:111–5. doi: 10.4142/jvs.2007.8.2.111
139. Foiani G, Guelfi G, Chiaradia E, Mancini F, Trivelli C, Vitellozzi G, et al. Somatostatin receptor 2 expression in canine meningioma. *J Comp Pathol*. (2019) 166:59–68. doi: 10.1016/j.jcpa.2018.11.002
140. Pierce JT, Cho SS, Nag S, Zeh R, Jeon J, Holt D, et al. Folate receptor overexpression in human and canine meningiomas-immunohistochemistry and case report of intraoperative molecular imaging. *Neurosurgery*. (2018) 85:359–68. doi: 10.1093/neuros/nyy356
141. Dickinson PJ, Surace EI, Cambell M, Higgins RJ, Leutenegger CM, Bollen AW, et al. Expression of the tumor suppressor genes NF2:4.1B, and TSLC1 in canine meningiomas. *Vet Pathol*. (2009) 46:884–92. doi: 10.1354/vp.08-VP-0251-D-FL
142. Coy S, Rashid R, Stemmer-Rachamimov A, Santagata S. An update on the CNS manifestations of neurofibromatosis type 2. *Acta Neuropathol*. (2019) 1–23. doi: 10.1007/s00401-019-02029-5. [Epub ahead of print].
143. Hao S, Huang G, Feng J, Li D, Wang K, Wang L, et al. Non-NF2 mutations have a key effect on inhibitory immune checkpoints and tumor pathogenesis in skull base meningiomas. *J Neurooncol*. (2019) 144:11–20. doi: 10.1007/s11060-019-03198-9
144. Muscatello LV, Avallone G, Serra F, Seuberlich T, Mandara MT, Siso S, et al. Glomeruloid microvascular proliferation, desmoplasia, and high proliferative index as potential indicators of high grade canine choroid plexus tumors. *Vet Pathol*. (2018) 55:391–401. doi: 10.1177/0300985817754124
145. Pastorello A, Constantino-Casas F, Archer J. Choroid plexus carcinoma cells in the cerebrospinal fluid of a staffordshire bull terrier. *Vet Clin Pathol*. (2010) 39:505–10. doi: 10.1111/j.1939-165X.2010.00270.x
146. Miller AD, Koehler JW, Donovan TA, Stewart JE, Porter BF, Rissi DR, et al. Canine ependymoma: diagnostic criteria and common pitfalls. *Vet Pathol*. (2019) 56:860–7. doi: 10.1177/0300985819859872
147. Choi EJ, Sloma EA, Miller AD. Kir7.1 immunoreactivity in canine choroid plexus tumors. *J Vet Diagn Invest*. (2016) 28:464–8. doi: 10.1177/1040638716650239
148. Ide T, Uchida K, Kikuta F, Suzuki K, Nakayama H. Immunohistochemical characterization of canine neuroepithelial tumors. *Vet Pathol*. (2010) 47:741–50. doi: 10.1177/0300985810363486
149. Nentwig A, Higgins RJ, Francey T, Doherr M, Zurbriggen A, Oevermann A. Aberrant E-cadherin, beta-catenin, and glial fibrillary acidic protein (GFAP) expression in canine choroid plexus tumors. *J Vet Diagn Invest*. (2012) 24:14–22. doi: 10.1177/1040638711425940
150. Reginato A, Girolami D, Menchetti L, Foiani G, Mandara MT. E-cadherin, N-cadherin expression and histologic characterization of canine choroid plexus tumors. *Vet Pathol*. (2016) 53:788–91. doi: 10.1177/0300985815620844
151. Ancona D, York D, Higgins RJ, Bannasch D, Dickinson PJ. Comparative cytogenetic analysis of dog and human choroid plexus tumors defines syntenic regions of genomic loss. *J Neuropathol Exp Neurol*. (2018) 77:413–9. doi: 10.1093/jnen/nly020
152. Dickinson PJ. Advances in diagnostic and treatment modalities for intracranial tumors. *J Vet Intern Med*. (2014) 28:1165–85. doi: 10.1111/jvim.12370
153. Rossmeisl J. New treatment modalities for brain tumors in dogs and cats. *Vet Clin North Am Small Anim Pract*. (2014) 44:1013–38. doi: 10.1016/j.cvsm.2014.07.003
154. Hu H, Barker A, Harcourt-Brown T, Jeffery N. Systematic review of brain tumor treatment in dogs. *J Vet Intern Med*. (2015) 29:1456–63. doi: 10.1111/jvim.13617
155. De Stefani A, De Risio L, Platt SR, Matiasek L, Lujan-Feliu-Pascual A, Garosi LS. Surgical technique, postoperative complications and outcome in 14 dogs treated for hydrocephalus by ventriculoperitoneal shunting. *Vet Surg*. (2011) 40:183–91. doi: 10.1111/j.1532-950X.2010.00764.x
156. Moore SA. Managing neuropathic pain in dogs. *Front Vet Sci*. (2016) 3:12. doi: 10.3389/fvets.2016.00012
157. Heidner GL, Kornegay JN, Page RL, Dodge RK, Thrall DE. Analysis of survival in a retrospective study of 86 dogs with brain tumors. *J Vet Intern Med*. (1991) 5:219–26. doi: 10.1111/j.1939-1676.1991.tb00952.x
158. Van Meervenne S, Verhoeven PS, De Vos J, Gielen IM, Polis I, Van Ham LM. Comparison between symptomatic treatment and lomustine supplementation in 71 dogs with intracranial, space-occupying lesions. *Vet Comp Oncol*. (2014) 12:67–77. doi: 10.1111/j.1476-5829.2012.00336.x
159. Moirano SJ, Dewey CW, Wright KZ, Cohen PW. Survival times in dogs with presumptive intracranial gliomas treated with oral lomustine: a comparative retrospective study (2008-2017). *Vet Comp Oncol*. (2018) 16:459–66. doi: 10.1111/vco.12401
160. Dolera M, Malfassi L, Bianchi C, Carrara N, Finesso S, Marcarini S, et al. Frameless stereotactic radiotherapy alone and combined with temozolomide for presumed canine gliomas. *Vet Comp Oncol*. (2018) 16:90–101. doi: 10.1111/vco.12316
161. Mohammed SI, Craig BA, Mutsaers AJ, Glickman NW, Snyder PW, Degortari AE, et al. Effects of the cyclooxygenase inhibitor, piroxicam, in combination with chemotherapy on tumor response, apoptosis, and angiogenesis in a canine model of human invasive urinary bladder cancer. *Mol Cancer Ther*. (2003) 2:183–8.
162. Roth P, Regli L, Tonder M, Weller M. Tumor-associated edema in brain cancer patients: pathogenesis and management. *Expert Rev Anticancer Ther*. (2013) 13:1319–25. doi: 10.1586/14737140.2013.852473
163. Rossmeisl JH Jr, Robertson JL, Zimmerman KL, Higgins MA, Geiger DA. Cyclooxygenase-2 (COX-2) expression in canine intracranial meningiomas. *Vet Comp Oncol*. (2009) 7:173–80. doi: 10.1111/j.1476-5829.2009.00188.x
164. Dickinson PJ, Roberts BN, Higgins RJ, Leutenegger CM, Bollen AW, Kass PH, et al. Expression of receptor tyrosine kinases VEGFR-1 (FLT-1), VEGFR-2 (KDR), EGFR-1, PDGFRalpha and c-Met in canine primary brain tumours. *Vet Comp Oncol*. (2006) 4:132–40. doi: 10.1111/j.1476-5829.2006.00101.x
165. Neal RE II, Rossmeisl JH Jr, D'alfonso V, Robertson JL, Garcia PA, Elankumaran S, Davalos RV. *In vitro* and numerical support for combinatorial irreversible electroporation and electrochemotherapy glioma treatment. *Ann Biomed Eng*. (2014) 42:475–87. doi: 10.1007/s10439-013-0923-2
166. Bentley RT, Thomovsky SA, Miller MA, Knapp DW, Cohen-Gadol AA. Canine (Pet Dog) tumor microsurgery and intratumoral concentration and safety of metronomic chlorambucil for spontaneous glioma: a phase i clinical trial. *World Neurosurg*. (2018) 116:e534–42. doi: 10.1016/j.wneu.2018.05.027
167. Rossmeisl JH Jr, Garcia PA, Daniel GB, Bourland JD, Debinski W, Dervisis N, et al. Invited review–neuroimaging response assessment criteria for brain

tumors in veterinary patients. *Vet Radiol Ultrasound*. (2014) 55:115–32. doi: 10.1111/vru.12118
168. Nanda A, Bir SC, Maiti TK, Konar SK, Missios S, Guthikonda B. Relevance of Simpson grading system and recurrence-free survival after surgery for World Health Organization Grade I meningioma. *J Neurosurg*. (2017) 126:201–11. doi: 10.3171/2016.1.JNS151842
169. Chow KE, Tyrrell D, Long SN. Early postoperative magnetic resonance imaging findings in five dogs with confirmed and suspected brain tumors. *Vet Radiol Ultrasound*. (2015) 56:531–9. doi: 10.1111/vru.12248
170. Kostolich M, Dulisch ML. A surgical approach to the canine olfactory bulb for meningioma removal. *Vet Surg*. (1987) 16:273–7. doi: 10.1111/j.1532-950X.1987.tb00952.x
171. Axlund TW, Mcglasson ML, Smith AN. Surgery alone or in combination with radiation therapy for treatment of intracranial meningiomas in dogs: 31 cases (1989-2002). *J Am Vet Med Assoc*. (2002) 221:1597–600. doi: 10.2460/javma.2002.221.1597
172. Rossmeisl J. Craniectomy for the treatment of canine meningiomas. In: *Proceedings of the American College of Veterinary Surgery Symposium*. Washington, DC. (2003).
173. Klopp LS, Rao S. Endoscopic-assisted intracranial tumor removal in dogs and cats: long-term outcome of 39 cases. *J Vet Intern Med*. (2009) 23:108–15. doi: 10.1111/j.1939-1676.2008.0234.x
174. Sunol A, Mascort J, Font C, Bastante AR, Pumarola M, Feliu-Pascual AL. Long-term follow-up of surgical resection alone for primary intracranial rostrotentorial tumors in dogs: 29 cases (2002-2013). *Open Vet J*. (2017) 7:375–83. doi: 10.4314/ovj.v7i4.14
175. Andersen BM, Pluhar GE, Seiler CE, Goulart MR, Santacruz KS, Schutten MM, et al. Vaccination for invasive canine meningioma induces in situ production of antibodies capable of antibody-dependent cell-mediated cytotoxicity. *Cancer Res*. (2013) 73:2987–97. doi: 10.1158/0008-5472.CAN-12-3366
176. Greco JJ, Aiken SA, Berg JM, Monette S, Bergman PJ. Evaluation of intracranial meningioma resection with a surgical aspirator in dogs: 17 cases (1996-2004). *J Am Vet Med Assoc*. (2006) 229:394–400. doi: 10.2460/javma.229.3.394
177. Keyerleber MA, Mcentee MC, Farrelly J, Thompson MS, Scrivani PV, Dewey CW. Three-dimensional conformal radiation therapy alone or in combination with surgery for treatment of canine intracranial meningiomas. *Vet Comp Oncol*. (2015) 13:385–97. doi: 10.1111/vco.12054
178. Thankey K, Faissler D, Kavirayani A, Keating JH, Mcdonnell JJ. Clinical presentation and outcome in dogs with histologically confirmed choroid plexus papillomas. *J Vet Intern Med*. (2006) 20:782–3.
179. Marino DJ, Dewey CW, Loughin CA, Marino LJ. Severe hyperthermia, hypernatremia, and early postoperative death after transethmoidal cavitron ultrasonic surgical aspirator (CUSA)-assisted diencephalic mass removal in 4 dogs and 2 cats. *Vet Surg*. (2014) 43:888–94. doi: 10.1111/j.1532-950X.2014.12238.x
180. Maclellan JD, Arnold SA, Dave AC, Hunt MA, Pluhar GE. Association of magnetic resonance imaging-based preoperative tumor volume with postsurgical survival time in dogs with primary intracranial glioma. *J Am Vet Med Assoc*. (2018) 252:98–102. doi: 10.2460/javma.252.1.98
181. Packer R, Engel S. Onscreen-guided brain tumor resection through registration of a variable-suction tissue resection device with a neuronavigation system. *J Vet Intern Med*. (2015) 29:1264.
182. Nakano Y, Nakata K, Shibata S, Heishima Y, Nishida H, Sakai H, et al. Fluorescein sodium-guided resection of intracranial lesions in 22 dogs. *Vet Surg*. (2018) 47:302–9. doi: 10.1111/vsu.12763
183. Forward AK, Volk HA, De Decker S. Postoperative survival and early complications after intracranial surgery in dogs. *Vet Surg*. (2018) 47:549–54. doi: 10.1111/vsu.12785
184. Lester NV, Hopkins AL, Bova FJ, Friedman WA, Buatti JM, Meeks SL, et al. Radiosurgery using a stereotactic headframe system for irradiation of brain tumors in dogs. *J Am Vet Med Assoc*. (2001) 219:1562–7:1550. doi: 10.2460/javma.2001.219.1562
185. Turrel JM, Fike JR, Lecouteur RA, Pflugfelder CM, Borcich JK. Radiotherapy of brain tumors in dogs. *J Am Vet Med Assoc*. (1984) 184:82–6.
186. Evans SM, Dayrell-Hart B, Powlis W, Christy G, Vanwinkle T. Radiation therapy of canine brain masses. *J Vet Intern Med*. (1993) 7:216–9. doi: 10.1111/j.1939-1676.1993.tb01010.x
187. Brearley MJ, Jeffery ND, Phillips SM, Dennis R. Hypofractionated radiation therapy of brain masses in dogs: a retrospective analysis of survival of 83 cases (1991-1996). *J Vet Intern Med*. (1999) 13:408–12. doi: 10.1111/j.1939-1676.1999.tb01454.x
188. Spugnini EP, Thrall DE, Price GS, Sharp NJ, Munana K, Page RL. Primary irradiation of canine intracranial masses. *Vet Radiol Ultrasound*. (2000) 41:377–80. doi: 10.1111/j.1740-8261.2000.tb02091.x
189. Bley CR, Sumova A, Roos M, Kaser-Hotz B. Irradiation of brain tumors in dogs with neurologic disease. *J Vet Intern Med*. (2005) 19:849–54. doi: 10.1111/j.1939-1676.2005.tb02776.x
190. Mariani CL, Schubert TA, House RA, Wong MA, Hopkins AL, Barnes Heller HL, et al. Frameless stereotactic radiosurgery for the treatment of primary intracranial tumours in dogs. *Vet Comp Oncol*. (2015) 13:409–23. doi: 10.1111/vco.12056
191. Schwarz P, Meier V, Soukup A, Drees R, Besserer J, Beckmann K, et al. Comparative evaluation of a novel, moderately hypofractionated radiation protocol in 56 dogs with symptomatic intracranial neoplasia. *J Vet Intern Med*. (2018) 32:2013–20. doi: 10.1111/jvim.15324
192. Khanna C, London C, Vail D, Mazcko C, Hirschfeld S. Guiding the optimal translation of new cancer treatments from canine to human cancer patients. *Clin Cancer Res*. (2009) 15:5671–7. doi: 10.1158/1078-0432.CCR-09-0719
193. Leblanc AK, Mazcko C, Brown DE, Koehler JW, Miller AD, Miller CR, et al. Creation of an NCI comparative brain tumor consortium: informing the translation of new knowledge from canine to human brain tumor patients. *Neuro Oncol*. (2016) 18:1209–18. doi: 10.1093/neuonc/now051
194. Schwartz JA, Shetty AM, Price RE, Stafford RJ, Wang JC, Uthamanthil RK, et al. Feasibility study of particle-assisted laser ablation of brain tumors in orthotopic canine model. *Cancer Res*. (2009) 69:1659–67. doi: 10.1158/0008-5472.CAN-08-2535
195. Rossmeisl JH Jr, Garcia PA, Pancotto TE, Robertson JL, Henao-Guerrero N, Neal RE II, Ellis TL, et al. Safety and feasibility of the NanoKnife system for irreversible electroporation ablative treatment of canine spontaneous intracranial gliomas. *J Neurosurg*. (2015) 123:1008–25. doi: 10.3171/2014.12.JNS141768
196. Latouche EL, Arena CB, Ivey JW, Garcia PA, Pancotto TE, Pavlisko N, et al. High-frequency irreversible electroporation for intracranial meningioma: a feasibility study in a spontaneous canine tumor model. *Technol Cancer Res Treat*. (2018) 17:1533033818785285. doi: 10.1177/1533033818785285
197. Rossmeisl JH, Herpai D, Robertson JL, Dickinson PJ, Tatter SB, Debinksi W. Tolerability and intial efficacy of convection-enhanced delivery of combinatorial IL-12RA2 and EphA2 targeted cytotoxins to dogs with spontaneous intracranial malignant gliomas. *Neuro Oncol*. (2017) 19:iii56. doi: 10.1093/neuonc/nox036.202
198. 198. Dickinson PJ, Lecouteur RA, Higgins RJ, Bringas JR, Larson RF, Yamashita Y, et al. Canine spontaneous glioma: a translational model system for convection-enhanced delivery. *Neuro Oncol*. (2010) 12:928–40. doi: 10.1093/neuonc/noq046
199. Robbins JM, Dickinson PJ, York D, Sturges BK, Martin B, Higgins RJ, et al. Evaluation of delivery of retroviral replicating vector, TOCA 511, in spontaneous canine brain tumor. *Neuro Oncol*. (2012) 14:vi48.
200. Rossmeisl JH, Hall-Manning K, Robertson JL, King JN, Davalos RV, Debinski W, et al. Expression and activity of the urokinase plasminogen activator system in canine primary brain tumors. *Onco Targets Ther*. (2017) 10:2077–85. doi: 10.2147/OTT.S132964
201. Freeman AC, Platt SR, Holmes S, Kent M, Robinson K, Howerth E, et al. Convection-enhanced delivery of cetuximab conjugated iron-oxide nanoparticles for treatment of spontaneous canine intracranial gliomas. *J Neurooncol*. (2018) 137:653–63. doi: 10.1007/s11060-018-2764-1
202. Young JS, Bernal G, Polster SP, Nunez L, Larsen GF, Mansour N, et al. Convection-enhanced delivery of polymeric nanoparticles encapsulating chemotherapy in canines with spontaneous supratentorial tumors. *World Neurosurg*. (2018) 117:e698–704. doi: 10.1016/j.wneu.2018.06.114

203. Kent M, Leung P, Dickinson P, Sturges B, Ng S, Bedard C, et al. Use of the novel oxygen carrier protein, ZOX, in dogs with intracranial masses. *J Vet Intern Med*. (2016) 30:1530.
204. Macdiarmid JA, Langova V, Bailey D, Pattison ST, Pattison SL, Christensen N, et al. Targeted doxorubicin delivery to brain tumors via minicells: proof of principle using dogs with spontaneously occurring tumors as a model. *PLoS ONE*. (2016) 11:e0151832. doi: 10.1371/journal.pone.0151832
205. Joshi AD, Botham RC, Schlein LJ, Roth HS, Mangraviti A, Borodovsky A, et al. Synergistic and targeted therapy with a procaspase-3 activator and temozolomide extends survival in glioma rodent models and is feasible for the treatment of canine malignant glioma patients. *Oncotarget*. (2017) 8:80124–38. doi: 10.18632/oncotarget.19085
206. Yaghi NK, Wei J, Hashimoto Y, Kong LY, Gabrusiewicz K, Nduom EK, et al. Immune modulatory nanoparticle therapeutics for intracerebral glioma. *Neuro Oncol*. (2017) 19:372–82. doi: 10.1093/neuonc/now198
207. Pluhar GE, Grogan PT, Seiler C, Goulart M, Santacruz KS, Carlson C, et al. Anti-tumor immune response correlates with neurological symptoms in a dog with spontaneous astrocytoma treated by gene and vaccine therapy. *Vaccine*. (2010) 28:3371–8. doi: 10.1016/j.vaccine.2010.02.082
208. Xiong W, Candolfi M, Liu C, Muhammad AK, Yagiz K, Puntel M, et al. Human Flt3L generates dendritic cells from canine peripheral blood precursors: implications for a dog glioma clinical trial. *PLoS ONE*. (2010) 5:e11074. doi: 10.1371/journal.pone.0011074
209. Olin MR, Ampudia-Mesias E, Pennell CA, Sarver A, Chen CC, Moertel CL, et al. Treatment combining CD200 immune checkpoint inhibitor and tumor-lysate vaccination after surgery for pet dogs with high-grade glioma. *Cancers*. (2019) 11:137. doi: 10.3390/cancers11020137
210. Lai SR, Castello SA, Robinson AC, Koehler JW. *In vitro* anti-tubulin effects of mebendazole and fenbendazole on canine glioma cells. *Vet Comp Oncol*. (2017) 15:1445–54. doi: 10.1111/vco.12288
211. Rossmeisl J. Maximizing local access to therapeutic deliveries in glioblastoma. Part V: Clinically relevant model for testing new therapeutic approaches. In: DeVlesschouwer S, editor. *Glioblastoma*. Brisbane, AU: Codon Publications. (2017) 21:405–25. doi: 10.15586/codon.glioblastoma.2017.ch21

Conflict of Interest: The authors declare that the research was conducted in the absence of any commercial or financial relationships that could be construed as a potential conflict of interest.

The reviewer MRC declared a shared affiliation, with no collaboration, with one of the authors, CRM, to the handling editor at time of review.

Copyright © 2019 Miller, Miller and Rossmeisl. This is an open-access article distributed under the terms of the Creative Commons Attribution License (CC BY). The use, distribution or reproduction in other forums is permitted, provided the original author(s) and the copyright owner(s) are credited and that the original publication in this journal is cited, in accordance with accepted academic practice. No use, distribution or reproduction is permitted which does not comply with these terms.

frontiers in Oncology

REVIEW
published: 15 November 2019
doi: 10.3389/fonc.2019.01257

Canine Cancer: Strategies in Experimental Therapeutics

Douglas H. Thamm [1,2,3]*

[1] Flint Animal Cancer Center, Colorado State University, Fort Collins, CO, United States, [2] Cell and Molecular Biology Graduate Program, Colorado State University, Fort Collins, CO, United States, [3] University of Colorado Cancer Center, Anschutz Medical Campus, Aurora, CO, United States

Cancer is the most common cause of death in adult dogs. Many features of spontaneously developing tumors in pet dogs contribute to their potential utility as a human disease model. These include similar environmental exposures, similar clonal evolution as it applies to important factors such as immune avoidance, a favorable body size for imaging and serial biopsy, and a relatively contracted time course of disease progression, which makes evaluation of temporal endpoints such as progression free or overall survival feasible in a comparatively short time frame. These criteria have been leveraged to evaluate novel local therapies, demonstrate proof of tumor target inhibition or tumor localization, evaluate potential antimetastatic approaches, and assess the efficacy, safety and immune effects of a variety of immune-based therapeutics. Some of these canine proof of concept studies have been instrumental in informing subsequent human clinical trials. This review will cover key aspects of clinical trials in dogs with spontaneous neoplasia, with examples of how these studies have contributed to human cancer therapeutic development.

Keywords: dog, tumor, clinical trial, translational, animal model

OPEN ACCESS

Edited by:
Mark W. Dewhirst,
Duke University, United States

Reviewed by:
Terence S. Herman,
University of Oklahoma Health Sciences Center, United States
Allison B. Warner,
Memorial Sloan Kettering Cancer Center, United States
Amy LeBlanc,
National Cancer Institute (NCI), United States

***Correspondence:**
Douglas H. Thamm
dthamm@colostate.edu

Specialty section:
This article was submitted to Cancer Molecular Targets and Therapeutics, a section of the journal Frontiers in Oncology

Received: *31 July 2019*
Accepted: *31 October 2019*
Published: *15 November 2019*

Citation:
Thamm DH (2019) Canine Cancer: Strategies in Experimental Therapeutics. Front. Oncol. 9:1257. doi: 10.3389/fonc.2019.01257

INTRODUCTION

Common concerns with regard to the clinical applicability of many murine models of human cancer include immune status, significantly reduced clonal heterogeneity, relative tumor burden, tumor location (orthotopic vs. heterotopic), species-specific differences in drug distribution/metabolism, and differences in *in vivo* drug concentrations that are achievable, among others. These contribute to the observation of extremely poor correlation between results of murine studies and early human clinical trials with anticancer agents (1). More predictive animal models are clearly needed.

More than 1 million new cases of cancer are thought to occur in dogs each year in the United States, and in retrospective studies describing canine mortality, cancer is the most common cause of death with an estimated rate of ∼30% (2–4). This large cancer burden in dogs indicates a group of spontaneously occurring tumors, many of which are histologically similar to human tumors. Commonly encountered histotypes include non-Hodgkin lymphoma, malignant melanoma, osteosarcoma (OSA), bladder carcinoma, and multiple brain cancer types among others (2, 5). Client-owned dogs with cancer are being increasingly recognized as a resource for preclinical interrogation of the tolerability, pharmacology, pharmacodynamic effects, and potential efficacy of novel anticancer therapies. This model's potential was discussed in a National Academy of Medicine Workshop on Comparative Oncology that occurred in 2015 (http://www.nap.edu/21830) (6).

Clinical trials in client-owned dogs with spontaneous cancer are potentially important translational models, owing to dogs' relative outbreeding, large size, immunocompetence, and physiological/biological similarity to humans. Spontaneous canine tumors naturally develop treatment resistance, as well as spontaneous recurrence and metastasis. Absolute tumor burdens in dogs are more similar to humans, which may be informative with regard to biological factors such as clonal heterogeneity and hypoxia. The comparatively large size of canine tumors (vs. rodent tumors) also allows for serial tissue collection and imaging over time (2, 7). This is due partly to the fact that these patients are commonly sedated or anesthetized for procedures, moderating concerns over patient discomfort. While clinical case management and data collection are of very high quality, the relative cost of veterinary oncology clinical trials are 10–20% of what similar trials in physician-based oncology would be.

Dogs may also be more reliable models for assessing toxicity of novel therapies than are rodents. As in human patients, canine patients are monitored for hematologic and biochemical toxicities via routine clinical pathology, and sophisticated monitoring (e.g., 24 hour continuous electrocardiographic telemetry, continuous blood pressure measurement, ophthalmologic monitoring, echocardiography, gait analysis, advanced imaging) can be performed as-needed. Unlike in laboratory settings, supportive care (e.g., antiemetics, antidiarrheals, antibiotics, etc.) is also used in client-owned animals similarly to its employment in human patients. Universally accepted grading systems for adverse events from antineoplastic therapy (8, 9), as well as universally accepted tumor response criteria (10, 11), are published.

The Comparative Oncology Trials Consortium (COTC: https://ccr.cancer.gov/Comparative-Oncology-Program/sponsors/consortium) is a network of more than 20 academic veterinary oncology centers, centrally managed by the Comparative Oncology Program, housed within the NIH-NCI-Center for Cancer Research. Its central goal is to plan and perform clinical trials in dogs with cancer to evaluated novel potential therapies for human cancer, with the goal of answering biological questions to inform development for future human clinical trials. COTC sponsored trials are usually pharmacokinetically/pharmacodynamically intensive, with the results incorporated into the design of future human studies. The launch of this network has improved the ability of potential sponsors and collaborators to access a national cooperative group for the conduct of proof of concept studies in dogs. Potential sponsors work with COTC management to iteratively develop a clinical protocol to address a specific drug development question/questions, which is then put out to the membership for potential participation. COTC sites have the opportunity to participate or decline based on capacity, specialized equipment/techniques that may be required, and/or competing trials at the institution. Trial conduct is governed by a single memorandum of understanding between the participating sites, which streamlines the contractual process.

These important attributes have allowed the preclinical evaluation of novel cancer therapeutics that fall into several broad categories: (1) Local therapy approaches such as surgery, radiation therapy and locally-delivered drug therapy; (2) Proof of target inhibition and proof of tumor targeting; (3) Studies in the minimal residual disease setting; (4) Immunotherapy studies.

LOCAL THERAPY APPROACHES

As a result of dogs' comparatively large body size and the relative size of their tumors, tumor-bearing dogs can be a unique and informative model for the evaluation of novel local therapies. Surgical and radiation therapy (RT) related studies can utilize the same techniques and equipment as would be used in human patients, without the need for the significant adaptation or miniaturization which could be required for rodents. As stated above, the comparatively similar size and growth rate of dog tumors results in similarities in important microenvironmental parameters such as oxygenation, pH, and interstitial fluid pressure (12–18), and the large tumor size facilitates serial biopsy and measurement of intratumoral parameters over time. As a result, tumor-bearing dogs have been utilized in translational studies of novel surgical approaches, RT, hyperthermia, and regionally-delivered drug therapy.

Translational Surgical Studies

National Cancer Institute sponsored work by Withrow et al. in the 1980's pioneered surgical protocols for cortical allografts for limb-salvage in bone sarcoma patients. These procedures were co-developed by veterinary and human surgical oncologists and refined in a large number of dogs with spontaneous OSA, mostly of the distal radius. Effects of neoadjuvant RT and chemotherapy on surgical outcome and allograft incorporation were also assessed (19–21). These observations and subsequent refinements developed in dogs led directly to the use of these approaches in human limb-sparing surgery (22). An observation was made regarding the postoperative development of bacterial osteomyelitis and improved metastasis-free and overall survival times in dogs (23). This was subsequently observed in at least one study of humans with OSA (24). Further study of this observation in a murine syngeneic OSA model suggested NK- and monocyte-mediated angiogenesis inhibition as a putative mechanism of action (25).

Radiation Therapy

Studies of radiation by Gillette et al. in the 1970's and 1980's in both normal and tumor-bearing dogs established many normal tissue RT dose constraints still in use today in human patients (19, 26–37). More recently, studies in tumor-bearing dogs provided critical proof of concept for accurate dosimetry and conformal avoidance during the development of helical tomotherapy, a slice-by-slice image-guided intensity modulated RT strategy that is now commercially available (38, 39).

Translational Studies of Hyperthermia and Radiation Therapy

A substantial body of literature documents pioneering NCI-funded work by Dewhirst et al. evaluating the effects of hyperthermia and hyperthermia/RT combinations on the tumor microenvironment in canine tumors, especially soft-tissue

sarcomas. As a result of their common subcutaneous location and the relative ease with which procedures such as serial biopsy and interstitial probe placement can be performed, meaningful insights into thermal dosimetry, alterations in tumor perfusion and tumor oxygenation, and predictors of clinical response were identified (36, 40–42).

Locally/Regionally Delivered Therapeutics

Multiple studies of inhaled/pulmonary delivered therapeutics have evaluated safety and provided preliminary evidence of antitumor efficacy in support of human trials. These include evaluation of inhaled doxorubicin, paclitaxel and gemcitabine for the treatment of measurable primary or metastatic pulmonary tumors (43, 44), and nebulized inhaled interleukin-2 (IL-2) containing liposomes for treatment of pulmonary metastatic OSA (45). In addition to the observed objective antitumor responses, the latter study included serially collected bronchoalveolar lavage (BAL) fluid to characterize the local leukocyte population before and after IL-2 therapy. Post-IL-2 BAL samples contained a more than four-fold increase in lymphocytes, with a shifted CD4:CD8 ratio and increased cytolytic activity *ex vivo* (45).

Various intratumor treatments have been evaluated in tumor-bearing dog models. These include attenuated *Clostridium* spores (46), and various intralesional gene therapy approaches (47–50). In many of these studies, serial biopsy was performed to evaluate and characterize immune infiltrates and/or confirm transgene expression. Several novel intralesional chemotherapy approaches (± other local treatments such as RT or hyperthermia) have likewise been evaluated, demonstrating tolerability and preliminary evidence of efficacy (50–55).

PROOF OF TARGET INHIBITION OR PROOF OF TUMOR TARGETING/ACCUMULATION

Owing again to the relative ease of serial biopsy, as well as comparably favorable pharmacokinetic parameters in dogs such as organ-specific blood flow and hepatic enzyme homologies, canine tumors can serve as very useful translational models for evaluation of pharmacokinetic/pharmacodynamic (PK/PD) relationships, demonstration of target inhibition, and/or demonstration of tumor targeting. In these cases, substantial preliminary *in vitro* work is often necessary to confirm target expression, demonstrate similar drug behavior in canine and human tumor cells, and potentially validate reagents and protocols necessary for PD assessment. Importantly, there are certain situations where molecular targets may be present in canine tumors that are histologically very different from human tumors expressing the same target. Examples include expression of mutant KIT protein in canine mast cell tumors (MCT) with a similar mutation expressed in human gastrointestinal stromal tumors (56), and expression of the V600E BRAF mutation, commonly expressed in human melanomas, in canine bladder cancer (57, 58).

Proof of Drug Target Inhibition

An early example of successful evaluation of a novel targeted agent in dogs with spontaneous neoplasia involves the preclinical evaluation of the "split kinase" inhibitor SU11654 (toceranib phosphate, Palladia™), in dogs with MCT. SU11654 is a structural analog of the human multi-kinase inhibitor sunitinib (Sutent™) with very similar physicochemical properties and IC50's against their intended targets, which include KIT, VEGFR2 and PDGFR-alpha. After initial *in vitro* studies demonstrating canine MCT growth inhibition, apoptosis induction and inhibition of KIT phosphorylation (59), pilot studies were performed in tumor-bearing dogs demonstrating achievement of likely therapeutic drug concentrations in plasma with good tolerability and evidence of antitumor activity (60). Furthermore, inhibition of KIT activation and downstream signaling was demonstrated in biopsy samples prior to and 8 h following the first dose of drug (61). These data provided critical information in support of the human development of sunitinib, which is now approved by the U.S. Food and Drug Administration (FDA) for human renal cell carcinoma, pancreatic neuroendocrine tumors, and gastrointestinal stromal tumors, and led to the FDA approval of toceranib for the treatment of canine MCT (62).

A similar "next to lead" approach has been taken with the selective inhibitor of nuclear export verdinexor (KPT-335), which was evaluated *in vitro* for activity in canine tumor cells, then in tumor-bearing dogs to provide supporting data for development of the human analog selinexor (KPT-330, Xpovio™) (63), now approved by the FDA for the treatment of human multiple myeloma. Verdinexor is now in clinical development as a canine cancer therapeutic.

Rather than evaluating a structural analog to generate preclinical data in tumor-bearing dogs in support of a human clinical candidate, another recent study evaluated PCI-32765 (ibrutinib, Imbruvica™), a first-in-class inhibitor of the Bruton tyrosine kinase (Btk), in dogs with spontaneous B-cell lymphoma prior to first-in-in-human studies (64). Goals of the study were 2-fold: (1) To validate a PD assay to be used in subsequent human trials; (2) To generate preliminary evidence of efficacy, since reliable murine B-cell lymphoma models demonstrating intact B cell receptor signaling were not available. Btk receptor occupancy following ibrutinib treatment was similar in lymphoma tissue and peripheral blood following treatment, providing support that measurement in blood alone would likely be accurate in humans. Furthermore, major antitumor responses were observed in three of eight dogs treated, providing strong impetus to accelerate human clinical development of ibrutinib. Ibrutinib now has FDA approval in humans for the treatment of certain B cell lymphoma subtypes, chronic lymphocytic leukemia, Waldenstrom's macroglobulinemia and graft-vs.-host disease.

Proof of Tumor Targeting

Canine tumors have been utilized to confirm tumor-specific targeting and/or tumor accumulation of therapeutics. The inaugural COTC trial evaluated a tumor vasculature targeted adeno-associated virus phage vector targeted to alphaV integrins expressed on tumor endothelium and delivering tumor necrosis factor (TNF), in preparation

for human trials. Selective targeting of tumor (vs. normal) vasculature was documented through serial biopsy of tumor and proximate normal tissues after intravenous infusion, and tumor-directed expression of TNF was documented. Furthermore, objective antitumor responses were noted in 2 of 14 dogs (65).

Certain bacteria, especially facultative anaerobes, demonstrate tropism for tumor tissues. VNP20009 is a *Salmonella typhimurium* strain that was attenuated through deletion of the *MsbB* gene, contributing to endotoxin production, and the PurI gene, requiring an exogenous source of purines for survival. These deletions reduce toxicity and further restrict colonization to tumor tissues *in vivo,* while diminishing or eliminating survival in the environment. Intravenous infusion of VNP20009 was evaluated in tumor-bearing dogs for safety and evidence of tumor colonization (66). While blood cultures were uniformly negative 7 days following infusion, the organism was isolated from tumor tissue in 42% of dogs. The objective response rate was 15% (10% complete responses). These data supported an NCI-sponsored clinical trial of VNP20009 in human metastatic melanoma (67). No objective antitumor responses were observed in the human melanoma study, however; this could be due to selection of melanoma as the sole human tumor type for study, or due to differences in either tolerability or host (e.g., immune, vascular) response to the bacterium between dog and human. Strategies for geographically targeted cytotoxic drug delivery via hyperthermia and thermosensitive liposomes have also been investigated in canine soft tissue sarcomas (68).

Proof of Tumor Drug Accumulation

A recent canine clinical trial of the autophagy modulating agent hydroxychloroquine (HCQ), which was published concurrently with a series of human clinical trials, was the first to document substantial accumulation (∼100-fold) of HCQ in tumor tissue when compared with plasma, and to demonstrate that there was no correlation between drug concentrations or changes in autophagy in the two compartments. This suggested that peripheral blood is not a good surrogate for tumor HCQ concentration or autophagy-modulatory activity, and that future clinical trials should aim to identify more accurate surrogates of HCQ activity (69).

Another large COTC trial evaluated a series of three distinct indenoisoquinolone-class topoisomerase I inhibitors in dogs with spontaneous lymphoma. Eighty-four dogs with lymphoma were allocated to receive one of three drugs. Tolerability, pharmacokinetics, target engagement and antitumor effects were evaluated. One of the three drugs, LMP744, demonstrated significantly increased accumulation in tumor tissue vs. the other two drugs, and enhanced antitumor activity was ascribed to this increased tumor accumulation (70). Although LMP744 was not originally selected for further human development, the unexpected positive results of the canine trial encouraged the NCI to evaluate LMP744 in humans (ClinicalTrials.gov identifier NCT03030417). This human trial is currently accruing and thus human safety/efficacy data are not currently available.

ANTIMETASTATIC EFFICACY

Another potential advantage of canine clinical cancer research is the relatively compressed time line for tumor progression and the spontaneous development of local recurrence, metastasis, and drug resistance. These characteristics allow surgical adjuvant studies against "microscopic residual disease," with temporal endpoints such as progression free or overall survival, to be conducted relatively expediently. This may be useful especially for agents designed primarily as antimetastatic therapies. Several candidate human therapies have been investigated in this context in tumor-bearing dogs.

Extensive work by Macewen, Kurzman et al. with the peptidoglycan recognition protein agonist and non-specific immune stimulant liposome muramyl tripeptide phosphatidylethanolamine (L-MTP-PE) was performed in dogs with hemangiosarcoma (HSA) and OSA. Randomized placebo controlled trials demonstrated meaningful delays in metastasis and prolongation of overall survival times when surgery and chemotherapy were combined with L-MTP-PE (71, 72). Furthermore, bronchoalveolar lavage performed before and after L-MTP-PE indicated significant enhancement of activation status and *ex vivo* antitumor cytotoxicity in pulmonary alveolar macrophages (73). This work provided critical proof of principle showing delay of metastasis in OSA, which led directly to the performance of a randomized, placebo-controlled trial of surgery, chemotherapy ± L-MTP-PE in human OSA (74). Subsequently, L-MTP-PE (mifamurtide, Mepact™) was granted regulatory approval by the European Medicines Agency for treatment of human OSA.

Another randomized, multicenter surgical adjuvant study compared standard-of-care therapy with carboplatin to treatment with the novel liposomal cisplatin drug SPI-77 in dogs with appendicular OSA. Despite SPI-77's capacity to deliver five times more cisplatin vs. the maximum tolerated dose of free cisplatin, there were no improvements in progression free survival time or overall survival time when compared with conventionally dosed carboplatin. These results, combined with other factors, contributed significantly to the decision to suspend SPI-77's clinical development (75).

In a recent study, dogs with splenic HSA were treated after splenectomy with a combination of doxorubicin and an epidermal growth factor receptor- and urokinase-targeted *Pseudomonas* exotoxin, referred to as eBAT. These targets appear to be conserved in certain human sarcomas, and thus canine HSA may be a valuable translational model despite the distinct histotype and rareness of its human homolog. In addition to very good tolerability, there was the suggestion of improved outcome when eBAT-treated patients were compared with historical canine patients receiving doxorubicin alone (76). The human development path for eBAT is not currently known.

IMMUNOTHERAPY

In addition to the advantages discussed above, a unique advantage of spontaneous canine tumors that has been somewhat overlooked is that these tumors have evolved, by necessity,

TABLE 1 | Immunotherapy approaches investigated in canine cancer trials.

Category	Therapy type	References
Passive, nonspecific	BCG/other bacterial products	(46, 66, 96–100)
	L-MTP-PE	(71–73, 101)
	Recombinant cytokines	(45, 101–107)
	Intralesional immuno/gene therapy	(47, 48, 108–110)
Passive, specific	Tumor-targeting antibodies	(111, 112)
	Checkpoint inhibitors	(113)
	Whole cell vaccines	(114–119)
	Gene/peptide vaccines	(120–124)
Active, nonspecific	Activated T cells	(125, 126)
	Oncolytic virotherapy	(127, 128)
Active, specific	CAR-T cells	(129)

immune-avoidance strategies that are very similar to those utilized by human cancers. This is in stark contrast to syngeneic murine tumor models, where immune tolerance does not evolve similarly. These immune-avoidance strategies include upregulation of immune-suppressive cytokines such as IL-8, IL-10, and transforming growth factor beta (77–80), cooptation of innate immune-suppressive cells such as regulatory T cells (81–83), myeloid-derived suppressor cells (84–86), and "steady state" macrophages (87–90), and upregulation of immune checkpoint molecules such as PD-L1 and B7x (91–95). Thus, successful cancer immunotherapy in dogs requires overcoming of these conserved immune-avoidance strategies just as is required in humans.

In addition to the approaches mentioned in previous sections, a variety of immunotherapy strategies have been investigated in dogs over decades. These range from passive non-specific immunotherapy approaches to early studies with canine chimeric antigen receptor-engineered T (CAR-T) cells. A partial list of immunotherapy approaches investigated in dogs with cancer is provided in **Table 1**. An exhaustive discussion of these approaches is beyond the scope of this review; however, this issue contains a dedicated article discussing canine tumor immunology and immunotherapy. Several of the approaches outlined in the Table have led to human clinical trials (74, 130, 131).

CONCLUSIONS AND FUTURE DIRECTIONS

In conclusion, there is great potential for studies in dogs with spontaneous cancer to inform development of novel human therapeutics and diagnostics. In general, these studies have a higher potential for success when there is a focused, *a priori* question that canine studies seek to answer, and a plan for utilization of the data generated is in place prior to study commencement. Additionally, utilizing the strengths of the model, especially vis a vis the ability to repeatedly sample tumor tissue, to generate robust PK/PD related data is value-added. These types of data are perhaps more critical in answering questions regarding why a treatment did not work than in supporting how a treatment did work. Was it an issue of insufficient drug exposure? Was there adequate exposure in plasma but not tumor? Was the target appropriately inhibited despite a lack of antitumor activity?

Additionally, successful implementation of studies in dogs generally requires some amount of preclinical work for validation of target expression, validation of drug activity against the canine analog of the target, and selection/validation of PD endpoints to be implemented in subsequent canine clinical trials. A lack of canine-specific reagents often requires some legwork for the validation of cross-reactive antibodies for these types of applications.

Ongoing foundational work has the potential to significantly expand the molecular underpinnings of canine cancer, and facilitate comparisons with human cancer. A number of 1 year administrative supplements to existing NIH P30 grants were recently approved, with the goals of utilizing next-gen sequencing (whole-exome sequencing, RNASeq) to characterize a variety of canine tumor types for quantification of mutational load, identification of driver mutations, and characterization of potential neoantigens for MHC binding. Furthermore, a series of U01 grants were recently funded by the NIH to explore novel immunotherapy approaches in canine cancer to inform human cancer immunotherapy studies. These studies have the potential to expand understanding of the molecular drivers of canine cancer and uncover novel shared molecular targets and pathways for future study.

Several ongoing large-scale longitudinal studies are taking advantage of dogs' foreshortened life spans to answer a variety of questions about life style, environment, aging and cancer incidence, as well as evaluating novel interventions. The Golden Retriever Lifetime Health Study (www.morrisanimalfoundation.org/golden-retriever-lifetime-study) is following 3,000 US golden retrievers from young adulthood to death, to identify environmental, nutritional, genetic, and lifestyle risk factors for cancer and other diseases in dogs. The University of Washington Dog Aging Project (https://dogagingproject.org) seeks to profile and follow up to 10,000 dogs to determine incidence and risk factors for a variety of age-related diseases, as well as pursuing smaller-scale trials with novel anti-aging (and potentially anti-cancer) interventions. The Vaccination Against Canine Cancer Study (www.vaccs.org) is an 800-dog, randomized, placebo-controlled, prospective, multi-center clinical trial seeking to evaluate the evaluate the ability of a multivalent frameshift vaccine to delay or prevent cancer development in healthy older dogs. These three long-term studies have the potential to shed significant light on genetic, environmental, lifestyle, and immunologic risk factors for cancer that may have significant translatability. The results are eagerly anticipated.

AUTHOR CONTRIBUTIONS

The author confirms being the sole contributor of this work and has approved it for publication.

REFERENCES

1. Johnson JI, Decker S, Zaharevitz D, Rubinstein LV, Venditti JM, Schepartz S, et al. Relationships between drug activity in NCI preclinical *in vitro* and *in vivo* models and early clinical trials. *Br J Cancer*. (2001) 84:1424–31. doi: 10.1054/bjoc.2001.1796
2. Paoloni M, Khanna C. Translation of new cancer treatments from pet dogs to humans. *Nat Rev Cancer*. (2008) 8:147–56. doi: 10.1038/nrc2273
3. Fleming JM, Creevy KE, Promislow DE. Mortality in North American dogs from 1984 to 2004: an investigation into age-, size-, and breed-related causes of death. *J Vet Intern Med*. (2011) 25:187–98. doi: 10.1111/j.1939-1676.2011.0695.x
4. Alvarez CE. Naturally occurring cancers in dogs: insights for translational genetics and medicine. *ILAR J*. (2014) 55:16–45. doi: 10.1093/ilar/ilu010
5. Leblanc AK, Mazcko CN, Khanna C. Defining the value of a comparative approach to cancer drug development. *Clin Cancer Res*. (2016) 22:2133–8. doi: 10.1158/1078-0432.CCR-15-2347
6. Leblanc AK, Breen M, Choyke P, Dewhirst M, Fan TM, Gustafson DL, et al. Perspectives from man's best friend: National Academy of Medicine's Workshop on Comparative Oncology. *Sci Transl Med*. (2016) 8:324ps325. doi: 10.1126/scitranslmed.aaf0746
7. Vail DM, Thamm DH. Spontaneously occurring tumors in companion animals as models for drug development. In: Teicher BA, Andrews PA, editors. *Anticancer Drug Development Guide: Preclinical Screening, Clinical Trials, and Approval,* 2nd ed. Totowa, NJ: Humana Press (2004). p. 259–84.
8. Ladue T, Klein MK, Veterinary Radiation Therapy Oncology G. Toxicity criteria of the veterinary radiation therapy oncology group. *Vet Radiol Ultrasound*. (2001) 42:475–6. doi: 10.1111/j.1740-8261.2001.tb00973.x
9. Veterinary Cooperative Oncology Group. Veterinary Cooperative Oncology Group - common terminology criteria for adverse events (VCOG-CTCAE) following chemotherapy or biological antineoplastic therapy in dogs and cats v1.1. *Vet Comp Oncol*. (2016) 14:417–46. doi: 10.1111/vco.283
10. Vail DM, Michels GM, Khanna C, Selting KA, London CA, Veterinary Cooperative Oncology G. Response evaluation criteria for peripheral nodal lymphoma in dogs (v1.0)–a Veterinary Cooperative Oncology Group (VCOG) consensus document. *Vet Comp Oncol*. (2010) 8:28–37. doi: 10.1111/j.1476-5829.2009.00200.x
11. Nguyen SM, Thamm DH, Vail DM, London CA. Response evaluation criteria for solid tumours in dogs (v1.0): a Veterinary Cooperative Oncology Group (VCOG) consensus document. *Vet Comp Oncol*. (2015) 13:176–83. doi: 10.1111/vco.12032
12. Cline JM, Thrall DE, Page RL, Franko AJ, Raleigh JA. Immunohistochemical detection of a hypoxia marker in spontaneous canine tumours. *Br J Cancer*. (1990) 62:925–31. doi: 10.1038/bjc.1990.411
13. Zeman EM, Calkins DP, Cline JM, Thrall DE, Raleigh JA. The relationship between proliferative and oxygenation status in spontaneous canine tumors. *Int J Radiat Oncol Biol Phys*. (1993) 27:891–8. doi: 10.1016/0360-3016(93)90465-8
14. Cline JM, Thrall DE, Rosner GL, Raleigh JA. Distribution of the hypoxia marker CCI-103F in canine tumors. *Int J Radiat Oncol Biol Phys*. (1994) 28:921–33. doi: 10.1016/0360-3016(94)90113-9
15. Raleigh JA, Zeman EM, Calkins DP, Mcentee MC, Thrall DE. Distribution of hypoxia and proliferation associated markers in spontaneous canine tumors. *Acta Oncol*. (1995) 34:345–9. doi: 10.3109/02841869509093987
16. Cline JM, Rosner GL, Raleigh JA, Thrall DE. Quantification of CCI-103F labeling heterogeneity in canine solid tumors. *Int J Radiat Oncol Biol Phys*. (1997) 37:655–62. doi: 10.1016/S0360-3016(96)00559-7
17. Thrall DE, Rosner GL, Azuma C, Mcentee MC, Raleigh JA. Hypoxia marker labeling in tumor biopsies: quantification of labeling variation and criteria for biopsy sectioning. *Radiother Oncol*. (1997) 44:171–6. doi: 10.1016/S0167-8140(97)01931-2
18. Zachos TA, Aiken SW, Diresta GR, Healey JH. Interstitial fluid pressure and blood flow in canine osteosarcoma and other tumors. *Clin Orthop Relat Res*. (2001) 230–6. doi: 10.1097/00003086-200104000-00034
19. Larue SM, Withrow SJ, Powers BE, Wrigley RH, Gillette EL, Schwarz PD, et al. Limb-sparing treatment for osteosarcoma in dogs. *J Am Vet Med Assoc*. (1989) 195:1734–44.
20. Thrall DE, Withrow SJ, Powers BE, Straw RC, Page RL, Heidner GL, et al. Radiotherapy prior to cortical allograft limb sparing in dogs with osteosarcoma: a dose response assay. *Int J Radiat Oncol Biol Phys*. (1990) 18:1351–7. doi: 10.1016/0360-3016(90)90308-7
21. Withrow SJ, Thrall DE, Straw RC, Powers BE, Wrigley RH, Larue SM, et al. Intra-arterial cisplatin with or without radiation in limb-sparing for canine osteosarcoma. *Cancer*. (1993) 71:2484–90. doi: 10.1002/1097-0142(19930415)71:8<2484::AID-CNCR2820710810>3.0.CO;2-D
22. Withrow SJ, Wilkins RM. Cross talk from pets to people: translational osteosarcoma treatments. *ILAR J*. (2010) 51:208–13. doi: 10.1093/ilar.51.3.208
23. Lascelles BD, Dernell WS, Correa MT, Lafferty M, Devitt CM, Kuntz CA, et al. Improved survival associated with postoperative wound infection in dogs treated with limb-salvage surgery for osteosarcoma. *Ann Surg Oncol*. (2005) 12:1073–83. doi: 10.1245/ASO.2005.01.011
24. Jeys LM, Grimer RJ, Carter SR, Tillman RM, Abudu A. Post operative infection and increased survival in osteosarcoma patients: are they associated? *Ann Surg Oncol*. (2007) 14:2887–95. doi: 10.1245/s10434-007-9483-8
25. Sottnik JL, U'Ren LW, Thamm DH, Withrow SJ, Dow SW. Chronic bacterial osteomyelitis suppression of tumor growth requires innate immune responses. *Cancer Immunol Immunother*. (2010) 59:367–78. doi: 10.1007/s00262-009-0755-y
26. Gillette EL, Maurer GD, Severin GA. Endothelial repair of radiation damage following beta irradiation. *Radiology*. (1975) 116:175–7. doi: 10.1148/116.1.175
27. Fike JR, Gillette EL, Clow DJ. Repair of sublethal radiation damage by capillaries. *Int J Radiat Oncol Biol Phys*. (1979) 5:339–42. doi: 10.1016/0360-3016(79)91213-6
28. Gavin PR, Gillette EL. Radiation response of the canine cardiovascular system. *Radiat Res*. (1982) 90:489–500. doi: 10.2307/3575726
29. Gillette EL, Mcchesney SL, Hoopes PJ. Isoeffect curves for radiation-induced cardiomyopathy in the dog. *Int J Radiat Oncol Biol Phys*. (1985) 11:2091–7. doi: 10.1016/0360-3016(85)90089-6
30. Hoopes PJ, Gillette EL, Benjamin SA. The pathogenesis of radiation nephropathy in the dog. *Radiat Res*. (1985) 104:406–19. doi: 10.2307/3576600
31. Powers BE, Mcchesney SL, Gillette EL. Late radiation response of the canine trachea with change in dose per fraction. *Int J Radiat Oncol Biol Phys*. (1987) 13:1673–80. doi: 10.1016/0360-3016(87)90164-7
32. Ahmadu-Suka F, Gillette EL, Withrow SJ, Husted PW, Nelson AW, Whiteman CE. Exocrine pancreatic function following intraoperative irradiation of the canine pancreas. *Cancer*. (1988) 62:1091–5. doi: 10.1002/1097-0142(19880915)62:6<1091::AID-CNCR2820620611>3.0.CO;2-A
33. Ching SV, Gillette SM, Powers BE, Roberts SM, Gillette EL, Withrow SJ. Radiation-induced ocular injury in the dog: a histological study. *Int J Radiat Oncol Biol Phys*. (1990) 19:321–8. doi: 10.1016/0360-3016(90)90540-Z
34. Gillette SM, Powers BE, Orton EC, Gillette EL. Early radiation response of the canine heart and lung. *Radiat Res*. (1991) 125:34–40. doi: 10.2307/3577979
35. Powers BE, Gillette EL, Gillette SL, Lecouteur RA, Withrow SJ. Muscle injury following experimental intraoperative irradiation. *Int J Radiat Oncol Biol Phys*. (1991) 20:463–71. doi: 10.1016/0360-3016(91)90058-C
36. Gillette SM, Dewhirst MW, Gillette EL, Thrall DE, Page RL, Powers BE, et al. Response of canine soft tissue sarcomas to radiation or radiation plus hyperthermia: a randomized phase II study. *Int J Hyperthermia*. (1992) 8:309–20. doi: 10.3109/02656739209021786
37. McChesney SL, Gillette EL, Powers BE. Response of the canine lung to fractionated irradiation: pathologic changes and isoeffect curves. *Int J Radiat Oncol Biol Phys*. (1989) 16:125–32. doi: 10.1016/0360-3016(89)90019-9
38. Mackie TR, Kapatoes J, Ruchala K, Lu W, Wu C, Olivera G, et al. Image guidance for precise conformal radiotherapy. *Int J Radiat Oncol Biol Phys*. (2003) 56:89–105. doi: 10.1016/S0360-3016(03)00090-7
39. Forrest LJ, Mackie TR, Ruchala K, Turek M, Kapatoes J, Jaradat H, et al. The utility of megavoltage computed tomography images from a helical tomotherapy system for setup verification purposes. *Int J Radiat Oncol Biol Phys*. (2004) 60:1639–44. doi: 10.1016/j.ijrobp.2004.08.016
40. Thrall DE, Larue SM, Pruitt AF, Case B, Dewhirst MW. Changes in tumour oxygenation during fractionated hyperthermia and radiation therapy in

spontaneous canine sarcomas. *Int J Hyperthermia*. (2006) 22:365–73. doi: 10.1080/02656730600836386
41. Chi JT, Thrall DE, Jiang C, Snyder S, Fels D, Landon C, et al. Comparison of genomics and functional imaging from canine sarcomas treated with thermoradiotherapy predicts therapeutic response and identifies combination therapeutics. *Clin Cancer Res*. (2011) 17:2549–60. doi: 10.1158/1078-0432.CCR-10-2583
42. Thrall DE, Maccarini P, Stauffer P, Macfall J, Hauck M, Snyder S, et al. Thermal dose fractionation affects tumour physiological response. *Int J Hyperthermia*. (2012) 28:431–40. doi: 10.3109/02656736.2012.689087
43. Hershey AE, Kurzman ID, Forrest LJ, Bohling CA, Stonerook M, Placke ME, et al. Inhalation chemotherapy for macroscopic primary or metastatic lung tumors: proof of principle using dogs with spontaneously occurring tumors as a model. *Clin Cancer Res*. (1999) 5:2653–9.
44. Rodriguez CO Jr., Crabbs TA, Wilson DW, Cannan VA, Skorupski KA, et al. Aerosol gemcitabine: preclinical safety and *in vivo* antitumor activity in osteosarcoma-bearing dogs. *J Aerosol Med Pulm Drug Deliv*. (2010) 23:197–206. doi: 10.1089/jamp.2009.0773
45. Khanna C, Anderson PM, Hasz DE, Katsanis E, Neville M, Klausner JS. Interleukin-2 liposome inhalation therapy is safe and effective for dogs with spontaneous pulmonary metastases. *Cancer*. (1997) 79:1409–21. doi: 10.1002/(SICI)1097-0142(19970401)79:7<1409::AID-CNCR19>3.0.CO;2-3
46. Roberts NJ, Zhang L, Janku F, Collins A, Bai RY, Staedtke V, et al. Intratumoral injection of Clostridium novyi-NT spores induces antitumor responses. *Sci Transl Med*. (2014) 6:249ra111. doi: 10.1126/scitranslmed.3008982
47. Dow SW, Elmslie RE, Willson AP, Roche L, Gorman C, Potter TA. *In vivo* tumor transfection with superantigen plus cytokine genes induces tumor regression and prolongs survival in dogs with malignant melanoma. *J Clin Invest*. (1998) 101:2406–14. doi: 10.1172/JCI510
48. Thamm DH, Kurzman ID, Macewen EG, Feinmehl R, Towell TL, Longhofer SL, et al. Intralesional lipid-complexed cytokine/superantigen immunogene therapy for spontaneous canine tumors. *Cancer Immunol Immunother*. (2003) 52:473–80. doi: 10.1007/s00262-003-0387-6
49. Finocchiaro LM, Villaverde MS, Gil-Cardeza ML, Riveros MD, Glikin GC. Cytokine-enhanced vaccine and interferon-beta plus suicide gene as combined therapy for spontaneous canine sarcomas. *Res Vet Sci*. (2011) 91:230–4. doi: 10.1016/j.rvsc.2010.12.012
50. Westberg S, Sadeghi A, Svensson E, Segall T, Dimopoulou M, Korsgren O, et al. Treatment efficacy and immune stimulation by AdCD40L gene therapy of spontaneous canine malignant melanoma. *J Immunother*. (2013) 36:350–8. doi: 10.1097/CJI.0b013e31829d8a1b
51. Theon AP, Madewell BR, Moore AS, Stephens C, Krag DN. Localized thermo-cisplatin therapy: a pilot study in spontaneous canine and feline tumours. *Int J Hyperthermia*. (1991) 7:881–92. doi: 10.3109/02656739109056456
52. Kitchell BE, Brown DM, Luck EE, Woods LL, Orenberg EK, Bloch DA. Intralesional implant for treatment of primary oral malignant melanoma in dogs. *J Am Vet Med Assoc*. (1994) 204:229–36.
53. Theon AP, Madewell BR, Ryu J, Castro J. Concurrent irradiation and intratumoral chemotherapy with cisplatin: a pilot study in dogs with spontaneous tumors. *Int J Radiat Oncol Biol Phys*. (1994) 29:1027–34. doi: 10.1016/0360-3016(94)90398-0
54. Kitchell BK, Orenberg EK, Brown DM, Hutson C, Ray K, Woods L, et al. Intralesional sustained-release chemotherapy with therapeutic implants for treatment of canine sun-induced squamous cell carcinoma. *Eur J Cancer*. (1995) 31A:2093–8. doi: 10.1016/0959-8049(95)00446-7
55. Venable RO, Worley DR, Gustafson DL, Hansen RJ, Ehrhart EJ III, Cai S, et al. Effects of intratumoral administration of a hyaluronan-cisplatin nanoconjugate to five dogs with soft tissue sarcomas. *Am J Vet Res*. (2012) 73:1969–76. doi: 10.2460/ajvr.73.12.1969
56. London CA, Galli SJ, Yuuki T, Hu ZQ, Helfand SC, Geissler EN. Spontaneous canine mast cell tumors express tandem duplications in the proto-oncogene c-kit. *Exp Hematol*. (1999) 27:689–97. doi: 10.1016/S0301-472X(98)00075-7
57. Decker B, Parker HG, Dhawan D, Kwon EM, Karlins E, Davis BW, et al. Homologous mutation to human BRAF V600E is common in naturally occurring canine bladder cancer–evidence for a relevant model system and urine-based diagnostic test. *Mol Cancer Res*. (2015) 13:993–1002. doi: 10.1158/1541-7786.MCR-14-0689
58. Mochizuki H, Breen M. Sequence analysis of RAS and RAF mutation hot spots in canine carcinoma. *Vet Comp Oncol*. (2017) 15:1598–605. doi: 10.1111/vco.12275
59. Liao AT, Chien MB, Shenoy N, Mendel DB, Mcmahon G, Cherrington JM, et al. Inhibition of constitutively active forms of mutant kit by multitargeted indolinone tyrosine kinase inhibitors. *Blood*. (2002) 100:585–93. doi: 10.1182/blood-2001-12-0350
60. London CA, Hannah AL, Zadovoskaya R, Chien MB, Kollias-Baker C, Rosenberg M, et al. Phase I dose-escalating study of SU11654, a small molecule receptor tyrosine kinase inhibitor, in dogs with spontaneous malignancies. *Clin Cancer Res*. (2003) 9:2755–68.
61. Pryer NK, Lee LB, Zadovaskaya R, Yu X, Sukbuntherng J, Cherrington JM, et al. Proof of target for SU11654: inhibition of KIT phosphorylation in canine mast cell tumors. *Clin Cancer Res*. (2003) 9:5729–34.
62. London CA, Malpas PB, Wood-Follis SL, Boucher JF, Rusk AW, Rosenberg MP, et al. Multi-center, placebo-controlled, double-blind, randomized study of oral toceranib phosphate (SU11654), a receptor tyrosine kinase inhibitor, for the treatment of dogs with recurrent (either local or distant) mast cell tumor following surgical excision. *Clin Cancer Res*. (2009) 15:3856–65. doi: 10.1158/1078-0432.CCR-08-1860
63. London CA, Bernabe LF, Barnard S, Kisseberth WC, Borgatti A, Henson M, et al. Preclinical evaluation of the novel, orally bioavailable Selective Inhibitor of Nuclear Export (SINE) KPT-335 in spontaneous canine cancer: results of a phase I study. *PLoS ONE*. (2014) 9:e87585. doi: 10.1371/journal.pone.0087585
64. Honigberg LA, Smith AM, Sirisawad M, Verner E, Loury D, Chang B, et al. The Bruton tyrosine kinase inhibitor PCI-32765 blocks B-cell activation and is efficacious in models of autoimmune disease and B-cell malignancy. *Proc Natl Acad Sci USA*. (2010) 107:13075–80. doi: 10.1073/pnas.1004594107
65. Paoloni MC, Tandle A, Mazcko C, Hanna E, Kachala S, Leblanc A, et al. Launching a novel preclinical infrastructure: comparative oncology trials consortium directed therapeutic targeting of TNFalpha to cancer vasculature. *PLoS ONE*. (2009) 4:e4972. doi: 10.1371/journal.pone.0004972
66. Thamm DH, Kurzman ID, King I, Li Z, Sznol M, Dubielzig RR, et al. Systemic administration of an attenuated, tumor-targeting Salmonella typhimurium to dogs with spontaneous neoplasia: phase I evaluation. *Clin Cancer Res*. (2005) 11:4827–34. doi: 10.1158/1078-0432.CCR-04-2510
67. Toso JF, Gill VJ, Hwu P, Marincola FM, Restifo NP, Schwartzentruber DJ, et al. Phase I study of the intravenous administration of attenuated Salmonella typhimurium to patients with metastatic melanoma. *J Clin Oncol*. (2002) 20:142–52. doi: 10.1200/JCO.20.1.142
68. Hauck ML, Larue SM, Petros WP, Poulson JM, Yu D, Spasojevic I, et al. Phase I trial of doxorubicin-containing low temperature sensitive liposomes in spontaneous canine tumors. *Clin Cancer Res*. (2006) 12:4004–10. doi: 10.1158/1078-0432.CCR-06-0226
69. Barnard RA, Wittenburg LA, Amaravadi RK, Gustafson DL, Thorburn A, Thamm DH. Phase I clinical trial and pharmacodynamic evaluation of combination hydroxychloroquine and doxorubicin treatment in pet dogs treated for spontaneously occurring lymphoma. *Autophagy*. (2014) 10:1415–25. doi: 10.4161/auto.29165
70. Burton JH, Mazcko C, Leblanc A, Covey JM, Ji J, Kinders RJ, et al. NCI Comparative Oncology Program testing of non-camptothecin indenoisoquinoline topoisomerase i inhibitors in naturally occurring canine lymphoma. *Clin Cancer Res*. (2018) 24:5830–40. doi: 10.1158/1078-0432.CCR-18-1498
71. Kurzman ID, Macewen EG, Rosenthal RC, Fox LE, Keller ET, Helfand SC, et al. Adjuvant therapy for osteosarcoma in dogs: results of randomized clinical trials using combined liposome-encapsulated muramyl tripeptide and cisplatin. *Clin Cancer Res*. (1995) 1:1595–601.
72. Vail DM, Macewen EG, Kurzman ID, Dubielzig RR, Helfand SC, Kisseberth WC, et al. Liposome-encapsulated muramyl tripeptide phosphatidylethanolamine adjuvant immunotherapy for splenic hemangiosarcoma in the dog: a randomized multi-institutional clinical trial. *Clin Cancer Res*. (1995) 1:1165–70.
73. Kurzman ID, Shi F, Vail DM, Macewen EG. *In vitro* and *in vivo* enhancement of canine pulmonary alveolar macrophage cytotoxic activity

against canine osteosarcoma cells. *Cancer Biother Radiopharm*. (1999) 14:121–8. doi: 10.1089/cbr.1999.14.121
74. Meyers PA, Schwartz CL, Krailo M, Kleinerman ES, Betcher D, Bernstein ML, et al. Osteosarcoma: a randomized, prospective trial of the addition of ifosfamide and/or muramyl tripeptide to cisplatin, doxorubicin, and high-dose methotrexate. *J Clin Oncol*. (2005) 23:2004–11. doi: 10.1200/JCO.2005.06.031
75. Vail DM, Kurzman ID, Glawe PC, O'Brien MG, Chun R, Garrett LD, et al. STEALTH liposome-encapsulated cisplatin (SPI-77) versus carboplatin as adjuvant therapy for spontaneously arising osteosarcoma (OSA) in the dog: a randomized multicenter clinical trial. *Cancer Chemother Pharmacol*. (2002) 50:131–6. doi: 10.1007/s00280-002-0469-8
76. Borgatti A, Koopmeiners JS, Sarver AL, Winter AL, Stuebner K, Todhunter D, et al. Safe and effective sarcoma therapy through bispecific targeting of EGFR and uPAR. *Mol Cancer Ther*. (2017) 16:956–65. doi: 10.1158/1535-7163.MCT-16-0637
77. Itoh H, Horiuchi Y, Nagasaki T, Sakonju I, Kakuta T, Fukushima U, et al. Evaluation of immunological status in tumor-bearing dogs. *Vet Immunol Immunopathol*. (2009) 132:85–90. doi: 10.1016/j.vetimm.2009.04.020
78. De Andres PJ, Illera JC, Caceres S, Diez L, Perez-Alenza MD, Pena L. Increased levels of interleukins 8 and 10 as findings of canine inflammatory mammary cancer. *Vet Immunol Immunopathol*. (2013) 152:245–51. doi: 10.1016/j.vetimm.2012.12.010
79. Kim JH, Frantz AM, Anderson KL, Graef AJ, Scott MC, Robinson S, et al. Interleukin-8 promotes canine hemangiosarcoma growth by regulating the tumor microenvironment. *Exp Cell Res*. (2014) 323:155–64. doi: 10.1016/j.yexcr.2014.02.020
80. Troyer RM, Ruby CE, Goodall CP, Yang L, Maier CS, Albarqi HA, et al. Exosomes from osteosarcoma and normal osteoblast differ in proteomic cargo and immunomodulatory effects on T cells. *Exp Cell Res*. (2017) 358:369–76. doi: 10.1016/j.yexcr.2017.07.011
81. Biller BJ, Elmslie RE, Burnett RC, Avery AC, Dow SW. Use of FoxP3 expression to identify regulatory T cells in healthy dogs and dogs with cancer. *Vet Immunol Immunopathol*. (2007) 116:69–78. doi: 10.1016/j.vetimm.2006.12.002
82. O'Neill K, Guth A, Biller B, Elmslie R, Dow S. Changes in regulatory T cells in dogs with cancer and associations with tumor type. *J Vet Intern Med*. (2009) 23:875–81. doi: 10.1111/j.1939-1676.2009.0333.x
83. Biller BJ, Guth A, Burton JH, Dow SW. Decreased ratio of CD8+ T cells to regulatory T cells associated with decreased survival in dogs with osteosarcoma. *J Vet Intern Med*. (2010) 24:1118–23. doi: 10.1111/j.1939-1676.2010.0557.x
84. Goulart MR, Pluhar GE, Ohlfest JR. Identification of myeloid derived suppressor cells in dogs with naturally occurring cancer. *PLoS ONE*. (2012) 7:e33274. doi: 10.1371/journal.pone.0033274
85. Sherger M, Kisseberth W, London C, Olivo-Marston S, Papenfuss TL. Identification of myeloid derived suppressor cells in the peripheral blood of tumor bearing dogs. *BMC Vet Res*. (2012) 8:209. doi: 10.1186/1746-6148-8-209
86. Goulart MR, Hlavaty SI, Chang YM, Polton G, Stell A, Perry J, et al. Phenotypic and transcriptomic characterization of canine myeloid-derived suppressor cells. *Sci Rep*. (2019) 9:3574. doi: 10.1038/s41598-019-40285-3
87. Beirao BC, Raposo T, Pang LY, Argyle DJ. Canine mammary cancer cells direct macrophages toward an intermediate activation state between M1/M2. *BMC Vet Res*. (2015) 11:151. doi: 10.1186/s12917-015-0473-y
88. Regan DP, Escaffi A, Coy J, Kurihara J, Dow SW. Role of monocyte recruitment in hemangiosarcoma metastasis in dogs. *Vet Comp Oncol*. (2017) 15:1309–22. doi: 10.1111/vco.12272
89. Monteiro LN, Rodrigues MA, Gomes DA, Salgado BS, Cassali GD. Tumour-associated macrophages: relation with progression and invasiveness, and assessment of M1/M2 macrophages in canine mammary tumours. *Vet J*. (2018) 234:119–25. doi: 10.1016/j.tvjl.2018.02.016
90. Seung BJ, Lim HY, Shin JI, Kim HW, Cho SH, Kim SH, et al. CD204-expressing tumor-associated macrophages are associated with malignant, high-grade, and hormone receptor-negative canine mammary gland tumors. *Vet Pathol*. (2018) 55:417–24. doi: 10.1177/0300985817750457
91. Maekawa N, Konnai S, Ikebuchi R, Okagawa T, Adachi M, Takagi S, et al. Expression of PD-L1 on canine tumor cells and enhancement of IFN-gamma production from tumor-infiltrating cells by PD-L1 blockade. *PLoS ONE*. (2014) 9:e98415. doi: 10.1371/journal.pone.0098415
92. Maekawa N, Konnai S, Okagawa T, Nishimori A, Ikebuchi R, Izumi Y, et al. Immunohistochemical analysis of PD-L1 expression in canine malignant cancers and PD-1 expression on lymphocytes in canine oral melanoma. *PLoS ONE*. (2016) 11:e0157176. doi: 10.1371/journal.pone.0157176
93. Ambrosius LA, Dhawan D, Ramos-Vara JA, Ruple A, Knapp DW, Childress MO. Quantification and prognostic value of programmed cell death ligand-1 expression in dogs with diffuse large B-cell lymphoma. *Am J Vet Res*. (2018) 79:643–9. doi: 10.2460/ajvr.79.6.643
94. Hartley G, Elmslie R, Dow S, Guth A. Checkpoint molecule expression by B and T cell lymphomas in dogs. *Vet Comp Oncol*. (2018) 16:352–60. doi: 10.1111/vco.12386
95. Chand SK, Pendharkar SA, Bharmal SH, Bartlett AS, Pandol SJ, Petrov MS. Frequency and risk factors for liver disease following pancreatitis: a population-based cohort study. *Dig Liver Dis*. (2019) 51:551–8. doi: 10.1016/j.dld.2018.11.001
96. Bech-Nielsen S, Brodey RS, Fidler IJ, Abt DA, Reif JS. The effect of BCG on *in vitro* immune reactivity and clinical course in dogs treated surgically for osteosarcoma. *Eur J Cancer*. (1977) 13:33–41. doi: 10.1016/0014-2964(77)90227-4
97. Bostock DE, Gorman NT. Intravenous BCG therapy of mammary carcinoma in bitches after surgical excision of the primary tumour. *Eur J Cancer*. (1978) 14:879–83. doi: 10.1016/0014-2964(78)90104-4
98. Meyer JA, Dueland RT, Macewen EG, Macy DW, Hoefle WD, Richardson RC, et al. Canine osteogenic sarcoma treated by amputation and MER: an adverse effect of splenectomy on survival. *Cancer*. (1982) 49:1613–6. doi: 10.1002/1097-0142(19820415)49:8<1613::AID-CNCR2820490814>3.0.CO;2-R
99. Parodi AL, Misdorp W, Mialot JP, Mialot M, Hart AA, Hurtrel M, et al. Intratumoral BCG and Corynebacterium parvum therapy of canine mammary tumours before radical mastectomy. *Cancer Immunol Immunother*. (1983) 15:172–7. doi: 10.1007/BF00199160
100. Henry CJ, Downing S, Rosenthal RC, Klein MK, Meleo K, Villamil JA, et al. Evaluation of a novel immunomodulator composed of human chorionic gonadotropin and bacillus Calmette-Guerin for treatment of canine mast cell tumors in clinically affected dogs. *Am J Vet Res*. (2007) 68:1246–51. doi: 10.2460/ajvr.68.11.1246
101. Macewen EG, Kurzman ID, Vail DM, Dubielzig RR, Everlith K, Madewell BR, et al. Adjuvant therapy for melanoma in dogs: results of randomized clinical trials using surgery, liposome-encapsulated muramyl tripeptide, and granulocyte macrophage colony-stimulating factor. *Clin Cancer Res*. (1999) 5:4249–58.
102. Moore AS, Theilen GH, Newell AD, Madewell BR, Rudolf AR. Preclinical study of sequential tumor necrosis factor and interleukin 2 in the treatment of spontaneous canine neoplasms. *Cancer Res*. (1991) 51:233–8.
103. Mito K, Sugiura K, Ueda K, Hori T, Akazawa T, Yamate J, et al. IFNγ markedly cooperates with intratumoral dendritic cell vaccine in dog tumor models. *Cancer Res*. (2010) 70:7093–101. doi: 10.1158/0008-5472.CAN-10-0600
104. Henson MS, Curtsinger JM, Larson VS, Klausner JS, Modiano JF, Mescher MF, et al. Immunotherapy with autologous tumour antigen-coated microbeads (large multivalent immunogen), IL-2 and GM-CSF in dogs with spontaneous B-cell lymphoma. *Vet Comp Oncol*. (2011) 9:95–105. doi: 10.1111/j.1476-5829.2010.00234.x
105. Konietschke U, Teske E, Jurina K, Stockhaus C. Palliative intralesional interleukin-2 treatment in dogs with urinary bladder and urethral carcinomas. *In Vivo*. (2012) 26:931–5.
106. Haagsman AN, Witkamp AC, Sjollema BE, Kik MJ, Kirpensteijn J. The effect of interleukin-2 on canine peripheral nerve sheath tumours after marginal surgical excision: a double-blind randomized study. *BMC Vet Res*. (2013) 9:155. doi: 10.1186/1746-6148-9-155
107. Ziekman PG, Otter WD, Tan JF, Teske E, Kirpensteijn J, Koten JW, et al. Intratumoural interleukin-2 therapy can induce regression of non-resectable mastocytoma in dogs. *Anticancer Res*. (2013) 33:161–5.
108. Finocchiaro LM, Fondello C, Gil-Cardeza ML, Rossi UA, Villaverde MS, Riveros MD, et al. Cytokine-enhanced vaccine and interferon-beta plus

suicide gene therapy as surgery adjuvant treatments for spontaneous canine melanoma. *Hum Gene Ther*. (2015) 26:367–76. doi: 10.1089/hum.2014.130
109. Monjazeb AM, Kent MS, Grossenbacher SK, Mall C, Zamora AE, Mirsoian A, et al. Blocking indolamine-2,3-dioxygenase rebound immune suppression boosts antitumor effects of radio-immunotherapy in murine models and spontaneous canine malignancies. *Clin Cancer Res*. (2016) 22:4328–40. doi: 10.1158/1078-0432.CCR-15-3026
110. Cicchelero L, Denies S, Haers H, Vanderperren K, Stock E, Van Brantegem L, et al. Intratumoural interleukin 12 gene therapy stimulates the immune system and decreases angiogenesis in dogs with spontaneous cancer. *Vet Comp Oncol*. (2017) 15:1187–205. doi: 10.1111/vco.12255
111. Paoloni M, Mazcko C, Selting K, Lana S, Barber L, Phillips J, et al. Defining the pharmacodynamic profile and therapeutic index of NHS-IL12 immunocytokine in dogs with malignant melanoma. *PLoS ONE*. (2015) 10:e0129954. doi: 10.1371/journal.pone.0129954
112. London CA, Gardner HL, Rippy S, Post G, La Perle K, Crew L, et al. KTN0158, a humanized anti-KIT monoclonal antibody, demonstrates biologic activity against both normal and malignant canine mast cells. *Clin Cancer Res*. (2017) 23:2565–74. doi: 10.1158/1078-0432.CCR-16-2152
113. Maekawa N, Konnai S, Takagi S, Kagawa Y, Okagawa T, Nishimori A, et al. A canine chimeric monoclonal antibody targeting PD-L1 and its clinical efficacy in canine oral malignant melanoma or undifferentiated sarcoma. *Sci Rep*. (2017) 7:8951. doi: 10.1038/s41598-017-09444-2
114. Hogge GS, Burkholder JK, Culp J, Albertini MR, Dubielzig RR, Keller ET, et al. Development of human granulocyte-macrophage colony-stimulating factor-transfected tumor cell vaccines for the treatment of spontaneous canine cancer. *Hum Gene Ther*. (1998) 9:1851–61. doi: 10.1089/hum.1998.9.13-1851
115. Turek MM, Thamm DH, Mitzey A, Kurzman ID, Huelsmeyer MK, Dubielzig RR, et al. Human granulocyte-macrophage colony-stimulating factor DNA cationic-lipid complexed autologous tumour cell vaccination in the treatment of canine B-cell multicentric lymphoma. *Vet Comp Oncol*. (2007) 5:219–31. doi: 10.1111/j.1476-5829.2007.00128.x
116. Bird RC, Deinnocentes P, Church Bird AE, Van Ginkel FW, Lindquist J, Smith BF. An autologous dendritic cell canine mammary tumor hybrid-cell fusion vaccine. *Cancer Immunol Immunother*. (2011) 60:87–97. doi: 10.1007/s00262-010-0921-2
117. Sorenmo KU, Krick E, Coughlin CM, Overley B, Gregor TP, Vonderheide RH, et al. CD40-activated B cell cancer vaccine improves second clinical remission and survival in privately owned dogs with non-Hodgkin's lymphoma. *PLoS ONE*. (2011) 6:e24167. doi: 10.1371/journal.pone.0024167
118. Marconato L, Frayssinet P, Rouquet N, Comazzi S, Leone VF, Laganga P, et al. Randomized, placebo-controlled, double-blinded chemoimmunotherapy clinical trial in a pet dog model of diffuse large B-cell lymphoma. *Clin Cancer Res*. (2014) 20:668–77. doi: 10.1158/1078-0432.CCR-13-2283
119. U'Ren LW, Biller BJ, Elmslie RE, Thamm DH, Dow SW. Evaluation of a novel tumor vaccine in dogs with hemangiosarcoma. *J Vet Intern Med*. (2007) 21:113–20. doi: 10.1111/j.1939-1676.2007.tb02936.x
120. Bergman PJ, Mcknight J, Novosad A, Charney S, Farrelly J, Craft D, et al. Long-term survival of dogs with advanced malignant melanoma after DNA vaccination with xenogeneic human tyrosinase: a phase I trial. *Clin Cancer Res*. (2003) 9:1284–90.
121. Bergman PJ, Camps-Palau MA, Mcknight JA, Leibman NF, Craft DM, Leung C, et al. Development of a xenogeneic DNA vaccine program for canine malignant melanoma at the Animal Medical Center. *Vaccine*. (2006) 24:4582–5. doi: 10.1016/j.vaccine.2005.08.027
122. Kamstock D, Elmslie R, Thamm D, Dow S. Evaluation of a xenogeneic VEGF vaccine in dogs with soft tissue sarcoma. *Cancer Immunol Immunother*. (2007) 56:1299–309. doi: 10.1007/s00262-007-0282-7
123. Gavazza A, Lubas G, Fridman A, Peruzzi D, Impellizeri JA, Luberto L, et al. Safety and efficacy of a genetic vaccine targeting telomerase plus chemotherapy for the therapy of canine B-cell lymphoma. *Hum Gene Ther*. (2013) 24:728–38. doi: 10.1089/hum.2013.112
124. Mason NJ, Gnanandarajah JS, Engiles JB, Gray F, Laughlin D, Gaurnier-Hausser A, et al. Immunotherapy with a HER2-targeting listeria induces HER2-specific immunity and demonstrates potential therapeutic effects in a phase I trial in canine osteosarcoma. *Clin Cancer Res*. (2016) 22:4380–90. doi: 10.1158/1078-0432.CCR-16-0088
125. Mie K, Shimada T, Akiyoshi H, Hayashi A, Ohashi F. Change in peripheral blood lymphocyte count in dogs following adoptive immunotherapy using lymphokine-activated T killer cells combined with palliative tumor resection. *Vet Immunol Immunopathol*. (2016) 177:58–63. doi: 10.1016/j.vetimm.2016.06.007
126. O'Connor CM, Sheppard S, Hartline CA, Huls H, Johnson M, Palla SL, et al. Adoptive T-cell therapy improves treatment of canine non-Hodgkin lymphoma post chemotherapy. *Sci Rep*. (2012) 2:249. doi: 10.1038/srep00249
127. Hwang CC, Igase M, Sakurai M, Haraguchi T, Tani K, Itamoto K, et al. Oncolytic reovirus therapy: pilot study in dogs with spontaneously occurring tumours. *Vet Comp Oncol*. (2018) 16:229–38. doi: 10.1111/vco.12361
128. Naik S, Galyon GD, Jenks NJ, Steele MB, Miller AC, Allstadt SD, et al. Comparative oncology evaluation of intravenous recombinant oncolytic vesicular stomatitis virus therapy in spontaneous canine cancer. *Mol Cancer Ther*. (2018) 17:316–26. doi: 10.1158/1535-7163.MCT-17-0432
129. Panjwani MK, Smith JB, Schutsky K, Gnanandarajah J, O'Connor CM, Powell DJ, et al. Feasibility and safety of RNA-transfected CD20-specific chimeric antigen receptor T cells in dogs with spontaneous B Cell lymphoma. *Mol Ther*. (2016) 24:1602–14. doi: 10.1038/mt.2016.146
130. Walsh P, Gonzalez R, Dow S, Elmslie R, Potter T, Glode LM, et al. A phase I study using direct combination DNA injections for the immunotherapy of metastatic melanoma. *Univ Colorado Cancer Center Clinical Trial Hum Gene Ther*. (2000) 11:1355–68. doi: 10.1089/104303400500 32447
131. Yuan J, Ku GY, Adamow M, Mu Z, Tandon S, Hannaman D, et al. Immunologic responses to xenogeneic tyrosinase DNA vaccine administered by electroporation in patients with malignant melanoma. *J Immunother Cancer*. (2013) 1:20. doi: 10.1186/2051-1426-1-20

Conflict of Interest: The author declares that the research was conducted in the absence of any commercial or financial relationships that could be construed as a potential conflict of interest.

Copyright © 2019 Thamm. This is an open-access article distributed under the terms of the Creative Commons Attribution License (CC BY). The use, distribution or reproduction in other forums is permitted, provided the original author(s) and the copyright owner(s) are credited and that the original publication in this journal is cited, in accordance with accepted academic practice. No use, distribution or reproduction is permitted which does not comply with these terms.

frontiers in Oncology

REVIEW
published: 22 November 2019
doi: 10.3389/fonc.2019.01291

Emerging Translational Opportunities in Comparative Oncology With Companion Canine Cancers: Radiation Oncology

Michael W. Nolan[1,2,3]*, *Michael S. Kent*[4] *and Mary-Keara Boss*[5]

[1] Department of Clinical Sciences, North Carolina State University, Raleigh, NC, United States, [2] Comparative Medicine Institute, North Carolina State University, Raleigh, NC, United States, [3] Duke Cancer Institute, Duke University, Durham, NC, United States, [4] Department of Surgical and Radiological Sciences, School of Veterinary Medicine, University of California, Davis, Davis, CA, United States, [5] Department of Environmental and Radiological Health Sciences, Flint Animal Cancer Center, Colorado State University, Fort Collins, CO, United States

OPEN ACCESS

Edited by:
Mark W. Dewhirst,
Duke University, United States

Reviewed by:
Maria Shoshan,
Karolinska Institutet (KI), Sweden
Karishma Rajani,
Mayo Clinic, United States
Mark A. Ritter,
University of Wisconsin-Madison, United States

***Correspondence:**
Michael W. Nolan
mwnolan@ncsu.edu

Specialty section:
This article was submitted to Cancer Molecular Targets and Therapeutics, a section of the journal Frontiers in Oncology

Received: 27 August 2019
Accepted: 07 November 2019
Published: 22 November 2019

Citation:
Nolan MW, Kent MS and Boss M-K (2019) Emerging Translational Opportunities in Comparative Oncology With Companion Canine Cancers: Radiation Oncology. Front. Oncol. 9:1291. doi: 10.3389/fonc.2019.01291

It is estimated that more than 6 million pet dogs are diagnosed with cancer annually in the USA. Both primary care and specialist veterinarians are frequently called upon to provide clinical care that improves the quality and/or quantity of life for affected animals. Because these cancers develop spontaneously in animals that often share the same environment as their owners, have intact immune systems and are of similar size to humans, and because the diagnostic tests and treatments for these cancers are similar to those used for management of human cancers, canine cancer provides an opportunity for research that simultaneously helps improve both canine and human health care. This is especially true in the field of radiation oncology, for which there is a rich and continually evolving history of learning from the careful study of pet dogs undergoing various forms of radiotherapy. The purpose of this review article is to inform readers of the potential utility and limitations of using dogs in that manner; the peer-reviewed literature will be critically reviewed, and current research efforts will be discussed. The article concludes with a look toward promising future directions and applications of this pet dog "model."

Keywords: radiation oncology, radiobiology, canine comparative radiation oncology, medical physics, animal models of cancer, imaging, theranostics, translational research

INTRODUCTION

Radiotherapy (RT) is most frequently applied to pet animals with naturally-occurring cancer as a means for improving animal health. However, there is also a long and rich history of studying radiation responses in the tumors and normal tissues of dogs, with a goal of informing therapeutic development in a manner that directly benefits both canine and human cancer patients. Such research forms the basis for the field of canine comparative radiation oncology and radiobiology. The purpose of this review article is to inform readers of the potential utility and limitations of using dogs in that manner; the peer-reviewed literature will be critically reviewed, and current research efforts will be discussed. The article will conclude with a look toward promising future directions and applications of this pet dog "model"; but we will begin with a brief overview of current practices in veterinary radiation oncology, which will enable readers to gain an appreciation for how the field

of canine comparative radiation oncology has developed, and how canine cancer studies can be efficiently, effectively and ethically conducted.

The American Veterinary Medical Association estimated that 38% of households in the Unites States owned a pet dog in 2018, and the National Cancer Institute's Comparative Oncology Program reports that nationwide ∼6 million new canine cancer diagnoses are made annually. RT is an important component of cancer care for dogs; external beam RT is the most common form of treatment. But despite the high rate of canine cancers, and the efficacy of RT, it is actually quite uncommon for dogs to be treated as such; this is largely attributable to limited accessibility. Financial cost is another important barrier to pet owners who might otherwise want to pursue advanced cancer treatments. The economics of veterinary RT are not well-documented. The cost of care varies with geographic location and type of center (university run academic veterinary teaching hospitals vs. private practice specialty clinics), but anecdotally, a course of palliative-intent RT in the US currently costs between ∼$1,000 and $3,500, and the cost for a definitive-intent course of therapy is often between $5,000 and $12,000. This is challenging because fewer than 10% of households carry pet health insurance, and so for most families, veterinary care represents an out-of-pocket expense. Another important factor that limits accessibility is the distance that must be traveled to pursue care; a 2010 report identified 66 veterinary-specific external beam RT centers in the United States (1). While that number is low relative to the number of canine cancer cases, geographic access is improving; indeed, there were only 42 US-based veterinary RT centers in 2001 (2).

Dogs develop a wide range of neoplasms that are treated with RT. Some of the most common indications with translational relevance to humans include soft tissue sarcoma, extremity osteosarcoma, glioma, and genitourinary carcinomas (both muscle-invasive urothelial carcinomas of the urinary bladder, and prostatic carcinomas). Many of these canine cancers share striking similarities with the equivalent human diseases, not only clinically and histologically, but also at a molecular and genomic level. For example, the most commonly altered gene in both canine and human osteosarcoma is TP53; the genomic imbalance in the two species is similar, and expression of several genes (including PTEN and RUNX2) are correlated with ploidy (3–5). Likewise, in addition to certain similarities between human and canine glioma, the process of PDGF-induced gliomagenesis seems to be well-conserved across mammalian species (6, 7).

A majority of canine radiotherapy patients are treated using conventional C-arm linear accelerators. Due to the need for general anesthesia, full-course definitive-intent, treatment protocols tend to be hypofractionated relative to protocols in common use for humans; often a total of 16–20 daily (Monday through Friday) fractions are administered, with fractional doses used for dogs typically ranging from 2.5 to 4 Gy. As with physician-based oncology, there has also been a tremendous shift in recent years toward much higher doses per fraction, with a rapid increase in access to, and application of, stereotactic radiosurgery (SRS) and stereotactic body RT (SBRT) for various malignancies (1).

HISTORICAL USES OF DOGS IN TRANSLATIONAL RADIATION RESEARCH

Normal Tissue Toxicity

In an online query of the US National Library of Medicine's PubMed database for the terms "canine" and "radiation," the earliest return was a 1922 article that was written by Stafford Warren and George Whipple; it was published in the Journal of Experimental Medicine, and described small intestinal radiosensitivity in dogs (8). This early use of dogs for radiobiology research may have been driven at least in part by the ease of housing and handling dogs, as well as access to hospital-grade irradiation equipment (X- and gamma-ray) for which it would have been straightforward to perform partial or total body irradiations. The similar anatomy of dogs and humans would also have been favorable, thus allowing experiments to be performed with similar radiation field sizes, and targets, as compared with other research species of the times, including various large animal agricultural species (e.g., swine, cattle) and small fish (9–11). Fortuitously, it was later learned that DNA repair mechanisms are highly conserved between mammalian species, and that there is high homology between key DNA damage response genes in humans and dogs (12–14).

Dogs have been used to model radiation injury in a wide range of normal tissues. And indeed, just as veterinarians have borrowed from physicians to inform the practice of veterinary radiation oncology, lessons learned from canine radiobiology research have also had important influences to optimize human cancer care. Through the 1980's and 1990's significant efforts at both Colorado State University and the National Cancer Institute (NCI) were directed toward defining the tolerance of canine tissues to intra-operative RT (IORT); similar studies were performed with multi-fraction irradiation protocols to estimate alpha-to-beta ratios for various normal tissues. These studies evaluated both conventional pathologic endpoints, and a wide range of clinically-relevant functional endpoints. For example, in a canine study, the volume of lung irradiated was found to be a critical limiting factor in thoracic RT (15). The assumption had already been made that a dose-volume relationship existed for lung tissue (16); the $TD_{50/5}$ (the radiation dose that causes toxicity in 50% of patients, 5 years after irradiation) was estimated to be 65 Gy when 33% of the total lung volume was irradiated. However, there were no cases of severe symptomatic pneumonitis in dogs for whom 33% of lung received up to 72 Gy; this suggests that when patients have otherwise healthy lungs (with normal compensatory function) the dose tolerance limits for lung may actually be higher than those originally proposed by Emami et al. (16).

It is beyond the scope of this manuscript to review all normal tissue injury studies for which dogs were utilized; however, another noteworthy endeavor was the use dogs to investigate tolerance of peripheral nerves to IORT. In the 1990's, investigators at NCI demonstrated a progressive sciatic neuropathy in American Foxhounds: with 3.5 years of follow-up, doses of up to 20 Gy were not found to cause clinically significant neuropathies, but 5 years after irradiation, doses of 15 Gy or more of IORT were injurious (17, 18). Similar findings

were reported in beagles, whose nerve function was evaluated via histology, neurologic examination, and electrophysiology (19). These experiments confirmed that nerves are dose-limiting for IORT, and that the neurovasculature plays a critical role in nerve injury. These studies also yielded insight regarding combinatorial therapies; while combining IORT with external beam RT resulted in a similar incidence and latency of neuropathy vs. IORT alone, the combination of IORT with hyperthermia led to increased incidence and decreased time to onset of nerve damage. More recently, hounds were used to demonstrate that both altered function of the internal pudendal artery, and pudendal nerve, accompany erectile dysfunction that follows treatment of prostate cancer with SBRT (20). That study identified potential strategies for mitigating radiation-induced sexual dysfunction in men. It also provided data to support the clinical observation that high-dose SBRT may lead to severe colorectal injury, for which latency can be increased, and incidence reduced via either reduction of the radiation dose, or increasing the duration of the interfraction interval (21, 22).

While some laboratory groups have studied both purpose-bred and tumor-bearing pet dogs, the latter have largely been used to study radiation effects on tumors, rather than normal tissue. Rainer Storb's team at the Fred Hutchinson Cancer Research Center has taken this approach for many years, demonstrating dose, fractionation and dose rate effects of total body irradiation in research colony animals, and providing proof-of-principle for clinical applications in the management of lymphomatous diseases in pet dogs (23–36). With rising clinical interest in bone marrow transplantation (including total body irradiation for marrow ablation) in pet dogs with high grade (non-Hodgkin's) multicentric lymphomas, opportunities exist to test novel radiomitigators (37). Certainly, infrastructure exists to enable canine clinical trials to study radiation-modifying drugs and devices. A classic example is a 1986 paper describing the role of canine comparative radiation oncology research in early development of the FDA-approved radioprotector amifostine (WR-2721); a bi-institutional canine clinical trial was performed, in which 73 pet dogs with spontaneously occurring soft tissue sarcomas were randomized (over a period of 3 years) to two dose response assays to receive irradiation alone, or with the radioprotector WR-2721 (38). With the dose and schedule used (40 mg/kg given intravenously, 15 min before each of 10 radiation fractions), WR-2721 provided no protection against acute skin reactions, little to no protection against late complications, and there was a suggestion that the drug protocol provided protection of the tumors at the low end of the radiation dose range. A contemporary example of how a similar study design can be deployed is provided by ongoing research by two authors of this review; both Nolan and Boss are involved in an NIH-sponsored bi-institutional canine clinical trial (5R01CA232148-02) which is currently enrolling 104 dogs with spontaneously occurring soft tissue sarcomas (over a 5 year period) to determine the safety of, and radiation enhancement provided by ultrasound-guided oxygen release from microbubbles. Conduct of these large-scale studies has historically been overseen and facilitated by clinical study coordinators and study teams at the local institutions. Today, large-scale multi-center trials can be coordinated by the Comparative Oncology Program (COP), which is a core resource of the Center for Cancer Research at the National Cancer Institute. The COP centrally manages a network of 20 academic comparative oncology centers; these centers comprise the Comparative Oncology Trials Consortium (COTC). Similarly, and with support from the V-Foundation, a second trials network is currently being planned. As envisioned, that group, called the Canine Oncology Research Consortium (CORC), will include multiple academic partners, with each partner defined as an academic veterinary center paired with an NCI-designated Comprehensive Cancer Center. Both the COP/COTC and CORC exemplify the expanded support that is now available for efficient conduct of canine comparative oncology clinical trials.

Another contemporary example of how normal tissue toxicity data can be directly gathered from pet dogs is provided by an author of this review; while not yet published, Nolan et al., have presented an abstract which describes how pain can be measured and modeled in dogs in pet dogs that develop acute radiodermatitis while undergoing post-operative RT for incompletely excised extremity soft tissue sarcomas (39). Their work not only indicated that mechanical quantitative sensory testing can be used as a reliable tool for preclinical evaluation of novel analgesic strategies, but also provides evidence that localized RT-induced pain is accompanied by widespread somatosensory sensitization. That set of experiments provides a template for how pet dog studies might fit into the traditional paradigm of therapeutic development: (1) hypothesis generating observations can first be made in people or dogs undergoing cancer therapy; (2) mechanistic studies can then be performed in more conventional preclinical models; (3) novel therapies that arise from the preclinical work can then be efficiently testing in dogs, to provide proof-of-concept for safety and clinical efficacy, before advancing to early phase human clinical trials.

Tumor Microenvironment

Tumor hypoxia is associated with relative radioresistance and aggressive biological behavior. Canine comparative oncology research has contributed meaningfully to the advancement of radiobiology research through tumor oxygenation studies. To validate canine cancer as a translationally relevant model of tumor hypoxia, Cline et al. detected the *in vivo* binding of a 2-nitroimidazole hypoxia (CCI-103F) marker in histochemical sections of canine tumors (40). The binding pattern was consistent with the expected location of hypoxic cells in tissues for which oxygen concentration gradients have been established by diffusion. The hypoxic fractions appeared in regions adjacent to necrosis, but also in regions free of necrosis. In addition to interest in hypoxic cells, populations of both non-cycling quiescent cells and rapidly-cycling proliferating cells can also influence tumor radioresponses. Zeman et al. investigated the relationships between hypoxia and proliferative status semi-quantitatively via immunohistochemical analysis of CCI-103F and proliferating cell nuclear antigen (PCNA), respectively, in canine tumor samples (41). Tumors with both high and low hypoxic and proliferative area fractions were identified; the hypoxic and proliferative cell populations overlapped to varying extents.

Direct, real-time quantification of tissue oxygenation was enabled by emergence of the Eppendorf method of direct oxygen partial pressure measurements. This technique, which involves intratumoral placement of polargraphic oxygen needle electrodes, opened the door for comparative veterinary trials characterizing the tumor microenvironmental effects of hypoxia in spontaneous canine tumors; it also allowed trials designed to investigate the impact of tumor oxygenation on treatment outcomes. Achermann et al. evaluated the oxygenation of canine soft tissue sarcomas via the Eppendorf method and determined that 44% of tumors had oxygenation measurements consistent with hypoxia (42). Soon after, trials were performed in dogs undergoing fractionated RT. Polarographic needle electrodes and OxyLite fluorescence probes were used to document the presence and changes of hypoxia during fractionated RT; 58% of the dog tumors in one study were hypoxic prior to treatment (43). The pO_2 of initially hypoxic tumors remained unchanged during fractionated RT, whereas the pO_2 decreased in initially normoxic tumors. Brurberg et al. evaluated pO_2 fluctuations in spontaneous canine tumors prior to and during RT (44). It was found that overall oxygenation status differed substantially among the tumors, and RT had no consistent effect on overall oxygenation status. Fluctuations in pO_2 were detected in both unirradiated and irradiated tumors, and those fluctuations were independent of the baseline tumor oxygenation status. This study was important as it demonstrated for the first time in canine cancer the dynamic changes in tumor oxygenation in spontaneous tumors over an extended time period. The influence of tumor oxygenation status on the response to RT was first described for spontaneous canine tumors by Bley et al. (45). Pretreatment oxygen level measurements in spontaneous canine tumors were correlated with local tumor response after RT; after curative-intent full-course irradiation, hypoxic tumors had a significantly shorter median progression-free interval and a shorter overall survival time compared to better oxygenated tumors.

Comparative canine oncology trials were instrumental to understanding how hyperthermia can be combined with RT to improve tumor control. A number of positive randomized studies in dogs provided initial evidence supporting the therapeutic benefit of such combinatorial therapy (46–48). In canine soft tissue sarcomas (STS), Vujaskovic et al. identified changes in tumor oxygenation, extracellular pH, and blood flow after hyperthermia (49). They also found that hyperthermia has biphasic effects on tumor physiologic parameters: lower temperatures tend to favor improved perfusion and oxygenation, whereas higher temperatures are more likely to cause vascular damage, leading to greater hypoxia.

EMERGING USES OF DOGS IN TRANSLATIONAL RADIATION RESEARCH

Imaging/Theranostics

Canine comparative oncology studies that incorporate functional imaging technologies have been used to characterize the tumor microenvironment, improve target delineation, optimize biological dose delivery, and correlate imaging characteristics with clinical outcomes. Building upon the early oxygenation and radioresponse research which relied on tissue sampling or direct insertion of electrodes for measurements, functional imaging studies provide opportunities for serial, non-invasive, quantitative or semi-quantitative analyses of the tumor microenvironment without tissue disruption (**Figure 1**).

Various positron emission tomography (PET) radiotracers have been used in comparative oncology studies to characterize the tumor microenvironment. The glucose analog 2-deoxy-2-[^{18}F]-Fluoro-D-glucose (FDG), a marker of glucose uptake, is the most commonly used PET tracer in clinical oncology, and canine cancer patients were among the earliest to be imaged with FDG PET (51). FDG PET/CT has become increasingly available in veterinary medicine (52), and it has been used to characterize tumor biology and treatment responses (53–57).

As tumor hypoxia is associated with both radioresistance and tumor aggressiveness, PET-based approaches have been developed for measuring tumor hypoxia (**Figure 2**). Bruehlmeier et al. were the first to examine tumor hypoxia in canine STS using [^{18}F]-fluoromisonidazole ([^{18}F]-FMISO); FMISO tumor oxygenation measurements correlated well with Eppendorf electrode measurements (58). However, when evaluating tumor hypoxia via [^{18}F]-FMISO in cats with fibrosarcomas, the polarographic pO_2 measurements did not confirm PET results; this lack of concordance was attributed to extensive tumor necrosis, and heterogeneous patterns of hypoxia (59). An alternative hypoxia imaging tracer is ^{64}Cu-ATSM. Hansen et al. performed a study to compare uptake characteristics of pimonidazole immunohistochemistry (IHC) to ^{64}Cu-ATSM autoradiography, and to PET uptake levels of ^{64}Cu-ATSM and [^{18}F]-FDG in spontaneous canine sarcomas and carcinomas (60). Tumors with high levels of pimonidazole staining displayed high uptake of [^{18}F]-FDG and ^{64}Cu-ATSM; the regional distribution of ^{64}Cu-ATSM and pimonidazole correlated with each other in heterogeneous tumor regions. The potential of using ^{64}Cu-ATSM to characterize the tumor microenvironment longitudinally over time was evaluated in canine tumors by measuring tumor uptake and distribution characteristics between consecutive PET scans (61). In this study, ^{64}Cu-ATSM uptake was also compared to uptake and spatial distributions of [^{18}F]-FDG and dynamic contrast enhanced perfusion CT perfusion maps. ^{64}Cu-ATSM uptake was positively correlated to FDG, signal was relatively stable between PET scans, and temporal changes were observed in hypo-perfused regions. ^{64}Cu-ATSM PET/CT scan has also been used to detect hypoxia in feline head and neck squamous cell carcinoma (HNSCC), with PET/CT results verified by pimonidazole IHC and O_2 detection probes (62).

Comparative canine oncology trials have supported investigations into the kinetics of established and novel PET/CT approaches, as well as characterization of the spatial distribution of these biological markers (63–65). Bradshaw et al. concurrently evaluated the predictive value of numerous quantitative imaging biomarkers derived from multitracer PET imaging in tumors before and during RT in dogs with sinonasal tumors (66). The strongest predictors of poor outcome were derived from fluorothymidine (FLT) imaging, a marker of proliferation. The

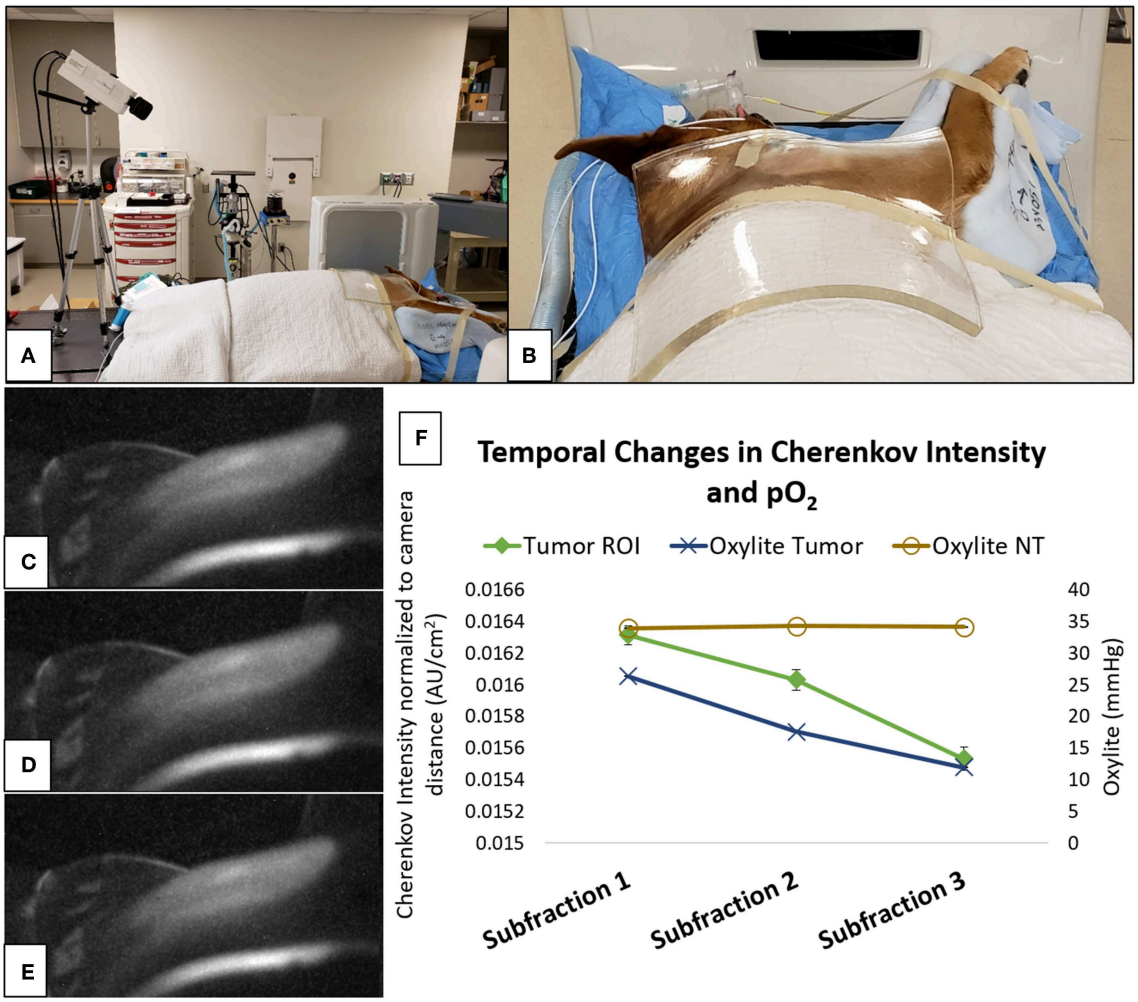

FIGURE 1 | Cherenkov imaging represents a non-invasive method for quantification of tumor oxygenation during radiation delivery, and is currently being validated in a canine clinical trial (50). **(A)** camera setup for Cherenkov image acquisition during irradiation of a soft tissue sarcoma on the right shoulder of a dog, including a clear/colorless 1 centimeter thick bolus material overlying the tumor and used for radiation dose-buildup; **(B)** "camera's-eye" view of the irradiation target—fur overlying the tumor has been removed; **(C–E)** representative Cherenkov images taken during a single radiation fraction that was delivered using the setup depicted in **(A,B)**; **(F)** relative to stable normal tissue (NT) oxygenation, reductions in both Oxylite measurements and Cherenkov intensity within the tumor region of interest (ROI) demonstrate that the tumor became progressively more hypoxic during delivery of this 6 Gy radiation fraction. Subtle visible changes within the tumor ROI (the centrally-located light areas on Cherenkov images **C–E**) correspond to reductions in signal intensity (subfractions 1–3, respectively, on the graph) that were measured using digital image processing tools (images courtesy of Ashlyn Rickard, Duke University).

combination of high mid-treatment standardized uptake values (SUV_{max}) and large decreases in FLT signal from pretreatment to mid-treatment was associated with worse clinical outcome. In this study, neither FDG PET nor Cu-ATSM PET were predictive of outcome. PET/CT has also been utilized in comparative oncology studies to investigate the potential for radiation "dose painting," which aims to improve therapeutic outcomes by increasing radiation dose in tumor regions that are identified as being at risk of relative radioresistance based upon imaging features (67, 68). Early results have been mixed.

Dynamic contrast-enhanced magnetic resonance imaging (DCE-MRI) can be used to assess tumor physiology by exploiting abnormal tumor microvasculature (**Figure 3**). This enables quantitative assessment of tissue vessel density, integrity, and permeability (69). In a canine STS study, DCE-MRI was performed before and following the first hyperthermia treatment, and parameters associated with increased tumor perfusion were predictive for overall and metastasis-free survival (70). This was the first time that DCE-MRI was shown to be predictive of clinical outcome for STS. A subsequent study performed an integrative analysis of gene expression and diffusion weighted imaging (DWI) parameters, pre- and post-treatment, in dogs with STS treated with thermoradiotherapy. DWI is an MRI-based technique which quantifies the diffusion of water to characterize tumor tissue (71). Significant correlations were identified between gene expression and DWI. An unsupervised

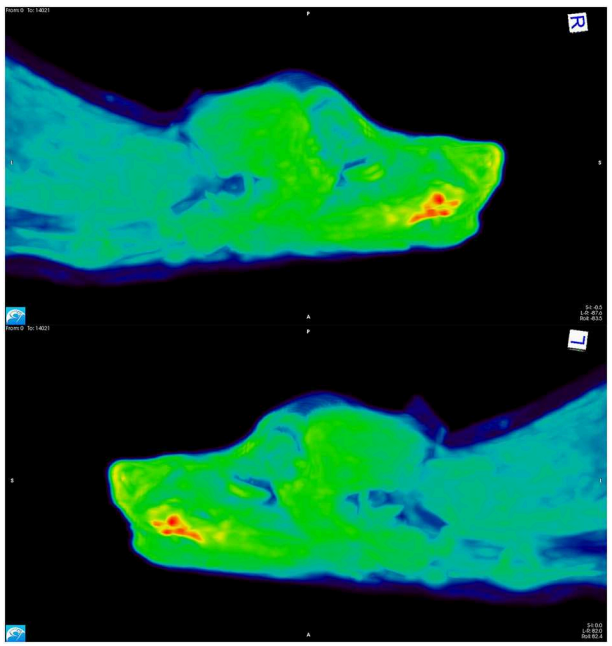

FIGURE 2 | [^{18}F]-FAZA PET scan images from a dog with a squamous cell carcinoma on the ventral aspect of the tongue. The areas depicted in red have high uptake of the tracer, indicating hypoxia; the yellow and green regions have intermediate uptake, and the blue areas have low tracer uptake, thus indicating the presence of well-oxygenated tissue.

analysis of the gene sets revealed two clusters: (1) tumors with an increase in tissue water content (corresponding to an increased ADC on the DWI) after treatment showed increases in genes associated with tissue remodeling (e.g., IL1β, IL6, IL8, IL10) and inflammation (e.g., MMP1, TGFβ); (2) tumors with less change in the ADC had more signs of more mature vasculature (i.e., higher gene expression of CD31 and vWF). These observations demonstrated how one can link changes in tumor physiology to changes in gene expression. This work demonstrates how early changes in functional imaging parameters might be used to aid in prognostication. Furthermore, the authors provided a blueprint for how such data can be manipulated to identify potential new drug targets.

DNA Damage Responses

The DNA damage response (DDR) is a complex network of pathways that responds to both endogenous and exogenous DNA damage. DDR deficiencies can be targeted for cancer therapy. For example, the DDR can be inhibited as a radiosensitization strategy. Additionally, because DNA damage drives chronic inflammation and various molecular and cellular pathways of the DDR activate immune signaling (72) and since checkpoint inhibitors may work best in the setting of tumors with high mutation load, DDR inhibition during RT can generate and preserve treatment-induced DNA damage which sensitizes the tumor to subsequent checkpoint blockade (73). There are many DDR components that can be inhibited to sensitize cancer cells to DNA damaging agents, including PARP, DNA-PK$_{cs}$, ATM, ATR, Chk1, and Chk2.

Many novel agents that show great promise in mice ultimately fail to prove efficacious in humans. Despite improved rodent models, methodologies, and study designs, many factors still contribute to these failures (74). With specific regard to DDR modifiers, a recent review suggested that better predictive biomarkers are needed to identify patients that would benefit from treatment, and that better therapeutic response biomarkers are also needed to quantify the pharmacodynamic impact and clinical gains that are achieved in humans (75). Successful and efficient translation of DDR inhibitors will rely upon preclinical studies that are designed to evaluate appropriate endpoints that can also be measured in human trials; when possible, they should also determine whether synthetic lethality contributes to efficacy of the drug as a chemo-radiosensitizer.

Dogs have previously been proposed as a model for studying the DDR (76). Indeed, the intrinsic radiosensitivity of various canine tumors and tumors cell lines is increasingly well-understood (77, 78), and methods for measuring the canine DDR have also been developed, including validation of the comet assay and immunohistochemistry for phosphorylated H2AX (79).

Canine extremity osteosarcoma (OS) may be particularly useful in the development of novel DDR inhibitors that can be combined with RT—ATR, ATM, and DNA-PK inhibitors in particular. As with pediatric OS, tumor resection plus chemotherapy is the standard treatment for canine OS. However, because RT can also provide significant analgesia and local tumor control, and because tumor necrosis is a validated surrogate for local control of canine OS, an intriguing study design would be to treat OS-bearing dogs with chemoRT, with or without a novel DDR inhibitor, and subsequently pursue tumor removal to provide standard-of-care treatment to the dog, and to provide investigators access to the resected tumor, which would thus allow robust measurement of treatment effects. Furthermore, approximately half of canine OS tumors have aberrant p53 function, making it possible to compare the effects of chemo-radiosensitizing effects of ATR or DNA-PK inhibition in normal tissues and tumors that may or may not benefit from synthetic lethality (80, 81). Thus, by studying canine OS, investigators would be able to learn about both mechanisms of interaction and clinically relevant biomarkers that directly translate to a variety of human cancers in a manner that is essentially agnostic of tumor histology.

Immuno-Radiotherapy

Advanced metastatic disease is the most common cause of death in human patients and is a significant cause of death in dogs as well (82). Cancer immunotherapy is not a new concept, but interest re-emerged when in 2010 a phase 3 clinical trial in people with metastatic melanoma showed a survival advantage for those treated with ipilimumab, a monoclonal antibody that targets CTLA-4 (83). Since then, the use of immunotherapy in human clinical trials has expanded rapidly, with some amazing successes. The problem remains that the majority of patients do not respond favorably; furthermore, unacceptable and sometimes fatal toxicities have occurred (84, 85).

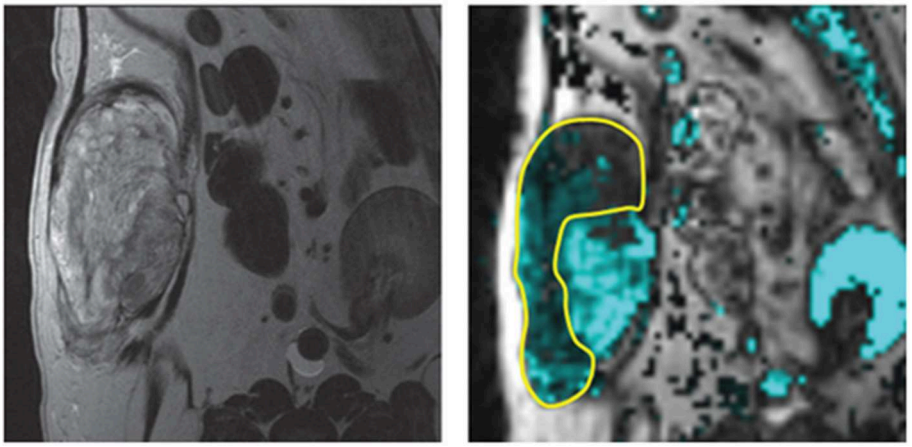

FIGURE 3 | Canine soft tissue sarcoma. Pre-treatment quantification of $iAUGC_{100}$ (initial area under the gadolinium concentration vs. time curve; this is a semi-quantitative parameter defined as a measure of the amount of contrast agent delivered to and retained by a tumor in a given time period). Outlined area represents the region with reduced perfusion and suspected hypoxic tissue. Radiation dose could be intensified to this area with the attempt to improve treatment outcome to suspected resistant tumor cell population. With permission from Boss et al. (69).

The idea that RT could induce a tumor response distant from the irradiated field has been around since the 1950s when the so-called "abscopal effect" was first proposed (86). In the context of RT, the abscopal effect refers to regression of metastatic lesions that are distant from the primary tumor and irradiated field. These are rare events; one study found 46 cases reported in the literature between 1969 and 2014 (87). That the abscopal effect occurs secondary to an immune response was first demonstrated in a 2004 mouse study which characterized radiation-induced abscopal effects as being a T-cell dependent event (88). Since that time it has become obvious that the mechanism is actually more complex, and involves a multi-faceted immune response (89).

While local irradiation can result in immunogenic cell kill by releasing neoantigens and creating local inflammation, irradiation can also attract immunosuppressive cells into the tumor microenvironment. This includes myeloid-derived suppressor cells, M2 tumor-associated macrophages and T regulatory cells; this cellular response is associated with release of cytokines (e.g., TGF-β and IL-10) which causes local immunosuppression (90). Given the clinical rarity of measurably and clinically beneficial RT-induced immune responses, and because of the potential for post-irradiation immunosuppression, it is logical that patients may benefit from a combination of RT plus immunotherapeutics that can more reliably induce beneficial systemic immune responses (91).

The dog immune system has been fairly well-characterized and shows great homology to humans (92). Because of these similarities, pet dogs with cancer can provide a useful model when looking to translate potential new radioimmunotherapies from mouse studies to human clinical trials.

Several small clinical trials using radio-immunotherapy protocols in dogs have been published. One recent example involved testing a novel immunotherapy combination in dogs with metastatic melanomas and sarcomas. Immediately after each fraction of primary tumor irradiation, intratumoral injections of canine CpG oligodeoxynucleotides [CpG ODNs; immune stimulatory toll-like receptor 9 (TLR9) agonists] were done; dogs were also orally dosed with 1-methyl-tryptophan [an indolamine-2,3 dioxygenase (IDO) inhibitor] (93). The idea was that localized tumor irradiation would induce immunogenic cell death, the CpG ODNs would stimulate an immune response, and the IDO checkpoint inhibitor would counter tumor-induced immunosuppression. The dog trial was paired with mouse studies which revealed a rebound immunosuppression after mice were treated with radiation or CpG ODNs alone. While all dogs showed a local response to irradiation, there were also abscopal responses in their metastatic lesions with one dog having a complete response, two having partial responses, one with stable disease and one with progressive disease (**Figure 4**). There was no toxicity beyond what was expected for a palliative course of localized RT. Interestingly, both circulating and tumoral T regulatory cells were decreased in the dogs who responded and increased in the dog with progressive disease—suggesting this as a potential biomarker. Due to the promising preliminary results and the lack of toxicity in dogs a clinical trial using this same strategy has now opened for people with advanced metastatic cancers (94).

In another study using an adoptive immunotherapy approach combined with RT, dog natural killer cells were isolated from peripheral blood (95). Those cells could be expanded and activated, and NK cells were capable of killing osteosarcoma tumor cells *in vitro*. Furthermore, cytotoxicity was improved when tumor cells were pretreated with ionizing radiation. This was repeated *in vivo* using canine patient-derived xenograft (PDX) tumors; adoptively-transferred canine NK cells delayed the growth of tumors in mice, and focal irradiation increased

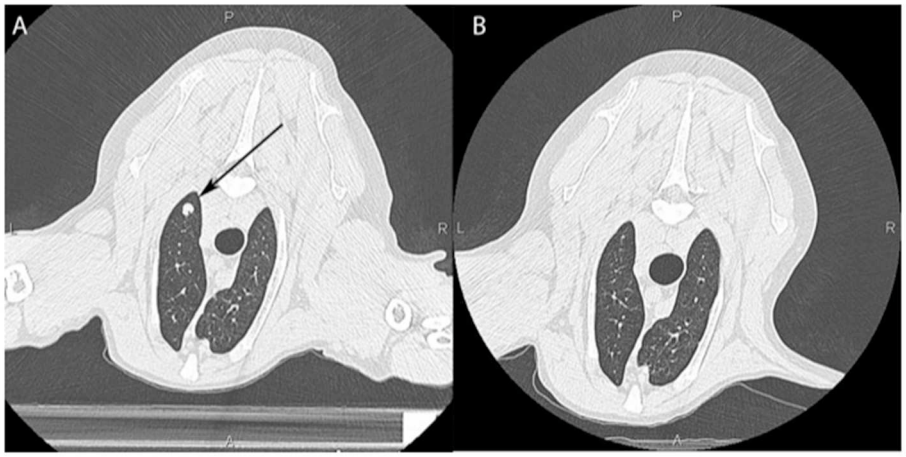

FIGURE 4 | Computed tomographic image of a dog's lungs showing a metastatic lesion (arrow) taken prior to local irradiation of an oral tumor **(A)** and 3 months post treatment **(B)** showing an abscopal effect with near complete resolution of the mass.

NK cell homing to these sarcoma xenografts. As part of the same study, a proof of concept clinical trial was carried out in 10 dogs with osteosarcoma. Treatment consisted of a course of palliative-intent RT followed by two intra-lesional injections of autologous activated canine NK cells. The NK cells were isolated, expanded, and activated *ex vivo* and supplemented with rhIL-2. The study demonstrated that NK cells persisted at the local tumor site for at least 1 week after injection. There was acceptable toxicity and in one of the cases there was resolution of a suspected metastatic lung nodule suggesting a possible abscopal effect.

Despite these early successes, there are several challenges in carrying out immune-RT trials in dogs, including: (1) limited availability of validated reagents, canine-specific monoclonal antibodies, and canine interleukins; and (2) limited access to properly staffed and equipped veterinary radiation oncology and RT centers (92). Work is ongoing to better characterize the canine immune system, and while many canine-specific antibodies are still not commercially available, this is improving. The majority of available checkpoint inhibitors are humanized monoclonal antibodies for which commercially available caninized versions do not exist. Furthermore, while it is possible to use recombinant human interleukins in dogs (they have been shown to be effective), there is concern that with prolonged use dogs could develop neutralizing antibodies and/or adverse immune reactions to the human-derived products. Thus, it will be difficult to fully realize the potential of this model until more immunotherapies become available for safe use in dogs.

FUTURE DIRECTIONS

The existing experimental animal models (e.g., rodents, zebrafish) are, and will remain, vitally important for *in vivo* radiation oncology research. Yet, there are opportunities in using pet dogs that have not been fully explored; pet dogs with spontaneously arising tumors can better inform the use of RT for clinical management of various human cancers. All of the topics discussed above will continue to spawn new research. Some of the additional areas where companion animal studies could make an impact in human medicine include radiobiology studies looking at different dosing and fractionation schemes, *in vivo* dosimetry, and testing of newly developed radiation sensitizing and radiation mitigating agents.

Small animal irradiators used in rodent research are increasingly sophisticated, but remain unable to recapitulate medical linear accelerators in terms of beam energy and dose rate (96, 97). Because companion animal oncology patients are routinely treated using standard clinical linear accelerators, they are also readily available for studies that seek to better understand the radiobiological effects of such factors as spatial fractionation (e.g., GRID and Lattice RT) and dose rate (e.g., FLASH-RT) (98, 99). For example, canine tumors are particularly well-suited to understanding the underlying biology of FLASH-RT. This is because the apparent selective normal tissue sparing (vs. tumor sparing) achieved by FLASH-RT is likely dependent upon pO_2; and as discussed above, because the size and growth rate of canine tumors is more similar to human cancers than experimentally-induced tumors in rodents, the oxygen (hypoxia) profiles of canine tumors also tend to be similar to those of human tumors. FLASH-RT also provides a particularly good example of how studies in companion animal species can be used as an intermediate step in scaling technologies from geometries that work for rodents, to those that would work well in the context of human tumors (100). In much the same way that treatment of canine intranasal tumors was used in the early development of helical Tomotherapy, these types of companion animal studies provide an excellent vehicle for testing the safety of, and establishing feasible clinical workflows for, novel treatment devices and approaches (101).

One area where dog studies may be particularly useful is understanding the interplay between radiation dose and immune responses. Some *in vivo* work suggests that the ideal fractional

dose for radioimmunotherapy may be 6–8 Gy per fraction, rather than the more extreme doses that are commonly used in modern SRS/SBRT (89, 102). Interestingly, a recent study showed an inverse relationship between radiation dose and survival in humans having undergone RT for stage III non-small cell lung cancer; worsening outcomes with increasing radiation dose was counterintuitive but may have been attributable to delivery of higher radiation doses to tumor-infiltrating immune cells. Hypofractionation is commonly used in veterinary medicine both for palliation, and in SRS/SBRT; this practice pattern makes it relatively straightforward to interpose scientific research into clinical practice in order to use dogs as a model for studying the biology of hypofractionation.

Research in the field of therapeutic radiation physics could also benefit from a canine comparative radiation oncology approach. Because of similarities between human and canine anatomy and treatment approach, dogs can be a valuable model for validation of new techniques and methods; this use of canine comparative radiation oncology research has been exemplified for *in vivo* dosimetry (103).

There are also several limitations of the canine "model" that must be addressed. First, access to clinical outcomes data, and canine cancer tissues is limited; at the present time, there are no canine cancer registries in the United States, there are few well-validated canine cancer cell lines, and there are very few well-curated canine cancer tissue banks exist. Second, while dogs and their cancers more closely recapitulate the geometry of human cancers than do tumors of rodents, it should be noted that many pet dogs weigh far less than half the average human adult. Third, while there are many similarities between various human and canine malignancies, important differences also exist. For example, while human prostate cancer most often arises from the glandular acini, carcinomas of the canine prostate seem to most often be of urothelial origin. And although IDH1 and IDH2 mutations are frequent in human gliomas, they are not a consistent or common feature of the canine condition (104). The value of any model system is maximized by understanding its strengths and limitations; thus, moving forward, it will be of utmost importance to focus significant energy on describing the biology of canine cancers, and making rigorous comparisons with the analogous human conditions.

Though the field of canine comparative radiation oncology research is still in its infancy, canine studies have already helped advance the understanding of human tumor biology and treatment. Through continued efforts to improve our understanding of canine tumor biology, and careful application of the canine comparative oncology model, we expect that man's best friend will be key to reducing the global burden of cancer and improving cancer care.

AUTHOR CONTRIBUTIONS

MN, MK, and M-KB each contributed to the drafting and editing of this manuscript, and each also approved the final version.

FUNDING

This work was supported in part by NIH R01 CA204723-03, and a seed grant from the Consortium for Canine Comparative Oncology (a joint initiative of the NC State University College of Veterinary Medicine, and Duke University's Duke Cancer Institute).

ACKNOWLEDGMENTS

The authors thank Ms. Ashlyn Rickard (Duke University) for her assistance with figure preparation.

REFERENCES

1. Farrelly J, McEntee MC. A survey of veterinary radiation facilities in 2010. *Vet Radiol Ultrasound.* (2014) 55:638–43. doi: 10.1111/vru.12161
2. McEntee MC. A survey of veterinary radiation facilities in the United States during 2001. *Vet Radiol Ultrasound.* (2004) 45:476–9. doi: 10.1111/j.1740-8261.2004.04082.x
3. Angstadt AY, Motsinger-Reif A, Thomas R, Kisseberth WC, Guillermo Couto C, Duval DL, et al. Characterization of canine osteosarcoma by array comparative genomic hybridization and RT-qPCR: signatures of genomic imbalance in canine osteosarcoma parallel the human counterpart. *Genes Chromosomes Cancer.* (2011) 50:859–74. doi: 10.1002/gcc.20908
4. Angstadt AY, Thayanithy V, Subramanian S, Modiano JF, Breen M. A genome-wide approach to comparative oncology: high-resolution oligonucleotide aCGH of canine and human osteosarcoma pinpoints shared microaberrations. *Cancer Genet.* (2012) 205:572–87. doi: 10.1016/j.cancergen.2012.09.005
5. Sakthikumar S, Elvers I, Kim J, Arendt ML, Thomas R, Turner-Maier J, et al. SETD2 is recurrently mutated in whole-exome sequenced canine osteosarcoma. *Cancer Res.* (2018) 78:3421–31. doi: 10.1158/0008-5472.CAN-17-3558
6. Connolly NP, Shetty AC, Stokum JA, Hoeschele I, Siegel MB, Miller CR, et al. Cross-species transcriptional analysis reveals conserved and host-specific neoplastic processes in mammalian glioma. *Sci Rep.* (2018) 8:1180. doi: 10.1038/s41598-018-19451-6
7. Koehler JW, Miller AD, Miller CR, Porter B, Aldape K, Beck J, et al. A revised diagnostic classification of canine glioma: towards validation of the canine glioma patient as a naturally occurring preclinical model for human glioma. *J Neuropathol Exp Neurol.* (2018) 77:1039–54. doi: 10.1093/jnen/nly085
8. Warren SL, Whipple GH. Roentgen ray intoxication: I. Unit dose over thorax negative over abdomen lethal Epithelium of small intestine sensitive to X-rays. *J Exp Med.* (1922) 35:187–202. doi: 10.1084/jem.35.2.187
9. Trum BF, Shively JN, Kuhn USG, Carll WT. Radiation injury and recovery in swine. *Radiat Res.* (1959) 11:326–42. doi: 10.2307/3570681
10. Brown DG, Thomas RE, Jones LP, Cross FH, Sasmore DP. Lethal dose studies with cattle exposed to whole-body Co^{60} gamma radiation. *Radiat Res.* (1961) 15:675–83. doi: 10.2307/3571149
11. Shechmeister IL, Watson LJ, Cole VW, Jackson LL. The effect of x-irradiation on goldfish. I The effect of x-irradiation on survival and susceptibility of the goldfish, *Carassius auratus*, to infection by *Aeromonas salmonicida* and *Gyrodactylus* spp. *Radiat Res.* (1962) 16:89–97. doi: 10.2307/3571133
12. Gentilini F, Turba ME, Forni M, Cinotti S. Complete sequencing of full-length canine ataxia telangiectasia mutated mRNA and characterization of its putative promoter. *Vet Immunol Immunopathol.* (2009) 128:437–40. doi: 10.1016/j.vetimm.2008.12.006
13. Koike M, Yutoku Y, Koike A. Cloning, localization and focus formation at DNA damage sites of canine Ku70. *J Vet Med Sci.* (2017) 79:554–61. doi: 10.1292/jvms.16-0649

14. Koike M, Yutoku Y, Koike A. Cloning, localization and focus formation at DNA damage sites of canine XLF. *J Vet Med Sci.* (2017) 79:22–8. doi: 10.1292/jvms.16-0440
15. Poulson JM, Vujaskovic Z, Gillette SM, Chaney EL, Gillette EL. Volume and dose-response effects for severe symptomatic pneumonitis after fractionated irradiation of canine lung. *Int J Radiat Biol.* (2000) 76:463–8. doi: 10.1080/095530000138457
16. Emami B, Lyman J, Brown A, Coia L, Goitein M, Munzenrider JE, et al. Tolerance of normal tissue to therapeutic irradiation. *Int J Radiat Oncol Biol Phys.* (1991) 21:109–22. doi: 10.1016/0360-3016(91)90171-Y
17. Kinsella TJ, DeLuca AM, Barnes M, Anderson W, Terrill R, Sindelar WF. Threshold dose for peripheral neuropathy following intraoperative radiotherapy (IORT) in a large animal model. *Int J Radiat Oncol Biol Phys.* (1991) 20:697–701. doi: 10.1016/0360-3016(91)90011-R
18. Johnstone PAS, Deluca AM, Bacher JD, Hampshire VA, Terrill RE, Anderson WJ, et al. Clinical toxicity of peripheral nerve to intraoperative radiotherapy in a canine model. *Int J Radiat Oncol Biol Phys.* (1995) 32:1031–4. doi: 10.1016/0360-3016(95)00028-W
19. LeCouteur RA, Gillette EL, Powers BE, Child G, McChesney SL, Ingram JT. Peripheral neuropathies following experimental intraoperative radiation therapy (IORT). *Int J Radiat Oncol Biol Phys.* (1989) 17:583–90. doi: 10.1016/0360-3016(89)90110-7
20. Nolan MW, Marolf AJ, Ehrhart EJ, Rao S, Kraft SL, Engel S, et al. Pudendal nerve and internal pudendal artery damage may contribute to radiation-induced erectile dysfunction. *Int J Radiat Oncol Biol Phys.* (2015) 91:796–806. doi: 10.1016/j.ijrobp.2014.12.025
21. King CR, Brooks JD, Gill H, Presti JC Jr. Long-term outcomes from a prospective trial of stereotactic body radiotherapy for low-risk prostate cancer. *Int J Radiat Oncol Biol Phys.* (2012) 82:877–82. doi: 10.1016/j.ijrobp.2010.11.054
22. Kim DW, Cho LC, Straka C, Christie A, Lotan Y, Pistenmaa D, et al. Predictors of rectal tolerance observed in a dose-escalated phase 1–2 trial of stereotactic body radiation therapy for prostate cancer. *Int J Radiat Oncol Biol Phys.* (2014) 89:509–17. doi: 10.1016/j.ijrobp.2014.03.012
23. Storb R, Epstein RB, Ragde H, Bryant J, Thomas ED. Marrow engraftment by allogeneic leukocytes in lethally irradiated dogs. *Blood.* (1967) 30:805–11. doi: 10.1182/blood.V30.6.805.805
24. Weiden PL, Storb R, Lerner KG, Kao GF, Graham TC, Thomas ED. Treatment of canine malignancies by 1200 R total body irradiation and autologous marrow grafts. *Exp Hematol.* (1975) 3:124–34.
25. Deeg HJ, Meyers JD, Storb R, Graham TC, Weiden PL. Effect of trimethoprim-sulfamethoxazole on hematological recovery after total body irradiation and autologous marrow infusion in dogs. *Transplantation.* (1979) 28:243–6. doi: 10.1097/00007890-197909000-00017
26. Kolb H, Sale GE, Lerner KG, Storb R, Thomas ED. Pathology of acute graft-versus-host disease in the dog. An autopsy study of ninety-five dogs. *Am J Pathol.* (1979) 96:581–94.
27. Weiden PL, Storb R, Deeg HJ, Graham TC, Thomas ED. Prolonged disease-free survival in dogs with lymphoma after total-body irradiation and autologous marrow transplantation consolidation of combination-chemotherapy-induced remissions. *Blood.* (1979) 54:1039–49. doi: 10.1182/blood.V54.5.1039.1039
28. Deeg HJ, Storb R, Prentice R, Fritz TE, Weiden PL, Sale GE, et al. Increased cancer risk in canine radiation chimeras. *Blood.* (1980) 55:233–9. doi: 10.1182/blood.V55.2.233.233
29. Deeg HJ, Prentice R, Fritz TE, Sale GE, Lombard LS, Thomas ED, et al. Increased incidence of malignant tumors in dogs after total body irradiation and marrow transplantation. *Int J Radiat Oncol Biol Phys.* (1983) 9:1505–11. doi: 10.1016/0360-3016(83)90325-5
30. Shulman HM, Luk K, Deeg HJ, Shuman WB, Storb R. Induction of hepatic veno-occlusive disease in dogs. *Am J Pathol.* (1987) 126:114–25.
31. Deeg HJ, Storb R, Longton G, Graham TC, Shulman HM, Appelbaum F, et al. Single dose or fractionated total body irradiation and autologous marrow transplantation in dogs: effects of exposure rate, fraction size, and fractionation interval on acute and delayed toxicity. *Int J Radiat Oncol Biol Phys.* (1988) 15:647–53. doi: 10.1016/0360-3016(88)90307-0
32. Storb R, Raff RF, Graham T, Appelbaum FR, Deeg HJ, Schuening FG, et al. Marrow toxicity of fractionated vs. single dose total body irradiation is identical in a canine model. *Int J Radiat Oncol Biol Phys.* (1993) 26:275–83. doi: 10.1016/0360-3016(93)90207-C
33. Storb R, Raff RF, Appelbaum FR, Deeg HJ, Graham TC, Schuening FG, et al. Fractionated versus single-dose total body irradiation at low and high dose rates to condition canine littermates for DLA-identical marrow grafts. *Blood.* (1994) 83:3384–9. doi: 10.1182/blood.V83.11.3384.3384
34. Storb R, Raff R, Deeg HJ, Graham T, Appelbaum FR, Schuening FG, et al. Dose rate-dependent sparing of the gastrointestinal tract by fractionated total body irradiation in dogs given marrow autografts. *Int J Radiat Oncol Biol Phys.* (1998) 40:961–6. doi: 10.1016/S0360-3016(97)00913-9
35. Storb R, Raff RF, Graham T, Appelbaum FR, Deeg HJ, Schuening FG, et al. Dose rate-dependent marrow toxicity of TBI in dogs and marrow sparing effect at high dose rate by dose fractionation. *Biol Blood Marrow Transplant.* (1999) 5:155–61. doi: 10.1053/bbmt.1999.v5.pm10392961
36. Graves SS, Storer BE, Butts TM, Storb R. Comparing high and low total body irradiation dose rates for minimum-intensity conditioning of dogs for dog leukocyte antigen-identical bone marrow grafts. *Biol Blood Marrow Transplant.* (2013) 19:1650–4. doi: 10.1016/j.bbmt.2013.08.007
37. Gieger TL, Nolan MW, Roback DM, Suter SE. Implementation of total body photon irradiation as part of an institutional bone marrow transplant program for the treatment of canine lymphoma and leukemias. *Vet Radiol Ultrasound.* (2019) 60:586–93. doi: 10.1111/vru.12776
38. McChesney SL, Gillette EL, Dewhirst MW, Withrow SJ. Influence of WR 2721 on radiation response of canine soft tissue sarcomas. *Int J Radiat Oncol Biol Phys.* (1986) 12:1957–63. doi: 10.1016/0360-3016(86)90132-X
39. Kelsey KL, Lascelles BDX, Enomoto M, Gieger TL, Nolan MW. Widespread central sensitization is associated with acute radiation dermatitis in pet dogs undergoing radiotherapy for spontaneous tumors. In: *63rd Annual Meeting of the Radiation Research Society*. Cancun (2017).
40. Cline J, Thrall D, Page R, Franko A, Raleigh J. Immunohistochemical detection of a hypoxia marker in spontaneous canine tumours. *Br J Cancer.* (1990) 62:925. doi: 10.1038/bjc.1990.411
41. Zeman EM, Calkins DP, Cline JM, Thrall DE, Raleigh JA. The relationship between proliferative and oxygenation status in spontaneous canine tumors. *Int J Radiat Oncol Biol Phys.* (1993) 27:891–8. doi: 10.1016/0360-3016(93)90465-8
42. Achermann R, Ohlerth S, Fidel J, Gardelle O, Gassmann M, Roos M, et al. Ultrasound guided, pre-radiation oxygen measurements using polarographic oxygen needle electrodes in spontaneous canine soft tissue sarcomas. *In Vivo.* (2002) 16:431–7.
43. Achermann RE, Ohlerth SM, Bley CR, Gassmann M, Inteeworn N, Roos M, et al. Oxygenation of spontaneous canine tumors during fractionated radiation therapy. *Strahlenther Onkol.* (2004) 180:297–305. doi: 10.1007/s00066-004-1193-6
44. Brurberg KG, Skogmo HK, Graff BA, Olsen DR, Rofstad EK. Fluctuations in pO_2 in poorly and well-oxygenated spontaneous canine tumors before and during fractionated radiation therapy. *Radiother Oncol.* (2005) 77:220–6. doi: 10.1016/j.radonc.2005.09.009
45. Bley CR, Ohlerth S, Roos M, Wergin M, Achermann R, Kaser-Hotz B. Influence of pretreatment polarographically measured oxygenation levels in spontaneous canine tumors treated with radiation therapy. *Strahlenther Onkol.* (2006) 182:518–24. doi: 10.1007/s00066-006-1519-7
46. Dewhirst MW, Sim DA, Sapareto S, Connor WG. Importance of minimum tumor temperature in determining early and long-term responses of spontaneous canine and feline tumors to heat and radiation. *Cancer Res.* (1984) 44:43–50.
47. Gillette EL, McChesney SL, Dewhirst MW, Scott RJ. Response of canine oral carcinomas to heat and radiation. *Int J Radiat Oncol Biol Phys.* (1987) 13:1861–7. doi: 10.1016/0360-3016(87)90353-1
48. Gillette SM, Dewhirst M, Gillette E, Thrall D, Page R, Powers B, et al. Response of canine soft tissue sarcomas to radiation or radiation plus hyperthermia: a randomized phase II study. *Int J Hyperthermia.* (1992) 8:309–20. doi: 10.3109/02656739209021786
49. Vujaskovic Z, Poulson JM, Gaskin AA, Thrall DE, Page RL, Charles HC, et al. Temperature-dependent changes in physiologic parameters of spontaneous canine soft tissue sarcomas after combined radiotherapy and hyperthermia treatment. *Int J Radiat Oncol Biol Phys.* (2000) 46:179–85. doi: 10.1016/S0360-3016(99)00362-4

50. Zhang X, Lam SK, Palmer G, Das S, Oldham M, Dewhirst M. Noninvasive measurement of tissue blood oxygenation with Cerenkov imaging during therapeutic radiation delivery. *Opt Lett.* (2017) 42:3101–4. doi: 10.1364/OL.42.003101
51. Paul R, Johansson R, Kiuru A, Illukka T, Talvio T, Roeda D, et al. Imaging of canine cancers with 18F-2-fluoro-2-deoxy-D-glucose (FDG) suggests further applications for cancer imaging in man. *Nucl Med Commun.* (1984) 5:641–6. doi: 10.1097/00006231-198410000-00006
52. Hansen AE, McEvoy F, Engelholm SA, Law I, Kristensen AT. FDG PET/CT imaging in canine cancer patients. *Vet Radiol Ultrasound.* (2011) 52:201–6. doi: 10.1111/j.1740-8261.2010.01757.x
53. LeBlanc AK, Miller AN, Galyon GD, Moyers TD, Long MJ, Stuckey AC, et al. Preliminary evaluation of serial 18fdg-pet/ct to assess response to toceranib phosphate therapy in canine cancer. *Vet Radiol Ultrasound.* (2012) 53:348–57. doi: 10.1111/j.1740-8261.2012.01925.x
54. Yoshikawa H, Randall EK, Kraft SL, LaRue SM. Comparison between 2-18f-fluoro-2-deoxy-d-glucose positron emission tomography and contrast-enhanced computed tomography for measuring gross tumor volume in cats with oral squamous cell carcinoma. *Vet Radiol Ultrasound.* (2013) 54:307–13. doi: 10.1111/vru.12016
55. Randall E, Kraft S, Yoshikawa H, LaRue S. Evaluation of 18F-FDG PET/CT as a diagnostic imaging and staging tool for feline oral squamous cell carcinoma. *Vet Comp Oncol.* (2016) 14:28–38. doi: 10.1111/vco.12047
56. Griffin LR, Thamm DH, Selmic LE, Ehrhart E, Randall E. Pilot study utilizing Fluorine-18 fluorodeoxyglucose-positron emission tomography/computed tomography for glycolytic phenotyping of canine mast cell tumors. *Vet Radiol Ultrasound.* (2018) 59:461–8. doi: 10.1111/vru.12612
57. Griffin LR, Thamm DH, Brody A, Selmic LE. Prognostic value of fluorine18 flourodeoxyglucose positron emission tomography/computed tomography in dogs with appendicular osteosarcoma. *J Vet Int Med.* (2019) 33:820–6. doi: 10.1111/jvim.15453
58. Bruehlmeier M, Kaser-Hotz B, Achermann R, Bley CR, Wergin M, Schubiger PA, et al. Measurement of tumor hypoxia in spontaneous canine sarcomas. *Vet Radiol Ultrasound.* (2005) 46:348–54. doi: 10.1111/j.1740-8261.2005.00065.x
59. Allemann K, Wyss M, Wergin M, Ohlerth S, Rohrer-Bley C, Evans S, et al. Measurements of hypoxia ([18F]-FMISO,[18F]-EF5) with positron emission tomography (PET) and perfusion using PET ([15O]-H2O) and power Doppler ultrasonography in feline fibrosarcomas. *Vet Comp Oncol.* (2005) 3:211–21. doi: 10.1111/j.1476-5810.2005.00081.x
60. Hansen AE, Kristensen AT, Jørgensen JT, McEvoy FJ, Busk M, van der Kogel AJ, et al. 64 Cu-ATSM and 18 FDG PET uptake and 64 Cu-ATSM autoradiography in spontaneous canine tumors: comparison with pimonidazole hypoxia immunohistochemistry. *Radiat Oncol.* (2012) 7:89. doi: 10.1186/1748-717X-7-89
61. Hansen AE, Kristensen AT, Law I, McEvoy FJ, Kjær A, Engelholm SA. Multimodality functional imaging of spontaneous canine tumors using 64Cu-ATSM and 18FDG PET/CT and dynamic contrast enhanced perfusion CT. *Radiother Oncol.* (2012) 102:424–8. doi: 10.1016/j.radonc.2011.10.021
62. Ballegeer EA, Madrill NJ, Berger KL, Agnew DW, McNiel EA. Evaluation of hypoxia in a feline model of head and neck cancer using 64 Cu-ATSM positron emission tomography/computed tomography. *BMC Cancer.* (2013) 13:218. doi: 10.1186/1471-2407-13-218
63. Black NF, McJames S, Rust TC, Kadrmas DJ. Evaluation of rapid dual-tracer 62Cu-PTSM+ 62Cu-ATSM PET in dogs with spontaneously occurring tumors. *Phys Med Biol.* (2007) 53:217. doi: 10.1088/0031-9155/53/1/015
64. Bradshaw TJ, Bowen SR, Jallow N, Forrest LJ, Jeraj R. Heterogeneity in intratumor correlations of 18F-FDG, 18F-FLT, and 61Cu-ATSM PET in canine sinonasal tumors. *J Nucl Med.* (2013) 54:1931–7. doi: 10.2967/jnumed.113.121921
65. Simoncic U, Jeraj R. Heterogeneity in stabilization phenomena in FLT PET images of canines. *Phys Med Biol.* (2014) 59:7937. doi: 10.1088/0031-9155/59/24/7937
66. Bradshaw TJ, Bowen SR, Deveau MA, Kubicek L, White P, Bentzen SM, et al. Molecular imaging biomarkers of resistance to radiation therapy for spontaneous nasal tumors in canines. *Int J Radiat Oncol Biol Phys.* (2015) 91:787–95. doi: 10.1016/j.ijrobp.2014.12.011
67. Clausen MM, Hansen AE, Af Rosenschold PM, Kjær A, Kristensen AT, McEvoy FJ, et al. Dose escalation to high-risk sub-volumes based on non-invasive imaging of hypoxia and glycolytic activity in canine solid tumors: a feasibility study. *Radiat Oncol.* (2013) 8:262. doi: 10.1186/1748-717X-8-262
68. Bradshaw T, Fu R, Bowen S, Zhu J, Forrest L, Jeraj R. Predicting location of recurrence using FDG, FLT, and Cu-ATSM PET in canine sinonasal tumors treated with radiotherapy. *Phys Med Biol.* (2015) 60:5211. doi: 10.1088/0031-9155/60/13/5211
69. Boss MK, Muradyan N, Thrall DE. DCE-MRI: a review and applications in veterinary oncology. *Vet Comp Oncol.* (2013) 11:87–100. doi: 10.1111/j.1476-5829.2011.00305.x
70. Viglianti BL, Lora-Michiels M, Poulson JM, Lan L, Yu D, Sanders L, et al. Dynamic contrast-enhanced magnetic resonance imaging as a predictor of clinical outcome in canine spontaneous soft tissue sarcomas treated with thermoradiotherapy. *Clin Cancer Res.* (2009) 15:4993–5001. doi: 10.1158/1078-0432.CCR-08-2222
71. Chi JT, Thrall DE, Jiang C, Snyder S, Fels D, Landon C, et al. Comparison of genomics and functional imaging from canine sarcomas treated with thermoradiotherapy predicts therapeutic response and identifies combination therapeutics. *Clin Cancer Res.* (2011) 17:2549–60. doi: 10.1158/1078-0432.CCR-10-2583
72. Nakad R, Schumacher B. DNA damage response and immune defense: links and mechanisms. *Front Genet.* (2016) 7:147. doi: 10.3389/fgene.2016.00147
73. Liontos M, Anastasiou I, Bamias A, Dimopoulos M-A. DNA damage, tumor mutational load and their impact on immune responses against cancer. *Ann Transl Med.* (2016) 4:264. doi: 10.21037/atm.2016.07.11
74. Coleman CN, Higgins GS, Brown JM, Baumann M, Kirsch DG, Willers H, et al. Improving the predictive value of preclinical studies in support of radiotherapy clinical trials. *Clin Cancer Res.* (2016) 22:3138–47. doi: 10.1158/1078-0432.CCR-16-0069
75. Weber AM, Ryan AJ. ATM and ATR as therapeutic targets in cancer. *Pharmacol Ther.* (2015) 149:124–38. doi: 10.1016/j.pharmthera.2014.12.001
76. Grosse N, van Loon B, Rohrer Bley C. DNA damage response and DNA repair - dog as a model? *BMC Cancer.* (2014) 14:203. doi: 10.1186/1471-2407-14-203
77. Maeda J, Froning CE, Brents CA, Rose BJ, Thamm DH, Kato TA. Intrinsic radiosensitivity and cellular characterization of 27 canine cancer cell lines. *PLoS ONE.* (2016) 11:e156689. doi: 10.1371/journal.pone.0156689
78. Yoshikawa H, Sunada S, Hirakawa H, Fujimori A, Elmegerhi S, Leary D, et al. Radiobiological characterization of canine malignant melanoma cell lines with different types of ionizing radiation and efficacy evaluation with cytotoxic agents. *Int J Mol Sci.* (2019) 20:841. doi: 10.3390/ijms20040841
79. Schulz N, Chaachouay H, Nytko KJ, Weyland MS, Roos M, Fuchslin RM, et al. Dynamic *in vivo* profiling of DNA damage and repair after radiotherapy using canine patients as a model. *Int J Mol Sci.* (2017) 18:16. doi: 10.3390/ijms18061176
80. Loukopoulos P, Thornton JR, Robinson WF. Clinical and pathologic relevance of p53 index in canine osseous tumors. *Vet Pathol.* (2003) 40:237–48. doi: 10.1354/vp.40-3-237
81. Kirpensteijn J, Kik M, Teske E, Rutteman GR. TP53 gene mutations in canine osteosarcoma. *Vet Surg.* (2008) 37:454–60. doi: 10.1111/j.1532-950X.2008.00407.x
82. Seyfried TN, Huysentruyt LC. On the origin of cancer metastasis. *Crit Rev Oncog.* (2013) 18:43–73. doi: 10.1615/CritRevOncog.v18.i1-2.40
83. Hodi FS, O'Day SJ, McDermott DF, Weber RW, Sosman JA, Haanen JB, et al. Improved survival with ipilimumab in patients with metastatic melanoma. *N Engl J Med.* (2010) 363:711–23. doi: 10.1056/NEJMoa 1003466
84. Puzanov I, Diab A, Abdallah K, Bingham CO III, Brogdon C, Dadu R, et al. Managing toxicities associated with immune checkpoint inhibitors: consensus recommendations from the Society for Immunotherapy of Cancer (SITC) Toxicity Management Working Group. *J Immunother Cancer.* (2017) 5:95. doi: 10.1186/s40425-017-0300-z
85. Ventola CL. Cancer immunotherapy, part 3: challenges and future trends. *Pharm Ther.* (2017) 42:514–21.
86. Mole RH. Whole body irradiation; radiobiology or medicine? *Br J Radiol.* (1953) 26:234–41. doi: 10.1259/0007-1285-26-305-234

87. Abuodeh Y, Venkat P, Kim S. Systematic review of case reports on the abscopal effect. *Curr Probl Cancer.* (2016) 40:25–37. doi: 10.1016/j.currproblcancer.2015.10.001
88. Demaria S, Ng B, Devitt ML, Babb JS, Kawashima N, Liebes L, et al. Ionizing radiation inhibition of distant untreated tumors (abscopal effect) is immune mediated. *Int J Radiat Oncol Biol Phys.* (2004) 58:862–70. doi: 10.1016/j.ijrobp.2003.09.012
89. Siva S, MacManus MP, Martin RF, Martin OA. Abscopal effects of radiation therapy: a clinical review for the radiobiologist. *Cancer Lett.* (2015) 356:82–90. doi: 10.1016/j.canlet.2013.09.018
90. Shevtsov M, Sato H, Multhoff G, Shibata A. Novel approaches to improve the efficacy of immuno-radiotherapy. *Front Oncol.* (2019) 9:156. doi: 10.3389/fonc.2019.00156
91. Baird JR, Monjazeb AM, Shah O, McGee H, Murphy WJ, Crittenden MR, et al. Stimulating innate immunity to enhance radiation therapy-induced tumor control. *Int J Radiat Oncol Biol Phys.* (2017) 99:362–73. doi: 10.1016/j.ijrobp.2017.04.014
92. Park JS, Withers SS, Modiano JF, Kent MS, Chen M, Luna JI, et al. Canine cancer immunotherapy studies: linking mouse and human. *J Immunother Cancer.* (2016) 4:97. doi: 10.1186/s40425-016-0200-7
93. Monjazeb AM, Kent MS, Grossenbacher SK, Mall C, Zamora AE, Mirsoian A, et al. Blocking indolamine-2,3-dioxygenase rebound immune suppression boosts antitumor effects of radio-immunotherapy in murine models and spontaneous canine malignancies. *Clin Cancer Res.* (2016) 22:4328–40. doi: 10.1158/1078-0432.CCR-15-3026
94. Monjazeb AM. *A Phase I/II Trial of an Indolamine 2,3 Dioxygenase Blockade, Intralesional Toll-receptor 9 Agonist, and Radiotherapy in Patients with Advanced Solid Tumors and Lymphomas.* (2019). Available online at: https://ccresources.ucdmc.ucdavis.edu/csr/clinicaltrialdisplay.csr?studynumdisplayed=UCDCC%23271&orgid=51&searchtext=-1&agegroup=-1&cancercategory=-1&piid=1551&piname=Arta%20Monjazeb&studynumber=-1&phaseid=-1 (accessed July 31, 2019).
95. Canter RJ, Grossenbacher SK, Foltz JA, Sturgill IR, Park JS, Luna JI, et al. Radiotherapy enhances natural killer cell cytotoxicity and localization in pre-clinical canine sarcomas and first-in-dog clinical trial. *J Immunother Cancer.* (2017) 5:98. doi: 10.1186/s40425-017-0305-7
96. Sharma S, Narayanasamy G, Przybyla B, Webber J, Boerma M, Clarkson R, et al. Advanced small animal conformal radiation therapy device. *Technol Cancer Res Treat.* (2017) 16:45–56. doi: 10.1177/1533034615626011
97. Verhaegen F, Dubois L, Gianolini S, Hill MA, Karger CP, Lauber K, et al. ESTRO ACROP: technology for precision small animal radiotherapy research: optimal use and challenges. *Radiother Oncol.* (2018) 126:471–8. doi: 10.1016/j.radonc.2017.11.016
98. Nolan MW, Gieger TL, Karakashian AA, Nikolova-Karakashian MN, Posner LP, Roback DM, et al. Outcomes of spatially fractionated radiotherapy (GRID) for bulky soft tissue sarcomas in a large animal model. *Technol Cancer Res Treat.* (2017) 16:357–65. doi: 10.1177/1533034617690980
99. Harrington KJ. Ultrahigh dose-rate radiotherapy: next steps for FLASH-RT. *Clin Cancer Res.* (2019) 25:3–5. doi: 10.1158/1078-0432.CCR-18-1796
100. Vozenin MC, De Fornel P, Petersson K, Favaudon V, Jaccard M, Germond JF, et al. The advantage of FLASH radiotherapy confirmed in mini-pig and cat-cancer patients. *Clin Cancer Res.* (2019) 25:35–42. doi: 10.1158/1078-0432.CCR-17-3375
101. Forrest LJ, Mackie TR, Ruchala K, Turek M, Kapatoes J, Jaradat H, et al. The utility of megavoltage computed tomography images from a helical tomotherapy system for setup verification purposes. *Int J Radiat Oncol Biol Phys.* (2004) 60:1639–44. doi: 10.1016/j.ijrobp.2004.08.016
102. Deloch L, Derer A, Hartmann J, Frey B, Fietkau R, Gaipl US. Modern radiotherapy concepts and the impact of radiation on immune activation. *Front Oncol.* (2016) 6:141. doi: 10.3389/fonc.2016.00141
103. Hsieh ES, Hansen KS, Kent MS, Saini S, Dieterich S. Can a commercially available EPID dosimetry system detect small daily patient setup errors for cranial IMRT/SRS? *Pract Radiat Oncol.* (2017) 7:e283–90. doi: 10.1016/j.prro.2016.12.005
104. Reitman ZJ, Olby NJ, Mariani CL, Thomas R, Breen M, Bigner DD, et al. IDH1 and IDH2 hotspot mutations are not found in canine glioma. *Int J Cancer.* (2010) 127:245–6. doi: 10.1002/ijc.25017

Conflict of Interest: The authors declare that the research was conducted in the absence of any commercial or financial relationships that could be construed as a potential conflict of interest.

Copyright © 2019 Nolan, Kent and Boss. This is an open-access article distributed under the terms of the Creative Commons Attribution License (CC BY). The use, distribution or reproduction in other forums is permitted, provided the original author(s) and the copyright owner(s) are credited and that the original publication in this journal is cited, in accordance with accepted academic practice. No use, distribution or reproduction is permitted which does not comply with these terms.

frontiers in Oncology

ORIGINAL RESEARCH
published: 12 December 2019
doi: 10.3389/fonc.2019.01397

Array Comparative Genomic Hybridization Analysis Reveals Significantly Enriched Pathways in Canine Oral Melanoma

Ginevra Brocca[1], Serena Ferraresso[1], Clarissa Zamboni[1], Elena M. Martinez-Merlo[2], Silvia Ferro[1], Michael H. Goldschmidt[3] and Massimo Castagnaro[1]*

[1] Department of Comparative Biomedicine and Food Science, University of Padua, Legnaro, Italy, [2] Department of Animal Medicine and Surgery, Complutense University, Madrid, Spain, [3] School of Veterinary Medicine, University of Pennsylvania, Philadelphia, PA, United States

OPEN ACCESS

Edited by:
Mark W. Dewhirst,
Duke University, United States

Reviewed by:
Jason Somarelli,
Duke University, United States
William Eward,
Duke University, United States
Steven Fiering,
Dartmouth College, United States
Miriam Kleiter,
University of Veterinary Medicine Vienna, Austria

***Correspondence:**
Ginevra Brocca
ginevra.brocca@gmail.com

Specialty section:
This article was submitted to Cancer Genetics, a section of the journal Frontiers in Oncology

Received: *23 July 2019*
Accepted: *26 November 2019*
Published: *12 December 2019*

Citation:
Brocca G, Ferraresso S, Zamboni C, Martinez-Merlo EM, Ferro S, Goldschmidt MH and Castagnaro M (2019) Array Comparative Genomic Hybridization Analysis Reveals Significantly Enriched Pathways in Canine Oral Melanoma. Front. Oncol. 9:1397. doi: 10.3389/fonc.2019.01397

Human Mucosal Melanoma (hMM) is an aggressive neoplasm of neuroectodermal origin with distinctive features from the more common cutaneous form of malignant melanoma (cMM). At the molecular level, hMMs are characterized by large chromosomal aberrations rather than single-nucleotide mutations, typically observed in cMM. Given the scarcity of available cases, there have been many attempts to establish a reliable animal model. In pet dogs, Canine Oral Melanoma (COM) is the most common malignant tumor of the oral cavity, sharing clinical and histological aspects with hMM. To improve the knowledge about COM's genomic DNA alterations, in the present work, formalin-fixed, paraffin-embedded (FFPE) samples of COM from different European archives were collected to set up an array Comparative Genomic Hybridization (aCGH) analysis to estimate recurrent Copy Number Aberrations (CNAs). DNA was extracted in parallel from tumor and healthy fractions and 19 specimens were successfully submitted to labeling and competitive hybridization. Data were statistically analyzed through GISTIC2.0 and a pathway-enrichment analysis was performed with ClueGO. Recurrent gained regions were detected, affecting chromosomes CFA 10, 13 and 30, while lost regions involved chromosomes CFA 10, 11, 22, and 30. In particular, CFA 13 showed a whole-chromosome gain in 37% of the samples, while CFA 22 showed a whole-chromosome loss in 25%. A distinctive sigmoidal trend was observed in CFA 10 and 30 in 25 and 30% of the samples, respectively. Comparative analysis revealed that COM and hMM share common chromosomal changes in 32 regions. MAPK- and PI3K-related genes were the most frequently involved, while pathway analysis revealed statistically significant perturbation of cancer-related biological processes such as immune response, drug metabolism, melanocytes homeostasis, and neo-angiogenesis. The latter is a new evidence of a significant involvement of neovascularization-related pathways in COMs and can provide the rationale for future application in anti-cancer targeted therapies.

Keywords: angiogenesis, array comparative genomic hybridization, canine oral melanoma, comparative oncology, copy number aberrations, mucosal melanoma, pathway enrichment analysis

INTRODUCTION

Human melanomas of mucosal sites (human Mucosal Melanoma, hMM) are neoplastic diseases of neuroectodermal origin, arising from non-cutaneous melanocytes migrated from the neural crest during embryogenesis (1–4). Although still not fully characterized, hMMs show to rely on numerous copy number changes and whole chromosomes gains or losses, rather than on single-nucleotide mutations, and they lack the typical UV-signature of the cutaneous malignant melanomas (cMM) (4–8). Large chromosomal aberrations, known to be deeply involved in solid tumors development (9), were investigated in hMMs through numerous techniques. Up to date, promising recurrent regions of gains and losses were identified (5) and confirmed by several investigations (4, 7, 8), in particular amplified portions of HSA 12q and 5p, which encode for genes as CDK4 and TERT, respectively (7). In addition, CCND1, KIT, and VEGFRA were proposed by a recent review (10) as targets for future investigations. hMMs represent only the 1.3% of all reported melanomas (1) and they may arise from different sites, as head-and-neck, female genital tract, and anal/rectal mucosa, with a respective 5 years survival rate of 31.7, 11.4, and 19.8%, while cMM has a 5 years survival rate of 80.8% (1). The highly aggressive biological behavior of hMMs (11) and the scarcity of available cases led to many attempts to establish a reliable animal model for the study of this life-threatening disease. Various *in vivo* models have been proposed for melanocytic derived-tumors through genetically engineered mice and zebrafish (12). Relevant limitations of these models are the lack of tumor population heterogeneity, combined with the longtime of tumor formation (12, 13). Altogether, these studies revealed the necessity of a spontaneous tumor model in non-engineered animals. Among companion animals, equine's primary melanomas have been taken into consideration as a model for hMMs' aberrations (8); however, they showed to have fewer copy number changes compared to hMM, making them a non-fitting model. On the basis of their greater genetic proximity with humans than other models proposed, dogs appear to be a more adequate preclinical surrogate (14). Canine tumors arise spontaneously in an intact immune system, often at a higher rate than in humans, and pet dogs share the same environmental risk factors with the owners. Moreover, dogs have a shorter lifespan and a more rapid neoplastic disease course (15, 16). Canine Oral Melanomas (COMs), the most common malignant tumor of the canine oral cavity (2, 17, 18), are characterized by a clinical evolution and progression, a tendency for local invasion and metastasis (2, 19–22), and a resistance to chemotherapy and radiation therapy (15, 20, 23), similar to hMM. In 2012, the National Cancer Institute Comparative Melanoma Tumor Board compared histological features of COM and canine melanomas arising in other sites (skin and acral) with hMM and cMM, finding a complete concordance between COMs and hMMs, and suggesting a common enrichment of PI3K and MAPK pathways (13). Given these promising results, the Board strongly encouraged validation of COM as a clinical model for hMM, by deepening the correlation of possible chromosomal, epigenetic and transcriptomic alterations. Molecular studies on COMs detected recurrent gains in CFA 13 and 17, and recurrent losses in CFA 2 and 22 (8, 24). A distinctive sigmoidal trend was also highlighted in CFA 30, with the alternation of gained and lost regions (8, 24). Although a large variety of gained and deleted genes was detected, some studies revealed discordant results indicating the need for further investigation on COMs' genetic landscape. In this work, DNA from formalin-fixed, paraffin-embedded (FFPE) samples of COM was collected from two European archives and analyzed through array Comparative Genomic Hybridization (aCGH). This technique takes advantage of the competitive hybridization of matched healthy and pathologic genomic DNA in parallel-extracted from FFPE samples, to estimate recurrent somatic Copy Number Aberrations (CNAs) characteristic of the cluster analyzed.

MATERIALS AND METHODS

Samples Collection and Selection

FFPE samples were collected from the archives of the Universities of Padua and Madrid. Initial inclusion criteria for the collection of the samples were a certain diagnosis of COM and sufficient material for nucleic acid extraction. Once collected, one 4 μm-thick slide was cut from each block and stained with a routine hematoxylin-eosin (H&E) protocol for a second evaluation. To be included in the study, the H&E slides were reviewed independently by two board-certified veterinary pathologists (American and European) and one expert veterinary pathologist to unequivocally confirm the initial diagnosis of COM, and to assess the presence of an adequate amount of healthy tissue suitable for the nucleic acid extraction. Diagnostic criteria were based upon the guidelines of the World Health Organization (25) and amelanotic specimens were evaluated through anti-Melan-A and anti-PNL2 antibodies. Forty samples were finally evaluated as adequate.

Nucleic Acid Extraction and Purification From FFPE Tissue

By using H&E stained slides as a guide, the paraffin blocks were incised in order to separate the tumor bulk from the healthy tissue. Sections 20 μm-thick were then cut from the blocks using a microtome with disposable blades. Tumor and healthy tissues were then scraped from the slides and put in two different 1.5 ml Eppendorf to be extracted separately. When necessary, more sections were cut in order to provide an adequate amount of healthy tissue material. Care was taken to avoid any possible contamination between tumor and healthy tissue and between different samples, by cleaning microtome, blades, and instruments after processing each specimen. Genomic DNA was extracted using the All-Prep DNA-RNA FFPE KIT (Qiagen®) according to the manufacturer's instructions, with the use of a heptane solution for deparaffinization steps. Quality and quantity of the extracted DNA were assessed via spectrophotometry with a Nanodrop ND-1000 (Life Technologies®), while its integrity was checked with an agarose gel electrophoresis, showing a marked degree of degradation in all samples. Only samples with a A^{260}/A^{230} ratio of at least 1.5 and a yield of DNA of at least 450

ng (for both pathological and healthy sections) were admitted to the following steps.

Array Comparative Genomic Hybridization

Genomic DNA from 24 samples was subjected to the cyanine labeling using the SureTag DNA Labeling Kit: DNA extracted from pathological and healthy fractions was labeled independently with Cy 3-deoxyuridine triphosphate (dUTP) and cyanine 5-dUTP, respectively. Cyanine incorporation and final concentration were calculated via spectrophotometry with a Nanodrop ND-1000 and the specific activity was calculated for each sample. Twenty samples, which reached an adequate matched tumor/healthy Cy3 and Cy5 specific activity, were then co-hybridized to a 180,000-feature SurePrint G3 Canine CGH Microarray (4–180 K, Agilent Technologies), comprising repeat-masked 60-mer oligonucleotides distributed at ∼2.7 Kb intervals throughout the dog CanFam2 genome assembly. After 24 h of incubation at 65° and 20 rpm, arrays were washed following the manufacturer's instruction and scanned at 3 μm using an Agilent G2565CA scanner. Image data were processed using Feature Extraction version 11.5, and Genomic Workbench version 7.0.

CNAs Analysis

Data were filtered to exclude probes exhibiting non-uniform hybridization or signal saturation and were normalized using the centralization algorithm with a threshold of eight and fuzzy ON. The ADM-2 algorithm was applied to define CNAs using a "three probes minimum" filter. Only autosomes were analyzed. The Cy5/Cy3 intensity ratios for each spot were converted into log2 ratios. Aberrant chromosome intervals were selected by using Agilent Genomic Workbench v. 7.0. A copy number gain was defined as a log2 ratio >0.25 and a copy number loss was defined as a log2 ratio <-0.25. Chromosomal locations were defined in terms of their Megabase (Mb) position. To identify significant CNAs the Genomic Identification of Significant Targets in Cancer (GISTIC2.0) (26) algorithm was also applied, as implemented in CGHtools software. The GISTIC2.0 module identifies regions of the genome that are significantly amplified or deleted across samples. Each aberration is assigned a G-score that considers the amplitude as well as the frequency of its occurrence across samples. False Discovery Rate q-values are then calculated for the aberrant regions, and regions with q-values below a user-defined threshold are considered significant. Log2ratios ≥0.25 and ≤−0.25 were assigned as the threshold for gain and loss detection, while amplification and deletion were defined as having a log2 ratio ≥1 and ≤−1. False Discovery Rate (FDR) ≤0.05 was set as the limit of significance.

Comparison Between Canine and Human CNAs

To compare the canine CNA profile with aberrations already described in the recent human literature, orthologous regions were identified using the Liftover Batch Coordinate Conversion Tool (http://genome.ucsc.edu/cgi-bin/hgLiftOver), as already done in previous studies (8, 24). In summary, the genome coordinates of the 180.000 60-mer probes of each array were mapped firstly to the canine reference genome CanFam3.1, and then to the human reference genome GRCh38/hg38. The syntenic human regions were then compared with published data (5, 7, 8, 24), to detect those regions shared by both hMMs and COMs. A comparative analysis between data produced herein, and recently published studies regarding the detection of CNAs in the canine genome through several techniques (as WES, WGS, aCGH, and FISH) (8, 24, 27, 28), was also performed.

Pathway Enrichment Analysis

Orthologous human genes were identified using the Ensemble Genome Browser (http://www.ensembl.org/index.html) and four lists of genes were employed for pathway analysis: (i) Gains with penetrance ≥25% (GR25), (ii) Gains with penetrance ≥40% (GR40), (iii) Losses with penetrance ≥25% (LR25) and (iv) regions highlighted as significant by Gistic analysis (GS). Genes were analyzed as human orthologs using the ClueGo plugin (29) for the software Cytoscape 3.7.1, an open-source Java tool that extracts the non-redundant biological information for large clusters of genes. In ClueGO, the kappa score is used to define term-term interrelations (edges), and functional groups based on shared genes between terms. Here, *Homo sapiens* was used as the control organism, and genes were uploaded as human orthologs named by the SymbolID. The genes were assigned to a network based on the updated ontologies: KEGG, GO Biological process, GO Immuno, REACTOME, and WIKIPATHWAYS. The significance of each term was calculated with a standard hypergeometric two-sided test. Networks were created on the basis of a kappa score threshold of 0.5 and a minimum of 3 genes in every network forming at least 10% of the total associated genes in each particular network, as previously done (28). Pathways' *P*-values were adjusted with Benjamini-Hochberg and the "fusion" option was also applied to reduce the redundancy. Pathways were then represented taking advantage of Cytoscape's complex visualization environment, as kappa score-based functional groups, and named by the most significant term of each group.

Immunohistochemistry and Immunohistochemical Assessment

For each of the 20 samples analyzed through the aCGH technique, a 4 μm-thick section was cut and mounted on a polarized glass slide (Superfrost® Plus, Thermo Scientific®), and tested with the mouse monoclonal antibody Ki67 (Dako®) diluted 1:50. Immunohistochemistry was performed with an automatic immunostainer (Ventana Benchmark GX, Roche-Diagnostic) using an ultraView universal alkaline phosphatase RED detection kit (Ventana Medical System Inc.), which provides a red chromogen reaction, and hematoxylin counterstain. The use of the red chromogen allowed avoiding bleaching reactions in pigmented COMs, in which DAB chromogen is often unusable, preserving the integrity of antigens. A Ki67 index was established for each sample on the base of the methodology described by Bergin et al. (30), which showed to be prognostic with a cutoff of 19.5 average cells per high power field (hpf).

Data Access

The data discussed in this publication have been deposited in NCBI's Gene Expression Omnibus (31), and are accessible through GEO Series accession number GSE131923 (https://www.ncbi.nlm.nih.gov/geo/query/acc.cgi?acc=~GSE131923).

RESULTS

Collected Samples and Immunohistochemical Analysis

A total of 20 samples, inclusive of the tumor and matched normal tissue, were selected for cyanine labeling and showed both an adequate yield and an adequate specific activity to be further subjected to the aCGH analysis. Only one case showed poor quality of hybridization and was excluded from this study, bringing the number of samples to 19. For each sample, an IHC with the Ki67 antibody was successfully performed, and the Ki67 index was established. Based on the study conducted by Bergin et al. (30), we established a threshold Ki67 value of >19.5 for the prediction of death (or euthanasia) due to melanoma by 1 year post-diagnosis. Based on the Ki67 value, samples were then classified as with a GOOD (G) or BAD (B) possible prognosis. The G group included 5/20 samples, and the B group 15/20 (including the one excluded from the aCGH cohort). Samples and available clinical data of dogs from which they were collected are listed in **Table S1** in Supplementary Materials.

Genomic Pattern of Aberration

CNA analysis allowed the identification of both focal and broad (near the size of a chromosome arm) chromosomal aberrations, distinguished in gains and losses (**Figure 1**). Two samples (A5, A35) did not present any aberration, while in the remaining ones, the mean number of aberrations per sample was 27.6 (range: 2–71). The pattern of genomic aberrations was evaluated for gained and lost regions with a penetrance ≥25% and consisted of 53 gained regions, with size ranging from 12.7 Kb to 30.9 Mb (with a mean length of 0.7 Mb), and 20 lost regions ranging from 60 bp to 40.5 Mb (mean length of 2 Mb).

The most frequently gained regions (penetrance ≥25%) affected chromosomes CFA 10, 13, and 30, while lost regions involved most frequently chromosomes CFA 10, 11, 22, and 30. Among the regions with gains, 8 showed a penetrance ≥40%, with regions chr30:17522685–17773010 and chr30:17847674–18058012 showing 45% penetrance. Among regions with losses, nine had a penetrance ≥30% and the most frequent loss was chr11:41248370–41248429, with a 35% penetrance. CNAs with penetrance ≥25% and corresponding genes are listed in **Table S2** in Supplementary Materials. Chromosomes that appeared to be more affected by gains and losses were CFA 13 and 22. CFA 13 showed a whole-chromosome gain in the 37% (7/19) of the samples, while CFA 22 showed a whole-chromosome loss in the 25% (5/19) of the samples, with the loss of region 0.2 to 54 Mb that reached a 30% penetrance. Additionally, a recurrent and distinctive alternation of gained and lost regions (sigmoidal trend) was observed on CFA 10 (25% of the samples, 5/19) and 30 (30% of the samples, 6/19). No aberrations significantly associated with a Ki67 index greater or lower than 19.5 were identified. The most frequent aberration observed was the loss of region chr11:41248370–41248429 in the G group, recurrent in three out of five samples. Microarray data were then interrogated using the GISTIC2.0 algorithm, to identify CNAs with a statistically significant frequency. A total of 20 significant gained regions were located on CFA 9, 10, 13, and 30. Those regions and the corresponding genes (reported in **Table S3** in Supplementary Materials) were mostly overlapping

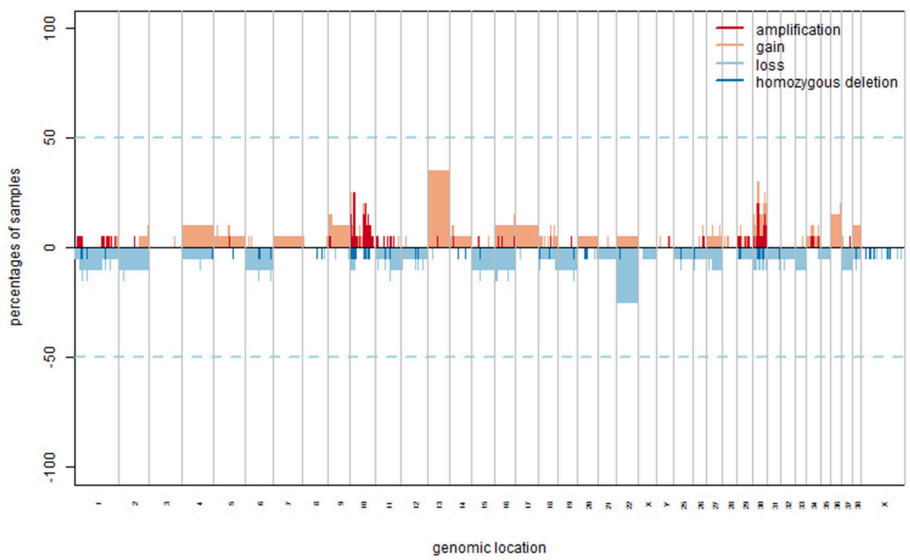

FIGURE 1 | CNAs in COM. Copy number gains and amplification are indicated in orange and red, respectively representing a $\log_2$ ratio ≥0.25 and ≥1. Copy number losses and deletion are indicated in light and dark blue, respectively representing a $\log_2$ ratio ≤–0.25 and ≤–1.

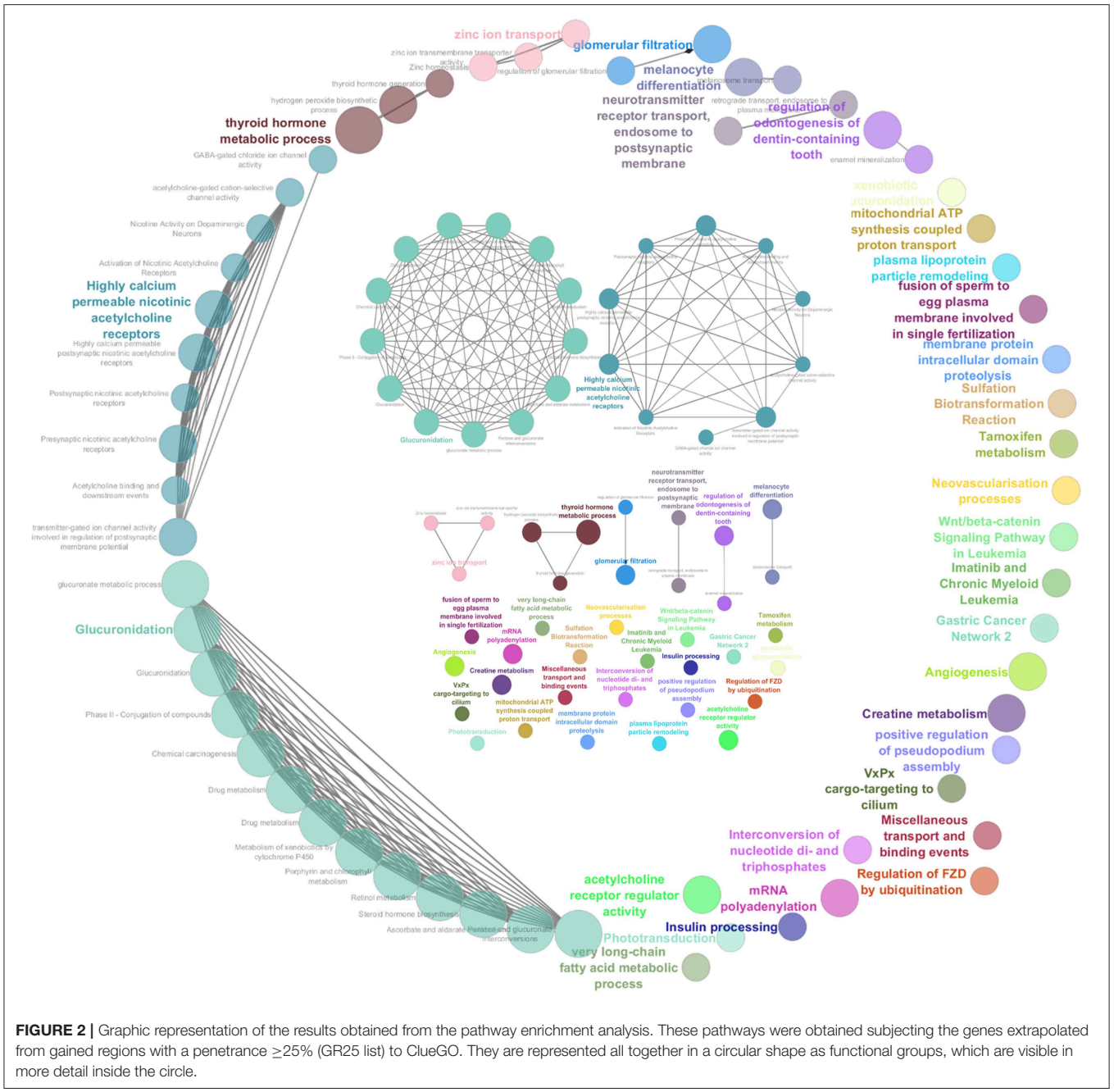

FIGURE 2 | Graphic representation of the results obtained from the pathway enrichment analysis. These pathways were obtained subjecting the genes extrapolated from gained regions with a penetrance ≥25% (GR25 list) to ClueGO. They are represented all together in a circular shape as functional groups, which are visible in more detail inside the circle.

with those showing higher penetrance across samples. The regions' size ranged from 33.9 Kb to 52.3 Mb, with a mean length of 4.2 Mb. CFA 10 and CFA 30 were affected by significant amplification in 36.8% (7/19) and 26.3% (5/19) of the samples, respectively. The three most frequent minimum common regions (MCRs) of CFA 10 were 1.7 to 1.9 Mb, 10.9 to 11.8 Mb and 43.6 to 45 Mb, while the most frequent MCRs of CFA 30 were 13.6 to 13.9 Mb, and 16.2 to 17.9 Mb. The GISTIC2.0 algorithm failed to identify statistically significant lost regions. A hierarchical clustering technique aimed to identify molecular features potentially correlated with the Ki67 index showed inconsistent results.

Pathway Enrichment Analysis

To generate a summary of the pathways likely involved in the tumorigenesis of COMs, four separate lists (i.e., GR25, GR40, LR25, and GS, see Methods) were submitted to the ClueGO tool to identify significantly enriched pathways. Pathways were considered significant if having an adjusted Benjamini-Hochberg $P < 0.05$. The enrichment analysis identified 60 significant pathways for the group GR25 (**Figure 2**), 10 significant pathways for the group LR25, and 49 significant pathways for the group GS. No pathways were found significantly enriched when analyzing the GR40 group. The complete list of significant pathways and genes is reported in **Table S4** in Supplementary Materials, while

TABLE 1 | List of part of the significantly enriched pathways.

Pathways	cPValue	Associated genes found	Source
Angiogenesis	<0.01	ANGPT1, KDR, PDGFRA, PTK2	GR25, GS
Glucuronidation	<0.01	UGT2A1, UGT2A3, UGT2B10, UGT2B11, UGT2B15, UGT2B17, UGT2B28, UGT2B4, UGT2B7	GR25, GS
Highly calcium permeable nicotinic acetylcholine receptors	<0.01	CHRNA3, CHRNA5, CHRNB4	GR25, GS
Wnt/beta-catenin Signaling Pathway in Leukemia	0.03	FZD6, MYC, PYGO1, WIF1	GR25, GS
Drug metabolism	<0.01	DPYS, DUT, MGST3, RRM2B, UGT2A1, UGT2A3, UGT2B10, UGT2B11, UGT2B15, UGT2B17, UGT2B28, UGT2B4, UGT2B7	GR25, GS
Tamoxifen metabolism	0.02	SULT1E1, UGT2B15, UGT2B7	GR25, GS
Imatinib and Chronic Myeloid Leukemia	0.02	KIT, MYC, PDGFRA	GR25, GS
Gastric Cancer Network 2	0.01	ATAD2, DSCC1, FAM91A1, MYC	GR25, GS
Chemical carcinogenesis	<0.01	MGST3, UGT2A1, UGT2A3, UGT2B10, UGT2B11, UGT2B15, UGT2B17, UGT2B28, UGT2B4, UGT2B7	GR25, GS
Regulation of odontogenesis of dentin-containing tooth	<0.01	AMTN, ENAM, RSPO2, TNFRSF11B	GR25, GS
Insulin processing	0.01	EXOC1, MYO5A, RAB27A, SLC30A8	GR25
Melanocyte differentiation	<0.01	BLOC1S6, KIT, MYO5A, RAB27A, SLC24A5	GR25
T-helper 1 type immune response	<0.01	IL18R1, IL18RAP, IL1RL1, SOCS5, TRAPPC9, UTP3	GS
Hippo-Yap signaling	0.01	MAP4K4, NDRG1, STK3	GS
Negative regulation of cell migration involved in sprouting angiogenesis	<0.01	DLL4, SPRED1, THBS1	LR25
Hydrolysis of LPC	<0.01	JMJD7-PLA2G4B, PLA2G4B, PLA2G4D, PLA2G4E	LR25

cPValue, P-value corrected with Benjamini-Hochberg; GR25, gains with penetrance ≥25%; LR25, losses with penetrance ≥25%; GS, regions highlighted as significant by Gistic analysis.

the most interesting, together with corresponding genes, are listed in **Table 1**. Pathways found enriched in the GR25 group included *Angiogenesis* ($P < 0.01$), *Glucuronidation* ($P < 0.01$), *Highly calcium permeable nicotinic acetylcholine receptors* ($P < 0.01$), and *Wnt/beta-catenin Signaling Pathway in Leukemia* ($P = 0.03$). Interestingly, many pathways related to *Drug metabolism* ($P < 0.01$) were also found significantly enriched (see **Table 1**). Other significant pathways were *Gastric Cancer Network 2* ($P = 0.01$), *Chemical carcinogenesis* ($P < 0.01$), and *Insulin processing* ($P = 0.01$). Most of the other pathways found to be enriched were melanocytes-related, such as *Melanocyte differentiation* ($P < 0.01$), or linked to the dental apparatus, e.g., *Regulation of odontogenesis of dentin-containing tooth* ($P < 0.01$). Noteworthy, in the GR25 group and GS group, enriched pathways were mostly overlapping. Additionally, GS enriched pathways included the *T-helper 1 type immune response* ($P < 0.01$) and *Hippo-Yap signaling* pathways ($P = 0.01$). Regarding the LR25 group, the most enriched pathways were *Negative regulation of cell migration involved in sprouting angiogenesis* ($P < 0.01$), and *Hydrolysis of LPC* ($P < 0.01$).

Comparative Analysis Between Canine and Human CNAs

Orthologous chromosomal regions in canine and human genome were examined to assess conserved CNAs between COMs and hMMs. In human literature, frequent gains of regions of human chromosomes HSA 1, 4, 5, 6, 7, 8, 11, 12, 17, 20, and losses of regions of HSA 3, 4, 6, 8, 9, 10, 11, 17, 21, have been reported (5, 7). The comparative analysis revealed 32 regions shared between COMs and hMMs, and regarded gains on CFA 9, 10, and 13, orthologous to HSA 17, 12, and 8–4 (respectively), and losses on CFA 11, 22 and 30, orthologous to HSA 9, 13, and 15 (respectively). A representation is visible in **Tables 2A–C**, while more details about the syntenic human regions are given in **Table 3**. In particular, the region characterized by the greatest recurrence was CFA 13:1722286–32543593, corresponding to HSA 8:99748261–136957380, already reported (5, 8, 24), and detected with a penetrance of 35% in this work. Regarding genes proposed as candidates for the tumorigenesis by other studies, a further concordance between COMs and hMMs was observed with the detection from gained regions of MYC, KIT and, for the first time, PDGFRA, although the latter was found gained only in the 12.5% of the hMMs analyzed (6) (**Table 4A**). A concordance can also be found in the loss of regions coding for BUB1B, KNSTRN, CYSLTR2, and SPRED1 (8) (**Table 4B**). Interestingly, also B2M was found imbalanced in both COMs and hMMs (8), but affected by a gain in the present work, instead of a loss. Other frequently reported events in hMMs are usually gains of BRAF (6, 8, 24), MDM2 (6, 8), CDK4 (5–7, 24), and CCND1 (5, 6, 24); losses of CDKN2A, PTEN (5, 6, 24), and TP53 (4, 6). However, aberrations involving the latter candidate genes were not found in the present study. A new promising target gene was also absent: PTPRJ was found lost in both hMMs and COMs (8), and was reported as inactivated by somatic mutations in COMs (28), but was not involved in the present cohort.

Comparison With Published Canine CNAs

Recently, several studies focused on COM's genetic landscape. The most frequently reported aberrations are gains on CFA 13, 17, and losses on CFA 11, 15,

TABLE 2 | Representation of the aberrated regions detected in the present study (CanFam3.1 annotation), showing a correspondent canine or human syntenic region in other studies, which are indicated through the bibliographic number: Wong et al. (8), Poorman et al. (24), Giannuzzi et al. (27), Hendricks et al. (28), Hayward et al. (6), Curtin et al. (5), Lyu et al. (7), and Furney et al. (4). CNAs are listed on the base of the chromosomal location, and divided into 3 groups: **(A)** gained regions with a penetrance ≥25% (GR25); **(B)** lost regions with a penetrance ≥25% (LR25); **(C)** represents gained regions found statistically significant by Gistic analysis (GS).

		CANINE studies				HUMAN studies					
CHR	**Present study**	**Wong et al. (8)**	**Poorman et al. (24)**	**Giannuzzi et al. (27)**	**Hendricks et al. (28)**	**Wong et al. (8)**	**Poorman et al. (24)**	**Hayward et al. (6)**	**Curtin et al. (5)**	**Lyu et al. (7)**	**Furney et al. (4)**
(A) GR25											
10	7814333–7827061					V					
	7827061–7896552					V					
	7896552–8860169					V					
	8860169–8889136					V					
	8889136–9197582					V					
	9225870–9593296					V					
	9593296–9724425					V					
	9724425–9752955					V					
13	1722286–32543593				V	V	V		V		
	32543593–34917864					V			V		
	34917864–60030824*					V			V		
							V		V		
	60030824–60110727						V				
30	16069762:16221290		V		V						
	16221290:16599297		V		V						
	16599298:16724522		V								
	16724522:16973676		V								
	16973676:17914975		V								
(B) LR25											
11	38095457–38199500								V		
	38199500–38219624								V		
	38219624–38219683								V		
	38219683–38263483								V		
	38263483–38372087								V		
22	102563–10473893						V				
30	1305764–2530849					V					
	2530849–2552538					V					
	2552538–2770691					V					
	2770691–4634866					V					
	4634866–5314049					V					
	5314049–9109654					V					
(C) GS											
9	1839468–1890597								V		
	2038907–2071775								V		
10	6204314–9752896					V					
	9948113–10047999					V					
13	101–23829651				V	V			V		
	23906345–60168042*					V	V		V		
									V		

*Canine regions marked with * were syntenic to human regions belonging to two different chromosomes, and were split accordingly (view **Table 3** for details).*

22 (8, 24, 27, 28) together with a sigmoidal trend (a complex alternation of copy number gains followed immediately by copy number losses), in CFA 10 and 30 (8, 24, 28). In this study, CFA 10 and CFA 30 also showed the sigmoidal trend, and 7 of the regions found imbalanced were already reported in recent literature (**Tables 2A,C**). Among them, CFA 30:16069762:16221290 and 30:16221290:16599297, in particular, are reported in 2 other

TABLE 3 | Comparison between canine CNAs detected in the present study (on the left, CanFam3.1 annotation), and corresponding syntenic human CNAs reported in literature (on the right, GRCh38/hg38 annotation).

Shared canine-human regions					
Canine gains (present study)	**Human gains**	**Canine loss (present study)**	**Human loss**	**Canine gistic (present study)**	**Human gains**
chr10:7814333–7827061	chr12:65226703–65241894[†]	chr11:38095457–38199500	chr9:18137869–18249633[§]	chr9:1839468–1890597	chr17:79737002–79797355[§]
chr10:7827061–7896552	chr12:65242092–65311784[†]	chr11:38199500–38219624	chr9:18249633–18271087[§]	chr9:2038907–2071775	chr17:79475861–79519528[§]
chr10:7896552–8860169	chr12:65311784–66424954[†]	chr11:38219624–38219683	chr9:18271087–18271147[§]	chr10:6204314–9752896	chr12:63095367–67388213[†]
chr10:8860169–8889136	chr12:66428185–66458897[†]	chr11:38219683–38263483	chr9:18271147–18348934[§]	chr10:9948113–10047999	chr12:67602904–67721312[†]
chr10:8889136–9197582	chr12:66458897–66810207[†]	chr11:38263483–38372087	chr9:18348934–18473616[§]	chr13:101–23829651	chr8:97763559–126022421[†§]
chr10:9225870–9593296	chr12:66840570–67211059[†]	chr22:102563–10473893	chr13:40898353–52112457[‡]	chr13:23906345–60168042	chr8:100M–140M[†‡§]
chr10:9593296–9724425	chr12:67213347–67350366[†]	chr30:1305764–2530849	chr15:32610232–33724875[†]		chr4:38M–65M[§]
chr10:9724425–9752955	chr12:67353025–67388264[†]	chr30:2530849–2552538	chr15:34810295–34839288[†]		
chr13:1722286–32543593	chr8:99748261–136957380[†‡§]	chr30:2552538–2770691	chr15:34839288–35104379[†]		
chr13:32543593–34917864	chr8:136957380-140179206[†§]	chr30:2770691-4634866	chr15:35104379-37107511[†]		
chr13:34917864–60030824	chr8:139727725–145066685[†§]	chr30:4634866–5314049	chr15:37107511–37907031[†]		
	chr4:41359607–70807315[‡§]	chr30:5314049–9109654	chr15:37907031–42087634[†]		
chr13:60030824–60110727	chr4:70738662–70861730[‡]				

With [†] the syntenic regions reported also by Wong et al. (8); with [‡] the syntenic regions reported also by Poorman et al. (24); with an [§] the syntenic regions reported by Curtin et al. (5); no regions were shared with Lyu et al. (7).

studies (24, 28), and had a penetrance ≥30% and ≥25% in this work, respectively.

Several genes which have been indicated to play a significant role in the development of COMs and hMMs were involved in CNAs, comprising gains of TRPM7 (24, 27), MYC (8, 24), KIT (24, 28), WIF1 (8), SLC27A2, GABPB1, USP8, SPPL2A, CYP19A1 (27) (**Table 4A**) and losses of RB1 (8, 24), LCP1, BUB1B, KNSTRN, CYSLTR2 (8), SPRED1 (24, 27), and FAM98B (27) (**Table 4B**). On the contrary, other genes such as MDM2 (27, 28) or CDK4 (8, 28), were not confirmed by our study. Finally, it is noteworthy that other genes involved in CNAs such as ADAM10, and genes belonging to gene families SNORA, SNORD, SLC25A, RPL, and RBM, have been recently shown to be highly expressed in metastatic COMs (32).

More details about the target genes taken into consideration (from both canine and human studies) are graphically represented in **Tables 4A,B**.

DISCUSSION

In the present study, more than 250 FFPE samples have been collected from archive material. However, due to the stringent inclusion criteria aimed to analyze only samples with a sufficient amount of paired healthy DNA, only 40 were considered adequate candidates for the aCGH analysis. The low number of samples has been a limitation, and a likely cause of the inconsistent results obtained from the hierarchical clustering, with only 5/20 cases with a Ki67 value <19.5. Since the presence of healthy tissue was a major restriction in the recruitment of cases, to ease future analysis the inclusion of a portion of presumed healthy tissue in the diagnostic sample is therefore recommended. The highly homogeneous cohort of samples obtained and the matching DNA for each sample allowed to overcome all potential discrepancies deriving from the use of genomic dog pools, which could have led to false correlations with race, age, sex, and health conditions.

A 50% increase in the DNA extraction yield was obtained by using the heptane as deparaffinization agent instead of the more toxic xylene (33). Precipitation of the extracted DNA with ethanol allowed to obtain a good DNA quality in some of the samples with an initial poor A^{260}/A^{230} ratio.

Chromosomal aberrations detected in this study partially overlap with those already documented in other works on canine species, and the software analysis showed both new and known enriched pathways. Only the GR40 group failed to identify significantly enriched pathways, probably due to the limited number of genes included in the list.

The most characteristic aberration is confirmed to be the sigmoidal pattern of CFA 10 and CFA30 (8, 24, 28). However, the biological significance of these recurrently lost-gained regions is still unclear. Future studies correlating the presence of lost-gained regions and clinical data could improve our understanding of this specific molecular feature of COM.

MDM2 (8, 27, 28), CDK4 (8, 28), and CDKN2A (24, 27, 28), which were found altered by other authors, were not identified as significantly aberrated by GISTIC algorithm in

TABLE 4 | Comparison of the target genes found gained **(A)** or lost **(B)** in this and other studies, which are indicated through the bibliographic number: Wong et al. (8), Poorman et al. (24), Giannuzzi et al. (27), Hendricks et al. (28), Hayward et al. (6), Curtin et al. (5), Lyu et al. (7), and Furney et al. (4).

	Present study	CANINE studies				HUMAN studies					
		Wong et al. (8)	Poorman et al. (24)	Giannuzzi et al. (27)	Hendricks et al. (28)	Wong et al. (8)	Poorman et al. (24)	Hayward et al. (6)	Curtin et al. (5)	Lyu et al. (7)	Furney et al. (4)
(A) GAINED GENES											
MYC	V	V	V			V	V				
KIT	V		V		V		V				
PDGFRA	V							V			
B2M*	V	V				V					
BRAF						V	V	V			
MDM2		V		V	V	V		V			
CDK4		V			V		V	V	V	V	
CCND1*		V	V			V	V	V	V		
TRPM7	V		V	V							
WIF1	V	V									
SLC27A2	V			V							
GABPB1	V			V							
USP8	V			V							
SPPL2A	V			V							
CYP19A1	V			V							
NOTCH1						V					
SMO		V				V					
TERT										V	
(B) LOST GENES											
BUB1B	V	V				V					
KNSTRN	V	V				V					
CYSLTR2	V	V				V					
SPRED1	V		V	V		V					
CDKN2A			V	V	V		V	V	V		
PTEN			V				V	V	V		
TP53								V			V
RB1	V	V	V								
LCP1	V	V									
FAM98B	V			V							
PTPRJ		V				V					
ARID1B						V					

*With * the genes B2M and CCND1: B2M was found gained in the present study, but was reported as lost by Wong et al. (8); CCND1 was reported as gained in hMMs, but lost in COMs, by Wong et al. (8) and Poorman et al. (24).*

this study. As reported also in hMM (4), MDM2 is known to favor tumor formation by acting on the tumor suppressor gene p53 (34). Although the reason for this discrepancy is not known, a significant gain of the MDM2 binding protein (MTBP) was instead present in our samples. These data, together with a copy number gain involving the p53 binding protein (TP53BP1), confirm the dysregulation of p53 family members in COMs. Moreover, a significant enrichment of the Hippo-Yap signaling pathway, which is strongly and sometimes contradictorily intertwined with the p53 pathway (35), was also detected.

CDK4 and its inhibitor CDKN2A are main actors of the cell cycle proliferation since they regulate Cyclin D1, allowing or not the transition from G1 to S phase. Although a direct involvement of CCND1 has been identified only in human acral and mucosal melanomas (5), and not in COMs (24), high expression of Cyclin D1 protein in COMs has been recently documented (36). Furthermore, a gain of the coding gene for Cyclin B2 (CCNB2), and a copy number imbalance of Eukaryotic Translation Initiation Factor family members (EIF2C2, EIF2AK4, EIF3E, EIF3H, EIF3J), were detected. Interestingly, the member EIF4E of the family is reported to increase the level of Cyclin D1 protein *in vitro* (37, 38), while other members (components of the EIF3 complex, in particular), have been correlated to human cancer (39–49), and human melanoma (41, 50, 51).

Another notable aberration is the loss of the tumor suppressor gene Retinoblastoma 1 (RB1), considered the governor of the cell cycle. RB1 has been already associated with other human and canine cancer types and it is strictly correlated to the cyclins' family. Even if with a mechanism different from those proposed in other works, cyclins activation appears then highly involved also in our cohort of COMs.

Among the genes related to cell proliferation and mitosis, GRHL2, a transcription factor able to bind the promoter region of TERT, was found to be gained. Although TERT is one of the most frequently involved genes in human non UV-induced melanomas (7, 10) it has never been found amplified in COMs. However, the gain of GRHL2 suggests that TERT expression may play a role in COMs.

A loss of mitosis-related genes was also highlighted. Loss of KNSTRN, required for correct chromosome segregation, BUB1, a checkpoint for mitosis progression, and TACC3, a stabilizer of the mitotic spindle, were detected.

COM is known to share with hMM the activation of MAPK and PI3K pathways, showing also similar responses to targeted therapies (52, 53). Aberrations are recognized to be part of the activation mechanism, and many MAPK-related genes are encoded by CFA 30 (orthologous to HSA 15) (8, 24, 28). Genes responsible for MAPK and PI3K activation found in this work comprise RASGRP1, MYC, FGF7, ANGPT1, TRPM7 (gained), and SPRED1 (lost). As reported in other works (6, 24), an imbalance of a wide variety of genes coding for tyrosine kinases receptors was also detected. These genes are abnormally activated in a wide range of human and animal tumors, inducing uncontrolled tumor proliferation (54). Our data showed an imbalance of the proto-oncogene c-KIT, and of other kinases such as PTK2, STK3, TEC, PDGFRA, VEGFR2, and CD63. It is noteworthy that VEGF receptors are involved in metastatic behavior in human melanoma studies (55), while PDGF receptors' expression has been shown to bear prognostic significance in COMs (22). Finally, CD63, a well-known melanoma-associated antigen (also called "Melanoma-Associated Antigen ME491"), has a role in VEGFA signaling.

As reported by other authors (28), the involvement of PI3K/mTOR/AKT signaling pathway is also suggested by the significant enrichment of the *Insulin processing* pathway, which is well-known to activate PI3K. The latter is also regulated by DEPTOR and MAP2K1 genes, which have been found altered in our study. Noteworthy, PI3K and mTOR are essential for the maintenance of the stem cell status in neural progenitor cells (56), and their abnormal involvement appears strategical for the tumorigenesis of neural crest-derived tumors such as COM.

Interestingly, the *Angiogenesis* pathway was enriched in both GR25 and GS lists (derived from the gained regions), and its suppressive pathway (*Negative regulation of cell migration involved in sprouting angiogenesis*) was enriched in LR25 list (derived from the lost regions). In addition, other vascular-related pathways, such as *Neovascularization processes*, were found enriched. Vessels proliferation, which plays an important role in several types of human melanomas (57), appears then to be deeply implicated in COMs' pathogenesis, and likely in their metastatic behavior. Neoangiogenesis is an obligatory phenotypic step for the establishment of distant metastases throughout the body: without an angiogenic process, the freshly-proliferated cells would incur into hypoxia and lack of nutrients, making the microenvironment adverse for the metastases survival (57). The main genes involved in endothelial and vascular cell proliferation, and reported by the ClueGo analysis, were ANGPT1, VEGFR2, PDGFRA, PTK2 for both GR25 and GS groups, and DLL4, SPRED1, THBS1, which are involved in the negative regulation of vessel sprouting, for LR25. Additionally, an imbalance (gains and losses) on the endothelin receptor type B gene (EDNRB), which role is crucial for melanocytes development (3) and for vessel homeostasis, was also detected. Interestingly, antibody-drug conjugates (ADC) targeting the endothelin B receptor (ET_BR) both *in vitro* and *in vivo* systems (58, 59), show anti-tumor activity (even if partial) in hMMs (59). Given these premises, further evaluation of ET_BR's expression in COMs could be promising to evaluate the application of ADC therapies also in dogs.

Furthermore, our data show the involvement of many other genes closely related to an angiogenic phenotype. Many genes coding for interleukin receptors, inflammatory molecules that contribute to neovascularization through endothelial cells migration and proliferation, and through metalloproteinases overexpression (as MMP19), were found gained in this study. Significantly, in hMM, a close relationship between IL-8, its receptor CXCR2, and MMP-2, is well-established (60, 61). Additional involved genes were those coding for fibroblast growth factors (FGF7 and FGF14), for lipid lysophosphatidic acids (LPAR6)—which are known to contribute to angiogenesis and lymphangiogenesis (57)—and for melanoma proliferation- and migration-related properties such as ZIC5 (62).

The GISTIC2.0 algorithm indicated the *T-helper 1 type immune response* pathway was significantly enriched (genes are listed in **Table 1**). Although in dogs therapeutic trials based on immunomodulation did not reach consistent results (63–65), these data strengthen the view of melanoma as a promising target for immunogenic therapies (66).

A general loss of many components of the T-cell homeostasis such as LCP1, TNFSF11, LRCH1, TRIM13 (which acts together with MDM2), RASGRP1, and GPR18 was found. On the contrary, the gain of PDCD7, involved in glucocorticoid-induced apoptosis in mouse T-cells (67), was detected.

Pathways related to drug metabolism were also found to be enriched, with *Glucuronidation* being the most significant. The cause is attributable to the high representation of the UGT-family genes, which are involved in the activity of the enzyme glucuronosyltransferase and phase II metabolism, and constitute an important pathway for xenobiotic elimination from the organism. Although the involvement of *Glucuronidation* in COM's behavior is still unclear, its potential role should be taken into consideration for future clinical trials and drug testing.

Not surprisingly, genes involved in the pathogenesis of other tumors were found to be altered. Significant gains of genes ATAD2, DSCC1, FAM91A1, and MYC brought to the enrichment of the *Gastric Cancer Network 2* pathway, and ATAD2 is a cancer-associated protein which can also induce the expression of Cyclin D1 and MYC (68).

Another enriched pathway, which has been frequently associated with cancer, was the *Wnt/beta-catenin Signaling Pathway in Leukemia*, which mediates the cell transduction signal. Gains of genes such as FZD6, PYGO1, and WIF1, causing Wnt inhibition, and MYC, were found. The involvement of Wnt signaling has been associated to numerous types of cancer, as glioblastoma (69), esophageal (70), ovarian (71), breast (72), colorectal (73), prostate (74), and lung (75) cancers and also to cutaneous melanomas (76). Gains of Wnt inhibitory genes in COM may still have a role in the complex deregulation of the Wnt pathway, which leads to carcinogenesis. However, further studies are needed to clarify this point.

The enrichment of pathways related to melanocytes' development (from neural stem cells) and pigmentation have been already reported in hMMs (7). In accordance, a significant enrichment of the *Highly calcium permeable nicotinic acetylcholine receptors*, and of the *Melanocyte differentiation* pathways were found in our study. Finally, the *Regulation of odontogenesis of dentin-containing tooth* pathway was also significantly enriched. Genes involved in the enrichment of this last pathway, namely AMTN, ENAM, RSPO2, and TNFRSF11B, encode, respectively, for the ameloblast protein amelotin, teeth component enamelin (a Wnt activator), and a TNF receptor. The involvement of these genes may be related to the frequent tendency of COMs to affect the oral cavity, and gingiva in particular (77). The application of aCGH on 19 COMs contributed to increase our knowledge of genetic aberrations in this canine tumor. We confirmed aberrational patterns noted also by other authors, as the sigmoidal trend in CFA 10 and 30. Thirty-two regions here detected showed to be syntenic with hMM-related regions and confirmed a common involvement of MAPK and PI3K pathways in COMs and hMMs. Moreover, our data suggest a strong involvement in COM's tumorigenesis of neovascularization-related pathways. These new data, together with the encouraging evidence of anti-angiogenic factors target therapies in human melanomas, remark the role of the dog as a model for hMMs and encourage new studies aimed to test the application of anti-angiogenic factors in the treatment of advanced and/or metastatic COMs.

DATA AVAILABILITY STATEMENT

The datasets generated for this study can be found in the NCBI's Gene Expression Omnibus, accession number: GSE131923.

ETHICS STATEMENT

Ethical review and approval was not required for the animal study because only formalin-fixed, paraffin-embedded surgical biopsies from canine tumors were used in the present work. Tissues were provided by the archives of the Department of Comparative Biomedicine and Food Science (University of Padova) and of the Department of Animal Medicine and Surgery (Complutense University). Written informed consent for participation was not obtained from the owners because the biopsies collected from the archives had already been approved for research purposes by the attending veterinarians, at the moment they sent the material to our facilities.

AUTHOR CONTRIBUTIONS

SeF and MC conceptualized the study design. MC acquired the funds and supervised the whole project. CZ and EM-M collected and recruited the cases and their available information. GB and CZ performed the IHC analysis when necessary. SiF, MG, and MC reviewed H&E and IHC slides to confirm the diagnosis. GB and SeF performed the aCGH analysis. GB curated the processed data and wrote the original draft. All authors reviewed and approved the final manuscript.

FUNDING

This present work was financed with internal resources of the University of Padua.

ACKNOWLEDGMENTS

The authors thank Dr. Annamaria Di Meglio and Dr. Stefano Capomaccio, for the helpful support in data processing. The authors also thank the Journal of Comparative Pathology Educational Trust, which supported the submission of some preliminary data of this work to the 2019 ESVP–ECVP Congress.

SUPPLEMENTARY MATERIAL

The Supplementary Material for this article can be found online at: https://www.frontiersin.org/articles/10.3389/fonc.2019.01397/full#supplementary-material

REFERENCES

1. Chang AE, Karnell LH, Menck HR. The National Cancer Data Base report on cutaneous and noncutaneous melanoma. *Cancer*. (1998) 83:1664–78. doi: 10.1002/(SICI)1097-0142(19981015)83:8<1664::AID-CNCR23>3.0.CO;2-G
2. Smith SH, Goldschmidt MH, McManus PM. A comparative review of melanocytic neoplasms. *Vet Pathol*. (2002) 39:651–78. doi: 10.1354/vp.39-6-651
3. Dupin E, Le Douarin NM. Development of melanocyte precursors from the vertebrate neural crest. *Oncogene*. (2003) 22:3016–23. doi: 10.1038/sj.onc.1206460
4. Furney SJ, Turajlic S, Stamp G, Nohadani M, Carlisle A, Thomas JM, et al. Genome sequencing of mucosal melanomas reveals that they are driven by distinct mechanisms from cutaneous melanoma. *J Pathol*. (2013) 230:261–9. doi: 10.1002/path.4204
5. Curtin JA, Fridlyand J, Kageshita T, Patel HN, Busam KJ, Kutzner H, et al. Distinct sets of genetic alterations in melanoma. *N Engl J Med*. (2005) 353:2135–47. doi: 10.1056/NEJMoa050092
6. Hayward NK, Wilmott JS, Waddell N, Johansson PA, Field MA, Nones K, et al. Whole-genome landscapes of major melanoma subtypes. *Nature*. (2017) 545:175–80. doi: 10.1038/nature22071

7. Lyu J, Song Z, Chen J, Shepard MJ, Song H, Ren G, et al. Whole-exome sequencing of oral mucosal melanoma reveals mutational profile and therapeutic targets. *J Pathol*. (2018) 244:358–66. doi: 10.1002/path.5017
8. Wong K, van der Weyden L, Schott CR, Foote A, Constantino-Casas F, Smith S, et al. Cross-species genomic landscape comparison of human mucosal melanoma with canine oral and equine melanoma. *Nat Commun*. (2019) 10:353. doi: 10.1038/s41467-018-08081-1
9. Albertson DG, Collins C, McCormick F, Gray JW. Chromosome aberrations in solid tumors. *Nat Genet*. (2003) 34:369–76. doi: 10.1038/ng1215
10. Merkel EA, Gerami P. Malignant melanoma of sun-protected sites: a review of clinical, histological, and molecular features. *Lab Invest*. (2017) 97:630–5. doi: 10.1038/labinvest.2016.147
11. Carvajal RD, Spencer SA, Lydiatt W. Mucosal melanoma: a clinically and biologically unique disease entity. *J Natl Compr Cancer Netw*. (2012) 10:345–56. doi: 10.6004/jnccn.2012.0034
12. van der Weyden L, Patton EE, Wood GA, Foote AK, Brenn T, Arends MJ, et al. Cross-species models of human melanoma. *J Pathol*. (2016) 238:152–65. doi: 10.1002/path.4632
13. Simpson RM, Bastian BC, Michael HT, Webster JD, Prasad ML, Conway CM, et al. Sporadic naturally occurring melanoma in dogs as a preclinical model for human melanoma. *Pigment Cell Melanoma Res*. (2014) 27:37–47. doi: 10.1111/pcmr.12185
14. Lindblad-Toh K, Wade CM, Mikkelsen TS, Karlsson EK, Jaffe DB, Kamal M, et al. Genome sequence, comparative analysis and haplotype structure of the domestic dog. *Nature*. (2005) 438:803–19. doi: 10.1038/nature04338
15. Vail DM, MacEwen EG. Spontaneously occurring tumors of companion animals as models for human cancer. *Cancer Invest*. (2000) 18:781–92. doi: 10.3109/07357900009012210
16. Paoloni M, Khanna C. Translation of new cancer treatments from pet dogs to humans. *Nat Rev Cancer*. (2008) 8:147–56. doi: 10.1038/nrc2273
17. Todoroff RJ, Brodey RS. Oral and pharyngeal neoplasia in the dog: a retrospective survey of 361 cases. *J Am Vet Med Assoc*. (1979) 175:567–71.
18. Goldschmidt MH. Benign and malignant melanocytic neoplasms of domestic animals. *Am J Dermatopathol*. (1985) 7:203–12. doi: 10.1097/00000372-198501001-00039
19. Ramos-Vara JA, Beissenherz ME, Miller MA, Johnson GC, Pace LW, Fard A, et al. Retrospective study of 338 canine oral melanomas with clinical, histologic, and immunohistochemical review of 129 cases. *Vet Pathol*. (2000) 37:597–608. doi: 10.1354/vp.37-6-597
20. Patrick RJ, Fenske NA, Messina JL. Primary mucosal melanoma. *J Am Acad Dermatol*. (2007) 56:828–34. doi: 10.1016/j.jaad.2006.06.017
21. Gillard M, Cadieu E, De Brito C, Abadie J, Vergier B, Devauchelle P, et al. Naturally occurring melanomas in dogs as models for non-UV pathways of human melanomas. *Pigment Cell Melanoma Res*. (2014) 27:90–102. doi: 10.1111/pcmr.12170
22. Iussich S, Maniscalco L, Di Sciuva A, Iotti B, Morello E, Martano M, et al. PDGFRs expression in dogs affected by malignant oral melanomas: correlation with prognosis. *Vet Comp Oncol*. (2017) 15:462–9. doi: 10.1111/vco.12190
23. Bergman PJ, Wolchok JD. Of Mice and Men (and Dogs): development of a xenogeneic DNA vaccine for canine oral malignant melanoma. *Cancer Ther*. (2008) 6:817–26.
24. Poorman K, Borst L, Moroff S, Roy S, Labelle P, Motsinger-Reif A, et al. Comparative cytogenetic characterization of primary canine melanocytic lesions using array CGH and fluorescence *in situ* hybridization. *Chromosome Res*. (2015) 23:171–86. doi: 10.1007/s10577-014-9444-6
25. Goldschmidt MH, Dunstan RW, Stannard AA, von Tscharner C, Walder EJ, Yager JA. *Histological Classification of Epithelial and Melanocytic Tumors of the Skin of Domestic Animals*. Washington, DC: Armed Forces Institute of Pathology in cooperation with the American Registry of Pathology and TheWorld Health Organization Colaborating Center for Worldwide Reference on Comparative Oncology (1998). p. 38–40.
26. Mermel CH, Schumacher SE, Hill B, Meyerson ML, Beroukhim R, Getz G. GISTIC2.0 facilitates sensitive and confident localization of the targets of focal somatic copy-number alteration in human cancers. *Genome Biol*. (2011) 12:R41. doi: 10.1186/gb-2011-12-4-r41
27. Giannuzzi D, Marconato L, Elgendy R, Ferraresso S, Scarselli E, Fariselli P, et al. Longitudinal transcriptomic and genetic landscape of radiotherapy response in canine melanoma. *Vet Comp Oncol*. (2019) 17:308–16. doi: 10.1111/vco.12473
28. Hendricks WPD, Zismann V, Sivaprakasam K, Legendre C, Poorman K, Tembe W, et al. Somatic inactivating PTPRJ mutations and dysregulated pathways identified in canine malignant melanoma by integrated comparative genomic analysis. *PLoS Genet*. (2018) 14:e1007589. doi: 10.1371/journal.pgen.1007589
29. Bindea G, Mlecnik B, Hackl H, Charoentong P, Tosolini M, Kirilovsky A, et al. ClueGO : a Cytoscape plug-in to decipher functionally grouped gene ontology and pathway annotation networks. *Bioinformatics*. (2009) 25:1091–3. doi: 10.1093/bioinformatics/btp101
30. Bergin IL, Smedley RC, Esplin DG, Spangler WL, Kiupel M. Prognostic evaluation of Ki67 threshold value in canine oral melanoma. *Vet Pathol*. (2011) 48:41–53. doi: 10.1177/0300985810388947
31. Edgar R, Domrachev M, Lash AE. Gene Expression Omnibus: NCBI gene expression and hybridization array data repository. *Nucleic Acids Res*. (2002) 30:207–10. doi: 10.1093/nar/30.1.207
32. Bowlt Blacklock KL, Birand Z, Selmic LE, Nelissen P, Murphy S, Blackwood L, et al. Genome-wide analysis of canine oral malignant melanoma metastasis-associated gene expression. *Sci Rep*. (2019) 9:6511. doi: 10.1038/s41598-019-42839-x
33. Stockert JC, López-Arias B, Del Castillo P, Romero A, Blázquez-Castro A. Replacing xylene with n-heptane for paraffin embedding. *Biotech Histochem*. (2012) 87:464–7. doi: 10.3109/10520295.2012.701764
34. Forslund A, Zeng Z, Qin LX, Rosenberg S, Ndubuisi M, Pincas H, et al. MDM2 gene amplification is correlated to tumor progression but not to the presence of SNP309 or TP53 mutational status in primary colorectal cancers. *Mol Cancer Res*. (2008) 6:205–11. doi: 10.1158/1541-7786.MCR-07-0239
35. Furth N, Aylon Y, Oren M. p53 shades of Hippo. *Cell Death Differ*. (2018) 25:81–92. doi: 10.1038/cdd.2017.163
36. Zamboni C, Brocca G, Ferraresso S, Ferro S, Sammarco A, Dal Corso C, et al. Cyclin D1 immunohistochemical expression and somatic mutations in canine oral melanoma. *Vet Comp Oncol*. (2019) 1–8:12539. doi: 10.1111/vco.12539
37. Rosenwald IB, Lazaris-Karatzas A, Sonenberg N, Schmidt EV. Elevated levels of cyclin D1 protein in response to increased expression of eukaryotic initiation factor 4E. *Mol Cell Biol*. (1993) 13:7358–63. doi: 10.1128/MCB.13.12.7358
38. Rosenwald IB, Kaspar R, Rousseau D, Gehrke L, Leboulch P, Chen JJ, et al. Eukaryotic translation initiation factor 4E regulates expression of cyclin D1 at transcriptional and post-transcriptional levels. *J Biol Chem*. (1995) 270:21176–80. doi: 10.1074/jbc.270.36.21176
39. Avdulov S, Li S, Michalek V, Burrichter D, Peterson M, Perlman DM, et al. Activation of translation complex eIF4F is essential for the genesis and maintenance of the malignant phenotype in human mammary epithelial cells. *Cancer Cell*. (2004) 5:553–63. doi: 10.1016/j.ccr.2004.05.024
40. Lin L, Holbro T, Alonso G, Gerosa D, Burger MM. Molecular interaction between human tumor marker protein p150, the largest subunit of eIF3, and intermediate filament protein K7. *J Cell Biochem*. (2001) 80:483–90. doi: 10.1002/1097-4644(20010315)80:4%3C483::aid-jcb1002%3E3.0.co;2-b
41. Gillis LD, Lewis SM. Decreased eIF3e/Int6 expression causes epithelial-to-mesenchymal transition in breast epithelial cells. *Oncogene*. (2013) 32:3598–605. doi: 10.1038/onc.2012.371
42. Shi J, Kahle A, Hershey JW, Honchak BM, Warneke JA, Leong SP, et al. Decreased expression of eukaryotic initiation factor 3f deregulates translation and apoptosis in tumor cells. *Oncogene*. (2006) 25:4923–36. doi: 10.1038/sj.onc.1209495
43. Pincheira R, Chen Q, Zhang JT. Identification of a 170-kDa protein over-expressed in lung cancers. *Br J Cancer*. (2001) 84:1520–7. doi: 10.1054/bjoc.2001.1828
44. Rothe M, Ko Y, Albers P, Wernert N. Eukaryotic initiation factor 3 p110 mRNA is overexpressed in testicular seminomas. *Am J Pathol*. (2000) 157:1597–604. doi: 10.1016/S0002-9440(10)64797-9
45. Nupponen NN, Porkka K, Kakkola L, Tanner M, Persson K, Borg A, et al. Amplification and overexpression of p40 subunit of eukaryotic translation initiation factor 3 in breast and prostate cancer. *Am J Pathol*. (1999) 154:1777–83. doi: 10.1016/S0002-9440(10)65433-8

46. Miyazaki S, Imatani A, Ballard L, Marchetti A, Buttitta F, Albertsen H, et al. The chromosome location of the human homolog of the mouse mammary tumor—associated gene INT6 and its status in human breast carcinomas. *Genomics*. (1997) 46:155–8. doi: 10.1006/geno.1997.4996
47. Doldan A, Chandramouli A, Shanas R, Bhattacharyya A, Cunningham JT, Nelson MA, et al. Loss of the eukaryotic initiation factor 3f in pancreatic cancer. *Mol Carcinog*. (2008) 47:235–44. doi: 10.1002/mc.20379
48. Li Z, Lin S, Jiang T, Wang J, Lu H, Tang H, et al. Overexpression of eIF3e is correlated with colon tumor development and poor prognosis. *Int J Clin Exp Pathol*. (2014) 7:6462–74.
49. Sesen J, Cammas A, Scotland SJ, Elefterion B, Lemarié A, Millevoi S, et al. Int6/eIF3e is essential for proliferation and survival of human glioblastoma cells. *Int J Mol Sci*. (2014) 15:2172–90. doi: 10.3390/ijms15022172
50. Doldan A, Chandramouli A, Shanas R, Bhattacharyya A, Leong SP, Nelson MA, et al. Loss of the eukaryotic initiation factor 3f in melanoma. *Mol Carcinog*. (2008) 47:806–13. doi: 10.1002/mc.20436
51. Li H, Zhou F, Wang H, Lin D, Chen G, Zuo X, et al. Knockdown of EIF3D suppresses proliferation of human melanoma cells through G2/M phase arrest. *Biotechnol Appl Biochem*. (2015) 62:615–20. doi: 10.1002/bab.1305
52. Fowles JS, Denton CL, Gustafson DL. Comparative analysis of MAPK and PI3K/AKT pathway activation and inhibition in human and canine melanoma. *Vet Comp Oncol*. (2015) 13:288–304. doi: 10.1111/vco.12044
53. Wei BR, Michael HT, Halsey CH, Peer CJ, Adhikari A, Dwyer JE, et al. Synergistic targeted inhibition of MEK and dual PI3K/mTOR diminishes viability and inhibits tumor growth of canine melanoma underscoring its utility as a preclinical model for human mucosal melanoma. *Pigment Cell Melanoma Res*. (2016) 29:643–55. doi: 10.1111/pcmr.12512
54. London CA. Tyrosine kinase inhibitors in veterinary medicine. *Top Companion Anim Med*. (2009) 24:106–12. doi: 10.1053/j.tcam.2009.02.002
55. Helal-Neto E, Brandão-Costa RM, Saldanha-Gama R, Ribeiro-Pereira C, Midlej V, Benchimol M, et al. Priming endothelial cells with a melanoma-derived extracellular matrix triggers the activation of αvβ3/VEGFR2 axis. *J Cell Physiol*. (2016) 231:2464–73. doi: 10.1002/jcp.25358
56. Sato A, Sunayama J, Matsuda K, Tachibana K, Sakurada K, Tomiyama A, et al. Regulation of neural stem/progenitor cell maintenance by PI3K and mTOR. *Neurosci Lett*. (2010) 470:115–20. doi: 10.1016/j.neulet.2009.12.067
57. Braeuer RR, Watson IR, Wu CJ, Mobley AK, Kamiya T, Shoshan E, et al. Why is melanoma so metastatic? *Pigment Cell Melanoma Res*. (2014) 27:19–36. doi: 10.1111/pcmr.12172
58. Asundi J, Reed C, Arca J, McCutcheon K, Ferrando R, Clark S, et al. An antibody-drug conjugate targeting the endothelin B receptor for the treatment of melanoma. *Clin Cancer Res*. (2011) 17:965–75. doi: 10.1158/1078-0432.CCR-10-2340
59. Sandhu S, McNeil CM, LoRusso P, Patel MR, Kabbarah O, Li C, et al. Phase I study of the anti-endothelin B receptor antibody-drug conjugate DEDN6526A in patients with metastatic or unresectable cutaneous, mucosal, or uveal melanoma. *Invest New Drugs*. (2019) 1–11. doi: 10.1007/s10637-019-00832-1
60. Luca M, Huang S, Gershenwald JE, Singh RK, Reich R, Bar-Eli M. Expression of interleukin-8 by human melanoma cells up-regulates MMP-2 activity and increases tumor growth and metastasis. *Am J Pathol*. (1997) 151:1105–13.
61. Varney ML, Johansson SL, Singh RK. Distinct expression of CXCL8 and its receptors CXCR1 and CXCR2 and their association with vessel density and aggressiveness in malignant melanoma. *Am J Clin Pathol*. (2006) 125:209–16. doi: 10.1309/VPL5R3JR7F1D6V03
62. Satow R, Nakamura T, Kato C, Endo M, Tamura M, Batori R, et al. ZIC5 drives melanoma aggressiveness by PDGFD-mediated activation of FAK and STAT3. *Cancer Res*. (2017) 77:366–77. doi: 10.1158/0008-5472.CAN-16-0991
63. Ottnod JM, Smedley RC, Walshaw R, Hauptman JG, Kiupel M, Obradovich JE. A retrospective analysis of the efficacy of Oncept vaccine for the adjunct treatment of canine oral malignant melanoma. *Vet Comp Oncol*. (2013) 11:219–29. doi: 10.1111/vco.12057
64. Treggiari E, Grant JP, North SM. A retrospective review of outcome and survival following surgery and adjuvant xenogeneic DNA vaccination in 32 dogs with oral malignant melanoma. *J Vet Med Sci*. (2016) 78:845–50. doi: 10.1292/jvms.15-0510
65. Verganti S, Berlato D, Blackwood L, Amores-Fuster I, Polton GA, Elders R, et al. Use of Oncept melanoma vaccine in 69 canine oral malignant melanomas in the UK. *J Small Anim Pract*. (2017) 58:10–6. doi: 10.1111/jsap.12613
66. Castelli C, Rivoltini L, Andreola G, Carrabba M, Renkvist N, Parmiani G. T-cell recognition of melanoma-associated antigens. *J Cell Physiol*. (2000) 182:323–31. doi: 10.1002/(SICI)1097-4652(200003)182:3%3C323::AID-JCP2%3E3.0.CO;2-%23
67. Park EJ, Kim JH, Seong RH, Kim CG, Park SD, Hong SH. Characterization of a novel mouse cDNA, ES18, involved in apoptotic cell death of T-cells. *Nucleic Acids Res*. (1999) 27:1524–30. doi: 10.1093/nar/27.6.1524
68. Zou JX, Revenko AS, Li LB, Gemo AT, Chen HW. ANCCA, an estrogen-regulated AAA+ ATPase coactivator for ERα, is required for coregulator occupancy and chromatin modification. *Proc Natl Acad Sci USA*. (2007) 104:18067–72. doi: 10.1073/pnas.0705814104
69. Lee Y, Lee JK, Ahn SH, Lee J, Nam DH. WNT signaling in glioblastoma and therapeutic opportunities. *Lab Investig*. (2016) 96:137–50. doi: 10.1038/labinvest.2015.140
70. Song Y, Li L, Ou Y, Gao Z, Li E, Li X, et al. Identification of genomic alterations in oesophageal squamous cell cancer. *Nature*. (2014) 509:91–5. doi: 10.1038/nature13176
71. Arend RC, Londoño-Joshi AI, Straughn JM Jr, Buchsbaum DJ. The Wnt/β-catenin pathway in ovarian cancer: a review. *Gynecol Oncol*. (2013) 131:772–9. doi: 10.1016/j.ygyno.2013.09.034
72. Howe LR, Brown AM. Wnt signaling and breast cancer. *Cancer Biol Ther*. (2004) 3:36–41. doi: 10.4161/cbt.3.1.561
73. Deitrick J, Pruitt WM. Wnt/β catenin-mediated signaling commonly altered in colorectal cancer. *Prog Mol Biol Transl Sci*. (2016) 144:49–68. doi: 10.1016/bs.pmbts.2016.09.010
74. Schneider JA, Logan SK. Revisiting the role of Wnt/β-catenin signaling in prostate cancer. *Mol Cell Endocrinol*. (2018) 462:3–8. doi: 10.1016/j.mce.2017.02.008
75. Rapp J, Jaromi L, Kvell K, Miskei G, Pongracz JE. WNT signaling - lung cancer is no exception. *Respir Res*. (2017) 18:167. doi: 10.1186/s12931-017-0650-6
76. Kaur A, Webster MR, Weeraratna AT. In the Wnt-er of life: Wnt signalling in melanoma and ageing. *Br J Cancer*. (2016) 115:1273–9. doi: 10.1038/bjc.2016.332
77. Bergman PJ. Canine oral melanoma. *Clin Tech Small Anim Pract*. (2007) 22:55–60. doi: 10.1053/j.ctsap.2007.03.004

Conflict of Interest: The authors declare that the research was conducted in the absence of any commercial or financial relationships that could be construed as a potential conflict of interest.

Copyright © 2019 Brocca, Ferraresso, Zamboni, Martinez-Merlo, Ferro, Goldschmidt and Castagnaro. This is an open-access article distributed under the terms of the Creative Commons Attribution License (CC BY). The use, distribution or reproduction in other forums is permitted, provided the original author(s) and the copyright owner(s) are credited and that the original publication in this journal is cited, in accordance with accepted academic practice. No use, distribution or reproduction is permitted which does not comply with these terms.

frontiers in Immunology

REVIEW
published: 17 January 2020
doi: 10.3389/fimmu.2019.02935

A Role for Dogs in Advancing Cancer Immunotherapy Research

*Steven Dow**

Flint Animal Cancer Center, Department of Clinical Sciences, College of Veterinary Medicine and Biomedical Sciences, Colorado State University, Fort Collins, CO, United States

While rodent cancer models are essential for early proof-of-concept and mechanistic studies for immune therapies, these models have limitations with regards to predicting the ultimate effectiveness of new immunotherapies in humans. As a unique spontaneous, large animal model of cancer, the value of conducting studies in pet dogs with cancer has been increasingly recognized by the research community. This review will therefore summarize key aspects of the dog cancer immunotherapy model and the role that these studies may play in the overall immunotherapy drug research effort. We will focus on cancer types and settings in which the dog model is most likely to impact clinical immuno-oncology research and drug development. Immunological reagent availability is discussed, along with some unique opportunities and challenges associated with the dog immunotherapy model. Overall it is hoped that this review will increase awareness of the dog cancer immunotherapy model and stimulate additional collaborative studies to benefit both man and man's best friend.

Keywords: canine, immune, cell, cytokine, oncology

OPEN ACCESS

Edited by:
Mark W. Dewhirst,
Duke University, United States

Reviewed by:
Silvia C. Formenti,
Weill Cornell Medicine, Cornell University, United States
Xiaobo Zhang,
Zhejiang University, China
Elizabeth Ann Repasky,
Roswell Park Comprehensive Cancer Center, University at Buffalo, United States

***Correspondence:**
Steven Dow
sdow@colostate.edu

Specialty section:
This article was submitted to Comparative Immunology, a section of the journal Frontiers in Immunology

Received: *02 August 2019*
Accepted: *29 November 2019*
Published: *17 January 2020*

Citation:
Dow S (2020) A Role for Dogs in Advancing Cancer Immunotherapy Research. Front. Immunol. 10:2935. doi: 10.3389/fimmu.2019.02935

INTRODUCTION

Cancer immunotherapy continues to make remarkable strides in just the few years since the first checkpoint molecule targeted therapeutic antibodies were evaluated in trials and approved by the FDA. Indeed, there is the sense by the author and colleagues in the veterinary immune-oncology community (Personal Communication, 2019) that the field of human immune-oncology is advancing so rapidly that new immunotherapy combinations are being evaluated before there is time to determine whether the combinations are truly effective, as judged by evidence of synergistic or additive antitumor activity in realistic animal models (1, 2). Thus, there is a need for additional animal models with which to evaluate new cancer immunotherapies, particularly novel immunotherapy combinations, including immunotherapy combined with targeted therapies, chemotherapy, and radiation therapy. Current rodent cancer models have certain limitations with regards to predicting the ultimate effectiveness of new immunotherapies in humans (3–5).

Increasingly the NIH and pharmaceutical and biotechnology companies are looking to alternative animal models with which to screen immunotherapeutic drugs. The dog spontaneous cancer model has received considerable attention recently (4, 6–13). Several factors drive interest in the dog model. For example, dogs spontaneously develop cancer that resembles human malignancies in many important respects, including phenotype, biological behavioral, histology, mutational signatures and signaling pathways, and immune responses. Indeed, the value of the dog cancer model was recently recognized by the National Institute of Medicine (9).

Therefore, this review will summarize key aspects of the dog cancer model that make it particularly well-suited to evaluating cancer immunotherapies and drug combinations. This will

not however be a comprehensive review of all dog cancer immunotherapy studies, which have been reviewed elsewhere and are beyond the scope of this work (3, 14–20). We will instead focus on areas of investigation in which the dog model currently may be most likely to impact clinical immuno-oncology research and new drug development. Reagent availability is also discussed, along with some challenges faced by the dog immunotherapy model along with strategies to overcome these challenges. The intent of this review is to increase awareness of the dog cancer model and stimulate additional studies, which in many cases may benefit both man and man's best friend.

THE CANINE CANCER MODEL AND RELEVANCE TO IMMUNOLOGICAL STUDIES

The uniquely valuable aspects of the canine cancer model have been well-covered in recent reviews (6, 7, 13). With regards to immunological studies in general, there are several key differences between dogs and rodents. For one, dogs are considered an immunologically outbred species, though there are genetic bottlenecks (i.e., limited genotypic or phenotypic diversity within breeds due to extensive inbreeding) for certain breeds of dogs (13). In fact, the availability of dog breeds can in some cases make it possible to map genetic loci to certain immunological traits, as in the example of susceptibility to lymphoma in dogs (21). For example, it was reported that usage of certain VH genes has been associated with improved survival times in canine B cell lymphoma, a dog model for human non-Hodgkin lymphoma (22). Other cancer traits have also been mapped to specific genetic loci in dogs by taking advantage of dog breed genetics (23–26).

Another relevant aspect of the dog model is that the immune system of dogs in cancer immunotherapy studies is typically already very immunologically experienced, with animals having experienced exposure to multiple immunizations during their early years, and to multiple different viral and bacterial infections prior to development of cancer. These immunological events all shape the immune repertoire of dogs and consequently render the dog much more immunologically experienced than rodents raised in sterile cages and fed sterilized water and chow. Dogs also share the same environment of their human companions, and are therefore exposed to many of the same allergens, food antigens, and environmental chemicals (6, 8). Thus, it is not surprising that dogs may react to an immunotherapeutic drug in a different manner than rodents, and behave in many ways more analogously to humans.

Dogs also develop tumors spontaneously, which means that the immune system has typically had weeks to months to recognize the tumor and mount immune responses prior to the appearance of a tumor large enough to diagnose. This long-term exposure to tumor antigens and secreted factors thus educates and conditions the canine immune system in a way that cannot be recapitulated in rodent implanted or induced tumor models (3, 5, 27). Moreover, the canine immune system is much more broadly "educated" which will shape the development of antitumor immunity.

From the standpoint of dosing immunotherapy drugs (other than vaccines), dogs with their similar body sizes and metabolic pathways also fill a gap not currently addressed by rodent studies. Drugs dosed based on weight or body surface area in dogs are much more likely to predict drug activity and toxicity than drugs dosed in mice frequently treated at much higher drug concentrations than can be tolerated by human patients (8). This feature of studies in dogs would be particularly relevant for dosing small molecule drugs and biologics such as monoclonal antibodies, where volume of distribution is critical for determining activity and toxicity (6, 8, 10, 13). The larger size of dogs and their tumors also makes repeated access to blood and tumor tissue biopsies a possibility, which is often important in immunological studies to assess the progression of immune responses, as for example changes in immune infiltrates in tumor tissues.

COMPARISON OF DOG AND HUMAN IMMUNE CELLS AND IMMUNE RESPONSES

The canine immune system and immune responses in general are very similar to those of humans, with a few notable differences. In broad terms, numbers and proportions of T cells (CD4 and CD8) and B cells in blood of adult dogs closely resemble those of humans (Schalm's Veterinary Hematology, 7th edition and Clinical Immunology of the Dog and Cat, 2nd edition). Moreover, the ratio of CD4 to CD8 T cells (∼2:1) in blood and lymph nodes is similar in dogs and humans. Numbers and percentages of neutrophils and monocytes in blood of both species are also very similar. However, recent reagent development for canine NK cells may improve our ability to quantitate dog NK cell responses (28, 29). Dogs also have circulating gamma-delta T cells, though little is known regarding how their numbers may change in disease states (30). Regulatory T cells (CD4+FoxP3+) in dogs have also been defined, and their numbers shown to be significantly increased in dogs with cancer, in both blood and tumor-draining lymph nodes (31–33).

Circulating concentrations of immunoglobulins in adult dogs are approximately the same as those of adult humans, though much less is known about normal immunoglobulin concentrations in young dogs and when final adult IgG concentrations are attained (Schalm's Veterinary Hematology, 7th edition and Clinical Immunology of the Dog and Cat, 2nd edition). Canine IgG molecules can be classified into four functional subclasses (A–D), similar to the human IgG subclasses, with two subclasses capable of binding Fc receptors and two subclasses being Fc functionally negative (34).

T cells in dogs express many of the same co-stimulatory or co-inhibitory molecules as present in humans, including CD28, PD-1, OX40, TIGIT, TIM-3, and Lag3. Like human T cells, canine T cells constitutively express low levels of MHCII, which can be upregulated following T cell activation. In addition,

canine effector T cells upregulate production of granzyme B, in addition to CD25 and MHCII (35). Antigen presenting cell (B cells, DC, and monocyte and macrophages) in dogs also share many co-stimulatory or inhibitory molecules with human APC, including MHCII, CD40, CD80, CD86, PD-L1 expression (36–40). In addition, responses to activation, as for example with TLR ligands, is also similar, with upregulated expression of co-stimulatory molecules, and production of pro-inflammatory cytokines such TNF-a, IL-1b, and IL-6, and anti-inflammatory cytokines including IL-10 and TGF-b. In addition, canine monocytes express the chemokine receptor CCR2 and migrate in response to an MCP-1 gradient (41).

An unusual feature of dog neutrophils, which differs from neutrophils in humans, is their expression of CD4 (Schalm's Veterinary Hematology, 7th edition and Clinical Immunology of the Dog and Cat, 2nd edition). The function of CD4 molecule expression by canine neutrophils is unclear, and CD4 is not expressed by other myeloid lineage cells such as monocytes in dogs. Dogs also appear to have a greater abundance of mast cells than humans, especially in mucosal sites such as the skin and airways, and mast cell tumors are much more common in dogs than in humans. Dogs also develop malignancies of cells of the DC and macrophage lineage (e.g., malignant histiosarcoma) at a much higher rate than in humans (e.g., Langerhans histiocytosis) (42–44).

SELECTED CANINE CANCER IMMUNOTHERAPY STUDIES WITH HIGH RELEVANCE TO HUMAN IMMUNO-ONCOLOGY

Dogs will never replace rodent cancer models for cancer immunotherapy drug research and development, since early drug screening and mechanism of action studies can realistically only be done in rodent models. However, there are several tumor models where the dog may offer clear advantages, particularly for assessment of new immunotherapies and their potential efficacy against metastatic disease (3, 9, 45). For example, the dog model may be uniquely valuable to address the following issues with respect to cancer immunotherapy: Can new cancer vaccines control advanced metastatic disease?; Can adoptive CAR T cell or NK cell therapy be both safe and active against solid tumors, and what is the safety profile?; How well do tumor microenvironment modifying agents work when combined with existing immunotherapies such as targeted drugs or checkpoint molecule antibodies?; Can checkpoint targeted therapeutics be effectively combined with other cancer treatment modalities (e.g., radiation therapy, cytotoxic chemotherapy) to control or prevent tumor metastases? These examples are discussed in greater detail below. A summary of key recent dog immunotherapy studies is provided in **Table 1**.

TABLE 1 | Summary of relevant canine cancer immunotherapy trials and results.

Trial	Delivery	Tumor type	Number enrolled	Study primary endpoints	Secondary endpoints	Outcomes	References
Her2 neu vaccine	Listeria vectored (IV)	Osteosarcoma	18	Time to metastasis	T cell responses	Increase OST vs. historical control	(46)
TERT vaccine	AAV vectored (IM)	B cell lymphoma	14	Time to progression, OST	TERT antibodies	Increase OST vs. historical control	(47)
Vaccine plus surgery	Autologous tumor lysate (SC)	Meningioma	11	Tumor progression	Antibody response	No tumor progression over 6 months	(48)
CD20 CAR T	Transduced autologous T cells	B cell lymphoma	1	Safety	Tumor regression	Safely tolerated, partial tumor response	(49)
NK cell ACT	Intratumoral administration	Osteosarcoma	10	Safety, tumor regression	Tumor infiltrates	Improved DFI, NK localization	(50)
Liposomal clodronate	IV, repeat infusions	Soft tissue sarcoma	13	Safety, macrophage depletion	Tumor regression	Macrophage depletion, no tumor responses	(51)
CCR4 blockade	Antagonist antibody (IV)	Bladder cancer	26	Treg infiltrates	Survival, toxicity	Improved OST, Treg depletion	(52)
IDO inhibitor wth XRT	Oral	Melanoma, soft tissue sarcom	5	Safety, tumor response	Reduction in Tregs	Partial tumor response, immune response	(53)
Allogeneic tumor vaccine	Tumor lysate with adjuvant (SC)	Hemangiosarcoma	28	OST, tumor progression	Antibody response	Increase survival vs. historical control	(54)
Bacterial immunotherapy	Attenuated Salmonella (IV)	Multiple tumor types	41	Tumor regression	Bacterial localization	15% overall response rate; dose dependent toxicity	(55)
Local superantigen immunotherapy	Plasmid DNA, intratumoral	Melanoma	26	Tumor regression, OST	Immune infiltrates	Increased survival vs. historical control; CTL activity	(56)
Liposomal MTP	IV, repeat infusions	Osteosarcoma	98	DFI and OST	Macrophage activation	DFI and OST significantly increased	(57)

Cancer Vaccines

A key question related to the new generation of cancer vaccines currently under development, which is difficult to fully address in rodent models, is whether they can effectively prevent metastatic disease, or control metastases once they develop. As noted above, dogs develop several highly metastatic cancers closely related to human cancers, including in particular osteosarcoma and melanoma (6, 20, 57). These cancers in dogs therefore offer an opportunity to test new cancer vaccine approaches in immunologically realistic settings. As an example, studies are currently underway in dogs with osteosarcoma to determine whether a newly conditionally approved canine osteosarcoma Listeria-vectored vaccine targeting HER2/neu can effectively prevent tumor metastases, and control the growth of macroscopic metastases (46). This novel vaccine approach has demonstrated remarkable early evidence of activity as adjuvant therapy for dogs with osteosarcoma at high risk for tumor metastases. Another example is a plasmid-DNA based tumor vaccine targeting the TERT antigen, which has been evaluated in dogs with lymphoma in combination with CHOP chemotherapy (47, 58). The vaccine has also demonstrated impressive antitumor activity, as reflected in prolonged disease-free intervals compared to relevant chemotherapy only control animals. A number of other cancer vaccine targets are currently being evaluated in canine immunotherapy studies, including the GD3 antigen in canine melanoma studies (59).

Adoptive Cellular Therapy

Adoptive cell therapy (ACT) with CAR T cells has transformed the treatment of certain leukemias and several other hematopoietic cancers in humans. However, progress in using CAR T cells to treat solid tumors in humans has been more fraught with difficulty, including serious and occasionally fatal toxicities, as well as less overall anti-tumor activity. The adverse events associated with CAR T cell treatment of solid tumors were unfortunately not predicted by rodent cancer models. Given the strong similarities between canine and human immune responses, dogs with solid tumors offer a unique opportunity to evaluate the safety and potential efficacy of new ACTs such as CAR T cell therapy before initiating human clinical trials. Indeed, ACT with CAR T cells has been evaluated in small scale studies in dogs, including CAR T cell studies with a CD20 targeted CAR T cells in dogs with B cell lymphoma (49). Other opportunities for use of the dog tumor model include evaluation of ACT with CAR T or CAR NK cells specific for other widely expressed tumor antigens in dogs, including HER2/neu, EGFR, and GD2 (60). For example, ACT using activated canine NK cells has shown early promise in conjunction with radiation therapy in a dog osteosarcoma model (50).

Tumor Microenvironment Modification

Increasingly studies point to the essential role of the tumor microenvironment (TME) in regulating overall anti-tumor immune responses. Thus, a new wave of therapeutics that target the TME are under development and evaluation in clinical trials. Our studies have identified a wide spectrum of immune responses in tumor tissues of dogs, ranging from highly inflammatory tumors (e.g., melanoma) to tumors that are immunologically "cold" (e.g., soft tissue sarcoma, mast cell tumors, osteosarcoma) (Regan D; Flint Animal Cancer Center, unpublished data). Each of these tumor models in dogs therefore offers the opportunity for evaluation of agents that target the TME, particularly for those designed to remove immune suppressive cells to help activate immunologically "cold" tumors. For example, depleting target tumor-associated macrophages by administration of agents such as liposomal clodronate that deplete tumor macrophages outright has been evaluated in dogs (51, 61). We also found that modifying the TME by direct tumor transfection with a potent T cell activating molecule such as a bacterial superantigen could stimulate T cell infiltration and activation and significant tumor regression in dogs with melanoma [**Figure 1**; (56)].

A second strategy to eliminate the immune suppressive tumor macrophage population is to prevent their recruitment to tumor tissues by administering agents that block signaling by the

FIGURE 1 | Tumor response to TME modification with a T cell activator. A dog with oral malignant melanoma (left panel) was treated with a series of every 2 week intratumoral injections of plasmid DNA encoding a bacterial superantigen gene (SEB), along with an IL-2 encoding plasmid. Tumor depigmentation was evident after the first injection (middle image) and complete tumor regression was noted after the second intratumoral injection (right panel).

chemokine receptor CCR2. Given that there are no currently approved (or affordable) pure CCR2 antagonists available for evaluation in dogs, our group has identified several drugs, most notably angiotensin receptor antagonists (ARBs), that can be repurposed as monocyte migration inhibitors. For example, we reported recently that the ARB losartan exerts potent antitumor activity by blocking signaling via the CCR2 chemokine receptor, thereby inhibiting the recruitment of inflammatory monocytes into tumor tissues, leading to overall tumor macrophage depletion (62). A recently completed clinical trial in dogs with metastatic osteosarcoma treated with high-dose losartan immunotherapy demonstrated significant antitumor activity and systemic suppression of monocyte migration (Regan et al., in review).

As another strategy to modify the TME, it was recently reported that blockade of CCR4 signaling with humanized antibodies could significantly deplete Tregs in a canine model of invasive bladder cancer (52). In that study, treatment with an anti-CCR4 antibody depleted Tregs in bladder tumor tissues in dogs, and was associated with sustained tumor regression, and prolonged survival.

Other groups have investigated indoleamine deoxygenase inhibitors, which target an immune suppressive metabolic pathway in the TME (53, 63). The hypoxic TME in brain cancer can also be modified by administering agents that increase tumor oxygenation in dogs, in conjunction with radiation (64). Thus, the dog cancer model offers multiple opportunities to evaluate TME modulating drugs, particularly because many of these studies have relatively simple PD endpoints and may be of relatively short duration if the primary study endpoints are changes in the TME rather than tumor responses *per se*.

Checkpoint Molecule Targeted Immunotherapies

Checkpoint targeted therapeutics are far advanced in development and approval for treatment of multiple cancers in humans. As new checkpoint molecule targeted drugs become available in dogs, opportunities exist where the dog model may provide important new information, particularly with respect rational combination therapies of immune targeted drugs given with checkpoint inhibitors. A fully canine PD-1 antibody is currently nearing phase I trial completion in dogs with a variety of different cancers and a product launch is possible in 2020 (40). Other canine checkpoint targeted antibodies are also in the pipeline, including PD-L1 and OX40 antibodies. In addition, several small molecule inhibitors of checkpoint molecules are being investigated in clinical tumor vaccine trials in dogs with brain cancer (64–66).

Thus, the anticipated availability of new checkpoint immunotherapy reagents will make it possible to conduct creative trials in dogs. For example, a number of questions could be addressed, including: Are checkpoint molecule therapeutics effective when administered in an adjuvant setting in dogs with highly metastatic disease such as osteosarcoma or hemangiosarcoma? Or can checkpoint inhibitors be effectively combined with cytotoxic drugs such as CHOP for treatment of lymphoma? Or does co-administration of a checkpoint inhibitor with a tumor vaccine such as the Her2/neu vaccine improve vaccine efficacy in the setting of advanced, bulky tumors? As these examples suggest, a number of important questions related to adjuvant therapy and checkpoint therapy combinations can be addressed in targeted populations of dogs with relevant cancers.

TABLE 2 | Immunological reagents for cell identification and functional assessment in dogs with cancer.

Molecule	Cellular expression	Usage
CD3	T cells	FC, IHC
CD5	T cells	FC
CD4	Th subset, neutrophils	FC, IHC
CD8	Tc subset	FC, IHC
CD9	Myeloid cells, T cells	FC
CD11a	Leukocytes, memory T cells	FC
CD11b	Myeloid cells	FC, IHC
CD11c	DC, some macrophages	FC, IHC
CD14	Monocytes, some neutrophils	FC
CD18	Myeloid cells, MH	FC, IHC
CD19, CD20, CD21	B cells, lymphoma	FC
CD25	Activated T cells, Tregs	FC
CD31	Endothelial cells	IHC
CD34	Hematopoietic stem cells	FC
CD40	APC	FC
CD45	All hematopoietic cells	FC
CD61	Platelets	FC
CD79a	Pre-B cell	IHC
CD86	APC	FC
MHCII	T cells, APC	FC, IHC
FoxP3	Regulatory T cells	FC, IHC
Granzyme B	T cells	FC, IHC
TNF-a	T cells, APC	FC, IHC
IFN-g	T cells, NK cells	FC, IHC
EOMES	T cell (exhausted; memory)	FC
Tim-3	T cell (exhausted)	FC
PD-1	T cell (exhausted); also recently activated	FC
PD-L1	Monocyte, macrophage, DC	FC, IHC
Ki67	Proliferating cells	FC, IHC

Other Immunotherapy Approaches

Additional promising cancer immunotherapy strategies are also under evaluation in the dog cancer model. These include the use of viral vectored cytokine delivery approaches (brain cancer), systemic administration of IL-12 nanoparticles (soft tissue sarcoma), bacterial delivered therapeutics (e.g., engineered hypoxia targeting *Salmonella* in soft tissue sarcoma), regulatory T cell depletion with metronomically delivered chemotherapeutics (e.g., toceranib), adoptive transfer of non-specifically activated T cells and IL-15 activated NK cells (osteosarcoma), along with a variety of different cancer vaccines (50, 55, 67). Thus, the canine oncology field has widely embraced the potential for immunotherapy, and it is likely this trend will

TABLE 3 | Cytokine reagents for dogs.

Cytokine	Expression	Format
IL-1b	Monocyte, macrophage	ELISA, multiplex
IL-2	T cells, NK cells, B cells	ELISA, multiplex
IL-4	Th2 T cells	ELISA
IL-6	Macrophage, T cells	ELISA, multiplex
IL-7	Multiple	multiplex
IL-8	Multiple	ELISA, multiplex
IL-10	APC, T cells	ELISA
IL-12	APC	ELISA
IL-15	Monocytes, others	multiplex
IL-18	APC	multiplex
MCP-1	Multiple	ELISA, multiplex
TNF-a	APC, T cells	ELISA, multiplex
GM-CSF	Multiple	multiplex
IFN-g	T cell, NK cell	ELISA, multiplex

continue in the future. Data from rigorously conducted trials of immunotherapy in dogs, paired with immune biomarker correlates (9) will help increase the impact of these studies on the human immuno-oncology.

Challenges for Immunotherapy Studies in Dogs

While there is great promise for studies in dogs with cancer to contribute to the advancement of immunotherapy for both dogs and humans, there are still challenges inherent to the dog immunotherapy model that must be addressed. Among these challenges is a perceived lack of necessary immunological reagents. Though this issue is often cited as a major impediment to immunotherapy studies in dogs, the reality is different (see **Tables 2** and **3**). For example, there are currently more than sufficient reagents available for evaluating immune responses to cancer, including T and B cell responses (activation, exhaustion, proliferation), monocyte and macrophage responses (numbers, functional phenotype), regulatory T cells (numbers), neutrophils (numbers, function), and NK cells (numbers, function) (**Table 2**). In addition, there are now a large variety of cytokine reagents for dog studies, including cytokine ELISAs, cytokine multiplexing kits, and antibodies for intracellular cytokine staining and analysis by flow cytometry (**Table 3**). It is also possible to assess immune responses in archived tissues and cells, using qRT-PCR and Nanostring technology, as well as next generation sequencing technologies (e.g., RNA sequencing).

Another important challenge of the dog model is related to the costs associated with upscaling drugs and immunological reagents for conducting pre-clinical studies in dogs, given their larger body size vs. mice. Moreover, there are substantial costs in terms of personnel (veterinarians, technicians, laboratory personnel) required to support such studies. However, all of these challenges are surmountable, given sufficient support from funding agencies, including more recently the NIH. The setting of realistic expectations at the outset of studies also helps minimize the impacts of these challenges.

Summary and Conclusions

The era of effective cancer immunotherapy represents a major change in how cancer is treated, and the dog cancer model undoubtedly has an opportunity to play an important role in advancing this field. The value of the dog cancer model for immunotherapy has been demonstrated previously, with the best example being the essential role played by dogs with osteosarcoma development of the non-specific immunotherapeutic L-MTP (liposomal muramyl tripeptide) as an approved immunotherapy for pediatric osteosarcoma (57, 68). The key to leveraging the dog model to advance such studies will be to identify questions that cannot be answered currently in rodent models, and to move nimbly to propose studies that can be informative within a short time frame (months), since the immunotherapy field moves so rapidly. Procuring adequate drug supplies and reagents for large animal studies is also essential. Finally, broad collaborations will always advance the field more effectively than single institution studies, particularly in situations where essential reagents must be shared or where access to patients with certain tumor types is limited. The best possible outcomes will be studies where the results can be translated promptly to benefit both dogs and humans, with their shared tumor types and strong bonds.

AUTHOR CONTRIBUTIONS

The author confirms being the sole contributor of this work and has approved it for publication.

FUNDING

The author wishes to acknowledge support from grants U01 CA224182-01 (SD) and an administrative supplement to CA143971(D. Theodorescu, University of Colorado Denver) from the National Cancer Institute of the National Institutes of Health, the Canine Health Foundation, and the Charles Shipley Foundation.

REFERENCES

1. Wege AK. Humanized mouse models for the preclinical assessment of cancer immunotherapy. *BioDrugs.* (2018) 32:245–66. doi: 10.1007/s40259-018-0275-4
2. Garden OA, Volk SW, Mason NJ, Perry JA. Companion animals in comparative oncology: one Medicine in action. *Vet J.* (2018) 240:6–13. doi: 10.1016/j.tvjl.2018.08.008
3. Park JS, Withers SS, Modiano JF, Kent MS, Chen M, Luna JI, et al. Canine cancer immunotherapy studies: linking mouse and human. *J Immunother Cancer.* (2016) 4:97. doi: 10.1186/s40425-016-0200-7
4. Withrow SJ, Khanna C. Bridging the gap between experimental animals and humans in osteosarcoma. *Cancer Treat Res.* (2009) 152:439–46. doi: 10.1007/978-1-4419-0284-9_24
5. Buque A, Galluzzi L. Modeling tumor immunology and immunotherapy in mice. *Trends Cancer.* (2018) 4:599–601. doi: 10.1016/j.trecan.2018.07.003

6. Khanna C, Lindblad-Toh K, Vail D, London C, Bergman P, Barber L, et al. The dog as a cancer model. *Nat Biotechnol.* (2006) 24:1065–6. doi: 10.1038/nbt0906-1065b
7. Khanna C, Gordon I. Catching cancer by the tail: new perspectives on the use of kinase inhibitors. *Clin Cancer Res.* (2009) 15:3645–7. doi: 10.1158/1078-0432.CCR-09-0132
8. Khanna C, London C, Vail D, Mazcko C, Hirschfeld S. Guiding the optimal translation of new cancer treatments from canine to human cancer patients. *Clin Cancer Res.* (2009) 15:5671–7. doi: 10.1158/1078-0432.CCR-09-0719
9. LeBlanc AK, Breen M, Choyke P, Dewhirst M, Fan TM, Gustafson DL, et al. Perspectives from man's best friend: National Academy of Medicine's Workshop on Comparative Oncology. *Sci Transl Med.* (2016) 8:324ps5. doi: 10.1126/scitranslmed.aaf0746
10. Paoloni M, Khanna C. Translation of new cancer treatments from pet dogs to humans. *Nat Rev Cancer.* (2008) 8:147–56. doi: 10.1038/nrc2273
11. Paoloni MC, Khanna C. Comparative oncology today. *Vet Clin North Am Small Anim Pract.* (2007) 37:1023–32. doi: 10.1016/j.cvsm.2007.08.003
12. Paoloni MC, Tandle A, Mazcko C, Hanna E, Kachala S, Leblanc A, et al. Launching a novel preclinical infrastructure: comparative oncology trials consortium directed therapeutic targeting of TNFalpha to cancer vasculature. *PLoS ONE.* (2009) 4:e4972. doi: 10.1371/journal.pone.0004972
13. Vail DM, MacEwen EG. Spontaneously occurring tumors of companion animals as models for human cancer. *Cancer Invest.* (2000) 18:781–92. doi: 10.3109/07357900009012210
14. Addissie S, Klingemann H. Cellular immunotherapy of canine cancer. *Vet Sci.* (2018) 5:E100. doi: 10.3390/vetsci5040100
15. Almela RM, Anson A. A Review of immunotherapeutic strategies in canine malignant melanoma. *Vet Sci.* (2019) 6:15. doi: 10.3390/vetsci6010015
16. Bergman PJ. Immunotherapy in veterinary oncology. *Vet Clin North Am Small Anim Pract.* (2014) 44:925–39. doi: 10.1016/j.cvsm.2014.05.002
17. Klingemann H. Immunotherapy for dogs: running behind humans. *Front Immunol.* (2018) 9:133. doi: 10.3389/fimmu.2018.00133
18. O'Connor CM, Wilson-Robles H. Developing T cell cancer immunotherapy in the dog with lymphoma. *ILAR J.* (2014) 55:169–81. doi: 10.1093/ilar/ilu020
19. Regan D, Dow S. Manipulation of innate immunity for cancer therapy in dogs. *Vet Sci.* (2015) 2:423–39. doi: 10.3390/vetsci2040423
20. Regan D, Guth A, Coy J, Dow S. Cancer immunotherapy in veterinary medicine: current options and new developments. *Vet J.* (2016) 207:20–8. doi: 10.1016/j.tvjl.2015.10.008
21. Elvers I, Turner-Maier J, Swofford R, Koltookian M, Johnson J, Stewart C, et al. Exome sequencing of lymphomas from three dog breeds reveals somatic mutation patterns reflecting genetic background. *Genome Res.* (2015) 25:1634–45. doi: 10.1101/gr.194449.115
22. Chen HW, Small GW, Motsinger-Reif A, Suter SE, Richards KL. VH1-44 gene usage defines a subset of canine B-cell lymphomas associated with better patient survival. *Vet Immunol Immunopathol.* (2014) 157:125–30. doi: 10.1016/j.vetimm.2013.10.020
23. Ostrander EA, Dreger DL, Evans JM. Canine cancer genomics: lessons for canine and human health. *Annu Rev Anim Biosci.* (2019) 7:449–72. doi: 10.1146/annurev-animal-030117-014523
24. Tarone L, Barutello G, Iussich S, Giacobino D, Quaglino E, Buracco P, et al. Naturally occurring cancers in pet dogs as pre-clinical models for cancer immunotherapy. *Cancer Immunol Immunother.* (2019) 68:1839–53. doi: 10.1007/s00262-019-02360-6
25. Dhawan D, Paoloni M, Shukradas S, Choudhury DR, Craig BA, Ramos-Vara JA, et al. Comparative gene expression analyses identify luminal and basal subtypes of canine invasive urothelial carcinoma that mimic patterns in human invasive bladder cancer. *PLoS ONE.* (2015) 10:e0136688. doi: 10.1371/journal.pone.0136688
26. Davis BW, Ostrander EA. Domestic dogs and cancer research: a breed-based genomics approach. *ILAR J.* (2014) 55:59–68. doi: 10.1093/ilar/ilu017
27. Abdelmegeed SM, Mohammed S. Canine mammary tumors as a model for human disease. *Oncol Lett.* (2018) 15:8195–205. doi: 10.3892/ol.2018.8411
28. Foltz JA, Somanchi SS, Yang Y, Aquino-Lopez A, Bishop EE, Lee DA. NCR1 expression identifies canine natural killer cell subsets with phenotypic similarity to human natural killer cells. *Front Immunol.* (2016) 7:521. doi: 10.3389/fimmu.2016.00521
29. Graves SS, Gyurkocza B, Stone DM, Parker MH, Abrams K, Jochum C, et al. Development and characterization of a canine-specific anti-CD94 (KLRD-1) monoclonal antibody. *Vet Immunol Immunopathol.* (2019) 211:10–8. doi: 10.1016/j.vetimm.2019.03.005
30. Ortiz AL, Carvalho S, Leo C, Riondato F, Archer J, Cian F. Gamma delta T-cell large granular lymphocyte lymphoma in a dog. *Vet Clin Pathol.* (2015) 44:442–7. doi: 10.1111/vcp.12265
31. Biller BJ, Elmslie RE, Burnett RC, Avery AC, Dow SW. Use of FoxP3 expression to identify regulatory T cells in healthy dogs and dogs with cancer. *Vet Immunol Immunopathol.* (2007) 116:69–78. doi: 10.1016/j.vetimm.2006.12.002
32. Biller BJ, Guth A, Burton JH, Dow SW. Decreased ratio of CD8+ T cells to regulatory T cells associated with decreased survival in dogs with osteosarcoma. *J Vet Intern Med.* (2010) 24:1118–23. doi: 10.1111/j.1939-1676.2010.0557.x
33. O'Neill K, Guth A, Biller B, Elmslie R, Dow S. Changes in regulatory T cells in dogs with cancer and associations with tumor type. *J Vet Intern Med.* (2009) 23:875–81. doi: 10.1111/j.1939-1676.2009.0333.x
34. Bergeron LM, McCandless EE, Dunham S, Dunkle B, Zhu Y, Shelly J, et al. Comparative functional characterization of canine IgG subclasses. *Vet Immunol Immunopathol.* (2014) 157:31–41. doi: 10.1016/j.vetimm.2013.10.018
35. Lee SH, Shin DJ, Kim Y, Kim CJ, Lee JJ, Yoon MS, et al. Comparison of phenotypic and functional characteristics between canine Non-B, Non-T natural killer lymphocytes and CD3(+)CD5(dim)CD21(-) cytotoxic large granular lymphocytes. *Front Immunol.* (2018) 9:841. doi: 10.3389/fimmu.2018.00841
36. Wheat WH, Chow L, Kurihara JN, Regan DP, Coy JW, Webb TL, et al. Suppression of canine dendritic cell activation/maturation and inflammatory cytokine release by mesenchymal stem cells occurs through multiple distinct biochemical pathways. *Stem Cells Dev.* (2017) 26:249–62. doi: 10.1089/scd.2016.0199
37. Hartley G, Regan D, Guth A, Dow S. Regulation of PD-L1 expression on murine tumor-associated monocytes and macrophages by locally produced TNF-alpha. *Cancer Immunol Immunother.* (2017) 66:523–35. doi: 10.1007/s00262-017-1955-5
38. Hartley G, Faulhaber E, Caldwell A, Coy J, Kurihara J, Guth A, et al. Immune regulation of canine tumour and macrophage PD-L1 expression. *Vet Comp Oncol.* (2017) 15:534–49. doi: 10.1111/vco.12197
39. Hartley G, Elmslie R, Dow S, Guth A. Checkpoint molecule expression by B and T cell lymphomas in dogs. *Vet Comp Oncol.* (2018) 16:352–60. doi: 10.1111/vco.12386
40. Coy J, Caldwell A, Chow L, Guth A, Dow S. PD-1 expression by canine T cells and functional effects of PD-1 blockade. *Vet Comp Oncol.* (2017) 15:1487–502. doi: 10.1111/vco.12294
41. Regan DP, Escaffi A, Coy J, Kurihara J, Dow SW. Role of monocyte recruitment in hemangiosarcoma metastasis in dogs. *Vet Comp Oncol.* (2017) 15:1309–22. doi: 10.1111/vco.12272
42. Friedrichs KR, Young KM. Histiocytic sarcoma of macrophage origin in a cat: case report with a literature review of feline histiocytic malignancies and comparison with canine hemophagocytic histiocytic sarcoma. *Vet Clin Pathol.* (2008) 37:121–8. doi: 10.1111/j.1939-165X.2008.00005.x
43. Coomer AR, Liptak JM. Canine histiocytic diseases. *Compend Contin Educ Vet.* (2008) 30:202–4, 208–16; quiz 216-17.
44. Moore PF. A review of histiocytic diseases of dogs and cats. *Vet Pathol.* (2014) 51:167–84. doi: 10.1177/0300985813510413
45. Killick DR, Stell AJ, Catchpole B. Immunotherapy for canine cancer–is it time to go back to the future? *J Small Anim Pract.* (2015) 56:229–41. doi: 10.1111/jsap.12336
46. Mason NJ, Gnanandarajah JS, Engiles JB, Gray F, Laughlin D, Gaurnier-Hausser A, et al. Immunotherapy with a HER2-targeting listeria induces HER2-specific immunity and demonstrates potential therapeutic effects in a phase I trial in canine osteosarcoma. *Clin Cancer Res.* (2016) 22:4380–90. doi: 10.1158/1078-0432.CCR-16-0088
47. Peruzzi D, Gavazza A, Mesiti G, Lubas G, Scarselli E, Conforti A, et al. A vaccine targeting telomerase enhances survival of dogs affected by B-cell lymphoma. *Mol Ther.* (2010) 18:1559–67. doi: 10.1038/mt.2010.104

48. Andersen BM, Pluhar GE, Seiler CE, Goulart MR, SantaCruz KS, Schutten MM, et al. Vaccination for invasive canine meningioma induces in situ production of antibodies capable of antibody-dependent cell-mediated cytotoxicity. *Cancer Res.* (2013) 73:2987–97. doi: 10.1158/0008-5472.CAN-12-3366
49. Panjwani MK, Smith JB, Schutsky K, Gnanandarajah J, O'Connor CM, Powell DJ Jr., et al. Feasibility and safety of RNA-transfected CD20-specific chimeric antigen receptor T cells in dogs with spontaneous B cell lymphoma. *Mol Ther.* (2016) 24:1602–14. doi: 10.1038/mt.2016.146
50. Canter RJ, Grossenbacher SK, Foltz JA, Sturgill IR, Park JS, Luna JI, et al. Radiotherapy enhances natural killer cell cytotoxicity and localization in pre-clinical canine sarcomas and first-in-dog clinical trial. *J Immunother Cancer.* (2017) 5:98. doi: 10.1186/s40425-017-0305-7
51. Guth AM, Hafeman SD, Elmslie RE, Dow SW. Liposomal clodronate treatment for tumour macrophage depletion in dogs with soft-tissue sarcoma. *Vet Comp Oncol.* (2013) 11:296–305. doi: 10.1111/j.1476-5829.2012.00319.x
52. Maeda S, Murakami K, Inoue A, Yonezawa T, Matsuki N. CCR4 blockade depletes regulatory T cells and prolongs survival in a canine model of bladder cancer. *Cancer Immunol Res.* (2019) 7:1175–87. doi: 10.1158/2326-6066.CIR-18-0751
53. Monjazeb AM, Kent MS, Grossenbacher SK, Mall C, Zamora AE, Mirsoian A, et al. Blocking indolamine-2,3-dioxygenase rebound immune suppression boosts antitumor effects of radio-immunotherapy in murine models and spontaneous canine malignancies. *Clin Cancer Res.* (2016) 22:4328–40. doi: 10.1158/1078-0432.CCR-15-3026
54. U'Ren LW, Biller BJ, Elmslie RE, Thamm DH, Dow SW. Evaluation of a novel tumor vaccine in dogs with hemangiosarcoma. *J Vet Intern Med.* (2007) 21:113–20. doi: 10.1892/0891-6640(2007)21[113:eoantv]2.0.co;2
55. Thamm DH, Kurzman ID, King I, Li Z, Sznol M, Dubielzig RR, et al. Systemic administration of an attenuated, tumor-targeting *Salmonella typhimurium* to dogs with spontaneous neoplasia: phase I evaluation. *Clin Cancer Res.* (2005) 11:4827–34. doi: 10.1158/1078-0432.CCR-04-2510
56. Dow SW, Elmslie RE, Willson AP, Roche L, Gorman C, Potter TA. *In vivo* tumor transfection with superantigen plus cytokine genes induces tumor regression and prolongs survival in dogs with malignant melanoma. *J Clin Invest.* (1998) 101:2406–14. doi: 10.1172/JCI510
57. MacEwen EG, Kurzman ID, Vail DM, Dubielzig RR, Everlith K, Madewell BR, et al. Adjuvant therapy for melanoma in dogs: results of randomized clinical trials using surgery, liposome-encapsulated muramyl tripeptide, and granulocyte macrophage colony-stimulating factor. *Clin Cancer Res.* (1999) 5:4249–58.
58. Thalmensi J, Pliquet E, Liard C, Chamel G, Kreuz C, Bestetti T, et al. A DNA telomerase vaccine for canine cancer immunotherapy. *Oncotarget.* (2019) 10:3361–72. doi: 10.18632/oncotarget.26927
59. Milner RJ, Salute M, Crawford C, Abbot JR, Farese J. The immune response to disialoganglioside GD3 vaccination in normal dogs: a melanoma surface antigen vaccine. *Vet Immunol Immunopathol.* (2006) 114:273–84. doi: 10.1016/j.vetimm.2006.08.012
60. Yin Y, Boesteanu AC, Binder ZA, Xu C, Reid RA, Rodriguez JL, et al. Checkpoint blockade reverses anergy in IL-13Rα2 humanized scFv-based CAR T cells to treat murine and canine gliomas. *Mol Ther Oncolytics.* (2018) 11:20–38. doi: 10.1016/j.omto.2018.08.002
61. Guth AM, Hafeman SD, Dow SW. Depletion of phagocytic myeloid cells triggers spontaneous T cell- and NK cell-dependent antitumor activity. *Oncoimmunology.* (2012) 1:1248–57. doi: 10.4161/onci.21317
62. Regan DP, Coy JW, Chahal KK, Chow L, Kurihara JN, Guth AM, et al. The angiotensin receptor blocker losartan suppresses growth of pulmonary metastases via AT1R-independent inhibition of CCR2 signaling and monocyte recruitment. *J Immunol.* (2019) 202:3087–102. doi: 10.4049/jimmunol.1800619
63. Porcellato I, Brachelente C, De Paolis L, Menchetti L, Silvestri S, Sforna M, Vichi G, et al. FoxP3 and IDO in canine melanocytic tumors. *Vet Pathol.* (2019) 56:189–99. doi: 10.1177/0300985818808530
64. Rossmeisl JH. New treatment modalities for brain tumors in dogs and cats. *Vet Clin North Am Small Anim Pract.* (2014) 44:1013–38. doi: 10.1016/j.cvsm.2014.07.003
65. Olin MR, Pluhar GE, Andersen BM, Shaver R, Waldron NN, Moertel CL. Victory and defeat in the induction of a therapeutic response through vaccine therapy for human and canine brain tumors: a review of the state of the art. *Crit Rev Immunol.* (2014) 34:399–432. doi: 10.1615/CritRevImmunol.2014011577
66. Hubbard ME, Arnold S, Bin Zahid A, McPheeters M, Gerard O'Sullivan M, Tabaran AF, et al. Naturally occurring canine glioma as a model for novel therapeutics. *Cancer Invest.* (2018) 36:415–23. doi: 10.1080/07357907.2018.1514622
67. Paoloni M, Mazcko C, Selting K, Lana S, Barber L, Phillips J, et al. Defining the pharmacodynamic profile and therapeutic index of NHS-IL12 immunocytokine in dogs with malignant melanoma. *PLoS ONE.* (2015) 10:e0129954. doi: 10.1371/journal.pone.0129954
68. Kurzman ID, MacEwen EG, Rosenthal RC, Fox LE, Keller ET, Helfand SC, et al. Adjuvant therapy for osteosarcoma in dogs: results of randomized clinical trials using combined liposome-encapsulated muramyl tripeptide and cisplatin. *Clin Cancer Res.* (1995) 1:1595–601.

Disclaimer: The content of the publication is the responsibility of the author and does not necessarily reflect the official views of the National Institutes of Health, the Canine Health Foundation, nor the Shipley Foundation.

Conflict of Interest: The author declares that the research was conducted in the absence of any commercial or financial relationships that could be construed as a potential conflict of interest.

Copyright © 2020 Dow. This is an open-access article distributed under the terms of the Creative Commons Attribution License (CC BY). The use, distribution or reproduction in other forums is permitted, provided the original author(s) and the copyright owner(s) are credited and that the original publication in this journal is cited, in accordance with accepted academic practice. No use, distribution or reproduction is permitted which does not comply with these terms.

frontiers in Oncology

REVIEW
published: 21 January 2020
doi: 10.3389/fonc.2019.01493

Naturally-Occurring Invasive Urothelial Carcinoma in Dogs, a Unique Model to Drive Advances in Managing Muscle Invasive Bladder Cancer in Humans

Deborah W. Knapp[1,2], Deepika Dhawan[1], José A. Ramos-Vara[2,3], Timothy L. Ratliff[2,3], Gregory M. Cresswell[2], Sagar Utturkar[2], Breann C. Sommer[1†], Christopher M. Fulkerson[1,2] and Noah M. Hahn[4]*

[1] Department of Veterinary Clinical Sciences, Purdue University, West Lafayette, IN, United States, [2] Purdue University Center for Cancer Research, Purdue University, West Lafayette, IN, United States, [3] Department of Comparative Pathobiology, Purdue University, West Lafayette, IN, United States, [4] Department of Oncology and Urology, Sidney Kimmel Comprehensive Cancer Center, Johns Hopkins University School of Medicine, Baltimore, MD, United States

There is a great need to improve the outlook for people facing urinary bladder cancer, especially for patients with invasive urothelial carcinoma (InvUC) which is lethal in 50% of cases. Improved outcomes for patients with InvUC could come from advances on several fronts including emerging immunotherapies, targeted therapies, and new drug combinations; selection of patients most likely to respond to a given treatment based on molecular subtypes, immune signatures, and other characteristics; and prevention, early detection, and early intervention. Progress on all of these fronts will require clinically relevant animal models for translational research. The animal model(s) should possess key features that drive success or failure of cancer drugs in humans including tumor heterogeneity, genetic-epigenetic crosstalk, immune cell responsiveness, invasive and metastatic behavior, and molecular subtypes (e.g., luminal, basal). Experimental animal models, while essential in bladder cancer research, do not possess these collective features to accurately predict outcomes in humans. These key features, however, are present in naturally-occurring InvUC in pet dogs. Canine InvUC closely mimics muscle-invasive bladder cancer in humans in cellular and molecular features, molecular subtypes, immune response patterns, biological behavior (sites and frequency of metastasis), and response to therapy. Thus, dogs can offer a highly relevant animal model to complement other models in research for new therapies for bladder cancer. Clinical treatment trials in pet dogs with InvUC are considered a win-win-win scenario; the individual dog benefits from effective treatment, the results are expected to help other dogs, and the findings are expected to translate to better treatment outcomes in humans. In addition, the high breed-associated risk for InvUC in dogs (e.g., 20-fold increased risk in Scottish Terriers)

OPEN ACCESS

Edited by:
Rodney L. Page, Colorado State University, United States

Reviewed by:
Suresh Kumar Kalangi, Amity University Gurgaon, India
Jenna Hart Burton, University of California, Davis, United States

***Correspondence:**
Deborah W. Knapp
knappd@purdue.edu

†Present address:
Breann C. Sommer, VCA Veterinary Emergency Service & Veterinary Specialty Center, Middleton, WI, United States

Specialty section:
This article was submitted to Cancer Molecular Targets and Therapeutics, a section of the journal Frontiers in Oncology

Received: *20 September 2019*
Accepted: *11 December 2019*
Published: *21 January 2020*

Citation:
Knapp DW, Dhawan D, Ramos-Vara JA, Ratliff TL, Cresswell GM, Utturkar S, Sommer BC, Fulkerson CM and Hahn NM (2020) Naturally-Occurring Invasive Urothelial Carcinoma in Dogs, a Unique Model to Drive Advances in Managing Muscle Invasive Bladder Cancer in Humans. Front. Oncol. 9:1493. doi: 10.3389/fonc.2019.01493

offers an unparalleled opportunity to test new strategies in primary prevention, early detection, and early intervention. This review will provide an overview of canine InvUC, summarize the similarities (and differences) between canine and human InvUC, and provide evidence for the expanding value of this canine model in bladder cancer research.

Keywords: animal models, bladder cancer, cancer prevention, dog, immunotherapy, targeted therapy, transitional cell carcinoma, urothelial carcinoma

INTRODUCTION

Urinary bladder cancer (urothelial carcinoma, also referred to as transitional cell carcinoma) is a major human health issue worldwide with more than 400,000 new cases per year (1, 2). Broadly speaking, human bladder cancer can be divided into two general types. The more common form which comprises approximately two thirds of cases, consists of low-grade non-invasive cancer that can typically be managed with transurethral resection and intravesical therapy (3). Although this cancer is manageable, it can negatively impact the patients' quality of life, frequently recurs, and can progress to invasive cancer (3). The less common, but more serious form of bladder cancer consists of high-grade muscle-invasive urothelial carcinoma (InvUC). InvUC is associated with a 50% lethality rate, marked reduction in quality of life from the cancer and its treatment (cystectomy, radiation therapy, chemotherapy), and high medical costs ($150,000 to >$200,000 per patient) (4–10). In the last two to three decades, only modest improvement has occurred in the outcome of patients with InvUC. This review will focus on this challenging form of bladder cancer, InvUC.

Encouraging progress has recently been made in new therapies aimed at molecular, epigenetic, and immune targets in InvUC (10–12). The finding of differential treatment responses based on molecular InvUC subtypes (luminal, basal, etc.) along with combinations of these new drugs, is expected to lead to dramatic improvements in InvUC therapy (11–18). There are, however, insufficient numbers of patients to test even a fraction of the new drugs, especially when considering various possible drug combinations, in order to optimize therapy. The numbers of patients with metastases who could still be eligible for trials after failing standard of care therapies are especially limited. This puts higher demands on pre-clinical animal studies to identify the most promising therapies to move forward into humans. Current experimental models, however, do not accurately predict drug outcomes in humans (19, 20). Although *in vitro* systems, and carcinogen-induced, engraftment, and genetically-engineered mouse models are essential in bladder cancer research, they do not possess the collective features (cancer heterogeneity, molecular complexity, invasion, metastasis, immune cell response) that are crucial to predicting success or failure of emerging therapies in humans (19–23). With the resurgence of immunotherapy and the understanding that the immune system plays a major role in the outcomes of many types of therapies (16–18, 24–29), it is especially critical that animal models possess a level of immunocompetence similar to that in human cancer patients. There is compelling evidence that dogs with naturally-occurring InvUC possess these collective features and can serve as a highly relevant animal model for the human condition to complement other models (30–32). This review will summarize the similarities (and differences) between InvUC in dogs and humans, and discuss some of the settings in which the canine model could be most useful. Expanding the application of this canine InvUC model is expected to greatly improve the outlook for humans and dogs facing urinary bladder cancer.

CLINICAL AND PATHOLOGICAL CHARACTERISTICS OF CANINE InvUC AND SIMILARITIES AND DIFFERENCES BETWEEN InvUC IN DOGS AND HUMANS

Frequency and Clinical Presentation of InvUC

Bladder cancer comprises ∼1.5–2% of all naturally-occurring cancers in dogs, a rate similar to that reported in humans (1, 2, 30). With estimates that 4–6 million pet dogs develop cancer in the US each year, this equates to more than 60,000 cases of InvUC in dogs each year (31). It is acknowledged that many of these cases will go undiagnosed and untreated, but this still leaves large numbers of dogs diagnosed with InvUC who could participate in clinical trials.

As in humans, InvUC is typically a disease of older age dogs with the reported mean and median ages at diagnosis ranging from 9 to 11 years (30, 31). A minority of dogs develop the cancer at a younger age, i.e., as young as 4–6 years of age. The female to male ratio of dogs with InvUC has been reported to range from 1.71:1 to 1.95:1 (30). Interestingly, in dogs in high risk breeds, the female to male risk is less pronounced (30). The female gender predilection in dogs differs from that in humans in which males are more likely to be affected (15). The reasons for this difference between the species are not known. One possible reason relates to smoking in humans, a causative factor for up to 50% of human bladder cancer (15, 33, 34). Over several decades, smoking has been more prevalent in men than women (34). Men have also traditionally had more occupational exposures to chemicals (34). With a long latency period (up to 30–40 years) between carcinogen exposure and cancer development in humans, the differences in exposures between men and women decades ago can be reflected in current InvUC cases. Another factor to consider regarding the gender differences between bladder cancer in humans and dogs is that most dogs diagnosed with InvUC have been neutered, typically at a young age, and this could affect their bladder cancer risk (30). In fact, the risk of InvUC is ∼2-fold higher in dogs who have been spayed or neutered than it is for intact dogs (30, 35). Interestingly, dogs who have been spayed

or neutered also have a higher risk for other cancers (35–37). The reasons for this are not yet known, but the differences are likely to be important in gaining a better understanding of the processes leading to the development of InvUC and other cancers, and dog studies could be very informative.

The presenting clinical signs of InvUC are similar between dogs and humans, with hematuria being the most common change observed (30). Pain and urgency are not usually noted in the early stages of the cancer, but can emerge as the cancer progresses. A history of urinary tract infections is common in InvUC cases in humans and dogs. When cancer and infection are present concurrently, the clinical signs improve with antibiotic administration, but typically recur after the course of antibiotics is completed. As the cancer progresses, signs associated with metastases can emerge. Bone metastases, while uncommon, can lead to severe pain in both species.

Pathological Features

The diagnosis of InvUC in dogs and humans is made by histologic examination of tissue biopsies. In dogs, these tissues are collected by surgery, cystoscopy, or catheter biopsy (30). The vast majority of bladder cancer in dogs (>90% of cases) consists of intermediate- to high-grade InvUC, the focus of this review (**Figure 1**) (30). Great similarity is noted in the microscopic features between canine and human InvUC (30). It is interesting to note that superficial, low-grade bladder cancer is very uncommon in dogs. Another interesting difference between bladder cancer in dogs and humans is the location of the cancer within the bladder. The majority of InvUC in dogs is found in the trigone region of the bladder, and extension down the urethra is common (reported in >50% of cases) (**Figure 1**), whereas in humans there is a more balanced distribution of the cancer across different areas of the bladder (30). In male dogs, 29% of cases have been reported to have prostate involvement based on evidence from imaging studies or pathology (30). In humans, prostate involvement of the urothelial carcinoma has been found in cystoprostatecomy sections in 15–48% of cases across multiple studies, with higher rates of involvement noted with more detailed pathologic examination of the tissues (38). Interestingly, incidental prostatic adenocarcinoma has been found in 12–51% of cystoprostatectomy sections from men with InvUC (39). Primary urothelial carcinoma of the prostatic urethra and ducts (in the absence of bladder disease) is not uncommon in dogs, but is considered rare in humans (40). It is possible that the growing practice of neutering male pet dogs, especially at an early age, could reduce the risk of prostatic adenocarcinoma in dogs, while enhancing the development of urothelial carcinoma, although confirmation of this requires further study. Upper tract, i.e., renal pelvic, urothelial carcinoma is reported in 5–10% of humans (41). Similar lesions are found in dogs (especially at necropsy), but the frequency at which they occur has not yet been established.

Several classification and grading schemes have been published for canine urothelial neoplasms, particularly InvUC, and these have been summarized in a prior review (30). By growth pattern, InvUCs are divided into papillary (50%) or non-papillary (50%) tumors and infiltrating (≥90%) or non-infiltrating (≤10%) tumors. Although non-infiltrating tumors comprise the majority of human InvUCs (≥65% of cases), this form of bladder cancer is uncommon in dogs.

When surgical specimens are examined, there is typically sufficient tissue to assess growth pattern, depth of invasion, vascular invasion, etc. When tissue biopsies are obtained by cystoscopy, however, the size of the biopsy is often small, especially in dogs. Nuclear grade has been established as one of the few constant features that can be evaluated even in small tissue samples (30). In a retrospective study using nuclear grade as the only feature to assign grade, of 232 canine InvUCs (biopsies or postmortem specimens), two InvUCs were grade I; 67 InvUCs were grade II; and 163 InvUCs were grade III (30). Although this work utilized a three tier grading system, a four tier grading system is currently in use in dogs, reflecting that used in humans (42).

Histologic variants of urothelial carcinoma (also called urothelial carcinoma with divergent differentiation) have been increasingly reported in humans, and in some cases may have prognostic significance (43–45). Interestingly, the percentage of cells showing divergent differentiation does not appear to influence patient outcomes (44). Some of the urothelial carcinoma variants have been observed in dogs including plasmacytoid and rhabdoid types (46). While there have been very few reports of such variants to determine their clinical significance in dogs, in one study, canine InvUC with fibromyxoid stroma was associated with invasion of the muscle layer, suggesting a more aggressive behavior (47). Perhaps of more importance from a clinical perspective, will be to determine which genetic fingerprints within these variants can be exploited for targeted therapies.

Local Invasion and Metastatic Behavior

InvUC in humans is characterized by locally aggressive cancer with growth into and often through the bladder wall, as well as distant metastases in ∼50% of patients (15, 16). One of the reasons there is great enthusiasm for the canine InvUC model is the model replicates this local invasion and distant metastases of human InvUC, while these features are difficult to produce in experimental models. In dogs, nodal and distant metastases have been reported in ∼16% of dogs at diagnosis and 50–60% of dogs at death (30). When applying World Health Organization (WHO) criteria for staging canine bladder tumors (**Table 1**) (48), 78% of dogs have been reported to have T2 tumors and 20% of dogs to have T3 tumors (30). There is a difference in the TNM staging system between dogs and humans, with T2 tumors in dogs including muscle invasive disease, whereas muscle invasive tumors in humans are typically classified as T3 or higher. Interestingly in a recent report of 65 dogs with InvUC that had whole body computed tomography (CT) performed at diagnosis, iliosacral lymphadenomegaly, sternal lymphadenomegaly, bone metastasis, and lung metastasis were suspected in 48, 18, 25, and 35% of the dogs, respectively (49). These rates of metastases appear higher than reported in other studies (30). It is possible that this group of dogs had later diagnoses when the cancer had become more advanced or that the CT imaging revealed more metastases than are typically observed with other imaging modalities.

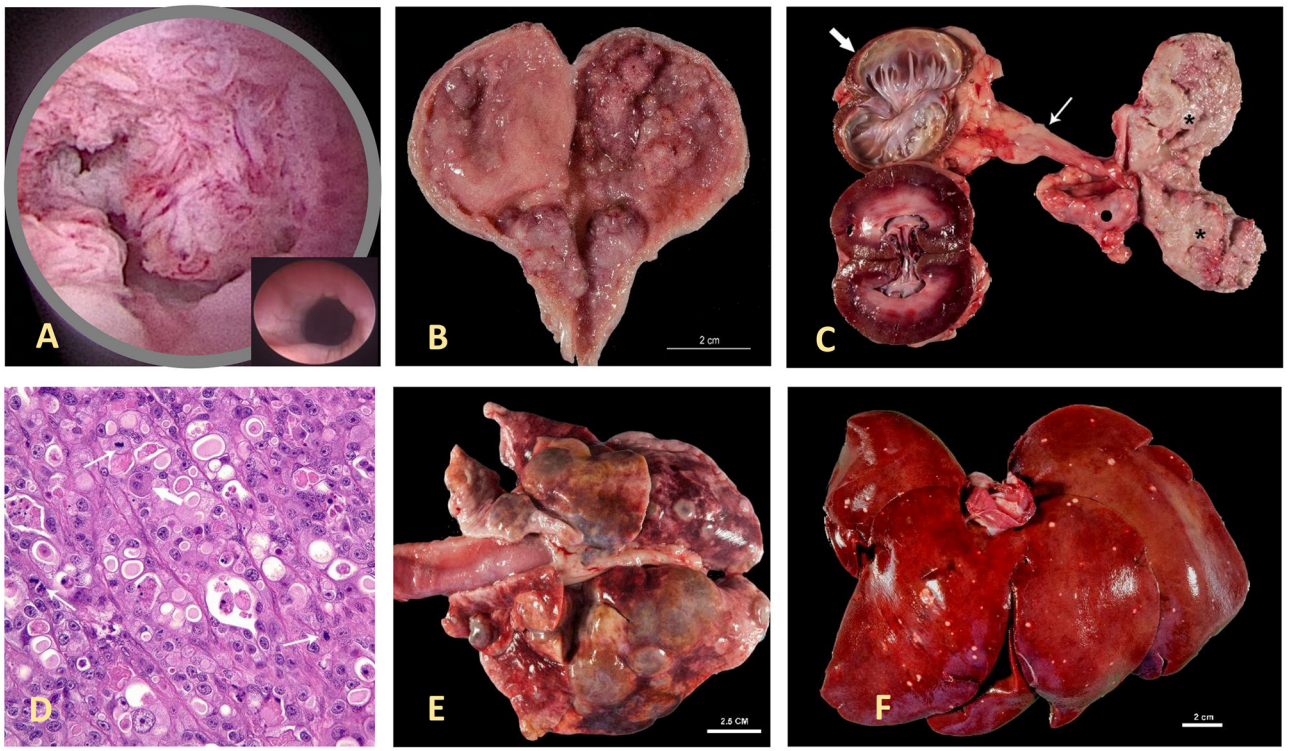

FIGURE 1 | Canine invasive urothelial carcinoma (InvUC). Canine InvUC often produces papillary lesions extending into the lumen of the urethra (as seen in the cystoscopic image in **A**) and bladder (as seen on post mortem specimen in **B,C**), along with deep invasion into the bladder wall. For comparison, in **(A)**, the inset demonstrates the normal appearance of this region of the urinary tract in the absence of cancer. In (C), note the transmural growth in the entire bladder (please see the 2* on the right side of the panel), hydroureter (thin arrow), and hydronephrosis (thick arrow) caused by obstruction of the ureteral orifice by tumor growth in the bladder. An adjacent iliac lymph node (dark dot) is also infiltrated by this neoplasm. The photomicrograph in **(D)** (H&E 40X) is typical of high-grade InvUC. There is lack of normal cell maturation and marked nuclear atypia with some binucleated and multinucleated cells, and mitotic figures (arrows). Note the presence of cytoplasmic vacuoles within neoplastic cells, a common but not unique finding to InvUC. Canine InvUC is locally aggressive and metastasizes to distant sites in more than 50% of cases. Note metastases to the lung **(E)** and liver **(F)**. The gross appearance of metastases range from single to multiple nodules that can become confluent as observed in the lung **(E)**.

TABLE 1 | WHO TNM clinical staging system for canine bladder cancer (48).

T—Primary tumor	
Tis	Carcinoma *in situ*
T0	No evidence of a primary tumor
T1	Superficial papillary tumor
T2	Tumor invading the bladder wall, with induration
T3	Tumor invading neighboring organs (prostate, uterus, vagina, and pelvic canal)
N—Regional lymph node (internal and external iliac lymph node)	
N0	No regional lymph node involvement
N1	Regional lymph node involved
N2	Regional lymph node and juxtaregional lymph node involved
M—Distant metastases	
M0	No evidence of metastasis
M1	Distant metastasis present

To better characterize the distribution of InvUC metastases in dogs as the cancer progresses, necropsy findings were compiled from 137 dogs with InvUC evaluated at Purdue University (**Table 2**) (30). Of the 137 dogs, 92 dogs (67%) had metastasis to at least one site. Nodal metastases alone (in the absence of distant metastases) were found in 9% of dogs, distant metastases alone were found in 25% of dogs, and a combination of nodal and distant metastases were identified in 33% of dogs at the time of death (30). The frequency of metastasis and the sites involved were similar between dogs and humans (**Table 2**), with lung being the most common site of distant metastasis (50). In addition to visceral and nodal metastasis, InvUC also spreads to the abdominal wall through instruments and needles used in surgical and non-surgical procedures and naturally along ligaments that support the bladder (51). In this location, the cancer typically grows aggressively and is poorly responsive to medical therapy.

Bone metastases are also important metastatic sites in dogs, as well as in humans. To assess the frequency of bone metastases in dogs, 188 dogs with InvUC undergoing necropsy were retrospectively studied (52). Of the 188 cases, 17 (9%) had histologically confirmed skeletal metastasis, mainly to the vertebrae. This was followed by a prospective study of 21 dogs with InvUC that underwent total body CT at the time of euthanasia followed by a standardized pathologic examination (52). In four dogs, skeletal lesions suspicious for bone metastases

TABLE 2 | Metastases identified in 137 dogs with invasive urothelial carcinoma undergoing necropsy at Purdue University (2005–2013) with comparison to published autopsy findings from 308 humans with urothelial carcinoma (30, 50).

Location of metastases	Number of dogs with metastasis in that location (% of 137 dogs undergoing necropsy) (30)	Number of humans with metastases in that location (% of 308 humans undergoing autopsy) (50)
Any metastases	92 (67%)	214 (69%)
Any nodal metastases	57 (42%)	180 (58%)
Regional nodes (abdominal, pelvic inguinal nodes)	40 (29%)[a]	158 (51%)
Thoracic nodes	17 (12%)[b]	80 (26%)
Other nodes	1 (1%)	8 (3%)
Any distant metastases	80 (58%)	147 (48%)
Lung	69 (50%)	96 (31%)
Bone	15 (11%)	71 (23%)
Liver	10 (7%)	103 (33%)
Kidney	10 (7%)[c]	30 (10%)
Adrenal gland	8 (6%)	28 (10%)
Skin	8 (6%)	4 (1.5%)
Spleen	6 (4%)	11 (3.6%)
Gastrointestinal	3 (2%)[d]	45 (15%)
Heart	5 (4%)	13 (4%)
Brain	2 (1.5%)	8 (2.5%)

[a] *Nodes included 32 iliac, sacral, and other "sub lumbar," three inguinal, two mesenteric, two pancreatic, and one hypogastric node.*
[b] *Nodes included nine tracheobronchial, four sternal, three mediastinal, and one hilar node.*
[c] *It was not always possible to determine if the InvUC represented a second primary site in the kidney or a metastatic lesion.*
[d] *Tumor location included stomach in one dog, jejunum in one dog, and pancreas in one dog.*

were detected on CT, and were confirmed to be InvUC metastases histologically in three (14%) dogs (52).

There was an additional interesting finding from the necropsy study of the 137 dogs with InvUC (30). Of the 137 dogs, 18 dogs (13%) had second primary tumors including hemangiosarcoma ($n = 3$), marginal zone lymphoma ($n = 3$), hepatocholangiocarcinoma ($n = 2$), follicular thyroid carcinoma ($n = 2$), B cell lymphoma ($n = 2$), adrenal adenocarcinoma ($n = 1$), meningioma ($n = 1$), nasal adenocarcinoma ($n = 1$), cutaneous squamous cell carcinoma ($n = 1$), oral melanoma ($n = 1$), pancreatic adenocarcinoma ($n = 1$), undifferentiated neuroendocrine tumor ($n = 1$), histiocytic sarcoma ($n = 1$), and splenic sarcoma ($n = 1$). Second primary tumors are also noted in humans with InvUC. In an autopsy study of 376 humans with InvUC, 74 patients (20%) had second primary tumors with other carcinomas being most common (53).

MOLECULAR FEATURES IN InvUC, AND SIMILARITIES BETWEEN DOGS AND HUMANS

Molecular Subtypes

One of the compelling recent advances in InvUC is the identification of gene expression patterns that segregate human InvUC into molecular subtypes including basal, luminal, and others initially described in human breast cancer (13–17, 54, 55). The subtypes are important because there is strong evidence that cancer behavior and response to therapy differ between subtypes, and thus subtypes could emerge as parameters to use in individualizing cancer treatment (13–17).

To briefly summarize some of the findings regarding subtypes, basal subtype InvUCs are more prevalent in women than men, are associated with squamous features, and are enriched for *STAT3, TP63, KRT5/6A*, and *CD44*; and NFkB, c-Myc, and HIF signaling (13–17). Some basal InvUC also express epithelial-mesenchymal transition markers of claudin-low breast cancer (56). Basal InvUC is thought to be inherently more aggressive than other subtype tumors, and is associated with more advanced stage and metastatic disease at diagnosis, although basal InvUC can be responsive to chemotherapy and immunotherapy. Luminal subtype InvUC is associated with papillary histologic features and better clinical outcomes. The luminal tumors are enriched for *ER, TRIM24, FOXA1, GATA3, PPARG*, and activating *FGFR3* mutations (with good response to FGFR inhibitors) (14, 17, 57, 58).

It is clear that modeling drug effects across molecular subtypes is essential. Work by our group provides strong evidence that the molecular subtypes present in human InvUC are also present in canine InvUC. Briefly, RNA-seq data were analyzed from 29 canine InvUCs and normal control bladder tissues from four dogs with no evidence of bladder disease (59). In unsupervised clustering, the tumors clearly segregated into two groups. When the same data were analyzed using a panel of genes known to distinguish luminal from basal bladder tumors in humans, the two groups from the unsupervised clustering analyses were identified as luminal and basal subtype. This finding is depicted in **Figure 2** in which additional cases have been added.

Other Molecular Features

The molecular characterization of canine InvUC is still in the early stages, especially in regards to mutation signatures and epigenetic events. Some of the initial findings are summarized in **Table 3** and in the following text.

Several important molecular features of InvUC were identified in the 2014 Cancer Genome Atlas Research Network (TCGA) comprehensive molecular characterization of human urothelial carcinomas (54). This study provided insight into the molecular pathogenesis of human InvUC, and identified potential treatment targets (54). Genomic alternations involving PI3K/AKT/mTOR, CDKN2A/CDK4/CCND1, and RTK/RAS pathways were noted, and thus receptor tyrosine kinases such as EGFR, ERBB2 (Her-2), ERBB3, and FGFR3 were identified as potential targets for therapy (54). Multiple sequencing studies of InvUC in dogs have been reported, some with cross species analyses, and many similarities across the species have been identified (59, 62, 68–71).

Overexpression of epidermal growth factor receptor (EGFR) has been reported in 73% of canine InvUC, which is comparable to that found in humans (62, 66, 67, 72). Inhibitors of EGFR family proteins have been evaluated in multiple human bladder cancer trials with varying success (73–75). EGFR inhibitors appear to be most useful in patients that are chemotherapy

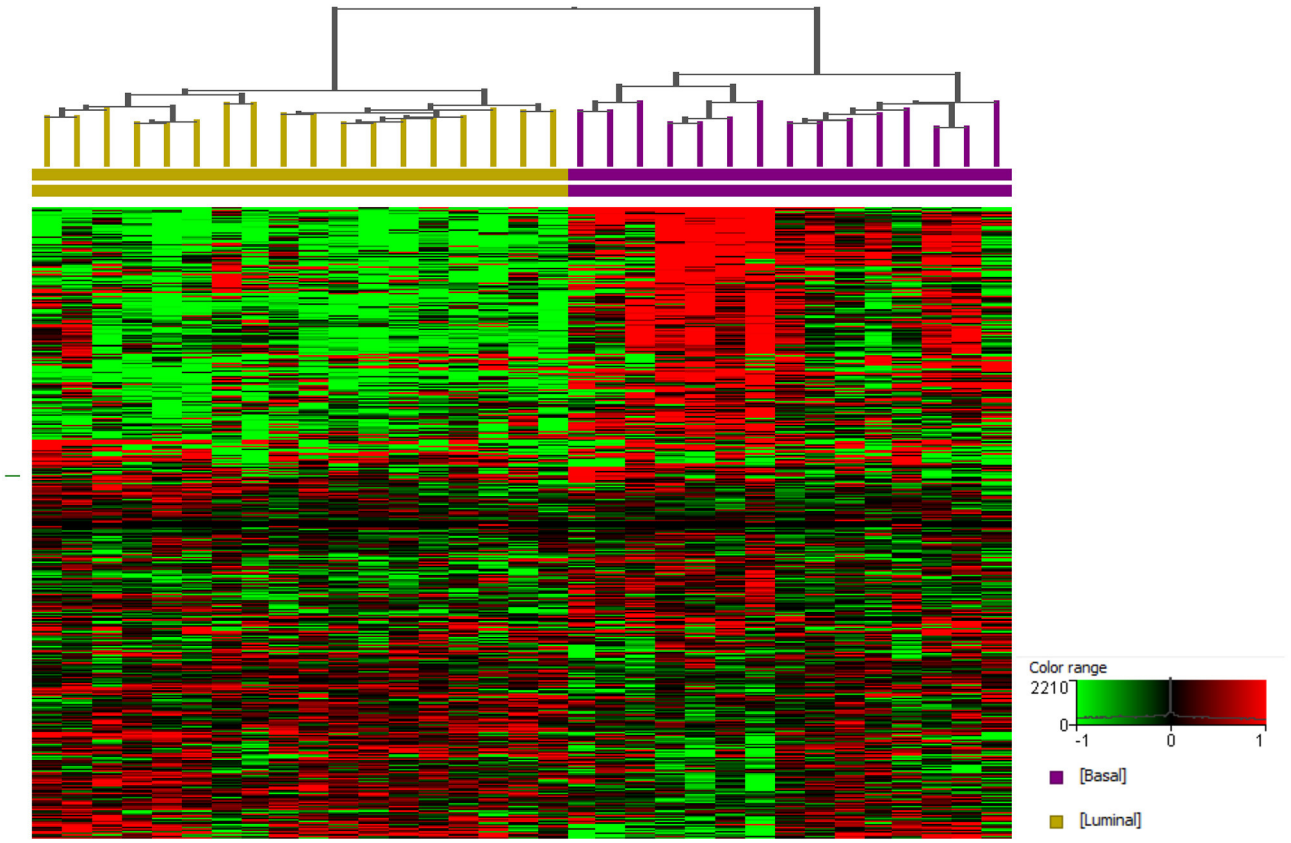

FIGURE 2 | Basal and luminal subtypes in canine invasive urothelial carcinoma. RNA-seq data from canine InvUC ($n = 33$) and normal bladder mucosal samples ($n = 4$) were normalized using TMM and DESeq concurrently using Strand NGS (Strand, Bengaluru, India). Statistical analyses were conducted using edge R (on TMM normalized data) and DESeq2 (on DESeq normalized data) with p corr ≤ 0.05 and $\geq$2-fold change from each analysis. These two lists of differentially expressed genes were pooled as described previously (59). A prediction model reported earlier was employed to assign luminal and basal subtypes (59). Supervised hierarchical clustering was performed using genes that assign basal and luminal subtypes in human InvUC (17). Two distinct groups were identified as basal ($n = 15$) and luminal ($n = 18$).

naïve and that have cancer overexpressing EGFR or ERBB2 (76). Prior treatment with chemotherapy can result in resistance to EGFR inhibitors, although the mechanisms of this are not well-defined. Canine studies could lead to a better understanding of the mechanisms of resistance, and to better identify subsets of patients who could benefit from EGFR inhibitor therapy.

One approach under investigation is to target EGFR with a photoimmunotherapy conjugate (Can225-IR700 conjugate), an approach which has shown promise in canine InvUC cell lines *in vitro* and in rodent models (77). The Can225-IR700 conjugate was shown to bind specifically and cause killing of EGFR expressing cells *in vitro*. In mice there was accumulation of the Can225-IR700 conjugate in the tumors with high tumor-to-background ratio, and tumor growth was significantly inhibited by near infrared photoimmunotherapy application (77). Using a different approach to exploit EGFR expression, a study of an EGFR-targeted toxin has recently been reported with antitumor activity observed in dogs with InvUC (78). These canine studies are being conducted to determine promising approaches to take into human clinical trials.

In considering a different molecular target, HER-2 (EGFR2/ERBB2/NEU) has been found to be significantly overexpressed in canine InvUC samples when compared to non-neoplastic urothelium (79), as is the case in human InvUC (80, 81). In two immunohistochemical studies HER-2 immunoreactivity was noted in 13 of 23 (56%) and in 14 of 23 (60.9%) cases of canine InvUC, respectively (79, 82).

The *p53* tumor suppressor gene product has an important role in differentiation of the urothelium (60). Loss of p53 expression has been noted in human InvUC, and has been associated with lymph node metastasis, advanced TNM stage, and shorter survival times (60, 83). Similar to the reports in humans, p63 expression, a homolog of p53, has been reported to be significantly lower in dogs with InvUC, compared to dogs with polypoid cystitis and normal urothelium (61). Expression of p53, the p53 inducible gene 14-3-3σ protein, and vimentin have been documented in canine InvUC *in vitro* and *in vivo* (63, 84). Expression of vimentin in human InvUC has been associated with epithelial-mesenchymal transition, cancer progression, and metastasis (85). The 14-3-3σ protein, which is expressed in

TABLE 3 | Early findings of molecular features in canine InvUC, and similarities and differences between canine and human InvUC.

Molecular feature	Human InvUC	Canine InvUC
Molecular subtypes	Luminal and basal are the main subtypes. Subgroupings within these occur (13–17)	Luminal and basal are the main subtypes. Early data indicating subgroupings requires confirmation in larger studies (59)
P53 pathway	p53 protein (presumed mutant) is detected by immunohistochemistry (IHC). Note: wildtype p53 protein is typically degraded faster than mutant p53, and thus mutant p53 is the form that is thought to be more commonly detected by IHC (15, 60)	p63 (homolog of p53) protein (presumed wildtype) is less abundant in InvUC than in normal bladder in IHC studies (61)
	Loss of function mutations in p53 occur in 50% of cases. Thus, the tumor suppressor pathway is inactivated (15)	P53 mutations are not well defined in canine InvUC. Enrichment has been noted in genes that negatively regulate the expression of p53 in microarray and RNA-seq analyses (59, 62)
	Loss of p53 function is often accompanied by loss of RB1 and amplification of MDM2 and CDKN2A (15)	RB1 expression is reduced in 5 of 8 canine InvUC cell lines (63). RB1 status has not yet been reported in clinical studies. MDM2 is overexpressed in InvUC in RNA-seq data. CDKN2B is overexpressed in RNA-seq data; CDKN2A has not been reported (59)
PTEN/PI3K/AKT/ mTOR pathway	Aberrant pathway activation occurs in 40% of human cases (13)	Overexpression of some genes in the pathway have been observed, but further study is needed to better characterize the pathway in dogs and to define similarities and differences between dogs and humans (59)
RTK/RAS pathway	FGFR3 mutations occur in 20% of cases (13)	FGFR3 mutations have not yet been defined
	BRAF mutations are rare (13)	$BRAF^{V600E}$ mutations are common (∼80% of cases) (64, 65)
EGFR	EGFR is overexpressed in 75% of high grade tumors detected by IHC (66, 67)	EGFR is overexpressed in 73% of cases as detected by IHC (62)
Cox-2	Cox-2 is overexpressed in >80% of cases as detected by IHC	Cox-2 is overexpressed in >80% of cases as detected by IHC and RNA-seq analyses (30)

human and canine bladder cancer, has also been linked to tumorigenesis (86, 87).

Mutations in several other genes implicated in the development and progression of InvUC and other cancers in humans have been identified in canine InvUC (64, 69). Examples include *CDKN2B*, *PIK3CA*, *BRCA2*, *NFkB, ARHGEF4, XPA, NCOA4, MDC1, UBR5, RB1CC1, RPS6, CIITA, MITF,* and *WT1* (16, 54, 64, 69, 88–93). It is anticipated that other shared molecular targets will be found. In early microarray analysis, more than 450 genes were identified that were differentially expressed between InvUC and normal bladder and that were shared between dogs and humans ($P < 0.05$; 2FC) (62, 94). In one report involving RNA-seq analysis, 1,589 genes were identified that were differentially expressed between normal bladder and bladder cancer in dogs and in humans (69).

Along with the notable similarities between canine and human InvUC, there is one intriguing difference. The majority (67–85%) of canine InvUCs harbor a $BRAF^{V595E}$ mutation, which is homologous to the $BRAF^{V600E}$ mutation in humans (64, 65). This mutation is considered a driver mutation of 8% of all human cancer across cancer types, and is especially common in human metastatic melanoma (64, 95). This mutation leads to constitutive activation of the MAPK pathway. While *BRAF* mutations are common in certain forms of human cancer, these mutations are rare in human InvUC. Other mutations within the MAPK pathway, however, occur in ∼30% of human InvUC cases (54). It is intriguing that even though *BRAF* mutations are common in canine InvUC and that different molecular drivers are more common in human InvUC, the cancer in both species converges into a disease possessing the same molecular subtypes.

In addition to traditional methods to assess molecular features in cancer, canine InvUC has been used as a test case for other methodologies. For example, the methods for desorption electrospray ionization (DESI), an ambient ionization mass spectrometry approach, were developed using canine tissues (96). In DESI analyses, lipid patterns were identified that distinguish InvUC from normal urothelium in the canine tissues. In a follow up study, similar lipid patterns were found in human bladder cancer tissues (96, 97). Recently a new ambient ionization MS approach, touch spray MS (TS-MS), has been tested in canine tissues, and this technique rapidly identified lipid patterns that distinguished InvUC from normal tissues (98). This technique is especially intriguing because optimization of this form of MS could lead to a point-of-care instrument for use in the operating room or cystoscopy suite.

SIMILARITIES IN TREATMENT RESPONSE BETWEEN DOGS AND HUMANS WITH InvUC

Standard Treatments for InvUC in Humans and Dogs

Some of the key features concerning the treatment of InvUC in humans and dogs are summarized in **Table 4**. In humans, the standard treatment for bladder-confined InvUC is cystectomy, usually combined with neoadjuvant chemotherapy (8, 9). In half of patients, distant metastases emerge over the next 1–2 years and sometimes later, and the metastatic disease is treated with chemotherapy or immunotherapy (4, 10, 12). For patients who are not eligible for cystectomy, bladder sparing therapies combining radiation therapy and chemotherapy have been defined (99).

TABLE 4 | Treatment options for invasive urinary bladder cancer in humans and dogs.

Type of Therapy	Human InvUC	Canine InvUC
Cystectomy	Cystectomy is the frontline treatment of choice in eligible patients with bladder-confined cancer. It is typically combined with neoadjuvant chemotherapy (8, 9)	Cystectomy is not usually performed in pet dogs due to the morbidity and cost of the procedure, and frequent extension of the cancer down the urethra which could preclude surgical cure (30–32)
Radiotherapy	Radiotherapy is used in trimodal therapies (maximum transurethral resection, radiotherapy, chemotherapy) in bladder sparing protocols. This is typically reserved for patients who are not eligible for or choose to forego cystectomy (99)	Studies to determine the efficacy of radiotherapy in dogs are limited. Trimodal therapy has not been investigated in dogs (100–102)
Chemotherapy	Chemotherapy is most often used in the neoadjuvant setting and in the treatment of emergent metastasis. Chemotherapy protocols can include: MVAC (methotrexate, vinblastine, doxorubicin, cisplatin), or in recent years less toxic combinations such as cisplatin-gemcitabine or carboplatin-taxol (103, 104)	Since cystectomy is rarely performed in dogs, chemotherapy is used to treat the primary cancer in the urinary tract, as well as to treat metastasis. Chemotherapy drugs with activity in dogs include: cisplatin, carboplatin, vinblastine, mitoxantrone, and others. Cisplatin is considered one of the most active agents in humans and dogs, but is rarely used in dogs due to consistent renal toxicity (10, 30)
Cyclooxygenase (Cox) inhibitors	Cox inhibitors are not routinely used as anticancer agents in human bladder cancer. In humans, Cox inhibitors induce biological changes in tumor tissues similar to those noted in canine bladder cancer (105, 106)	Cox inhibitors are a mainstay of canine bladder cancer treatment. These drugs are appealing because of the antitumor effects (single agent remission rate 20%, stable disease rate 55–60%), oral delivery, relatively low cost and risk of side effects, and positive benefits on quality of life. Cox inhibitors are also used to improve remission rates with chemotherapy, e.g., doubling the remission rate with cisplatin and vinblastine (30, 107–112)
Immunotherapy	Immune checkpoint inhibitors approved for use in humans include those targeting PD-L1 (atezolizumab, durvalumab, avelumab) and those targeting PD-1 (pembrolizumab, nivolumab) (12, 113–120)	Immune checkpoint inhibitors are not yet available for use in dogs
Targeted agents	An FGFR inhibitor (Erdafitinib) is approved for use in human bladder cancer	FGFR mutations are less common in canine bladder cancer, and agents targeting FGFR have not been tested in dogs. Targeted therapies tested in dogs include an EGF-toxin conjugate, and folate targeted therapies (78, 121, 122)

The treatment of InvUC in dogs can include surgery, radiation therapy, chemotherapy and other drugs, or combinations of these, although surgery and radiation therapy are used less often than drug therapy in dogs (30–32). Complete cystectomy is not typically performed in pet dogs because of the frequent extension of cancer beyond the bladder (urethra, prostate, other organs), the morbidity of the procedure, and the expense involved (30–32). Most InvUC lesions in dogs are not in a location where complete surgical excision is possible. Early reports of radiation therapy in dogs with InvUC were discouraging because of the side effects (100), although newer radiation therapy approaches have been much better tolerated, allowing further study (101, 102). Currently, drugs are the mainstay for treatment of InvUC in dogs (30). Pet owners insist that the drug protocols be well-tolerated; anything beyond mild side effects is not considered acceptable. This is not unreasonable, and low adverse event profiles are also desirable for humans. Although InvUC is not usually curable in dogs with current therapies, the disease can be controlled in 80% or more of dogs, and the dogs can enjoy many months to beyond a year, with a minority of dogs living more than 3 years with good quality of life (30). It should be noted that since the bladder is not removed, dogs can be used to study treatments of organ-confined disease, metastases, or both. It is recognized that having the primary tumor intact will lead to continued emergence of cells with metastatic potential.

Chemotherapy Responses

The response to chemotherapy for InvUC is similar between dogs and humans. Platinum agents are considered to be the most active agents in both species (10, 30, 103, 104). Cisplatin-based combination chemotherapy protocols are not often used in dogs because of side effects considered unacceptable in dogs, although a comparison of single-agent activity between dogs and humans is possible. The remission rate with single-agent cisplatin has been reported to be 12–20% in dogs and 17–34% in humans (30, 104). Carboplatin has activity in both species, although it is considered less active than cisplatin (30, 104, 123). The previous standard protocol for InvUC treatment in humans was methotrexate, vinblastine, doxorubicin, and cisplatin (104). Although this protocol was considered too toxic for acceptable use in pet dogs, an important component of the protocol, vinblastine, has been evaluated in dogs with remission and stable disease rates of 36 and 50%, respectively (124). Vinblastine has single-agent activity in humans and contributes to combination therapy protocols (125, 126). Gemcitabine is also considered an active drug in both species (127, 128).

ENTHUSIASM FOR CANINE CLINICAL TRIALS IN InvUC, AND EXAMPLES OF TRANSLATIONAL STUDIES

Canine Clinical Trials, a Win-Win-Win Scenario

Treatment studies in dogs are expected to be a win–win–win scenario (30). The individual dog receives treatment that is expected to help them and that often provides hope when other

treatments are not effective or not feasible. The study results are expected to help other dogs and ultimately help humans with InvUC. The subsidized cost for treatment in many of the trials allows some pet owners to pursue treatment for their dog even if they cannot afford any other therapies. For all of these reasons, in the Purdue University Veterinary Teaching Hospital, more than 90% of owners of dogs with InvUC elect to enroll their pet in a clinical trial. Parallel mechanism studies are feasible in dogs with samples of blood, urine, and, in some cases, tumor tissues collected by cystoscopy available before, during, and after therapy. Most pet owners will also allow a necropsy of the dog when it dies or is euthanized (because of declining quality of life due to cancer progression or other conditions). This provides crucial information on the disease process and response to therapy, and the opportunity to bank tissue samples for future studies. Although most treatments tested in dogs have been systemic therapies, dog studies can also be used to evaluate intravesical therapy (129).

Evaluation of Emerging Targeted Therapies in Dogs With InvUC

There are published examples of studies of targeted therapies in dogs with InvUC of translational value (121, 122, 130). One example is a canine clinical study performed to determine the expression of high affinity folate receptors (folate receptor alpha) in InvUC and the safety and efficacy of folate-targeted therapy (121). Briefly, folate receptor alpha expression was detected in 78% of canine InvUC tissues, and folate uptake *in vivo* was confirmed by scintigraphy. An escalating dose of folate-targeted vinblastine (EC0905) was administered to pet dogs with biopsy-confirmed folate receptor-positive InvUC. The maximum tolerated dose was determined, with neutropenia and gastrointestinal upset being dose limiting toxicities. The drug was well-tolerated at the maximum tolerated dose, and good antitumor activity was observed (121). Folate receptor expression was identified in human InvUC (121), and further work is ongoing to define the percentage of cases with folate receptor expression. Although the folate-vinblastine conjugate had good antitumor activity in dogs with InvUC, the duration of remission was limited in many cases. Thus, a follow up study was performed in dogs using a different folate conjugate, folate-tubulysin (EC0531) (122). Unlike vinblastine, tubulysin is not a substrate for the P-glycoprotein drug efflux pump, and therefore, longer remission times were anticipated (122). In the EC0531 study, the maximum tolerated dose was defined, and again neutropenia and gastrointestinal toxicity were observed at higher doses, as were observed with folate-vinblastine treatment. Of 28 dogs treated, three dogs had partial remission and 17 dogs had stable disease (122). The progression free interval appeared longer than that noted in dogs treated with folate-vinblastine, although a head-to-head comparison would be required to confirm this. Unlike human neutrophils, canine neutrophils were found to express folate receptors, which contributes to the neutropenia at higher doses of folate-targeted therapies in dogs (122). This suggest that humans may tolerate higher, potentially more effective, doses of folate-targeted therapies.

Evaluation of Cox Inhibitors in InvUC

An intriguing discovery was made in dogs with InvUC and other types of cancer which is expected to translate into benefit in humans. Briefly, non-selective cyclooxygenase inhibitors (Cox inhibitors, i.e., non-steroidal anti-inflammatory drugs) have had unexpected antitumor effects in dogs with cancer (107). The interest in Cox inhibitors in dogs with cancer stemmed from the observation of dramatic remission of a poorly differentiated sarcoma of the thoracic wall in one dog and of complete remission of advanced metastatic carcinoma of unknown primary in another dog who were receiving the non-selective Cox inhibitor, piroxicam, but no other drugs (107). These initial observations made more than three decades ago subsequently led to phase I, II, and III clinical trials of Cox inhibitors in dogs with InvUC which confirmed the antitumor effects and safety of the drugs (30, 107–110). In 76 dogs with InvUC treated with single-agent piroxicam, tumor responses included two (3%) complete remission (complete resolution of all clinical evidence of cancer), 14 (18%) partial remission ($\geq$50% reduction in tumor volume and no new tumor lesions), 45 (59%) stable disease (<50% change in tumor volume and no new lesions), and 15 (20%) progressive disease ($\geq$50% increase in tumor volume or the development of new tumor lesions) (30).

In addition to the antitumor effects of single agent Cox inhibitor treatment, these drugs also enhance the activity of chemotherapy (109–111). In dogs, Cox inhibitors have enhanced the activity of cisplatin in multiple studies including randomized trials (109, 111, 112). The remission rate with cisplatin alone was <20%, while the remission rate with cisplatin combined with the Cox inhibitor ranged from 50–70% across randomized trials (109, 111, 112). Similarly, in another randomized trial in dogs with InvUC, the remission rate was significantly higher in dogs receiving vinblastine combined with piroxicam (58%) than in dogs receiving vinblastine alone (23%) (110).

The findings from the Cox inhibitor studies in dogs have been translated into humans with InvUC (105). Intriguingly, the biological effects associated with Cox inhibitor-induced remission in dogs (e.g., induction of apoptosis) were found to occur to the same degree in humans with InvUC receiving the Cox-2 inhibitor, celecoxib prescribed between initial diagnosis and cystectomy (105, 106). Cox inhibitors have also reduced the recurrence of superficial bladder tumors in humans in some, but not all studies (131, 132).

Proposed mechanisms of the antitumor effects of Cox inhibitors have included antiangiogenic effects, immunologic effects, modulation of cancer stem cells, and direct induction of apoptosis (105, 106, 133, 134). There are growing numbers of studies of the immunologic effects. Cox-2 is upregulated in canine and human InvUC (135, 136). Cox and the Cox product PGE2 in tumor-associated macrophages and tumors, have been reported to decrease the activation and proliferation of T cells (CD4+, CD8+), increase release of IDO1, reduce the function of NK cells, cause a shift from Th1 to Th2 response, increase the infiltration of regulatory cells into the tumor and release of immunosuppressive cytokines, decrease immunostimulatory cytokines, and to drive negative DAMPs (damage-associated molecular patterns) (137–141). Cox blockade (via knockdown

or drugs) has been shown to reverse all of these effects (137–141). Of special current interest, aspirin enhanced the effects of immune checkpoint inhibitor treatment of melanoma and colon tumors in mice (141). These and other reports prompted our group to re-examine H&E slides from patients with InvUC in the celecoxib trial (105). Interestingly, the number of tumor-infiltrating lymphocytes (TILs) increased multifold in 73% of cases receiving celecoxib, compared to 38% of control cases (Dhawan and Knapp, unpublished data). Clearly, further studies of the effects of Cox inhibitors in InvUC treatment are indicated, and dogs offer an ideal animal model for this work.

GROWING ROLE FOR THE DOG MODEL TO DRIVE ADVANCES IN EMERGING IMMUNOTHERAPIES FOR InvUC

Emerging Role and Need for Advances in Immunotherapy

The medical community has seen an unprecedented resurgence in immunotherapy, as impressive remissions have been documented in patients with advanced chemotherapy-refractory cancer (12, 24, 25, 113–120). There is clear promise for immunotherapies, yet a crucial need to improve the effectiveness of these agents. This has heightened the demand for relevant immunocompetent animal models of cancer that can predict the outcomes (efficacy, toxicity) of immunotherapies (alone and when combined with other agents) when given to humans.

Among emerging immunotherapies, there is particularly high interest in immune checkpoint inhibitors (12, 24, 25, 113–120). Immune checkpoints, including PD-L1, PD-1, CTLA-4, B7x, and others, are critical regulatory components of the immune system that are essential for maintaining self-tolerance (24, 113). Immune checkpoints also modulate the amplitude and length of physiological immune responses in peripheral tissues in order to minimize collateral tissue damage. Many types of cancer, however, exploit these immune checkpoints to evade immune attack especially by T cells specific for tumor antigens (24, 113). Cancer cells upregulate PD-L1 (and other immune checkpoints) in response to oncogenic signals or endogenous antitumor immune responses. The binding of PD-L1 to PD-1 on activated T cells causes cell anergy or death (24, 113). PD-L1 is also expressed by antigen presenting cells, natural killer cells, and T cells, and can interfere with the function of these cells.

The finding of dramatic durable complete remissions in heavily pre-treated patients in multiple studies provides compelling evidence that immune checkpoint inhibitors can drive new success in treating InvUC and other cancers (25, 113–120). Much more work must be done, however, before immune checkpoint inhibitors reach their potential in saving the lives of cancer patients. Although impressive remissions are seen in patients with advanced cancer, only a minority of patients (∼20%) have this level of benefit (25, 113, 115–120). In addition, immune checkpoint inhibitors can unleash a plethora of autoimmune processes, and special attention must be paid to monitoring and treating these "toxicities" (120). Studies of biomarkers to predict immune checkpoint inhibitor activity have had conflicting results, indicating the need for continued study (25, 113, 114, 142–145).

The limited rate of remission with immune checkpoint inhibitors and the absence of clear biomarkers of response are not surprising because the immune system can fail at multiple points in attacking the cancer (24, 26, 114). Causes of immune failure can include low antigenicity (e.g., lack of antigens, MHC downregulation), deficient adjuvanticity (e.g., lack of DAMPs) to signal the immune system, ineffective T cell trafficking, immunosuppressive cells and cytokines, exhausted T cells, and deficient numbers or function of immune effector cells in general (24, 146, 147). It is expected that combining drugs that positively affect different parts of the immune system will substantially increase the success rate of immune checkpoint inhibitors (26–29). This again highlights the need for relevant animal models to help select the most promising approaches to take into human trials.

There are multiple reports of the expression of immune checkpoints in InvUC and other cancers in dogs (148–157). In addition to the well-known checkpoints PD-1, PD-L1, CTLA-4, other checkpoints have been identified in canine InvUC (59, 157). B7x (B7-H4/B7S1/VTCN1), for example, is an inhibitory immune checkpoint molecule and is considered a potential therapeutic target because of its immunosuppressive effects and well-known expression in cancers (157). The expression of B7x in canine InvUC has recently been reported (157). In RNA-seq analysis, a 5–7-fold increase in the expression of B7x in canine InvUC was noted compared to the expression in the normal bladder. B7x protein expression was confirmed by immunohistochemistry (IHC) with medium to high expression in 18 of 50 (20%) canine InvUC samples studied (157). For comparison, TCGA and Genotype-Tissue Expression (GTEx) data sets were used to examine B7x expression in 599 human urothelial carcinomas. B7x expression was significantly ($p = 0.02$) associated with worse overall survival in humans (157).

The scientific community is eagerly awaiting the availability of immune checkpoint inhibitors for studies in dogs. Human monoclonal antibodies that target immune checkpoints have not yet been shown to bind and functionally disrupt canine checkpoints. In addition, neutralizing antibodies would form in dogs in response to the administration of human antibodies, i.e., foreign protein, making the antibody treatment ineffective and potentially leading to allergic and anaphylactic reactions in the dogs.

There are reports of canine PD-L1 (cPD-L1) antibodies developed by academic laboratories (155, 156). A canine chimeric PD-L1 antibody has been administered to nine dogs with oral melanoma or soft tissue sarcomas (155). Although tumor regression was observed in two dogs, the extent of the cPD-L1 inhibitor's activity is not known because the dogs were allowed to receive concurrent non-steroidal anti-inflammatory drugs that have been documented to have antitumor effects in those cancers in dogs and in canine xenograft models (107, 158, 159). The lack of immune-mediated toxicity (which is common in humans) in the dogs also calls the drug's activity into question.

As immune checkpoint inhibitors become available for dogs, studies to evaluate the antitumor effects, determine

mechanisms of response and resistance, test potential combination therapies, and develop strategies to minimize adverse events will be high priorities. It is likely that dogs will develop adverse events similar to the autoimmune-related adverse events in humans because dogs naturally develop immune mediated diseases such as hemolytic anemia, thrombocytopenia, myasthenia gravis, polyarthritis, inflammatory bowel disease, and others (160). The adverse events are expected to be manageable in dogs, just as they are in humans. Dog studies of the antitumor effects, safety, and mechanisms of response and resistance to immune checkpoint inhibitors are anticipated to be key to advancing these therapies in humans.

Next to immune checkpoint inhibitors, chimeric antigen receptor T cells (CAR T cells) which are T lymphocytes engineered to express a specific chimeric antigen receptor, are gaining the most attention in immunotherapy, and are perhaps showing more promise than other current immunotherapy strategies (161). CAR T cell therapy has been successfully delivered to dogs with naturally-occurring lymphoma (162). Briefly, autologous RNA-transfected CAR T cells were generated, expanded, and administered to pet dogs with relapsed B cell lymphoma. The treatment was well-tolerated and resulted in reduction of CD20+ B cells in target lymph nodes. The results from this proof-of-concept study validate further evaluation of CAR T cell therapy in dogs, and the opportunity to fill the gap between mouse models and translation into humans (162).

Monitoring the Immune Response in Dogs With InvUC

Although the fairly extensive "tool kit" available to assess immune cells and the activity of the immune system in humans is much more limited in dogs, methods do exist to analyze immune cells and cytokines in circulation and in the tumor masses. A few of those used to study the immune infiltrates in the tumor will be highlighted in this review.

Immune cells infiltrating the tumor can be visualized with IHC (163–166). While all of the markers for various immune cells in humans are not available for dogs, CD3 IHC is a popular approach to assess tumor infiltrating lymphocytes (TILs) in canine cancer, including application to formalin fixed tissues (166). IHC protocols have also been described to detect regulatory T cells in canine tumors (167, 168). More specific immune cells can be detected in frozen sections of canine tumors (169). Using IHC, the pattern of TILs in human InvUC have been classified in some studies as: (1) immune desert (no or very few TILs observed), (2) immune excluded (TILs on the periphery of the tumor mass but no TILs within the mass itself), or (3) immune infiltrated (TILs in the mass), with further distinctions made for the presence of TILs in the stroma in and around the tumor or between tumor cells in the tumor mass (163–165). An effective immune attack is expected to require TILs within the tumor mass, and there is great interest in developing strategies to convert the immune desert or immune excluded state to an immune infiltrated state. It is therefore important to note that

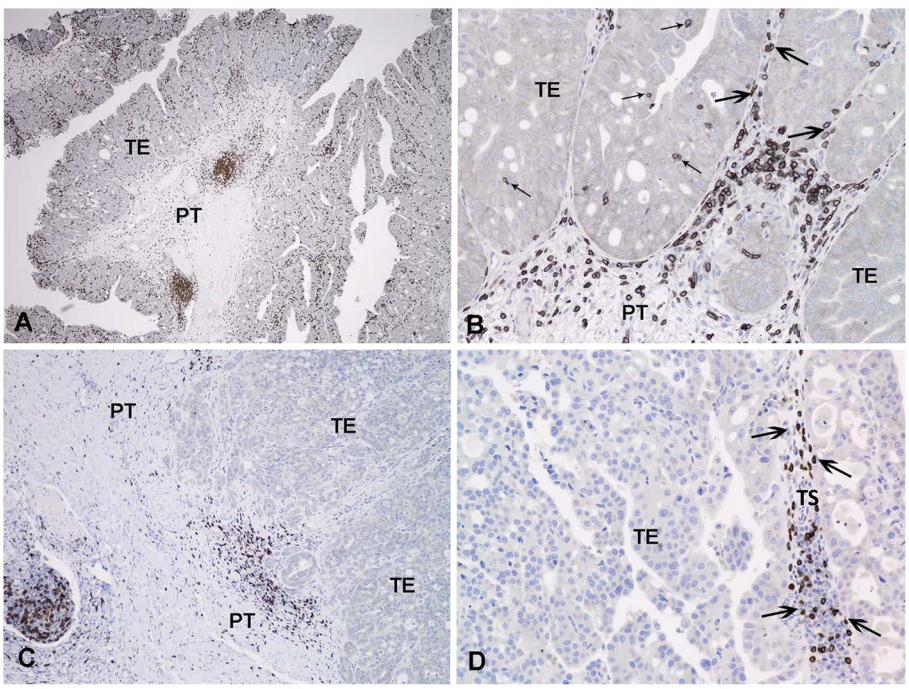

FIGURE 3 | Immunohistochemical detection of T lymphocytes with an antibody to CD3 in canine invasive urothelial carcinoma. In **(A)** all areas examined (intraepithelial, tumor stroma, and peritumoral) contain CD3 positive cells. In **(B)** a detail of the triphasic pattern of CD3 expression is noted. In **(C)** only the peritumoral lymphoid infiltrate expresses CD3 in this tumor. In **(D)** the tumoral stroma contains numerous CD3 positive lymphocytes, but the tumor epithelium is negative. TE, tumoral epithelium; TS, tumoral stroma; PT, peritumoral stroma; Small arrow, intraepithelial T-lymphocytes; Large arrow, tumoral stroma T lymphocytes.

these same patterns of TILs have been observed in canine InvUC (**Figure 3**).

Sequencing studies have also been used to characterize the immune state in InvUC tissues (13, 16, 54, 59, 170–173). Whole exome sequencing analyses can be used to determine tumor mutation burden and neoantigen load, factors that are thought to influence the immune attack on the cancer (171–173). Patterns in RNA-seq data have been defined to classify tumors broadly as "immune hot" (immune infiltrated) or "immune cold" (non-infiltrated), with mixed patterns also present (13, 16, 163, 170). The immune hot tumors are expected to be primed to respond well to immunotherapy and other therapies, whereas the immune cold tumors are thought to be largely incapable of responding to immunotherapy. Similar RNA-seq analyses have been used to demonstrate an immune hot vs. cold state in canine InvUC (**Figure 4**) (59). This demonstrates that the canine InvUC model can be used to develop and test strategies to convert immune cold tumors to immune hot tumors in order to sensitize the tumor to immunotherapy. There are also intriguing initial findings from single cell RNA-seq analyses of canine InvUC (**Figure 5**) (174, 175). When performing single cell RNA-seq on InvUC tissues, the tumor biopsy is digested into a single cell suspension. The cells are segregated into CD45+ (immune cells) and CD45– (tumor cells, stromal cells). Each cell is barcoded and the sequence of each cell generated. This makes it possible to identify the different immune cell populations present in the cancer, to determine the gene expression in those immune cells indicating the activity of the cells, and to determine changes in the number and activity of the immune cells in each population over time. In the future, this is expected to allow the characterization of each step in the immune response in the individual patient. This could facilitate the development of interventions aimed at specific parts of the immune response in need of "help" in the individual.

While canine tumor immunology has lagged behind human tumor immunology, the field is advancing rapidly and will set the stage for high impact studies in dogs to improve immunotherapies across both species.

PREVENTION, EARLY DETECTION, AND EARLY INTERVENTION, AND VALUE OF CANINE STUDIES

Challenges in Cancer Prevention Research

It is well-recognized that prevention of cancer holds the greatest promise for reducing cancer morbidity and mortality, as well as decreasing health care costs (176). This includes primary cancer prevention aimed at stopping cancer from

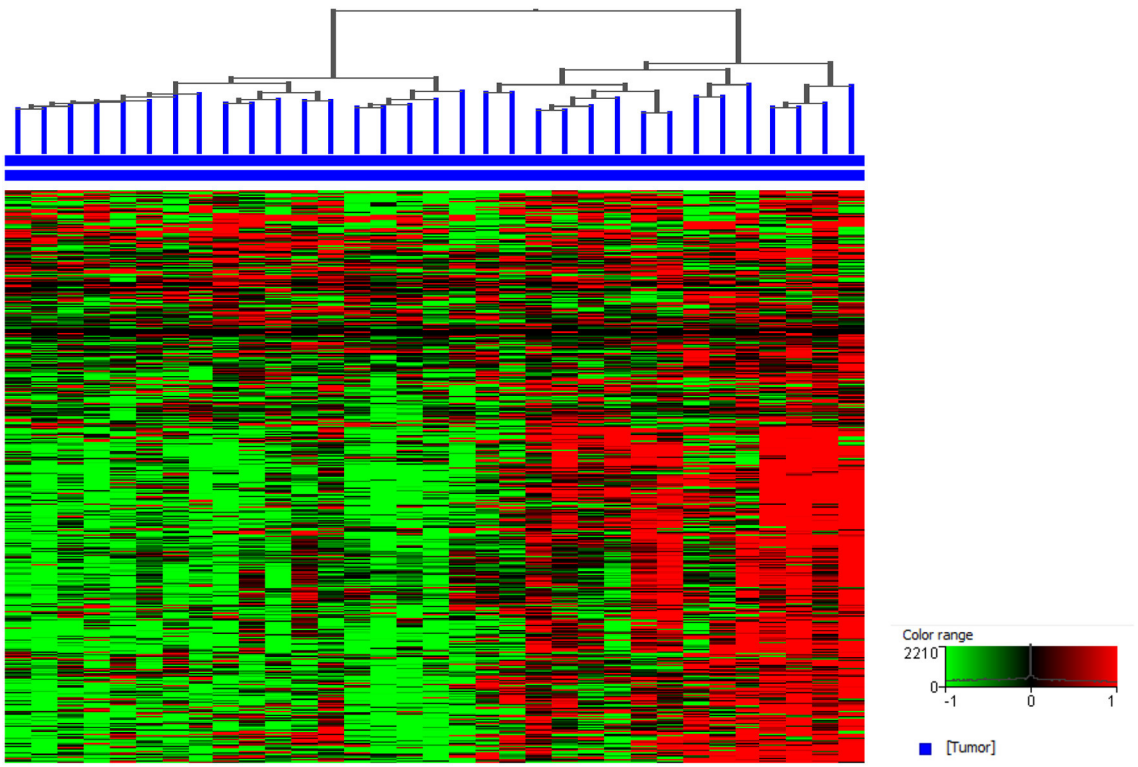

FIGURE 4 | Canine invasive urothelial carcinoma (InvUC) samples display gene expression patterns classifying the tumors as immune infiltrated (immune "hot") or non-immune infiltrated (immune "cold"). A list of immune signature genes known to be upregulated in T-cell inflamed human InvUC samples were used (170) to visualize the immune patterns that exist in canine InvUC. Normalized intensity values were used for supervised hierarchical clustering using Euclidean distance metrics and Ward's linkage algorithm as a distance metric. Note the predominantly high expression of immune genes in the right cluster of the canine InvUC samples ($n = 15$, 45%) classifying them as immune "hot" (immune infiltrated).

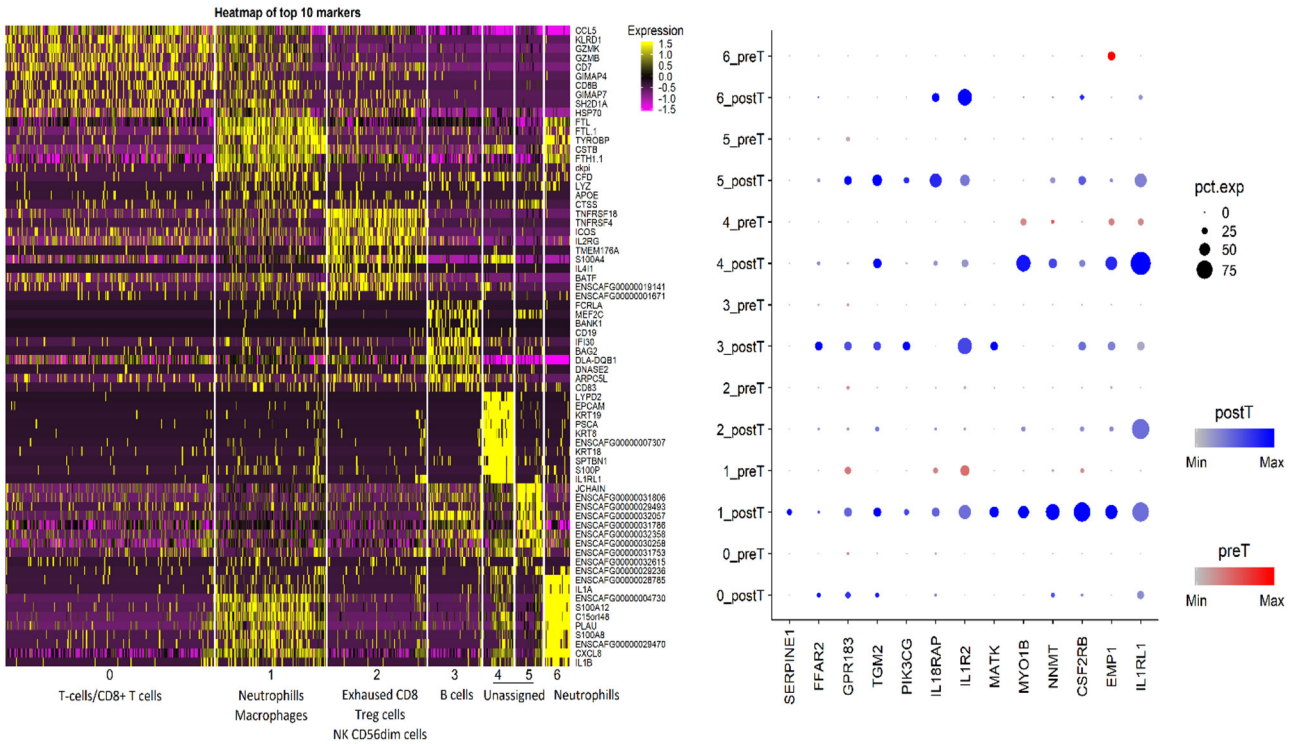

FIGURE 5 | Single cell RNA-seq analysis of canine invasive urothelial carcinoma. Unsupervised clustering of the canine InvUC sample was performed (Seurat package, Satija Lab). The cells segregated into seven different clusters. Putative cell type assignment was based on marker gene expression and abundance within the cluster. The gene expression heatmap focused on the CD45+ cells (immune cells) shows the cell clusters with putative immune cell type assignments on x-axis and top 10 marker genes in each cluster on Y-axis. The split dotplot on right shows the intensity (dot color) and percentage of cells expressing (dot size) 13 marker genes (x axis) analyzed in InvUC tissue across clusters before and after treatment (y axis). This type of data can be used to study mechanisms and generate new hypotheses. For example, GPR183 which increases in cluster 1 cells, is known for its role in lymphoid organ development and positioning of activated CD4 T cells in lymphoid follicles, but its role in the immune state of InvUC has not been elucidated (174).

developing, and secondary cancer prevention aimed at detecting cancer early and intervening early to stop its progression. In order to most effectively prevent cancer, crucial information is needed including: (1) environmental and host (genetic) risk factors and gene-environment interactions that lead to cancer, (2) effective methods for screening and early detection, and (3) successful strategies for early intervention (i.e., chemoprevention, diet, drugs, others). This crucial information is very difficult to elucidate in humans. Unlike the case for breast cancer and colon cancer, specific well-defined groups of people with high familial susceptibility for InvUC have not been identified (15). Heritable risks which are likely to exist have not yet been defined, and therefore, cohorts of people who would provide the best study subjects and who would most likely benefit from prevention, early detection, and early intervention have not been established. To further complicate matters, more than half of bladder cancer patients are not aware of any exposures or risk factors that contributed to their cancer (15, 34). And, for people with known carcinogen exposures, the latency period between the carcinogen exposure (i.e., cigarette smoke, specific chemicals) and the development of bladder cancer can extend to decades (15, 33, 34, 177).

Testing prevention strategies can also be challenging. Such research would often require more years of study than would be feasible. If an investigator wanted to test a cancer prevention strategy in humans that would be applied from middle age to the age of typical cancer diagnosis (e.g., from age 40 to age 65 years), the study would require 25 years or more for completion. Clearly, relevant animal models with more compressed life spans are needed for prevention studies in order to select the strategies most likely to be successful in humans. There are many compelling reasons why dogs who have InvUC or who are at risk for developing InvUC can be key models in prevention research.

Unique Opportunities for Studies in Dogs to Advance Cancer Prevention Research

There are many reasons why dogs are ideally suited to study strategies for prevention, early detection, and early intervention of InvUC (30). The similarities between InvUC in dogs and humans have been detailed in this review. The compressed life span in dogs makes prevention studies feasible in a reasonable length of time. Further, dogs of specific breeds have a much higher risk for developing InvUC than mixed breed dogs as summarized in **Table 5** (30).

TABLE 5 | Breed-associated risk for InvUC in dogs (30)*.

Breed	Number of dogs in that breed in VMDB	Number of InvUC cases in that breed	OR compared to mixed breed	95% confidence intervals
Mixed breed dog (reference category)	42,777	269	1.0	NA
Scottish Terrier	670	79	21.12	16.23–27.49
Eskimo Dog	225	9	6.58	3.34–12.96
Shetland Sheepdog	2,521	93	6.05	4.76–7.69
West Highland White Terrier	1,234	44	5.84	4.23–8.08
Keeshond	381	10	4.26	2.25–8.07
Samoyed	471	10	3.43	1.81–6.49
Beagle	3236	62	3.09	2.34–4.08
Dalmatian	1253	19	2.43	1.52–3.89

**Data are summarized from the Veterinary Medical Database (VMDB). The odds ratios (ORs) of InvUC risk compared with the risk in mixed breed dogs are included for breeds with an OR > 2.0 and at least nine cases of InvUC in the breed recorded in the VMDB.*

Scottish Terriers especially stand out for having a 20-fold increased risk for InvUC compared to mixed breed dogs (30). This provides a unique resource to identify existing genes and new genes that have not yet been characterized that contribute to cancer risk and to then assess the expression of those genes in human InvUC patients. Dogs offer a great opportunity to assess environmental risk and gene-environment interactions leading to InvUC. In Scottish Terriers, for example, exposure to lawn chemicals increases the risk of InvUC 7-fold on top of the already existing heritable risk (178). On a more positive front, Scottish Terriers who consume vegetables three times per week in addition to regular dog food have a 70% reduced risk for InvUC (179).

Dogs can also be used to track chemical exposures. With interest arising from the association between lawn chemical exposure and InvUC risk, a study was undertaken to track herbicide exposure and specifically to measure herbicide concentrations in the urine of exposed pet dogs in a community setting. In one study, three chemicals used in lawn care products (2,4-dichlorophenoxyacetic acid, 4-chloro-2-methylphenoxypropionic acid, dicamba) were measured on the grass and in the urine of dogs from 25 households that used lawn chemicals and from eight control households that did not use lawn chemicals (180). Urine samples from the dogs were collected prior to lawn treatment and at 24 and 48 h after lawn treatment. The results were concerning in that after lawn chemicals were applied, the chemicals were detected in the urine of dogs in 19 of 25 treated households. Of even greater concern, chemicals were found in the urine of dogs in 14 of the 25 households before the lawn was treated, and in four of eight control households. This indicated widespread exposure to the chemicals, most likely due in part to chemical drift from other treated areas.

The compressed lifespan of dogs greatly facilitates timely prevention studies. A study in humans from age 40–65 (25 years) could be accomplished in dogs of "similar physiological ages" in 2–4 years. Shorter term interventional strategies could be tested over weeks to several months in dogs. Also, in conducting research to assess the value of a prevention strategy in dogs, it is much more feasible to control other variables (diet, smoking, etc.) than is possible in humans. Regarding establishing the means for cancer screening and early detection, dogs again offer an excellent opportunity because of the compressed life span of dogs, the motivation by pet owners to have cancer detected early in their dog, and the feasibility of non-invasive screening tests and then follow-up confirmatory tests to determine if cancer is or is not present.

CONCLUSIONS

In conclusion, there is strong evidence that dogs with naturally-occurring InvUC can represent a relevant predictive model for InvUC treatment and prevention. Further validation of the canine model could come from parallel human and canine InvUC trials in which the outcome in dogs is predictive of the outcome in humans. Dogs are anticipated to fill an essential niche in cancer drug development and prevention research, and to ultimately transform the outlook for humans (and dogs) facing InvUC.

AUTHOR CONTRIBUTIONS

All authors listed have made a substantial, direct and intellectual contribution to the work, and approved it for publication.

FUNDING

This review article summarizes findings from many different studies at Purdue University and other institutions. These studies were made possible by support from public agencies, foundations, private donors, industry partners, and others. Specific funding information is listed in the individual study publications.

ACKNOWLEDGMENTS

The authors wish to thank the clinicians and staff of the Purdue Comparative Oncology Program and the Canine Bladder Cancer Clinic in the Purdue University Veterinary Teaching Hospital for their dedicated work. The authors also wish to thank all of the families of the pet dogs that participated in the studies summarized in this review. The authors are also very grateful for the financial gift support for bladder cancer research at Purdue University.

REFERENCES

1. Antoni S, Ferlay J, Soerjomataram I, Znaor A, Jemal A, Bray F. Bladder cancer incidence and mortality: a global overview and recent trends. *Eur Urol.* (2017) 71:96–108. doi: 10.1016/j.eururo.2016.06.010
2. Siegel RL, Miller KD, Jemal A. Cancer statistics, 2019. *CA Cancer J Clin.* (2019) 69:7–34. doi: 10.3322/caac.21551
3. Monteiro LL, Witjes JA, Agarwal PK, Anderson CB, Bivalacqua TJ, Bochner BH, et al. ICUD-SIU International Consultation on Bladder Cancer 2017: management of non-muscle invasive bladder cancer. *World J Urol.* (2019) 37:51–60. doi: 10.1007/s00345-018-2438-9
4. Lobo N, Mount C, Omar K, Nair R, Thurairaja R, Khan MS. Landmarks in the treatment of muscle-invasive bladder cancer. *Nat Rev Urol.* (2017) 14:565–74. doi: 10.1038/nrurol.2017.82
5. Niegisch G, Retz M, Siener R, Albers P. Quality of life in patients with cisplatin-resistant urothelial cancer: typical ailments and effect of paclitaxel-based salvage therapy. *Urol Oncol.* (2016) 34:256.e15–21. doi: 10.1016/j.urolonc.2016.02.002
6. Svatek RS, Hollenbeck BK, Holmäng S, Lee R, Kim SP, Stenzl A, et al. The economics of bladder cancer: costs and considerations of caring for this disease. *Eur Urol.* (2014) 66:253–62. doi: 10.1016/j.eururo.2014.01.006
7. Verma V, Sprave T, Haque W, Simone CB, Chang JY, Welsh JW, et al. A systematic review of the cost and cost-effectiveness studies of immune checkpoint inhibitors. *J Immunother Cancer.* (2018) 6:128. doi: 10.1186/s40425-018-0442-7
8. Tyson MD, Barocas DA. Quality of life after radical cystectomy. *Urol Clin N Am.* (2018) 45:249–56. doi: 10.1016/j.ucl.2017.12.008
9. Massari F, Santoni M, di Nunno V, Cheng L, Lopez-Beltran A, Cimadamore A, et al. Adjuvant and neoadjuvant approaches for urothelial cancer: updated indications and controversies. *Cancer Treat Rev.* (2018) 68:80–5. doi: 10.1016/j.ctrv.2018.06.002
10. Merseburger AS, Apolo AB, Chowdhury S, Hahn NM, Galsky MD, Milowsky MI, et al. SIU-ICUD recommendations on bladder cancer: systemic therapy for metastatic bladder cancer. *World J Urol.* (2019) 37:95–105. doi: 10.1007/s00345-018-2486-1
11. Rouanne M, Loriot Y, Lebret T, Soria J-C. Novel therapeutic targets in advanced urothelial carcinoma. *Crit Rev Oncol Hematol.* (2016) 98:106–15. doi: 10.1016/j.critrevonc.2015.10.021
12. Kim HS, Seo HK. Immune checkpoint inhibitors for urothelial carcinoma. *Investig Clin Urol.* (2018) 59:285–96. doi: 10.4111/icu.2018.59.5.285
13. Robertson AG, Kim J, Al-Ahmadie H, Bellmunt J, Guo G, Cherniack AD, et al. Comprehensive molecular characterization of muscle-invasive bladder cancer. *Cell.* (2018) 174:1033. doi: 10.1016/j.cell.2018.07.036
14. Choi W, Porten S, Kim S, Willis D, Plimack ER, Hoffman-Censits J, et al. Identification of distinct basal and luminal subtypes of muscle-invasive bladder cancer with different sensitivities to frontline chemotherapy. *Cancer Cell.* (2014) 25:152–65. doi: 10.1016/j.ccr.2014.01.009
15. Czerniak B, Dinney C, McConkey D. Origins of bladder cancer. *Annu Rev Pathol.* (2016) 11:149–74. doi: 10.1146/annurev-pathol-012513-104703
16. McConkey DJ, Choi W. Molecular subtypes of bladder cancer. *Curr Oncol Rep.* (2018) 20:77. doi: 10.1007/s11912-018-0727-5
17. Damrauer JS, Hoadley KA, Chism DD, Fan C, Tiganelli CJ, Wobker SE, et al. Intrinsic subtypes of high-grade bladder cancer reflect the hallmarks of breast cancer biology. *Proc Natl Acad Sci USA.* (2014) 111:3110–5. doi: 10.1073/pnas.1318376111
18. Soria F, Krabbe L-M, Todenhöfer T, Dobruch J, Mitra AP, Inman BA, et al. Molecular markers in bladder cancer. *World J Urol.* (2019) 37:31–40. doi: 10.1007/s00345-018-2503-4
19. Kobayashi T, Owczarek TB, McKiernan JM, Abate-Shen C. Modelling bladder cancer in mice: opportunities and challenges. *Nat Rev Cancer.* (2015) 15:42–54. doi: 10.1038/nrc3858
20. Mak IW, Evaniew N, Ghert M. Lost in translation: animal models and clinical trials in cancer treatment. *Am J Transl Res.* (2014) 6:114–8.
21. Zhang N, Li D, Shao J, Wang X. Animal models for bladder cancer: the model establishment and evaluation (Review). *Oncol Lett.* (2015) 9:1515–9. doi: 10.3892/ol.2015.2888
22. He Z, Kosinska W, Zhao Z-L, Wu X-R, Guttenplan JB. Tissue-specific mutagenesis by N-butyl-N-(4-hydroxybutyl)nitrosamine as the basis for urothelial carcinogenesis. *Mutat Res.* (2012) 742:92–5. doi: 10.1016/j.mrgentox.2011.11.015
23. Vang DP, Wurz GT, Griffey SM, Kao C-J, Gutierrez AM, Hanson GK, et al. Induction of invasive transitional cell bladder carcinoma in immune intact human MUC1 transgenic mice: a model for immunotherapy development. *J Vis Exp.* (2013) 80:e50868. doi: 10.3791/50868
24. Pardoll DM. The blockade of immune checkpoints in cancer immunotherapy. *Nat Rev Cancer.* (2012) 12:252–64. doi: 10.1038/nrc3239
25. Rosenberg JE, Hoffman-Censits J, Powles T, van der Heijden MS, Balar AV, Necchi A, et al. Atezolizumab in patients with locally advanced and metastatic urothelial carcinoma who have progressed following treatment with platinum-based chemotherapy: a single-arm, multicentre, phase 2 trial. *Lancet.* (2016) 387:1909–20. doi: 10.1016/S0140-6736(16)00561-4
26. Galluzzi L, Zitvogel L, Kroemer G. Immunological mechanisms underneath the efficacy of cancer therapy. *Cancer Immunol Res.* (2016) 4:895–902. doi: 10.1158/2326-6066.CIR-16-0197
27. Pfirschke C, Engblom C, Rickelt S, Cortez-Retamozo V, Garris C, Pucci F, et al. Immunogenic chemotherapy sensitizes tumors to checkpoint blockade therapy. *Immunity.* (2016) 44:343–54. doi: 10.1016/j.immuni.2015.11.024
28. Bracci L, Schiavoni G, Sistigu A, Belardelli F. Immune-based mechanisms of cytotoxic chemotherapy: implications for the design of novel and rationale-based combined treatments against cancer. *Cell Death Differ.* (2014) 21:15–25. doi: 10.1038/cdd.2013.67
29. Peng J, Hamanishi J, Matsumura N, Abiko K, Murat K, Baba T, et al. Chemotherapy induces programmed cell death-ligand 1 overexpression via the nuclear factor-κB to foster an immunosuppressive tumor microenvironment in ovarian cancer. *Cancer Res.* (2015) 75:5034–45. doi: 10.1158/0008-5472.CAN-14-3098
30. Knapp DW, Ramos-Vara JA, Moore GE, Dhawan D, Bonney PL, Young KE. Urinary bladder cancer in dogs, a naturally occurring model for cancer biology and drug development. *ILAR J.* (2014) 55:100–18. doi: 10.1093/ilar/ilu018
31. Sommer BC, Dhawan D, Ratliff TL, Knapp DW. Naturally-occurring canine invasive urothelial carcinoma: a model for emerging therapies. *Bladder Cancer.* (2018) 4:149–59. doi: 10.3233/BLC-170145
32. Fulkerson CM, Dhawan D, Ratliff TL, Hahn NM, Knapp DW. Naturally occurring canine invasive urinary bladder cancer: a complementary animal model to improve the success rate in human clinical trials of new cancer drugs. *Int J Genomics.* (2017) 2017:6589529. doi: 10.1155/2017/6589529
33. Al Hussein Al Awamlh B, Shoag JE, Ravikumar V, Posada L, Taylor BL, et al. Association of smoking and death from genitourinary malignancies: analysis of the national longitudinal mortality study. *J Urol.* (2019) 202:1248–54. doi: 10.1097/JU.0000000000000433.
34. Burger M, Catto JWF, Dalbagni G, Grossman HB, Herr H, Karakiewicz P, et al. Epidemiology and risk factors of urothelial bladder cancer. *Eur Urol.* (2013) 63:234–41. doi: 10.1016/j.eururo.2012.07.033
35. Bryan JN, Keeler MR, Henry CJ, Bryan ME, Hahn AW, Caldwell CW. A population study of neutering status as a risk factor for canine prostate cancer. *Prostate.* (2007) 67:1174–81. doi: 10.1002/pros.20590
36. Cooley DM, Beranek BC, Schlittler DL, Glickman NW, Glickman LT, Waters DJ. Endogenous gonadal hormone exposure and bone sarcoma risk. *Cancer Epidemiol Biomarkers Prev.* (2002) 11:1434–40.
37. Villamil JA, Henry CJ, Hahn AW, Bryan JN, Tyler JW, Caldwell CW. Hormonal and sex impact on the epidemiology of canine lymphoma. *J Cancer Epidemiol.* (2009) 2009:591753. doi: 10.1155/2009/591753
38. Autorino R, Di Lorenzo G, Damiano R, Giannarini G, De Sio M, Cheng L, et al. Pathology of the prostate in radical cystectomy specimens: a critical review. *Surg Oncol.* (2009) 18:73–84. doi: 10.1016/j.suronc.2008.07.006
39. Jønck S, Helgstrand JT, Røder MA, Klemann N, Grønkaer Toft B, Brasso K. The prognostic impact of incidental prostate cancer following radical cystoprostatectomy: a nationwide analysis. *Scand J Urol.* (2018) 52:358–63. doi: 10.1080/21681805.2018.1534885
40. Zhou J, Yang C, Lu Z, Zhang L, Yin Y, Tai S, Liang C. Primary urothelial carcinoma of the prostate: a rare case report. *Medicine.* (2019) 98:e14155. doi: 10.1097/MD.0000000000014155
41. Froemming A, Potretzke T, Takahashi N, Kim B. Upper tract urothelial cancer. *Eur J Radiol.* (2018) 98:50–60. doi: 10.1016/j.ejrad.2017.10.021
42. Cheng L, MacLennan GT, Lopez-Beltran A. Histologic grading of urothelial carcinoma: a reappraisal. *Hum Pathol.* (2012) 43:2097–108. doi: 10.1016/j.humpath.2012.01.008
43. Black PC, Brown GA, Dinney CPN. The impact of variant histology on the outcome of bladder cancer treated with curative

intent. *Urol Oncol.* (2009) 27:3–7. doi: 10.1016/j.urolonc.2007.07.010
44. Humphrey PA, Moch H, Cubilla AL, Ulbright TM, Reuter VE. The 2016 WHO Classification of tumours of the urinary system and male genital organs-part b: prostate and bladder tumours. *Eur Urol.* (2016) 70:106–19. doi: 10.1016/j.eururo.2016.02.028
45. Monn MF, Kaimakliotis HZ, Pedrosa JA, Cary KC, Bihrle R, Cheng L, et al. Contemporary bladder cancer: variant histology may be a significant driver of disease. *Urol Oncol.* (2015) 33:18.e15–20. doi: 10.1016/j.urolonc.2014.10.001
46. Lin SJ-H, Kao C-F, Wang F-I, Jeng C-R, Lee J-J, Wang L-Y, et al. Urothelial carcinomas of the urinary bladder with plasmacytoid or rhabdoid features and tendency of epithelial-mesenchymal transition in 3 dogs. *Vet Pathol.* (2018) 55:673–7. doi: 10.1177/0300985818771151
47. de Brot S, Grau-Roma L, Stirling-Stainsby C, Dettwiler M, Guscetti F, Meier D, et al. A fibromyxoid stromal response is associated with muscle invasion in canine urothelial carcinoma. *J Comp Pathol.* (2019) 169:35–46. doi: 10.1016/j.jcpa.2019.04.003
48. Owen LN. *TNM Classification of Tumours in Domestic Animals*. Geneva: World Health Organization (1980).
49. Iwasaki R, Shimosato Y, Yoshikawa R, Goto S, Yoshida K, Murakami M, et al. Survival analysis in dogs with urinary transitional cell carcinoma that underwent whole-body computed tomography at diagnosis. *Vet Comp Oncol.* (2019) 17:385–93. doi: 10.1111/vco.12483
50. Wallmeroth A, Wagner U, Moch H, Gasser TC, Sauter G, Mihatsch MJ. Patterns of metastasis in muscle-invasive bladder cancer (pT2-4): an autopsy study on 367 patients. *Urol Int.* (1999) 62:69–75. doi: 10.1159/000030361
51. Higuchi T, Burcham GN, Childress MO, Rohleder JJ, Bonney PL, Ramos-Vara JA, et al. Characterization and treatment of transitional cell carcinoma of the abdominal wall in dogs: 24 cases (1985-2010). *J Am Vet Med Assoc.* (2013) 242:499–506. doi: 10.2460/javma.242.4.499
52. Charney VA, Miller MA, Heng HG, Weng HY, Knapp DW. Skeletal metastasis of canine urothelial carcinoma: pathologic and computed tomographic features. *Vet Pathol.* (2017) 54:380–6. doi: 10.1177/0300985816677152
53. Kotake T, Kiyohara H. Multiple primary cancers (MPC) associated with bladder cancer: an analysis of the clinical and autopsy cases in Japan. *Jpn J Clin Oncol.* (1985) 15(Suppl. 1):201–10.
54. Cancer Genome Atlas Research Network. Comprehensive molecular characterization of urothelial bladder carcinoma. *Nature.* (2014) 507:315–22. doi: 10.1038/nature12965
55. Choi W, Ochoa A, McConkey DJ, Aine M, Höglund M, Kim WY, et al. Genetic alterations in the molecular subtypes of bladder cancer: illustration in the cancer genome atlas dataset. *Eur Urol.* (2017) 72:354–65. doi: 10.1016/j.eururo.2017.03.010
56. Aine M, Sjödahl G, Eriksson P, Veerla S, Lindgren D, Ringnér M, et al. Integrative epigenomic analysis of differential DNA methylation in urothelial carcinoma. *Genome Med.* (2015) 7:23. doi: 10.1186/s13073-015-0144-4
57. Tabernero J, Bahleda R, Dienstmann R, Infante JR, Mita A, Italiano A, et al. Phase I dose-escalation study of JNJ-42756493, an oral pan-fibroblast growth factor receptor inhibitor, in patients with advanced solid tumors. *J Clin Oncol.* (2015) 33:3401–8. doi: 10.1200/JCO.2014.60.7341
58. Rebouissou S, Bernard-Pierrot I, de Reyniès A, Lepage M-L, Krucker C, Chapeaublanc E, et al. EGFR as a potential therapeutic target for a subset of muscle-invasive bladder cancers presenting a basal-like phenotype. *Sci Transl Med.* (2014) 6:244ra91. doi: 10.1126/scitranslmed.3008970
59. Dhawan D, Hahn NM, Ramos-Vara JA, Knapp DW. Naturally-occurring canine invasive urothelial carcinoma harbors luminal and basal transcriptional subtypes found in human muscle invasive bladder cancer. *PLoS Genet.* (2018) 14:e1007571. doi: 10.1371/journal.pgen.1007571
60. Watanabe R, Tomita Y, Nishiyama T, Tanikawa T, Sato S. Correlation of p53 protein expression in human urothelial transitional cell cancers with malignant potential and patient survival. *Int J Urol.* (1994) 1:43–8. doi: 10.1111/j.1442-2042.1994.tb00007.x
61. Hanazono K, Nishimori T, Fukumoto S, Kawamura Y, Endo Y, Kadosawa T, et al. Immunohistochemical expression of p63, Ki67 and β-catenin in canine transitional cell carcinoma and polypoid cystitis of the urinary bladder. *Vet Comp Oncol.* (2016) 14:263–9. doi: 10.1111/vco.12095
62. Dhawan D, Paoloni M, Shukradas S, Choudhury DR, Craig BA, Ramos-Vara JA, et al. Comparative gene expression analyses identify luminal and basal subtypes of canine invasive urothelial carcinoma that mimic patterns in human invasive bladder cancer. *PLoS ONE.* (2015)10:e0136688. doi: 10.1371/journal.pone.0136688
63. Dhawan D, Ramos-Vara JA, Stewart JC, Zheng R, Knapp DW. Canine invasive transitional cell carcinoma cell lines: *in vitro* tools to complement a relevant animal model of invasive urinary bladder cancer. *Urol Oncol.* (2009) 27:284–92. doi: 10.1016/j.urolonc.2008.02.015
64. Decker B, Parker HG, Dhawan D, Kwon EM, Karlins E, Davis BW, et al. Homologous mutation to human BRAF V600E is common in naturally occurring canine bladder cancer–evidence for a relevant model system and urine-based diagnostic test. *Mol Cancer Res.* (2015) 13:993–1002. doi: 10.1158/1541-7786.MCR-14-0689
65. Mochizuki H, Shapiro SG, Breen M. Detection of BRAF mutation in urine DNA as a molecular diagnostic for canine urothelial and prostatic carcinoma. *PLoS ONE.* (2015) 10:e0144170. doi: 10.1371/journal.pone.0144170
66. Chaux A, Cohen JS, Schultz L, Albadine R, Jadallah S, Murphy KM, et al. High epidermal growth factor receptor immunohistochemical expression in urothelial carcinoma of the bladder is not associated with EGFR mutations in exons 19 and 21: a study using formalin-fixed, paraffin-embedded archival tissues. *Hum Pathol.* (2012) 43:1590–5. doi: 10.1016/j.humpath.2011.11.016
67. Chow NH, Chan SH, Tzai TS, Ho CL, Liu HS. Expression profiles of ErbB family receptors and prognosis in primary transitional cell carcinoma of the urinary bladder. *Clin Cancer Res.* (2001) 7:1957–62.
68. Ramsey SA. A method for cross-species visualization and analysis of RNA-sequence data. *Methods Mol Biol.* (2018) 1702:291–305. doi: 10.1007/978-1-4939-7456-6_14
69. Ramsey SA, Xu T, Goodall C, Rhodes AC, Kashyap A, He J, et al. Cross-species analysis of the canine and human bladder cancer transcriptome and exome. *Genes Chromosomes Cancer.* (2017) 56:328–43. doi: 10.1002/gcc.22441
70. Kent MS, Zwingenberger A, Westropp JL, Barrett LE, Durbin-Johnson BP, Ghosh P, et al. MicroRNA profiling of dogs with transitional cell carcinoma of the bladder using blood and urine samples. *BMC Vet Res.* (2017) 13:339. doi: 10.1186/s12917-017-1259-1
71. Maeda S, Tomiyasu H, Tsuboi M, Inoue A, Ishihara G, Uchikai T, et al. Comprehensive gene expression analysis of canine invasive urothelial bladder carcinoma by RNA-Seq. *BMC Cancer.* (2018) 18:472. doi: 10.1186/s12885-018-4409-3
72. Hanazono K, Fukumoto S, Kawamura Y, Endo Y, Kadosawa T, Iwano H, et al. Epidermal growth factor receptor expression in canine transitional cell carcinoma. *J Vet Med Sci.* (2015) 77:1–6. doi: 10.1292/jvms.14-0032
73. Pruthi RS, Nielsen M, Heathcote S, Wallen EM, Rathmell WK, Godley P, et al. A phase II trial of neoadjuvant erlotinib in patients with muscle-invasive bladder cancer undergoing radical cystectomy: clinical and pathological results. *BJU Int.* (2010) 106:349–54. doi: 10.1111/j.1464-410X.2009.09101.x
74. Petrylak DP, Tangen CM, Van Veldhuizen PJ, Goodwin JW, Twardowski PW, Atkins JN, et al. Results of the Southwest Oncology Group phase II evaluation (study S0031) of ZD1839 for advanced transitional cell carcinoma of the urothelium. *BJU Int.* (2010) 105:317–21. doi: 10.1111/j.1464-410X.2009.08799.x
75. Wülfing C, Machiels J-PH, Richel DJ, Grimm M-O, Treiber U, De Groot MR, et al. A single-arm, multicenter, open-label phase 2 study of lapatinib as the second-line treatment of patients with locally advanced or metastatic transitional cell carcinoma. *Cancer.* (2009) 115:2881–90. doi: 10.1002/cncr.24337
76. Mooso BA, Vinall RL, Mudryj M, Yap SA, deVere White RW, et al. The role of EGFR family inhibitors in muscle invasive bladder cancer: a review of clinical data and molecular evidence. *J Urol.* (2015) 193:19–29. doi: 10.1016/j.juro.2014.07.121
77. Nagaya T, Okuyama S, Ogata F, Maruoka Y, Knapp DW, Karagiannis SN, et al. Near infrared photoimmunotherapy targeting bladder cancer with a canine anti-epidermal growth factor receptor (EGFR) antibody. *Oncotarget.* (2018) 9:19026–38. doi: 10.18632/oncotarget.24876
78. Jack S, Madhivanan K, Ramadesikan S, Subramanian S, Edwards DF ii, Elzey BD, et al. A novel, safe, fast and efficient treatment for Her2-positive and negative bladder cancer utilizing an EGF-anthrax toxin chimera. *Int J Cancer.* (2019) 146:449–60. doi: 10.1002/ijc.32719
79. Millanta F, Impellizeri J, McSherry L, Rocchigiani G, Aurisicchio L, Lubas G. Overexpression of HER-2 via immunohistochemistry in canine urinary bladder transitional cell carcinoma - A marker of malignancy

and possible therapeutic target. *Vet Comp Oncol.* (2018) 16:297–300. doi: 10.1111/vco.12345
80. Eriksson P, Sjödahl G, Chebil G, Liedberg F, Höglund M. HER2 and EGFR amplification and expression in urothelial carcinoma occurs in distinct biological and molecular contexts. *Oncotarget.* (2017) 8:48905–14. doi: 10.18632/oncotarget.16554
81. Cimpean AM, Tarlui V, Cumpănaş AA, Bolintineanu S, Cumpănaş A, Raica M. Critical overview of HER2 assessement in bladder cancer: what is missing for a better therapeutic approach? *Anticancer Res.* (2017) 37:4935–42. doi: 10.21873/anticanres.11903
82. Tsuboi M, Sakai K, Maeda S, Chambers JK, Yonezawa T, Matsuki N, et al. Assessment of HER2 expression in canine urothelial carcinoma of the urinary bladder. *Vet Pathol.* (2019) 56:369–76. doi: 10.1177/0300985818817024
83. Chatterjee SJ, Datar R, Youssefzadeh D, George B, Goebell PJ, Stein JP, et al. Combined effects of p53, p21, and pRb expression in the progression of bladder transitional cell carcinoma. *J Clin Oncol.* (2004) 22:1007–13. doi: 10.1200/JCO.2004.05.174
84. Suárez-Bonnet A, Herráez P, Aguirre M, Suárez-Bonnet E, Andrada M, Rodríguez F, et al. Expression of cell cycle regulators, 14-3-3σ and p53 proteins, and vimentin in canine transitional cell carcinoma of the urinary bladder. *Urol Oncol.* (2015) 33:332.e1–7. doi: 10.1016/j.urolonc.2015.04.006
85. Baumgart E, Cohen MS, Silva Neto B, Jacobs MA, Wotkowicz C, Rieger-Christ KM, et al. Identification and prognostic significance of an epithelial-mesenchymal transition expression profile in human bladder tumors. *Clin Cancer Res.* (2007) 13:1685–94. doi: 10.1158/1078-0432.CCR-06-2330
86. Kunze E, Wendt M, Schlott T. Promoter hypermethylation of the 14-3-3 sigma, SYK and CAGE-1 genes is related to the various phenotypes of urinary bladder carcinomas and associated with progression of transitional cell carcinomas. *Int J Mol Med.* (2006) 18:547–57. doi: 10.3892/ijmm.18.4.547
87. Mhawech P, Benz A, Cerato C, Greloz V, Assaly M, Desmond JC, et al. Downregulation of 14-3-3sigma in ovary, prostate and endometrial carcinomas is associated with CpG island methylation. *Mod Pathol.* (2005) 18:340–8. doi: 10.1038/modpathol.3800240
88. Ross JS, Wang K, Al-Rohil RN, Nazeer T, Sheehan CE, Otto GA, et al. Advanced urothelial carcinoma: next-generation sequencing reveals diverse genomic alterations and targets of therapy. *Mod Pathol.* (2014) 27:271–80. doi: 10.1038/modpathol.2013.135
89. Bilgrami SM, Qureshi SA, Pervez S, Abbas F. Promoter hypermethylation of tumor suppressor genes correlates with tumor grade and invasiveness in patients with urothelial bladder cancer. *Springerplus.* (2014) 3:178. doi: 10.1186/2193-1801-3-178
90. Wang X, Ji P, Zhang Y, LaComb JF, Tian X, Li E, Williams JL. Aberrant DNA methylation: implications in racial health disparity. *PLoS ONE.* (2016) 11:e0153125. doi: 10.1371/journal.pone.0153125
91. Zhi Y, Ji H, Pan J, He P, Zhou X, Zhang H, et al. Downregulated XPA promotes carcinogenesis of bladder cancer via impairment of DNA repair. *Tumour Biol.* (2017) 39:1010428317691679. doi: 10.1177/1010428317691679
92. Lee J-H, Park S-J, Kim SW, Hariharasudhan G, Jung S-M, Jun S, et al. c-Fos-dependent miR-22 targets MDC1 and regulates DNA repair in terminally differentiated cells. *Oncotarget.* (2017) 8:48204–21. doi: 10.18632/oncotarget.18389
93. Eissa S, Matboli M, Awad N, Kotb Y. Identification and validation of a novel autophagy gene expression signature for human bladder cancer patients. *Tumour Biol.* (2017) 39:1010428317698360. doi: 10.1177/1010428317698360
94. Dhawan D, Ramos-Vara JA, Hahn NM, Waddell J, Olbricht GR, Zheng R, et al. DNMT1: an emerging target in the treatment of invasive urinary bladder cancer. *Urol Oncol.* (2013) 31:1761–9. doi: 10.1016/j.urolonc.2012.03.015
95. Roskoski R. Targeting oncogenic Raf protein-serine/threonine kinases in human cancers. *Pharmacol Res.* (2018) 135:239–58. doi: 10.1016/j.phrs.2018.08.013
96. Dill AL, Ifa DR, Manicke NE, Costa AB, Ramos-Vara JA, Knapp DW, et al. Lipid profiles of canine invasive transitional cell carcinoma of the urinary bladder and adjacent normal tissue by desorption electrospray ionization imaging mass spectrometry. *Anal Chem.* (2009) 81:8758–64. doi: 10.1021/ac901028b
97. Dill AL, Eberlin LS, Costa AB, Zheng C, Ifa DR, Cheng L, et al. Multivariate statistical identification of human bladder carcinomas using ambient ionization imaging mass spectrometry. *Chemistry.* (2011) 17:2897–902. doi: 10.1002/chem.201001692
98. D'Hue CA, Dhawan D, Peat T, Ramos-Vara J, Jarmusch A, Knapp DW, et al. Fatty acid patterns detected by ambient ionization mass spectrometry in canine invasive urothelial carcinoma from dogs of different breeds. *Bladder Cancer.* (2018) 4:283–91. doi: 10.3233/BLC-170125
99. El-Achkar A, Souhami L, Kassouf W. Bladder preservation therapy: review of literature and future directions of trimodal therapy. *Curr Urol Rep.* (2018) 19:108. doi: 10.1007/s11934-018-0859-z
100. Anderson CR, McNiel EA, Gillette EL, Powers BE, LaRue SM. Late complications of pelvic irradiation in 16 dogs. *Vet Radiol Ultrasound.* (2002) 43:187–92. doi: 10.1111/j.1740-8261.2002.tb01668.x
101. Nolan MW, Kogan L, Griffin LR, Custis JT, Harmon JF, Biller BJ, et al. Intensity-modulated and image-guided radiation therapy for treatment of genitourinary carcinomas in dogs. *J Vet Intern Med.* (2012) 26:987–95. doi: 10.1111/j.1939-1676.2012.00946.x
102. Choy K, Fidel J. Tolerability and tumor response of a novel low-dose palliative radiation therapy protocol in dogs with transitional cell carcinoma of the bladder and urethra. *Vet Radiol Ultrasound.* (2016) 57:341–51. doi: 10.1111/vru.12339
103. Lei AQ, Cheng L, Pan C. Current treatment of metastatic bladder cancer and future directions. *Expert Rev Anticancer Ther.* (2011) 11:1851–62. doi: 10.1586/era.11.181
104. Ismaili N, Amzerin M, Flechon A. Chemotherapy in advanced bladder cancer: current status and future. *J Hematol Oncol.* (2011) 4:35. doi: 10.1186/1756-8722-4-35
105. Dhawan D, Craig BA, Cheng L, Snyder PW, Mohammed SI, Stewart JC, et al. Effects of short-term celecoxib treatment in patients with invasive transitional cell carcinoma of the urinary bladder. *Mol Cancer Ther.* (2010) 9:1371–7. doi: 10.1158/1535-7163.MCT-10-0049
106. Mohammed SI, Bennett PF, Craig BA, Glickman NW, Mutsaers AJ, Snyder PW, et al. Effects of the cyclooxygenase inhibitor, piroxicam, on tumor response, apoptosis, and angiogenesis in a canine model of human invasive urinary bladder cancer. *Cancer Res.* (2002) 62:356–8.
107. Knapp DW, Richardson RC, Bottoms GD, Teclaw R, Chan TC. Phase I trial of piroxicam in 62 dogs bearing naturally occurring tumors. *Cancer Chemother Pharmacol.* (1992) 29:214–8. doi: 10.1007/BF00686255
108. Knapp DW, Richardson RC, Chan TC, Bottoms GD, Widmer WR, DeNicola DB, et al. Piroxicam therapy in 34 dogs with transitional cell carcinoma of the urinary bladder. *J Vet Intern Med.* (1994) 8:273–8. doi: 10.1111/j.1939-1676.1994.tb03232.x
109. Knapp DW, Glickman NW, Widmer WR, DeNicola DB, Adams LG, Kuczek T, et al. Cisplatin versus cisplatin combined with piroxicam in a canine model of human invasive urinary bladder cancer. *Cancer Chemother Pharmacol.* (2000) 46:221–6. doi: 10.1007/s002800000147
110. Knapp DW, Ruple-Czerniak A, Ramos-Vara JA, Naughton JF, Fulkerson CM, Honkisz SI. A nonselective cyclooxygenase inhibitor enhances the activity of vinblastine in a naturally-occurring canine model of invasive urothelial carcinoma. *Bladder Cancer.* (2016) 2:241–50. doi: 10.3233/BLC-150044
111. Knapp DW, Henry CJ, Widmer WR, Tan KM, Moore GE, Ramos-Vara JA, et al. Randomized trial of cisplatin versus firocoxib versus cisplatin/firocoxib in dogs with transitional cell carcinoma of the urinary bladder. *J Vet Intern Med.* (2013) 27:126–33. doi: 10.1111/jvim.12013
112. Mohammed SI, Craig BA, Mutsaers AJ, Glickman NW, Snyder PW, deGortari AE, et al. Effects of the cyclooxygenase inhibitor, piroxicam, in combination with chemotherapy on tumor response, apoptosis, and angiogenesis in a canine model of human invasive urinary bladder cancer. *Mol Cancer Ther.* (2003) 2:183–8.
113. Zhou TC, Sankin AI, Porcelli SA, Perlin DS, Schoenberg MP, Zang X. A review of the PD-1/PD-L1 checkpoint in bladder cancer: from mediator of immune escape to target for treatment. *Urol Oncol.* (2017) 35:14–20. doi: 10.1016/j.urolonc.2016.10.004
114. Brahmer JR, Drake CG, Wollner I, Powderly JD, Picus J, Sharfman WH, et al. Phase I study of single-agent anti-programmed death-1 (MDX-1106) in refractory solid tumors: safety, clinical activity,

pharmacodynamics, and immunologic correlates. *J Clin Oncol.* (2010) 28:3167–75. doi: 10.1200/JCO.2009.26.7609
115. Balar AV, Galsky MD, Rosenberg JE, Powles T, Petrylak DP, Bellmunt J, et al. Atezolizumab as first-line treatment in cisplatin-ineligible patients with locally advanced and metastatic urothelial carcinoma: a single-arm, multicentre, phase 2 trial. *Lancet.* (2017) 389:67–76. doi: 10.1016/S0140-6736(16)32455-2
116. Sharma P, Retz M, Siefker-Radtke A, Baron A, Necchi A, Bedke J, et al. Nivolumab in metastatic urothelial carcinoma after platinum therapy (CheckMate 275): a multicentre, single-arm, phase 2 trial. *Lancet Oncol.* (2017) 18:312–22. doi: 10.1016/S1470-2045(17)30065-7
117. Inman BA, Longo TA, Ramalingam S, Harrison MR. Atezolizumab: a PD-L1-blocking antibody for bladder cancer. *Clin Cancer Res.* (2017) 23:1886–90. doi: 10.1158/1078-0432.CCR-16-1417
118. Bellmunt J, de Wit R, Vaughn DJ, Fradet Y, Lee J-L, Fong L, et al. Pembrolizumab as second-line therapy for advanced urothelial carcinoma. *N Engl J Med.* (2017) 376:1015–26. doi: 10.1056/NEJMoa1613683
119. Bellmunt J, Powles T, Vogelzang NJ. A review on the evolution of PD-1/PD-L1 immunotherapy for bladder cancer: the future is now. *Cancer Treat Rev.* (2017) 54:58–67. doi: 10.1016/j.ctrv.2017.01.007
120. Hahn AW, Gill DM, Agarwal N, Maughan BL. PD-1 checkpoint inhibition: toxicities and management. *Urol Oncol.* (2017) 35:701–7. doi: 10.1016/j.urolonc.2017.08.005
121. Dhawan D, Ramos-Vara JA, Naughton JF, Cheng L, Low PS, Rothenbuhler R, et al. Targeting folate receptors to treat invasive urinary bladder cancer. *Cancer Res.* (2013) 73:875–84. doi: 10.1158/0008-5472.CAN-12-2101
122. Szigetvari NM, Dhawan D, Ramos-Vara JA, Leamon CP, Klein PJ, Ruple AA, et al. Phase I/II clinical trial of the targeted chemotherapeutic drug, folate-tubulysin, in dogs with naturally-occurring invasive urothelial carcinoma. *Oncotarget.* (2018) 9:37042–53. doi: 10.18632/oncotarget.26455
123. Boria PA, Glickman NW, Schmidt BR, Widmer WR, Mutsaers AJ, Adams LG, et al. Carboplatin and piroxicam therapy in 31 dogs with transitional cell carcinoma of the urinary bladder. *Vet Comp Oncol.* (2005) 3:73–80. doi: 10.1111/j.1476-5810.2005.00070.x
124. Arnold EJ, Childress MO, Fourez LM, Tan KM, Stewart JC, Bonney PL, et al. Clinical trial of vinblastine in dogs with transitional cell carcinoma of the urinary bladder. *J Vet Intern Med.* (2011) 25:1385–90. doi: 10.1111/j.1939-1676.2011.00796.x
125. Blumenreich MS, Yagoda A, Natale RB, Watson RC. Phase II trial of vinblastine sulfate for metastatic urothelial tract tumors. *Cancer.* (1982) 50:435–8. doi: 10.1002/1097-0142(19820801)50:3<435::AID-CNCR2820500309>3.0.CO;2-B
126. von der Maase H, Sengelov L, Roberts JT, Ricci S, Dogliotti L, Oliver T, et al. Long-term survival results of a randomized trial comparing gemcitabine plus cisplatin, with methotrexate, vinblastine, doxorubicin, plus cisplatin in patients with bladder cancer. *J Clin Oncol.* (2005) 23:4602–8. doi: 10.1200/JCO.2005.07.757
127. de Brito Galvao JF, Kisseberth WC, Murahari S, Sutayatram S, Chew DJ, Inpanbutr N. Effects of gemcitabine and gemcitabine in combination with carboplatin on five canine transitional cell carcinoma cell lines. *Am J Vet Res.* (2012) 73:1262–72. doi: 10.2460/ajvr.73.8.1262
128. Haggag R, Farag K, Abu-Taleb F, Shamaa S, Zekri A-R, Elbolkainy T, et a. Low-dose versus standard-dose gemcitabine infusion and cisplatin for patients with advanced bladder cancer: a randomized phase II trial-an update. *Med Oncol.* (2014) 31:811. doi: 10.1007/s12032-013-0811-5
129. Abbo AH, Jones DR, Masters AR, Stewart JC, Fourez L, Knapp DW. Phase I clinical trial and pharmacokinetics of intravesical mitomycin C in dogs with localized transitional cell carcinoma of the urinary bladder. *J Vet Intern Med.* (2010) 24:1124–30. doi: 10.1111/j.1939-1676.2010.0569.x
130. Gustafson TL, Biller B. Use of toceranib phosphate in the treatment of canine bladder tumors: 37 cases. *J Am Anim Hosp Assoc.* (2019) 55:243–8. doi: 10.5326/JAAHA-MS-6905
131. Pastore A, Palleschi G, Fuschi A, Silvestri L, Al Salhi Y, Costantini E, et al. Can daily intake of aspirin and/or statins influence the behavior of non-muscle invasive bladder cancer? A retrospective study on a cohort of patients undergoing transurethral bladder resection. *BMC Cancer.* (2015) 15:120. doi: 10.1186/s12885-015-1152-x
132. Sabichi AL, Lee JJ, Grossman HB, Liu S, Richmond E, Czerniak BA, et al. A randomized controlled trial of celecoxib to prevent recurrence of nonmuscle-invasive bladder cancer. *Cancer Prev Res.* (2011) 4:1580–9. doi: 10.1158/1940-6207.CAPR-11-0036
133. Hashemi Goradel N, Najafi M, Salehi E, Farhood B, Mortezaee K. Cyclooxygenase-2 in cancer: a review. *J Cell Physiol.* (2019) 234:5683–99. doi: 10.1002/jcp.27411
134. Kurtova AV, Xiao J, Mo Q, Pazhanisamy S, Krasnow R, Lerner SP, et al. Blocking PGE2-induced tumour repopulation abrogates bladder cancer chemoresistance. *Nature.* (2015) 517:209–13. doi: 10.1038/nature14034
135. Cekanova M, Uddin MJ, Bartges JW, Callens A, Legendre AM, Rathore K, et al. Molecular imaging of cyclooxygenase-2 in canine transitional cell carcinomas *in vitro* and *in vivo*. *Cancer Prev Res.* (2013) 6:466–76. doi: 10.1158/1940-6207.CAPR-12-0358
136. Agrawal U, Kumari N, Vasudeva P, Mohanty NK, Saxena S. Overexpression of COX2 indicates poor survival in urothelial bladder cancer. *Ann Diagn Pathol.* (2018) 34:50–5. doi: 10.1016/j.anndiagpath.2018.01.008
137. Sreeramkumar V, Fresno M, Cuesta N. Prostaglandin E2 and T cells: friends or foes? *Immunol Cell Biol.* (2012) 90:579–86. doi: 10.1038/icb.2011.75
138. Obermajer N, Wong JL, Edwards RP, Odunsi K, Moysich K, Kalinski P. PGE(2)-driven induction and maintenance of cancer-associated myeloid-derived suppressor cells. *Immunol Invest.* (2012) 41:635–57. doi: 10.3109/08820139.2012.695417
139. Gabrilovich DI. Myeloid-derived suppressor cells. *Cancer Immunol Res.* (2017) 5:3–8. doi: 10.1158/2326-6066.CIR-16-0297
140. Hangai S, Ao T, Kimura Y, Matsuki K, Kawamura T, Negishi H, et al. PGE2 induced in and released by dying cells functions as an inhibitory DAMP. *Proc Natl Acad Sci USA.* (2016) 113:3844–9. doi: 10.1073/pnas.1602023113
141. Zelenay S, van der Veen AG, Böttcher JP, Snelgrove KJ, Rogers N, Acton SE, et al. Cyclooxygenase-dependent tumor growth through evasion of immunity. *Cell.* (2015) 162:1257–70. doi: 10.1016/j.cell.2015.08.015
142. Johnson DB, Frampton GM, Rioth MJ, Yusko E, Xu Y, Guo X, et al. Targeted next generation sequencing identifies markers of response to PD-1 blockade. *Cancer Immunol Res.* (2016) 4:959–67. doi: 10.1158/2326-6066.CIR-16-0143
143. Tumeh PC, Harview CL, Yearley JH, Shintaku IP, Taylor EJM, Robert L, et al. PD-1 blockade induces responses by inhibiting adaptive immune resistance. *Nature.* (2014) 515:568–71. doi: 10.1038/nature13954
144. Yarchoan M, Johnson BA, Lutz ER, Laheru DA, Jaffee EM. Targeting neoantigens to augment antitumour immunity. *Nat Rev Cancer.* (2017) 17:209–22. doi: 10.1038/nrc.2016.154
145. Topalian SL, Taube JM, Anders RA, Pardoll DM. Mechanism-driven biomarkers to guide immune checkpoint blockade in cancer therapy. *Nat Rev Cancer.* (2016) 16:275–87. doi: 10.1038/nrc.2016.36
146. Wu AA, Drake V, Huang H-S, Chiu S, Zheng L. Reprogramming the tumor microenvironment: tumor-induced immunosuppressive factors paralyze T cells. *Oncoimmunology.* (2015) 4:e1016700. doi: 10.1080/2162402X.2015.1016700
147. Pauken KE, Wherry EJ. Overcoming T cell exhaustion in infection and cancer. *Trends Immunol.* (2015) 36:265–76. doi: 10.1016/j.it.2015.02.008
148. Shosu K, Sakurai M, Inoue K, Nakagawa T, Sakai H, Morimoto M, et al. Programmed Cell Death Ligand 1 expression in canine cancer. *In Vivo.* (2016) 30:195–204.
149. Ambrosius LA, Dhawan D, Ramos-Vara JA, Ruple A, Knapp DW, Childress MO. Quantification and prognostic value of programmed cell death ligand-1 expression in dogs with diffuse large B-cell lymphoma. *Am J Vet Res.* (2018) 79:643–9. doi: 10.2460/ajvr.79.6.643
150. Filley A, Henriquez M, Bhowmik T, Tewari BN, Rao X, Wan J, et al. Imunologic and gene expression profiles of spontaneous canine oligodendrogliomas. *J Neurooncol.* (2018) 137:469–79. doi: 10.1007/s11060-018-2753-4
151. Hartley G, Elmslie R, Dow S, Guth A. Checkpoint molecule expression by B and T cell lymphomas in dogs. *Vet Comp Oncol.* (2018) 16:352–60. doi: 10.1111/vco.12386
152. Hartley G, Faulhaber E, Caldwell A, Coy J, Kurihara J, Guth A, et al. Immune regulation of canine tumour and macrophage PD-L1 expression. *Vet Comp Oncol.* (2017) 15:534–49. doi: 10.1111/vco.12197

153. Maekawa N, Konnai S, Okagawa T, Nishimori A, Ikebuchi R, Izumi Y, et al. Immunohistochemical analysis of PD-L1 expression in canine malignant cancers and PD-1 expression on lymphocytes in canine oral melanoma. *PLoS ONE.* (2016) 11:e0157176. doi: 10.1371/journal.pone.0157176
154. Tagawa M, Kurashima C, Takagi S, Maekawa N, Konnai S, Shimbo G, et al. Evaluation of costimulatory molecules in dogs with B cell high grade lymphoma. *PLoS ONE.* (2018) 13:e0201222. doi: 10.1371/journal.pone.0201222
155. Maekawa N, Konnai S, Takagi S, Kagawa Y, Okagawa T, Nishimori A, et al. A canine chimeric monoclonal antibody targeting PD-L1 and its clinical efficacy in canine oral malignant melanoma or undifferentiated sarcoma. *Sci Rep.* (2017) 7:8951. doi: 10.1038/s41598-017-09444-2
156. Nemoto Y, Shosu K, Okuda M, Noguchi S, Mizuno T. Development and characterization of monoclonal antibodies against canine PD-1 and PD-L1. *Vet Immunol Immunopathol.* (2018) 198:19–25. doi: 10.1016/j.vetimm.2018.02.007
157. Chand D, Dhawan D, Sankin A, Ren X, Lin J, Schoenberg M, et al. Immune Checkpoint B7x (B7-H4/B7S1/VTCN1) is over expressed in spontaneous canine bladder cancer: the first report and its implications in a preclinical model. *Bladder Cancer.* (2019) 5:63–71. doi: 10.3233/BLC-180204
158. Boria PA, Murry DJ, Bennett PF, Glickman NW, Snyder PW, Merkel BL, et al. Evaluation of cisplatin combined with piroxicam for the treatment of oral malignant melanoma and oral squamous cell carcinoma in dogs. *J Am Vet Med Assoc.* (2004) 224:388–94. doi: 10.2460/javma.2004.224.388
159. Choisunirachon N, Jaroensong T, Yoshida K, Saeki K, Mochizuki M, Nishimura R, et al. Effects of low-dose cyclophosphamide with piroxicam on tumour neovascularization in a canine oral malignant melanoma-xenografted mouse model. *Vet Comp Oncol.* (2015) 13:424–32. doi: 10.1111/vco.12059
160. Gershwin LJ. Current and newly emerging autoimmune diseases. *Vet Clin North Am Small Anim Pract.* (2018) 48:323–38. doi: 10.1016/j.cvsm.2017.10.010
161. Gomes-Silva D, Ramos CA. Cancer immunotherapy using CAR-T cells: from the research bench to the assembly line. *Biotechnol J.* (2018) 13. doi: 10.1002/biot.201700097
162. Panjwani MK, Smith JB, Schutsky K, Gnanandarajah J, O'Connor CM, Powell DJ, et al. Feasibility and safety of RNA-transfected CD20-specific Chimeric Antigen Receptor T Cells in dogs with spontaneous B cell lymphoma. *Mol Ther.* (2016) 24:1602–14. doi: 10.1038/mt.2016.146
163. Pfannstiel C, Strissel PL, Chiappinelli KB, Sikic D, Wach S, Wirtz RM, et al. The tumor immune microenvironment drives a prognostic relevance that correlates with bladder cancer subtypes. *Cancer Immunol Res.* (2019) 7:923–38. doi: 10.1158/2326-6066.CIR-18-0758
164. Chen DS, Mellman I. Elements of cancer immunity and the cancer-immune set point. *Nature.* (2017) 541:321–30. doi: 10.1038/nature21349
165. Hegde PS, Karanikas V, Evers S. The where, the when, and the how of immune monitoring for cancer immunotherapies in the era of checkpoint inhibition. *Clin Cancer Res.* (2016) 22:1865–74. doi: 10.1158/1078-0432.CCR-15-1507
166. Dalton MF, Stilwell JM, Krimer PM, Miller AD, Rissi DR. Clinicopathologic features, diagnosis, and characterization of the immune cell population in canine choroid plexus tumors. *Front Vet Sci.* (2019) 6:224. doi: 10.3389/fvets.2019.00224
167. Withers SS, York D, Choi JW, Woolard KD, Laufer-Amorim R, Sparger EE, et al. Metastatic immune infiltrates correlate with those of the primary tumour in canine osteosarcoma. *Vet Comp Oncol.* (2019) 17:242–52. doi: 10.1111/vco.12459
168. Porcellato I, Brachelente C, De Paolis L, Menchetti L, Silvestri S, Sforna M, et al. FoxP3 and IDO in canine melanocytic tumors. *Vet Pathol.* (2019) 56:189–99. doi: 10.1177/0300985818808530
169. Franzoni MS, Brandi A, de Oliveira Matos Prado JK, Elias F, Dalmolin F, de Faria Lainetti P, et al. Tumor-infiltrating CD4+ and CD8+ lymphocytes and macrophages are associated with prognostic factors in triple-negative canine mammary complex type carcinoma. *Res Vet Sci.* (2019)126:29–36. doi: 10.1016/j.rvsc.2019.08.021
170. Sweis RF, Spranger S, Bao R, Paner GP, Stadler WM, Steinberg G, et al. Molecular drivers of the non-T-cell-inflamed tumor microenvironment in urothelial bladder Cancer. *Cancer Immunol Res.* (2016) 4:563–8. doi: 10.1158/2326-6066.CIR-15-0274
171. Chan TA, Yarchoan M, Jaffee E, Swanton C, Quezada SA, Stenzinger A, et al. Development of tumor mutation burden as an immunotherapy biomarker: utility for the oncology clinic. *Ann Oncol.* (2019) 30:44–56. doi: 10.1093/annonc/mdy495
172. Leko V, McDuffie LA, Zheng Z, Gartner JJ, Prickett TD, Apolo AB, et al. Identification of neoantigen-reactive tumor-infiltrating lymphocytes in primary bladder cancer. *J Immunol.* (2019) 202:3458–67. doi: 10.4049/jimmunol.1801022
173. Arora S, Velichinskii R, Lesh RW, Ali U, Kubiak M, Bansal P, et al. Existing and emerging biomarkers for immune checkpoint immunotherapy in solid tumors. *Adv Ther.* (2019) 36:2638–78. doi: 10.1007/s12325-019-01051-z
174. Emgård J, Kammoun H, García-Cassani B, Chesné J, Parigi SM, Jacob J-M, et al. Oxysterol sensing through the receptor GPR183 promotes the lymphoid-tissue-inducing function of innate lymphoid cells and colonic inflammation. *Immunity.* (2018) 48:120–32.e8. doi: 10.1016/j.immuni.2017.11.020
175. Tanaka N, Katayama S, Reddy A, Nishimura K, Niwa N, Hongo H, et al. Single-cell RNA-seq analysis reveals the platinum resistance gene COX7B and the surrogate marker CD63. *Cancer Med.* (2018) 7:6193–204. doi: 10.1002/cam4.1828
176. Valle I, Tramalloni D, Bragazzi NL. Cancer prevention: state of the art and future prospects. *J Prev Med Hyg.* (2015) 56:E21–7.
177. Case RA, Hosker ME, McDonald DB, Pearson JT. Tumours of the urinary bladder in workmen engaged in the manufacture and use of certain dyestuff intermediates in the British chemical industry. Part I. The role of aniline, benzidine, alpha-naphthylamine, and beta-naphthylamine. *Br J Ind Med.* (1954) 50:389–411. doi: 10.1136/oem.50.5.389-a
178. Glickman LT, Raghavan M, Knapp DW, Bonney PL, Dawson MH. Herbicide exposure and the risk of transitional cell carcinoma of the urinary bladder in Scottish Terriers. *J Am Vet Med Assoc.* (2004) 224:1290–7. doi: 10.2460/javma.2004.224.1290
179. Raghavan M, Knapp DW, Bonney PL, Dawson MH, Glickman LT. Evaluation of the effect of dietary vegetable consumption on reducing risk of transitional cell carcinoma of the urinary bladder in Scottish Terriers. *J Am Vet Med Assoc.* (2005) 227:94–100. doi: 10.2460/javma.2005.227.94
180. Knapp DW, Peer WA, Conteh A, Diggs AR, Cooper BR, Glickman NW, et al. Detection of herbicides in the urine of pet dogs following home lawn chemical application. *Sci Total Environ.* (2013) 456–7:34–41. doi: 10.1016/j.scitotenv.2013.03.019

Conflict of Interest: NH acknowledges that he receives an Honoraria—Bladder Cancer Academy, PeerView, PlatformQ Health; that he engages in consulting activity with Bristol-Myers Squibb, AstraZeneca/MedImmune, Pieris Pharmaceuticals, Inovio Pharmaceuticals, Genentech/Roche, Health Advances, Merck, Ferring, Principia, Champions Oncology, Taris Biomedical, Seattle Genetics/Astellas, Incyte, TransMed, Rexahn Pharmaceuticals, CicloMed, Janssen, Celgene, GlaxoSmithKline, Mirati Therpeutics; and that he receives institutional support provided by Genentech/Roche, Merck, Bristol-Myers Squibb, AstraZeneca/MedImmune, Principia Biopharma, Acerta Pharma, Incyte, Seattle Genetics/Astellas, Astex Pharmaceuticals, and Pieris Pharmaceuticals. None of this support or consulting work was related to the content of this manuscript.

The remaining authors declare that the research was conducted in the absence of any commercial or financial relationships that could be construed as a potential conflict of interest.

Copyright © 2020 Knapp, Dhawan, Ramos-Vara, Ratliff, Cresswell, Utturkar, Sommer, Fulkerson and Hahn. This is an open-access article distributed under the terms of the Creative Commons Attribution License (CC BY). The use, distribution or reproduction in other forums is permitted, provided the original author(s) and the copyright owner(s) are credited and that the original publication in this journal is cited, in accordance with accepted academic practice. No use, distribution or reproduction is permitted which does not comply with these terms.

frontiers in Oncology

REVIEW
published: 24 January 2020
doi: 10.3389/fonc.2020.00023

The Genetic and Molecular Basis for Canine Models of Human Leukemia and Lymphoma

*Anne C. Avery**

Department of Microbiology, Immunology and Pathology, College of Veterinary Medicine and Biomedical Science, Colorado State University, Fort Collins, CO, United States

Emerging details of the gene expression and mutational features of canine lymphoma and leukemia demonstrate areas of similarities and differences between disease subsets in the humans and dogs. Many features of canine diffuse large B-cell lymphoma resemble the ABC form of human DLBCL, including constitutive activation of the NF-kB pathway, and almost universal presence of double expressing MYC/BCL2 lymphomas. Frequent *TRAF3* mutations and absence of BCL6 expression are differences with the human disease that need further exploration. Canine peripheral T-cell lymphoma is more common in dogs than in people and behaves in a similarly aggressive manner. Common features of canine and human PTCL include activation of the PI3 kinase pathways, loss of PTEN, and the tumor suppressor CDKN2. There is insufficient data available yet to determine if canine PTCL exhibits the GATA3-TBX21 dichotomy seen in people. Common to all forms of canine lymphoproliferative disease are breed-specific predilections for subsets of disease. This is particularly striking in PTCL, with the Boxer breed being dramatically overrepresented. Breed-specific diseases provide an opportunity for uncovering genetic and environmental risk factors that can aid early diagnosis and prevention.

Keywords: diffuse large B cell lymphoma, chronic lymphocytic leukemia, peripheral T cell lymphoma, acute myeloid leukemia, acute lymphoid leukemia, dog, canine

OPEN ACCESS

Edited by:
Mark W. Dewhirst,
Duke University, United States

Reviewed by:
Tracy Stokol,
Cornell University, United States
Matthew Breen,
North Carolina State University, United States

***Correspondence:**
Anne C. Avery
anne.avery@colostate.edu

Specialty section:
This article was submitted to Hematologic Malignancies, a section of the journal Frontiers in Oncology

Received: *15 October 2019*
Accepted: *08 January 2020*
Published: *24 January 2020*

Citation:
Avery AC (2020) The Genetic and Molecular Basis for Canine Models of Human Leukemia and Lymphoma. Front. Oncol. 10:23. doi: 10.3389/fonc.2020.00023

INTRODUCTION

Hematopoietic malignancies are a complex group of disorders that are commonly diagnosed in dogs. When faced with the diagnosis of any kind of cancer in their pet, an owner's decision to treat is based on a myriad of personal and financial factors, but lymphomas are among the most frequently diagnosed and treated types of cancer with chronic lymphocytic leukemia, acute myeloid leukemia, and acute lymphoid leukemia less commonly observed. Chemotherapy protocols, primarily CHOP-based (cyclophosphamide, doxorubricin, vincristine, prednisone), are the current standard of care for aggressive malignancies, and are standardized in the veterinary oncology community. Many dog owners are motivated to participate in clinical trials to help their pet. Thus, dogs can be a useful pre-clinical model for human hematopoietic neoplasia. Discovery of new therapies and refinement of existing ones have the potential to benefit both species. Given the enormous heterogeneity of these types of cancers, however, the utility of the dog as a model will be strengthened by identifying those diseases in each species which share common cell of origin, gene expression profile and driver mutations.

The terms "lymphoma" and "leukemia" encompass an enormous variety of cancers, derived from a broad range of lymphocytes, and myeloid cells from different stages of development, with different functions. The most recent iteration of the WHO classification system for human hematopoietic malignancies uses a combination of histology, epidemiology, immunophenotyping, chromosomal aberrations, mutational analysis, and gene expression profiling to identify different subtypes (1, 2). Discovering the normal cellular counterpart of these tumors drives understanding of the pathogenesis, development of therapies, and preventative measures.

The value of the canine model has been the subject of several recent reviews (3, 4) and generally lies in four areas: a pre-clinical model that has a shortened clinical course compared to human patients, fewer regulatory hurdles to experimental therapies and repeated sampling, the presence of a shared environment, and a degree of in-breeding which has created remarkable breed-specific patterns of disease for the discovery of genetic risk factors.

The goal of this review is to examine hematopoietic malignancies in dogs that may have a human counterpart, and discuss the clinical and molecular basis for their commonalities and differences. The data described here will suggest that, rather than representing an entire WHO subtype, canine tumors may be more similar to a discrete subset of malignancies within one sub-classification. For example, human diffuse large B cell lymphoma (DLBCL) is a heterogeneous disease with an expanding range of subtypes including GC (germinal center) and ABC (activated B cell) forms. DLBCL in dogs appears to be most similar to the ABC form, rather than covering the entire spectrum of disease as seen in people.

GENERAL APPROACH TO THE DIAGNOSIS AND TREATMENT OF CANINE HEMATOPOIETIC MALIGNANCY

A consortium of veterinary pathologists applied the WHO classification system to canine lymphoma (5) utilizing immunophenotype and histologic appearance. The comparative features of canine and human lymphoid neoplasms are the subject of a recent review (6). Diagnosis generally begins with analysis of a fine needle aspirate by a clinical pathologist. Often this can lead treatment without further characterization, but more commonly fine needle aspiration is followed by histology (± immunohistochemistry), flow cytometry, or immunocytochemistry. Histology with immunohistochemistry (IHC) can provide a WHO subtype in most cases. Flow cytometry can be used to subclassify most forms of T cell lymphoma (7, 8) but not different forms of B cell lymphoma. Clonality testing is also widely used for those cases where it is difficult to distinguish a reactive from a neoplastic process (9). Although further characterization of canine hematopoietic neoplasms using gene expression, mutational landscape, and chromosomal aberrations are active areas of investigation in many laboratories, these methods have yet to reach routine diagnostic utility. Bone marrow evaluation is often not included in the initial diagnostic workup with the exception of some cases of acute leukemia (see below).

TYPES OF CANINE LYMPHOPROLIFERATIVE DISORDERS

Although the WHO recognizes more than 60 forms of human lymphoma and leukemia, fewer lymphoma subtypes have been clearly established in the dog [reviewed in Seelig et al. (6)]. WHO subtype is assigned to a canine tumor based on histology and immunohistochemistry (IHC), or for cases of leukemia where the primary disease is in the blood/marrow, by cytologic appearance, and immunophenotyping by flow cytometry. Hodgkin's lymphoma has not been recognized in dogs. Although the frequency of acute leukemias and CLL have not been estimated in dogs, a detailed analysis of over 600 lymphomas categorized by WHO subtype (10) is shown in **Figure 1**, and this data is supported by one subsequent large study (11).

Precursor neoplasms, mature B cell tumors and mature T cell tumors are all recognized in the dog. Diffuse large B cell lymphoma (DLBCL) is the most common B cell neoplasm in both people and dogs, and peripheral T cell lymphoma the most common T cell neoplasm (10, 11). The frequency of other types differs substantially between breeds, and some tumor types are unique to each. Malignancies derived from human-specific viral infections, such as adult T cell leukemia/lymphoma and Epstein-Barr virus associated tumors do not have common counterparts in dogs. Tumors which appear to be driven by specific translocations, such as follicular lymphoma are rare in dogs, most likely because chromosomal structure differs between species, resulting in barriers to translocation (12). Treatment-associated lymphomas are also not seen in dogs. By contrast, some common canine lymphoid tumors, such as T zone lymphoma (7, 13) and CD8+ T cell leukemias (14), are seen infrequently in people.

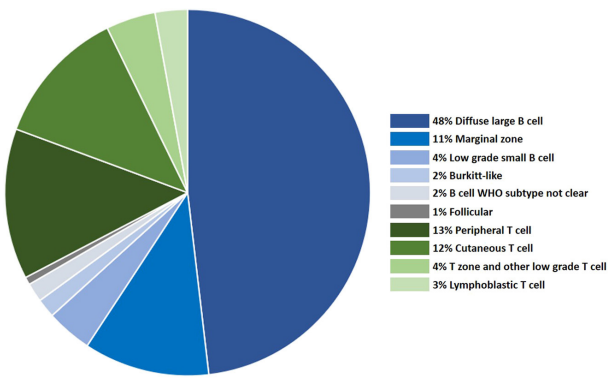

FIGURE 1 | The distribution of canine lymphoma categorized by WHO subtype, based on histology and immunophenotyping.

PRECURSOR NEOPLASMS: ACUTE LEUKEMIA

Diagnosis

Canine acute leukemias of lymphoid and myeloid lineage are identified by their clinical presentation, cytologic appearance, and immunophenotype. The diagnosis is most commonly made on peripheral blood. With the exception of rare plasma cell tumors (15) and some cases of B cell lymphoma (16), the expression of CD34 on circulating cells is considered diagnostic for acute myeloid and lymphoid leukemia, but absence of CD34 expression does not rule out the disease. Expression of TdT would be evidence of a precursor neoplasm, but antibodies recognizing canine TdT are not available. Bone marrow evaluation is not common if the diagnosis can be made using peripheral blood, but would be performed if there are peripheral cytopenias and to determine the blast count in acute myeloid leukemia.

Epidemiology

Epidemiologically, both acute myeloid leukemia (AML) and acute lymphoid leukemia (ALL) appear to be diseases of middle aged dogs; in four separate studies of provisionally diagnosed AML and ALL including over 100 dogs, the median age was reported to be between 7 and 8 years (17–19), and a male predominance was indicated in two studies (17, 19). Both Golden retrievers and German shepherds appear to be frequently affected. It is possible that this observation reflects the popularity of these breeds, but further investigation of this breed association is warranted. If these two breeds are truly predisposed, they would be useful populations for studying underlying genetic risk factors.

Lineage Determination and Outcome

Once the diagnosis of acute leukemia is established, differentiating AML from ALL is not always straightforward. A combination of morphology, expression of myeloid-lineage proteins (CD11b, CD11c, CD14) and cytochemical analysis (20, 21) is used to diagnose AML. Morphology and lack of myeloid features or antigens is generally used to diagnose ALL, with intracellular expression of CD3 and CD20/Pax5/CD79a used for further lineage assignment. A significant proportion of cases of potential ALL, however, do not express any lineage-defining antigens, and are considered unclassified.

In the author's opinion, canine acute lymphoid leukemias are almost always T cell in origin. Several pieces of evidence support this conclusion: (1) The tissue equivalent (lymphoblastic B cell lymphoma) is almost never diagnosed by histopathology, whereas lymphoblastic T cell lymphoma, while not common, has been identified in several studies (5, 10), (2) When examining copy number variation in canine ALL, recurrent losses in the T cell receptor α/δ, and T cell receptor β region were observed, consistent with T cell receptor rearrangements, but similar losses were not identified in immunoglobulin heavy or light chain regions (22), (3) Evidence for B cell lineage in reports describing B-cell ALL have relied entirely on the expression of CD79a which does not have high lineage fidelity (23, 24). Despite these observations, further proof of this hypothesis will require additional immunophenotypic and gene expression studies.

Regardless of lineage, outcomes in acute leukemia are dismal, even with aggressive chemotherapy (14, 17–19). Median survivals are reported to be 25–50 days.

Mutational Analysis

There are limited studies of the molecular features of acute leukemia and it is too early to determine if canine ALL and AML will be appropriate models for their human counterparts. Some commonalities, however, have been described. *FLT3, NPM, DNMT3A*, *RAS*, and *KIT* are among the most frequently mutated genes in human AML (25, 26) and FLT3, RAS, and KIT are potential therapeutic targets. In two studies that encompassed a total of 43 dogs with AML or ALL, a FLT3 internal tandem duplication (ITD) was found 5 cases (12%) (27, 28). Because of the difficulty in lineage assignment, it is unclear if these cases were myeloid or lymphoid. Treatment with a FLT3 inhibitor resulted in marginal decreases in the growth characteristics of a canine cell line containing the ITD and inhibition of downstream signaling pathways (28). In the same study (27), 25% of AMLs were noted to have *NRAS* missense mutations and 20% had *KIT* mutations. In a separate investigation of the DNA methylation status of AMLs, *DNMT3A* mutations were not identified (29).

Taken together the data suggest that canine acute leukemias, in particular AMLs, may share some common mutations with human AML, and with further characterization of the canine disease may provide a useful model for testing new therapies. The very poor outcomes currently seen in canine acute leukemia mean that such testing would benefit both dogs and humans, and owners would be eager to try new therapies that could promise better results.

MATURE B CELL NEOPLASMS

Diffuse Large B Cell Lymphoma

Diagnosis

Diffuse large B cell lymphoma (cDLBCL) is the most common subtype recognized in dogs and people. In dogs, the histologic diagnosis relies on recognition of a diffuse pattern with uniformly large nuclei (5). Pax5, CD79a, and CD20 (cytoplasmic) are all used to indicate B cell lineage by IHC. Immunophenotyping can also be performed by flow cytometry. Antibodies to cell surface CD19 and CD20 are not available for dogs, but anti-CD21 and anti-CD22 reliably identify B-cell lineage tumors, and intracellular staining for CD79a can also be used but is less specific. Although the lineage (B or T cell) can be determined by flow cytometry, different forms of B cell lymphomas (BCL) cannot be identified using this method.

Epidemiology

cDLBCL affects dogs over a wide range of ages, with the median age of 7–9 years (10, 30, 31). It is not clear if there is a breed-specific predilection for this disease, but several studies of histologically confirmed cDLBCL indicate Golden retrievers, Labrador retrievers, Bernese mountain dogs and

German shepherds are commonly affected breeds (10, 30, 31). Dogs are typically treated with CHOP, with overall survival times varying between studies, from 300 to 500 days (31–33). Although a number of clinical trials of anti-CD20 therapy in dogs with B cell lymphoma are in progress, to date clinically efficacious antibody therapy is not available for dogs with BCL.

Gene Expression Profiling and Mutation Status

Gene expression profiling has demonstrated that the majority of human DLBCL (hDLBCL) arise from cells within the germinal center (GC DBLCL), or from cells immediately post-germinal center differentiating toward plasma cells (activated B cell or ABC DBLCL) (34). Although histologically indistinguishable, these forms of DLBCL most likely represent molecularly distinct entities at different points along the B cell differentiation pathway, because mutations, large scale chromosomal aberrations and the pathways that drive their proliferation differ between the groups (35, 36). Notably, activation of the NF-kB/B cell receptor signaling pathways are characteristic of ABC DLBCL, but not GC DLBCL [reviewed in Young et al. (37)].

Global gene expression profiling of cDLBCL does not precisely parallel either subtype, but appears to have more in common with human ABC DLBCL. Several lines of evidence support this idea. Gene expression profiling from cDLBCL compared with normal lymph nodes shows an enrichment for genes in the B cell receptor signaling pathway (38, 39) and the NF-kB signaling pathway (38–40). These observations were corroborated by biochemical studies demonstrating that 24/24 dogs with cDLBCL exhibited constitutive activation of the canonical NF-kB pathway (the non-canonical pathway was not investigated in this study) (41, 42). The expression of downstream anti-apoptotic genes (*BCL2*, *c-FLIP,* and *XIAP*) was increased in the majority of these cases. Inhibition of the upstream IKK complex using a NEMO binding domain peptide inhibited phosphorylation of IkB and increased apoptosis *in vitro* (41), and showed some degree of efficacy in these same assays when administered intra-nodally or intravenously (41, 42).

To some extent, analysis of mutations harbored by cDLBCL also point to activation of the NF-kB pathway, but with some confounding observations. Three studies have investigated mutational features of canine BCL—either specifically subtyped cDLBCL, or pooled cases of BCL which were most likely dominated by cDLBCL. Together they included 129 total dogs (43–45). Notably, 20–30% of these lymphomas had inhibitory mutations in *TRAF3*. TRAF3 is a negative regulator of the non-canonical NF-kB signaling pathway, and when inactivated leads to constitutive processing of p100 to p52 for translocation into the nucleus with its partner, RelB (46, 47). In contrast to signals through the B cell receptor and toll like receptors (through MyD88), the non-canonical NF-kB pathway is activated in response to differentiation signals such as those transmitted through CD40 and BAFF. Although *TRAF3* mutations in hDLBCL were rare (36) or not found at all (43) in both studies a subset of hDLBCL, 9% of cases exhibited chromosomal loss in the region containing *TRAF3*, a finding further supported by Green et al. (48). ABC DLBCL had the most frequent losses (36).

Other mutations that promote constitutive NF-kB activation associated with the canonical NF-kB pathway were found in cDLBCL at low levels in only one study: *TNFAIP3* (14% of 14 cases) and CD79b (7% of 14 cases) (43). Thus the overall implication of the available mutational analyses is consistent with the idea that the NF-kB pathway is important to cDLBCL.

Further support for the idea that cDLBCL more closely resembles the ABC form is the observation that virtually all cDLBCL are "double expressers"—a very high proportion of cells in canine DLBCL express both MYC and BCL2 (49), a feature which is associated with significantly poorer outcomes in people, and more frequently seen in ABC DLBCL (although can be present in all forms) (50). A parallel finding is the enrichment for genes in the MYC pathway in cDLBCL (39). High expression of MYC and BCL2 in some human cases is the result of translocations which free the genes from transcriptional constraints, but not all cases with high levels of protein expression have the translocation. *MYC-IGH* translocations have been observed in the dog, but only in Burkitt's lymphoma (51). Dog cancers of all types, including lymphomas, frequently have gain of part or all of chromosome 13, which carries *MYC* and *KIT* (52, 53). This may be the most common reason for the high level of *MYC* expression.

Differences Between Canine and Human DLBCL

Despite the accumulating data on similarities between cDLBCL and human ABC DLBCL, there are some significant differences that need to be clarified in order to fully exploit the dog as a pre-clinical model. Perhaps most importantly, cDLBCL appears to almost never express the BCL6 protein (1 positive case of 59 total tested) (38, 54). BCL6 is readily detectable in germinal centers of normal canine B cells by IHC (54). BCL6 is a transcriptional repressor that is key to the germinal center reaction. One of its major roles is to inhibit terminal differentiation of B cells to plasma cells or memory cells, thereby maintaining cells within the germinal center cycling between light and dark zones to undergo proliferation, somatic hypermutation and selection. *BCL6* is downregulated when cells exit the germinal center.

While ABC DLBCL are more frequently BCL6 negative than GC DLBCL (55), the lack of any evidence of BCL6 expression in dogs is unusual. Furthermore, while upregulation of IRF4 (Mum1) is a feature of post-germinal center B cells that have down-regulated BCL6, and seen more frequently in ABC DLBCL (34), IRF4 does not appear to be expressed in most cDLBCL when assessed using IHC (38).

Overall, the evidence suggests that cDCBCL is dissimilar to GC DCLBL. In addition to the data described above, mutation analysis did not identify genes that are commonly found in GC DLBCL such as *KMT2D, MYD88*, *CARD11*, *EZH2*, and *CREBBP* (36, 56, 57). Given that the ABC subtype of DLBCL is most closely associated with activation of the NF-kB pathway, the combined findings of mutation analysis, gene expression profiling and IHC suggest that canine DLBCL is more similar to the ABC form that GC form.

Immunoglobulin Heavy Chain Gene Mutation Status

B cells that have been through the germinal center have hypermutated immunoglobulin variable region genes (IGHV) as a result of affinity maturation and selection and presence of hypermutated IGHV genes indicates a B cell has (in most cases) traveled through the germinal center. To determine mutation status in B cell neoplasms, IGHV gene sequences from the tumor are compared to unmutated sequences—the latter data taken from compiled germline sequences from a large number of individuals (http://www.imgt.org). In people, IGHV genes are considered to have undergone hypermutation if there is <98% sequence similarity compared to germline counterpart (58). The analysis of IGHV mutation status in dogs is complicated by the fact that there is only one germline sequence available for each of the 80+ IGHV genes. This allele is from the Boxer originally sequenced for the canine genome (59). Because only one allele for each V gene has been sequenced, the degree of allelic variation in IGHV gene is unknown in the dog. When comparing the sequence of a neoplastic IGHV to the available germline, differences may be due to either hypermutation or due to allelic variation.

With this caveat in mind, IGHV genes in 52/52 cases of canine B cell lymphoma from various breeds (29 definitively established to be cDLBCL) had >98% identity with their germline counterpart from the Boxer (60), indicating, as expected, that they were derived from germinal center or post germinal center B cells. A separate study, which examined only Boxer large cell B cell lymphomas (not further classified by histology) found that only 64% exhibited hypermutation (61). Thus, while it is likely that most cDLBCL have evidence of being derived from germinal center B cells based on IGHV mutation status, a precise enumeration IGHV mutation status in canine B cell lymphoma will depend on a larger database of IGHV alleles.

Summary

Although much work needs to be done, the available evidence suggests that cDLBCL is most similar to ABC DLBCL. Gene expression, biochemical data and mutation analysis point to a role for the NF-kB signaling pathway, which is central to ABC DLBCL. Co-expression of high levels of BCL2 and MYC is seen in virtually all cDLBCL, a feature more common to the ABC subtype. cDLBCL has some unique characteristics as well, including the possibility that the non-canonical NF-kB pathway may be prevalent in some cases, and the observation that BCL6 is not expressed. As noted for acute leukemias and T cell lymphoma, it is likely that cDLBCL will be analogous to discreet subsets of hDLBLC, rather than reflecting the entire range of subtypes in this diverse disease.

Other Mature B Cell Neoplasms

Follicular lymphoma and mantle cell lymphoma have been described in dogs, but are uncommon, and little information beyond descriptive data is available. Some information is available for two more common B cell tumors, marginal zone and B-cell CLL.

Marginal Zone Lymphoma

Canine marginal zone lymphoma (MZL) is defined by a nodular pattern and intermediate-sized cells with a central nucleolus. This disease can be found in both the spleen and lymph nodes. While originally considered to be a single disease, studies have shown that while splenic marginal zone lymphoma has good long-term survival with splenectomy alone (62), nodal marginal zone lymphoma is as aggressive as cDLBCL (63). In later stages of the disease, pathologists can have difficulty distinguishing DLBCL from NMZL, often referring to NMZL as "late NMZL" to reflect the fact that the tumor contains marginal zone-like cells, but the characteristic nodular pattern is lost (38). Molecular characterization of this disease is lacking, other than the observation that gene expression profiling was unable to distinguish histologically diagnosed cDLBCL from nodal marginal zone lymphoma in three separate analyses (38, 64, 65).

B Cell CLL

B cell chronic lymphocytic leukemia (B-CLL) in dogs is diagnosed by expansion of small, mature-appearing B cells in the blood, and an indolent clinical course (14). Unlike the human disease, canine B-CLL cells do not express CD5. It is seen primarily in small breed, older dogs (66). Strikingly, despite the prevalence of large breed dogs such as German shepherds and Golden retrievers in the population of cDLBLC, these breeds virtually never develop B-CLL (66). Small breed dogs tend to have longer lifespans than large breeds, but this not the entire reason for the observation. Golden retrievers are the most common breed to develop indolent T zone lymphoma, which is also a disease of older dogs (median age at presentation 10 years for both diseases) (67). Thus, the intriguing breed-specific resistance to B-CLL most likely has a more complex explanation than age.

No comprehensive gene expression or mutational analysis has been performed for canine B-CLL, but analysis of copy number variation highlighted a region of shared aberration with the human disease (22). Twelve percent of canine B-CLL cases exhibited loss of a chromosomal region encoding miR-15a/miR16-1—loss of this region is present in approximately 55% of human patients [reviewed in Spina et al. (68)]. These microRNAs are thought to control expression of *BCL2*, and loss of expression results in *BCL2* upregulation. A variety of other shared regions of gain and loss between human and canine B-CLL were observed, but all await further confirmation by gene expression and functional studies.

One of the most important prognostic factors in human B-CLL is the mutation status of the IGVH gene (69). Patients with unmutated IGHV genes tend to have more aggressive disease. We have started to explore the role of IGHV mutation status in canine B-CLL, and found that the majority of cases exhibit IGHV mutation, with one exception. B-CLL in the Boxer breed carry unmutated IGHV genes (61), but mutation status and outcome has not yet been linked in individual dogs. Nonetheless, with further confirmation and gene expression studies, which are currently underway, the Boxer breed may be a useful model for aggressive B-CLL.

MATURE T CELL NEOPLASMS

Peripheral T Cell Lymphoma

The frequency of peripheral T cell lymphoma in dogs, and early indications of genetic similarities with the human disease, perhaps offers the most fruitful avenue for comparative investigation between the two species. The two most frequent forms of nodal T cell lymphoma in dogs are peripheral T cell lymphoma not otherwise specified (PTCL-NOS) and T zone lymphoma. The latter is classified as a very rare form of human PTCL in the WHO system, but it is discussed separately from PTCL in veterinary medicine because it is common, and clearly distinct from the other types—dogs are older, the disease is indolent and often not treated, and the defining feature of T zone lymphoma is loss of CD45 expression (7, 70), which is not seen in other canine lymphomas. Anaplastic large cell lymphoma (71) and angioimmunoblastic T cell lymphoma (AITL) are diagnosed rarely if at all in dogs (5).

Epidemiology

Canine PTCL-NOS (cPTCL) is most common in the Boxer breed. This breed-specific predilection is striking and has been noted in numerous studies in both the U.S. and Europe (10, 72–74). cPTCL affects middle age dogs (median 7 years) and has a slight male predominance (8, 72). Mediastinal involvement is seen in approximately half of cPTCL cases, and half of all cases are hypercalcemic (these features overlap but also exist independently). Peripheral blood involvement, including the presence of circulating cells and peripheral cytopenias, is very rare. Median survival is approximately 158 days with CHOP or modified CHOP chemotherapy (72, 75, 76).

Diagnosis

A study of 73 cases of nodal cPTCL with paired histology and immunophenotyping by flow cytometry demonstrated that cPTCL can be reliably diagnosed by flow cytometry alone (8). cPTCL most commonly expresses CD4, high levels of CD3, low levels of class II MHC and often exhibits loss of CD5 expression, similar to hPTCL. A smaller number of cases express CD8, neither CD4 nor CD8, or both antigens. The cells do not express CD34, and gene expression profiling on a limited number of cases did not identify upregulated *TdT* expression compared to normal CD4 T cells (8). These findings support the classification of these tumors as mature T cell lymphomas, rather than precursor neoplasms despite the frequent mediastinal involvement.

Gene Expression Profiling and Mutation Status

Human PTCL-NOS (hPTCL) has been divided by gene expression profiling into two main subtypes—those which are characterized by upregulation of the transcription factor GATA3 and the downstream pathways it controls, and those characterized by upregulation of the transcription factor TBX21 (T-bet), and downstream pathways (77, 78). GATA3 and TBX21 are drivers of Th2 and Th1 helper T cell differentiation, respectively, and the GATA3 subtype is associated with reduced survival. There is some evidence that GATA3-dominant hPTCL affect the tumor microenvironment by driving macrophages toward an alternative, suppressive phenotype (79) which may contribute to poor outcomes.

Gene expression profiling by RNA seq (8), mutational analysis (44, 80), and copy number variation (52, 53) have been described in separate studies of canine T cell lymphoma. There is insufficient gene expression data currently available to determine the extent of heterogeneity of cPTCL, and if this disease can be subdivided into GATA3 and TBX21 associated tumors. However, gene expression studies did provide some information about possible relevant pathways. In an RNA seq study of 6 cPTCL, increased expression of the *MTOR* gene and decreased expression of *PTEN* was observed in all 6 cases when compared with purified normal CD4 T cells (8). Gene set enrichment analysis confirmed the transcriptional programs associated with upregulation of *MTOR* and down-regulation of *PTEN* were consistent with this observation. PTEN is an inhibitor of the phosphatidylinositol 3-kinase (PI3K) pathway, and release of inhibition results in downstream activation of a variety of cell survival pathways (81). In hPTCL, dysregulation of this pathway is seen in PTCL-GATA3 (78) and a clinical trial using a PI3K inhibitor showed some degree of efficacy in hPTCL (82).

Gene expression data is supported to some extent by mutational analysis. Elvers et al. described exome sequencing from 41 cases of canine T cell lymphoma (44). Samples were derived from two breeds, Boxers and Golden retrievers, which exhibited a different array of mutations. These tumors were not subtyped by histology, but the high frequency of T zone lymphoma in Goldens, and the high frequency of PTCL in Boxers suggests the histologic subtypes were probably quite different in these two groups. When focusing on the likely cPTCL mutations (Boxer breed, 16 dogs), this study found that 25% of cases had *PTEN* mutations, consistent with the gene expression data. Targeted sequencing of cancer genes similarly identified *PTEN* mutation in a subset of T cell lymphomas (80).

Another observation from both exome sequencing and analysis of variants in RNA seq data is that 16–25% of canine PTCL have a functional mutation in the SATB1 gene (8, 44). SATB1 is a transcriptional repressor that is predominately found in thymocytes and plays a key role in T-cell development (83). It has variable effects when dysregulated in human cutaneous T cell lymphomas and anaplastic T cell lymphomas (84). It is possible that a subset of cPTCL (particularly those with mediastinal involvement) are derived from a mature, naïve T cell precursor, and *SATB1* mutation may be functionally relevant to this group of tumors.

cPTCL have more extensive chromosomal aberrations than canine B cell lymphomas (53). In addition to frequent gains of chromosomes 13 (containing the *MYC* gene) and 31 (also noted for B cell lymphomas), cPTCL exhibited frequent losses of chromosomes 11, 17, 22, 28, and 38. The CDKN2 gene (p16) is found on canine chromosome 11, and loss of CDKN2 was further validated in a follow up study (85) which found that CDKN2 loss was specific to PTCL and not seen in low grade T cell lymphomas or B cell lymphomas. This finding is particularly notable because CDKN2 is a tumor suppressor: loss of expression was noted in 45% of human PTCL-GATA3 tumors (78) and was associated with a poorer prognosis.

Characterization of canine PTCL is clearly in its early stages. Important questions to be answered included the nature of the driver mutations and the identification of the cell of origin of discreet subsets of disease. As with cDLBCL, dogs may not represent the entire spectrum of human PTCL, but could be used to focus attention on particular subsets of the disease.

EXPLOITING BREED-SPECIFIC DISEASES FOR PREVENTION AND DISEASE PREDICTION

Several instances of breed-specific patterns of disease are noted above. Such observations mean that genetic and environmental risk factors for cancer may be identified in smaller prospective studies, taking less time, than would be necessary in people. The leading cause of death in Golden retrievers is hematopoietic malignancy (86), and in 2012 a prospective study of >3,000 Goldens, enrolled at age 2 or younger, was undertaken (87). The goal of this study was to collect environmental and biological data for correlation with the future diagnoses of malignancy and other diseases. Sadly, in this group of dogs, the oldest of which is 7, 42 cases of lymphoma have already been identified (1.3%) (Diehl, K. personal communication). It will be several years before the prospective data can be compiled to examine risk factors, but this study is an example of how the dog may not only be used to investigate treatments, but to identify possible interventions before cancer gains a foothold.

FUTURE DIRECTIONS

The short-term goals that will allow the dog to be deployed as a pre-clinical model for human hematopoietic malignancy include a comprehensive analysis of gene expression, mutational landscape and epigenetic features for each subtype of disease. These goals are readily achievable with the tools currently available to researchers, with some caveats—the canine genome is less well-annotated than the human genome, and a full catalog of population level polymorphisms is still being developed. A greater challenge will be creating more focused diagnostics (small gene expression panels, better antibody-based classification using IHC or flow cytometry) for routine clinical use. The availability of such focused diagnostics will be essential for taking full advantage of the canine model for investigating new therapies, allowing for rapid classification of cases and enrollment in drug trials. An additional benefit of more precise classification of canine hematopoietic malignancies will be the identification of even more breed-specific tendencies allowing for discovery of additional genetic risk factors. While the specific risk genes are unlikely to be identical between species, the pathways or processes affected may be similar. Evaluation of genetic and environmental risk factors, coupled with the ability to test new therapies, can make the dog a comprehensive large animal model for one of the most important cancers affecting both species.

AUTHOR CONTRIBUTIONS

AA designed and wrote the review.

REFERENCES

1. Arber DA, Orazi A, Hasserjian R, Thiele J, Borowitz MJ, Le Beau MM, et al. The 2016 revision to the World Health Organization classification of myeloid neoplasms and acute leukemia. *Blood.* (2016) 127:2391–405. doi: 10.1182/blood-2016-03-643544
2. Swerdlow SH, Campo E, Pileri SA, Harris NL, Stein H, Siebert R, et al. The 2016 revision of the World Health Organization classification of lymphoid neoplasms. *Blood.* (2016) 127:2375–90. doi: 10.1182/blood-2016-01-643569
3. Richards KL, Suter SE. Man's best friend: what can pet dogs teach us about non-Hodgkin's lymphoma? *Immunol Rev.* (2015) 263:173–91. doi: 10.1111/imr.12238
4. Villarnovo D, McCleary-Wheeler A, Richards KL. Barking up the right tree: advancing our understanding and treatment of lymphoma with a spontaneous canine model. *Curr Opin Hematol.* (2017) 24:359–66. doi: 10.1097/MOH.0000000000000357
5. Valli VE, San Myint M, Barthel A, Bienzle D, Caswell J, Colbatzky F, et al. Classification of canine malignant lymphomas according to the World Health Organization criteria. *Vet Pathol.* (2011) 48:198–211. doi: 10.1177/0300985810379428
6. Seelig DM, Avery AC, Ehrhart E, Linden MA. The comparative diagnostic features of canine and human lymphoma. *Vet Sci.* (2016) 3:11. doi: 10.3390/vetsci3020011
7. Seelig DM, Avery P, Webb T, Yoshimoto J, Bromberek J, Ehrhart EJ, et al. Canine T-zone lymphoma: unique immunophenotypic features, outcome, and population characteristics. *J Vet Intern Med.* (2014) 28:878–86. doi: 10.1111/jvim.12343
8. Harris LJ, Hughes KL, Ehrhart EJ, Labadie JD, Yoshimoto J, Avery AC. Canine CD4+ T-cell lymphoma identified by flow cytometry exhibits a consistent histomorphology and gene expression profile. *Vet Comp Oncol.* (2019) 17:253–64. doi: 10.1111/vco.12460
9. Keller SM, Vernau W, Moore PF. Clonality testing in veterinary medicine: a review with diagnostic guidelines. *Vet Pathol.* (2016) 53:711–25. doi: 10.1177/0300985815626576
10. Ponce F, Marchal T, Magnol JP, Turinelli V, Ledieu D, Bonnefont C, et al. A morphological study of 608 cases of canine malignant lymphoma in France with a focus on comparative similarities between canine and human lymphoma morphology. *Vet Pathol.* (2010) 47:414–33. doi: 10.1177/0300985810363902
11. Valli VE, Kass PH, San Myint M, Scott F. Canine lymphomas: association of classification type, disease stage, tumor subtype, mitotic rate, and treatment with survival. *Vet Pathol.* (2013) 50:738–48. doi: 10.1177/0300985813478210
12. Thomas R, Demeter Z, Kennedy KA, Borst L, Singh K, Valli VE, et al. Integrated immunohistochemical and DNA copy number profiling analysis provides insight into the molecular pathogenesis of canine follicular lymphoma. *Vet Comp Oncol.* (2017) 15:852–67. doi: 10.1111/vco.12227
13. Flood-Knapik KE, Durham AC, Gregor TP, Sanchez MD, Durney M, Sorenmo KU. Clinical, histopathological and immunohistochemical characterization of canine indolent lymphoma. *Vet Comp Oncol.* (2013) 11:272–86. doi: 10.1111/j.1476-5829.2011.00317.x
14. Williams MJ, Avery AC, Lana SE, Hillers KR, Bachand A, Avery PR. Canine lymphoproliferative disease characterized by lymphocytosis: immunophenotypic markers of prognosis. *J Vet Intern Med.* (2008) 22:596–601. doi: 10.1111/j.1939-1676.2008.0041.x
15. Rout ED, Shank AM, Waite AH, Siegel A, Avery A, Avery PR. Progression of cutaneous plasmacytoma to plasma cell leukemia in a dog. *Vet Clin Pathol.* (2017) 46:77–84. doi: 10.1111/vcp.12463
16. Rao S, Lana S, Eickhoff J, Marcus E, Avery PR, Morley PS, et al. Class II major histocompatibility complex expression and cell size independently predict survival in canine B-cell lymphoma. *J Vet Intern Med.* (2011) 25:1097–105. doi: 10.1111/j.1939-1676.2011.0767.x

17. Novacco M, Comazzi S, Marconato L, Cozzi M, Stefanello D, Aresu L, et al. Prognostic factors in canine acute leukaemias: a retrospective study. *Vet Comp Oncol.* (2015) 14:409–16. doi: 10.1111/vco.12136
18. Bennett AL, Williams LE, Ferguson MW, Hauck ML, Suter SE, Lanier CB, et al. Canine acute leukaemia: 50 cases. (1989-2014). *Vet Comp Oncol.* (2017) 15:1101–14. doi: 10.1111/vco.12251
19. Davis LL, Hume K, Stokol T. A retrospective review of acute myeloid leukaemia in 35 dogs diagnosed by a combination of morphologic findings, flow cytometric immunophenotyping and cytochemical staining results (2007-2015). *Vet Comp Oncol.* (2018) 16:268–75. doi: 10.1111/vco.12377
20. Stokol T, Schaefer DM, Shuman M, Belcher N, Dong L. Alkaline phosphatase is a useful cytochemical marker for the diagnosis of acute myelomonocytic and monocytic leukemia in the dog. *Vet Clin Pathol.* (2015) 44:79–93. doi: 10.1111/vcp.12227
21. Stokol T, Nickerson GA, Shuman M, Belcher N. Dogs with acute myeloid leukemia have clonal rearrangements in T and B cell receptors. *Front Vet Sci.* (2017) 4:76. doi: 10.3389/fvets.2017.00076
22. Roode SC, Rotroff D, Avery AC, Suter SE, Bienzle D, Schiffman JD, et al. Genome-wide assessment of recurrent genomic imbalances in canine leukemia identifies evolutionarily conserved regions for subtype differentiation. *Chromosome Res.* (2015) 23:681–708. doi: 10.1007/s10577-015-9475-7
23. Lai R, Juco J, Lee SF, Nahirniak S, Etches WS. Flow cytometric detection of CD79a expression in T-cell acute lymphoblastic leukemias. *Am J Clin Pathol.* (2000) 113:823–30. doi: 10.1309/391R-93YF-DB4D-1L35
24. Kozlov I, Beason K, Yu C, Hughson M. CD79a expression in acute myeloid leukemia t(8;21) and the importance of cytogenetics in the diagnosis of leukemias with immunophenotypic ambiguity. *Cancer Genet Cytogenet.* (2005) 163:62–7. doi: 10.1016/j.cancergencyto.2005.06.002
25. Papaemmanuil E, Gerstung M, Bullinger L, Gaidzik VI, Paschka P, Roberts ND, et al. Genomic classification and prognosis in acute myeloid leukemia. *N Engl J Med.* (2016) 374:2209–21. doi: 10.1056/NEJMoa1516192
26. Medinger M, Passweg JR. Acute myeloid leukaemia genomics. *Br J Haematol.* (2017) 179:530–42. doi: 10.1111/bjh.14823
27. Usher SG, Radford AD, Villiers E, Blackwood L. RAS, FLT3, and C-KIT mutations in immunophenotyped canine leukemias. *Exp Hematol.* (2009) 37:65–77. doi: 10.1016/j.exphem.2008.09.005
28. Suter SE, Small GW, Seiser EL, Thomas R, Breen M, Richards KL. FLT3 mutations in canine acute lymphocytic leukemia. *BMC Cancer.* (2011) 11:38. doi: 10.1186/1471-2407-11-38
29. Bronzini I, Aresu L, Paganin M, Marchioretto L, Comazzi S, Cian F, et al. DNA methylation and targeted sequencing of methyltransferases family genes in canine acute myeloid leukaemia, modelling human myeloid leukaemia. *Vet Comp Oncol.* (2017) 15:910–8. doi: 10.1111/vco.12231
30. Martini V, Aresu L, Riondato F, Marconato L, Cozzi M, Stefanello D, et al. Prognostic role of non-neoplastic lymphocytes in lymph node aspirates from dogs with diffuse large B-cell lymphoma treated with chemo-immunotherapy. *Res Vet Sci.* (2019) 125:130–5. doi: 10.1016/j.rvsc.2019.06.003
31. Wolf-Ringwall A, Lopez L, Elmslie R, Fowler B, Lori J, Sfiligoi G, et al. Prospective evaluation of flow cytometric characteristics, histopathologic diagnosis and clinical outcome in dogs with naive B-cell lymphoma treated with a 19-week CHOP protocol. *Vet Comp Oncol.* (2019) doi: 10.1111/vco.12553. [Epub ahead of print].
32. Ponce F, Magnol JP, Ledieu D, Marchal T, Turinelli V, Chalvet-Monfray K, et al. Prognostic significance of morphological subtypes in canine malignant lymphomas during chemotherapy. *Vet J.* (2004) 167:158–66. doi: 10.1016/j.tvjl.2003.10.009
33. Marconato L, Aresu L, Stefanello D, Comazzi S, Martini V, Ferrari R, et al. Opportunities and challenges of active immunotherapy in dogs with B-cell lymphoma: a 5-year experience in two veterinary oncology centers. *J Immunother Cancer.* (2019) 7:146. doi: 10.1186/s40425-019-0624-y
34. Alizadeh AA, Eisen MB, Davis RE, Ma C, Lossos IS, Rosenwald A, et al. Distinct types of diffuse large B-cell lymphoma identified by gene expression profiling. *Nature.* (2000) 403:503–11. doi: 10.1038/35000501
35. Lenz G, Wright GW, Emre NC, Kohlhammer H, Dave SS, Davis RE, et al. Molecular subtypes of diffuse large B-cell lymphoma arise by distinct genetic pathways. *Proc Natl Acad Sci USA.* (2008) 105:13520–5. doi: 10.1073/pnas.0804295105
36. Schmitz R, Wright GW, Huang DW, Johnson CA, Phelan JD, Wang JQ, et al. Genetics and pathogenesis of diffuse large B-cell lymphoma. *N Engl J Med.* (2018) 378:1396–407. doi: 10.1056/NEJMoa1801445
37. Young RM, Phelan JD, Wilson W, Staudt LM. Pathogenic B-cell receptor signaling in lymphoid malignancies: new insights to improve treatment. *Immunol Rev.* (2019) 291:190–213. doi: 10.1111/imr.12792
38. Richards KL, Motsinger-Reif AA, Chen HW, Fedoriw Y, Fan C, Nielsen DM, et al. Gene profiling of canine B-cell lymphoma reveals germinal center and postgerminal center subtypes with different survival times, modeling human DLBCL. *Cancer Res.* (2013) 73:5029–39. doi: 10.1158/0008-5472.CAN-12-3546
39. Aresu L, Ferraresso S, Marconato L, Cascione L, Napoli S, Gaudio E, et al. New molecular and therapeutic insights into canine diffuse large B-cell lymphoma elucidates the role of the dog as a model for human disease. *Haematologica.* (2019) 104:e256–9. doi: 10.3324/haematol.2018.207027
40. Mudaliar MA, Haggart RD, Miele G, Sellar G, Tan KA, Goodlad JR, et al. Comparative gene expression profiling identifies common molecular signatures of NF-kappaB activation in canine and human diffuse large B cell lymphoma (DLBCL). *PLoS ONE.* (2013) 8:e72591. doi: 10.1371/journal.pone.0072591
41. Gaurnier-Hausser A, Patel R, Baldwin AS, May M, Mason NJ. NEMO-binding domain peptide inhibits constitutive NF-kappaB activity and reduces tumor burden in a canine model of relapsed, refractory diffuse large B-cell lymphoma. *Clin Cancer Res.* (2011) 17:4661–71. doi: 10.1158/1078-0432.CCR-10-3310
42. Habineza Ndikuyeze G, Gaurnier-Hausser A, Patel R, Baldwin AS, May MJ, Flood P, et al. A phase I clinical trial of systemically delivered NEMO binding domain peptide in dogs with spontaneous activated B-cell like diffuse large B-cell lymphoma. *PLoS ONE.* (2014) 9:e95404. doi: 10.1371/journal.pone.0095404
43. Bushell KR, Kim Y, Chan FC, Ben-Neriah S, Jenks A, Alcaide M, et al. Genetic inactivation of TRAF3 in canine and human B-cell lymphoma. *Blood.* (2015) 125:999–1005. doi: 10.1182/blood-2014-10-602714
44. Elvers I, Turner-Maier J, Swofford R, Koltookian M, Johnson J, Stewart C, et al. Exome sequencing of lymphomas from three dog breeds reveals somatic mutation patterns reflecting genetic background. *Genome Res.* (2015) 25:1634–45. doi: 10.1101/gr.194449.115
45. Giannuzzi D, Marconato L, Cascione L, Comazzi S, Elgendy R, Pegolo S, et al. Mutational landscape of canine B-cell lymphoma profiled at single nucleotide resolution by RNA-seq. *PLoS ONE.* (2019) 14:e0215154. doi: 10.1371/journal.pone.0215154
46. Shih VF, Tsui R, Caldwell A, Hoffmann, A. A single NFkappaB system for both canonical and non-canonical signaling. *Cell Res.* (2011) 21:86–102. doi: 10.1038/cr.2010.161
47. Tegowski M, Baldwin A. Noncanonical NF-kappaB in Cancer. *Biomedicines.* (2018) 6:E66. doi: 10.3390/biomedicines6020066
48. Green MR, Vicente-Duenas C, Romero-Camarero I, Long Liu C, Dai B, Gonzalez-Herrero I, et al. Transient expression of Bcl6 is sufficient for oncogenic function and induction of mature B-cell lymphoma. *Nat Commun.* (2014) 5:3904. doi: 10.1038/ncomms4904
49. Curran KM, Schaffer PA, Frank CB, Lana SE, Hamil LE, Burton JH, et al. BCL2 and MYC are expressed at high levels in canine diffuse large B-cell lymphoma but are not predictive for outcome in dogs treated with CHOP chemotherapy. *Vet Comp Oncol.* (2016) 15:1269–79. doi: 10.1111/vco.12263
50. Rosenthal A, Younes A. High grade B-cell lymphoma with rearrangements of MYC and BCL2 and/or BCL6: double hit and triple hit lymphomas and double expressing lymphoma. *Blood Rev.* (2017) 31:37–42. doi: 10.1016/j.blre.2016.09.004
51. Breen M, Modiano JF. Evolutionarily conserved cytogenetic changes in hematological malignancies of dogs and humans–man and his best friend share more than companionship. *Chromosome Res.* (2008) 16:145–54. doi: 10.1007/s10577-007-1212-4
52. Thomas R, Smith KC, Ostrander EA, Galibert F, Breen M. Chromosome aberrations in canine multicentric lymphomas detected with comparative genomic hybridisation and a panel of single locus probes. *Br J Cancer.* (2003) 89:1530–7. doi: 10.1038/sj.bjc.6601275
53. Thomas R, Seiser EL, Motsinger-Reif A, Borst L, Valli VE, Kelley K, et al. Refining tumor-associated aneuploidy through

'genomic recoding' of recurrent DNA copy number aberrations in 150 canine non-Hodgkin lymphomas. *Leuk Lymphoma.* (2011) 52:1321–35. doi: 10.3109/10428194.2011.559802
54. Sato M, Kanemoto H, Kagawa Y, Kobayashi T, Goto-Koshino Y, Mochizuki H, et al. Evaluation of the prognostic significance of BCL6 gene expression in canine high-grade B-cell lymphoma. *Vet J.* (2012) 191:108–14. doi: 10.1016/j.tvjl.2010.12.006
55. Iqbal J, Greiner TC, Patel K, Dave BJ, Smith L, Ji J, et al. Distinctive patterns of BCL6 molecular alterations and their functional consequences in different subgroups of diffuse large B-cell lymphoma. *Leukemia.* (2007) 21:2332–43. doi: 10.1038/sj.leu.2404856
56. Lohr JG, Stojanov P, Lawrence MS, Auclair D, Chapuy B, Sougnez C, et al. Discovery and prioritization of somatic mutations in diffuse large B-cell lymphoma (DLBCL) by whole-exome sequencing. *Proc Natl Acad Sci USA.* (2012) 109:3879–84. doi: 10.1073/pnas.1121343109
57. Pasqualucci L, Dalla-Favera R. Genetics of diffuse large B-cell lymphoma. *Blood.* (2018) 131:2307–19. doi: 10.1182/blood-2017-11-764332
58. Rosenquist R, Ghia P, Hadzidimitriou A, Sutton LA, Agathangelidis A, Baliakas P, et al. Immunoglobulin gene sequence analysis in chronic lymphocytic leukemia: updated ERIC recommendations. *Leukemia.* (2017) 31:1477–81. doi: 10.1038/leu.2017.125
59. Lindblad-Toh K, Wade CM, Mikkelsen TS, Karlsson EK, Jaffe DB, Kamal M, et al. Genome sequence, comparative analysis and haplotype structure of the domestic dog. *Nature.* (2005) 438:803–19. doi: 10.1038/nature04338
60. Chen H-WW, Small GW, Motsinger-Reif A, Suter S, Richards KL. VH1-44 gene usage defines a subset of canine B-cell lymphomas associated with better patient survival. *Vet Immunol Immunopathol.* (2014) 157:125–30. doi: 10.1016/j.vetimm.2013.10.020
61. Rout ED, Burnett RC, Labadie JD, Yoshimoto J, Avery AC. Preferential use of unmutated immunoglobulin heavy variable region genes in Boxer dogs with chronic lymphocytic leukemia. *PLoS ONE.* (2018) 13:e0191205. doi: 10.1371/journal.pone.0191205
62. van Stee LL, Boston SE, Singh A, Romanelli G, Rubio-Guzman A, Scase TJ. Outcome and prognostic factors for canine splenic lymphoma treated by splenectomy (1995-2011). *Vet Surg.* (2015) 44:976–82. doi: 10.1111/vsu.12405
63. Cozzi M, Marconato L, Martini V, Aresu L, Riondato F, Rossi F, et al. Canine nodal marginal zone lymphoma: descriptive insight into the biological behaviour. *Vet Comp Oncol.* (2017) 16:246–52. doi: 10.1111/vco.12374
64. Frantz AM, Sarver AL, Ito D, Phang TL, Karimpour-Fard A, Scott MC, et al. Molecular profiling reveals prognostically significant subtypes of canine lymphoma. *Vet Pathol.* (2013) 50:693–703. doi: 10.1177/0300985812465325
65. Cascione L, Giudice L, Ferraresso S, Marconato L, Giannuzzi D, Napoli S, et al. Long non-coding RNAs as molecular signatures for canine B-cell lymphoma characterization. *Noncoding RNA.* (2019) 5:47. doi: 10.3390/ncrna5030047
66. Bromberek JL, Rout ED, Agnew MR, Yoshimoto J, Morley P, Avery AC. Breed distribution and clinical characteristics of B cell chronic lymphocytic leukemia in dogs. *J Vet Intern Med.* (2016) 30:215–22. doi: 10.1111/jvim.13814
67. Labadie JD, Magzamen S, Morley PS, Anderson GB, Yoshimoto J, Avery AC. Associations of environment, health history, T-zone lymphoma, and T-zone-like cells of undetermined significance: a case-control study of aged Golden Retrievers. *J Vet Intern Med.* (2019) 33:764–75. doi: 10.1111/jvim.15405
68. Spina V, Rossi, D. Overview of non-coding mutations in chronic lymphocytic leukemia. *Mol Oncol.* (2019) 13:99–106. doi: 10.1002/1878-0261.12416
69. International, CLLIPIwg. An international prognostic index for patients with chronic lymphocytic leukaemia (CLL-IPI): a meta-analysis of individual patient data. *Lancet Oncol.* (2016) 17:779–90. doi: 10.1016/S1470-2045(16)30029-8
70. Martini V, Melega M, Riondato F, Marconato L, Cozzi M, Bernardi S, et al. A retrospective study of flow cytometric characterization of suspected extranodal lymphomas in dogs. *J Vet Diagn Invest.* (2018) 30:830–6. doi: 10.2307/j.ctt21217bt.11
71. Stranahan LW, Whitley D, Thaiwong T, Kiupel M, Oliveira F. Anaplastic large T-cell lymphoma in the intestine of dogs. *Vet Pathol.* (2019) 56:878–84. doi: 10.1177/0300985819852132
72. Avery PR, Burton J, Bromberek JL, Seelig DM, Elmslie R, Correa S, et al. Flow cytometric characterization and clinical outcome of CD4+ T-cell lymphoma in dogs: 67 cases. *J Vet Intern Med.* (2014) 28:538–46. doi: 10.1111/jvim.12304
73. Comazzi S, Marelli S, Cozzi M, Rizzi R, Finotello R, Henriques J, et al. Breed-associated risks for developing canine lymphoma differ among countries: an European canine lymphoma network study. *BMC Vet Res.* (2018) 14:232. doi: 10.1186/s12917-018-1557-2
74. Pinello KC, Niza-Ribeiro J, Fonseca L, de Matos AJ. Incidence, characteristics and geographical distributions of canine and human non-Hodgkin's lymphoma in the Porto region (North West Portugal). *Vet J.* (2019) 245:70–6. doi: 10.1016/j.tvjl.2019.01.003
75. Rebhun RB, Kent MS, Borrofka SA, Frazier S, Skorupski K, Rodriguez CO. CHOP chemotherapy for the treatment of canine multicentric T-cell lymphoma. *Vet Comp Oncol.* (2011) 9:38–44. doi: 10.1111/j.1476-5829.2010.00230.x
76. Angelo G, Cronin K, Keys D. Comparison of combination l-asparaginase plus CHOP or modified MOPP treatment protocols in dogs with multi-centric T-cell or hypercalcaemic lymphoma. *J Small Anim Pract.* (2019) 60:430–7. doi: 10.1111/jsap.12986
77. Iqbal J, Wright G, Wang C, Rosenwald A, Gascoyne RD, Weisenburger DD, et al. Gene expression signatures delineate biological and prognostic subgroups in peripheral T-cell lymphoma. *Blood.* (2014) 123:2915–223. doi: 10.1182/blood-2013-11-536359
78. Heavican TB, Bouska A, Yu J, Lone W, Amador C, Gong Q, et al. Genetic drivers of oncogenic pathways in molecular subgroups of peripheral T-cell lymphoma. *Blood.* (2019) 133:1664–76. doi: 10.1182/blood-2018-09-872549
79. Wang T, Feldman AL, Wada DA, Lu Y, Polk A, Briski R, et al. GATA-3 expression identifies a high-risk subset of PTCL, NOS with distinct molecular and clinical features. *Blood.* (2014) 123:3007–15. doi: 10.1182/blood-2013-12-544809
80. McDonald JT, Kritharis A, Beheshti A, Pilichowska M, Burgess K, Ricks-Santi L, et al. Comparative oncology DNA sequencing of canine T cell lymphoma via human hotspot panel. *Oncotarget.* (2018) 9:22693–702. doi: 10.18632/oncotarget.26114
81. Worby C, Dixon JE. Pten. *Annu Rev Biochem.* (2014) 83:641–69. doi: 10.1146/annurev-biochem-082411-113907
82. Horwitz SM, Koch R, Porcu P, Oki Y, Moskowitz A, Perez M, et al. Activity of the PI3K-delta, gamma inhibitor duvelisib in a phase 1 trial and preclinical models of T-cell lymphoma. *Blood.* (2018) 131:888–98. doi: 10.1182/blood-2017-08-802470
83. Alvarez JD, Yasui DH, Niida H, Joh T, Loh D, Kohwi-Shigematsu T. The MAR-binding protein SATB1 orchestrates temporal and spatial expression of multiple genes during T-cell development. *Genes Dev.* (2000) 14:521–35.
84. Poglio S, Merlio JP. SATB1 is a pivotal epigenetic biomarker in cutaneous T-cell lymphomas. *J Invest Dermatol.* (2018) 138:1694–6. doi: 10.1016/j.jid.2018.04.018
85. Fosmire SP, Thomas R, Jubala CM, Wojcieszyn JW, Valli VE, Getzy DM, et al. Inactivation of the p16 cyclin-dependent kinase inhibitor in high-grade canine non-Hodgkin's T-cell lymphoma. *Vet Pathol.* (2007) 44:467–78. doi: 10.1354/vp.44-4-467
86. Fleming JM, Creevy K, Promislow DE. Mortality in north american dogs from 1984 to 2004: an investigation into age-, size-, and breed-related causes of death. *J Vet Intern Med.* (2011) 25:187–98. doi: 10.1111/j.1939-1676.2011.0695.x
87. Simpson M, Searfoss E, Albright S, Brown DE, Wolfe B, Clark NK, et al. Population characteristics of golden retriever lifetime study enrollees. *Canine Genet Epidemiol.* (2017) 4:14. doi: 10.1186/s40575-017-0053-5

Conflict of Interest: The author declares that the research was conducted in the absence of any commercial or financial relationships that could be construed as a potential conflict of interest.

Copyright © 2020 Avery. This is an open-access article distributed under the terms of the Creative Commons Attribution License (CC BY). The use, distribution or reproduction in other forums is permitted, provided the original author(s) and the copyright owner(s) are credited and that the original publication in this journal is cited, in accordance with accepted academic practice. No use, distribution or reproduction is permitted which does not comply with these terms.

frontiers in Oncology

REVIEW
published: 31 January 2020
doi: 10.3389/fonc.2020.00013

Understanding and Modeling Metastasis Biology to Improve Therapeutic Strategies for Combating Osteosarcoma Progression

Timothy M. Fan[1]*, *Ryan D. Roberts*[2] and *Michael M. Lizardo*[3]

[1] Comparative Oncology Research Laboratory, Department of Veterinary Clinical Medicine, College of Veterinary Medicine, University of Illinois at Urbana-Champaign, Urbana, IL, United States, [2] Center for Childhood Cancer and Blood Disorders, Abigail Wexner Research Institute at Nationwide Children's Hospital, The James Comprehensive Cancer Center at The Ohio State University, Columbus, OH, United States, [3] Poul Sorensen Laboratory, Department of Molecular Oncology, BC Cancer, Part of the Provincial Health Services Authority in British Columbia, Vancouver, BC, Canada

OPEN ACCESS

Edited by:
Rodney L. Page,
Colorado State University,
United States

Reviewed by:
Christine F. Brainson,
University of Kentucky, United States
Justin V. Joseph,
Aarhus University, Denmark

***Correspondence:**
Timothy M. Fan
t-fan@illinois.edu

Specialty section:
This article was submitted to Cancer Molecular Targets and Therapeutics, a section of the journal Frontiers in Oncology

Received: 01 October 2019
Accepted: 07 January 2020
Published: 31 January 2020

Citation:
Fan TM, Roberts RD and Lizardo MM (2020) Understanding and Modeling Metastasis Biology to Improve Therapeutic Strategies for Combating Osteosarcoma Progression. Front. Oncol. 10:13. doi: 10.3389/fonc.2020.00013

Osteosarcoma is a malignant primary tumor of bone, arising from transformed progenitor cells with osteoblastic differentiation and osteoid production. While categorized as a rare tumor, most patients diagnosed with osteosarcoma are adolescents in their second decade of life and underscores the potential for life changing consequences in this vulnerable population. In the setting of localized disease, conventional treatment for osteosarcoma affords a cure rate approaching 70%; however, survival for patients suffering from metastatic disease remain disappointing with only 20% of individuals being alive past 5 years post-diagnosis. In patients with incurable disease, pulmonary metastases remain the leading cause for osteosarcoma-associated mortality; yet identifying new strategies for combating metastatic progression remains at a scientific and clinical impasse, with no significant advancements for the past four decades. While there is resonating clinical urgency for newer and more effective treatment options for managing osteosarcoma metastases, the discovery of druggable targets and development of innovative therapies for inhibiting metastatic progression will require a deeper and more detailed understanding of osteosarcoma metastasis biology. Toward the goal of illuminating the processes involved in cancer metastasis, a convergent science approach inclusive of diverse disciplines spanning the biology and physical science domains can offer novel and synergistic perspectives, inventive, and sophisticated model systems, and disruptive experimental approaches that can accelerate the discovery and characterization of key processes operative during metastatic progression. Through the lens of trans-disciplinary research, the field of comparative oncology is uniquely positioned to advance new discoveries in metastasis biology toward impactful clinical translation through the inclusion of pet dogs diagnosed with metastatic osteosarcoma. Given the spontaneous course of osteosarcoma development in the context of real-time tumor microenvironmental cues and immune mechanisms, pet dogs are distinctively valuable in translational modeling given their faithful recapitulation of metastatic disease

progression as occurs in humans. Pet dogs can be leveraged for the exploration of novel therapies that exploit tumor cell vulnerabilities, perturb local microenvironmental cues, and amplify immunologic recognition. In this capacity, pet dogs can serve as valuable corroborative models for realizing the science and best clinical practices necessary for understanding and combating osteosarcoma metastases.

Keywords: comparative oncology, metastasis biology, experimental models, translational therapeutics, canine cancer

TARGETING PULMONARY METASTASIS IN OSTEOSARCOMA

Since the institution of chemotherapy in the 1960s, relapse-free survival for osteosarcoma (OS) patients with localized disease has dramatically improved. The current standard of care involves surgical resection of the primary tumor and multi-agent chemotherapy (both in the neoadjuvant and adjuvant setting) which can result in 5-year survival rates up to 70% for patients with localized disease (1). For those patients who present with distant metastases (usually in the lung), outcomes are much poorer with a survival rate of about 20% (2). The negative prognoses associated with macroscopic disseminated OS burdens is not unique, but rather holds true for many types of cancers that metastasize (3); and underscores the broader need in combating metastatic progression across diverse solid tumor histologies. For OS patients, major hurdles that reduce overall survival include relapse, which occurs in 1/3 of patients with localized disease (4) and in the majority (∼75%) of patients presenting with systemic disease (5); and the development of chemo-resistance (6). Since overall survival rates have plateaued with multi-agent chemotherapy (7), there remains an impetus to discover and clinically deploy alternative non-cytotoxin based anti-metastatic therapeutics that inhibit lung metastasis progression and may lead to improved patient outcomes. Several investigators in the metastasis research community have advocated the idea that delaying or inhibiting metastatic progression (particularly the early stages of lung colonization) should be the most clinical and biologic relevant metric rather than the cytoreduction of the primary tumor in the evaluation of new drugs (3, 8, 9). The merit of this proposed paradigm shift in therapeutic assessment is supported by historical clinical data that micrometastases in the lung are already present in OS patients with localized tumors and that adjuvant chemotherapy has been shown to improve relapse-free survival (10). Additionally, preclinical effectiveness of molecularly-targeted therapy for targeting early stages of lung colonization or micrometastases have been shown previously (11, 12) (also see **Table 2**), and justify the exploration of precision medicine approaches for improving survival outcomes. To accelerate discovery to impact, the rational development of anti-metastatic therapeutics requires a convergent science approach including (1) a better understanding of OS metastasis biology in relation to the lung microenvironment and (2) the availability of engineered and natural model systems that most faithfully recapitulate the complexities of metastatic progression. Through transdisciplinary collaborative research, it is envisioned that novel and effective anti-metastatic therapeutics can be identified and translated to extend the lives of patients with OS by eradicating or thwarting the progression of subclinical micrometastatic disease that persisted following standard multi-agent chemotherapy.

BIOLOGY OF PULMONARY METASTASES

Dissemination From the Primary Tumor

The metastatic process, or more commonly referred to as the *metastatic cascade,* describes the progressive steps of tumor cell dissemination from the primary tumor, transit within the blood vasculature, and the establishment of clinically detectable pulmonary metastases (**Figure 1**). Since each step of the metastatic cascade is rate limiting, metastasis is considered to be a very inefficient process (30–32). The initial stages of metastasis involve the acquisition of an invasive phenotype and migration away from the primary tumor site (step 1, **Figures 1A,B**). Several studies have shown that OS cells secrete proteolytic enzymes such as matrix metalloproteinases (MMPs) and cathepsins which causes the degradation of local tissue extracellular matrix (ECM) and basement membranes (33). Modulation of TIMP3, MMP1, MMP3, MMP11 have been shown to influence *in vitro* invasiveness of OS cells, and enhance *in vivo* tumorigenicity (34–36). OS cell interactions with local stromal cells such as mesenchymal stem cells (37) and endothelial cells (38, 39), have been found to be pro-tumorigenic, whereas interactions with natural killer cells (40) or primed dendritic cells (41), were shown to have anti-tumor effects.

Intravasation and Transit Within the Blood Vasculature

Once tumor cells reach the local microvasculature, intravasation, or entry into blood vessels, is the next step in the metastatic cascade (step 2, **Figures 1A,B**). Entry into the local microvasculature requires OS cell interaction with endothelial cells. Several *in vitro* models exist to study tumor cell interactions with endothelial cells (42), with the simplest system being the co-culturing of tumor cells onto a monolayer of endothelial cells. Research from several groups have utilized this *in vitro* co-culture method and have shown that RUNX and osteopontin (43), uPAR (14), and $\alpha_v\beta_3$ (44) influence the physical interactions between OS cells and endothelial cells. More importantly, several of these studies have shown that interfering with these OS cell-endothelial interactions were found to inhibit metastasis formation *in vivo* (14, 43).

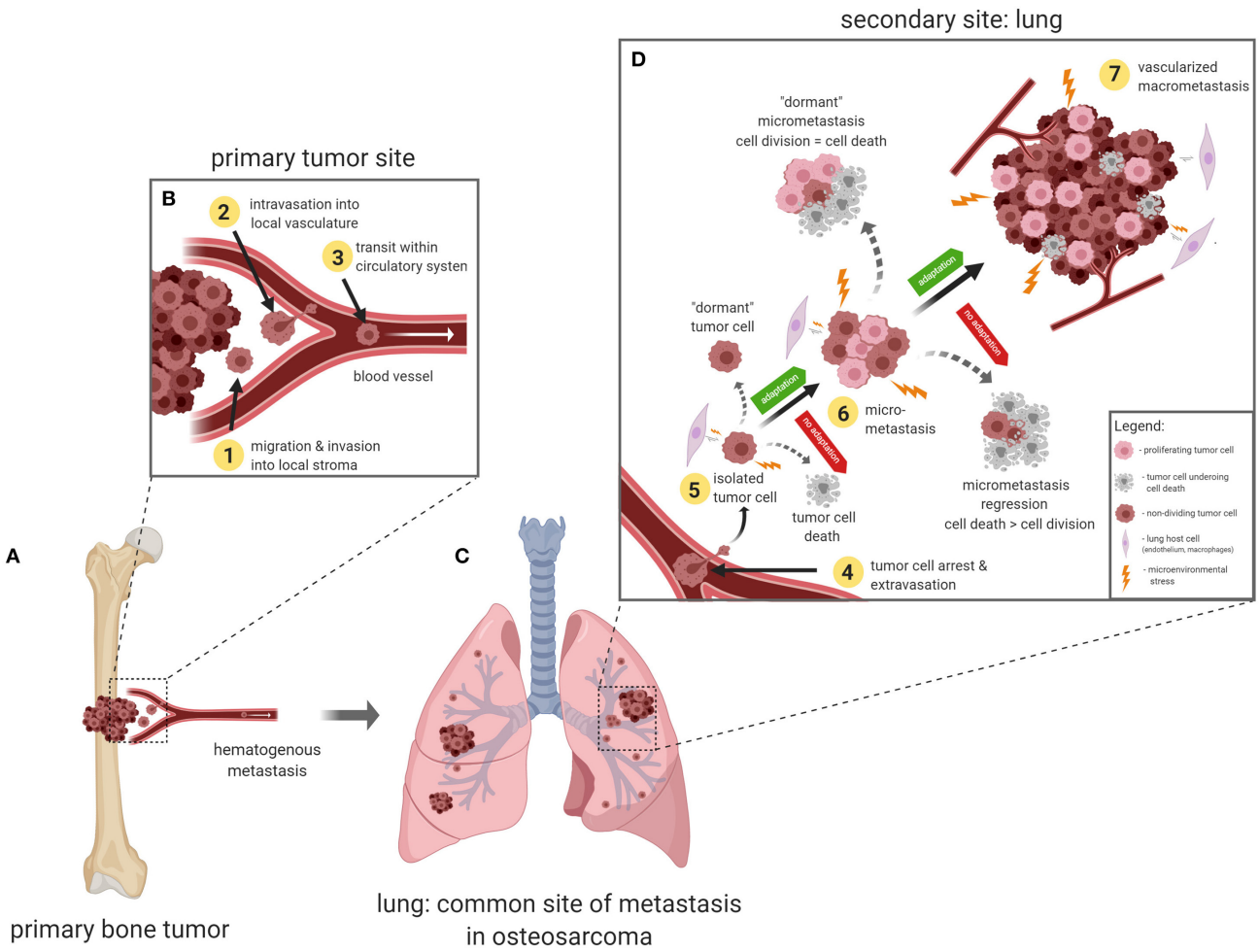

FIGURE 1 | The metastatic cascade in osteosarcoma. **(A)** Primary OS tumor, usually in the long bones. **(B)** Tumor cells acquire an invasive phenotype and migrate away from the primary tumor and invade into surrounding tissues (step 1). Tumor cells interact with the basement membrane and endothelial cells to intravasate into the blood microvasculature (step 2) and travel in the circulation (step 3). **(C)** Upon arrival at the secondary site (lung), tumor cells arrest via size restriction or adhesion interactions with the pulmonary microvascular endothelial cells (step 4). **(D)** Once tumor cells extravasate out of the blood vessels, they must be able to adapt and survive in the lung microenvironment (step 5). At this vulnerable stage, tumor cells can undergo a number of fates which include- enter cellular dormancy, die off, or if the stresses of the lung microenvironment can be successfully managed, tumor cells can proliferate into multi-cellular micrometastases (step 6). Micrometastases can enter into a state of "angiogenic dormancy" and remain the same size, or regress if cell death is greater than proliferation, or recruit local blood vessels and form a vascularized secondary tumor (step 7).

Once within the blood stream, OS cells must be able to resist *anoikis,* a specialized form of apoptosis induced by the disruption of cell-matrix interactions, as first described by Frisch and Francis (45). A number of key regulators of anoikis have been characterized since its initial discovery (e.g., Mcl-1, Cav-1, Bcl-x_L, c-FLIP) (46) and several of these genes have been linked to metastatic capacity in breast cancer cells (47) and OS cells (24, 48, 49).

Another type of stress OS cells encounter within the circulation is the physical hemodynamic forces of blood flow. Observations on the hemodynamic destruction of tumor cells were initially made by Weiss and Dimitrov (50). The major physical stressor in the blood circulation is fluid shear stress (FSS), which is defined as the frictional forces between moving layers, and is measured in Newtons per meter squared (N/m^2) or Dynes per centimeter squared (Dyn/cm^2) (51). FSS in the blood circulation ranges from 1 to 30 Dyn/cm^2 depending on the anatomical location (52). Lien and colleagues have demonstrated that OS cells (MG63) were found to have higher levels of apoptosis when exposed to FSS ranging from 0.5 to 12 Dyn/cm^2 when compared to control static cells in an *in vitro* flow chamber (53). The authors also demonstrated that the level of OS apoptosis correlated with increasing times of exposure of various FSS conditions. It would be interesting to assess whether MG63.3 cells, a highly metastatic variant of MG63 cells, characterized by Ren et al. (54), exhibit some level of resistance to FSS-induced apoptosis.

Lung Colonization and Microenvironmental Stressors

If OS cells can resist anoikis and adapt to damaging FSS in the blood circulation, arrest, and survival in the lung microvasculature presents the next significant challenge to metastatic OS cells. Several studies using the experimental metastasis model (tail vein injection of tumor cells) have demonstrated that the majority of tumor cells that arrive in the lung do not survive, and only a small subset of the initial population (1–6%) were able to successfully establish metastases (31, 32). These studies have carefully analyzed tumor cell fate over time and concluded that metastatic colonization of the lung is a non-linear process where tumor cells can undergo any number of fates, as illustrated in **Figure 1D**. Newly arrested tumor cells can either: (1) enter a dormant, viable but non-dividing state, as observed in several lung metastasis studies (32, 55, 56); (2) proliferate into a pre-angiogenic micrometastasis, or (3) undergo apoptotic cell death (57, 58). Micrometastases, in turn, can also undergo a number of fates which include: (1) enter a state "angiogenic dormancy" where tumor cell proliferation is balanced with cell death (59), (2) proliferate into a vascularized macrometastatic lesion (60), or (3) regress if tumor cell death is greater than cell proliferation. The ability to adapt quickly to a harsh new microenvironment is a prerequisite for metastatic cancer cell survival and proliferation in the lung. Stress adaptation pathways depend on the nature of the particular stress encountered, and several research groups have begun to shed light on this aspect of metastasis biology.

Redox stress is a major microenvironmental stressor that contributes to tumor cell clearance in the lung since several studies have provided microscopic imaging evidence and "omic" data supporting this notion. Qiu et al. (58) have shown that the physical arrest of murine melanoma cells in the lung stimulates the local microvascular endothelial cells to release a burst of nitric oxide (NO), which was cytotoxic to tumor cells. Inhibition of NO release by L-NAME (a nitric oxide synthase inhibitor) treatment or the use of endothelial nitric oxide synthase knock-out mice resulted in higher lung tumor burden. Piskounova et al. (61) have shown that metastatic melanoma cells adapt to the redox stress in the lung by upregulating the NADPH-generating enzyme ALDH1L2; and targeting shRNAs against ALDH1L2 resulted in lower lung tumor burden (61). NADPH is important in maintaining redox homeostasis (62), and a recent study by Basnet et al. (63) have shown that micrometastases of breast cancer cells in the mouse lung have elevated transcript and protein levels of antioxidant genes (e.g., NRF2 and GPX1). The notion that ROS can negatively regulate metastasis formation is somewhat controversial since other studies seem to suggest the opposite (64–66). These discrepancies may be due to cell type-specific responses, or the particular dose of ROS exposure. Low, sublethal concentrations of ROS can turn on antioxidant responses, whereas high concentrations of ROS can cause irreversible damage to proteins, lipids and DNA with consequent cell death.

Another type of cellular stress closely linked to redox stress is endoplasmic reticulum (ER) stress. Protein folding processes within the ER are exquisitely sensitive to perturbations in cellular redox state, Ca^{2+} concentration within ER lumen, and ATP supply (67). Redox stress can alter the oxidative protein folding environment of the ER lumen, which results in the accumulation of unfolded proteins, a condition known as ER stress (68). The unfolded protein response (UPR) is activated by various sensors on the ER membrane, and an adaptive transcriptional program is activated to increase the chaperone capacity of the ER and increase ER-associated degradation pathways to compensate for the sudden load of unfolded proteins (67). The UPR has been found to be dysregulated in many types of cancer, including OS (69, 70). Several highly metastatic human OS cell lines were found to upregulate the ER chaperone protein GRP78 at higher levels compared to their low metastatic counterparts during ER stress (12), and shRNAs and IT-139, a small molecule inhibitor of GRP78 under clinical investigation (71), were found to reduce lung metastatic burden. Translocation of the transcription factor ATF6α to the nucleus is also part of ER stress response, and human OS cells were found to have elevated levels of nuclear ATF6α compared to osteoblast controls under ER stress conditions (72). Downstream targets of ATF6α such as GRP78, PDI, and ERO1β where found to confer chemotherapy resistance in OS cells, and down-modulation of ATF6α resulted in increased sensitivity to cisplatin. Moreover, elevated levels of ATF6α in patient samples was predictive or poorer overall survival and poorer response to chemotherapy (72). Several groups have also found UPR-related pathways to be dysregulated in OS (73–75).

Although the microenvironmental stressors discussed above can contribute to tumor cell clearance in the lung, these observations do not explain the apparent "organotropism" of OS cells for the lung. Why do metastases in OS preferentially occur in the lung? The answer, in part, may be due to mechanical restriction of disseminated tumor cells in the lung microvasculature. Human alveolar capillaries range from 5 to 8 μm in diameter (76), whereas the average diameter of osteoblastic osteosarcoma cells ranges from 10 to 19 μm (estimated from histology micrographs) (77). Circulating tumor cells often arrest via size restriction within the first microvascular capillary bed they encounter, and video microscopic evidence from animal studies suggest that organs such as the lung and liver are efficient at "filtering" out circulating tumor cells from the blood (78). OS cell "organotropism" for the lung can also be explained by the concept of the "pre-metastatic niche" (PMN), in which growth factors from the primary tumor "prime" downstream metastatic sites for tumor cell engraftment (79–81). As to whether PMN contributes to lung colonization in OS, Murgai et al. (82) found that metastatic OS cells secret exosomes containing cytokines that can induce lung perivascular cells to secrete fibronectin. The same authors also demonstrated that fibronectin promoted tumor cell adhesion, migration, and proliferation *in vitro*. Additionally, Macklin et al. (83) also found that highly metastatic OS cells are capable of secreting extracellular vesicles that were preferentially retained in the lung, but not liver. More definitive studies will be needed to define OS-specific changes in the lung during PMN formation, and whether or not modulation of OS-specific PMN can influence the formation of lung metastasis.

MODEL SYSTEMS TO STUDY OSTEOSARCOMA METASTASES

Preclinical Models to Study and Image the Steps of Metastasis

Since lung metastasis progression involves complex 3 dimensional (3D) interactions between OS cells, ECM, and lung parenchymal cells, model systems that can maintain or partially recapitulate some aspects of these 3D interactions will allow researchers to interpret metastatic OS cell responses to gene therapy or pharmacologic intervention in a relevant microenvironmental context. Indeed, several studies have demonstrated that tumor cell response to therapeutics differ when comparing 2D vs. 3D growth conditions (84–86). To this end, several microscope-based models exist that permit researchers to directly visualize and study metastatic cancer cell behavior in a 3D microenvironment. Such models are described below, and the benefits and limitations of each model are discussed.

Chick Chorioallantoic Membrane Model

The chick chorioallantoic membrane (CAM) is a highly vascularized membrane that primarily functions as a gas-exchange organ for the developing embryo (87). The CAM is commonly studied in a shell-less format (*ex ovo*), where xenograft human tumor fragments or a tumor cell suspension (**Figure 2A**) can be placed onto the CAM or injected into blood vessels of the CAM. The CAM has proven to be a useful model in studying tumor angiogenesis (90, 91), tumor cell migration and invasion (92), intravasation into blood vessels (93), tumor cells in transit within the vasculature, extravasation out from blood vessels (**Figure 2B**) (94–98), and the outgrowth of patient derived xenografts (99). In OS research, the CAM model has been used to study tumor growth of a variety of OS cell lines (100), angiogenesis (101), and metastasis to distant sites (102). The main benefits of using the chick CAM model include: (1) amenable to *in vivo* imaging, (2) relatively inexpensive, and (3) can be used for high-throughput screening of targeted therapies. Disadvantages of the CAM model include: (1) short observation times (days), (2) inability to study tumor cell interactions with the immune system since the chick CAM is immunodeficient until developmental day 18 (87), and (3) fewer antibodies available for host chicken antigens (103). The chick CAM model is applicable to the study of tumor cell invasion (step 1, **Figure 1B**), interactions between endothelial cells during intravasation, transit within blood vessels, and extravasation (steps 2, 3, and 4, **Figures 1B,D**) since these steps are readily observable at the surface of the chick CAM. Tumor colonization of distant sites in the chick CAM are not accessible for imaging, and thus harvesting the organs for histology, or polymerase chain reaction assays for tumor specific DNA sequences are required. To study lung colonization in OS, other microscope-based models that can examine lung tissue would be more appropriate.

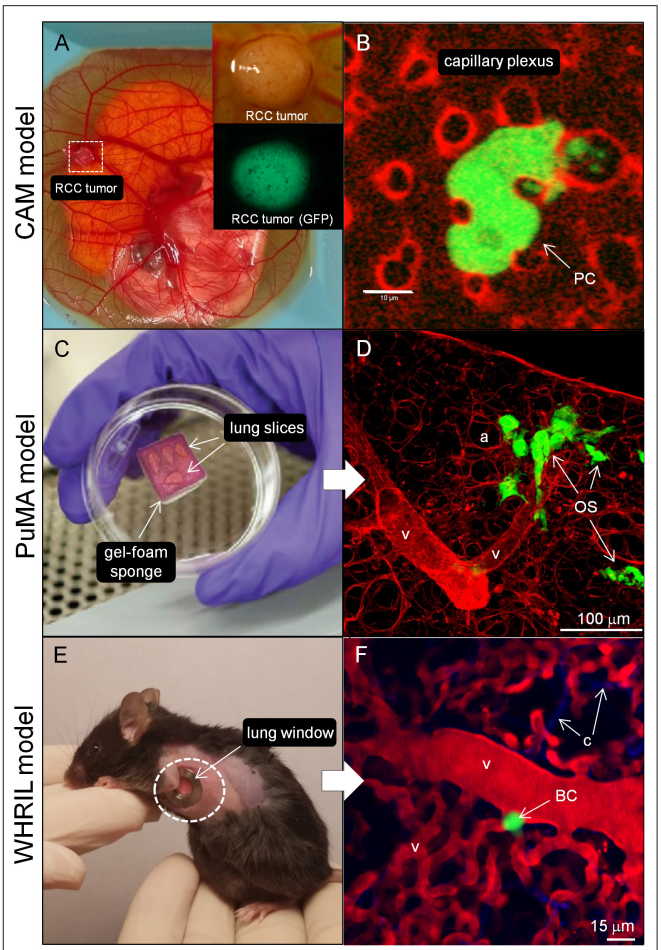

FIGURE 2 | Imaging models to study the metastatic cascade in cancer. **(A)** The CAM model (whole mount image) showing the chick embryo and highly vascularized CAM. A small renal cell carcinoma (RCC) explant can be seen growing in the dashed white box. Zoomed image of a different established GFP-expressing RCC tumor where the entire tumor, associated vasculature, and corresponding fluorescence image (below) are shown (Image courtesy of Matthew Lowerison and Pengfei Song, UIUC). **(B)** High magnification, single cell imaging of a GFP-labeled prostatic carcinoma cell (PC) migrating through capillary plexus (labeled with rhodamine-lectin) and forming invadopodia (yellow arrowheads) into the lumen of 2 adjacent capillaries in the CAM model (Image courtesy of Fabrice Lucien and Yohan Kim, Mayo Clinic). **(C)** The PuMA is an *ex vivo* lung explant model where tumor cells in viable lung tissue is maintained in cell culture. The lung slices are kept at an air-liquid interface on top of a gelatin sponge. **(D)** Shows the lung parenchyma (stained red with DAR4M) and eGFP-expressing MG63 OS cells (OS) interacting with vessel-like structures (v). Scalebar = 100 μm. See Lizardo and Sorensen (88) for methods. **(E)** The WHRIL model allows for the direct visualize of lung tissue through a window in the mouse chest cavity (89) as shown with the dashed white circle. **(F)** Fluorescent micrograph showing the lung microvasculature (v) (labeled red with tetramethylrhodamine) and GFP-expressing breast cancer cell (BC). Blue fibers represent second harmonic imaging of connective tissue (c) fibers. Scalebar = 15 μm (Images courtesy of David R. Entenberg, Albert Einstein College of Medicine). UIUC, University of Illinois at Urbana-Champaign.

Pulmonary Metastasis Assay (PuMA)

A technical advance that addresses the need to directly visualize and characterize the growth of metastatic OS cells in the lung microenvironment is called the pulmonary metastasis assay (PuMA), first developed by Mendoza et al. (104), and further refined by others (88, 105). The PuMA is an *ex vivo*, lung tissue

explant model where fluorescently labeled tumor cells in viable lung tissue (**Figures 2C,D**) can be maintained *in vitro* for up to 21 days of observation. High and low metastatic pairs of human and mouse OS cell lines, whose *in vivo* metastatic phenotypes were characterized elsewhere (54), retain their metastatic propensities in the *ex vivo* PuMA model. Such observations suggest that despite the lack of blood flow, certain cellular, and extracellular features of lung tissue still exert "microenvironmental pressures" that are not conducive to the growth of low metastatic tumor cells, but still permit the growth of highly metastatic tumor cells. Indeed, the histology and microarchitecture of PuMA tissue sections are virtually indistinguishable from that of *in vivo* lungs (104). The PuMA model has been used to assess how gene modulation or drug treatment affects metastatic OS growth in lung tissue (12, 21–23, 25, 106). The PuMA model has several advantages which include: (1) the ability to directly study metastatic OS cells at both the cellular and subcellular level while in a relevant 3D microenvironment, (2) amenable to molecular imaging (gene or signaling pathways) by labeling tumor cells with fluorescent dyes, fluorescent protein reporter or protein fusion constructs, and (3) the PuMA model has recently been adapted to a 96-well plate format for a high-throughput drug screen (20). For image analysis, proprietary software is not needed, and analysis can be done with publicly available software packages such as ImageJ. Image processing can be expedited through automation as described by Young et al. (105). One major drawback of the PuMA model is the limited number of cell lines that are compatible with the assay. For tumor cell lines that have not been previously published to work within the PuMA model, researchers must empirically determine whether their metastatic tumor cell line of interest is compatible with the B-media used in the PuMA model, and whether their cell line can grow into progressively larger lesions over time. Secondly, the length of observation in the PuMA model is limited to 21 days post-injection of tumor cells. Beyond 21 days, the PuMA lung tissue becomes devoid of lung parenchymal cells, leaving only connective tissue. The PuMA model is ideal in studying tumor cell arrest in the lung microvasculature, extravasation, interactions with the lung parenchyma, and the formation of micrometastases (steps 4, 5, and 6, **Figure 1D**). If a researcher's investigations require an intact microcirculation, then an intravital (within a living subject) imaging model of the lung would be more appropriate.

Intravital Video Microscopy of Lung Metastasis

Direct observation of labeled tumor cells in an intact lung perfusion model have been described previously (58, 107); however this method is an *ex vivo* perfusion model where the lungs were removed *en bloc* and imaged on an inverted microscope. Intravital imaging of the microcirculation of various organs (such as lung or liver) was reported by Varghese et al. (108), where an acute preparation of the organ of interest was stably imaged on an inverted microscope for 4–6 h in anesthetized mice. While innovative at the time, this technique was prone to motion artifact from physiologic processes such as breathing or heart beating, and necessitated movement artifact compensation through a post-processing image stabilization algorithm. More recently, imaging of labeled tumor cells in the lung of a live, free breathing mice was recently described by Entenberg et al. (89). In this intravital video microscopy model, called Window for High-Resolution Imaging in the Lung (WHRIL), a small circular window is implanted in the chest cavity of the mouse (**Figure 2E**) and permits serial imaging of the same area of the lung for a period of up to 2 weeks (protocol allowance). Using the WHRIL model, the authors were able to image tumor cells within the lung microvasculature (**Figure 2F**), tumor cell extravasation, cell division, and formation of micrometastases (89). The WHRIL model has capacity to thoroughly characterize the effects of targeted anti-metastatic therapeutics on pulmonary micrometastases and established metastases in a preclinical setting. Using fluorescent reporter genes or functional dyes, in combination with WHRIL model, would permit researchers to assess the effects of gene modulation or targeted therapies on metastatic OS cell biology in the lung, in real-time. The advantages of the WHRIL model include the unprecedented ability to study metastatic OS cells at the cellular, subcellular, and molecular level in live, free-breathing mice. Secondly, serial imaging can be performed to assess the effects of therapy over progressive (albeit limited) time points. One major drawback of this technique is the limited depth of imaging, which in turn is dependent on the type of microscope (single photon vs. multi-photon imaging) and the type of fluorophore used (109). Regular epifluorescence imaging would be limited to an imaging depth of 200 μm due to light scattering. In contrast, using a multi-photon confocal microscope and tumor cells labeled with near-infrared fluorophores (emission wavelengths between 650 and 900 nm) would push the imaging depth toward 700 μm (110). The WHRIL model can be implanted at a timepoint corresponding to tumor cell arrest, extravasation, colonization of extravascular lung tissue, formation of micrometastases, and vascularized macrometastases (steps 4, 5, 6, and 7, **Figure 1D**).

Mouse Models of Osteosarcoma Metastasis

Based upon the complexity of metastatic biology, scientific discoveries that lead to new and effective therapies for OS metastases are expected to be derived through experimental models which most faithfully recapitulate the biology and key regulatory pathways involved in the genesis and metastatic progression of OS. Furthermore, models that accurately reproduce the natural progression of spontaneous micrometastases in the absence of a primary tumor are necessary to investigate activities of novel anti-metastatic therapeutics, as this clinical setting is the most pressing scenario in which humans diagnosed with OS require advances in treatment. Although an ideal animal model of OS has yet to be universally recognized or accepted, the most desirable model characteristics should include spontaneous primary bone tumor and pulmonary metastases development within an immunocompetent host.

In whole organisms, such as humans and dogs, successful metastasis occurs only when cancer cells, singly or in groups, become able to dehisce from not only the surrounding normal tissues, but also from malignantly transformed neighboring

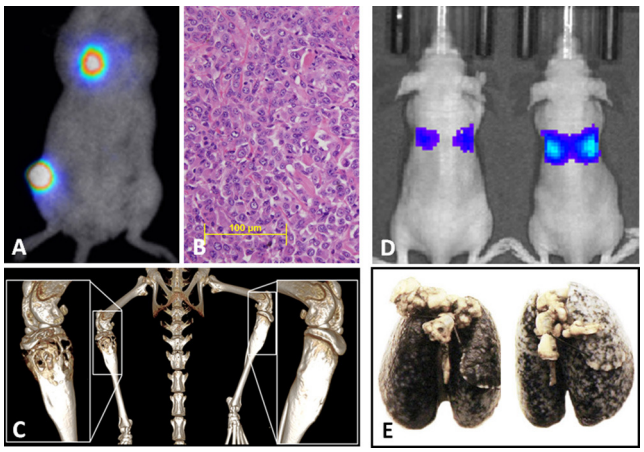

FIGURE 3 | (A) Syngeneic orthotopic mouse model of primary bone OS (K7M3) with concurrent spontaneous pulmonary metastases development visualized by bioluminescent imaging, **(B)** with corollary histology of established pulmonary metastatic lesions and **(C)** micro CT images of the OS primary lesion showing profound osteolysis and contralateral unaffected tibia. **(D)** Bioluminescent imaging of an experimental metastases model in athymic nude mice following tail vein injection with the Abrams (canine OS) luciferase cell line demonstrating correlation between luminescent signal and **(E)** gross macroscopic tumor burdens.

cells within the primary tumor. To be successful in seeding distant sites, these metastatic precursors must acquire the ability to invade through the tissue matrix, intravasate into the circulation, arrest within the target tissue, extravasate, survive within each of these diverse and heterotypic environments, and then proliferate within the target organ in ways that recapitulate the primary solid tumor (111). Doing so requires the acquisition of myriad behaviors not typical of the cells of origin, and these transformed phenotypes can arise from abnormal activation of cell-autonomous pathways that endow tumor cells with, for example, resistance to apoptosis (112) or the ability to affect unusually high levels of capped mRNA translation (22). Beyond these shifts in behavior that represent intrinsic properties of the malignant cells themselves, disseminated tumor cells often acquire additional malignancy-associated behaviors from interactions with the normal tissues that surround them within the metastatic niche (113). Interestingly, these interactions need not require close contact between the effector cells and the responder cells—they can occur at long distances, even being initiated by cells located within the primary tumor (114).

These complex interactions between malignant tumors and host cells and tissues make the study of metastasis difficult outside of whole organisms. As the laboratory workhorse for most biological systems, murine models have become those that researchers most often use for exploration into the mechanisms of OS metastasis (115). Murine models of metastasis are diverse and can facilitate the study of biology and therapeutic development through manipulation of the host (using genetically engineered mice, or GEMs), manipulation of the tumor cells themselves (using cell lines, xenografts, or allogeneic transplants), or both. Murine systems allow researchers to study elements critical to oncogenesis, as is evident in the multiple GEM models of spontaneous OS (116–118)—even facilitating whole-genome forward genetic screens into mechanisms of oncogenesis and metastasis (119). The use of immunodeficient mice has facilitated a recent explosion in the generation of patient-derived xenograft (PDX) models (120, 121) and their use in OS research (122), including orthotopic models of spontaneous metastasis which mimic the care patients receive through the implementation of hindlimb amputations (123, 124).

Generally, mouse models can be divided into three classes: (1) those that spontaneously develop primary tumors and subsequently develop metastasis, (2) those that are implanted orthotopically (usually into a leg bone) with spontaneous distant metastases (**Figures 3A–C**), and (3) those where tumor cells are inoculated directly into the circulation (often called experimental metastasis, **Figures 3D,E**) (115). Each of these approaches can ask different experimental questions, and each has unique strengths and weaknesses that should be recognized when interpreting results and formulating conclusions. Advantages and disadvantages associated with these models are summarized in **Table 1**.

Three Dimensional Engineered Models of Metastasis

Traditionally, the oncogenic transformation and malignant behaviors of cancer cells have been ascribed to perturbations involving multiple and interactive molecular factors rooted in genetic alterations and dysregulated biochemical signaling. While many aspects of cancer cell phenotype, including metastasis, can be adequately characterized and studied through the singular lens of biology, there is overwhelming evidence that mechanical forces exerted by and upon cancer cells, surrounding stromal elements, and ECM are integrally linked with oncologic activities, including cancer cell invasion and metastasis (51, 125). Living cells are capable of sensing mechanical stimuli (tensile, compressive, and shear forces), termed mechanotransduction, through specialized cellular structures including focal adhesions and stretch-gated ion channels (126, 127), which result in activation of gene and signaling pathways that regulate cellular behaviors. The realization that mechanical cues, in concert with biologic context, contribute collaboratively to diverse cancer processes has spurred rapid advancements in studying cancer metastasis through the deliberate inclusion of physical science, tumor bioengineering, and microfabrication approaches.

While a preponderance of cancer investigations includes studies based on two-dimensional (2D) cell models, such experimental methods that rely upon cancer cells grown in monolayer do not recapitulate the true interactions between cells-cells and cells-extracellular matrices encountered during solid tumor formation, evolution, and metastatic progression. The bidirectional interactions of cancer cells with the tumor microenvironment generates biological complexity, which can be more thoroughly studied through three-dimensional (3D) modeling strategies that include biomimetic engineered tumor models. Through the purposeful design of various mechanical platforms, it is now possible to ask and answer specific questions

TABLE 1 | Mouse models of osteosarcoma.

	Advantages	Disadvantages
TUMOR SOURCE		
Human cell lines	• Easy to expand • Easy to manipulate genetically • Able to compare across many studies • Those that colonize lung demonstrate tissue tropism	• Serial passage induces genetic and phenotypic drift • Must use immunodeficient mice • Few stable lines available, fewer that colonize murine lungs
Patient-derived xenografts	• Broad panels recapitulate diversity • Better fidelity to original tumor properties/clones • Many stable PDXs available	• Must use immunodeficient mice • Most do not show lung metastasis under traditional conditions • Still questionable retention of original tumor properties/clones
GEM-derived cell lines	• Implantable in immunocompetent mouse strains • High- and low-metastatic cell lines derived without multiple rounds of selection	• Uncertain how well GEM osteosarcoma recapitulates spontaneous disease • Less-well-characterized than human models (genetics/copy number)
Intact GEM mice	• Can engineer to study interplay with genes of interest • Can study earlier stages of malignant transformation	• Patterns of tumor development differ from human (axial/jaw) • Usually multiple primary lesions • Cannot resect/amputate
MODE OF INTRODUCTION		
Orthotopic injection	• May preserve original tumor properties/clones • Simple procedure requiring minimal investment in personnel • High take rates in most cell line/PDX models • Can be removed surgically, usually by amputation	• Humane endpoints occur faster and with smaller tumors • Difficult to distinguish procedure-related emboli from metastasis arising from primary tumor
Orthotopic implantation	• Same as for orthotopic injection, except: • Procedure-related tumor emboli unlikely	• Same as for orthotopic injection, except: • More complex procedure requiring large time investment • Lower take rate than for injections • Requires actively growing "donor" tumors
Subcutaneous implantation	• Simple procedure can be high throughput • Many PDX lines already propagated subcutaneously • Can be excised in a simple surgical procedure	• Serial passage in subcutaneous environment introduces phenotypic drift (less than in culture) • Low rates of metastasis from subcutaneous tumors
Intravenous inoculation	• Very high throughput procedure • High rates of metastasis formation in numerous models • Retains tissue tropism to lung • Short time courses for experimentation • Single-step experiments (no resection surgery required)	• Agnostic to early steps in metastasis • Inoculated cells may differ from those that disseminate hematogenously from a primary tumor • Tissue tropism may be weighted toward anatomic circulation patterns and site of injection
PROCEDURES/MANIPULATIONS		
Amputation	• Mimics patterns of clinical care in humans and dogs • Allows time for metastases to develop beyond humane endpoint for primary tumor • Mice tolerate procedure and recover well	• Complex procedure requires large investment of time, not high throughput • Morbidities associated with procedure can complicate interpretation
Surgical excision	• Excision of subcutaneous lesions less morbid than amputation • Procedure takes less time than amputation	• Low rates of metastasis from subcutaneous tumors • Adhesions surrounding large lesions can complicate excision

regarding how cancer cells respond to highly tunable variables including matrix stiffness, interfacial geometry, cell curvature, and other mechanotransduction gradients (128–131). By virtue of precise and reproducible fabrication techniques for generating engineered biomimetics, cancer cell reactivity in response to individual or collective stimuli can be investigated under controllable and quantitative experimental conditions. While providing unique opportunity to study cancer biology, awareness for the strengths and limitations of diverse mechanobiology platforms for elucidating cancer-associated processes is required to ensure their suitable applications. Given their capacity for high throughput data generation, bioengineered 3D cellular platforms are expected to complement existing biologic model systems for rapidly advancing the current state of knowledge regarding cancer metastasis. Several 3D *in vitro* biomimetic platforms currently used in cancer research are summarized, and their suitability for studying unique aspects related to OS metastasis are highlighted.

Scaffold-Free 3D Models: Tumor Spheroids

Tumor cell masses naturally grow in 3D and cellular behaviors are dependent upon multiple biochemical and mechanical cues heterogeneously distributed throughout the microenvironment (i.e., hypoxia and intercellular forces, respectively). Compared to conventional 2D cell culture methods, spherical 3D tumor models are superior for recapitulating the spatial cellular and biochemical heterogeneity of solid tumors. Tumor spheroids are cancer cell aggregates ranging in size from 20 to 1,000 μm

in diameter and can be formed through various techniques, with the easiest method reliant upon cell buoyancy (132). Additionally, allowing cells to aggregate by gravity (hanging drop method) or culturing cancer cells on non-adherent or cell-repulsive substrates are alternative strategies for reproducible spheroid formation (133). The simplest spheroid models focus on single cell populations which can self-aggregate and produce endogenous ECM, thereby recapitulating homotypic cell-cell, as well as heterotypic cell-ECM interactions operative during solid tumor formation. The generation of more biologically complex suspension models can be achieved through multicellular spheroids whereby diverse cell populations (cancer, stromal, immune) are intermixed to create more realistic physiologic cues and cellular interactions produced within the naturally occurring tumor microenvironment. Collectively, advantages of tumor spheroid models include high-throughput analysis (**Figure 4A**) and capacity for rapid scale up, while limitations of scaffold-free 3D spheroids include difficulty in studying more complex and dynamic processes such as angiogenesis, invasion, and metastasis. Based upon these characteristics and limitations, scaffold-free spheroid models are well-suited for preclinical anti-cancer drug screening, characterizing diffusion kinetics and drug resistance mechanisms, and unicellular responses including migration, spreading, ECM deposition, and soluble mediator secretions (133, 134).

Specific for OS, 3D culture systems with spheroids have been utilized for the past 2 decades for studying the effects of the tumor microenvironment on various aspects of OS biology and has been thoroughly summarized by De Luca et al. (135). Derived from these multiple investigations and relevant to therapeutic strategies specifically for OS metastasis, OS spheroids have shed illumination on drug resistance mechanisms to conventional chemotherapeutics (136–142), the maintenance of cancer stem cells and tumor-initiating cells (139, 143, 144), impact of ECM stiffness and composition on metastatic phenotype (145, 146), cues that promote vasculogenic mimicry (147, 148), and metastasis favoring pathways including the roles of specific transcription factors (NF-κB) (149, 150) and miRNAs (151). In addition, the feasibility of generating co-culture bicellular spheroids through the combination of HUVEC and MG-63 cells for the study of VEGF-mediated angiogenesis has recently been described (152).

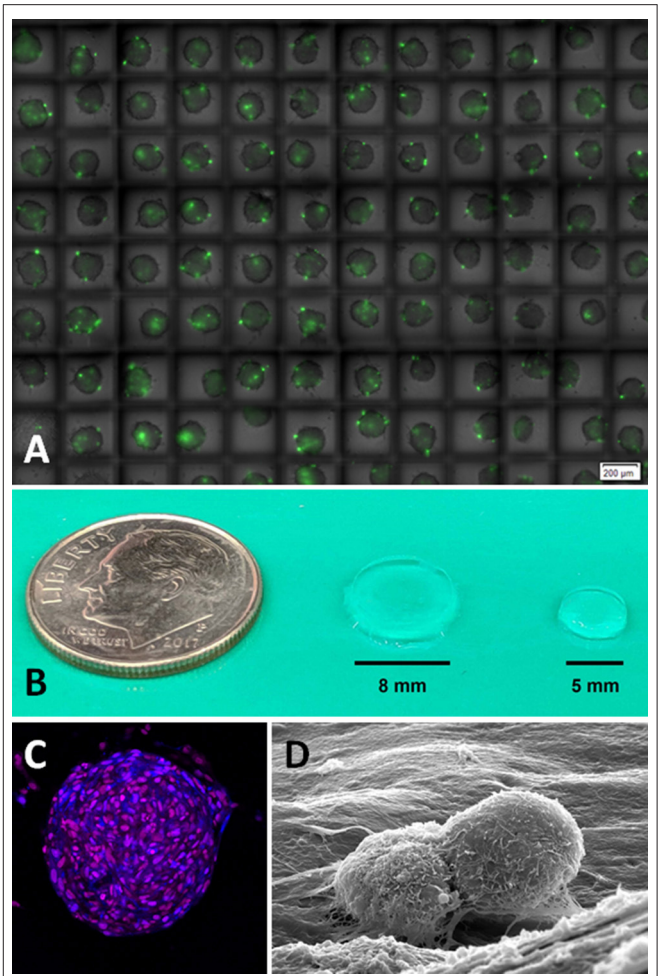

FIGURE 4 | (A) Glioblastoma spheroids in high throughput high-density hanging drop culture on a microchip. Method allows for the rapid screening of novel therapeutic agents in cancer cells growing in 3D whereby diffusional gradients and cell-cell interactions are more accurately recapitulated than 2D cell culture conditions (monolayer). Green dye (Celltox™ Promega) shows cell death after 24 h of culture (Image courtesy of Anurup Ganguli and Rashid Bashir, UIUC). **(B)** Relative size of hydrogel scaffolds for the study of **(C)** 3D glioblastoma spheroids by confocal fluorescent microscopy and associated **(D)** homotypic (cell-cell) and heterotypic (cell-ECM) interactions by scanning electron microscopy (Images courtesy of Emily Chen and Brendan Harley, UIUC). UIUC, University of Illinois at Urbana-Champaign.

Scaffold-Based 3D Models

The ECM is critical in shaping tumor biologic responses through mechanotransducive mechanisms, and the investigation of cancer cells embedded within scaffold-based constructs that vary in chemical composition, shape, density, structure, and porosity allows for researchers to dissect differential mechanotransductive contributions for the induction of diverse malignant phenotypes and cellular processes displayed by cancer cells. Scaffolds can be constructed from either natural or synthetic polymers, with both sharing conserved properties of biocompatibility and promotion of cellular adhesion. Natural scaffold materials are typical ECM proteins while synthetic scaffolds are derived from tunable and crosslinking materials including polyethylene glycol (PEG) and polylactide-co-glycolide acid (PLGA), as well as porous ceramic biomaterials such as bioactive hydroxyapatite and tricalcium phosphate.

Hydrogel scaffolds (**Figure 4B**), composed of natural or synthetic polymers, are widely used for studying biologic responses of cancer cells, as a gel medium mimics the natural *in vivo* microenvironment of nascent tumor mass growth in 3D (**Figure 4C**), whereby cell-to-cell and cell-to-matrix interactions are preserved for directing phenotypic behaviors including proliferation, migration, chemoresistance, and angiogenesis (153, 154). The most common biocompatible polymeric hydrogel materials include collagen type I, Matrigel, and alginate; and these natural materials facilitate cancer cell attachment through

heterotypic interactions via integrin receptors and ECM which regulate cell survival, growth, and differentiation (**Figure 4D**). In addition to natural biomolecules, synthetic constituents used for hydrogel formulation can include polyethylene glycol, polylactic acid, polyglycolic acid. By virtue of their chemistry, synthetic hydrogels have the advantage of being chemically tunable (stiffness, porosity, adhesion ligand density) via synthesis or crosslinking (155), and can recapitulate spatiotemporal changes in matrix heterogeneity encountered within the tumor microenvironment. Increasing sophistication of hydrogel-based models can be achieved through a combination of chemical engineering and biologic layering, including the construction of soluble mediator (growth factors, chemokines, peptidyl signaling molecules) gradients or combinatorial co-culturing of cancer cells with stromal cells including endothelial cells, fibroblasts, and immune cells. While hydrogels have been explored as a controlled drug release scaffold strategies for OS therapy (156–158), the study 3D scaffold tumor models for unraveling OS biology and metastasis remains limited, with some investigations describing differences in behavioral phenotype of malignant OS cells compared to non-transformed osteoblasts based upon matrix rigidity and elasticity (159, 160). In addition to hydrogel scaffolds, chitosan, silk, and synthetic polymers have served as adhesive constructs for 3D OS modeling and have illuminated mechanisms behind viral permissiveness (161), hypoxia-induced angiogenic mediator secretions (162), drug resistance (163), and maintenance of stem cell phenotype (164).

Microfluidic Platforms: Organ-on-a-Chip

While 3D spheroids with or without scaffolds provide valuable information on cell-cell and cell-ECM interactions, the static nature of nutrient and metabolic waste transport under typical 3D culture systems does not accurately replicate spatiotemporal diffusional gradients naturally formed from lymphatic or blood vessel formation within solid tumors. Microfluidic systems are precisely fabricated from molds and made of materials that are biocompatible, oxygen permeable, and tunable (stiffness, temperature, shear flow pressure, molecular gradients). Structurally, microfluidic systems can be fabricated to include diverse shapes on a micro- or nanoscale including channels and chambers with highly precise diameters, shapes, and flow control rates. When combined with 3D cell culture systems such as spheroids, microfluidic platforms can recapitulate diverse complex processes representing different stages of the cancer progression including tumor-vascular interface responses, diffusional effects of biomolecules on cell populations, and pathologic cancer processes including invasion, angiogenesis, and metastasis (165–170). Recently, specific metastasis-on-a-chip platforms have been fabricated allowing for real time tracking of fluorescently labeled cancer cells and their heterotypic interactions with both ECM and normal resident cells along the full continuum of the metastatic cascade (171, 172). Kong and colleagues recently reported the construction and use of a microfluidic platform for studying the organotropism of cancer cell metastasis and demonstrated the correlative value of their microfluidic system with athymic nude mice models for the evaluation of small molecule inhibiting anti-metastatic strategies (173). Specific for OS, 3D microfluidic platforms have been used to study OS cell adhesive properties under various physiologic conditions (pH, temperature, shear flow) (174), cell morphology in response to gradient molecules (175), and drug screening of nanoparticle encapsulated chemotherapeutics (176).

TABLE 2 | Druggable molecular targets in the metastatic cascade.

Step of the metastatic cascade	Actionable target(s)	Inhibitors	Inhibit lung metastasis in preclinical model? (cancer type)	References
Migration, intravasation	PAK1	IPA3	Yes (ESCC)	(13)
Intravasation	uPAR	SRSRY	Yes (OS)	(14)
Transit within blood	TDO2	680C91	Yes (BC)	(15)
	αvβ3	IH1062	Yes (Mel)	(16)
Extravasation	VCAM	α-VCAM Ab	Yes (Mel)	(17)
	α5β1	PHSCN	Yes (BC)	(18)
	CCR2	TC1-TSL	Yes (Mel, Col)	(19)
Lung colonization	GRP78	IT-139	Yes (OS)	(12)
	CDK12/13	THZ531	Yes (OS)	(20)
	BRD4	JQ1	Yes (OS)	(21)
	mTOR	Rapamycin	Yes (OS)	(22)
	Ezrin	NSC305787	Yes (OS)	(23)
		NSC668394	Yes (OS)	(23)
	HDACs	MS-275 (Entinostat)	Yes (OS)	(24)
	PKC	UCN-01	Yes (OS)	(25)
	IL-6ST	sc-144	Yes (OS)	(26)
	CXCR1/2	DF2156A	Yes (OS)	(26)
	PD-1/Lag-3/ NK activity	α-PD-1, α-Lag-3 Abs IL-2	Yes (BC)	(27)
Micrometastases	Cell surface-GRP78	BMTP-78	Yes (BC)	(11)
	PD-1	Anti-PD-1 mAb	Yes (OS)	(28)
Macrometastases*	Procaspase-3	PAC-1	Yes (OS)	(29)

**Studies using an animal protocol where treatment was given after establishment of lung metastases. OS, osteosarcoma; BC, breast cancer; Mel, melanoma; Col, colon cancer; ESCC, esophageal squamous cell carcinoma.*

Spontaneous and Immunocompetent Dog Model of Metastasis

Conventional OS models for studying experimental therapies most frequently are reliant upon xenogeneic and syngeneic transplant models conducted in mice, however, the inclusion of complementary model systems (CAM, PuMA, WHRIL, engineered 3D biomimetics) have gained wider appeal and scientific acceptance for improving predictive modeling of cancer biology and metastasis. While xenogeneic models, including patient derived xenografts, may provide information pertaining to the sensitivity of human OS tissues or cell lines to specific therapeutics, tumor-host interactions (especially immunobiologic responses) are poorly recapitulated in comparison to what occurs in people who develop OS spontaneously. Although syngeneic models more accurately represent immunologic tumor-host responses than xenogeneic systems, the process of tumor formation and spontaneous metastasis in any transplant model remains artificial, likely underestimating the complexity for how OS naturally progresses

in an immunocompetent host. To accurately identify and expedite the clinical translation of novel therapeutics to people with metastatic OS, the evaluation of experimental strategies, in particular immune-based, should be conducted in the most highly relevant and immunocompetent tumor model.

Besides people, canines are the only other large mammal that spontaneously develops OS with substantive frequency. Canine appendicular OS is the most common primary bone tumor in dogs of large to giant skeletal size, and has been estimated to affect at least 10,000 pet dogs every year in North America (58), which is 10 times greater than the number of pediatric OS patients diagnosed annually in the United States. The clinical presentation, biologic behavior, natural disease progression, and genetic signature of OS in dogs is similar to people (177–179), and collectively emphasizes the comparative relevance of dogs to serve as a model system for both discovery and therapeutic investigations (180–184). This modeling strategy has been advocated by leaders in the field of OS basic science and clinical research, and ascribes value on the inclusion of pet dogs with OS as a distinctively informative model system for prioritizing novel therapeutic agents that target metastatic progression (8).

STANDARD OF CARE AND THE UNMET NEED FOR NEW ANTI-METASTATIC THERAPIES

The current standard of care for human patients diagnosed with OS remains largely unchanged from that first used in the early 1980s (185), being neoadjuvant and adjuvant MAP chemotherapy (methotrexate, doxorubicin, cisplatin) together with aggressive local control by surgical excision (186). Building on techniques pioneered in pet dogs with OS (187, 188), most human patients diagnosed today benefit from limb salvage reconstructive techniques that preserve limb function. With these standard of care therapies, outcomes for patients with localized disease increased markedly, such that up to 60% of patients experience "cure" (5-year event-free survival) (189). However, these outcomes have changed little over the last four decades (190).

The factor that most strongly influences outcomes in human patients is the presence or absence of metastatic lesions, usually of the lung parenchyma. Patients who develop lung metastases, whether at diagnosis or years after completing therapy, face a dismal prognosis, with fewer than one in five patients surviving more than 5 years beyond this event (189, 191). Multiple efforts to improve this outcome through intensification of systemic therapy or the introduction of novel regimens have not succeeded.

Patients with both resectable and unresectable metastatic disease at relapse are usually offered systemic therapy, most commonly with high dose ifosfamide (192) or multi-tyrosine kinase inhibitors (193). Although these therapies do little to effect long-term outcomes, they can facilitate short-term disease control and prolong survival. While radiation has a relatively minor role in the curative care of patients with either localized or metastatic disease, modern techniques can be extremely helpful in the palliative setting, providing excellent disease and symptom control (194). The only intervention proven to offer hope for long-term "cure" of disease in patients with metastases remains surgical excision of all macrometastases, and several studies suggest that up to 30% of patients who achieve complete surgical remission will survive disease-free beyond 5 years (195–197).

NOVEL THERAPEUTIC STRATEGIES FOR COMBATING PULMONARY METASTASES

Tumor-Specific Molecular Vulnerabilities

As mentioned previously, each step of the metastatic cascade is a rate limiting step. For example, if a new drug can prevent OS cells from leaving the primary tumor, invading local tissue, or entering local blood vessels, then the metastatic cascade is stopped in its tracks. Indeed, every step of the metastatic cascade harbors several druggable targets in various types of cancer, as summarized in **Table 2**. In the clinical setting, however, it is presumed that patients with localized tumors already have subclinical micrometastatic disease in the lung. Thus, targeted therapies that act within the microenvironment of the primary tumor may not necessarily be effective on tumor cells have already spread to the lung since adaptation strategies depend on the particular microenvironment the tumor cells reside. In this scenario, therapeutic strategies that target the processes involved in lung colonization and micrometastases formation would be expected to be most effective in delaying metastatic progression. Further basic research into the molecular pathways underpinning OS lung colonization, micrometastases formation, and the establishment of macrometastases is needed to uncover more actionable targets.

Targeting the Tumor Microenvironment

Successful dissemination and colonization of distant tissues by a tumor cell requires navigating a gauntlet of interactions with normal cells and associated tissues (114). Each interaction can either help or hurt that cancer cell's chance of survival. The striking tropism that OS displays for lung tissues suggests that tumor cells elicit or receive signals from cells within the lung metastatic niche that facilitate their survival. Several emerging studies have defined characteristics of that environment that might support tumor growth, many of which constitute targetable vulnerabilities, including pathways that promote dormancy, alter susceptibility to chemotherapy, facilitate metastatic outgrowth, and the maintenance of stemness.

Stromal elements produced by both host cells and tumor cells may play a particular role in the survival of metastasis-initiating cells and in the maintenance of their stem-like features. Zhang and colleagues recently showed that FGF signaling within the metastatic environment triggers a fibrogenic program within disseminated tumor cells that promotes their stemness and survival (198). Signals transduced by way of mTOR complex 1 initiate this program, although the subsequent production of fibronectin by OS cells can then maintain this stem-like state independent of host signals, including FGF. These studies stop short of testing the therapeutic

potential of targeting these pathways, but existing agents should facilitate future assessment of their capacity to affect disease progression, most likely in preventing emergence of late metastases.

The laboratories of Roberts and Cam have identified targetable bi-directional signaling between OS cells and lung epithelial cells that appears critical for metastatic colonization. Using a combination of human tissues, xenografts, syngeneic mouse models, and canine models of disease, they have shown how a ΔNp63/IL6/CXCL8 signaling axis mediates tumor-host signaling events critical to the metastatic process. In their model, tumor cells primed by aberrant expression of ΔNp63 (112) (an alternative isoform of the p53 family member TP63) respond to signals from lung epithelial cells by producing high levels of IL6 and CXCL8 (199). Disruption of these cytokine/chemokine signals effectively reduced metastasis formation. Indeed, more than 80% of mice treated with inhibitors of both IL6 and CXCL8 signaling survived long term, while 100% of mice bearing the same tumors succumbed to metastatic disease (26). Interestingly, this antimetastatic effect was only achieved with combination therapy. Mice treated with one or the other inhibitor showed only modest inhibition of metastasis, suggesting some signaling pathway redundancies that remains undefined. Unfortunately, inhibitors that proved effective in their models are unlikely to be developed clinically. Work aimed at identifying critical signaling nodes up- or down- stream of these pathways may identify targets that are more effective and druggable with small molecule inhibitors well-suited for clinical implementation.

Signals that facilitate tumor cell survival within the metastatic niche can emerge from either lung-resident cells or from cells that invade that niche, often in response to tumor-derived signals. For example, Baglio and colleagues have shown that TGFβ expressed on the surface of extracellular vesicles from OS cells can also elicit production of large amounts of IL6 by mesenchymal stem cells (200). The release of this cytokine into the metastatic niche triggers activation of STAT3 within the tumor cells, which promoted proliferation of those metastatic cells in their models. In evaluating the therapeutic relevance of this phenomenon, they showed that the administration of anti-IL6 antibodies reduced the number of metastatic lesions that formed in their animals (200).

Some tumor-host interactions prove detrimental to the survival of disseminated tumor cells. Kleinerman's group has made a series of observations that suggest most disseminated tumor cells that reach the lung will be eliminated through activation of a suicide signal when the FAS receptor expressed on the surface of the tumor cells engages FAS ligand, which is expressed constitutively within the lung (201). This phenomenon results in the selection of a subpopulation of tumor cells that are FAS-negative (202). Interestingly, they have shown that FAS downregulation within this subset of malignant cells can be reversed, as exposure to inhaled gemcitabine drives re-expression of the FAS receptor, engaging the death-inducing signaling complex and triggering apoptosis (203). Such therapies have yet to be tested clinically in pediatric OS patients but seem viable. As proof-of-concept, a study by Rodriguez and colleagues demonstrated that pet dogs with macrometastatic pulmonary OS receiving treatment with aerosolized gemcitabine did result in the upregulation of FAS receptor and markers of cell death by OS cells within pulmonary metastatic lesions (204).

Searching for epigenetic changes that facilitate metastatic colonization of lung tissue by OS cells, Morrow and colleagues recently identified genetic loci that acquire enhancer activity in cells with high metastatic potential (21). Among genes regulated by these metastatic variant enhancer loci, Factor 3 (F3, a gene which can activate blood clotting) demonstrated particular importance for metastasis when evaluated functionally. Disruption of F3 production by OS cells significantly impeded metastatic colonization efficiency in animal models but did not affect primary tumor growth (21). Interestingly, the importance of blood clotting for lung colonization in OS may have been suggested in previous work, lending credence to these findings (205, 206). While this target has not been evaluated in a therapeutic setting, F3 signaling (which triggers both clotting and intracellular signal cascades) should be targetable using existing, FDA-approved drugs (207).

Potential Metabolic Vulnerabilities of OS

The unique metabolic demands of the primary tumor vs. metastasis are reflective of their different microenvironments (cellular and extracellular components), nutritional availabilities, and level of oxygenation. A rapidly growing primary tumor mass requires a constant supply of energy (ATP) and biomacromolecules (lipids, carbohydrates, and proteins) (208). During glycolysis in normal cells, ATP is obtained from glucose via the oxidation of its carbon bonds through mitochondrial respiration, a process which also requires oxygen. However in cancer cells, the glycolytic intermediate pyruvate is shuttled away from the tricarboxylic acid cycle, and is fermented into lactic acid, even in the presence or absence of oxygen—a phenomenon called the Warburg effect; and several theories on how the Warburg effect might benefit proliferating cancer cells has been discussed elsewhere (209). Not surprisingly, subversion of the Warburg effect has been observed in several OS cell lines such as LM7 and 143B (210). Furthermore in a preclinical mouse model, Hua and colleagues demonstrated LM8 tumor-bearing mice had elevated levels of serum pyruvic acid and lactic acid compared to healthy controls, which suggested that proliferating OS tumor cells were highly glycolytic. The serum from tumor-bearing mice also had higher levels of intermediate metabolites of the tricarboxylic acid cycle compared to healthy controls, further underscoring the higher energy demands of proliferating OS cells within localized and metastatic sites (211). Interestingly, the majority of circulating metabolites in serum were lowest at initial primary tumor formation (week 1) and again at metastatic progression (week 4) following LM8 inoculation, which could suggest that similar global metabolic transformation mechanisms were shared by OS cells during incipient primary tumor growth and distant metastases development. Mechanistically, Hua and colleagues suggested that the unexpected lower metabolic profile in tumor-bearing mice identified at week 4 (metastatic progression) may be due to tumor microenvironmental

hypoxia that restricted OS cell growth and reduced cellular metabolism, although this possibility wasn't confirmed in their study (211).

Surviving in the lung microenvironment presents a unique set of metabolic challenges that are distinct from the primary tumor. As mentioned previously, redox stress appears to be a major microenvironmental stressor in the lung. Reactive oxidative species (ROS) and reactive nitrogen species (RNS) produced by the lung parenchyma can affect tumor cell mitochondrial function in a number of ways (58, 212). For example, it is generally known that excess ROS, such as superoxide (O_2^-), can modify mitochondrial DNA, which in turn, can negatively affect the electron transport chain (ETC), mitochondrial membrane potential, and ATP production (213). Prolonged exposure to RNS such NO^- can irreversibly inhibit complex I of the ETC (214). Peroxynitrite ($ONOO^-$), another potent RNS, can inhibit multiple enzymes in the mitochondria such as complexes I–IV, as well as aconitase of the tricarboxylic acid cycle (214). Metabolic adaptation to such oxidative stress would be a pro-survival phenotype that would be selected for during the colonization process, and not surprisingly, anti-oxidant responses which consists of either the upregulation of redox-related enzymes or altered glutathione (GSH) metabolism have been observed in metastatic breast (63), melanoma (61), and osteosarcoma (21, 215). For example, Ren and colleagues have found that metabolites in the GSH metabolic pathway were found to be significantly altered in highly metastatic OS cells compared to their clonally related, low metastatic counterparts (215). Shuttling of metabolites into the GSH pathway is important for producing GSH, which in turn, react with and neutralize ROS and RNS to form less reactive intermediates (216, 217). Other metabolic pathways that were found to be altered in highly metastatic OS cells include arginine, inositol, and lipid metabolic pathways. The previously mentioned study by Hua and colleagues found that serum metabolites of lipid metabolism were found to be elevated in mice with lung metastases compared to tumor-bearing mice with no metastases (211). These observations noted by Hua and colleagues in a mouse model of OS are congruent with global lipidomic studies identifying differences between metastatic (143B) and non-metastatic (HOS) human OS cell lines (218), as well as the recognized importance of lipid metabolism in cancer metastases (219). Collectively, derived from preclinical studies inclusive of cell lines and murine models of cancer, evidence supports altered lipid metabolism being important for metastasis progression; where increased lipid production may address the heightened demand for membrane synthesis during cell growth and organelle biogenesis. As such, targeting unique metabolic demands of metastasis offers a new avenue of anti-metastatic therapy. Indeed, Ren and colleagues demonstrated that targeting the inositol metabolism of metastatic OS cells prevented their growth in the lung microenvironment (215). Further studies are needed to elucidate whether other metabolic susceptibilities exist in metastatic OS, and whether these metabolic susceptibilities can be exploited for new therapeutics.

Leveraging the Immune System to Combat OS Metastases

Recently, immunotherapy has been heralded as a breakthrough for the management of diverse liquid and solid tumors, and its ascension as a major therapeutic pillar is underscored by a rapidly increasing number of FDA approved immune-based treatments for cancers that are resistant to conventional modalities. The anticancer activities of immunotherapies can be ascribed to the cooperative effector functions exerted by both the innate and adaptive immune arms, and while immunotherapy is highly effective for certain solid tumors like melanoma, renal cell carcinoma, and others, its promise for benefiting patients diagnosed with metastatic OS remains largely disappointing to date (220–223). Paradoxically, there is convincing evidence that OS can be recognized by trafficking immunocytes, yet successful exploitation of immunotherapeutic strategies remains elusive. To accelerate the clinical deployment of effective antitumor immune approaches for combating OS, recent scientific investigations have focused on characterizing the quantity, phenotype, dynamics, and functional nature of immune cells that infiltrate into primary and metastatic OS lesions, and these collective findings have been recently and thoroughly summarized (223, 224).

By way of detailed analyses, several innate and adaptive immunocytes have been identified to putatively participate in the initiation or suppression of anti-OS immune responses and include a plethora of diverse myeloid and lymphoid cell types. Of the various immunocytes identified within the OS microenvironment, both innate affector and adaptive effector populations have been characterized, and include antigen-presenting cells (macrophages/dendritic cells) and T lymphocytes, respectively. Within primary OS lesions, tumor-associated macrophages (TAMs) that can be distinguished via genomic signatures, cell surface markers, and functional activities (inflammation vs. immunosuppression) have received considerable attention for their prognostic value and functional role in OS metastasis (225–230). Most, but not all, investigations have identified that increases in TAMs (quantity) or macrophage infiltrate profiles (quality) favoring a M1-subtype polarization ($INOS^+$; pro-inflammatory) rather than a M2-subtype profile ($CD163^+$; immunosuppressive) are associated with better overall survival in OS patients. Incongruent findings among studies regarding the role of TAMs in OS biology could be related to the inherent limitations of single timepoint tissue assessments which fail to capture the dynamic nature of immune cell infiltration within the tumor microenvironment. Nonetheless, the majority of histologic findings provide supportive justification to therapeutically manipulate TAMs profiles within OS lesions that have potential to either favor immune activation (Mifamurtide) (231) or inhibit M2-macrophage polarization (ATRA) (232, 233), for the intended purpose of inhibiting metastatic progression.

Complementing the participatory role of TAMs, several studies have focused on characterizing tumor infiltrating lymphocytes (TILs) and their contribution to metastasis immunobiology. Analyses of TILs within the OS microenvironment have shown that both effector and

suppressor T lymphocyte ($CD3^+$) phenotypes participate in shaping immunosurveillance of OS lesions (229, 230, 234–236). Furthermore, several studies suggest that the density (number) or phenotype (activated or exhausted) of effector TILs within OS primary tumors correlate with prognosis. With regards to TILs density, recent studies have demonstrated that increases in the absolute number of $CD8^+$ TILs or the ratio of $CD8^+/Foxp3^+$ TILs significantly correlate with improved overall survival (230, 234). Provocatively, the functional relevance of TILs and operative checkpoint blockade mechanisms might be especially important for metastases, as some studies have found the density of TILs to be enriched in metastatic lesions compared to primary tumors (236, 237). Despite the presence of TILs within OS lesions, several studies suggest that the activity of effector TILs might be attenuated, as supported by the expression of exhaustion markers (PD-1, CTLA-4, Tim3) by TILs and/or tumoral microenvironmental expression of PD-L1 (227–229, 235–237). Collectively, these detailed studies strongly suggest that OS lesions can be effectively infiltrated by T lymphocytes, and that therapeutic modulation of checkpoint blockade strategies could improve TILs effector capabilities.

With a basal understanding for the collection of immunocytes that are present within primary tumor and metastatic OS lesions, rational design of immunotherapeutic interventions can be constructed. Through these concerted efforts, the scientific and clinical oncology community can continue to forge toward understanding fundamental anticancer immune mechanisms and improving treatment outcomes in patients with OS metastases through diverse immunologic strategies, either singly or in combination with conventional therapies (radiochemotherapy).

Immune Modulators

Immunomodulatory agents modify immune responses by amplifying the recognition of cancer cells (immunostimulation) or by attenuating the immunosuppressive activities exerted by cancer cells within the local tumor microenvironment. The innate arm of the immune system comprised of natural killer cells, macrophages, dendritic cells, and primordial T cell subsets (natural killer and γδ) are predominant effector targets of immunomodulatory strategies. The clinical significance of immunomodulatory interventions relevant to sarcomas was noted over a century ago, when William Coley in 1891 reported objective responses in a small minority (10%) of patients with non-resectable sarcomas (bone and soft tissue) treated with heat-inactivated *Streptococcus pyogenes* and *Serratia marcescens* injections, termed Coley's toxin (238). The potent anticancer activities induced by bacterial products noted by Coley have been corroborated in both canine and human OS patients that develop surgical site infections (188, 239, 240), and mechanistically these favorable immunologic effects have been attributed to toll-like receptor activation with consequent amplified macrophage and natural killer cell effector functions in mouse models of OS (241).

The clinical translation of immunomodulatory agents which stimulate the innate immune arm for improving outcomes in OS patients remain limited, but include liposome-encapsulated muramyl tripeptide phosphatidylethanolamine (L-MTP-PE) and cytokine-based therapies. Based upon its mechanism *in vitro* and in preclinical investigations for activating monocytes and macrophage to a tumoricidal state (242, 243), as well as its unique evaluation singly or in combination with cisplatin in pet dogs with OS (243, 244), clinical investigations of MTP-based strategies have been conducted prospectively by the Children's Oncology Group consortium. In a seminal study by Meyers and colleagues, the addition of MTP to a MAP (methotrexate, doxorubicin, cisplatin) backbone in patients with localized OS significantly improved 6-year overall survival rate from 70 to 78% (245). Additionally in the setting of metastatic and/or recurrent OS, the 5-year event free survival rate of patients receiving chemotherapy alone (26%) vs. chemotherapy with L-MTP-PE (42%) appeared favorable (246), further supporting the clinical benefit of this immunomodulatory strategy for delaying the natural progression of OS pulmonary metastases. Complementing the mechanism of L-MTP-PE, exogenous cytokine therapies have also produced marginal improvements in patients diagnosed with OS. In particular, INF-α-2b and IL-2 have been evaluated in the adjuvant setting with either chemotherapy or other immune-based strategies. Recently, the 3-year event free survival benefit derived from adjuvant pegylated INF-α-2b with MAP has been described in a large consortium trial (EURAMOS-1) (247). While early results have not demonstrated significant improvements in event free survival between MAP alone (81%) vs. MAP with adjuvant pegylated INF-α-2b (84%), long term follow up remains active and will ultimately determine if adjuvant pegylated INF-α-2b has any definitive immune activating role for improving the control of OS micrometastases.

In the setting of macroscopic OS metastases, the tolerability and potential benefit exerted by exogenous IL-2 has been explored. In one study, Meazza and colleagues reported the outcomes of 35 pediatric OS patients with macroscopic OS treated with surgery and combinatorial chemoimmunotherapy comprised of IL-2, MAP, ifosfamide, and lymphokine-activated killer (LAK) cell infusion. While the study was not designed to determine the immunobiologic benefit derived from IL-2 and LAK cell infusion, adverse effects associated with IL-2 therapy were tolerable (grade I and II) with most common side effects being fever, flu-like symptoms, hypotension, and cytokine release syndrome (248). In a different study, Schwinger and colleagues reported the tolerability and activity of single-agent, high-dose IV IL-2 therapy in 10 pediatric patients, in which 4 adolescents had metastatic OS (249). While 2 of 4 OS patients achieved complete remission for 14 and 42 months in duration, systemic toxicity associated with high-dose IV IL-2 therapy was significant with 60–100% of treated patients experience some form of grade III or IV clinical toxicity (fatigue, anorexia, or diarrhea). Despite the high level of toxicity, this study clearly demonstrated the potential for IL-2 to amplify anticancer immune responses sufficient to regress macroscopic OS burdens. In attempts to reduce the toxicity associated with systemic IL-2, yet maintain favorable anticancer immune activities within the anatomic site of metastases (lungs), two significant studies have been conducted in pet dogs with pulmonary metastatic

OS, which leverage innovative drug delivery or site-specific gene transducing strategies. Khanna and colleagues evaluated the feasibility and activity of aerosolizing liposome encapsulating IL-2 in pet dogs and demonstrated that robust anticancer immune effects could be induced within the pulmonary parenchyma sufficient to cytoreduce macroscopic OS burdens (2 of 4, CR) without significant toxicity (250). A complementary study reported by Dow and colleagues investigated the activity of intravenously administered liposome-DNA complexes (LDC) encoding the IL-2 gene in dogs with macroscopic OS metastases (251). Infusions of LDC was well-tolerated, generated systemic immune activation, and transgene IL-2 expression within the lung parenchyma. Furthermore, objective cytoreductive activities (2 PR, 1 CR) were achieved in three of 20 dogs treated.

Monoclonal Antibodies

The engineering of monoclonal antibodies to enhance the immune system's attack on cancer cells has dramatically expanded therapeutic options for multiple hematopoietic and solid tumor histologies, and currently over a dozen antibodies have received FDA approval for treating different cancers (252). Upon binding to their cognate epitope, monoclonal antibodies exert anticancer activities through various methods including direct cell killing, immune-mediated cell killing (phagocytosis, complement activation, or antibody-dependent cellular cytotoxicity), or disruption of the tumor microenvironment through vascular and stromal cell ablation. While widely instituted and capable of dramatically improving survival outcomes in patients diagnosed with specific forms of hematopoietic cancers, the clinical impact of monoclonal antibodies remains more limited for solid tumors, and almost non-existent in aggressive sarcomas. In part, the restricted application of monoclonal antibodies for OS metastases therapy is driven by the limited expression of extracellular membrane epitopes, as underscored in the study reported by Ebb and colleagues whereby adjuvant trastuzumab (HER2 targeting antibody) combined with chemotherapy failed to improve outcomes in patients diagnosed with metastatic OS (253). Nonetheless, several OS expressing epitopes remain a focus of interest for improving the management of OS metastases, and include GD2, GPNMB, and RANKL (254–257). In particular, GD2 as a surface epitope on OS cells continues to be an actively explored target with several ongoing clinical trials evaluating various anti-GD2 antibody strategies.

In addition to monoclonal antibodies that target OS cells, considerable focus has been on manipulating tumor-specific or tumor microenvironmental (TME) cues with antibody strategies, specifically enhancing the quantity and quality of intratumoral infiltration with immune cell populations through blockade of checkpoint signaling (258). Checkpoint blocking antibodies have been a breakthrough for the management of diverse cancer types including melanoma, non-small cell lung cancer, renal cell carcinoma, bladder cancer, and head and neck cancers. For these collective solid tumors, blockade of immune checkpoints, including CTLA-4, PD-1, and PD-L1, with antibodies have provided life-saving anticancer activities to a subset of patients who would otherwise experience disease progression and death. While several pieces of basic and clinical evidence support the potential benefit of checkpoint inhibition for the treatment of OS metastases including mutational burden, neoantigen load, overexpression of PD-L1 by OS cells and tissue samples, and preclinical activity of checkpoint inhibition in mouse models of metastatic OS (259–262), the clinical activity of single- or combined- checkpoint blockade in treating patients with advanced OS have been largely unfavorable, with objective response rates (CR or PR) ranging from 0 to 5% (NCT011445379, Ipilimumab; NCT02500797 [Alliance A091401], Nivolumab + Ipilimumab; NCT02301039 [SARC028], Pembrolizumab) (263). Given these initial disappointing results, combination therapies have been proposed whereby small molecule agents (Nab-rapamycin, apatinib, axitinib) that target multiple signaling pathways (mTOR, VEGFR1, VEGFR2, PDGFRβ, c-kit) should be combined with checkpoint blockade antibodies in hopes of improving response rates (264).

Vaccines

Tumor vaccines are an active form of immunotherapy in which robust adaptive immunity is developed and cytotoxic T lymphocytes are generated for recognizing and killing cancer cells. The induction of antitumor responses against known or unidentified tumor antigens can be achieved through vaccine strategies inclusive of whole cells, lysates, proteins, DNA, RNA, or peptides. For vaccine strategies to be effective, dendritic cells must present tumor peptides within major histocompatibility complexes, as well as costimulatory signals, to fully activate the effector functions of cytotoxic T lymphocytes. Given the key role of dendritic cells for initiating the activation and proliferation of cytotoxic T lymphocytes with anticancer effector functions, dendritic cell vaccines have been explored in patients with metastatic OS through the conductance of two recent clinical studies (265, 266). Miwa and colleagues evaluated 14 patients with recurrent and/or metastatic OS who were treated with 6 weekly subcutaneous vaccinations with autologous dendritic cells pulsed with autologous tumor lysate, TNFα, and OK-432 (265). While treated patients did demonstrate systemic immune activation represented by increases in circulating INFγ and IL-12, none of the OS patients achieved an objective response to dendritic vaccination alone. These negative findings were consistent with an earlier study in which Himoudi and colleagues evaluated 13 patients with relapsing OS treated with intradermal vaccines of autologous dendritic cells matured with autologous tumor lysate and keyhole limpet hemocyanin (266). While the vaccination protocol was well-tolerated, tumor-specific immune activation assessed by the identification of INFγ secreting T cells (ELISPOT) was only observed in 3 patients, and none of the OS patients experience any measurable reduction in macroscopic tumor burden. In light of these initial disappointing studies with dendritic cell vaccination in OS patients, ongoing efforts are focusing on innovative combinatorial strategies to boost OS cell antigen expression, as well as attenuate the localized immunosuppression associated with the tumor microenvironment.

Recently, a vaccine strategy based upon the intravenous infusion of a genetically modified, live attenuated *Listeria*

monocytogenes which expresses three immunodominant epitopes of HER2 has been evaluated for in patients with HER2-expressing solid tumors (NCT02386501). This vaccine construct (ADXS31-164) was granted Fast Track designation by the FDA for treatment of patients with newly diagnosed, non-metastatic, surgically-resectable OS, and patients will be treated with this vaccine strategy through the Children's Oncology Group consortium. As a predecessor to the pediatric trial, ADXS31-164 was piloted in pet dogs with OS and provided valuable translational information. Mason and colleagues demonstrated that treatment with ADXS31-164 induced HER2-specific immunity in 15/18 dogs and resulted in a significant increase in median disease-free interval (615 days) and median survival (956 days) when compared to a historical control group. Overall survival rates at 1, 2, and 3 years for dogs treated with ADXS31-164 were 78, 61, and 50%, respectively (267).

Adoptive Cell Therapies

Adoptive cellular therapies involve the direct administration of either innate (natural killer cells) or adaptive (cytotoxic T lymphocytes) immune effector cell populations that have been genetically manipulated. The infusion of cellular therapies, specifically cytotoxic T lymphocytes into tumor-bearing patients, circumvents the reliance of vaccine strategies to successfully active a large population of tumor-specific effector lymphocytes in the recipient host. For T-cell based strategies, adoptive cell therapies rely upon the genetic engineering of T lymphocytes to either express a known T cell receptor (transgenic TCR) or chimeric antigen receptor (CAR), with both strategies resulting in the production of T cells with defined specificity, which can be MHC-restricted (transgenic TCR) or -unrestricted (CAR). While CAR technology has clinically impacted the management of hematopoietic cancers such as acute lymphoblastic leukemia and diffuse large B-cell lymphoma, the application of CARs for effectively treating OS metastases remains incompletely defined. Recently, the results of a phase I/II clinical study evaluating the tolerability and activity of HER2-CAR T cells were reported by Ahmed and colleagues. In this study, 16 patients with recurrent and/or metastatic OS were treated with escalating intravenous doses of T cells expressing an HER2-specific CAR with CD28ζ signaling domain (268). Treatment with HER2-CAR T cells was tolerable and induced systemic inflammatory responses represented by elevations of circulating IL-8. Additionally, following infusion persistence of HER2-CAR T cells in circulation could be demonstrate, as well as their trafficking to tumor sites. However, the clinical impact of HER2-CAR T cells was marginal, with three OS patients experiencing stable disease lasting 12-15 weeks, and the remainder of patients having disease progression. While initial results with CAR T cells have yet to meaningfully impact outcomes in metastatic OS patients, strong enthusiasm exists for the continued exploration of additional adoptive cell therapies that include anti-GD2 CAR T cells, natural killer cells, transgenic TCR cells, and γδ T cells.

The development and clinical assessment of adoptive cell therapies have been piloted in canine OS, providing valuable preclinical data regarding feasibility and activity. For CAR T cells, HER2 has also been explored as a target for canine OS, and Mata and colleagues reported the successful development of HER2-CAR T cells that killed HER2+ canine OS cell lines in an antigen dependent manner (269). Additionally, combining radiation and immunotherapy has been recently explored in a first-in-dog trial of autologous natural killer (NK) adoptive cell therapy (270). In this study, OS-bearing dogs were treated with a coarsely fractionated radiation protocol consisting of 9 Gy once weekly for 4 treatments, with NK cells being harvested and expanded *ex vivo*, and then delivered back to dogs by intratumoral injection following the completion of radiation therapy. Of the 10 dogs treated, 5 remained metastasis-free at 6 months, and one had regression of a suspicious pulmonary nodule detected at the time of diagnosis. While preliminary in nature, these studies in canine OS provide the underpinnings to prospectively evaluate different combinatorial strategies inclusive of adoptive cell therapies for combating OS metastatic progression.

RELEVANCE OF PET DOGS FOR REALIZING NOVEL OS METASTASES THERAPEUTICS

In order for animal models of human pathologies to be useful and informative, it is necessary for the experimental system to be readily available and accurately recapitulate the natural course of disease. For OS, where the genetic underpinnings are chaotic and the etiopathogenesis remains elusive, the creation of experimental model systems becomes fundamentally difficult, and potentially flawed; as the blueprint of models are derived from and constructed upon current understandings of disease processes. Pet dogs that spontaneously develop OS have potential to serve as excellent naturally-occurring models for diverse comparative pathologies, including OS. Through collaborative research efforts, canine OS can be uniquely positioned in the scientific discovery pathway for understanding metastasis biology, which can drive and accelerate the identification of new promising anti-metastatic therapies. Several characteristics of canine OS are noteworthy and with the continued inclusion and future innovative addition of pet dogs as comparative OS models, it would be expected that significant progress will be made toward improving the outcomes of patients diagnosed with OS metastases.

Abundance, Accelerated Natural Disease Course, and Limited Cure Rate

Pediatric OS, by definition is categorized as a rare tumor (<15 cases per 100,000 people per year). For localized OS, surgery and MAP chemotherapy in pediatric patients produces 5-year event free survival in the majority (60–70%) of patients treated. In this good responder population with favorable histologic Huvos grade, the opportunity to clinically evaluate and realize the anti-metastatic activity of novel therapies is narrow and temporally protracted. While patients with recurrent and/or metastatic OS can be readily included for investigating novel therapies, biologic responses to experimental agents might differ between macro- and microscopic disease settings, and confound

the accurate identification of new agents with reproducible anti-metastatic properties.

Canine OS is the most common primary bone tumor in large and giant breed dogs, and has been estimated to affect at least 10,000 pet dogs every year in North America (271), which is a log order greater than the number of pediatric OS patients diagnosed annually in the United States (800–1,000 new cases/year). Conventional treatment with surgery and chemotherapy improves outcomes in affected dogs, producing a median survival time of ∼9 months (272). However, even in treated dogs, death as a result of metastatic progression occurs in 85–90% of patients within 2-years of diagnosis. While these statistics for canine OS are sobering, when viewed through the lens of comparative oncology, pet dogs offer an unprecedented opportunity to be included in the evaluation and translation of new anti-metastatic agents. Ultimately, through their purposeful inclusion in drug assessment, pet dogs can accelerate the identification of new agents which hold promise to improve long term outcomes in both humans and canines diagnosed with metastatic OS.

Comparable Anatomic-Sized Tumor Burdens and Laws of Diffusion

Despite their accepted research value, some limitations of murine models remain irreconcilable including the $>10^3$ difference in anatomic size between mice (20 g) and humans (70 kg). Specifically for the evaluation of novel drugs or drug delivery strategies for combating OS metastatic progression, differences in anatomic size and corresponding dimensions of metastatic lesions can strongly bias treatment outcomes simply as a function of tumor volume and interstitial pressures, as therapeutics released into the pulmonary parenchyma are still governed by the physical laws of diffusion prior to reaching their intended targets, being OS metastatic foci. Fick's law of diffusion states that the rate of movement (mass flux) can be modeled mathematically by the following equation:

$$\mathbf{J} = -\mathbf{D}^* \, \Delta\mathbf{C}/\Delta\mathbf{x}$$

Where **J** represents mass flux, **D** represents molecular diffusivity of a specific therapeutic agent within a microenvironment, **ΔC** represents the change in concentration gradients, and **Δx** represents distance of diffusion. Although several determinants influence mass flux **J** (representing the movement of therapeutic agents), diffusional distances within a chosen experimental system directly affects the movement rates of therapeutics, thereby having the potential to either positively (small anatomic size and limited diffusion distances) or negatively (large anatomic size and expansive diffusion distances) bias treatment outcomes. As such, drugs that demonstrate potent activity in murine models of OS metastasis can be partially attributed to the diminutive diffusion distances required to be traversed by therapeutic agents. However, when translated to larger mammals including human or canine OS patients, where diffusion distances are log orders greater, achieving therapeutic response becomes more difficult (158), if not impossible as governed by the laws of diffusion. Governed by physical laws of diffusion, studies investigating novel therapies for OS metastases would be most predictive when evaluated in tumor model systems which most closely approximate anatomic sizes at both the organism (human) and target (OS metastases) levels. Under these assumptions, dogs with OS can serve as excellent comparative models for pediatric OS given comparable size in body mass and metastatic tumor burdens (**Figures 5A–D**) as occurs in both adolescents and giant breed dogs.

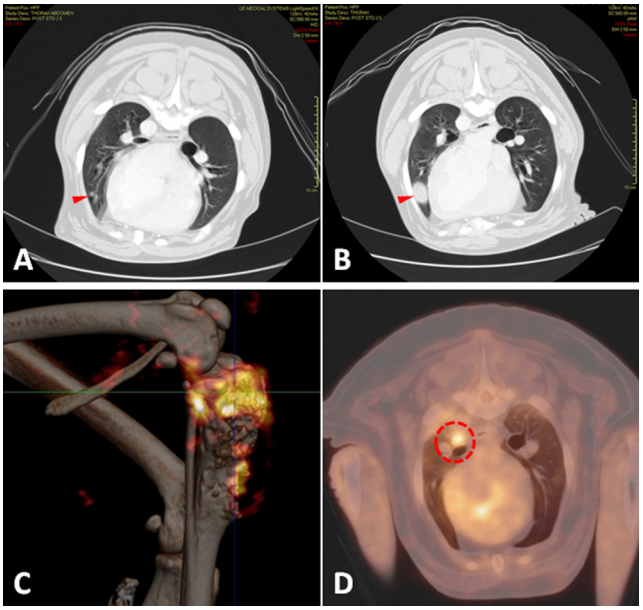

FIGURE 5 | Radiologic assessment and relevance of comparable anatomic size and metabolic activity of OS tumors arising in pet dogs. **(A)** Early detection of emerging pulmonary metastatic lesion (red arrowhead) with **(B)** subsequent rapid macroscopic growth (red arrowhead) over a period of 8 weeks documented by serial CT imaging. Metabolic activity of **(C)** primary bone OS (Image courtesy of Kim Selting, UIUC) and **(D)** pulmonary metastases (Image courtesy of Lynn Griffin, Colorado State University) using PET/CT imaging in pet dogs with OS. UIUC, University of Illinois at Urbana-Champaign.

Natural Evolution and Immune Competency

The natural development of cancer is dynamic, giving rise to heterogenous cell populations that in aggregate form solid tumors. Critically contributing to tumor mass evolution are stromal cells within the tumor microenvironment. While specific cell populations like fibroblasts and endothelial cells within the microenvironment can be modeled reasonably well in more sophisticated experimental systems, including mouse models and engineered biomimetics, it remains challenging to recapitulate the dynamic and heterogeneous processes of immune surveillance and editing through existing model systems. With the overwhelming focus on expanding immunotherapeutic strategies for treating various forms of cancer, the inclusion of a model system that firmly mimics immune interactions between cancer and immune effector cells remains of highest priority.

Given the abundance of scientific and clinical evidence supporting OS to be immunogenic in humans and dogs (273, 274), recent investigations have forged new ground which clearly demonstrate the conserved immunologic signatures and phenotypes shared between canine and human OS (275); and these correlative investigations underscore the unique and high valued information that might be gleaned from pet dogs in regards to systemic and immune microenvironment signatures that can be targeted and manipulated to thwart OS progression and metastasis.

A few salient examples of conserved immune targets include *Foxp3* regulatory T cells, tumor-infiltrating macrophages, and tumoral PD-L1 expressions. In dogs with OS, the participation and prognostic value of regulatory T cells in systemic and tumor microenvironmental immunosuppression has been characterized. Biller and colleagues reported that a decreased $CD8^{+}/T_{reg}$ ratio was associated with significantly shorter survival times in dogs with OS (276, 277), and these observations in dogs corroborate findings identified in human OS patient samples for the prognostic value of effector/suppressor T cell ratios in predicting long-term outcomes (234). Recently, the significance of tumor-infiltrating macrophages within primary OS lesions have been studied in both dogs and humans. Withers and colleagues characterized the innate and adaptive immune infiltrates within primary OS lesions from 30 dogs and correlated these findings with disease-free interval (278). In this study, the magnitude (dichotomous cutoff of 4.7%) of tumor infiltrating macrophages identified within the primary tumor correlated with survival time, suggesting that macrophages may play an integral role for inhibiting OS metastatic progression. These findings in pet dogs closely mirror some investigations in human OS patients, whereby tumor-infiltrating macrophages were also associated with reduced metastasis and improved survival in patients with high-grade OS (226). Lastly, PD-L1 expressions, which serve as a therapeutic target for checkpoint inhibitor strategies, have been studied in both canine and human OS samples. In canine OS primary samples, Maekawa and colleagues characterized PD-L1 expression across various canine tumor histologies and identified seven out of 10 OS samples to stain positively for PD-L1 (279). Comparatively, the expression of PD-L1 in human OS tissue samples appears more restricted (229), with potential enriched expressions in relapsed or metastatic lesions compared to primary tumors (236, 237). In aggregate, the immune signatures shared between canine and human OS are highly comparable, and provides a rational scientific foundation to leverage pet dogs for evaluating novel immune-based therapies against OS metastases.

FUTURE DIRECTIONS

Research Awareness and Emphasis

Compared to the state of metastasis research in other types of cancer such as breast (∼7,703 entries on PubMed) and prostate (∼2,653 entries), basic metastasis research in OS (∼860 entries) is taking its first furtive steps. Discovering new and critical processes that contribute to OS metastasis biology will pave the way for the development of novel anti-metastatic therapies that can be integrated in the current standard of care. Paradigm shifts in animal research should include a focus on lung colonization, clearing or halting the progression of micrometastases, and shrinkage of established metastases as being translational targets, as recognized and supported by leaders in the OS field (3, 8). Tumor cell dormancy in OS is also an area of much needed research since dormant tumor cells are thought of as a reservoir of future tumor recurrence (280, 281). Funding initiatives that focus on metastasis biology discovery, "omic" approaches in finding actionable targets involved in the metastatic cascade, or re-purposing of existing clinical drugs and assessing their anti-metastatic activity is sorely needed. Such experimental approaches require investment in more animal work, specialized equipment, and skilled personnel. Lastly, shifting the research landscape to include more metastasis-focused initiatives requires a voice from patient advocates, who are an integral part of research funding.

Necessity and Benefits of Collaborative Science

Fueled by increasing commitments of resources, veterinary oncology collaborative groups have rapidly become more organized, more agile, and more capable of efficiently conducting high-value pilot studies, complex biology studies, and large clinical trials in client-owned pets that develop cancer. The Comparative Oncology Trials Consortium, headquartered at NIH, has undertaken several initiatives to broaden the comparative biology of human and canine cancers and to improve the efficiency with which they can generate pharmacokinetic, pharmacodynamic, and initial efficacy data in canine clinical investigations that can guide human trial development. Recent initiatives arising from the NIH Cancer Moonshot program have recognized opportunities for incorporating canine clinical trials into the evaluation of immune-oncology approaches by funding several large grants and spawning new comparative immuno-oncology consortia.

Intelligent use of the data arising from this work should improve the likelihood of good outcomes in human clinical trials. Coordination across canine clinical consortia, basic scientists, and industry has become increasingly important. The ability to share data and to plan collaboratively has been enhanced by integration of veterinary oncologists into pediatric clinical trials groups and vice-versa. Efforts led by a handful of philanthropic groups to intensify dialog between these stakeholders have met with increasing interest and engagement. These achievements to date represent only initial forays into truly integrated drug development and science—with opportunity far surpassing the current actuality.

Growth of Comparative Oncology and Coordination of Clinical Trials

With continued and growing interest of the scientific community for including spontaneous tumor models to accelerate novel drug development, comparative oncology centers of excellence must keep pace and commensurately grow to meet the expectations of an ever increasing desire for executing high-value clinical

trials in an agile and efficient manner. To achieve these deliverables, existing comparative oncology centers must expand capacity, and new centers must develop. Incentivization for such development can be achieved through different mechanisms including active participation in Clinical and Translational Science Awards (CTSA) program and integration with existing Basic or Comprehensive Cancer Centers.

Central coordination and unification across participating comparative oncology centers should be strongly advocated, thereby increasing the efficiency and impact of ongoing and future prospective clinical trials. Regional consortia operating in silos will not likely maximize collaborative efforts, and have potential to dilute limited shared resources and manpower. Visionary and inclusive leadership in this arena is necessary, and will ensure that all participating teams can be maximally and directionally aligned for the greatest translational impact as possible.

CONCLUSIONS

Cancer metastasis remains the leading cause of mortality for people afflicted with diverse solid tumor histologies. While tremendous advances in therapy have been achieved over the past decade for some tumor types, the management and outcomes of aggressive sarcoma metastases, including OS, remains almost at a standstill. To impact the lives of patients suffering from OS metastases, it will be necessary to deepen our fundamental understanding of OS metastasis and its specific vulnerabilities at both the cellular and microenvironmental levels. Additionally, the translation of new and promising therapeutic discoveries must be evaluated using complementary model systems that faithfully recapitulate natural metastatic disease progression in people. Given the conserved biology of OS in humans and dogs, unique opportunities exist for human and comparative oncology researchers to engage in translationally impactful collaborations, which uniquely include pet dogs with OS to expand the understanding of metastasis biology and clinically realize the activity of novel investigational therapeutics that target OS metastatic progression.

ETHICS STATEMENT

All animal experiments were done with ethics approval of the local Animal Care Committees.

AUTHOR CONTRIBUTIONS

TF, RR, and ML: project conception and manuscript authorship.

FUNDING

A portion of results in this review article were supported by funding from the following agencies: TF: NIH R01-CA120439, Morris Animal Foundation D09CA-083, D14CA-035, and D19CA-064. RR: supported by NIH K08-CA201638 and St. Baldrick's Scholar award. ML: supported by the BC Cancer Foundation.

ACKNOWLEDGMENTS

Fluorescent images of tumor spheroids were generated using the Core Facilities at the Carl R. Woese Institute for Genomic Biology. Bioluminescent imaging of mouse OS models and micro-CT scans, as well as scanning electron images of homotypic and heterotypic interactions of tumor cells were generated in the Beckman Institute Imaging Technology Group and Biomedical Imaging Center at the University of Illinois at Urbana-Champaign. Development and maintenance of GBM PDX models was supported by Mayo Clinic, the Mayo SPORE in Brain Cancer, and the Mayo Clinic Brain Tumor Patient-Derived xenograft national resource.

REFERENCES

1. Lindsey BA, Markel JE, Kleinerman ES. Osteosarcoma overview. *Rheumatol Therapy.* (2017) 4:25–43. doi: 10.1007/s40744-016-0050-2
2. Geller DS, Gorlick R. Osteosarcoma: a review of diagnosis, management, and treatment strategies. *Clin Adv Hematol Oncol.* (2010) 8:705–18.
3. Steeg PS. Targeting metastasis. *Nat Rev Cancer.* (2016) 16:201–18. doi: 10.1038/nrc.2016.25
4. Fuchs N, Bielack SS, Epler D, Bieling P, Delling G, Korholz D, et al. Long-term results of the co-operative German-Austrian-Swiss osteosarcoma study group's protocol COSS-86 of intensive multidrug chemotherapy and surgery for osteosarcoma of the limbs. *Ann Oncol.* (1998) 9:893–9. doi: 10.1023/A:1008391103132
5. Marina NM, Pratt CB, Rao BN, Shema SJ, Meyer WH. Improved prognosis of children with osteosarcoma metastatic to the lung(s) at the time of diagnosis. *Cancer.* (1992) 70:2722–7.
6. He H, Ni J, Huang J. Molecular mechanisms of chemoresistance in osteosarcoma (Review). *Oncol Lett.* (2014) 7:1352–62. doi: 10.3892/ol.2014.1935
7. Longhi A, Errani C, De Paolis M, Mercuri M, Bacci G. Primary bone osteosarcoma in the pediatric age: state of the art. *Cancer Treat Rev.* (2006) 32:423–36. doi: 10.1016/j.ctrv.2006.05.005
8. Khanna C, Fan TM, Gorlick R, Helman LJ, Kleinerman ES, Adamson PC, et al. Toward a drug development path that targets metastatic progression in osteosarcoma. *Clin Cancer Res.* (2014) 20:4200–9. doi: 10.1158/1078-0432.CCR-13-2574
9. Anderson RL, Balasas T, Callaghan J, Coombes RC, Evans J, Hall JA, et al. A framework for the development of effective anti-metastatic agents. *Nat Rev Clin Oncol.* (2019) 16:185–204. doi: 10.1038/s41571-018-0134-8
10. Link MP, Goorin AM, Miser AW, Green AA, Pratt CB, Belasco JB, et al. The effect of adjuvant chemotherapy on relapse-free survival in patients with osteosarcoma of the extremity. *New Engl J Med.* (1986) 314:1600–6. doi: 10.1056/NEJM198606193142502
11. Miao YR, Eckhardt BL, Cao Y, Pasqualini R, Argani P, Arap W, et al. Inhibition of established micrometastases by targeted drug delivery via cell surface-associated GRP78. *Clin Cancer Res.* (2013) 19:2107–16. doi: 10.1158/1078-0432.CCR-12-2991

12. Lizardo MM, Morrow JJ, Miller TE, Hong ES, Ren L, Mendoza A, et al. Upregulation of glucose-regulated protein 78 in metastatic cancer cells is necessary for lung metastasis progression. *Neoplasia.* (2016) 18:699–710. doi: 10.1016/j.neo.2016.09.001
13. Chen L, Bi S, Hou J, Zhao Z, Wang C, Xie S. Targeting p21-activated kinase 1 inhibits growth and metastasis via Raf1/MEK1/ERK signaling in esophageal squamous cell carcinoma cells. *Cell Commun Signal.* (2019) 17:31. doi: 10.1186/s12964-019-0343-5
14. Ingangi V, Bifulco K, Yousif AM, Ragone C, Motti ML, Rea D, et al. The urokinase receptor-derived cyclic peptide [SRSRY] suppresses neovascularization and intravasation of osteosarcoma and chondrosarcoma cells. *Oncotarget.* (2016) 7:54474–87. doi: 10.18632/oncotarget.9976
15. D'Amato NC, Rogers TJ, Gordon MA, Greene LI, Cochrane DR, Spoelstra NS, et al. A TDO2-AhR signaling axis facilitates anoikis resistance and metastasis in triple-negative breast cancer. *Cancer Res.* (2015) 75:4651–64. doi: 10.1158/0008-5472.CAN-15-2011
16. Zhang Y, Yang M, Ji Q, Fan D, Peng H, Yang C, et al. Anoikis induction and metastasis suppression by a new integrin αvβ3 inhibitor in human melanoma cell line M21. *Invest New Drugs.* (2011) 29:666–73. doi: 10.1007/s10637-010-9616-y
17. Wieland E, Rodriguez-Vita J, Liebler SS, Mogler C, Moll I, Herberich SE, et al. Endothelial notch1 activity facilitates metastasis. *Cancer Cell.* (2017) 31:355–67. doi: 10.1016/j.ccell.2017.01.007
18. Yao H, Veine DM, Livant DL. Therapeutic inhibition of breast cancer bone metastasis progression and lung colonization: breaking the vicious cycle by targeting alpha5beta1 integrin. *Breast Cancer Res Treat.* (2016) 157:489–501. doi: 10.1007/s10549-016-3844-6
19. Roblek M, Calin M, Schlesinger M, Stan D, Zeisig R, Simionescu M, et al. Targeted delivery of CCR2 antagonist to activated pulmonary endothelium prevents metastasis. *J Control Release.* (2015) 220(Pt A):341–7. doi: 10.1016/j.jconrel.2015.10.055
20. Bayles I, Krajewska M, Pontius WD, Saiakhova A, Morrow JJ, Bartels C, et al. *Ex vivo* screen identifies CDK12 as a metastatic vulnerability in osteosarcoma. *J Clin Invest.* (2019) 129:4377–92. doi: 10.1172/JCI127718
21. Morrow JJ, Bayles I, Funnell APW, Miller TE, Saiakhova A, Lizardo MM, et al. Positively selected enhancer elements endow osteosarcoma cells with metastatic competence. *Nat Med.* (2018) 24:176–85. doi: 10.1038/nm.4475
22. Morrow JJ, Mendoza A, Koyen A, Lizardo MM, Ren L, Waybright TJ, et al. mTOR inhibition mitigates enhanced mRNA translation associated with the metastatic phenotype of osteosarcoma cells *in vivo*. *Clin Cancer Res.* (2016) 22:6129–41. doi: 10.1158/1078-0432.CCR-16-0326
23. Bulut G, Hong SH, Chen K, Beauchamp EM, Rahim S, Kosturko GW, et al. Small molecule inhibitors of ezrin inhibit the invasive phenotype of osteosarcoma cells. *Oncogene.* (2012) 31:269–81. doi: 10.1038/onc.2011.245
24. Rao-Bindal K, Koshkina NV, Stewart J, Kleinerman ES. The histone deacetylase inhibitor, MS-275 (entinostat), downregulates c-FLIP, sensitizes osteosarcoma cells to FasL, and induces the regression of osteosarcoma lung metastases. *Curr Cancer Drug Targets.* (2013) 13:411–22. doi: 10.2174/1568009611313040005
25. Hong SH, Ren L, Mendoza A, Eleswarapu A, Khanna C. Apoptosis resistance and PKC signaling: distinguishing features of high and low metastatic cells. *Neoplasia.* (2012) 14:249–58. doi: 10.1593/neo.111498
26. Gross AC, Cam H, Phelps DA, Saraf AJ, Bid HK, Cam M, et al. IL-6 and CXCL8 mediate osteosarcoma-lung interactions critical to metastasis. *JCI Insight.* (2018) 3:e99791. doi: 10.1172/jci.insight.99791
27. Ohs I, Ducimetiere L, Marinho J, Kulig P, Becher B, Tugues S. Restoration of natural killer cell antimetastatic activity by IL12 and checkpoint blockade. *Cancer Res.* (2017) 77:7059–71. doi: 10.1158/0008-5472.CAN-17-1032
28. Dhupkar P, Gordon N, Stewart J, Kleinerman ES. Anti-PD-1 therapy redirects macrophages from an M2 to an M1 phenotype inducing regression of OS lung metastases. *Cancer Med.* (2018) 7:2654–64. doi: 10.1002/cam4.1518
29. Botham RC, Roth HS, Book AP, Roady PJ, Fan TM, Hergenrother PJ. Small-molecule procaspase-3 activation sensitizes cancer to treatment with diverse chemotherapeutics. *ACS Cent Sci.* (2016) 2:545–59. doi: 10.1021/acscentsci.6b00165
30. Weiss L. Metastatic inefficiency. *Adv Cancer Res.* (1990) 54:159–211. doi: 10.1016/S0065-230X(08)60811-8
31. Fidler IJ. Metastasis: quantitative analysis of distribution and fate of tumor emboli labeled with 125 I-5-iodo-2'-deoxyuridine. *J Natl Cancer Inst.* (1970) 45:773–82.
32. Cameron MD, Schmidt EE, Kerkvliet N, Nadkarni KV, Morris VL, Groom AC, et al. Temporal progression of metastasis in lung: cell survival, dormancy, and location dependence of metastatic inefficiency. *Cancer Res.* (2000) 60:2541–6.
33. Kane SE, Gottesman MM. The role of cathepsin L in malignant transformation. *Semin Cancer Biol.* (1990) 1:127–36.
34. Waresijiang N, Sun J, Abuduaini R, Jiang T, Zhou W, Yuan H. The downregulation of miR125a5p functions as a tumor suppressor by directly targeting MMP11 in osteosarcoma. *Mol Med Rep.* (2016) 13:4859–64. doi: 10.3892/mmr.2016.5141
35. Chen CL, Zhang L, Jiao YR, Zhou Y, Ge QF, Li PC, et al. miR-134 inhibits osteosarcoma cell invasion and metastasis through targeting MMP1 and MMP3 *in vitro* and *in vivo*. *FEBS Lett.* (2019) 593:1089–101. doi: 10.1002/1873-3468.13387
36. Han XG, Li Y, Mo HM, Li K, Lin D, Zhao CQ, et al. TIMP3 regulates osteosarcoma cell migration, invasion, and chemotherapeutic resistances. *Tumour Biol.* (2016) 37:8857–67. doi: 10.1007/s13277-015-4757-4
37. Xu WT, Bian ZY, Fan QM, Li G, Tang TT. Human mesenchymal stem cells (hMSCs) target osteosarcoma and promote its growth and pulmonary metastasis. *Cancer Lett.* (2009) 281:32–41. doi: 10.1016/j.canlet.2009.02.022
38. Liao YY, Tsai HC, Chou PY, Wang SW, Chen HT, Lin YM, et al. CCL3 promotes angiogenesis by dysregulation of miR-374b/ VEGF-A axis in human osteosarcoma cells. *Oncotarget.* (2016) 7:4310–25. doi: 10.18632/oncotarget.6708
39. Zeng C, Wen M, Liu X. Fibroblast activation protein in osteosarcoma cells promotes angiogenesis via AKT and ERK signaling pathways. *Oncol Lett.* (2018) 15:6029–35. doi: 10.3892/ol.2018.8027
40. Fernandez L, Valentin J, Zalacain M, Leung W, Patino-Garcia A, Perez-Martinez A. Activated and expanded natural killer cells target osteosarcoma tumor initiating cells in an NKG2D-NKG2DL dependent manner. *Cancer Lett.* (2015) 368:54–63. doi: 10.1016/j.canlet.2015.07.042
41. Kawano M, Tanaka K, Itonaga I, Iwasaki T, Miyazaki M, Ikeda S, et al. Dendritic cells combined with anti-GITR antibody produce antitumor effects in osteosarcoma. *Oncol Rep.* (2015) 34:1995–2001. doi: 10.3892/or.2015.4161
42. van Moorst M, Dass CR. Methods for co-culturing tumour and endothelial cells: systems and their applications. *J Pharm Pharmacol.* (2011) 63:1513–21. doi: 10.1111/j.2042-7158.2011.01352.x
43. Villanueva F, Araya H, Briceno P, Varela N, Stevenson A, Jerez S, et al. The cancer-related transcription factor RUNX2 modulates expression and secretion of the matricellular protein osteopontin in osteosarcoma cells to promote adhesion to endothelial pulmonary cells and lung metastasis. *J Cell Physiol.* (2019) 234:13659–79. doi: 10.1002/jcp.28046
44. Duan X, Jia SF, Zhou Z, Langley RR, Bolontrade MF, Kleinerman ES. Association of alphavbeta3 integrin expression with the metastatic potential and migratory and chemotactic ability of human osteosarcoma cells. *Clin Exp Metastasis.* (2004) 21:747–53. doi: 10.1007/s10585-005-0599-6
45. Frisch SM, Francis H. Disruption of epithelial cell-matrix interactions induces apoptosis. *J Cell Biol.* (1994) 124:619–26. doi: 10.1083/jcb.124.4.619
46. Tan K, Goldstein D, Crowe P, Yang JL. Uncovering a key to the process of metastasis in human cancers: a review of critical regulators of anoikis. *J Cancer Res Clin Oncol.* (2013) 139:1795–805. doi: 10.1007/s00432-013-1482-5
47. Young AI, Law AM, Castillo L, Chong S, Cullen HD, Koehler M, et al. MCL-1 inhibition provides a new way to suppress breast cancer metastasis and increase sensitivity to dasatinib. *Breast Cancer Res.* (2016) 18:125. doi: 10.1186/s13058-016-0781-6
48. Sun T, Zhong X, Song H, Liu J, Li J, Leung F, et al. Anoikis resistant mediated by FASN promoted growth and metastasis of osteosarcoma. *Cell Death Dis.* (2019) 10:298. doi: 10.1038/s41419-019-1532-2
49. Zhao GS, Zhang Q, Cao Y, Wang Y, Lv YF, Zhang ZS, et al. High expression of ID1 facilitates metastasis in human osteosarcoma by regulating the

sensitivity of anoikis via PI3K/AKT depended suppression of the intrinsic apoptotic signaling pathway. *Am J Transl Res.* (2019) 11:2117–39.
50. Weiss L, Dimitrov DS. A fluid mechanical analysis of the velocity, adhesion, and destruction of cancer cells in capillaries during metastasis. *Cell Biophys.* (1984) 6:9–22. doi: 10.1007/BF02788577
51. Wirtz D, Konstantopoulos K, Searson PC. The physics of cancer: the role of physical interactions and mechanical forces in metastasis. *Nat Rev Cancer.* (2011) 11:512–22. doi: 10.1038/nrc3080
52. Huang Q, Hu X, He W, Zhao Y, Hao S, Wu Q, et al. Fluid shear stress and tumor metastasis. *Am J Cancer Res.* (2018) 8:763–77.
53. Lien SC, Chang SF, Lee PL, Wei SY, Chang MD, Chang JY, et al. Mechanical regulation of cancer cell apoptosis and autophagy: roles of bone morphogenetic protein receptor, Smad1/5, and p38 MAPK. *Biochim Biophys Acta.* (2013) 1833:3124–33. doi: 10.1016/j.bbamcr.2013.08.023
54. Ren L, Mendoza A, Zhu J, Briggs JW, Halsey C, Hong ES, et al. Characterization of the metastatic phenotype of a panel of established osteosarcoma cells. *Oncotarget.* (2015) 6:29469–81. doi: 10.18632/oncotarget.5177
55. Goodison S, Kawai K, Hihara J, Jiang P, Yang M, Urquidi V, et al. Prolonged dormancy and site-specific growth potential of cancer cells spontaneously disseminated from nonmetastatic breast tumors as revealed by labeling with green fluorescent protein. *Clin Cancer Res.* (2003) 9(10 Pt 1):3808–14.
56. Suzuki M, Mose ES, Montel V, Tarin D. Dormant cancer cells retrieved from metastasis-free organs regain tumorigenic and metastatic potency. *Am J Pathol.* (2006) 169:673–81. doi: 10.2353/ajpath.2006.060053
57. Wong CW, Lee A, Shientag L, Yu J, Dong Y, Kao G, et al. Apoptosis: an early event in metastatic inefficiency. *Cancer Res.* (2001) 61:333–8.
58. Qiu H, Orr FW, Jensen D, Wang HH, McIntosh AR, Hasinoff BB, et al. Arrest of B16 melanoma cells in the mouse pulmonary microcirculation induces endothelial nitric oxide synthase-dependent nitric oxide release that is cytotoxic to the tumor cells. *Am J Pathol.* (2003) 162:403–12. doi: 10.1016/S0002-9440(10)63835-7
59. Holmgren L, O'Reilly MS, Folkman J. Dormancy of micrometastases: balanced proliferation and apoptosis in the presence of angiogenesis suppression. *Nat Med.* (1995) 1:149–53. doi: 10.1038/nm0295-149
60. Almog N, Ma L, Raychowdhury R, Schwager C, Erber R, Short S, et al. Transcriptional switch of dormant tumors to fast-growing angiogenic phenotype. *Cancer Res.* (2009) 69:836–44. doi: 10.1158/0008-5472.CAN-08-2590
61. Piskounova E, Agathocleous M, Murphy MM, Hu Z, Huddlestun SE, Zhao Z, et al. Oxidative stress inhibits distant metastasis by human melanoma cells. *Nature.* (2015) 527:186–91. doi: 10.1038/nature15726
62. Xiao W, Wang RS, Handy DE, Loscalzo J. NAD(H) and NADP(H) redox couples and cellular energy metabolism. *Antioxid Redox Signal.* (2018) 28:251–72. doi: 10.1089/ars.2017.7216
63. Basnet H, Tian L, Ganesh K, Huang YH, Macalinao DG, Brogi E, et al. Flura-seq identifies organ-specific metabolic adaptations during early metastatic colonization. *Elife.* (2019) 8:e43627. doi: 10.7554/eLife.43627.037
64. Ferraro D, Corso S, Fasano E, Panieri E, Santangelo R, Borrello S, et al. Pro-metastatic signaling by c-Met through RAC-1 and reactive oxygen species (ROS). *Oncogene.* (2006) 25:3689–98. doi: 10.1038/sj.onc.1209409
65. Ishikawa K, Takenaga K, Akimoto M, Koshikawa N, Yamaguchi A, Imanishi H, et al. ROS-generating mitochondrial DNA mutations can regulate tumor cell metastasis. *Science.* (2008) 320:661–4. doi: 10.1126/science.1156906
66. Gill JG, Piskounova E, Morrison SJ. Cancer, oxidative stress, and metastasis. *Cold Spring Harb Symp Quant Biol.* (2016) 81:163–75. doi: 10.1101/sqb.2016.81.030791
67. Szegezdi E, Logue SE, Gorman AM, Samali A. Mediators of endoplasmic reticulum stress-induced apoptosis. *EMBO Rep.* (2006) 7:880–5. doi: 10.1038/sj.embor.7400779
68. Townsend DM. S-glutathionylation: indicator of cell stress and regulator of the unfolded protein response. *Mol Interv.* (2007) 7:313–24. doi: 10.1124/mi.7.6.7
69. Ojha R, Amaravadi RK. Targeting the unfolded protein response in cancer. *Pharmacol Res.* (2017) 120:258–66. doi: 10.1016/j.phrs.2017.04.003
70. Chaiyawat P, Sungngam P, Teeyakasem P, Sirikaew N, Klangjorhor J, Settakorn J, et al. Protein profiling of osteosarcoma tissue and soft callus unveils activation of the unfolded protein response pathway. *Int J Oncol.* (2019) 54:1704–18. doi: 10.3892/ijo.2019.4737
71. Burris HA, Bakewell S, Bendell JC, Infante J, Jones SF, Spigel DR, et al. Safety and activity of IT-139, a ruthenium-based compound, in patients with advanced solid tumours: a first-in-human, open-label, dose-escalation phase I study with expansion cohort. *ESMO Open.* (2016) 1:e000154. doi: 10.1136/esmoopen-2016-000154
72. Yarapureddy S, Abril J, Foote J, Kumar S, Asad O, Sharath V, et al. ATF6alpha activation enhances survival against chemotherapy and serves as a prognostic indicator in osteosarcoma. *Neoplasia.* (2019) 21:516–32. doi: 10.1016/j.neo.2019.02.004
73. Zhang R, Thamm DH, Misra V. The effect of Zhangfei/CREBZF on cell growth, differentiation, apoptosis, migration, and the unfolded protein response in several canine osteosarcoma cell lines. *BMC Vet Res.* (2015) 11:22. doi: 10.1186/s12917-015-0331-y
74. Yan M, Ni J, Song D, Ding M, Huang J. Activation of unfolded protein response protects osteosarcoma cells from cisplatin-induced apoptosis through NF-kappaB pathway. *Int J Clin Exp Pathol.* (2015) 8:10204–15.
75. Asling J, Morrison J, Mutsaers AJ. Targeting HSP70 and GRP78 in canine osteosarcoma cells in combination with doxorubicin chemotherapy. *Cell Stress Chaperon.* (2016) 21:1065–76. doi: 10.1007/s12192-016-0730-4
76. Weibel ER. Lung morphometry: the link between structure and function. *Cell Tissue Res.* (2017) 367:413–26. doi: 10.1007/s00441-016-2541-4
77. Huret J-L, Ahmad M, Arsaban M, Bernheim A, Cigna J, Desangles F, et al. Atlas of genetics and cytogenetics in oncology and haematology in 2013. *Nucleic Acids Res.* (2012) 41:D920–D4. doi: 10.1093/nar/gks1082
78. Chambers AF, Groom AC, MacDonald IC. Dissemination and growth of cancer cells in metastatic sites. *Nat Rev Cancer.* (2002) 2:563–72. doi: 10.1038/nrc865
79. Kaplan RN, Riba RD, Zacharoulis S, Bramley AH, Vincent L, Costa C, et al. VEGFR1-positive haematopoietic bone marrow progenitors initiate the pre-metastatic niche. *Nature.* (2005) 438:820–7. doi: 10.1038/nature04186
80. Hiratsuka S, Watanabe A, Aburatani H, Maru Y. Tumour-mediated upregulation of chemoattractants and recruitment of myeloid cells predetermines lung metastasis. *Nat Cell Biol.* (2006) 8:1369–75. doi: 10.1038/ncb1507
81. Psaila B, Lyden D. The metastatic niche: adapting the foreign soil. *Nat Rev Cancer.* (2009) 9:285–93. doi: 10.1038/nrc2621
82. Murgai M, Ju W, Eason M, Kline J, Beury DW, Kaczanowska S, et al. KLF4-dependent perivascular cell plasticity mediates pre-metastatic niche formation and metastasis. *Nat Med.* (2017) 23:1176–90. doi: 10.1038/nm.4400
83. Macklin R, Wang H, Loo D, Martin S, Cumming A, Cai N, et al. Extracellular vesicles secreted by highly metastatic clonal variants of osteosarcoma preferentially localize to the lungs and induce metastatic behaviour in poorly metastatic clones. *Oncotarget.* (2016) 7:43570–87. doi: 10.18632/oncotarget.9781
84. Ekert JE, Johnson K, Strake B, Pardinas J, Jarantow S, Perkinson R, et al. Three-dimensional lung tumor microenvironment modulates therapeutic compound responsiveness *in vitro* – implication for drug development. *PLoS ONE.* (2014) 9:e92248. doi: 10.1371/journal.pone.0092248
85. Luca AC, Mersch S, Deenen R, Schmidt S, Messner I, Schäfer K-L, et al. Impact of the 3D microenvironment on phenotype, gene expression, and EGFR inhibition of colorectal cancer cell lines. *PLoS ONE.* (2013) 8:e59689. doi: 10.1371/journal.pone.0059689
86. Pickl M, Ries CH. Comparison of 3D and 2D tumor models reveals enhanced HER2 activation in 3D associated with an increased response to trastuzumab. *Oncogene.* (2008) 28:461. doi: 10.1038/onc.2008.394
87. Ribatti D. The chick embryo chorioallantoic membrane (CAM) assay. *Reprod Toxicol.* (2017) 70:97–101. doi: 10.1016/j.reprotox.2016.11.004
88. Lizardo MM, Sorensen PH. Practical considerations in studying metastatic lung colonization in osteosarcoma using the pulmonary metastasis assay. *J Vis Exp.* (2018) 133:1–14. doi: 10.3791/56332
89. Entenberg D, Voiculescu S, Guo P, Borriello L, Wang Y, Karagiannis GS, et al. A permanent window for the murine lung enables high-resolution imaging of cancer metastasis. *Nat Methods.* (2018) 15:73–80. doi: 10.1038/nmeth.4511
90. Mangir N, Raza A, Haycock JW, Chapple C, Macneil S. An improved *in vivo* methodology to visualise tumour induced changes in vasculature using

the chick chorionic allantoic membrane assay. *In Vivo.* (2018) 32:461–72. doi: 10.21873/invivo.11262
91. Deryugina EI. Chorioallantoic membrane microtumor model to study the mechanisms of tumor angiogenesis, vascular permeability, and tumor cell intravasation. *Methods Mol Biol.* (2016) 1430:283–98. doi: 10.1007/978-1-4939-3628-1_19
92. Armstrong PB, Quigley JP, Sidebottom E. Transepithelial invasion and intramesenchymal infiltration of the chick embryo chorioallantois by tumor cell lines. *Cancer Res.* (1982) 42:1826–37.
93. Zhang Y, Thayele Purayil H, Black JB, Fetto F, Lynch LD, Masannat JN, et al. Prostaglandin E2 receptor 4 mediates renal cell carcinoma intravasation and metastasis. *Cancer Lett.* (2017) 391:50–8. doi: 10.1016/j.canlet.2017.01.007
94. Koop S, Khokha R, Schmidt EE, MacDonald IC, Morris VL, Chambers AF, et al. Overexpression of metalloproteinase inhibitor in B16F10 cells does not affect extravasation but reduces tumor growth. *Cancer Res.* (1994) 54:4791–7.
95. Deryugina EI, Quigley JP. Chick embryo chorioallantoic membrane model systems to study and visualize human tumor cell metastasis. *Histochem Cell Biol.* (2008) 130:1119–30. doi: 10.1007/s00418-008-0536-2
96. Kim Y, Williams KC, Gavin CT, Jardine E, Chambers AF, Leong HS. Quantification of cancer cell extravasation *in vivo*. *Nat Prot.* (2016) 11:937–48. doi: 10.1038/nprot.2016.050
97. Leong HS, Robertson AE, Stoletov K, Leith SJ, Chin CA, Chien AE, et al. Invadopodia are required for cancer cell extravasation and are a therapeutic target for metastasis. *Cell Rep.* (2014) 8:1558–70. doi: 10.1016/j.celrep.2014.07.050
98. Williams KC, Cepeda MA, Javed S, Searle K, Parkins KM, Makela AV, et al. Invadopodia are chemosensing protrusions that guide cancer cell extravasation to promote brain tropism in metastasis. *Oncogene.* (2019) 38:3598–615. doi: 10.1038/s41388-018-0667-4
99. DeBord LC, Pathak RR, Villaneuva M, Liu HC, Harrington DA, Yu W, et al. The chick chorioallantoic membrane (CAM) as a versatile patient-derived xenograft (PDX) platform for precision medicine and preclinical research. *Am J Cancer Res.* (2018) 8:1642–60.
100. Kunz P, Schenker A, Sahr H, Lehner B, Fellenberg J. Optimization of the chicken chorioallantoic membrane assay as reliable *in vivo* model for the analysis of osteosarcoma. *PLoS One.* (2019) 14:e0215312. doi: 10.1371/journal.pone.0215312
101. Manjunathan R, Ragunathan M. Chicken chorioallantoic membrane as a reliable model to evaluate osteosarcoma-an experimental approach using SaOS2 cell line. *Biol Proc Online.* (2015) 17:10. doi: 10.1186/s12575-015-0022-x
102. Haeckel C, Krueger S, Roessner A. Antisense inhibition of urokinase: effect on malignancy in a human osteosarcoma cell line. *Int J Cancer.* (1998) 77:153–60. doi: 10.1002/(SICI)1097-0215(19980703)77:1<153::AID-IJC23>3.0.CO;2-E
103. Lokman NA, Elder AS, Ricciardelli C, Oehler MK. Chick chorioallantoic membrane (CAM) assay as an *in vivo* model to study the effect of newly identified molecules on ovarian cancer invasion and metastasis. *Int J Mol Sci.* (2012) 13:9959–70. doi: 10.3390/ijms13089959
104. Mendoza A, Hong SH, Osborne T, Khan MA, Campbell K, Briggs J, et al. Modeling metastasis biology and therapy in real time in the mouse lung. *J Clin Invest.* (2010) 120:2979–88. doi: 10.1172/JCI40252
105. Young ED, Strom K, Tsue AF, Usset JL, MacPherson S, McGuire JT, et al. Automated quantitative image analysis for *ex vivo* metastasis assays reveals differing lung composition requirements for metastasis suppression by KISS1. *Clin Exp Metastasis.* (2018) 35:77–86. doi: 10.1007/s10585-018-9882-1
106. Nomura M, Rainusso N, Lee YC, Dawson B, Coarfa C, Han R, et al. Tegavivint and the beta-catenin/ALDH axis in chemotherapy-resistant and metastatic osteosarcoma. *J Natl Cancer Inst.* (2019) 111:1216–27. doi: 10.1093/jnci/djz026
107. Al-Mehdi AB, Tozawa K, Fisher AB, Shientag L, Lee A, Muschel RJ. Intravascular origin of metastasis from the proliferation of endothelium-attached tumor cells: a new model for metastasis. *Nat Med.* (2000) 6:100–2. doi: 10.1038/71429
108. Varghese HJ, MacKenzie LT, Groom AC, Ellis CG, Chambers AF, MacDonald IC. Mapping of the functional microcirculation in vital organs using contrast-enhanced *in vivo* video microscopy. *Am J Physiol Heart Circ Physiol.* (2005) 288:H185–93. doi: 10.1152/ajpheart.01022.2003
109. James ML, Gambhir SS. A molecular imaging primer: modalities, imaging agents, and applications. *Physiol Rev.* (2012) 92:897–965. doi: 10.1152/physrev.00049.2010
110. Weissleder R. Scaling down imaging: molecular mapping of cancer in mice. *Nat Rev Cancer.* (2002) 2:11–8. doi: 10.1038/nrc701
111. Vanharanta S, Massague J. Origins of metastatic traits. *Cancer Cell.* (2013) 24:410–21. doi: 10.1016/j.ccr.2013.09.007
112. Cam M, Gardner HL, Roberts RD, Fenger JM, Guttridge DC, London CA, et al. DeltaNp63 mediates cellular survival and metastasis in canine osteosarcoma. *Oncotarget.* (2016) 7:48533–46. doi: 10.18632/oncotarget.10406
113. Hanahan D, Coussens LM. Accessories to the crime: functions of cells recruited to the tumor microenvironment. *Cancer Cell.* (2012) 21:309–22. doi: 10.1016/j.ccr.2012.02.022
114. Liu Y, Cao X. Characteristics and significance of the pre-metastatic niche. *Cancer Cell.* (2016) 30:668–81. doi: 10.1016/j.ccell.2016.09.011
115. Khanna C, Hunter K. Modeling metastasis *in vivo*. *Carcinogenesis.* (2005) 26:513–23. doi: 10.1093/carcin/bgh261
116. Guijarro MV, Ghivizzani SC, Gibbs CP. Animal models in osteosarcoma. *Front Oncol.* (2014) 4:189. doi: 10.3389/fonc.2014.00189
117. Jones KB. Osteosarcomagenesis: modeling cancer initiation in the mouse. *Sarcoma.* (2011) 2011:694136. doi: 10.1155/2011/694136
118. Gupte A, Baker EK, Wan S-S, Stewart E, Loh A, Shelat AA, et al. Systematic screening identifies dual PI3K and mTOR inhibition as a conserved therapeutic vulnerability in osteosarcoma. *Clin Cancer Res.* (2015) 21:3216–29. doi: 10.1158/1078-0432.CCR-14-3026
119. Moriarity BS, Otto GM, Rahrmann EP, Rathe SK, Wolf NK, Weg MT, et al. A Sleeping Beauty forward genetic screen identifies new genes and pathways driving osteosarcoma development and metastasis. *Nat Genet.* (2015) 47:615–24. doi: 10.1038/ng.3293
120. Stewart E, Federico S, Karlstrom A, Shelat A, Sablauer A, Pappo A, et al. The childhood solid tumor network: a new resource for the developmental biology and oncology research communities. *Dev Biol.* (2016) 411:287–93. doi: 10.1016/j.ydbio.2015.03.001
121. Stewart E, Federico SM, Chen X, Shelat AA, Bradley C, Gordon B, et al. Orthotopic patient-derived xenografts of paediatric solid tumours. *Nature.* (2017) 549:96–100. doi: 10.1038/nature23647
122. Sayles LC, Breese MR, Koehne AL, Leung SG, Lee AG, Liu HY, et al. Genome-informed targeted therapy for osteosarcoma. *Cancer Discov.* (2019) 9:46–63. doi: 10.1158/2159-8290.CD-17-1152
123. Goldstein SD, Hayashi M, Albert CM, Jackson KW, Loeb DM. An orthotopic xenograft model with survival hindlimb amputation allows investigation of the effect of tumor microenvironment on sarcoma metastasis. *Clin Exp Metastasis.* (2015) 32:703–15. doi: 10.1007/s10585-015-9738-x
124. Goldstein SD, Trucco M, Bautista Guzman W, Hayashi M, Loeb DM. A monoclonal antibody against the Wnt signaling inhibitor dickkopf-1 inhibits osteosarcoma metastasis in a preclinical model. *Oncotarget.* (2016) 7:21114–23. doi: 10.18632/oncotarget.8522
125. Kumar S, Weaver VM. Mechanics, malignancy, and metastasis: the force journey of a tumor cell. *Cancer Metastasis Rev.* (2009) 28:113–27. doi: 10.1007/s10555-008-9173-4
126. Martino F, Perestrelo AR, Vinarsky V, Pagliari S, Forte G. Cellular mechanotransduction: from tension to function. *Front Physiol.* (2018) 9:824. doi: 10.3389/fphys.2018.00824
127. Martinac B. Mechanosensitive ion channels: molecules of mechanotransduction. *J Cell Sci.* (2004) 117(Pt 12):2449–60. doi: 10.1242/jcs.01232
128. Lee J, Abdeen AA, Wycislo KL, Fan TM, Kilian KA. Interfacial geometry dictates cancer cell tumorigenicity. *Nat Mater.* (2016) 15:856–62. doi: 10.1038/nmat4610
129. Wei SC, Fattet L, Tsai JH, Guo Y, Pai VH, Majeski HE, et al. Matrix stiffness drives epithelial-mesenchymal transition and tumour metastasis through a TWIST1-G3BP2 mechanotransduction pathway. *Nat Cell Biol.* (2015) 17:678–88. doi: 10.1038/ncb3157

130. Najafi M, Farhood B, Mortezaee K. Extracellular matrix (ECM) stiffness and degradation as cancer drivers. *J Cell Biochem.* (2019) 120:2782–90. doi: 10.1002/jcb.27681
131. Zhang D, Lee J, Sun MB, Pei Y, Chu J, Gillette MU, et al. Combinatorial discovery of defined substrates that promote a stem cell state in malignant melanoma. *ACS Cent Sci.* (2017) 3:381–93. doi: 10.1021/acscentsci.6b00329
132. Foty R. A simple hanging drop cell culture protocol for generation of 3D spheroids. *J Vis Exp.* (2011) 51:1–4. doi: 10.3791/2720
133. Sant S, Johnston PA. The production of 3D tumor spheroids for cancer drug discovery. *Drug Discov Today Technol.* (2017) 23:27–36. doi: 10.1016/j.ddtec.2017.03.002
134. Perche F, Torchilin VP. Cancer cell spheroids as a model to evaluate chemotherapy protocols. *Cancer Biol Ther.* (2012) 13:1205–13. doi: 10.4161/cbt.21353
135. De Luca A, Raimondi L, Salamanna F, Carina V, Costa V, Bellavia D, et al. Relevance of 3d culture systems to study osteosarcoma environment. *J Exp Clin Cancer Res.* (2018) 37:2. doi: 10.1186/s13046-017-0663-5
136. Baek N, Seo OW, Lee J, Hulme J, An SS. Real-time monitoring of cisplatin cytotoxicity on three-dimensional spheroid tumor cells. *Drug Des Devel Ther.* (2016) 10:2155–65. doi: 10.2147/DDDT.S108004
137. Baek N, Seo OW, Kim M, Hulme J, An SS. Monitoring the effects of doxorubicin on 3D-spheroid tumor cells in real-time. *Onco Targets Ther.* (2016) 9:7207–18. doi: 10.2147/OTT.S112566
138. Charoen KM, Fallica B, Colson YL, Zaman MH, Grinstaff MW. Embedded multicellular spheroids as a biomimetic 3D cancer model for evaluating drug and drug-device combinations. *Biomaterials.* (2014) 35:2264–71. doi: 10.1016/j.biomaterials.2013.11.038
139. Martins-Neves SR, Lopes AO, do Carmo A, Paiva AA, Simoes PC, Abrunhosa AJ, et al. Therapeutic implications of an enriched cancer stem-like cell population in a human osteosarcoma cell line. *BMC Cancer.* (2012) 12:139. doi: 10.1186/1471-2407-12-139
140. Leon IE, Cadavid-Vargas JF, Resasco A, Maschi F, Ayala MA, Carbone C, et al. *In vitro* and *in vivo* antitumor effects of the VO-chrysin complex on a new three-dimensional osteosarcoma spheroids model and a xenograft tumor in mice. *J Biol Inorg Chem.* (2016) 21:1009–20. doi: 10.1007/s00775-016-1397-0
141. Fujii H, Honoki K, Tsujiuchi T, Kido A, Yoshitani K, Takakura Y. Sphere-forming stem-like cell populations with drug resistance in human sarcoma cell lines. *Int J Oncol.* (2009) 34:1381–6.
142. Fallica B, Maffei JS, Villa S, Makin G, Zaman M. Alteration of cellular behavior and response to PI3K pathway inhibition by culture in 3D collagen gels. *PLoS ONE.* (2012) 7:e48024. doi: 10.1371/journal.pone.0048024
143. Pang LY, Gatenby EL, Kamida A, Whitelaw BA, Hupp TR, Argyle DJ. Global gene expression analysis of canine osteosarcoma stem cells reveals a novel role for COX-2 in tumour initiation. *PLoS ONE.* (2014) 9:e83144. doi: 10.1371/journal.pone.0083144
144. Schoeftner S, Scarola M, Comisso E, Schneider C, Benetti R. An Oct4-pRb axis, controlled by MiR-335, integrates stem cell self-renewal and cell cycle control. *Stem Cells.* (2013) 31:717–28. doi: 10.1002/stem.1315
145. Tanaka T, Yui Y, Naka N, Wakamatsu T, Yoshioka K, Araki N, et al. Dynamic analysis of lung metastasis by mouse osteosarcoma LM8: VEGF is a candidate for anti-metastasis therapy. *Clin Exp Metastasis.* (2013) 30:369–79. doi: 10.1007/s10585-012-9543-8
146. Elenjord R, Allen JB, Johansen HT, Kildalsen H, Svineng G, Maelandsmo GM, et al. Collagen I regulates matrix metalloproteinase-2 activation in osteosarcoma cells independent of S100A4. *FEBS J.* (2009) 276:5275–86. doi: 10.1111/j.1742-4658.2009.07223.x
147. Zhang LZ, Mei J, Qian ZK, Cai XS, Jiang Y, Huang WD. The role of VE-cadherin in osteosarcoma cells. *Pathol Oncol Res.* (2010) 16:111–7. doi: 10.1007/s12253-009-9198-1
148. Fu D, He X, Yang S, Xu W, Lin T, Feng X. Zoledronic acid inhibits vasculogenic mimicry in murine osteosarcoma cell line *in vitro*. *BMC Musculoskelet Disord.* (2011) 12:146. doi: 10.1186/1471-2474-12-146
149. Suzuki Y, Nishida Y, Naruse T, Gemba T, Ishiguro N. Pericellular matrix formation alters the efficiency of intracellular uptake of oligonucleotides in osteosarcoma cells. *J Surg Res.* (2009) 152:148–56. doi: 10.1016/j.jss.2008.02.037
150. Nishimura A, Akeda K, Matsubara T, Kusuzaki K, Matsumine A, Masuda K, et al. Transfection of NF-kappaB decoy oligodeoxynucleotide suppresses pulmonary metastasis by murine osteosarcoma. *Cancer Gene Ther.* (2011) 18:250–9. doi: 10.1038/cgt.2010.75
151. Guo X, Yu L, Zhang Z, Dai G, Gao T, Guo W. miR-335 negatively regulates osteosarcoma stem cell-like properties by targeting POU5F1. *Cancer Cell Int.* (2017) 17:29. doi: 10.1186/s12935-017-0398-6
152. Chaddad H, Kuchler-Bopp S, Fuhrmann G, Gegout H, Ubeaud-Sequier G, Schwinte P, et al. Combining 2D angiogenesis and 3D osteosarcoma microtissues to improve vascularization. *Exp Cell Res.* (2017) 360:138–45. doi: 10.1016/j.yexcr.2017.08.035
153. Park KM, Lewis D, Gerecht S. Bioinspired hydrogels to engineer cancer microenvironments. *Annu Rev Biomed Eng.* (2017) 19:109–33. doi: 10.1146/annurev-bioeng-071516-044619
154. Geckil H, Xu F, Zhang XH, Moon S, Demirci U. Engineering hydrogels as extracellular matrix mimics. *Nanomedicine.* (2010) 5:469–84. doi: 10.2217/nnm.10.12
155. Zhang YS, Khademhosseini A. Advances in engineering hydrogels. *Science.* (2017) 356:aaf3627. doi: 10.1126/science.aaf3627
156. Ali Gumustas S, Isyar M, Topuk S, Yilmaz I, Oznam K, Onay T, et al. Systematic evaluation of drug-loaded hydrogels for application in osteosarcoma treatment. *Curr Pharm Biotechnol.* (2016) 17:866–72. doi: 10.2174/1389201017666160519113104
157. Ma H, He C, Cheng Y, Yang Z, Zang J, Liu J, et al. Localized co-delivery of doxorubicin, cisplatin, and methotrexate by thermosensitive hydrogels for enhanced osteosarcoma treatment. *ACS Appl Mater Interfaces.* (2015) 7:27040–8. doi: 10.1021/acsami.5b09112
158. Yin Q, Tang L, Cai K, Tong R, Sternberg R, Yang X, et al. Pamidronate functionalized nanoconjugates for targeted therapy of focal skeletal malignant osteolysis. *Proc Natl Acad Sci USA.* (2016) 113:E4601–9. doi: 10.1073/pnas.1603316113
159. Jiang T, Zhao J, Yu S, Mao Z, Gao C, Zhu Y, et al. Untangling the response of bone tumor cells and bone forming cells to matrix stiffness and adhesion ligand density by means of hydrogels. *Biomaterials.* (2019) 188:130–43. doi: 10.1016/j.biomaterials.2018.10.015
160. Jiang T, Xu G, Chen X, Huang X, Zhao J, Zheng L. Impact of Hydrogel Elasticity and Adherence on Osteosarcoma Cells and Osteoblasts. *Adv Healthc Mater.* (2019) 8:e1801587. doi: 10.1002/adhm.201801587
161. Dey S, Laredj L, Damjanovic K, Muller M, Beard P. Growth of osteosarcoma cells in a three-dimensional bone-like matrix alters their susceptibility to adeno-associated virus. *J Gen Virol.* (2014) 95(Pt 7):1539–43. doi: 10.1099/vir.0.061945-0
162. Tan PH, Chia SS, Toh SL, Goh JC, Nathan SS. The dominant role of IL-8 as an angiogenic driver in a three-dimensional physiological tumor construct for drug testing. *Tissue Eng Part A.* (2014) 20:1758–66. doi: 10.1089/ten.tea.2013.0245
163. Bai C, Yang M, Fan Z, Li S, Gao T, Fang Z. Associations of chemo- and radio-resistant phenotypes with the gap junction, adhesion and extracellular matrix in a three-dimensional culture model of soft sarcoma. *J Exp Clin Cancer Res.* (2015) 34:58. doi: 10.1186/s13046-015-0175-0
164. Jabbari E, Sarvestani SK, Daneshian L, Moeinzadeh S. Optimum 3D matrix stiffness for maintenance of cancer stem cells is dependent on tissue origin of cancer cells. *PLoS ONE.* (2015) 10:e0132377. doi: 10.1371/journal.pone.0132377
165. Shang M, Soon RH, Lim CT, Khoo BL, Han J. Microfluidic modelling of the tumor microenvironment for anti-cancer drug development. *Lab Chip.* (2019) 19:369–86. doi: 10.1039/C8LC00970H
166. Turetta M, Ben FD, Brisotto G, Biscontin E, Bulfoni M, Cesselli D, et al. Emerging technologies for cancer research: towards personalized medicine with microfluidic platforms and 3D tumor models. *Curr Med Chem.* (2018) 25:4616–37. doi: 10.2174/0929867325666180605122633
167. Samatov TR, Shkurnikov MU, Tonevitskaya SA, Tonevitsky AG. Modelling the metastatic cascade by *in vitro* microfluidic platforms. *Prog Histochem Cytochem.* (2015) 49:21–9. doi: 10.1016/j.proghi.2015.01.001
168. Chaw KC, Manimaran M, Tay EH, Swaminathan S. Multi-step microfluidic device for studying cancer metastasis. *Lab Chip.* (2007) 7:1041–7. doi: 10.1039/b707399m

169. Ma YHV, Middleton K, You LD, Sun Y. A review of microfluidic approaches for investigating cancer extravasation during metastasis. *Microsyst Nanoeng.* (2018) 4:17104. doi: 10.1038/micronano.2017.104
170. Sontheimer-Phelps A, Hassell BA, Ingber DE. Modelling cancer in microfluidic human organs-on-chips. *Nat Rev Cancer.* (2019) 19:65–81. doi: 10.1038/s41568-018-0104-6
171. Skardal A, Devarasetty M, Forsythe S, Atala A, Soker S. A reductionist metastasis-on-a-chip platform for *in vitro* tumor progression modeling and drug screening. *Biotechnol Bioeng.* (2016) 113:2020–32. doi: 10.1002/bit.25950
172. Ruzycka M, Cimpan MR, Rios-Mondragon I, Grudzinski IP. Microfluidics for studying metastatic patterns of lung cancer. *J Nanobiotechnol.* (2019) 17:71. doi: 10.1186/s12951-019-0492-0
173. Kong J, Luo Y, Jin D, An F, Zhang W, Liu L, et al. A novel microfluidic model can mimic organ-specific metastasis of circulating tumor cells. *Oncotarget.* (2016) 7:78421–32. doi: 10.18632/oncotarget.9382
174. Stamp MEM, Jotten A, Kudella PW, Breyer D, Strobl FG, Geislinger TM, et al. Exploring the limits of cell adhesion under shear stress within physiological conditions and beyond on a chip. *Diagnostics.* (2016) 6:E38. doi: 10.3390/diagnostics6040038
175. Barata D, Spennati G, Correia C, Ribeiro N, Harink B, van Blitterswijk C, et al. Development of a shear stress-free microfluidic gradient generator capable of quantitatively analyzing single-cell morphology. *Biomed Microdevices.* (2017) 19:81. doi: 10.1007/s10544-017-0222-z
176. Mitxelena-Iribarren O, Zabalo J, Arana S, Mujika M. Improved microfluidic platform for simultaneous multiple drug screening towards personalized treatment. *Biosens Bioelectron.* (2019) 123:237–43. doi: 10.1016/j.bios.2018.09.001
177. Withrow SJ, Powers BE, Straw RC, Wilkins RM. Comparative aspects of osteosarcoma. Dog versus man. *Clin Orthop Relat Res.* (1991) 270:159–68. doi: 10.1097/00003086-199109000-00023
178. Paoloni M, Davis S, Lana S, Withrow S, Sangiorgi L, Picci P, et al. Canine tumor cross-species genomics uncovers targets linked to osteosarcoma progression. *BMC Genomics.* (2009) 10:625. doi: 10.1186/1471-2164-10-625
179. Mueller F, Fuchs B, Kaser-Hotz B. Comparative biology of human and canine osteosarcoma. *Anticancer Res.* (2007) 27:155–64.
180. Fenger JM, London CA, Kisseberth WC. Canine osteosarcoma: a naturally occurring disease to inform pediatric oncology. *ILAR J.* (2014) 55:69–85. doi: 10.1093/ilar/ilu009
181. Rankin KS, Starkey M, Lunec J, Gerrand CH, Murphy S, Biswas S. Of dogs and men: comparative biology as a tool for the discovery of novel biomarkers and drug development targets in osteosarcoma. *Pediatr Blood Cancer.* (2012) 58:327–33. doi: 10.1002/pbc.23341
182. Withrow SJ, Wilkins RM. Cross talk from pets to people: translational osteosarcoma treatments. *ILAR J.* (2010) 51:208–13. doi: 10.1093/ilar.51.3.208
183. Saraf AJ, Fenger JM, Roberts RD. Osteosarcoma: accelerating progress makes for a hopeful future. *Front Oncol.* (2018) 8:4. doi: 10.3389/fonc.2018.00004
184. LeBlanc AK, Breen M, Choyke P, Dewhirst M, Fan TM, Gustafson DL, et al. Perspectives from man's best friend: national academy of medicine's workshop on comparative oncology. *Sci Transl Med.* (2016) 8:324ps5. doi: 10.1126/scitranslmed.aaf0746
185. Winkler K, Beron G, Kotz R, Salzer-Kuntschik M, Beck J, Beck W, et al. Adjuvant chemotherapy in osteosarcoma - effects of cisplatinum, BCD, and fibroblast interferon in sequential combination with HD-MTX and adriamycin. Preliminary results of the COSS 80 study. *J Cancer Res Clin Oncol.* (1983) 106:1–7. doi: 10.1007/BF00625042
186. Roberts RD, Wedekind MF, Setty BA. Chemotherapy regimens for patients with newly diagnosed malignant bone tumors. In: Cripe TP, Yeager ND, editors. *Malignant Pediatric Bone Tumors - Treatment & Management*. Cham: Springer US (2015) 83–108. doi: 10.1007/978-3-319-18099-1_6
187. Kuntz CA, Asselin TL, Dernell WS, Powers BE, Straw RC, Withrow SJ. Limb salvage surgery for osteosarcoma of the proximal humerus: outcome in 17 dogs. *Vet Surg.* (1998) 27:417–22. doi: 10.1111/j.1532-950X.1998.tb00150.x
188. Liptak JM, Dernell WS, Ehrhart N, Lafferty MH, Monteith GJ, Withrow SJ. Cortical allograft and endoprosthesis for limb-sparing surgery in dogs with distal radial osteosarcoma: a prospective clinical comparison of two different limb-sparing techniques. *Vet Surg.* (2006) 35:518–33. doi: 10.1111/j.1532-950X.2006.00185.x
189. Marina NM, Smeland S, Bielack SS, Bernstein M, Jovic G, Krailo MD, et al. Comparison of MAPIE versus MAP in patients with a poor response to preoperative chemotherapy for newly diagnosed high-grade osteosarcoma (EURAMOS-1): an open-label, international, randomised controlled trial. *Lancet Oncol.* (2016) 17:1396–408. doi: 10.1016/S1470-2045(16)30214-5
190. Allison DC, Carney SC, Ahlmann ER, Hendifar A, Chawla S, Fedenko A, et al. A meta-analysis of osteosarcoma outcomes in the modern medical era. *Sarcoma.* (2012) 2012:704872. doi: 10.1155/2012/704872
191. Aljubran AH, Griffin A, Pintilie M, Blackstein M. Osteosarcoma in adolescents and adults: survival analysis with and without lung metastases. *Ann Oncol.* (2009) 20:1136–41. doi: 10.1093/annonc/mdn731
192. Berrak SGLN, Pearson M, Berberoglu S, Lhan NER, Jaffe N. High-dose ifosfamide in relapsed pediatric osteosarcoma: therapeutic effects and renal toxicity. *Pediatr Blood Cancer.* (2005) 44:215–9. doi: 10.1002/pbc.20228
193. Duffaud F, Mir O, Boudou-Rouquette P, Piperno-Neumann S, Penel N, Bompas E, et al. Efficacy and safety of regorafenib in adult patients with metastatic osteosarcoma: a non-comparative, randomised, double-blind, placebo-controlled, phase 2 study. *Lancet Oncol.* (2019) 20:120–33. doi: 10.1016/S1470-2045(18)30742-3
194. Chen EL, Yoo CH, Gutkin PM, Merriott DJ, Avedian RS, Steffner RJ, et al. Outcomes for pediatric patients with osteosarcoma treated with palliative radiotherapy. *Pediatr Blood Cancer.* (2019) 67:e27967. doi: 10.1002/pbc.27967
195. Chou AJ, Merola PR, Wexler LH, Gorlick RG, Vyas YM, Healey JH, et al. Treatment of osteosarcoma at first recurrence after contemporary therapy: the Memorial Sloan-Kettering Cancer Center experience. *Cancer.* (2005) 104:2214–21. doi: 10.1002/cncr.21417
196. Kempf-Bielack B, Bielack SS, Jurgens H, Branscheid D, Berdel WE, Exner GU, et al. Osteosarcoma relapse after combined modality therapy: an analysis of unselected patients in the Cooperative Osteosarcoma Study Group (COSS). *J Clin Oncol.* (2005) 23:559–68. doi: 10.1200/JCO.2005.04.063
197. Bacci G, Briccoli A, Longhi A, Ferrari S, Mercuri M, Faggioli F, et al. Treatment and outcome of recurrent osteosarcoma: experience at Rizzoli in 235 patients initially treated with neoadjuvant chemotherapy. *Acta Oncol.* (2005) 44:748–55. doi: 10.1080/02841860500327503
198. Zhang W, Ding M-L, Zhang J-N, Qiu J-R, Shen Y-H, Ding X-Y, et al. mTORC1 Maintains the tumorigenicity of SSEA-4+ high-grade osteosarcoma. *Sci Rep.* (2015) 5:9604. doi: 10.1038/srep09604
199. Bid HK, Roberts RD, Cam M, Audino A, Kurmasheva RT, Lin J, et al. DeltaNp63 promotes pediatric neuroblastoma and osteosarcoma by regulating tumor angiogenesis. *Cancer Res.* (2014) 74:320–9. doi: 10.1158/0008-5472.CAN-13-0894
200. Baglio SR, Lagerweij T, Perez-Lanzon M, Ho XD, Leveille N, Melo SA, et al. Blocking tumor-educated MSC paracrine activity halts osteosarcoma progression. *Clin Cancer Res.* (2017) 23:3721–33. doi: 10.1158/1078-0432.CCR-16-2726
201. Lafleur EA. Increased Fas expression reduces the metastatic potential of human osteosarcoma cells. *Clin Cancer Res.* (2004) 10:8114–9. doi: 10.1158/1078-0432.CCR-04-0353
202. Koshkina NV, Khanna C, Mendoza A, Guan H, DeLauter L, Kleinerman ES. Fas-negative osteosarcoma tumor cells are selected during metastasis to the lungs: the role of the Fas pathway in the metastatic process of osteosarcoma. *Mol Cancer Res.* (2007) 5:991–9. doi: 10.1158/1541-7786.MCR-07-0007
203. Gordon N, Koshkina NV, Jia SF, Khanna C, Mendoza A, Worth LL, et al. Corruption of the Fas pathway delays the pulmonary clearance of murine osteosarcoma cells, enhances their metastatic potential, and reduces the effect of aerosol gemcitabine. *Clin Cancer Res.* (2007) 13:4503–10. doi: 10.1158/1078-0432.CCR-07-0313
204. Rodriguez CO Jr, Crabbs TA, Wilson DW, Cannan VA, Skorupski KA, Gordon N, et al. Aerosol gemcitabine: preclinical safety and *in vivo* antitumor activity in osteosarcoma-bearing dogs. *J Aerosol Med Pulm Drug Deliv.* (2010) 23:197–206. doi: 10.1089/jamp.2009.0773
205. Hernández-Rodríguez NA, Correa E, Sotelo R, Gómez-Ruiz C, Contreras-Paredes A, Green L. Thrombin is present in the lungs of patients with primary extremity osteosarcoma and pulmonary metastases.

Int J Biol Markers. (2002) 17:189–95. doi: 10.1177/172460080201700308
206. Tieken C, Verboom MC, Ruf W, Gelderblom H, Bovée JVMG, Reitsma PH, et al. Tissue factor associates with survival and regulates tumour progression in osteosarcoma. *Thromb Haemost.* (2016) 115:1025–33. doi: 10.1160/TH15-07-0541
207. Van Den Berg YW, Osanto S, Reitsma PH, Versteeg HH. The relationship between tissue factor and cancer progression: insights from bench and bedside. *Blood.* (2012) 119:924–32. doi: 10.1182/blood-2011-06-317685
208. Lehuede C, Dupuy F, Rabinovitch R, Jones RG, Siegel PM. Metabolic plasticity as a determinant of tumor growth and metastasis. *Cancer Res.* (2016) 76:5201–8. doi: 10.1158/0008-5472.CAN-16-0266
209. Liberti MV, Locasale JW. The Warburg effect: how does it benefit cancer cells? *Trends Biochem Sci.* (2016) 41:211–8. doi: 10.1016/j.tibs.2015.12.001
210. Giang AH, Raymond T, Brookes P, de Mesy Bentley K, Schwarz E, O'Keefe R, et al. Mitochondrial dysfunction and permeability transition in osteosarcoma cells showing the Warburg effect. *J Biol Chem.* (2013) 288:33303–11. doi: 10.1074/jbc.M113.507129
211. Hua Y, Qiu Y, Zhao A, Wang X, Chen T, Zhang Z, et al. Dynamic metabolic transformation in tumor invasion and metastasis in mice with LM-8 osteosarcoma cell transplantation. *J Proteome Res.* (2011) 10:3513–21. doi: 10.1021/pr200147g
212. Connelly L, Barham W, Onishko HM, Chen L, Sherrill TP, Zabuawala T, et al. NF-kappaB activation within macrophages leads to an anti-tumor phenotype in a mammary tumor lung metastasis model. *Breast Cancer Res.* (2011) 13:R83. doi: 10.1186/bcr2935
213. Orrenius S, Gogvadze V, Zhivotovsky B. Mitochondrial oxidative stress: implications for cell death. *Annu Rev Pharmacol Toxicol.* (2007) 47:143–83. doi: 10.1146/annurev.pharmtox.47.120505.105122
214. Poderoso JJ, Helfenberger K, Poderoso C. The effect of nitric oxide on mitochondrial respiration. *Nitric Oxide.* (2019) 88:61–72. doi: 10.1016/j.niox.2019.04.005
215. Ren L, Hong ES, Mendoza A, Issaq S, Tran Hoang C, Lizardo M, et al. Metabolomics uncovers a link between inositol metabolism and osteosarcoma metastasis. *Oncotarget.* (2017) 8:38541–53. doi: 10.18632/oncotarget.15872
216. Winterbourn CC. Revisiting the reactions of superoxide with glutathione and other thiols. *Arch Biochem Biophys.* (2016) 595:68–71. doi: 10.1016/j.abb.2015.11.028
217. Ridnour LA, Thomas DD, Mancardi D, Espey MG, Miranda KM, Paolocci N, et al. The chemistry of nitrosative stress induced by nitric oxide and reactive nitrogen oxide species. Putting perspective on stressful biological situations. *Biol Chem.* (2004) 385:1–10. doi: 10.1515/BC.2004.001
218. Roy J, Dibaeinia P, Fan TM, Sinha S, Das A. Global analysis of osteosarcoma lipidomes reveal altered lipid profiles in metastatic versus nonmetastatic cells. *J Lipid Res.* (2019) 60:375–87. doi: 10.1194/jlr.M088559
219. Luo X, Cheng C, Tan Z, Li N, Tang M, Yang L, et al. Emerging roles of lipid metabolism in cancer metastasis. *Mol Cancer.* (2017) 16:76. doi: 10.1186/s12943-017-0646-3
220. Miwa S, Shirai T, Yamamoto N, Hayashi K, Takeuchi A, Igarashi K, et al. Current and emerging targets in immunotherapy for osteosarcoma. *J Oncol.* (2019) 2019:7035045. doi: 10.1155/2019/7035045
221. Dyson KA, Stover BD, Grippin A, Mendez-Gomez HR, Lagmay J, Mitchell DA, et al. Emerging trends in immunotherapy for pediatric sarcomas. *J Hematol Oncol.* (2019) 12:78. doi: 10.1186/s13045-019-0756-z
222. Wedekind MF, Wagner LM, Cripe TP. Immunotherapy for osteosarcoma: where do we go from here? *Pediatr Blood Cancer.* (2018) 65:e27227. doi: 10.1002/pbc.27227
223. Wang Z, Wang Z, Li B, Wang S, Chen T, Ye Z. Innate immune cells: a potential and promising cell population for treating osteosarcoma. *Front Immunol.* (2019) 10:1114. doi: 10.3389/fimmu.2019.01114
224. Heymann MF, Lezot F, Heymann D. The contribution of immune infiltrates and the local microenvironment in the pathogenesis of osteosarcoma. *Cell Immunol.* (2019) 343:103711. doi: 10.1016/j.cellimm.2017.10.011
225. Dumars C, Ngyuen JM, Gaultier A, Lanel R, Corradini N, Gouin F, et al. Dysregulation of macrophage polarization is associated with the metastatic process in osteosarcoma. *Oncotarget.* (2016) 7:78343–54. doi: 10.18632/oncotarget.13055
226. Buddingh EP, Kuijjer ML, Duim RA, Burger H, Agelopoulos K, Myklebost O, et al. Tumor-infiltrating macrophages are associated with metastasis suppression in high-grade osteosarcoma: a rationale for treatment with macrophage activating agents. *Clin Cancer Res.* (2011) 17:2110–9. doi: 10.1158/1078-0432.CCR-10-2047
227. Han Q, Shi H, Liu F. CD163(+) M2-type tumor-associated macrophage support the suppression of tumor-infiltrating T cells in osteosarcoma. *Int Immunopharmacol.* (2016) 34:101–6. doi: 10.1016/j.intimp.2016.01.023
228. Hingorani P, Maas ML, Gustafson MP, Dickman P, Adams RH, Watanabe M, et al. Increased CTLA-4(+) T cells and an increased ratio of monocytes with loss of class II (CD14(+) HLA-DR(lo/neg)) found in aggressive pediatric sarcoma patients. *J Immunother Cancer.* (2015) 3:35. doi: 10.1186/s40425-015-0082-0
229. Koirala P, Roth ME, Gill J, Piperdi S, Chinai JM, Geller DS, et al. Immune infiltration and PD-L1 expression in the tumor microenvironment are prognostic in osteosarcoma. *Sci Rep.* (2016) 6:30093. doi: 10.1038/srep30093
230. Gomez-Brouchet A, Illac C, Gilhodes J, Bouvier C, Aubert S, Guinebretiere JM, et al. CD163-positive tumor-associated macrophages and CD8-positive cytotoxic lymphocytes are powerful diagnostic markers for the therapeutic stratification of osteosarcoma patients: an immunohistochemical analysis of the biopsies fromthe French OS2006 phase 3 trial. *Oncoimmunology.* (2017) 6:e1331193. doi: 10.1080/2162402X.2017.1331193
231. Pahl JH, Kwappenberg KM, Varypataki EM, Santos SJ, Kuijjer ML, Mohamed S, et al. Macrophages inhibit human osteosarcoma cell growth after activation with the bacterial cell wall derivative liposomal muramyl tripeptide in combination with interferon-gamma. *J Exp Clin Cancer Res.* (2014) 33:27. doi: 10.1186/1756-9966-33-27
232. Shao XJ, Xiang SF, Chen YQ, Zhang N, Cao J, Zhu H, et al. Inhibition of M2-like macrophages by all-trans retinoic acid prevents cancer initiation and stemness in osteosarcoma cells. *Acta Pharmacol Sin.* (2019) 40:1343–50. doi: 10.1038/s41401-019-0262-4
233. Zhou Q, Xian M, Xiang S, Xiang D, Shao X, Wang J, et al. All-trans retinoic acid prevents osteosarcoma metastasis by inhibiting M2 polarization of tumor-associated macrophages. *Cancer Immunol Res.* (2017) 5:547–59. doi: 10.1158/2326-6066.CIR-16-0259
234. Fritzsching B, Fellenberg J, Moskovszky L, Sapi Z, Krenacs T, Machado I, et al. CD8(+)/FOXP3(+)-ratio in osteosarcoma microenvironment separates survivors from non-survivors: a multicenter validated retrospective study. *Oncoimmunology.* (2015) 4:e990800. doi: 10.4161/2162402X.2014.990800
235. Li X, Chen Y, Liu X, Zhang J, He X, Teng G, et al. Tim3/Gal9 interactions between T cells and monocytes result in an immunosuppressive feedback loop that inhibits Th1 responses in osteosarcoma patients. *Int Immunopharmacol.* (2017) 44:153–9. doi: 10.1016/j.intimp.2017.01.006
236. Sundara YT, Kostine M, Cleven AH, Bovee JV, Schilham MW, Cleton-Jansen AM. Increased PD-L1 and T-cell infiltration in the presence of HLA class I expression in metastatic high-grade osteosarcoma: a rationale for T-cell-based immunotherapy. *Cancer Immunol Immunother.* (2017) 66:119–28. doi: 10.1007/s00262-016-1925-3
237. Lussier DM, O'Neill L, Nieves LM, McAfee MS, Holechek SA, Collins AW, et al. Enhanced T-cell immunity to osteosarcoma through antibody blockade of PD-1/PD-L1 interactions. *J Immunother.* (2015) 38:96–106. doi: 10.1097/CJI.0000000000000065
238. Coley WB. The treatment of sarcoma of the long bones. *Ann Surg.* (1933) 97:434–60. doi: 10.1097/00000658-193303000-00010
239. Lascelles BD, Dernell WS, Correa MT, Lafferty M, Devitt CM, Kuntz CA, et al. Improved survival associated with postoperative wound infection in dogs treated with limb-salvage surgery for osteosarcoma. *Ann Surg Oncol.* (2005) 12:1073–83. doi: 10.1245/ASO.2005.01.011
240. Jeys LM, Grimer RJ, Carter SR, Tillman RM, Abudu A. Post operative infection and increased survival in osteosarcoma patients: are they associated? *Ann Surg Oncol.* (2007) 14:2887–95. doi: 10.1245/s10434-007-9483-8
241. Sottnik JL, U'Ren LW, Thamm DH, Withrow SJ, Dow SW. Chronic bacterial osteomyelitis suppression of tumor growth requires innate immune responses. *Cancer Immunol Immunother.* (2010) 59:367–78. doi: 10.1007/s00262-009-0755-y
242. Fidler IJ, Sone S, Fogler WE, Barnes ZL. Eradication of spontaneous metastases and activation of alveolar macrophages by intravenous injection

of liposomes containing muramyl dipeptide. *Proc Natl Acad Sci USA*. (1981) 78:1680–4. doi: 10.1073/pnas.78.3.1680

243. MacEwen EG, Kurzman ID, Rosenthal RC, Smith BW, Manley PA, Roush JK, et al. Therapy for osteosarcoma in dogs with intravenous injection of liposome-encapsulated muramyl tripeptide. *J Natl Cancer Inst.* (1989) 81:935–8. doi: 10.1093/jnci/81.12.935
244. Kurzman ID, MacEwen EG, Rosenthal RC, Fox LE, Keller ET, Helfand SC, et al. Adjuvant therapy for osteosarcoma in dogs: results of randomized clinical trials using combined liposome-encapsulated muramyl tripeptide and cisplatin. *Clin Cancer Res.* (1995) 1:1595–601.
245. Meyers PA, Schwartz CL, Krailo MD, Healey JH, Bernstein ML, Betcher D, et al. Osteosarcoma: the addition of muramyl tripeptide to chemotherapy improves overall survival–a report from the Children's Oncology Group. *J Clin Oncol.* (2008) 26:633–8. doi: 10.1200/JCO.2008.14.0095
246. Chou AJ, Kleinerman ES, Krailo MD, Chen Z, Betcher DL, Healey JH, et al. Addition of muramyl tripeptide to chemotherapy for patients with newly diagnosed metastatic osteosarcoma: a report from the Children's Oncology Group. *Cancer.* (2009) 115:5339–48. doi: 10.1002/cncr.24566
247. Bielack SS, Smeland S, Whelan JS, Marina N, Jovic G, Hook JM, et al. Methotrexate, doxorubicin, and cisplatin (MAP) plus maintenance pegylated interferon Alfa-2b versus MAP alone in patients with resectable high-grade osteosarcoma and good histologic response to preoperative MAP: first results of the EURAMOS-1 good response randomized controlled trial. *J Clin Oncol.* (2015) 33:2279–87. doi: 10.1200/JCO.2014.60.0734
248. Meazza C, Cefalo G, Massimino M, Daolio P, Pastorino U, Scanagatta P, et al. Primary metastatic osteosarcoma: results of a prospective study in children given chemotherapy and interleukin-2. *Med Oncol.* (2017) 34:191. doi: 10.1007/s12032-017-1052-9
249. Schwinger W, Klass V, Benesch M, Lackner H, Dornbusch HJ, Sovinz P, et al. Feasibility of high-dose interleukin-2 in heavily pretreated pediatric cancer patients. *Ann Oncol.* (2005) 16:1199–206. doi: 10.1093/annonc/mdi226
250. Khanna C, Anderson PM, Hasz DE, Katsanis E, Neville M, Klausner JS. Interleukin-2 liposome inhalation therapy is safe and effective for dogs with spontaneous pulmonary metastases. *Cancer.* (1997) 79:1409–21. doi: 10.1002/(SICI)1097-0142(19970401)79:7<1409::AID-CNCR19>3.0.CO;2-3
251. Dow S, Elmslie R, Kurzman I, MacEwen G, Pericle F, Liggitt D. Phase I study of liposome-DNA complexes encoding the interleukin-2 gene in dogs with osteosarcoma lung metastases. *Hum Gene Ther.* (2005) 16:937–46. doi: 10.1089/hum.2005.16.937
252. Chiavenna SM, Jaworski JP, Vendrell A. State of the art in anti-cancer mAbs. *J Biomed Sci.* (2017) 24:15. doi: 10.1186/s12929-016-0311-y
253. Ebb D, Meyers P, Grier H, Bernstein M, Gorlick R, Lipshultz SE, et al. Phase II trial of trastuzumab in combination with cytotoxic chemotherapy for treatment of metastatic osteosarcoma with human epidermal growth factor receptor 2 overexpression: a report from the children's oncology group. *J Clin Oncol.* (2012) 30:2545–51. doi: 10.1200/JCO.2011.37.4546
254. Weigel B, Malempati S, Reid JM, Voss SD, Cho SY, Chen HX, et al. Phase 2 trial of cixutumumab in children, adolescents, and young adults with refractory solid tumors: a report from the Children's Oncology Group. *Pediatr Blood Cancer.* (2014) 61:452–6. doi: 10.1002/pbc.24605
255. Roth M, Barris DM, Piperdi S, Kuo V, Everts S, Geller D, et al. Targeting glycoprotein NMB with antibody-drug conjugate, glembatumumab vedotin, for the treatment of osteosarcoma. *Pediatr Blood Cancer.* (2016) 63:32–8. doi: 10.1002/pbc.25688
256. Trinidad EM, Gonzalez-Suarez E. RANKL inhibitors for osteosarcoma treatment: hope and caution. *Ann Transl Med.* (2016) 4:534. doi: 10.21037/atm.2016.12.10
257. Roth M, Linkowski M, Tarim J, Piperdi S, Sowers R, Geller D, et al. Ganglioside GD2 as a therapeutic target for antibody-mediated therapy in patients with osteosarcoma. *Cancer.* (2014) 120:548–54. doi: 10.1002/cncr.28461
258. Galon J, Angell HK, Bedognetti D, Marincola FM. The continuum of cancer immunosurveillance: prognostic, predictive, and mechanistic signatures. *Immunity.* (2013) 39:11–26. doi: 10.1016/j.immuni.2013.07.008
259. Lussier DM, Johnson JL, Hingorani P, Blattman JN. Combination immunotherapy with alpha-CTLA-4 and alpha-PD-L1 antibody blockade prevents immune escape and leads to complete control of metastatic osteosarcoma. *J Immunother Cancer.* (2015) 3:21. doi: 10.1186/s40425-015-0067-z
260. Perry JA, Kiezun A, Tonzi P, Van Allen EM, Carter SL, Baca SC, et al. Complementary genomic approaches highlight the PI3K/mTOR pathway as a common vulnerability in osteosarcoma. *Proc Natl Acad Sci USA.* (2014) 111:E5564–73. doi: 10.1073/pnas.1419260111
261. Chen X, Bahrami A, Pappo A, Easton J, Dalton J, Hedlund E, et al. Recurrent somatic structural variations contribute to tumorigenesis in pediatric osteosarcoma. *Cell Rep.* (2014) 7:104–12. doi: 10.1016/j.celrep.2014.03.003
262. Wang D, Niu X, Wang Z, Song CL, Huang Z, Chen KN, et al. Multiregion sequencing reveals the genetic heterogeneity and evolutionary history of osteosarcoma and matched pulmonary metastases. *Cancer Res.* (2019) 79:7–20. doi: 10.1158/0008-5472.CAN-18-1086
263. Tawbi HA, Burgess M, Bolejack V, Van Tine BA, Schuetze SM, Hu J, et al. Pembrolizumab in advanced soft-tissue sarcoma and bone sarcoma (SARC028): a multicentre, two-cohort, single-arm, open-label, phase 2 trial. *Lancet Oncol.* (2017) 18:1493–501. doi: 10.1016/S1470-2045(17)30624-1
264. Thanindratarn P, Dean DC, Nelson SD, Hornicek FJ, Duan Z. Advances in immune checkpoint inhibitors for bone sarcoma therapy. *J Bone Oncol.* (2019) 15:100221. doi: 10.1016/j.jbo.2019.100221
265. Miwa S, Nishida H, Tanzawa Y, Takeuchi A, Hayashi K, Yamamoto N, et al. Phase 1/2 study of immunotherapy with dendritic cells pulsed with autologous tumor lysate in patients with refractory bone and soft tissue sarcoma. *Cancer.* (2017) 123:1576–84. doi: 10.1002/cncr.30606
266. Himoudi N, Wallace R, Parsley KL, Gilmour K, Barrie AU, Howe K, et al. Lack of T-cell responses following autologous tumour lysate pulsed dendritic cell vaccination, in patients with relapsed osteosarcoma. *Clin Transl Oncol.* (2012) 14:271–9. doi: 10.1007/s12094-012-0795-1
267. Mason NJ, Gnanandarajah JS, Engiles JB, Gray F, Laughlin D, Gaurnier-Hausser A, et al. Immunotherapy with a HER2-targeting listeria induces HER2-specific immunity and demonstrates potential therapeutic effects in a phase I trial in canine osteosarcoma. *Clin Cancer Res.* (2016) 22:4380–90. doi: 10.1158/1078-0432.CCR-16-0088
268. Ahmed N, Brawley VS, Hegde M, Robertson C, Ghazi A, Gerken C, et al. Human epidermal growth factor receptor 2 (HER2) -specific chimeric antigen receptor-modified T cells for the immunotherapy of HER2-positive sarcoma. *J Clin Oncol.* (2015) 33:1688–96. doi: 10.1200/JCO.2014.58.0225
269. Mata M, Vera JF, Gerken C, Rooney CM, Miller T, Pfent C, et al. Toward immunotherapy with redirected T cells in a large animal model: *ex vivo* activation, expansion, and genetic modification of canine T cells. *J Immunother.* (2014) 37:407–15. doi: 10.1097/CJI.0000000000000052
270. Canter RJ, Grossenbacher SK, Foltz JA, Sturgill IR, Park JS, Luna JI, et al. Radiotherapy enhances natural killer cell cytotoxicity and localization in pre-clinical canine sarcomas and first-in-dog clinical trial. *J Immunother Cancer.* (2017) 5:98. doi: 10.1186/s40425-017-0305-7
271. Chun R, de Lorimier LP. Update on the biology and management of canine osteosarcoma. *Vet Clin North Am Small Anim Pract.* (2003) 33:491–516, vi. doi: 10.1016/S0195-5616(03)00021-4
272. Selmic LE, Burton JH, Thamm DH, Withrow SJ, Lana SE. Comparison of carboplatin and doxorubicin-based chemotherapy protocols in 470 dogs after amputation for treatment of appendicular osteosarcoma. *J Vet Intern Med.* (2014) 28:554–63. doi: 10.1111/jvim.12313
273. Roberts SS, Chou AJ, Cheung NK. Immunotherapy of Childhood Sarcomas. *Front Oncol.* (2015) 5:181. doi: 10.3389/fonc.2015.00181
274. Wycislo KL, Fan TM. The immunotherapy of canine osteosarcoma: a historical and systematic review. *J Vet Intern Med.* (2015) 29:759–69. doi: 10.1111/jvim.12603
275. Scott MC, Temiz NA, Sarver AE, LaRue RS, Rathe SK, Varshney J, et al. Comparative transcriptome analysis quantifies immune cell transcript levels,

metastatic progression, and survival in osteosarcoma. *Cancer Res.* (2018) 78:326–37. doi: 10.1158/0008-5472.CAN-17-0576

276. Biller BJ, Guth A, Burton JH, Dow SW. Decreased ratio of CD8+ T cells to regulatory T cells associated with decreased survival in dogs with osteosarcoma. *J Vet Intern Med.* (2010) 24:1118–23. doi: 10.1111/j.1939-1676.2010.0557.x
277. Biller BJ, Elmslie RE, Burnett RC, Avery AC, Dow SW. Use of FoxP3 expression to identify regulatory T cells in healthy dogs and dogs with cancer. *Vet Immunol Immunopathol.* (2007) 116:69–78. doi: 10.1016/j.vetimm.2006.12.002
278. Withers SS, Skorupski KA, York D, Choi JW, Woolard KD, Laufer-Amorim R, et al. Association of macrophage and lymphocyte infiltration with outcome in canine osteosarcoma. *Vet Comp Oncol.* (2019) 17:49–60. doi: 10.1111/vco.12444
279. Maekawa N, Konnai S, Okagawa T, Nishimori A, Ikebuchi R, Izumi Y, et al. Immunohistochemical analysis of PD-L1 expression in canine malignant cancers and PD-1 expression on lymphocytes in canine oral melanoma. *PLoS ONE.* (2016) 11:e0157176. doi: 10.1371/journal.pone.0157176
280. Goss PE, Chambers AF. Does tumour dormancy offer a therapeutic target? *Nat Rev Cancer.* (2010) 10:871–7. doi: 10.1038/nrc2933
281. Zhu L, McManus M, Hughes D. Understanding the biology of bone sarcoma from early initiating events through late events in metastasis and disease progression. *Front Oncol.* (2013) 3:230. doi: 10.3389/fonc.2013.00230

Conflict of Interest: The authors declare that the research was conducted in the absence of any commercial or financial relationships that could be construed as a potential conflict of interest.

Copyright © 2020 Fan, Roberts and Lizardo. This is an open-access article distributed under the terms of the Creative Commons Attribution License (CC BY). The use, distribution or reproduction in other forums is permitted, provided the original author(s) and the copyright owner(s) are credited and that the original publication in this journal is cited, in accordance with accepted academic practice. No use, distribution or reproduction is permitted which does not comply with these terms.

frontiers in Oncology

HYPOTHESIS AND THEORY
published: 07 February 2020
doi: 10.3389/fonc.2020.00084

Advanced Cancer Imaging Applied in the Comparative Setting

David M. Vail[1,2*], *Amy K. LeBlanc*[3] *and Robert Jeraj*[2,4]

[1] Department of Medical Sciences, School of Veterinary Medicine, University of Wisconsin-Madison, Madison, WI, United States, [2] Carbone Cancer Center, University of Wisconsin-Madison, Madison, WI, United States, [3] Comparative Oncology Program, Center for Cancer Research, National Cancer Institute, Bethesda, MD, United States, [4] Department of Medical Physics, School of Medicine and Public Health, University of Wisconsin-Madison, Madison, WI, United States

The potential for companion (pet) species with spontaneously arising tumors to act as surrogates for preclinical development of advanced cancer imaging technologies has become more apparent in the last decade. The utility of the companion model specifically centers around issues related to body size (including spatial target/normal anatomic characteristics), physical size and spatial distribution of metastasis, tumor heterogeneity, the presence of an intact syngeneic immune system and a syngeneic tumor microenvironment shaped by the natural evolution of the cancer. Companion species size allows the use of similar equipment, hardware setup, software, and scan protocols which provide the opportunity for standardization and harmonization of imaging operating procedures and quality assurance across imaging protocols, imaging hardware, and the imaged species. Murine models generally do not replicate the size and spatial distribution of human metastatic cancer and these factors strongly influence image resolution and dosimetry. The following review will discuss several aspects of comparative cancer imaging in more detail while providing several illustrative examples of investigational approaches performed or currently under exploration at our institutions. Topics addressed include a discussion on interested consortia; image quality assurance and harmonization; image-based biomarker development and validation; contrast agent and radionuclide tracer development; advanced imaging to assess and predict response to cytotoxic and immunomodulatory anticancer agents; imaging of the tumor microenvironment; development of novel theranostic approaches; cell trafficking assessment via non-invasive imaging; and intraoperative imaging to inform surgical oncology decision making. Taken in totality, these comparative opportunities predict that safety, diagnostic and efficacy data generated in companion species with naturally developing and progressing cancers would better recapitulate the human cancer condition than that of artificial models in small rodent systems and ultimately accelerate the integration of novel imaging technologies into clinical practice. It is our hope that the examples presented should serve to provide those involved in cancer investigations who are unfamiliar with available comparative methodologies an understanding of the potential utility of this approach.

Keywords: canine, cancer, imaging, radiomics, biomarkers, PET/CT, theranostics, comparative

OPEN ACCESS

Edited by:
Rodney L. Page, Colorado State University, United States

Reviewed by:
Lynn Griffin, Colorado State University, United States
Natalie Julie Serkova, University of Colorado, United States

***Correspondence:**
David M. Vail
david.vail@wisc.edu

Specialty section:
This article was submitted to Cancer Molecular Targets and Therapeutics, a section of the journal Frontiers in Oncology

Received: *31 July 2019*
Accepted: *16 January 2020*
Published: *07 February 2020*

Citation:
Vail DM, LeBlanc AK and Jeraj R (2020) Advanced Cancer Imaging Applied in the Comparative Setting. Front. Oncol. 10:84. doi: 10.3389/fonc.2020.00084

INTRODUCTION

Historically, cancer imaging in comparative species (e.g., pet dogs and cats) followed (lagged) behind cancer imaging technology development in humans. That is, as a new modality (CT, MRI, PET) was developed and subsequently applied clinically in human cancer patients, only then would it become available to veterinarians for clinical application. However, in the last two decades, the potential for companion species with spontaneously arising tumors to act as surrogates for preclinical development of advanced imaging technologies has become more apparent. Indeed, the blueprint has begun to shift where investigations of novel cancer imaging technologies in companion species precede human application and are involved earlier in the development pipeline. For example, the conformal image-guided radiation therapy technology, tomotherapy®, was first tested by inclusion of companion dogs with spontaneous sinonasal tumors and subsequent PET/CT serial imaging in these patients was used to characterize and map hypoxic, metabolic, and proliferative areas of the tumors under treatment (1, 2). Several other examples will follow in subsequent sections of this review.

Opportunities, Advantages, and Obstacles for Comparative Cancer Imaging

The opportunities and potential advantages for a comparative approach to cancer investigation that involves the inclusion of companion species (e.g., pet dogs and cats) with spontaneously arising cancers as preclinical surrogates to human-centric studies have been collectively and generally discussed in several of the reviews within this special volume of Frontiers. With regards to cancer imaging in particular, the opportunities, and advantages more specifically center around issues related to body size (including spatial target/normal anatomic characteristics), physical size and spatial distribution of metastasis, tumor heterogeneity, the presence of an intact syngeneic immune system and a syngeneic tumor microenvironment shaped by the natural evolution of the cancer. Taken in totality, these comparative opportunities predict that safety, diagnostic, and efficacy data generated in companion species with naturally developing and progressing cancers would better recapitulate the human cancer condition than that of artificial models in small rodent systems.

The body size of companion species conveys several advantages in the imaging realm. Standard and advanced equipment designed for pediatric and adult human imaging of cancer can be readily applied without modification to companion species ensuring more global accessibility at both human and veterinary clinical research centers. Further, the use of similar equipment, hardware setup, software, and scan protocols provide the opportunity for standardization and harmonization of imaging operating procedures and quality assurance across imaging protocols, imaging hardware, and the imaged species. Spatial concerns regarding image resolution, radionuclide and other optically active compound wavelength and tissue penetration depth are also abrogated in companion species with larger body size. For example, when dealing with diagnostic and therapeutic radionuclides, the canine body size is more representative of human subjects than rodents with respect to radiation dosimetry calculations and are more reliable for extrapolation to humans. Murine models do not replicate the size and spatial distribution of human metastatic cancer and these factors strongly influence image resolution and dosimetry. This becomes even more important when investigating off-target effects of diagnostic and therapeutic radiation emitters where tumor and normal organ (e.g., bone marrow) proximity is critical to both efficacy and safety. Finally, body (and indeed tumor) size allows for serial and varied biospecimen procurement in companion species that are concomitant to image investigations. Since anesthesia is requisite for most advanced imaging modalities (CT, MRI, PET) in companion species, this allows greater ethical latitude for procurement of biospecimens concomitant to procuring advanced and functional images. Such procurements, whether they be from the peripheral blood compartment or the tumor/TME, would allow characterization of PK/PD for novel imaging agents, validation of potential imaging biomarkers, assessment of immune modulation, and safety evaluations.

Companion animals in general allow for achieving much higher quantitative imaging accuracy. Imaging under anesthesia allows much more reproducible positioning of companion animals within scanners and generally experience reduced motion artifact, very important in multiple sequential (treatment response assessment) types of studies. Similarly, anesthesia allows for prolonged scanning times, if necessary, therefore allowing more accurate assessment of PK (e.g., in dynamic PET studies of novel imaging or labeled treatment agents).

With the realization that tumor—tumor microenvironment (TME) interaction is critical for many aspects of tumor imaging, image-guided therapy, and image derived assessment of therapeutic response, the potential of syngeneic natural tumors in companion animals as surrogates for image technology development becomes self-evident. Further, an intact syngeneic immune system is a critical component of this tumor-TME interaction and further enhances the surrogate utility of cancer-bearing companion species in a comparative approach.

The following review will discuss the utility of comparative cancer imaging in more detail while providing several illustrative examples of investigational approaches performed or currently under exploration at our institutions. It is our hope that the examples presented should serve to provide those in cancer investigations who are unfamiliar with available comparative methodologies an understanding of the potential utility of this approach.

NCI Perspectives

In 2004, the intramural research program of the National Institutes of Health's National Cancer Institute created the Comparative Oncology Program (COP), with the explicit goal of advancing the tumor-bearing dog as a naturally-occurring complementary animal model of cancer. As a scientific discipline, comparative oncology has the overarching goal to advance knowledge of veterinary cancers and to rationally integrate such patients into studies of cancer biology and therapy. To that end, in 2015, a workshop was convened by the U.S.

National Academy of Medicine's National Cancer Policy Forum to define and explore the perceived and/or acknowledged gaps in knowledge that may impact the delivery of comparative oncology data to stakeholders in cancer drug development (3). Seven distinct topics, including opportunities in comparative cancer imaging, were discussed to gain insight into how the gaps could be addressed and the role of tumor-bearing dogs in cancer research strengthened. Since that time, several NCI-funded initiatives focused on canine cancer have been introduced to the cancer research community that begin to address these gaps in knowledge, including genomic characterization of canine tumors and the development of novel immunotherapeutic strategies.

As part of the U01-affiliated Immuno-Oncology Translational Network (https://www.cancer.gov/research/key-initiatives/moonshot-cancer-initiative/implementation/adult-immunotherapy-network) several exciting collaborative efforts are underway to realize the potential for dogs to inform the development and prioritization of novel immunotherapeutic approaches for human cancer treatment and many involve sophisticated imaging techniques (discussed later in this review).

Consortia [COTC, CBTC, CORC]

One of the most important achievements in comparative oncology over the last decade has been the development of successful and collaborative consortia that perform multicenter clinical trials in the comparative realm, several involving development of, or utilization of advanced cancer imaging. Consortium infrastructures allow larger scale clinical trials and provide the voice for collective advocacy in veterinary and comparative oncology. Examples include the comparative oncology trials consortia (COTC), comparative brain tumor consortia (CBTC) and the comparative oncology research consortia (CORC).

The COTC is an active network of 24 academic comparative oncology centers (https://ccr.cancer.gov/Comparative-Oncology-Program/sponsors/consortium), centrally managed by the National Institutes of Health–NCI's COP that functions to design and execute clinical trials in dogs with cancer to assess novel therapies (4–6). The goal of this effort is to answer biologic questions geared to inform the development path of these agents for use in human cancer patients. COTC trials are pharmacokinetically and pharmacodynamically rich, with the product of this work directly integrated into the design of human early and late phase clinical trials. They are focused to answer mechanistic questions and define dose-toxicity and dose-response relationships. They can be designed to compare varying schedules and routes of drug administration, validate target biology, model clinical standard operating procedures (SOPs), and assess biomarkers. Additionally, within this effort, the COTC PD Core was created. The COTC PD Core is a virtual laboratory of assays and services, including pathology, immunohistochemistry, immunocytochemistry, flow cytometry, genomics, proteomics, cell culture and drug screening, PKs, and cell biology designed to support COTC clinical trial biologic endpoints. As of 2019, the COTC has completed 14 clinical trials and has been successful in promoting the utility of comparative oncology modeling within the drug development community.

The CBTC was created by the NCI's COP in 2015 to specifically address gaps in knowledge that pertain to the translational relevance of canine brain tumors to their human counterparts (https://ccr.cancer.gov/comparative-oncology-program/research/cbtc). Further, the CBTC membership seeks to recognize the potential for these canine patients to participate in studies of cancer biology and therapy to benefit both humans and dogs. At the inaugural meeting of this consortium, a SWOT analysis (strengths, weaknesses, opportunities, threat) was carried out to define, through working group discussions, a list of prioritized projects that could begin to address the most critical unanswered questions and medical needs for both species (7). Since that time, a series of initiatives have been published that reflect the activity of this group of investigators. These include a comparative assessment of canine glioma pathology and harmonized magnetic resonance imaging (MRI) parameters to facilitate multicenter clinical trials in canine brain tumor patients (8, 9). Further, the first CBTC-specific clinical trial in canine brain tumors evaluates a theranostic strategy targeting apoptosis. In this ongoing trial, dogs with meningioma receive a novel CNS-penetrant small molecule activator of procaspsase-3 (PAC-1) and undergo serial PET imaging with a novel apoptosis-specific PET imaging agent (^{18}F-CSNAT4) to detect and semi-quantitatively measure tumoral apoptosis prior to and after PAC-1 exposure (10–12). Data generated from this work is directly linked to and is informing the clinical study of both PAC-1 and ^{18}F-CSNAT4 in human patients (clinicaltrials.gov identifier NCT02355535).

The CORC is a recently formed research consortia whose members represent academic comparative oncologists and scientists from partnered academic institutional programs where an NCI Comprehensive Cancer Center and academic veterinary oncology program have a formal affiliation. The CORC was designed to fulfill some of the clear mandates required to advance the discipline of comparative oncology. The V Foundation for Cancer Research committed to serve as the fiduciary agent, funding partner, and grant coordinator of CORC in order to support fundamental and translational research to more fully characterize cross-species opportunities. (https://www.v.org/research/specialfunds/canine-comparative-oncology/). Advanced cancer imaging in companion species comprise an important component of this consortia.

IMAGING BIOMARKERS IN COMPARATIVE ONCOLOGY

Quality Assurance, Standardization, and Harmonization of Imaging Technologies

Until recently, the primary goal for imaging has been diagnosis and staging, both in humans and companion animals. However, when imaging is used to define a treatment target (e.g., in radiation oncology), or assess changes from one scan to another scan to assess treatment efficacy (e.g., by RECIST evaluation), imaging signals need to be *quantified*. Quantification requirements are elevated in both, spatial quantification information (e.g., where exactly is tumor), as well as temporal quantification (e.g., how much has the tumor

changed). Because of the high spatio-temporal quantification nature, quantification imaging requirements are much more stringent; they require a high level of image quantification and minimal uncertainties of the imaging signal.

In order to obtain quantitative information from any images, several steps of the so-called "imaging chain" need to be followed. The key steps of the quantitative imaging chain include: (1) Imaging protocol, (2) Imaging data acquisition, (3) Image reconstruction, (4) Image analysis, and (5) Image measurement. In order to secure a high level of quantitative imaging accuracy, each step of the quantitative imaging chain needs to be carefully evaluated. As the overall image quantification accuracy depends on each step, it is essential to adequately control major uncertainties of the overall chain.

Because of the similarities of the imaging systems between human and larger companion animals, the same Quality Assurance (QA) steps as in humans should be followed in veterinary clinics [e.g., see Table 1 in Jeraj et al. (13)]. For quantitative imaging applications, the QA program needs to be even more elaborate (often requiring added scanner qualification using dedicated imaging phantoms), to minimize imaging bias and variance. In multi-center setting, the need for adequate QA at each participating site, is significantly increased. Furthermore, steps to ensure better "harmonization" of the scanners from multiple institutions (tuning them in a way to produce similar imaging quality), is warranted. While basic imaging QA is typically performed on scanners in veterinary use, a shortage of adequate expertise, particularly medical physics, which assures high quality imaging for human use, severely hampers ability to perform quantitative imaging in comparative oncology setting.

In order to help facilitating quantitative imaging, the Quantitative Imaging Biomarker Alliance (QIBA) has been established (https://www.rsna.org/en/research/quantitative-imaging-biomarkers-alliance). QIBA seeks to improve the value and practicality of Quantitative Imaging Biomarkers (QIBs) by reducing variability across devices, sites, patients and time (14). QIBA defines a QIB as "an objective characteristic derived from an *in vivo* image measured on a ratio or interval scale as indicators of normal biological processes, pathogenic processes, or a response to a therapeutic intervention." The technical performance of each QIB must then be assessed by establishing the physical phenomenon being measured, under what circumstances it can be measured, and what level of uncertainty is to be expected with each measurement. These points are all addressed by investigating the *bias*, *repeatability*, and *reproducibility* of measured imaging values.

While in humans, quantitative imaging has been rather well-established, realization of the needs and requirements for achieving adequate quantitative imaging accuracy in comparative oncology is significantly lagging behind. Too often imaging is used without adequate quantitative accuracy, and without understanding uncertainties, which can severely hamper interpretation of the imaging data. For example, QIBA has developed a number of "profiles" and "protocols (http://qibawiki.rsna.org/index.php/Profiles), in various stages of validation, which address necessary steps that need to be taken for achieving adequate image quality for a given type of imaging accuracy (e.g., FDG PET/CT). Ideally, one would derive similar "profiles" for companion animals. In the meantime, it is highly recommended that QIBA recommendations are also followed in comparative oncology studies.

UTILITY OF COMPARATIVE CANCER IMAGING

Imaging Technology Development

Contrast Agent Development

Owing to the similarities in size, spatial anatomy and physiologic parameters (e.g., ADME; absorption, distribution, metabolism, and excretion), cancer-bearing companion species enable proof-of-concept investigations of novel imaging agents with relevant lesion sizes on clinically-equivalent scanners. A recent investigation of a long-circulating liposomal iodinated CT contrast agent in dogs with naturally occurring tumors serves illustrative of this concept (15). Unlike conventional iodinated contrast agents which have rapid wash-in/wash-out tumor kinetics and renal clearance, long-circulating liposomes gradually extravasate, through the permeable tumor vasculature, and accumulate in tumors, a phenomenon known as enhanced permeation and retention (EPR) (16). Our trial in companion dogs characterized agent safety and ability to perform serial and prolonged visualization of small and large tumors over time without repeated infusions as is necessary in non-liposomal iodinated contrast agents. The agent allowed significant enhancement and uniform opacification of the vascular compartment in early-phase scans (15-min post-contrast infusion), demonstrated non-renal clearance which is preferable in patients with renal impairment, and took advantage of EPR characteristics of long-circulating liposomal products allowing intra-tumoral signal enhancement in the delayed-phase scans (24 h post-contrast infusion) (**Figure 1**).

Novel Radionuclide Tracer Development

The opportunities and advantages of the comparative approach also lends itself to development and validation of novel radionuclide tracers for functional imaging. In particular, spatial (lesion-normal tissue) considerations and our ability to perform serial biopsy and biospecimen procurement allow concomitant validation of novel tracer functional correlation. For example, the authors validated the non-invasive assessment of tumor proliferation of the thymidine-analog 3′-deoxy-3′[^{18}F]fluorothymidine (FLT) by comparing FLT uptake in companion dogs with non-Hodgkin's lymphoma (NHL) to gold-standard Ki-67 immunohistochemistry [**Figure 2**; (18)]. Comparisons of ^{18}F-FDG and ^{18}F-FLT may also allow distinction of tumor borders within areas of higher-than-average background tracer uptake, such as within liver or brain (**Figure 3**). Further, these studies illustrate the use of advanced imaging in companion species to document efficacy of investigational cytotoxic agents like the novel cytotoxic prodrug, GS-9219; and also to map areas of chemosensitive cells such as proliferating bone marrow (17, 19, 20). Access to such patients supports multiparametric imaging studies in a tractable period of time within their clinical management.

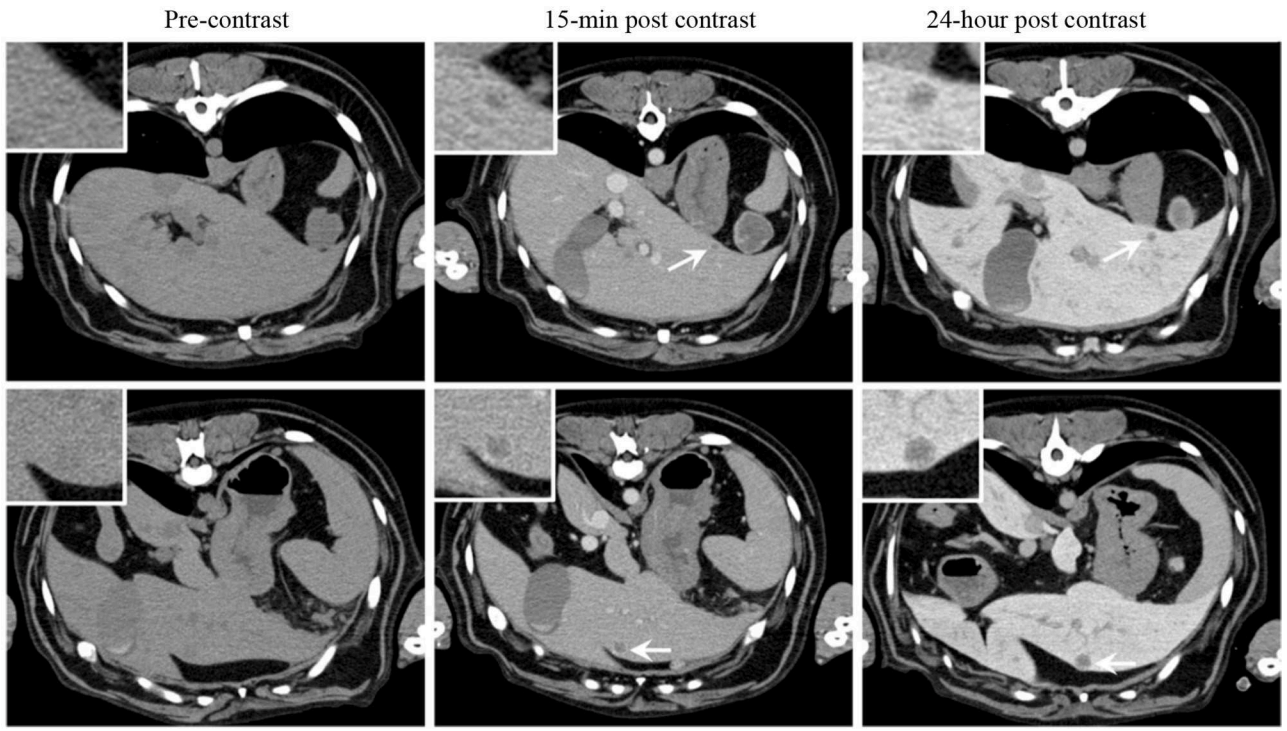

FIGURE 1 | Signal enhancement pattern of a long-circulating liposomal iodinated CT contrast agent investigated in a companion dog with metastatic liver tumors. Axial CT images demonstrating the effect of post-Liposomal-I imaging time point on visualization of metastatic liver lesions (white arrows). The 0.5 cm **(Top)** and 1 cm **(Bottom)** lesions are better visualized on the post-24 h images due to increased liver uptake of the contrast agent. Reprinted from Ghaghada et al. (15).

Other examples of novel tracer development and application by inclusion of companion species include 13-C pyruvate magnetic resonance spectroscopy (21), and ^{18}F-tetrafluoroborate (^{18}F-BF_4^- or ^{18}F-TFB) for expressed sodium-iodide symporter (NIS) PET imaging (**Figure 4**), which could be a useful tool for clinical thyroid and neuroendocrine tumor imaging, for preclinical imaging of NIS-expressing disease models and for cell trafficking studies (22–24). We have also explored the utility of an ^{18}F-radiolabeled fatty acid ^{18}F-fluoro-thia-heptadecandoic acid for metabolic imaging of fatty acid oxidation, which is an emerging field in the study of cancer metabolism (**Figure 5**) (25, 26). All of these concepts share the common theme of investigating advanced functional imaging technologies in a relevant large animal model that can develop spontaneous syngeneic tumors.

Assessment of Novel Cytotoxic Drug Efficacy

Inclusion of companion species in the pre-clinical assessments of efficacy and safety of novel cytotoxic drugs holds tremendous potential for informing subsequent or parallel human clinical trials and theoretically could accelerate the drug development and registration timeline. The inclusion of advanced cancer imaging in these comparative trials serves to provide compelling proof-of-concept characterizations of response in small treatment cohorts. Further, characterization of early imaging response may then be followed and validated as a predictive measure of temporal response such as progression-free and overall survival. As illustrated above in **Figure 2**, inclusion of companion dogs in a proof-of-concept investigation of a novel cytotoxic nucleotide analog prodrug (GS-9219), response assessment using advanced cancer imaging (e.g., ^{18}F-FLT PET/CT) could be performed early (within days of treatment) and was predictive of outcome (17–19). These studies also serve to highlight the potential bidirectional flow of comparative oncology advances; GS-9219 was eventually abandoned in the crowded human NHL therapeutic arena, but continued development in the veterinary arena and represents the first FDA-approved cytotoxic chemotherapeutic for use in pet dogs with lymphoma under the name Tanovea® (27–29).

As a second example, our group has used a comparative approach to use advanced imaging to temporally characterize the effects of a novel bisphosphonate-cytotoxic drug conjugate that targets primary or metastatic sites of cancer within bone (30). Prior to first-in-human trials we performed a proof-of-concept pilot trial of safety and efficacy in companion dogs with spontaneously arising osteosarcoma and applied serial ^{18}F-NaF/^{18}F-FLT PET/CT cancer imaging to assess primary tumor and associated bone proliferative activity [**Figure 6**; (31)]. The novel agent was found to induce an initial increase in proliferative activity at the tumor location at day 6 post-treatment followed by reduced primary tumor proliferation over the course of the next 28 days. These data were correlated with documentation of pain palliation using force-platform

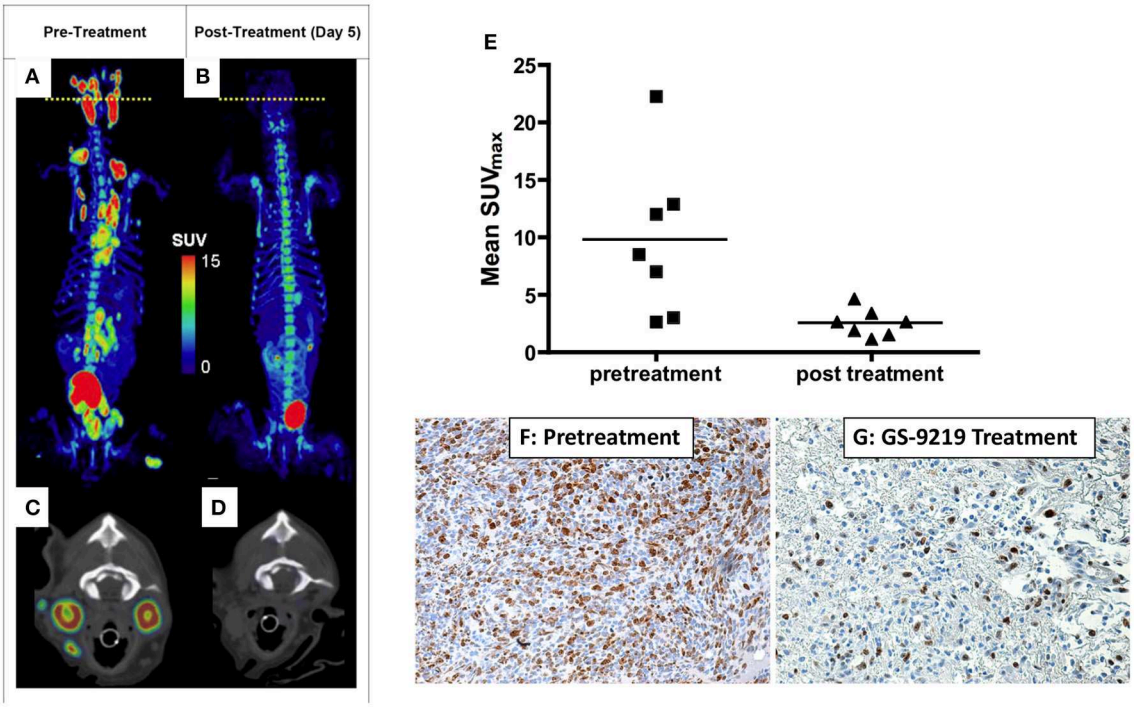

FIGURE 2 | PET/CT scan before **(A,C)** and 5 days after **(B,D)** a single dose of GS-9219 in a dog with NHL. The cell proliferation tracer ^{18}F-FLT was used to document significant anti-proliferative response in affected lymphoid tissues (popliteal, mesenteric, mediastinal, prescapular, and submandibular lymph nodes). Note that the signal in the urinary bladder and renal calyces is normal and represents urinary excretion. Low-level signal present in the vertebral bone marrow and the gastrointestinal tract reflects background uptake of tracer in the proliferating cell populations in these tissues. The axial views are displayed at the position of the yellow dotted lines on the whole-body PET scans and represent the level of the mandibular lymph nodes. **(E)** Mean FLT maximum body mass standardized uptake value (SUV_{max}) for seven dogs was significantly higher before treatment than after treatment. Mean FLT SUV_{max} predicted a significant decrease in tumor proliferation as confirmed using Ki-67 immunoreactivity as illustrated in **(F,G)**: Lymphoma tissue from the prescapular lymph node of a dog before treatment **(F)** compared with the contralateral prescapular lymph node in the same dog biopsied 4 days following treatment **(G)** (X600). Note the significant decrease in Ki-67 immunoreactivity following therapy indicating an antiproliferative effect. **(A–D)** Reprinted from Reiser et al. (17). **(E–G)** reprinted from Lawrence et al. (18).

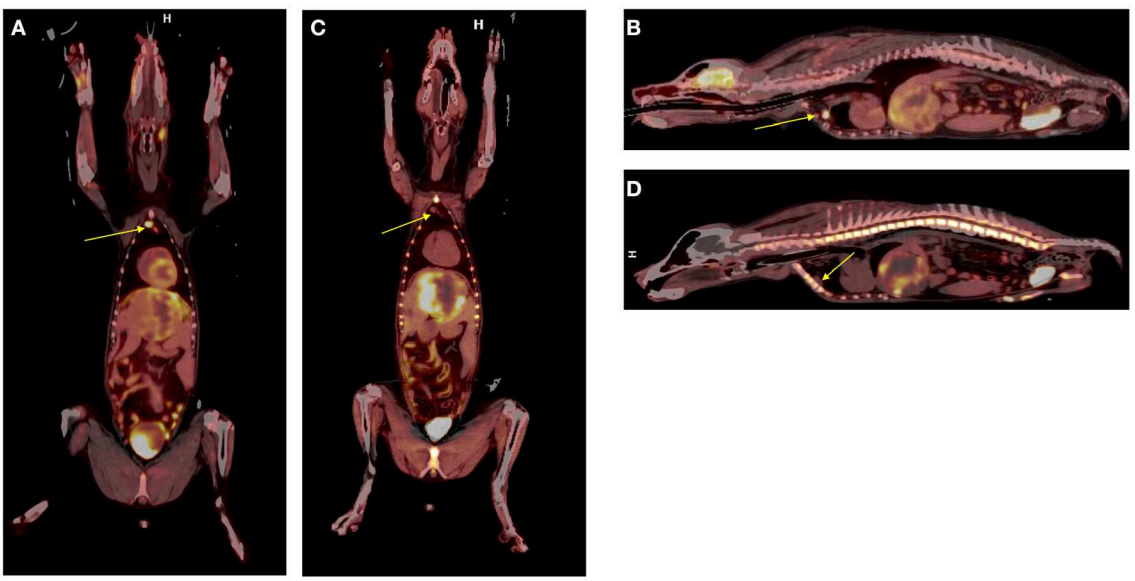

FIGURE 3 | Dual tracer ^{18}F-FDG **(A,B)** vs. ^{18}F-FLT **(C,D)** in canine hepatocellular carcinoma. Note the increased tumor conspicuity with ^{18}F-FLT particularly when discerning tumor borders from surrounding hepatic parenchyma. A reactive retrosternal lymph node is evident within the ^{18}FDG images (arrows, **A,B**) but does not exhibit significant ^{18}FLT uptake (arrows, **C,D**).

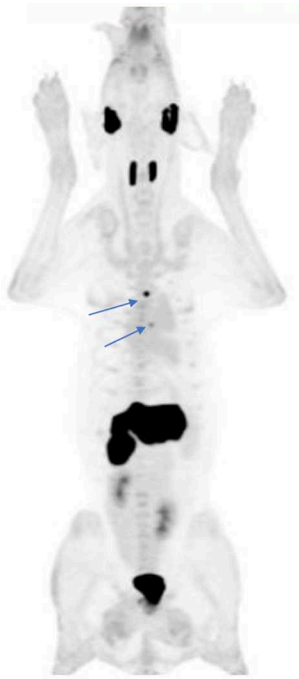

FIGURE 4 | ^{18}F-tetrafluoroborate, a PET imaging agent for the sodium-iodide symporter (NIS) protein, was used to document physiologic distribution in this 41 kg hound dog. Note the expected physiologic uptake within the salivary glands, thyroid, and stomach. Small foci of uptake in the thorax (arrows) represent ectopic thyroid tissue within the left ventricular outflow tract and mediastinum. There is evidence of tracer excretion within the urinary system (renal pelvis and bladder). A small amount of free F-, the product of tracer dehalogenation *in vivo*, is evident by the mild diffuse bone uptake in this MIP image.

analysis and significant suppression of the bone resorption marker urinary NTX-telopeptide (31). These results, along with adverse event profiling in companion dogs, justified further clinical advancement of MBC-11, and subsequent first-in-human investigations documented substantial reductions in metabolic activity of several solid bone cancers in human patients at well-tolerated doses (32).

Another example that highlights the utility of molecular imaging in gauging tumor response is an investigation of serial ^{18}F-FDG PET/CT during toceranib treatment in dogs with solid tumors (33). This study exemplifies the potential for discordance with the use of ^{18}F-FDG PET to gauge response to receptor tyrosine kinase inhibition and the need to consider the timing of such imaging studies, as well as applying multi-parametric imaging-based measures of response such as dual ^{18}F-FDG and ^{18}F-FLT PET/CT imaging, to gain a clearer understanding of drug impact. In the context of short drug exposures, an immediate anti-proliferative response (best assessed through ^{18}F-FLT PET imaging) may predate a metabolic response (as assessed through ^{18}F-FDG PET imaging), as suggested in a study of human patients receiving sunitinib treatment for renal cell carcinoma (34). Additionally, issues relating to structural changes within tumors, such as necrosis and hemorrhage, may have impacted the uptake of ^{18}F-FDG in the canine patients receiving toceranib thus leading to discordant results. It is also important to consider the clinical benefit patients may experience during therapy that may not be captured with standard treatment response assessment criteria (e.g., RECIST or PERCIST) alone. Nonetheless, the examples highlighted here serve to illustrate the utility of comparative cancer imaging within the drug development pathway for novel cytotoxic therapeutics, as well as the opportunities to explore various schedules for gathering imaging data to determine which are most informative.

Assessment of Tumor Microenvironment (TME)

Solid tumors are phenotypically heterogeneous, exhibiting an array of expressed characteristics that are rooted both in their origin and tumor microenvironment. Extracellular changes alter the tumor microenvironment in a manner that can cause further modifications of genes and their transcription at the epigenetic level. Temporal evolution of these heterogeneities is affected by the interplay between the dynamics of the tumor, tumor microenvironment, neovasculature, and any therapeutics administered, all of which elicit responses in the form of further genetic and phenotypic modifications. It is no surprise that assessment of tumor microenvironment has been of specifically high interest to investigators both in human and comparative oncology.

One of particularly impactful tumor microenvironment characteristics that has shown to have great influence over clinical outcome and response to therapy is hypoxia (35, 36). Non-invasive volumetric imaging of hypoxia markers continues to become a more ubiquitous technique for *in vivo* visualization and quantification. The most common imaging modality, also quite frequently used in comparative oncology setting, is PET using specific radiotracer surrogates of tumor hypoxia, such as ^{18}F-FMISO, ^{18}F-FAZA, and ^{61,64}Cu-Cu-ATSM, among others. FMISO is the most common PET hypoxia tracer due to its close chemical relationship with the marker pimonidazole. Low image contrast of FMISO was addressed with the synthesis of FAZA, a less lipophilic nitroimidazole that is not plagued by non-specific uptake in normal tissues. Similarly, Cu-ATSM lipophilicity from planar molecular geometry allows for rapid passive uptake in tumor cells, where it is preferentially reduced by cytochrome reductase enzymes forming the microsomal electron transport chain that leads to high image contrast.

Similarly, functional MRI can be used to indirectly image hypoxia. The BOLD technique in particular images the differential blood flow and the oxidation of hemoglobin via changes in magnetic susceptibility. Dynamic contrast-enhanced MRI (DCE-MRI) allows for assessment of vasculature parameters (e.g., perfusion/permeability), related to tumor microenvironment, and indirectly to tumor hypoxia, some of which has been shown to be predictive of outcome both in humans as well as in canines (37).

Imaging of tumor microenvironment, together with imaging of other clinically relevant tumor phenotypes such as proliferation, metabolism, and vasculature condition assessment, has shown to be of significant benefit to comparative oncology,

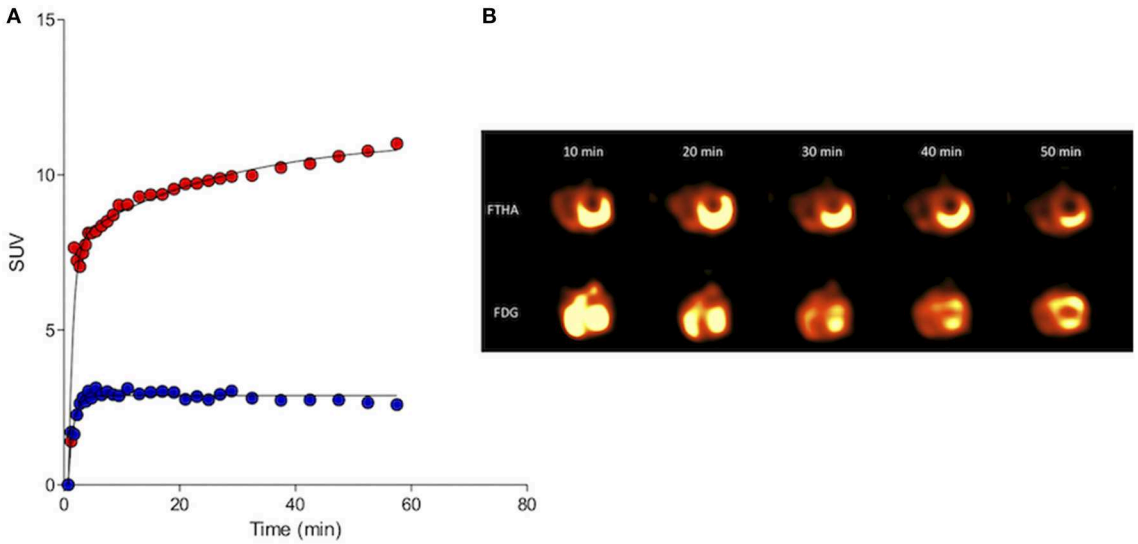

FIGURE 5 | Kinetic standardized uptake value (SUV) data (**A**; Red, 18FDG and blue, 18FTHA) and serial left ventricular images **(B)** gathered from the myocardium of a clinically normal purpose-bred cat. Both 18FDG and 18FTHA were evaluated 48 h apart, with DICOM data collected over a 1 h period beginning simultaneously with tracer injection. Note the early trapping and sustained retention of 18FTHA contrasting with continuously increasing uptake of 18FDG over the 60 min imaging period. This is consistent with the continuously gluconeogenic and glycolytic state of the domestic cat and its myocardium, respectively, even in the fasted state.

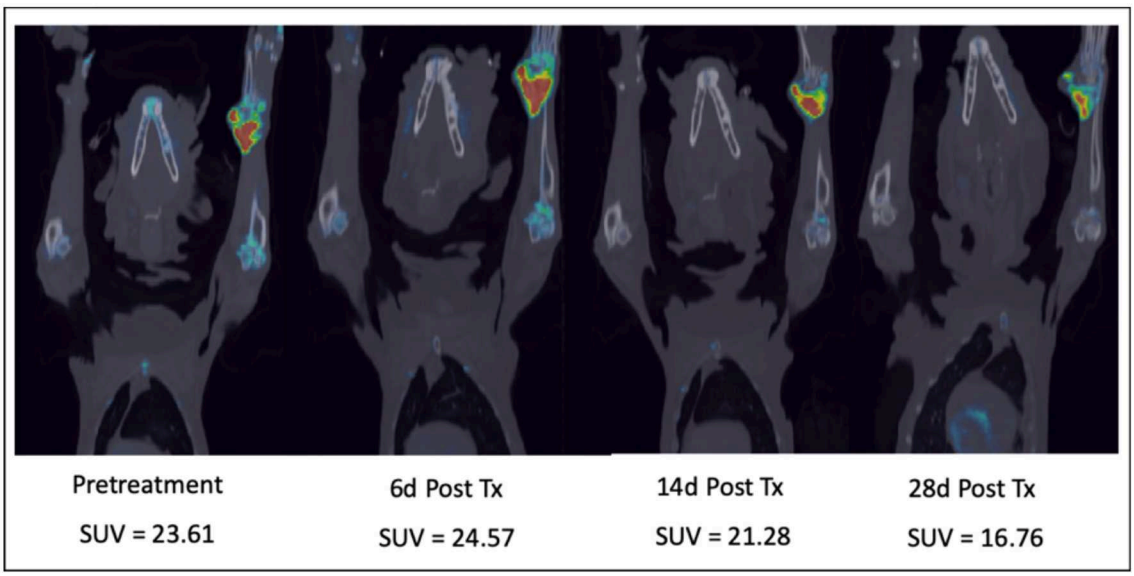

FIGURE 6 | Serial combination ^{18}F-NaF/^{18}F-FLT PET/CT scans in a dog with a right distal radial osteosarcoma treated with a novel bone-targeting bisphosphonate-cytotoxic drug conjugate. After an initial proliferative increase 6 days after a single IV drug treatment, tumor proliferation and bone turnover diminished over the 28-day treatment cycle. SUV, Maximum Standard Unit of Value.

as it allows better understanding of interplay between different tumor phenotypes, assessment of the response to therapeutic interventions, and ultimately deriving better and more effective treatments (2, 38–40). However, more research, and particularly broader adaption of advanced imaging technologies is needed to fully explore its potential.

Response Prediction and Assessment

Functional Assessments

The utility of advanced imaging to serially assess functional changes in tumors or TME to document or indeed predict response to cancer therapeutics has been covered in previous sections of this review [see sections Imaging Technology

Development, Assessment of Novel Cytotoxic Drug Efficacy, and Assessment of tumor microenvironment (TME)]. As the field of comparative oncology continues to advance and novel interventions and therapeutic strategies are investigated in companion species, the integration of advanced imaging technologies to document response and develop non-invasive image-based biomarkers will become more important and commonplace.

Immunotherapeutic Response Assessment

Although immunotherapy is becoming one of the cornerstones of modern cancer therapy, resulting in durable favorable outcomes for some patients, the assessment of clinical response to immunotherapy is still a very challenging task (41). Immunotherapy response patterns can be substantially different from those of classical cytotoxic therapies (42). A significant subset of patients first experience a pseudo-progression after the administration of immunotherapy, and the actual response/shrinkage of tumors can be delayed and only observed later in the time course of therapy. Four different distinct immunotherapy response patterns are associated with favorable survival (42); (a) shrinkage in baseline lesions with no new lesions, (b) long-term stable disease, (c) response after an initial increase (pseudoprogression) of tumors, and (d) response of initial lesions but with appearance of new lesions. Therefore, the standard Response Evaluation Criteria in Solid Tumors (RECIST 1.1.) (43) are not appropriate for assessing the effects of immunotherapy and can result in patients moving off of effective therapy due to an invalid parameter for progression. For example, as defined by RECIST, patients experiencing early pseudo-progression or patients with response in the presence of new lesions would be characterized as progressive disease (PD), indicating treatment failure and suggesting cessation of therapy. However, such treatment response patterns following immunotherapy can be associated with eventual tumor regression/stabilization and potentially long-term survival. In 2009, immune-related response criteria (irRC), based upon data from checkpoint blockade were recommended for use in immunotherapy (42). irRC is based on measuring the change in size of tumor burden and the change in the number of metastatic lesions at two different imaging time points, at least 4 weeks apart. While the irRC have been retrospectively validated, their usefulness and generalizability to other immunotherapy agents and cancer types is still undergoing prospective validation (42, 44–50). Broadly speaking, irRC only covers assessment of anatomical changes, which are known to be slow, compared to molecular and functional changes within the tumor and tumor microenvironment, and has been inconsistently implemented (45, 46, 49, 50).

Non-invasive imaging tools to assess and predict response to immunotherapy would greatly facilitate drug development and clinical decision-making in this era of growing incorporation of immune-modulating approaches for treatment. Ideally, methods that assess response to immunotherapeutic strategies as early as possible should allow non-responding patients to switch to other treatment modalities sooner and guard from the high cost and toxicities of continuing an ineffective therapy. Functional/molecular imaging is known to show tumor changes much earlier than anatomical changes. While ^{18}F-FDG PET/CT has become a standard tool to assess treatment response in oncology, in immunotherapy its interpretation is severely confounded by changes related to an active and responding immune response. The lack of specificity of FDG uptake (e.g., **Figure 3**) mandates a more specific indicator of tumor cell viability, which fortunately can be achieved with ^{18}F-FLT PET/CT or PET/MR imaging. We are currently exploring in companion species whether a positive immunotherapeutic response will be reflected by an increased FDG/FLT uptake ratio [termed the Imaging Immune Response (IMR) ratio] during and after therapy when compared with baseline. An increase in the IMR ratio is expected because of two premises: (1) effective immunotherapy elicits immune activation leading to increased "inflammation" in the tumor reflected by increased glycolytic activity in the tumor microenvironment by activated immune cells, which can be measured by FDG PET, and (2) effective immunotherapy will eventually result in antitumor effects, which can be measured by a decrease in proliferation as reflected by thymidine synthase activity in the tumor region measured using FLT PET. As antitumor effects can be delayed, and early changes on FDG PET/CT may reflect both inflammatory and tumor progression, we hypothesize that the change in the ratio of FDG to FLT will provide the necessary discriminatory information to characterize tumor lesions as having a *positive immune effect* (increase in IMR ratio) vs. *no effect* (no change or decrease in IMR ratio).

The use of imaging as a predictive biomarker is currently limited due to the contrasting reports and limited evidence about the predictive power of simple standardly applied PET metrics, such as the maximum standardized uptake value (SUV_{max}) (51–55). On the other hand, the rapidly expanding field of medical image analysis, so called "radiomics," is harnessing the full power of medical imaging by extracting numerous quantitative features (sometimes referred to as "texture features") out of the images of different modalities, including PET, CT and magnetic resonance imaging (MRI) (56). Several studies have reported predictive ability of radiomics texture features in different types of cancer therapies, but interestingly, no radiomics analyses have been performed in immunotherapy studies thus far.

Applied to immunotherapy, one would expect that the immune-radiomics (irRADIOMICS) signature of responders will be different from the irRADIOMIC signature of non-responders due to the different levels, spatial distribution and temporal dynamics of tumor infiltrating lymphocytes (TILs) and various other immunosuppressive cells, such as myeloid-derived suppressive cells (MDSC), regulatory T cells (Treg), tumor-associated macrophages (TAM), and regulatory dendritic cells (DCreg) (57). Thus, it may be possible to assess the response to immunotherapy much earlier than by conventional means, perhaps even at just one imaging time-point, preferably in the pseudoprogression phase. Based on the assumption that irRADIOMICS might be able to detect differences in the tumor immunosuppressive microenvironment, we further hypothesize that it may also be possible to predict which patients are most likely to benefit from immunotherapy before initiation

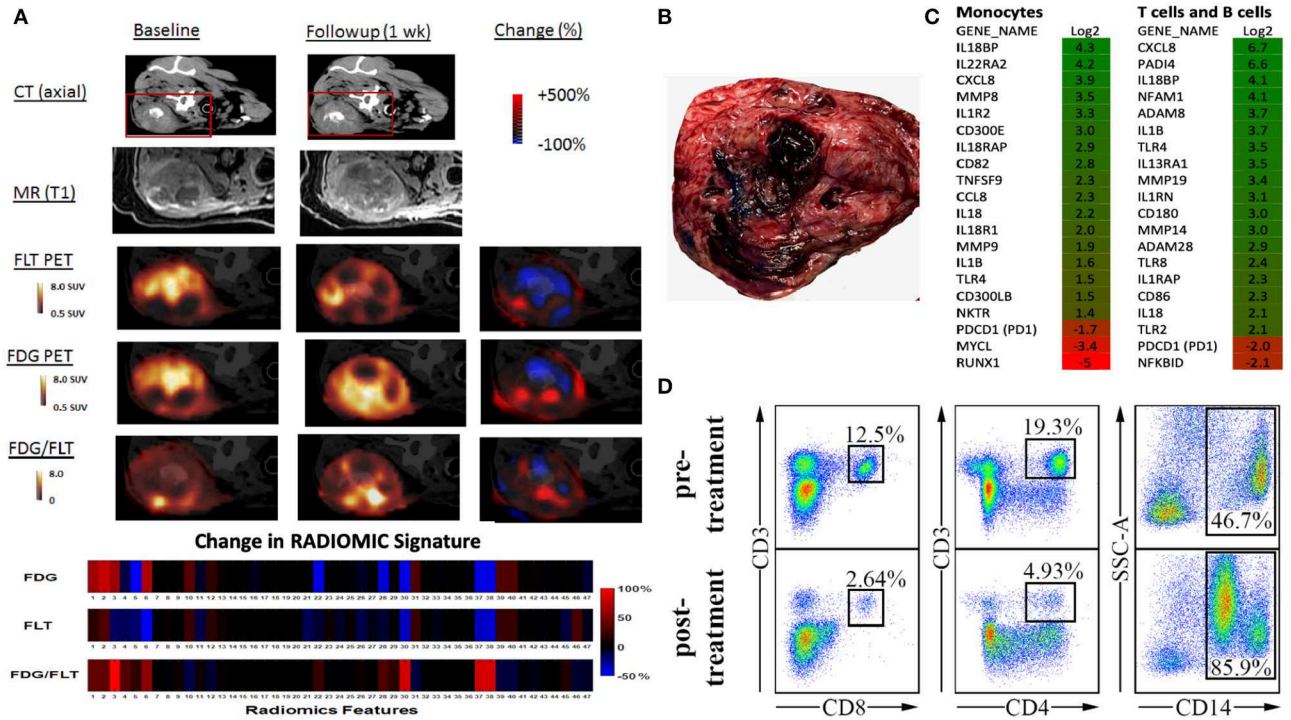

FIGURE 7 | Advanced imaging (irRADIOMICS) evaluation in a dog with osteosarcoma before and after immunotherapy and correlation with biomarkers of immunomodulation. **(A)**. CT, MRI, ^{18}F-FLT PET, ^{18}F-FDG PET, and FDG/FLT PET images of a dog with a stump recurrence osteosarcoma at baseline and 1 week post-L-MTP-PE immunotherapy. The change in image features using 47 extracted imaging features (RADIOMIC signature) extracted from ^{18}F-FLT PET to ^{18}F-FDG PET and the ratio of the FDG/FLT PET scans are presented in the lower bars. Analysis shows that the change in FDG PET radiomics signature is mostly positive, FLT PET radiomics signature mostly negative, and change in FDG/FLT PET ratio radiomics signature is uniformly positive, likely indicating effective immunotherapy. The RADIOMIC features can then be correlated with global tumor pathology/histology **(B)** and other biomarkers of immunomodulation such as single-cell gene expression profiling **(C)** and peripheral blood mononuclear cell subset **(D)** changes from baseline.

of the therapy. In other words, irRADIOMICS could have potential to serve as a pre-treatment biomarker of response to immunotherapeutic strategies.

To begin characterizing response assessment and predictive potential, we are currently creating irRADIOMIC signatures in companion dogs with metastatic osteosarcoma (**Figure 7**) and melanoma (**Figure 8**) before and after immunotherapeutic strategies. **Figure 7** represents a veterinary patient who developed a stump-recurrence osteosarcoma following forelimb amputation and platinum-based chemotherapy. The dog received systemically delivered liposomal muramyl tripeptide (L-MTP), an innate immune system stimulant known to have activity in canine and human osteosarcoma and to activate canine monocytes (58–60). In order to assess metabolic and proliferative response of this dogs tumors (and regional lymph nodes), and account for potential changes in perfusion/permeability, we then performed dynamic ^{18}F-FLT PET/CT and dynamic ^{18}F-FDG PET/MR scans before and 1 week after initiation of immunotherapy. Analysis revealed that the change in FDG PET radiomic signature was mostly positive, FLT PET radiomics signature mostly negative, and the change in FDG/FLT PET ratio (IMR ratio) radiomic signature was uniformly positive, suggesting an effective immune response. **Figure 8** represents a veterinary patient with a large prescapular metastatic malignant melanoma from a subungual primary who received intratumoral injections of an investigational immunocytokine-monoclonal antibody fusion protein. Pre and post-treatment FLT and FDG PET/CT images revealed reduced metabolism and proliferation in the prescapular metastatic lesion with increased metabolism and proliferation in the non-effaced reactive regional lymph node; also indicative of an effective immune response.

Through serial biospecimen procurement during serial scans, we have begun to correlate radiomic signatures with histologic and immunopathologic characterizations of the tumor, the tumor microenvironment, peripheral blood compartment and regional nodes. Our group, as part of the Moonshot U01-affiliated Immuno-Oncology Translational Network (IOTN: https://www.cancer.gov/research/key-initiatives/moonshot-cancer-initiative/implementation/adult-immunotherapy-network) has access to an ever-expanding catalog of validated canine-specific reagents and methodologies that will allow assessments that should prove meaningful and readily translatable. We have demonstrated an ability to apply sophisticated analytic interrogations in dogs with solid tumors and have demonstrated differences before and after a variety of immunomodulatory therapies. For example, in the dogs with metastatic OSA receiving immunotherapy (**Figure 7**), we assessed changes in PBMC lymphocyte subsets, flow-sorted immune cells, and documented changes in gene

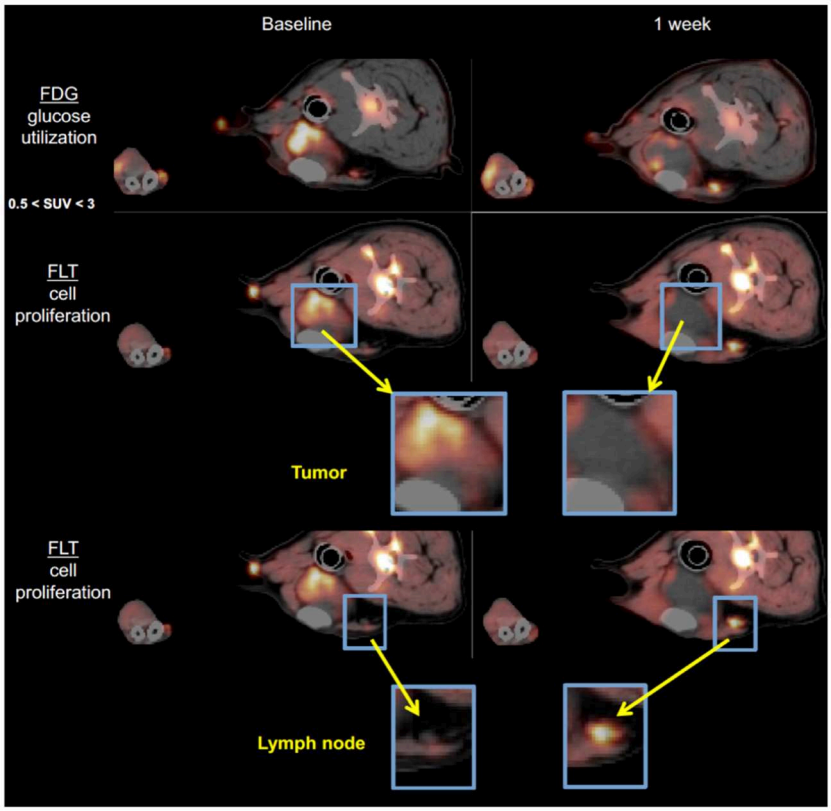

FIGURE 8 | ^{18}F-FDG PET and ^{18}F-FLT-PET images of a dog with metastatic melanoma before and after immunotherapy with intratumoral immunocytokine injections. Note the antiproliferative response in the index tumor and the conversely pro-proliferative response in the non-metastatic, reactive regional lymph node predicting a positive antitumor immune response.

expression for known activation pathways, and optimized a protocol for deep sequencing the canine T cell receptor (TCR) from PBMCs and showed increased TCR diversity after immunotherapy. These biospecimen-heavy pilot studies again illustrate the potential for the comparative approach to cancer image-based investigations. Much remains to be learned about standardization of irRADIOMICS imaging applications and analysis. Which textures are most critical to assess and the temporal nature of the signature changes that occur, are currently unknown and this knowledge is critical to determine the optimal timing of imaging events relative to the initiation of immunotherapy.

Development of Novel Theranostic Approaches

Much utility is gained in clinical practice if a single agent can be used for both diagnostic imaging and therapy; so called "theranostic" agents. For example, metaiodobenzylguanidine (mIBG) is such an agent for pediatric neuroblastoma where ^{123}I-mIBG is used for accurate staging and ^{131}I-mIBG is the correlate therapeutic (61). Similarly, ^{177}Lu prostate-specific membrane antigen (^{177}Lu-PSMA) is used as a theranostic for men with prostate cancer (62).

The inclusion of companion animals in the development of novel theranostic agents also has advantages owing to their physical size and spatial distribution of tumors (primary and metastatic) which more closely mimics that in humans with cancer. This is critical for studying the safety and efficacy of theranostic agents that deliver therapeutic agents in close proximity to organs at risk, particularly lymphoid organs (bone marrow, spleen, thymus, draining lymphatics). This is particularly requisite for theranostic agents used for molecularly targeted radionuclide therapy (MTRT). Dosimetry calculations using canines should be more reliable for extrapolation to humans than mouse models.

By way of illustration, our group is working with radiolabeled alkylphosphocholines (APCs) which selectively accumulate in tumor cells *in vivo* by exploiting the relative overabundance of lipid rafts in cancer vs. normal cells, a mechanism that is ubiquitous to most malignancies (63, 64). An APC analog, NM600, developed by members in our group targets numerous cancer types regardless of histology and anatomic location (63). NM600 chelates a variety of radiometals (e.g., ^{86}Y, ^{90}Y, ^{177}Lu, ^{225}Ac) and is currently being evaluated in multiple imaging/therapy trials. Members of our collaborative group have eloquently shown that distant metastatic sites serve as a nidus for immunosuppressive cells (e.g., Tregs), and these mediate

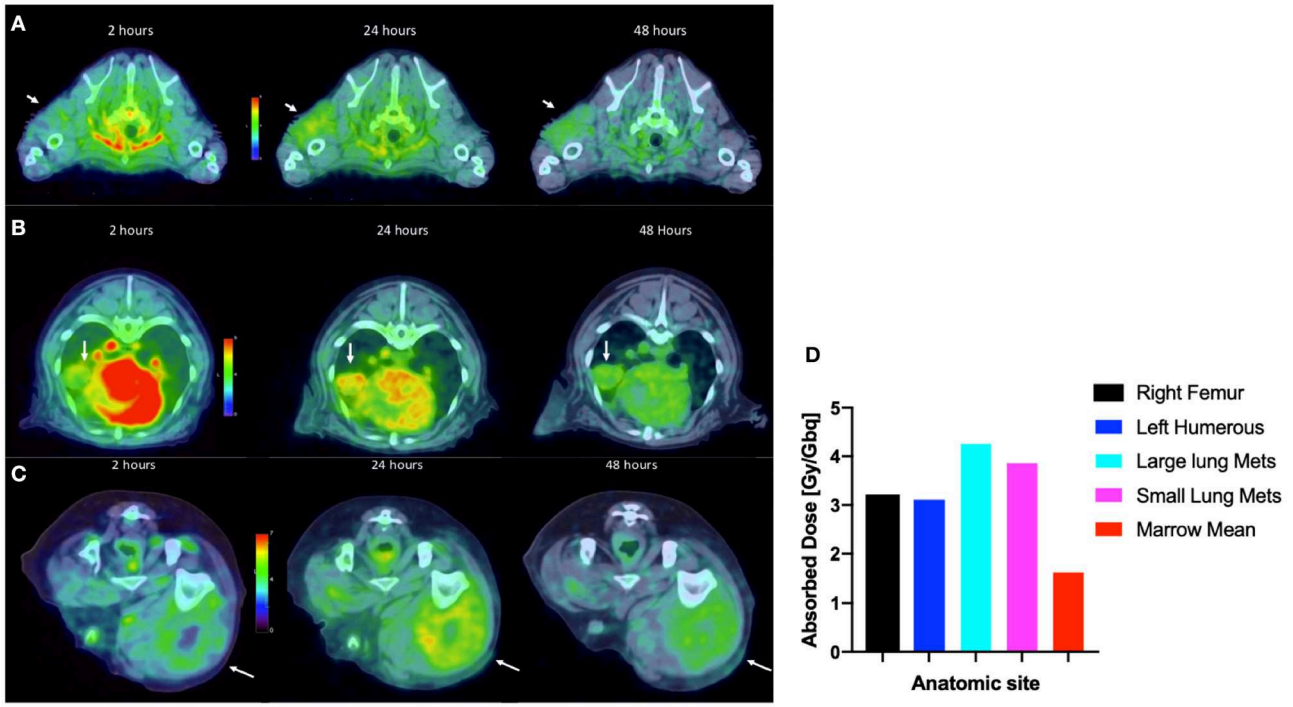

FIGURE 9 | Tumor selective uptake of ^{86}Y-NM600 as documented by PET/CT. 2-, 24-, and 48-h axial scans at the level of **(A)** left proximal humoral subcutaneous osteosarcoma metastasis (arrow); **(B)** left middle lung lobe metastasis (arrow); **(C)** right lateral femoral subcutaneous metastasis (arrow). Note the NM600 is primarily in the vascular compartment at the 20 h time point, then selectively disperses into all metastatic sites at subsequent time points. **(D)** Importantly, metastatic lesions had at least a 2:1 tumor to bone marrow uptake of ^{86}Y-NM600 predicting safe delivery of ^{90}Y-NM600.

systemic immunosuppressive effects that antagonize external beam radiation therapy (EBRT) generated *in situ* vaccination—a phenomenon called concomitant immune tolerance (CIT) (65). Fortunately, CIT is radiation sensitive; delivering low-dose (~2 Gy) RT to metastatic sites can overcome CIT and enable *in situ* vaccine regimens to destroy both primary and distant tumor. (66). While it is not typically feasible to deliver EBRT to all sites of metastatic disease (due to immune suppression and inability to specifically target all microscopic disease), it may be possible to use MTRT to immunomodulate the TME of all tumor sites in the setting of metastatic disease. We are currently investigating delivery of low dose molecularly targeted radionuclides to all tumor sites in the setting of metastatic disease by using the theranostic isotope pair, ^{86}Y-NM600 and ^{90}Y-NM600, to immunomodulate the collective TME in a way that will promote response to EBRT-based *in situ* vaccine. Radiolabeled NM600 enables tumor-specific PET imaging (^{86}Y-NM600) and targeted delivery of ionizing radiation (^{90}Y-NM600) at doses that theoretically will abrogate CIT. **Figure 9** shows a veterinary patient with widespread metastatic osteosarcoma undergoing serial ^{86}Y-NM600 PET/CT imaging at various metastatic sites. These data proved selective uptake of NM600 by all metastatic sites and allowed dosimetry calculations (**Figure 9D**) that predicted at least a 2:1 tumor to bone marrow differential uptake and safe delivery of ^{90}Y-NM600 to all metastatic tumors at doses likely to overcome CIT while sparing bone marrow. Indeed, this patient subsequently received the calculated ^{90}Y-NM600 dose without hematologic toxicity. This example further supports the utility of the companion animal model for bridging preliminary rodent data and clinical application in people.

Other examples of companion species utility in the development of theranostic approaches include the previously mentioned use of the novel apoptosis-specific PET imaging agent (^{18}F-CSNAT4) to detect and semi-quantitatively measure tumoral apoptosis prior to and after anti-apoptosis therapy (10–12).

Miscellaneous Utility of Comparative Imaging

Cellular Trafficking

With heightened interest for the inclusion of companion dogs with heterogenous spontaneous tumors occurring and progressing in the context of a syngeneic TME and an intact immune system, the ability to image, in real time, changes in tumor and TME infiltrating immune effector and suppressor cell trafficking would be highly advantageous to assess effectiveness of immunotherapeutic approaches and characterize cell-based immune approaches.

By way of example, we and others have been investigating the utility of natural killer cell (NK) based therapies in both

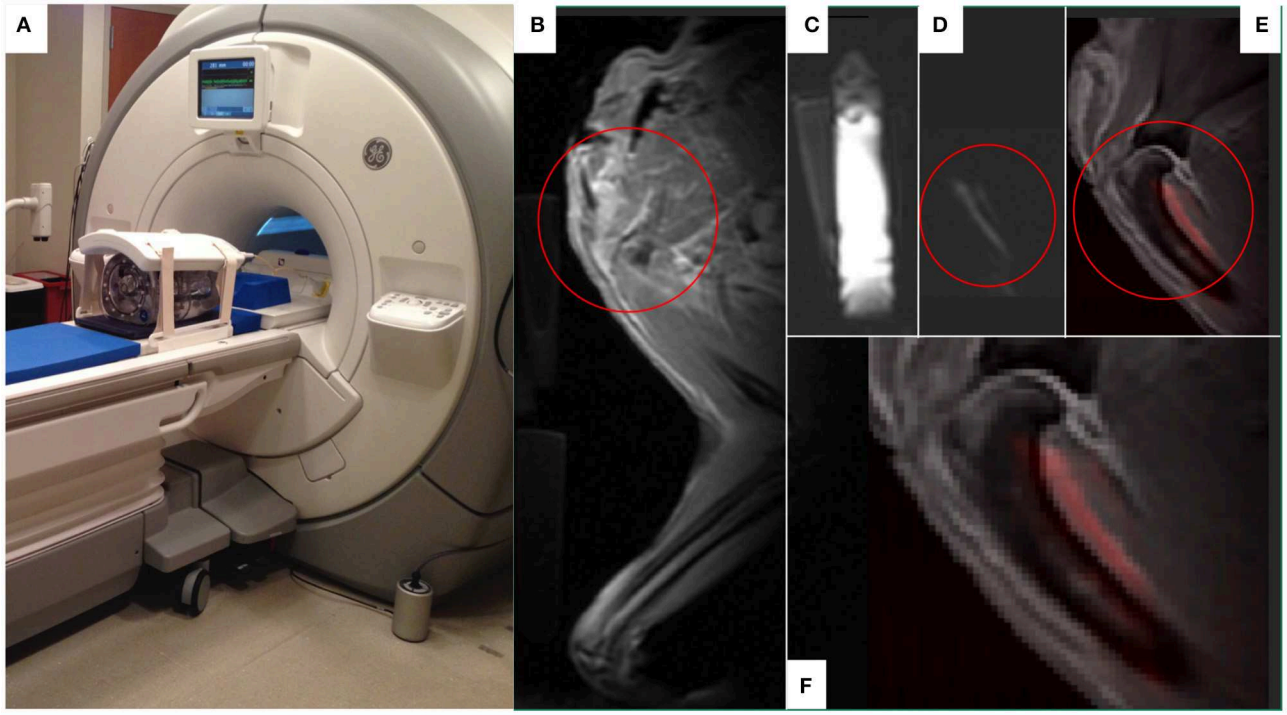

FIGURE 10 | The use of ^{19}F MR to develop *in vivo* imaging of ^{19}F-labeled immune effector cell persistence and trafficking. A customized ^{19}F MR coil system (MRI Tools, Berlin, Germany) that allows *in vivo* imaging of ^{19}F. The duel-frequency, 8-channel Transmit/Receive ^{1}H/^{19}F torso coil system (MRI Tools, Berlin, Germany) with a water phantom is demonstrated **(A)** on a 3.0T Discovery MR750w MRI scanner (GE Healthcare, Chicago, IL). A companion dog limb was imaged using this system after ^{19}F-emulsion was infused into the soft tissues on the caudal aspect of the proximal humerus, a common site for osteosarcoma. Fluorine images of the canine limb were acquired with a slice thickness of 10 mm via a T1-weighted gradient echo sequence (TR:20 ms, TE:2.1 ms, FA:20°, FOV: 380 × 380 mm, Matrix:128 × 128, resolution: 2.97 × 2.97 mm, number of averages: 64, $T = 16$ min). The MR proton anatomical image of the proximal humeral area of interest circled in red **(B)** were subsequently overlaid with the ^{19}F images (**C**, fiducial marker; **D,** limb) to create a composite image **(E,F)** with ^{19}F appearing as red in the composite images. Figures courtesy of Sean Fain and Paul Begovatz.

companion dogs and pediatric patients with solid tumors (67, 68). Currently, there are no FDA-approved agents available to label and track immune cells after infusion into patients, and current infusion treatments are "blind" without confirmation that cells are viable or trafficking to tumor sites. Confirming delivery of cell therapies to tumors and other sites of disease will become more important as treatments are tailored to individual patients or modulated over time with repeated dosing. In clinical trials, we rely on analyses of blood and bone marrow samplings to detect the persistence of donor-derived infused NK cells; biopsy of tumors to actually localize these infused NK cells are difficult due to the potential of sampling error and risk to the pediatric patient. Thus, the field of cancer immunotherapy is in need of a means by which to non-invasively track infused cells in both normal organs and tumors. According to the FDA Cellular, Tissue and Gene Therapy Advisory Committee, there is an urgent need to track immune cells *in vivo* to determine trafficking patterns and longevity. Also, the FDA's Center for Devices and Radiological Health has launched an initiative to reduce unnecessary radiation exposure from medical imaging. MRI is the clinical standard for obtaining non-radioactive high-resolution images of soft tissue including solid tumors. While conventional MRI detects tissue ^{1}H, and mainly differences in signal recovery of water and fat, multinuclear, and spectroscopic MRI has the potential to detect functional and cellular signals not visible with conventional ^{1}H MRI methods. ^{19}F MRI is a promising approach for tracking NK cells non-invasively without toxicity or ionizing radiation. Members of our collaborative group have developed methodology to label canine NK cells with non-radioactive ^{19}F without compromising NK cell function and they were the first group to enumerate and track NK cells within a tumor *in vivo* using hot spot ^{19}F-MRI (69, 70). We are currently evaluating the utility of a customized ^{19}F MR coil (**Figure 10**) large enough to acquire images from canines (and pediatric patients in future trials). We have collected and expanded canine NK cells from University of Wisconsin Veterinary Care patients and have begun investigations to refine ^{19}F-MR imaging protocols to characterize trafficking and persistence of autologous canine NK cells after intratumoral and intravenous infusion. Success of this line of investigation would offer a non-radioactive approach of tracking *ex vivo* activated NK cells (and other immune cells) in patients with solid tumors undergoing immune-based therapies.

As another example, one could envision the inclusion of companion dogs with cancer to bridge early investigations of dendritic cell migration in rodents using the novel

PET probe ^{18}F-tetrafluoroborate that was mentioned above (22–24).

Intraoperative Imaging

The use of advanced imaging modalities to inform surgical oncology decision making is another area where an opportunity for comparative oncologic investigations involving inclusion of companion animals with spontaneous tumors has and will play a role. Many of these technologies strive to discriminate between different tissue types (particularly between tumor and adjacent normal tissues) using intraoperative imaging. For example, the real-time intraoperative assessment of the completeness of surgical margins, sentinel node and distant regional metastasis at the time of tumor resection would be advantageous to waiting for time and labor intense *ex vivo* assessments and may abrogate the need for revision surgery. Examples where companion species have been involved in evaluating intra-operative surgical margins include optical coherence tomography (OCT) in dogs and cats with soft tissue sarcoma (STS) and fluorescence-guided surgical and sentinel node assessment for a variety of solid tumors (e.g., primary lung tumors, carcinomas, and STS) (71–78). Fluorescent probes used in these studies include agents with preferential/differential avidity for tumor cells such as protoporphyrins, lipid nanoparticles, integrin-targeting compounds ($\alpha_v\beta_3$), folate-targeting agents, modified chlorotoxins these technologies have also been used to assess surgical wound beds for residual tumor cells after tumor extirpation (72).

SUMMARY AND FUTURE DIRECTIONS

The myriad of opportunities and advantages inherent in the inclusion of cancer-bearing companion species in the investigation, development, and application of advanced imaging technologies stem primarily from similarities they share with cancer-bearing humans in body size, tumor heterogeneity, spatial distribution of metastatic disease, and the presence of an intact and syngeneic immune system and tumor microenvironment (TME).

The expansion of comparative consortia and funding opportunities that bring veterinary and physician-based basic researchers, medical physicists, and clinician-scientists to the cooperative table has the potential to harmonize the efforts applied in cancer imaging toward the common goal of diminishing the morbidity and mortality of cancer in all species. This bidirectional flow of new information should serve to streamline, inform and ultimately accelerate the development and application of non-invasive imaging technologies that can be applied to diagnosis, treatment and treatment planning, documentation of treatment response and indeed prediction of which individuals are likely to respond to a particular therapy. Further, the use of advanced functional imaging in companion species with spontaneous tumor-TME characteristics that better recapitulate human tumor-TME interplay would play an important role in novel tumor target identification, basic cancer growth and progression characterization, and the role of the immune system in cancer biology.

Much remains to be done to more successfully align and integrate companion species into cancer investigation pathways that involve advanced imaging. The harmonization of imaging protocols with consistent application of quality assurance and medical physics expertise is necessary to assure high quality and reproducible quantitative imaging in the comparative oncology setting. The integration of assurance endeavors such as those ongoing through the QIBA are essential to confidently interpret and apply the imaging data gathered in companion species. Additionally, some research tools readily available in rodent and human systems are currently lacking in companion species. In particular, immunologic and TME reagents that allow validation of immunomodulation and tumor-TME interactions are somewhat sparse in companion species; however, better organized and well-funded cooperative efforts such as the Immuno-Oncology Translational Network are rapidly expanding the available toolbox. Of course, no one model is perfect and not all research questions can be answered within the context of one model. In addition to the incomplete reagent toolbox, while some tumor histology's are genetically and phenotypically very similar between canines and humans (e.g., osteosarcoma) others have specific differences such as the near absence of BRAF mutations in canine melanoma. Such limitations, discussed in more detail in other manuscripts in this special volume of Frontiers, need to be considered when choosing a specific model to recapitulate human cancer biology. It is also not lost on the authors that the majority of examples compiled involve companion dogs and only one example of cats is presented. Unfortunately, companion cats have been relatively "orphaned" in the comparative oncology field in general and the advanced imaging area in particular. This may reflect several perceived limitations of the species, including smaller body size, clinical temperament, hepatic metabolism differences, species-specific reagent availability, and a lack of well-characterized histologies with human cancer correlates. The authors are aware of comparative trials about to begin that include cats with head and neck squamous cell carcinoma, a common cancer in the species and it is hoped that more attention will be paid the species in the comparative realm in the future.

The discussion and examples presented in this review serve to raise awareness of the utility of comparative oncology and companion species as a surrogate system that is ideal for bridging early preclinical small rodent investigations with clinical trials in humans.

AUTHOR CONTRIBUTIONS

DV, AL, and RJ conceived, produced, and edited this review article.

FUNDING

This work presented was funded in part by the following: U01CA233102-01 DHHS, PHS, NIH; AAC1164 UW Carbone Cancer Center (UWCCC) CCSG Program Pilot Grant, UW Foundation Immunotherapy/Tumor Immunology Pilot

Award and the Barbara A. Suran Comparative Oncology Research Endowment. Additionally, this work was partially supported (AL) by the Intramural Program of the National Cancer Institute, NIH (Z01-BC006161). The content of this publication does not necessarily reflect the views or policies of the Department of Health and Human Services, nor does mention of trade names, commercial products, or organizations imply endorsement by the U.S. Government.

ACKNOWLEDGMENTS

The authors acknowledge the contributions of Paul Sondel for his expertise in immunocytokine applications (**Figure 8**); Jamey Weichert, Reinier Hernandez, Zachary Morris, Bryan Bednarz, and Ian Marsh for their expertise in targeted radionuclide theranostics and dosimetry (**Figure 9**); and Sean Fain, Paul Begovatz, and Christian Capitini for their contribution to NK cell imaging (**Figure 10**).

REFERENCES

1. Forrest LJ, Mackie TR, Ruchala K, Turek M, Kapatoes J, Jaradat H, et al. The utility of megavoltage computed tomography images from a helical tomotherapy system for setup verification purposes. *Int J Radiat Oncol Biol Phys.* (2004) 60:1639–44. doi: 10.1016/j.ijrobp.2004.08.016
2. Bradshaw TJ, Bowen SR, Deveau MA, Kubicek L, White P, Bentzen SM, et al. Molecular imaging biomarkers of resistance to radiation therapy for spontaneous nasal tumors in canines. *Int J Radiat Oncol Biol Phys.* (2015) 91:787–95. doi: 10.1016/j.ijrobp.2014.12.011
3. LeBlanc AK, Breen M, Choyke P, Dewhirst M, Fan TM, Gustafson DL, et al. Perspectives from man's best friend: National Academy of Medicine's Workshop on Comparative Oncology. *Sci Transl Med.* (2016) 8:324ps5. doi: 10.1126/scitranslmed.aaf0746
4. Gordon I, Paoloni M, Mazcko C, Khanna. The comparative oncology trials consortium: using spontaneously occurring cancers in dogs to inform the cancer drug development pathway. *PLoS Med.* (2009) 6:e1000161. doi: 10.1371/journal.pmed.1000161
5. Paoloni M, Lana S, Thamm D, Mazcko C, Withrow S. The creation of the comparative oncology trials consortium pharmacodynamic core: infrastructure for a virtual laboratory. *Vet J.* (2010) 185:88–9. doi: 10.1016/j.tvjl.2010.04.019
6. Paoloni MC, Tandle A, Mazcko C, Hanna E, Kachala S, Leblanc A, et al. Launching a novel preclinical infrastructure: comparative oncology trials consortium directed therapeutic targeting of TNFalpha to cancer vasculature. *PLoS ONE.* (2009) 4:e4972. doi: 10.1371/journal.pone.0004972
7. LeBlanc AK, Mazcko C, Brown DE, Koehler JW, Miller AD, Miller CR, et al. Creation of an NCI comparative brain tumor consortium: informing the translation of new knowledge from canine to human brain tumor patients. *Neuro Oncol.* (2016) 18:1209–18. doi: 10.1093/neuonc/now051
8. Packer RA, Rossmeisl JH, Kent MS, Griffin JF, Mazcko C, LeBlanc AK. Consensus recommendations on standardized magnetic resonance imaging protocols for multicenter canine brain tumor clinical trials. *Vet Radiol Ultrasound.* (2018) 59:261–71. doi: 10.1111/vru.12608
9. Koehler JW, Miller AD, Miller CR, Porter B, Aldape K, Beck J, et al. A revised diagnostic classification of canine glioma: towards validation of the canine glioma patient as a naturally occurring preclinical model for human glioma. *J Neuropathol Exp Neurol.* (2018) 77:1039–54. doi: 10.1093/jnen/nly085
10. Chen Z, Rao. Positron emission tomography imaging of tumor apoptosis with a caspase-sensitive nano-aggregation tracer [(18)F]C-SNAT. *Methods Mol Biol.* (2018) 1790:181–95. doi: 10.1007/978-1-4939-7860-1_14
11. Schlein LJ, Fadl-Alla B, Pondenis HC, Lezmi S, Eberhart CG, LeBlanc AK, et al. Immunohistochemical characterization of procaspase-3 overexpression as a druggable target with PAC-1, a procaspase-3 activator, in canine and human brain cancers. *Front Oncol.* (2019) 9:96. doi: 10.3389/fonc.2019.00096
12. Witney TH, Hoehne A, Reeves RE, Ilovich O, Namavari M, Shen B, et al. A systematic comparison of 18F-C-SNAT to established radiotracer imaging agents for the detection of tumor response to treatment. *Clin Cancer Res.* (2015) 21:3896–905. doi: 10.1158/1078-0432.CCR-14-3176
13. Jeraj R, Bradshaw T, Simoncic U. Molecular imaging to plan radiotherapy and evaluate its efficacy. *J Nucl Med.* (2015) 56:1752–65. doi: 10.2967/jnumed.114.141424
14. Sullivan DC, Obuchowski NA, Kessler LG, Raunig DL, Gatsonis C, Huang EP, et al. Metrology standards for quantitative imaging biomarkers. *Radiology.* (2015) 277:813–25. doi: 10.1148/radiol.2015142202
15. Ghaghada KB, Sato AF, Starosolski ZA, Berg J, Vail DM. Computed tomography imaging of solid tumors using a liposomal-iodine contrast agent in companion dogs with naturally occurring cancer. *PLoS ONE.* (2016) 11:e0152718. doi: 10.1371/journal.pone.0152718
16. Hallouard F, Anton N, Choquet P, Constantinesco A, Vandamme T. Iodinated blood pool contrast media for preclinical X-ray imaging applications–a review. *Biomaterials.* (2010) 31:6249–68. doi: 10.1016/j.biomaterials.2010.04.066
17. Reiser H, Wang J, Chong L, Watkins WJ, Ray AS, Shibata R, et al. GS-9219–a novel acyclic nucleotide analogue with potent antineoplastic activity in dogs with spontaneous non-Hodgkin's lymphoma. *Clin Cancer Res.* (2008) 14:2824–32. doi: 10.1158/1078-0432.CCR-07-2061
18. Lawrence J, Vanderhoek M, Barbee D, Jeraj R, Tumas DB, Vail DM. Use of 3'-deoxy-3'-[18F]fluorothymidine PET/CT for evaluating response to cytotoxic chemotherapy in dogs with non-Hodgkin's lymphoma. *Vet Radiol Ultrasound.* (2009) 50:660–8. doi: 10.1111/j.1740-8261.2009.01612.x
19. Vail DM, Thamm DH, Reiser H, Ray AS, Wolfgang GH, Watkins WJ, et al. Assessment of GS-9219 in a pet dog model of non-Hodgkin's lymphoma. *Clin Cancer Res.* (2009) 15:3503–10. doi: 10.1158/1078-0432.CCR-08-3113
20. Rowe JA, Morandi F, Osborne DR, Wall JS, Kennel SJ, Reed RB, et al. Relative skeletal distribution of proliferating marrow in the adult dog determined using 3'-deoxy-3'-[(18) F]fluorothymidine. *Anat Histol Embryol.* (2019) 48:46–52. doi: 10.1111/ahe.12410
21. Hansen AE, Gutte H, Holst P, Johannesen HH, Rahbek S, Clemmensen AE, et al. Combined hyperpolarized (13)C-pyruvate MRS and (18)F-FDG PET (hyperPET) estimates of glycolysis in canine cancer patients. *Eur J Radiol.* (2018) 103:6–12. doi: 10.1016/j.ejrad.2018.02.028
22. Diocou S, Volpe A, Jauregui-Osoro M, Boudjemeline M, Chuamsaamarkkee K, Man F, et al. [(18)F]tetrafluoroborate-PET/CT enables sensitive tumor and metastasis *in vivo* imaging in a sodium iodide symporter-expressing tumor model. *Sci Rep.* (2017) 7:946. doi: 10.1038/s41598-017-01044-4
23. Jiang H, DeGrado TR. [(18)F]Tetrafluoroborate ([(18)F]TFB) and its analogs for PET imaging of the sodium/iodide symporter. *Theranostics.* (2018) 8:3918–31. doi: 10.7150/thno.24997
24. Lee SB, Lee HW, Lee H, Jeon YH, Lee SW, Ahn BC, et al. Tracking dendritic cell migration into lymph nodes by using a novel PET probe (18)F-tetrafluoroborate for sodium/iodide symporter. *EJNMMI Res.* (2017) 7:32. doi: 10.1186/s13550-017-0280-5
25. DeGrado TR, Coenen HH, Stocklin G. 14(R,S)-[18F]fluoro-6-thia-heptadecanoic acid (FTHA): evaluation in mouse of a new probe of myocardial utilization of long chain fatty acids. *J Nucl Med.* (1991) 32:1888–96. doi: 10.1002/jlcr.2580290903
26. Taylor M, Wallhaus TR, Degrado TR, Russell DC, Stanko P, Nickles RJ, et al. An evaluation of myocardial fatty acid and glucose uptake using PET with [18F]fluoro-6-thia-heptadecanoic acid and [18F]FDG in patients with congestive heart failure. *J Nucl Med.* (2001) 42:55–62.
27. Saba CF, Vickery KR, Clifford CA, Burgess KE, Phillips B, Vail DM, et al. Rabacfosadine for relapsed canine B-cell lymphoma: Efficacy and adverse event profiles of 2 different doses. *Vet Comp Oncol.* (2017) 16:E76–82. doi: 10.1111/vco.12337

28. Thamm DH, Vail DM, Post GS, Fan TM, Phillips BS, Axiak-Bechtel S, et al. Alternating Rabacfosadine/Doxorubicin: efficacy and tolerability in naive canine multicentric lymphoma. *J Vet Intern Med*. (2017) 31:872–8. doi: 10.1111/jvim.14700
29. De Clercq E. Tanovea® for the treatment of lymphoma in dogs. *Biochem Pharmacol*. (2018) 154:265–9. doi: 10.1016/j.bcp.2018.05.010
30. Farrell KB, Karpeisky A, Thamm DH, Zinnen S. Bisphosphonate conjugation for bone specific drug targeting. *Bone Rep*. (2018) 9:47–60. doi: 10.1016/j.bonr.2018.06.007
31. Zinnen DTS, Vail D, Fan T, Karpeisky A. Evaluation of a novel bone targeted aracytidine therapy in dogs with spontaneous osteosarcoma. *Bone*. (2011) 48:S22–55. doi: 10.1016/j.bone.2010.10.145
32. Zinnen SP, Karpeisky A, Von Hoff DD, Plekhova L, Alexandrov A. First-in-human phase I study of MBC-11, a novel bone-targeted cytarabine-etidronate conjugate in patients with cancer-induced bone disease. *Oncologist*. (2019) 24:303–e102. doi: 10.1634/theoncologist.2018-0707
33. Leblanc AK, Miller AN, Galyon GD, Moyers TD, Long MJ, Stuckey AC, et al. Preliminary evaluation of serial (18) FDG-PET/CT to assess response to toceranib phosphate therapy in canine cancer. *Vet Radiol Ultrasound*. (2012) 53:348–57. doi: 10.1111/j.1740-8261.2012.01925.x
34. Horn KP, Yap JT, Agarwal N, Morton KA, Kadrmas DJ, Beardmore B, et al. FDG and FLT-PET for early measurement of response to 37.5 mg daily sunitinib therapy in metastatic renal cell carcinoma. *Cancer Imaging*. (2015) 15:15. doi: 10.1186/s40644-015-0049-x
35. Rickard AG, Palmer GM, Dewhirst MW. Clinical and pre-clinical methods for quantifying tumor hypoxia. *Adv Exp Med Biol*. (2019) 1136:19–41. doi: 10.1007/978-3-030-12734-3_2
36. Snyder SA, Dewhirst MW, Hauck ML. The role of hypoxia in canine cancer. *Vet Comp Oncol*. (2008) 6:213–23. doi: 10.1111/j.1476-5829.2008.00163.x
37. Viglianti BL, Lora-Michiels M, Poulson JM, Lan L, Yu D, Sanders L, et al. Dynamic contrast-enhanced magnetic resonance imaging as a predictor of clinical outcome in canine spontaneous soft tissue sarcomas treated with thermoradiotherapy. *Clin Cancer Res*. (2009) 15:4993–5001. doi: 10.1158/1078-0432.CCR-08-2222
38. Bowen SR, Chappell RJ, Bentzen SM, Deveau MA, Forrest LJ, Jeraj R. Spatially resolved regression analysis of pre-treatment FDG, FLT and Cu-ATSM PET from post-treatment FDG PET: an exploratory study. *Radiother Oncol*. (2012) 105:41–8. doi: 10.1016/j.radonc.2012.05.002
39. Bradshaw T, Fu R, Bowen S, Zhu J, Forrest L, Jeraj R. Predicting location of recurrence using FDG, FLT, and Cu-ATSM PET in canine sinonasal tumors treated with radiotherapy. *Phys Med Biol*. (2015) 60:5211–24. doi: 10.1088/0031-9155/60/13/5211
40. Bradshaw TJ, Bowen SR, Jallow N, Forrest LJ, Jeraj R. Heterogeneity in intratumor correlations of 18F-FDG, 18F-FLT, and 61Cu-ATSM PET in canine sinonasal tumors. *J Nucl Med*. (2013) 54:1931–7. doi: 10.2967/jnumed.113.121921
41. Khoja L, Kibiro M, Metser U, Gedye C, Hogg D, Butler MO, et al. Patterns of response to anti-PD-1 treatment: an exploratory comparison of four radiological response criteria and associations with overall survival in metastatic melanoma patients. *Br J Cancer*. (2016) 115:1186–92. doi: 10.1038/bjc.2016.308
42. Wolchok JD, Hoos A, O'Day S, Weber JS, Hamid O, Lebbe C, et al. Guidelines for the evaluation of immune therapy activity in solid tumors: immune-related response criteria. *Clin Cancer Res*. (2009) 15:7412–20. doi: 10.1158/1078-0432.CCR-09-1624
43. Eisenhauer EA, Therasse P, Bogaerts J, Schwartz LH, Sargent D, Ford R, et al. New response evaluation criteria in solid tumours: revised RECIST guideline (version 1.1). *Eur J Cancer*. (2009) 45:228–47. doi: 10.1016/j.ejca.2008.10.026
44. Ascierto PA, Marincola FM. What have we learned from cancer immunotherapy in the last 3 years? *J Transl Med*. (2014) 12:141. doi: 10.1186/1479-5876-12-141
45. Chen TT, Statistical issues and challenges in immuno-oncology. *J Immunother Cancer*. (2013) 1:18. doi: 10.1186/2051-1426-1-18
46. Nishino M, Giobbie-Hurder A, Gargano M, Suda M, Ramaiya NH, Hodi FS. Developing a common language for tumor response to immunotherapy: immune-related response criteria using unidimensional measurements. *Clin Cancer Res*. (2013) 19:3936–43. doi: 10.1158/1078-0432.CCR-13-0895
47. Nishino M, Jagannathan JP, Krajewski KM, O'Regan K, Hatabu H, Shapiro G, et al. Personalized tumor response assessment in the era of molecular medicine: cancer-specific and therapy-specific response criteria to complement pitfalls of RECIST. *AJR Am J Roentgenol*. (2012) 198:737–45. doi: 10.2214/AJR.11.7483
48. Postow MA, Callahan MK, Wolchok JD. Immune checkpoint blockade in cancer therapy. *J Clin Oncol*. (2015) 33:1974–82. doi: 10.1200/JCO.2014.59.4358
49. Ribas A, Chmielowski B, Glaspy JA. Do we need a different set of response assessment criteria for tumor immunotherapy? *Clin Cancer Res*. (2009) 15:7116–8. doi: 10.1158/1078-0432.CCR-09-2376
50. Xing Y, Bronstein Y, Ross MI, Askew RL, Lee JE, Gershenwald JE, et al. Contemporary diagnostic imaging modalities for the staging and surveillance of melanoma patients: a meta-analysis. *J Natl Cancer Inst*. (2011) 103:129–42. doi: 10.1093/jnci/djq455
51. Burdick MJ, Stephans KL, Reddy CA, Djemil T, Srinivas SM, Videtic GM. Maximum standardized uptake value from staging FDG-PET/CT does not predict treatment outcome for early-stage non-small-cell lung cancer treated with stereotactic body radiotherapy. *Int J Radiat Oncol Biol Phys*. (2010) 78:1033–9. doi: 10.1016/j.ijrobp.2009.09.081
52. Clarke K, Taremi M, Dahele M, Freeman M, Fung S, Franks K, et al. Stereotactic body radiotherapy (SBRT) for non-small cell lung cancer (NSCLC): is FDG-PET a predictor of outcome? *Radiother Oncol*. (2012) 104:62–6. doi: 10.1016/j.radonc.2012.04.019
53. Hoopes DJ, Tann M, Fletcher JW, Forquer JA, Lin PF, Lo SS, et al. FDG-PET and stereotactic body radiotherapy (SBRT) for stage I non-small-cell lung cancer. *Lung Cancer*. (2007) 56:229–34. doi: 10.1016/j.lungcan.2006.12.009
54. Horne ZD, Clump DA, Vargo JA, Shah S, Beriwal S, Burton SA, et al. Pretreatment SUVmax predicts progression-free survival in early-stage non-small cell lung cancer treated with stereotactic body radiation therapy. *Radiat Oncol*. (2014) 9:41. doi: 10.1186/1748-717X-9-41
55. Takeda A, Yokosuka N, Ohashi T, Kunieda E, Fujii H, Aoki Y, et al. The maximum standardized uptake value (SUVmax) on FDG-PET is a strong predictor of local recurrence for localized non-small-cell lung cancer after stereotactic body radiotherapy (SBRT). *Radiother Oncol*. (2011) 101:291–7. doi: 10.1016/j.radonc.2011.08.008
56. Lambin P, Rios-Velazquez E, Leijenaar R, Carvalho S, van Stiphout RG, Granton P, et al. Radiomics: extracting more information from medical images using advanced feature analysis. *Eur J Cancer*. (2012) 48:441–6. doi: 10.1016/j.ejca.2011.11.036
57. Liu Y, Cao X. Immunosuppressive cells in tumor immune escape and metastasis. *J Mol Med*. (2016) 94:509–22. doi: 10.1007/s00109-015-1376-x
58. Kurzman ID, MacEwen EG, Rosenthal RC, Fox LE, Keller ET, Helfand SC, et al. Adjuvant therapy for osteosarcoma in dogs: results of randomized clinical trials using combined liposome-encapsulated muramyl tripeptide and cisplatin. *Clin Cancer Res*. (1995) 1:1595–601.
59. Kurzman ID, Shi F, Vail DM, MacEwen EG. *In vitro* and *in vivo* enhancement of canine pulmonary alveolar macrophage cytotoxic activity against canine osteosarcoma cells. *Cancer Biother Radiopharm*. (1999) 14:121–8. doi: 10.1089/cbr.1999.14.121
60. Meyers PA, Schwartz CL, Krailo MD, Healey JH, Bernstein ML, Betcher D, et al. Children's Oncology, Osteosarcoma: the addition of muramyl tripeptide to chemotherapy improves overall survival–a report from the Children's Oncology Group. *J Clin Oncol*. (2008) 26:633–8. doi: 10.1200/JCO.2008.14.0095
61. Parisi MT, Eslamy H, Park JR, Shulkin BL, Yanik GA. (1)(3)(1)I-Metaiodobenzylguanidine theranostics in neuroblastoma: historical perspectives; practical applications. *Semin Nucl Med*. (2016) 46:184–202. doi: 10.1053/j.semnuclmed.2016.02.002
62. Emmett L, Willowson K, Violet J, Shin J, Blanksby A, Lee J. Lutetium (177) PSMA radionuclide therapy for men with prostate cancer: a review of the current literature and discussion of practical aspects of therapy. *J Med Radiat Sci*. (2017) 64:52–60. doi: 10.1002/jmrs.227
63. Weichert JP, Clark PA, Kandela IK, Vaccaro AM, Clarke W, Longino MA, et al. Alkylphosphocholine analogs for broad-spectrum cancer imaging and therapy. *Sci Transl Med*. (2014) 6:240ra75. doi: 10.1126/scitranslmed.3007646

64. Baiu DC, Marsh IR, Boruch AE, Shahi A, Bhattacharya S, Jeffery JJ, et al. Targeted molecular radiotherapy of pediatric solid tumors using a radioiodinated alkyl-phospholipid ether analog. *J Nucl Med*. (2018) 59:244–50. doi: 10.2967/jnumed.117.193748
65. Morris ZS, Guy EI, Werner LR, Carlson PM, Heinze CM, Kler JS, et al. Tumor-specific inhibition of in situ vaccination by distant untreated tumor sites. *Cancer Immunol Res.* (2018) 6:825–34. doi: 10.1158/2326-6066.CIR-17-0353
66. Morris ZS, Guy EI, Francis DM, Gressett MM, Werner LR, Carmichael LL, et al. *In Situ* tumor vaccination by combining local radiation and tumor-specific antibody or immunocytokine treatments. *Cancer Res*. (2016) 76:3929–41. doi: 10.1158/0008-5472.CAN-15-2644
67. Canter RJ, Grossenbacher SK, Foltz JA, Sturgill IR, Park JS, Luna JI, et al. Radiotherapy enhances natural killer cell cytotoxicity and localization in pre-clinical canine sarcomas and first-in-dog clinical trial. *J Immunother Cancer*. (2017) 5:98. doi: 10.1186/s40425-017-0305-7
68. McDowell KA, Hank JA, DeSantes KB, Capitini CM, Otto M, Sondel PM. NK cell-based immunotherapies in pediatric oncology. *J Pediatr Hematol Oncol*. (2015) 37:79–93. doi: 10.1097/MPH.0000000000000303
69. Chapelin F, Capitini CM, Ahrens ET. Fluorine-19 MRI for detection and quantification of immune cell therapy for cancer. *J Immunother Cancer*. (2018) 6:105. doi: 10.1186/s40425-018-0416-9
70. Bouchlaka MN, Ludwig KD, Gordon JW, Kutz MP, Bednarz BP, Fain SB, et al. (19)F-MRI for monitoring human NK cells *in vivo*. *Oncoimmunology*. (2016) 5:e1143996. doi: 10.1080/2162402X.2016.1143996
71. Fidel J, Kennedy KC, Dernell WS, Hansen S, Wiss V, Stroud MR, et al. Preclinical validation of the utility of BLZ-100 in providing fluorescence contrast for imaging spontaneous solid tumors. *Cancer Res*. (2015) 75:4283–91. doi: 10.1158/0008-5472.CAN-15-0471
72. Holt D, Parthasarathy AB, Okusanya O, Keating J, Venegas O, Deshpande C, et al. Intraoperative near-infrared fluorescence imaging and spectroscopy identifies residual tumor cells in wounds. *J Biomed Opt*. (2015) 20:76002. doi: 10.1117/1.JBO.20.7.076002
73. Keating JJ, Runge JJ, Singhal S, Nims S, Venegas O, Durham AC, et al. Intraoperative near-infrared fluorescence imaging targeting folate receptors identifies lung cancer in a large-animal model. *Cancer*. (2017) 123:1051–60. doi: 10.1002/cncr.30419
74. Mery E, Golzio M, Guillermet S, Lanore D, Le Naour A, Thibault B, et al. Fluorescence-guided surgery for cancer patients: a proof of concept study on human xenografts in mice and spontaneous tumors in pets. *Oncotarget*. (2017) 8:109559–74. doi: 10.18632/oncotarget.22728
75. Mesa KJ, Selmic LE, Pande P, Monroy GL, Reagan J, Samuelson J, et al. Intraoperative optical coherence tomography for soft tissue sarcoma differentiation and margin identification. *Lasers Surg Med*. (2017) 49:240–8. doi: 10.1002/lsm.22633
76. Parrish-Novak J, Byrnes-Blake K, Lalayeva N, Burleson S, Fidel J, Gilmore R, et al. Nonclinical profile of BLZ-100, a tumor-targeting fluorescent imaging agent. *Int J Toxicol*. (2017) 36:104–12. doi: 10.1177/1091581817697685
77. Predina JD, Runge J, Newton A, Mison M, Xia L, Corbett C, et al. Evaluation of aminolevulinic acid-derived tumor fluorescence yields disparate results in murine and spontaneous large animal models of lung cancer. *Sci Rep*. (2019) 9:7629. doi: 10.1038/s41598-019-40334-x
78. Selmic LE, Samuelson J, Reagan JK, Mesa KJ, Driskell E, Li J, et al. Intra-operative imaging of surgical margins of canine soft tissue sarcoma using optical coherence tomography. *Vet Comp Oncol*. (2019) 17:80–8. doi: 10.1111/vco.12448

Conflict of Interest: The authors declare that the research was conducted in the absence of any commercial or financial relationships that could be construed as a potential conflict of interest.

Copyright © 2020 Vail, LeBlanc and Jeraj. This is an open-access article distributed under the terms of the Creative Commons Attribution License (CC BY). The use, distribution or reproduction in other forums is permitted, provided the original author(s) and the copyright owner(s) are credited and that the original publication in this journal is cited, in accordance with accepted academic practice. No use, distribution or reproduction is permitted which does not comply with these terms.

frontiers in Oncology

ORIGINAL RESEARCH
published: 07 February 2020
doi: 10.3389/fonc.2020.00020

SPECT-CT Imaging of Dog Spontaneous Diffuse Large B-Cell Lymphoma Targeting CD22 for the Implementation of a Relevant Preclinical Model for Human

Floriane Etienne[1,2†], Maxime Berthaud[1†], Frédérique Nguyen[1,2], Karine Bernardeau[1,3], Catherine Maurel[1], Caroline Bodet-Milin[1,4], Maya Diab[1], Jérôme Abadie[1,2], Valérie Gouilleux-Gruart[5], Aurélien Vidal[6], Mickaël Bourgeois[1,6], Nicolas Chouin[1,2], Catherine Ibisch[1,2] and François Davodeau[1]*

[1] CRCINA, INSERM, CNRS, Université de Nantes, Université d'Angers, Nantes, France, [2] AMaROC, Oniris (Nantes Atlantic College of Veterinary Medicine, Food Science and Engineering), Nantes, France, [3] P2R "Production de Protéines Recombinantes", CRCINA, SFR-Santé, INSERM, CNRS, UNIV Nantes, CHU Nantes, Nantes, France, [4] Nuclear Medicine, University Hospital, Nantes, France, [5] EA7501, GICC, Université de Tours, CHRU de Tours, Tours, France, [6] Groupement d'Intérêt Public ARRONAX Cyclotron, Saint-Herblain, France

Antibodies directed against CD22 have been used in radioimmunotherapy (RIT) clinical trials to treat patients with diffuse large B-cell lymphoma (DLBCL) with promising results. However, relevant preclinical models are needed to facilitate the evaluation and optimization of new protocols. Spontaneous DLBCL in dogs is a tumor model that may help accelerate the development of new methodologies and therapeutic strategies for RIT targeting CD22. Seven murine monoclonal antibodies specific for canine CD22 were produced by the hybridoma method and characterized. The antibodies' affinity and epitopic maps, their internalization capability and usefulness for diagnosis in immunohistochemistry were determined. Biodistribution and PET imaging on a mouse xenogeneic model of dog DLBCL was used to choose the most promising antibody for our purposes. PET-CT results confirmed biodistribution study observations and allowed tumor localization. The selected antibody, 10C6, was successfully used on a dog with spontaneous DLBCL for SPECT-CT imaging in the context of disease staging, validating its efficacy for diagnosis and the feasibility of future RIT assays. This first attempt at phenotypic imaging on dogs paves the way to implementing quantitative imaging methodologies that would be transposable to humans in a theranostic approach. Taking into account the feedback of existing human radioimmunotherapy clinical trials targeting CD22, animal trials are planned to investigate protocol improvements that are difficult to consider in humans due to ethical concerns.

Keywords: comparative oncology, dog, diffuse large B-cell lymphoma, monoclonal antibody, SPECT-CT imaging, CD22, internalization

OPEN ACCESS

Edited by:
Rodney L. Page, Colorado State University, United States

Reviewed by:
Rebecca A. Krimins, Johns Hopkins University, United States
Ana Ponce Kiess, Johns Hopkins Medicine, United States

***Correspondence:**
François Davodeau
francois.davodeau@inserm.fr

†These authors have contributed equally to this work and share first authorship

Specialty section:
This article was submitted to Cancer Molecular Targets and Therapeutics, a section of the journal Frontiers in Oncology

Received: *11 July 2019*
Accepted: *08 January 2020*
Published: *07 February 2020*

Citation:
Etienne F, Berthaud M, Nguyen F, Bernardeau K, Maurel C, Bodet-Milin C, Diab M, Abadie J, Gouilleux-Gruart V, Vidal A, Bourgeois M, Chouin N, Ibisch C and Davodeau F (2020) SPECT-CT Imaging of Dog Spontaneous Diffuse Large B-Cell Lymphoma Targeting CD22 for the Implementation of a Relevant Preclinical Model for Human. Front. Oncol. 10:20. doi: 10.3389/fonc.2020.00020

INTRODUCTION

Radioimmunotherapy (RIT) using an anti-CD20 antibody radiolabeled with yttrium-90 (ibritumomab tiuxetan/Zevalin®) is approved for the treatment of patients with relapsed or refractory follicular lymphoma (FL) or in consolidation after a front-line induction chemotherapy (1–4). Other clinical trials in the field of B-cell lymphoma RIT aim at demonstrating the value of RIT in front-line treatment (5, 6), high-dose treatment (7, 8), and fractionated RIT protocol with humanized monoclonal antibody (MAb) (9, 10) or using new monoclonal antibodies (MAbs) specific for lymphoma antigens (11, 12). Recently, antibodies directed against CD22 have been used in RIT clinical trials to treat patients with diffuse large B-cell lymphoma (DLBCL) and B-cell acute lymphoblastic leukemia (B-ALL) with encouraging results (13, 14). But performing RIT protocols in first-line treatment is not currently feasible until further clinical data is obtained regarding safety and efficacy in later-line treatment. For these reasons, relevant preclinical models are needed to facilitate the evaluation and optimization of new protocols. The relevance of rodent models of lymphoma is limited to the small number of lymphoma cell lines that are able to grow in vivo. Indeed, these few cell lines do not represent the large physiopathological diversity of human tumor subtypes and the inter-individual heterogeneity of patients (15, 16).

To improve the relevance of the preclinical approaches, pet dogs with spontaneous lymphomas diagnosed in veterinary practice would be an asset. Most of the B-cell lymphomas diagnosed in dogs are DLBCLs (17). Among NHLs, DLBCLs are more aggressive than FL and new therapeutic approaches are needed for relapsing patients. In humans, phase I/II clinical trials targeting CD22 for DLBCL therapy are promising. Spontaneous DLBCL in dogs is therefore a tumor model that may help to accelerate the development of new methodologies and therapeutic strategies with enhanced probability of success when transferred to the clinic (18, 19).

Whole-body molecular imaging of dogs with SPECT (single-photon emission computed tomography) or PET (positron emission tomography) using radiolabeled antibody specific for tumor antigens is non-invasive and enables to more accurately evaluate the disease extension at diagnosis before setting conventional treatment of dogs with DLBCL. In a theranostic approach, molecular quantitative imaging enables the calculation of the actual dose deposition to organs within the course of RIT performed with the same anti-CD22 antibody. This personalization of treatment requires defining specific methods such as population pharmacokinetics to evaluate the individual pharmacokinetic profiles of the patients treated (20, 21). Setting up these approaches requires sequential imaging, which is difficult to impose on human patients, but is realistic in the veterinary clinic. Since spontaneous tumor imaging in humans and dogs is performed using the same camera, the transfer from veterinary to human clinical trials will be facilitated. Based on the most promising phase I/II clinical trial of DLBCL RIT targeting CD22 in humans (14), it is relevant to perform clinical trials on sick dogs focusing on the rationale of dosing or treatment schedule with the hope of therapeutic benefit compared to conventional chemotherapy. Chemotherapy applied to dogs is adapted from human treatments. A current treatment of lymphoma in dogs includes L-asparaginase, vincristine, cyclophosphamide, prednisone, and doxorubicin (COPLA) induction followed by chlorambucil, vincristine, and prednisone (LVP). This treatment, however, rarely cures dogs and the median survival after chemotherapy is only 6 months. Finally, the less limiting ethical constraint in veterinary medicine and the possibility of proposing clinical trials for dogs whose owner opts for corticosteroid therapy may facilitate the evaluation of RIT in front-line treatment, while offering the animals and owners the opportunity to benefit from cancer treatment unavailable in the veterinary clinic, but currently in validation for human patients.

To develop the model of spontaneous DLBCL in dogs for molecular imaging and RIT, we isolated seven mouse monoclonal antibodies directed against the canine CD22 (CD22c) antigen. Here we describe the characterization and selection strategy of these antibodies for future molecular imaging and RIT in dogs. A dog with spontaneous DLBCL was subjected to a SPECT-CT imaging with an indium-111-radiolabeled anti-CD22 antibody as part of disease staging in order to obtain the proof of concept of the relevance of this antibody in a veterinary clinical trial.

MATERIALS AND METHODS

Cell Lines

The Chinese Hamster Ovary dihydrofolate reductase-deficient cell line (CHO DHFR$^-$) purchased from ECACC (European Collection of Cell Cultures, ref 94060607) was transfected for stable expression of soluble membranous canine CD22 (CD22c). CHO wild type (WT) and DHFR- cells were cultured in Roswell Park Memorial Institute medium 1640 (RPMI 1640) (Gibco BRL) containing 10% fetal bovine serum (Gibco BRL, ref 10270106), 1% glutamine (L-glutamine 200 mM; Gibco BRL, ref 25030149), and 1% antibiotic (penicillin 100 U/mL, streptomycin 100 U/mL; Gibco BRL, ref 15140148), and supplemented with 10 μg/mL of adenosine-deoxyadenosine-thymidine (ADT) (Sigma-Aldrich, ref T-1895). The CLBL-1 cell line is a canine diffuse large B-cell lymphoma cell line kindly supplied by Rütgen et al. (22). All cell lines were incubated at 37°C in a humidified atmosphere in 5% CO_2.

Antibodies

The 6H4 MAb, a mouse IgG_1 specific for human beta-2-microglobulin (β2m) produced and characterized in the laboratory, was used to screen and purify the canine CD22-human β2m fusion protein (CD22-β2m) as previously described (23).

A mouse anti-GFP monoclonal antibody [GFP Antibody (B-2); Santa Cruz Biotechnology, ref sc-9996] was used for Western blots using cell lysates of CD22c-GFP transfected CHO clones to detect the expression of the fusion protein CD22-β2m.

Vectors and Genes

The pKCR6 vector was used as an expression vector for CHO cell transfection (24). The soluble CD22c fused to human β2m as well as the entire canine CD22c-GFP coding sequences

were synthesized by GeneCust (Dudelange, Luxembourg). These sequences were received in a pBluescript II SK^+ vector with a *Xho I* and *Xba I* enzyme restriction sites at their 5′ end and 3′ end, respectively.

Production and Purification of CD22c-β2m Recombinant Protein

The soluble CD22c was produced as a fusion protein consisting of the ectodomain of CD22c (amino acids 1–683) fused to the human Beta-2-microglobulin (β2m) without the peptide signal (amino acids 21–119) via a linker of 15 amino acids constituted of three repeated $(SerGlyGlyGlyGly)_3$ motifs. The coding sequence of the soluble form of CD22c merged to β2m (CD22c-β2m) was cloned into the pKCR6 vector and transfected into CHO cells using Lipofectamine™ LTX Reagent with PLUS™ Reagent (Invitrogen, ref 15338030) according to the supplier's instructions. Cells were then cultured in 96-well plates in ADT-free RMPI medium to select transfected cells. The supernatant of the wells with surviving cells 2–3 weeks post-transfection were tested for the expression of CD22c-β2m with an ELISA assay. Briefly, the supernatants of growing clones were diluted in PBS and coated on Nunc MaxiSorp™ plates (ThermoFisher Scientific, ref 44-2404-21). Non-specific sites were blocked with 100 µL of PBS-0.5% BSA. The biotinylated anti-β2m antibody 6H4 was added to each well followed by 50 µL of horseradish peroxidase (HRP)-conjugated streptavidin (R&D Systems, ref DY998) and tetramethylbenzidine (TMB) substrate (R&D Systems, ref DY999). The reaction was stopped with 1 M of sulfuric acid (H_2SO_4). Optical density (OD) was measured at 405 and 570 nm by a spectrophotometer (Multiskan EX, Thermo Scientific, Ventana, Finland). The cells from the positive wells were then subcloned by limiting dilution. The supernatant of the clones was screened with the same ELISA assay, in order to select high-expressing CD22c-β2m clones.

The transfected CHO cell clone showing the highest production of canine CD22-β2m fusion protein was selected and expanded to produce 1 L of culture supernatant. The recombinant protein was then purified by affinity chromatography using HiTrap NHS-activated HP affinity column (GE Healthcare, ref 17071701) coated with the 6H4 antibody according to the supplier's instructions. Eluted canine CD22-β2m protein was further purified by size-exclusion chromatography (Superdex 200 10:300GL, GE Healthcare) and the fractions containing high CD22-β2m were pooled, concentrated using an ultrafiltration Amicon Ultra-15 membrane (30K—Millipore). Purified canine CD22-β2m fusion protein was then sterilized by filtration over a 0.22-µm Minisart® Syringe Filter (Sartorius, ref 16534) and stored in PBS at −20°C.

Gel Electrophoresis and Western Blotting

The purity of the CD22c-β2m protein produced was monitored by sodium dodecyl sulfate polyacrylamide gel electrophoresis (SDS-PAGE) with 5 µg of purified CD22c-β2m and human β2m (Sigma-Aldrich, ref M4890) used as a control. After electrophoresis on a 12% acrylamide gel under non-reducing conditions in 1x Tris Glycine SDS running buffer, the proteins were stained using Coomassie brilliant blue (National Diagnostics, ref HS-604) and the gel was scanned using a Bio-Rad scanner.

The SDS-PAGE gel was then transferred onto pore polyvinylidene fluoride (PVDF) membrane (Roche, ref 03010040001) in tris-glycine blotting buffer (Bio-Rad, ref 1610771). Non-specific sites were blocked using a TBS-0.1%-Tween-5% milk buffer, and PVDF membrane was incubated with the primary antibody 6H4 directed against human β2m for 2 h at room temperature. After washing, the membrane was incubated with a peroxidase-conjugated goat anti-mouse secondary antibody (Jackson ImmunoResearch, ref 115-035-003) (1:1,000 dilution) for 90 min. Target proteins were visualized with the Bio-Rad camera after revelation with the 3,3′-Diaminobenzidine (DAB) substrate.

Production of CHO Cells Expressing Membranous Canine CD22 Fused to GFP

The full-length CD22c coding sequence (aa 1–848) with a *Xho I* restriction site at the 5′ end and a *Bgl II* restriction site at the 3′ end was produced by GeneCust laboratories (Luxembourg) and cloned into the pCR™ 2.1-TOPO^R plasmid using the TOPO™ TA Cloning™ Kit (Invitrogen, ref K456001). The *Xbo I-Xba I* CD22c coding sequence was then inserted in pEGFP-N3 (Clontech) and digested by *Xho I* and *Bgl II* in order to merge the CD22c and EGFP coding sequences. The CD22c-EGFP coding sequence in pEGFP-N3 and the expression vector pKCR6 were then digested with *Xho I* and *Xba I*. The fragments of interest were purified and ligated. The pKCR6/CD22c-EGFP construct was then transfected into Chinese hamster ovary (CHO) cells using the Lipofectamine™ LTX Reagent with PLUS™ Reagent (Invitrogen, ref 15338030).

The transfected cell line was subcloned by limiting dilution and the clones with positive green fluorescence were selected by flow cytometry analysis. Cell lysates from the highest expressing clones were further analyzed with Western blot using an anti-EGFP antibody (B-2). The clones with a positive band at the expected size corresponding to CD22c-EGFP were amplified and used thereafter for hybridoma supernatant screening.

Mice Immunization Procedure

Three BALB/c JRj mice obtained from JANVIER laboratories (France) were immunized with the purified canine CD22-β2m recombinant protein. For each mouse, two immunizations 3 weeks apart were administered intraperitoneally with a constant amount of 50 µg of CD22c-β2m protein in PBS. These injections were performed with an equivalent volume of Freund's complete adjuvant (first injection) or incomplete adjuvant (second injection) (Sigma-Aldrich, ref F5881 and F5506) according to the supplier's instructions. One week after the second injection, blood was collected and antibody titers were assessed by flow cytometry analysis on the selected CD22c-EGFP expressing the CHO clone. The best responding mouse was selected and received a last intravenous boost of 50 µg of canine CD22c-β2m protein in PBS without adjuvant. Five days later, the mouse was sacrificed by cervical dislocation, the spleen was collected and splenocytes were harvested in RPMI 1640

medium for fusion. All experiments were conducted according to the National Institutes of Health (NIH) guidelines for handling experimental animals.

Hybridoma Cell Production

Hybridomas were generated by the fusion of spleen cells from the immunized mouse with murine myeloma cells SP2/0 (ATC, ref PTA-5817) at a 5/1 ratio using 50% polyethylene glycol (PEG 1500) (Roche, ref 10783641001) according to the supplier's instructions. Hybridomas were grown in RMPI culture medium containing 20% fetal bovine serum, penicillin (100 U/mL) and streptomycin (100 U/mL) and supplemented with interleukin-6 (50 U/mL) and 2% hypoxanthine-aminopterin-thymidine (HAT) (ATCC) for the selection of hybridomas. This medium was replaced after 1 week with 2% hypoxanthine-thymidine supplemented medium (ATCC). Ten to 15 days after fusion, hybridomas were established in the wells and culture supernatants were screened.

Hybridoma Supernatant Screening

The production of CD22c-specific antibodies was determined by flow cytometry analysis using the selected CHO cell clone expressing canine CD22c-EGFP. Hybridoma supernatants diluted in PBS-BSA 0.1% (1:1) were incubated with the canine CD22c-EGFP-positive CHO clone for 1 h at 4°C. A phycoerythrin-conjugated anti-mouse IgG (Jackson ImmunoResearch, ref 115-116-071) was used as a secondary antibody. Data acquisition and analysis were performed in a Becton Dickinson FACSCalibur flow cytometer (BD Biosciences) using FlowJo software (FlowJo LLC). The specificity of hybridomas for canine CD22c was confirmed using a similar flow cytometry method on WT CHO cells used as a negative control.

Monoclonal Antibody (MAb) Purification and Isotype Determination

Selected cloned hybridomas were cultured in RPMI 1640 medium supplemented with 10% IgG-depleted fetal bovine serum in a 1-L Erlenmeyer flask (Corning®) with stirring at 80 rpm for 4 days at 37°C and 5% CO_2 in an agitator. Clone supernatant cultures were collected and canine CD22-specific antibodies were purified over a HiTrap Protein G HP column (GE Healthcare, ref 29-0485-81). Briefly, supernatants from hybridoma cultures were diluted in phosphate buffer (1:1) to adjust the pH to 7. After passage through the column, antibodies were eluted using a glycine-HCl buffer pH 2.7 and dialyzed overnight against PBS pH 7.4 using 30,000 MWCO dialysis cassettes (Thermo Scientific). Purified antibodies were filtered through 0.2-μm filters and stored at 4°C and their production yields were determined.

Isotypes and light chains of purified antibodies were characterized using the IsoStrip™ Mouse Monoclonal Antibody Isotyping Kit (Roche, ref 11493027001) according to the kit instructions.

Determination of MAb Equilibrium Dissociation Constant (Kd)

The affinity of MAbs was determined by flow cytometry as described above. For each antibody, a series of concentrations from 4.10^{-7} to 3.10^{-11} M was tested with a constant number of 2×10^5 of the canine CD22c-EGFP-positive CHO cells. IgG1/K and IgG2b/K antibodies were used as control isotypes. Mean fluorescence intensities (MFI) were plotted against their corresponding antibody concentrations. Antibody dissociation constants were determined by a non-linear regression using the Prism software package (GraphPad Software Inc.).

Epitope Mapping

Competition tests using the indirect ELISA method were performed to evaluate the number of distinct epitopes recognized by the antibodies produced. For these tests, 1 mg of each antibody was biotinylated using an EZ-Link™ Sulfo-NHS-Biotinylation Kit (Thermo Scientific, ref 21425) according to the supplier's instructions. Antibody biotinylation was essential for revelation with Streptavidin-HRP. An ELISA plate was coated with 250 ng/well of the anti-β2m antibody (6H4). Non-specific sites were blocked with PBS-0.5% BSA and 125 ng/well of the CD22c-β2m was added. Each biotinylated antibody was separately incubated at a constant concentration, equal to its Kd, with a 100-fold excess of each of the unlabeled antibodies. Then the wells were washed three times and revelation was finally performed with 50 μL of horseradish peroxidase (HRP)-conjugated streptavidin, as described above.

For the analysis of the competition between antibodies, the wells containing biotinylated antibody with an excess of a mouse IgG control isotype were considered as controls of the absence of competition. Wells containing the same antibody in biotinylated and unlabeled forms were considered as positive controls of the competition.

Internalization

To estimate the internalization of anti-CD22 antibody, the CD22 proteins at the cell surface were quantified using the CLBL-1 cell line. We seeded 1.5×10^5 CLBL-1 cells in two 96-well plates. One plate was kept at 4°C and the other at 37°C. At 0, 15, 30, 60, 90, 120, 180, and 240 min after incubation, each anti-CD22 antibody produced was added to the wells of the plate at 4 and 37°C. Multiple assays were performed with antibody concentrations corresponding to 10-, 5-, 1-, and 0.1-fold their own Kd. At the end of the incubation time, the plates were placed on ice, the cells were washed twice with ice-cold PBS and stained with phycoerythrin goat anti-mouse F(ab)′2 at 4°C for 1 h. After washing in ice-cold PBS BSA 0.1%, cell fluorescence was measured using a FACSCalibur cytometer. For each incubation time, the percentage of internalization was calculated as = [(MFI at 4°C)–(MFI at 37°C)]*100/(MFI at 4°C).

To evaluate the percentage of internalization as a function of the antigenic site saturation, the maximum binding of antibodies (Bmax) was evaluated for each antibody at each concentration after 240 min at 4°C at a saturating amount of antibodies using non-linear regression (one phase exponential association equation, PRISM GraphPad software). The actual percentage

of saturated CD22c antigenic sites was also calculated for each antibody concentration 240 min after incubation at 4°C. The corresponding percentage of internalization was then plotted against the percentage of saturation of cell-surface CD22c.

Immunohistochemistry

Formalin-fixed, paraffin-embedded (FFPE) 5-μm-thick tissue blocks from dogs were cut for anti-CD22 immunohistochemistry (IHC). A normal dog lymph node was used to check immunoreactivity of the canine CD22-specific clones produced. Samples of canine diffuse large B-cell lymphomas consisted of 30 previously diagnosed cases, of which 10 were of the germinal-center phenotype (i.e., positive for CD10, or CD10-negative but positive for BCL6 expression and negative for MUM1), and 20 were of the non-germinal-center phenotype (i.e., negative for CD10 and BCL6, or CD10-negative but positive for both BCL6 and MUM1). All histologic slides were freshly cut before IHC analysis. Briefly, sections were dried at 60°C for 2 h, deparaffinized, pretreated at 95°C for 60 min in a basic buffer (CC1, cell conditioning medium-1, pH 8.4; Ventana Medical Systems, ref 950-124) for antigen retrieval, and stained at 37°C for 60 min. The antibody concentrations were 2 μg/mL for the CD22-specific clone 2D1, 10 μg/mL for the clones 1E3, 5C2, and 5F8, 15 μg/mL for the clones 5A3 and 10C6, and 20 μg/mL for the clone 6B7. All dilutions were performed in a commercially available antibody diluent (Ventana Medical Systems, ref 251-018). All IHC protocols were run in a Ventana BenchMark XT immunostainer (Ventana Medical Systems). Antibody incubation was followed by chromogenic detection with the OptiView DAB IHC detection kit (Ventana Medical Systems, ref 760-700), counterstaining with 1 drop of hematoxylin-II for 4 min and post-counterstaining with 1 drop of Bluing Reagent for 4 min. Subsequently, slides were removed from the immunostainer, washed in water with a drop of dishwashing detergent, and mounted. In each run, a negative control was obtained by replacing the primary antibody with normal mouse serum (Negative Control Monoclonal Ig, 1 μg/mL, Ventana Medical Systems).

Radiolabelling of Anti-CD22c MAbs

Radiolabeling of Anti-CD22c MAbs With Iodine-125

Anti-CD22c MAbs were labeled with ^{125}I (Perkin Elmer, ref NEZ033001) using the iodogen method, as previously described (25). The ^{125}I-labeled anti-CD22c MAbs were purified on a PD10 desalting column with sephadex G-25 (GE Healthcare, ref 17085101). Radiolabeling efficiencies, estimated by Instant Thin Layer Chromatography (ITLC), were above 95%.

Radiolabeling 10C6 MAb With Copper-64 and Indium-111

The 10C6 anti-CD22c clone was modified with p-SCN-Bn-DOTA (p-SCN-Bn-DOTA; Macrocyclics, ref B-205), as previously described (26). In brief, 10C6 MAb was incubated with 20 equivalents (mole/mole) of p-SCN-Bn-DOTA in borate buffer (0.2 M, pH 8.7) for 1 h at room temperature. The excess p-SCN-Bn-DOTA was removed by several filtration cycles on a centrifugal filter (Ultracel 30K, Amicon) using sodium acetate (0.2 M, pH 6). 10C6-DOTA was then radiolabeled with ^{64}Cu (ARRONAX cyclotron) by adding 50 MBq ^{64}Cu and adjusting the pH to 5.5 with sodium acetate (0.5 M, pH 5). The resulting ^{64}Cu-labeled 10C6-DOTA was separated from unbound ^{64}Cu by size-exclusion chromatography using a PD-10 column. Radiochemical purity, checked by ITLC, was >95%. The specific activity after purification was 216 MBq.mg^{-1}.

The 10C6 Mab was radiolabeled with indium-111 according to the same protocol as that used for radiolabeling with ^{64}Cu. Briefly, 1.0 mg 10C6-DOTA was mixed with indium-111 chloride adjusted to pH 5.5 with sodium acetate (0.5 M, pH 5) and incubated. The resulting ^{111}In-labeled 10C6-DOTA was separated from unbound ^{111}In by size-exclusion chromatography using a PD-10 column. Radiochemical purity, checked by ITLC, was 81%. The specific activity after purification was 128.8 MBq.mg^{-1}.

Xenogeneic Mouse Model of Canine DLBCL

All experiments were conducted according to the National Institutes of Health (NIH) guidelines for handling experimental animals (ethics committee of Pays de la Loire, CEEA 00143.01 and CEEA 2012.171).

Mouse Tumor Model

5.10^6 CLBL-1 cells (canine B-cell lymphoma cell line) in 0.1 mL PBS were injected in the flank of 8-week-old NMRI-nu female mice (JANVIER). Biodistribution and PET imaging were carried out 14 days after tumor cell injection.

Biodistribution of ^{125}I-Anti-CD22c MAbs

Biodistribution was carried out by injecting mice in the tail vein with 6 μg of ^{125}I-anti-CD22c MAbs in 0.1 mL PBS (30 Bq). At each time point, three mice were sacrificed, the organs were collected and weighed, and the amount of radionuclide activity in tissues was measured using a gamma scintillation counter (PerkinElmer). The results are expressed as a percentage of injected activity per gram of tissue.

PET-CT Imaging and Biodistribution of ^{64}Cu-10C6 MAb

For PET-CT imaging, three mice were injected in the tail vein with 10 MBq of ^{64}Cu-10C6 (50 μg). Images were acquired 16 h after injection using a microPET-CT scanner (Inveon Siemens Medical Solutions) under anesthesia (isoflurane-O_2). After imaging, the mice were sacrificed and biodistribution was performed.

SPECT-CT Imaging on Experimental Dogs and Dogs With Spontaneous DLBCL

The SPECT-CT protocols applied to experimental dogs and dogs with spontaneous DLBCL were identical. This imaging was conducted according to WSAVA Global Guidelines (World Small Animal Veterinary Association) and the protocol study was validated by the CERVO Ethics Committee (Comité d'Ethique pour la Recherche clinique et épidémiologique Vétérinaire d'Oniris, Nantes, France; CERVO-2016-21-V). For imaging on

sick privately owned dogs, the pet owner's informed consent was collected. The Mab content of endotoxin is within the range recommended for humans. The dogs were premedicated with methylprednisolone (Solu-Medrol® 20, PFIZER PFE France, 1 mg.kg^{-1} intravenously) and promethazine (Phenergan® 2.5%, UCB Pharma SA, 0.3 mg.kg^{-1} subcutaneously). The ^{111}In-10C6 was co-injected with naked 10C6 MAb under anesthesia for 30 min through an intravenous saline line in a front leg. A variable amount of cold antibody ranging from 0 to 1.5 mg.kg^{-1} was used. The injected activity of ^{111}In-10C6 was 3.7 MBq/kg of body weight. SPECT-CT was performed at 1 h and daily for 1 week for experimental dogs and at 48 h for sick dogs. SPECT-CT images were acquired on a SPECT-CT camera (Optima 640, GE Medical Systems) with a medium-energy general-purpose collimator (MEGP). The acquisition time was 30 s for each of the 60 projections. Energy windows (15% width) were centered on the two major peaks at 172 keV and 247 keV. The reconstruction was done using Xeleris software and the ordered subset expectation maximization (OSEM) algorithm with two iterations and 10 subsets. Images were corrected for attenuation, based on computed tomography (120 keV, 10 mA).

RESULTS

Production and Purification of Canine CD22 Immunogen for Mice Immunization

A soluble form of canine CD22 usable for mice immunization and for monoclonal antibody characterization was produced by stable transfection into CHO cells. In its NH2 end this immunogen comprises the canine CD22 extracellular domain merged to the human beta-2-microglobulin with a peptide linker. Human β2m was chosen because of the availability in the laboratory of a specific anti-hβ2m monoclonal antibody (6H4) (23). This antibody enables the screening by ELISA of transfected cell supernatants for the production of the canine recombinant protein. One clone of transfected CHO cells (named 13E12) showing the strongest signal was amplified. One liter of 13E12 supernatant was produced and purified using HiTrap NHS-activated HP affinity column coupled to 6H4 antibody (HiTrap-6H4). The protein obtained after one-step affinity chromatography on HiTrap-6H4 was then purified by size-exclusion chromatography Superdex 200 column (**Figure 1A**). The purification fractions were analyzed by Western blot using the 6H4 antibody. The fractions corresponding to the major peak were further analyzed by Western blot. The molecular weight of the highlighted protein corresponds to the CD22-β2m fusion protein (**Figure 1B**). After purification, 2 mg of the fusion protein was obtained at sufficient purity for use as an immunogen. This amount was sufficient for the immunization of several mice and characterization of the MAbs produced.

Production of a CHO Clone Expressing Canine CD22 at the Membrane for Hybridoma Screening

To screen hybridomas producing antibodies specific for canine CD22 using flow cytometry analysis, we produced CHO cells expressing membranous canine CD22. Since no antibodies specific for canine CD22 were available for the screening of transfected cells, the cytoplasmic domain of CD22 was merged with EGFP in order to be able to screen transfectants with flow cytometry. The polyclonal cell line was then cloned by limiting dilution and we selected the clones with the highest green fluorescence intensity, such as clones 5.2C2 and 5G10 (**Figure 1C**). Western blot analysis using an anti-EGFP antibody was performed on protein extracts from these clones and compared to CHO cells transfected with EGFP alone. A major band corresponding to the CD22c-EGFP molecular weight was highlighted for the 5G10 and 5.2C2 clones. However, an additional faint band (around 75,000 Da) and a strong band at lower molecular weight corresponding to EGFP alone were detected for the clone 5.2C2 (**Figure 1D**). The clone 5G10 that displayed the expected profile in Western blot was therefore selected for hybridoma supernatant screening.

Immunization of Mice Against Canine CD22

Three mice were immunized with the canine CD22c-β2m fusion protein. The serums of immunized mice were assessed for anti-CD22c antibody production by flow cytometry analysis using the CD22c-EGFP transfected CHO cell clone 5G10. The pre-immune serum at day 0, which was used as negative control, displayed a strong background on transfected CHO cells. However, at day 29 after the second antigen injection, significant labeling was obtained, attesting to the production of anti-CD22c by the mice immunized against the CD22c-β2m immunogen. It also validated the CD22c-EGFP transfected CHO cell clone 5G10 for the screening of hybridoma supernatant (**Figure 2A**). We further analyzed the serum of immunized mice using the canine diffuse large B-cell lymphoma (DLBCL) cell line CLBL-1. Because of the lack of available anti-CD22c antibody, we were not able to determine the expression level of this antigen on the canine DLBCL cells. Here we show that, as for the 5G10 clone, we detected a specific labeling of the CLBL-1 cell line at day 29 compared with the pre-immune serum (day 0) attesting, as expected, that CD22 is expressed by canine B-cell lymphoma and that the immunization with soluble CD22c-β2m is efficient at generating the production of antibodies able to bind the CD22c on its native form. Interestingly, the dilutions giving half of the maximum binding on the CD22c-EGFP transfected CHO cells and on CLBL-1 cells were very close (1:1,050 and 1:976, respectively, with the best immunized mouse), attesting that the anti-CD22 antibodies from the serum of immunized mouse recognized CD22c with the same affinity on both cell lines (**Figure 2A**). Even if the signal was specific, it was lower on CLBL-1 cells as compared to the 5G10 CHO clone. This is consistent with the low expression level of membrane CD22 described in human DLBCL (27). At the end of immunization process, the most potent immunized mouse was sacrificed, the spleen was harvested, and the splenocytes were fused with the mouse myeloma cell line SP2/0 in order to obtain hybridomas.

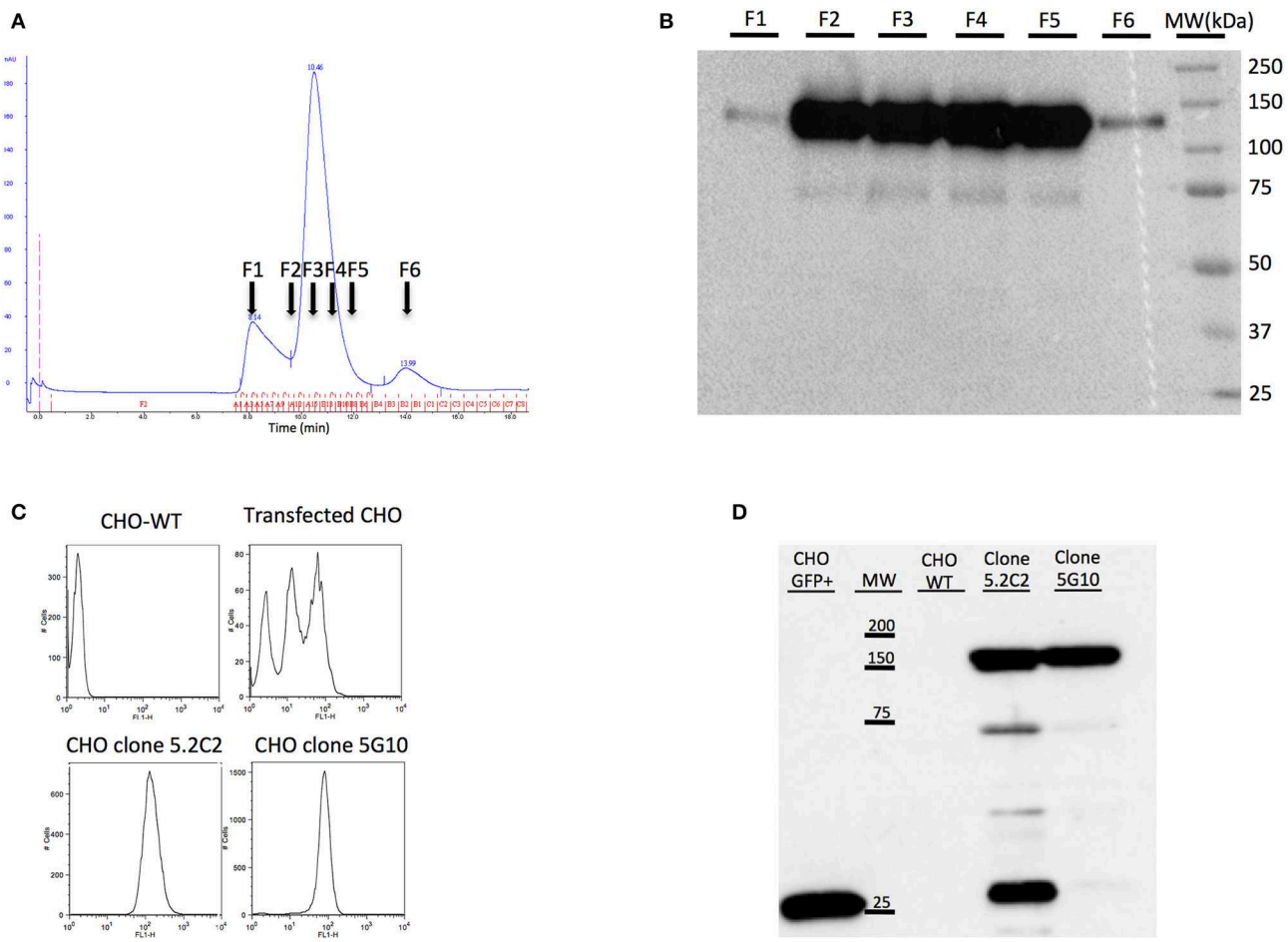

FIGURE 1 | Production of soluble CD22c for mice immunization and production of CD22c expressing CHO cell line for hybridoma screening. **(A)** The recombinant canine CD22c-Beta2M protein produced by the transfected CHO cell clone showing the highest expression was purified by affinity chromatography using the 6H4 MAb followed by a Superdex 200 column. The results of size-exclusion chromatography show three distinct peaks. **(B)** Further analysis of fractions F1–F6 by Western blot showed high expression of CD22c-Beta2M in the major peak. **(C)** At the same time, CHO cells were transfected with a full-length CD22c merged to GFP (CD22c-GFP) for hybridoma screening using cytofluorometry. The two upper panels show FACS analysis of WT CHO (left) and polyclonal transfected CHO cells (right). The transfected CHO cells were further subcloned to select high-expressing clones: **CHO** 5C.2 and **CHO** 5G10 (bottom panels). **(D)** Western blot analysis allowed us to select clone **CHO** 5G10, which expresses a unique protein at the size corresponding to CD22cGFP for hybridoma screening.

Screening of Hybridoma Supernatant

Ten to 15 days after the fusion of splenocytes, 500 hybridomas were screened to evaluate their efficiency in producing the anti-canine CD22 antibodies. We used the WT CHO cell line as a negative control and the CD22c-EGFP+ 5G10 CHO clone and the CLBL-1 cell line as positive controls. Seven hybridomas out of the 500 tested allowed strong labeling of the CD22c-EGFP+ 5G10 CHO clone and no staining on WT CHO cells, as expected for antibodies specific for canine CD22. The ability of the seven hybridoma supernatants to bind the CLBL-1 cell line confirmed this specificity for CD22c (**Figure 2B**). We confirmed the low expression level of CD22c on CLBL-1 cells compared to CD22c-EGFP+ 5G10 CHO clone observed with the plasma of immunized mice. Positive hybridomas were then cloned by limiting dilution. Once these clones were established, a pilot production of supernatant was performed to obtain a sufficient amount of MAb by purification with protein G to define their isotypes and affinity for CD22c by flow cytometry analysis. Six of the seven antibodies (5A3, 6B7, 1E3, 10C6, 5C2, 5F8) displayed an $IgG_{1,\kappa}$ isotype and the last, 2D1 MAb, is an $IgG_{2b,\kappa}$. The dissociation constants (Kd) of the seven MAbs were between 3.88 1E-8 M and 1.21 1E-10 M (**Table 1**). These affinities are satisfactory for nuclear medicine applications targeting tumor antigen for imaging and therapy.

Epitope Mapping

Apart from its use for mice immunization, the canine CD22-β2m fusion protein was also useful for characterizing the anti-canine CD22 antibodies. This construct was used in a sandwich ELISA assay to define an epitope mapping of the sites recognized on CD22 by the seven antibodies (**Figure 3**). For this purpose, each MAb was biotinylated and separately incubated with an

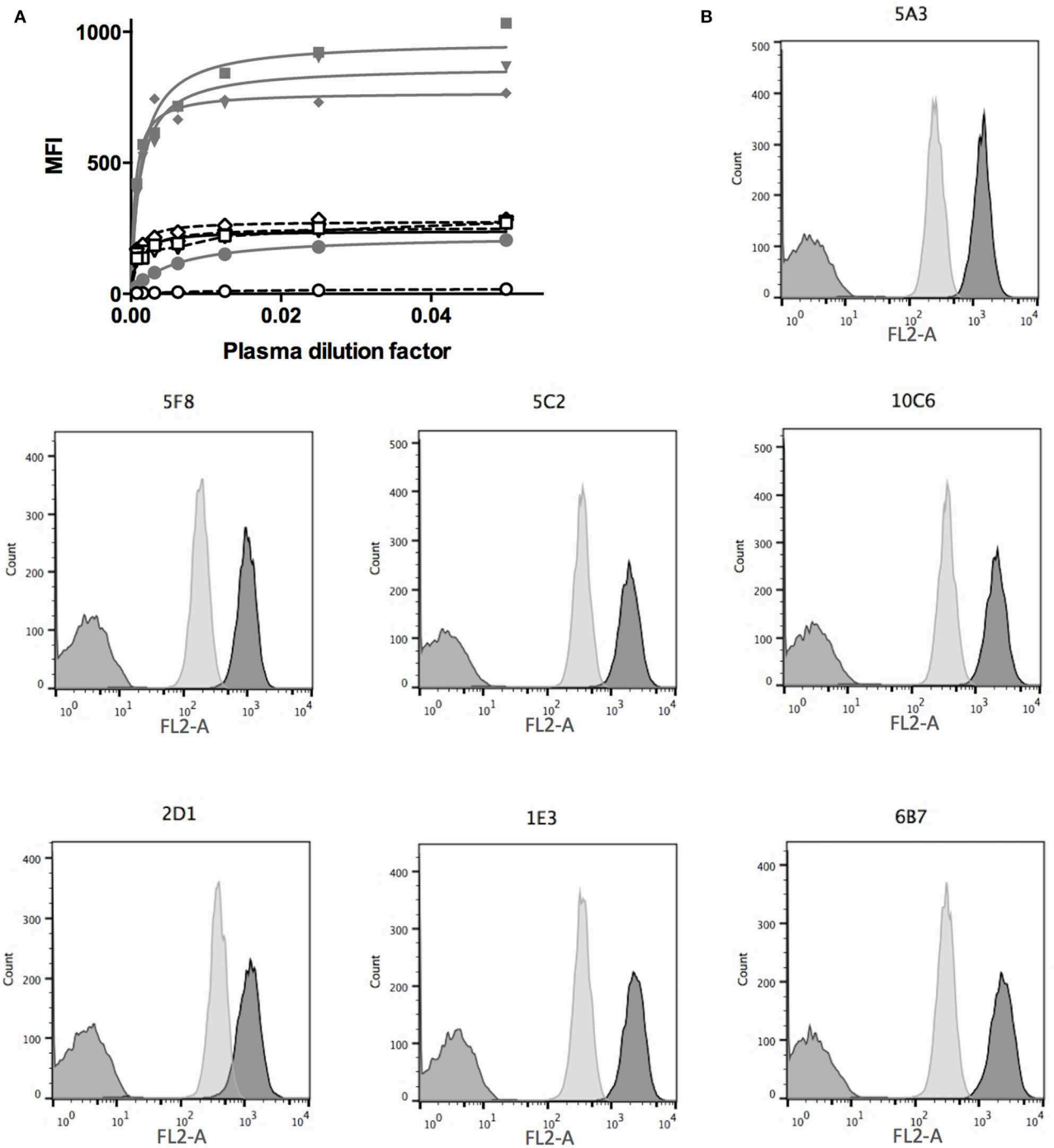

FIGURE 2 | Mice immunization and hybridoma screening. **(A)** Mice were first injected with CD22c-Beta2M in complete Freund adjuvant at day 0 and 15 days later with the same amount of CD22c-Beta2M in incomplete Freund adjuvant. At day 29, the plasma of mice were harvested and used at serial dilutions in a FACS assay to label CD22-EGFP CHO clone 5G10 (gray lines, closed symbols) and the canine DLBCL cell-line CLBL-1 (dashed lines, open symbols) and compared to the signal obtained at the same dilution factors of the plasma before antigen injection (close and open circles). A clear signal increase at day 29 attests for immunization of mice. The lower signal obtained on CLBL-1 is consistent with a low CD22 expression on canine DLBCL. **(B)** The hybridomas obtained after fusion of splenocytes of an immunized mouse were screened by FACS analysis using CD22-EGFP CHO cells (dark gray) as a positive control, WT CHO cells as a negative control (medium gray). The specificity for the CD22 antigen was confirmed on the CLBL-1 cell line (light gray). Here are shown the results obtained for the seven hybridomas specific for CD22c, isolated from the fusion of the splenocytes of one mouse.

TABLE 1 | Dissociation constants and isotypes of the seven MAbs specific for canine CD22.

	2D1	5A3	6B7	1E3	10C6	5C2	5F8
Kd (M)	8.47E-10	3.88E-08	2.23E-10	9.80E-10	1.21E-10	3.08E-10	5.61E-09
Std. error	*9.92E-11*	*9.90E-09*	*6.01E-11*	*1.35E-10*	*1.78E-11*	*3.61E-11*	*5.07E-10*
Isotype	IgG2b,k	IgG1,k	IgG1,k	IgG1,k	IgG1,k	IgG1,k	IgG1,k

Italic values indicates standard error.

excess of the seven anti-CD22c MAbs and a control isotype. Streptavidin HRP was used to detect antibody binding to CD22 in this competition assay regarding CD22 binding.

At least three different recognition patterns of CD22-β2m antibodies could be distinguished. The binding of the biotinylated 5A3 antibody on CD22-β2m was only inhibited by an excess of cold 5A3 MAb, indicating that it recognizes an epitope distinguishable from those recognized by the other MAbs on the CD22c molecule. The 10C6 and 5C2 antibodies recognized a single epitope, as indicated by their mutual binding inhibition. The antibodies 1E3, 5F8, and 6B7 also displayed a common pattern of cross inhibition for the binding on CD22c, indicating their specificity for a single epitope or overlapping epitopes. The 2D1 antibody displayed a more complex competition pattern: its binding was partially inhibited by 1E3, 5F8, and 6B7 antibodies, but 2D1 failed to impair 1E3, 5F8, and 6B7 binding to their own epitope. This could be consistent with a steric hindrance or in a non-mutually exclusive way with different conformational shapes of CD22 recognized by 2D1 and the 1E3, 5F8, and 6B7 group.

IHC on Canine Lymph Node and Diffuse Large B-Cell Lymphomas

First we tested the seven antibodies in immunohistochemistry (IHC) for the detection of CD22c on formalin-fixed paraffin-embedded samples of normal lymph node. Whereas, all these antibodies were efficient at labeling CD22c in its native form on the CLBL-1 cell line by flow cytometry analysis (**Figure 2B**), they displayed strong differences in their ability to stain the CD22c antigen on histological sections, probably because of antigen denaturation after exposure to organic solvents during the process of histological preparation (**Figure 4A**). The clones 2D1 and 5C2 did not yield any specific staining of canine lymphocytes in the B-cell areas of normal lymph node and were therefore considered improper for immunohistochemistry. The clones 5A3 and 6B7 labeled sparse B cells in canine normal lymph nodes, whereas the clones 1E3, 5F8, and 10C6 were the most sensitive for IHC applications, because they labeled the membrane of large B cells in the germinal centers (**Figure 4A**), as well as the membrane of plasma cells (not shown). The 10C6 antibody clearly gave the best staining on healthy lymph node. Interestingly, even though 10C6 and 5C2 shared the same epitope on canine CD22 (**Figure 3B**), the 5C2 MAb was improper for IHC application, contrary to the former. This was also true for the 1E3 and 5F8 clones, which share a common epitope with the 6B7 MAb: the two former gave a satisfactory and comparable signal on CD22c in normal lymph node, while the 6B7 clone was inefficient in labeling this antigen on tissue sections. It is noteworthy that the distribution pattern of CD22-positive cells observed in the normal canine lymph node indicated that CD22 is not a pan-B-cell marker in dogs and is expressed by plasma cells.

Since these MAbs are the first anti-canine CD22c isolated to our knowledge, the CD22c expression status of canine DLBCLs was unknown at the beginning of the study. A canine DLBCL sample was immunolabeled with the seven anti-CD22c MAbs, showing that the 2D1 and 5C2 clones failed to react with lymphoma cells; the 5A3 and 6B7 clones gave a positive signal at the membrane of most neoplastic large B cells; and the 1E3, 5F8, and 10C6 MAbs positively labeled all of the neoplastic B cells, with the best IHC results obtained with the 10C6 clone (**Figure 4A**). From this IHC assay, we retained the 10C6 MAb for further development, for diagnosis in IHC, and for nuclear medicine applications, i.e., SPECT imaging and radioimmunotherapy.

We then proceeded to a first evaluation of CD22 expression on 30 canine DLBCLs by IHC, using the 10C6 MAb (**Figure 4B**). Among the 30 cases analyzed, 17 were strongly labeled with 10C6, 11 displayed intermediate CD22c membrane expression, and only two cases were negative for CD22 expression on DLBCL cells. There was no significant correlation between CD22 expression and the germinal-center or non-germinal-center phenotype of these cases. The high frequency of membrane CD22 expression by canine DLBCLs validates CD22 as a good antigen for targeted therapy of canine DLBCL, in accordance with what has been described in human DLBCL.

Internalization Properties of Anti-CD22c MAbs

A characteristic of antibodies directed against human CD22 is their ability to internalize once bound to the antigen. This is of particular interest in the context of phenotypic imaging or radioimmunotherapy, because radiolabeled antibodies with a residualizing property would make it possible to sequester radioactivity within cell compartments after internalization, allowing higher activity deposition than a simpler membrane binding of the radiolabeled antibody (28). We thus determined the internalization ability of our CD22c-specific MAbs on the canine DLBCL CLBL-1 cell line, which naturally expresses CD22. Usually, CD22 internalization is evaluated on cells preloaded with saturating amounts of anti-CD22 MAb at 4°C to avoid membrane turnover. After washing, cells are placed at 37°C and internalization is evaluated at different time points. However, in nuclear medicine applications, DLBCL cells targeted

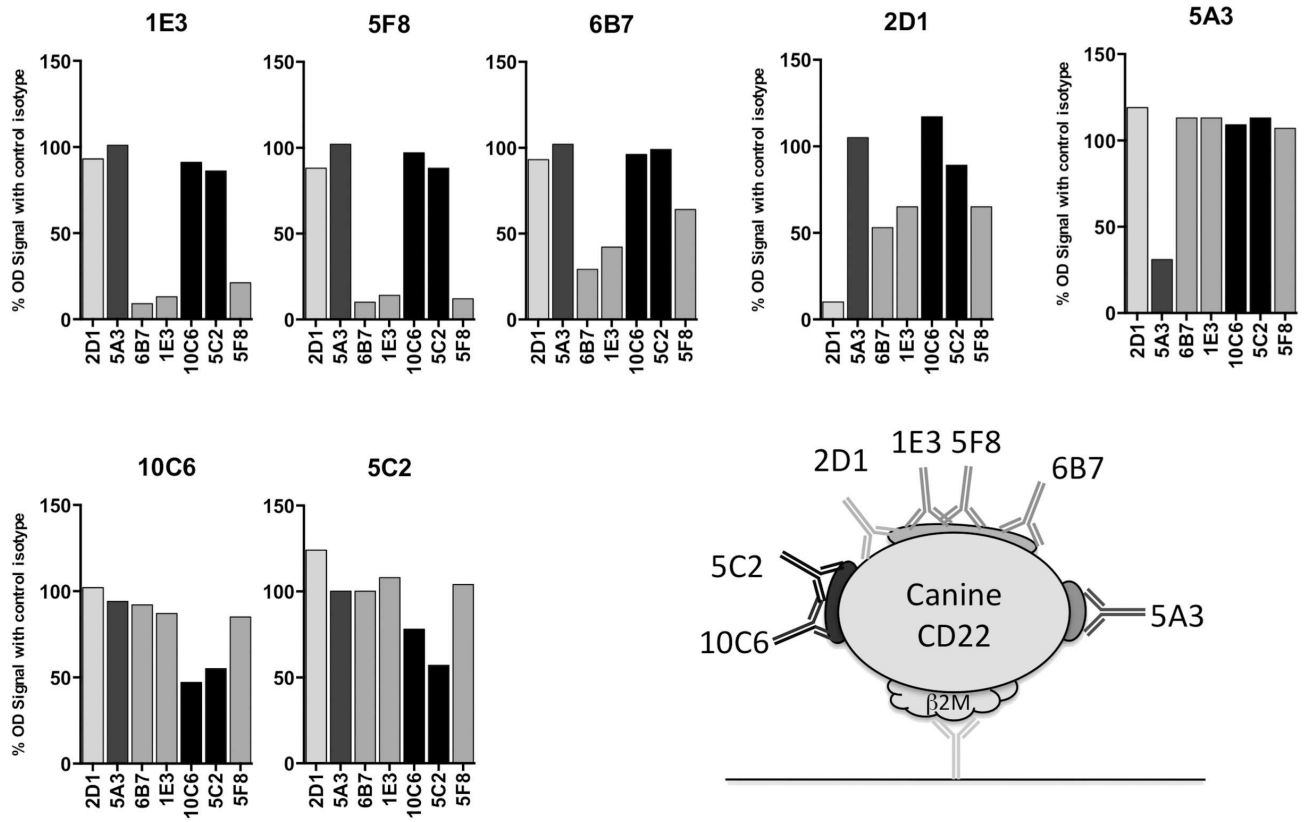

FIGURE 3 | Epitope mapping of anti-CD22c antibodies. The seven MAbs selected for their specificity against the CD22c antigen were biotinylated and used in an ELISA assay using the CD22c-Beta2M for coating and the Beta2M antibody 6H4 for protein detection. Each biotinylated antibody was mixed with a ten-fold excess of each anti-CD22c clone, in order to identify the competing antibodies for the binding on CD22c. The results are expressed as the percentage of binding in comparison to the results obtained with a control isotype. The binding inhibition of each antibody by itself reflects the maximum inhibition of the test and constitutes a positive control of the competition test. A schematic representation of CD22c and the different epitopes recognized by the anti-CD22c MAbs is shown.

by anti-CD22 antibodies are exposed to variable circulating antibody concentrations in the course of treatment, due to the mobilization of antibodies on healthy B cells and DLBCL cells, and due to antibody catabolism that progressively decreases the concentration of MAb in blood. We therefore wondered what the antibody binding to membrane CD22 antigen could be at various concentrations at 37°C compared to 4°C. Four MAb concentrations corresponding to 10-, 5-, 1-, and 0.1-fold their Kd value were used to compare the binding of the different anti-CD22 antibodies at comparable levels of antigen saturation. At different time points after the beginning of the incubation, the cells were placed at 4°C, washed with ice-cold PBS and labeled with an anti-mouse antibody to measure the mean fluorescence at each time point using flow cytometry. The membrane expression level of each antibody at 10- and 1-fold its Kd is shown in **Figure 5A**. A clear internalization of all MAbs is observed at 37°C with the antibody concentration corresponding to 10-fold the antibody Kd (saturation). However, a lower concentration corresponding to the Kd (half-saturation) results in higher membrane expression at 37°C than at 4°C of MAbs 1E3, 6B7, and 5A3, indicates that some antibodies may in some instances stabilize CD22 at the cell membrane, at least for the duration of the assay (6 h). The relative expression level at 37 vs. 4°C at the four concentrations investigated in this experiment is summarized in **Figure 5B**. Only the MAbs 5C2, 10C6, and 2D1 were able to internalize at low concentration (0.1-fold the MAb Kd), indicating that internalization not only depends on the antibody binding on its target, but also on the density of bound antibody at the cell surface. Indeed, the internalizations of the different antibodies were variously affected by saturation level, as shown in **Figure 5C** where the percentage of expression at 37°C relative to 4°C is plotted against the percentage of saturation at 4°C observed at each concentration used in the test. This graph emphasizes that a threshold of antigen occupation needs to be reached for internalization to take place. This threshold was low for 5C2, 10C6, and 2D1 because they were internalized at the lowest MAb concentrations used in the test. Conversely, internalization was observed for MAbs 1E3, 6B7, and 5F8 when the surface density reached 45–65% saturation and even more for the 5A3 MAb. It is puzzling that these strong, intermediate, and low internalizing capabilities segregate with the epitopes recognized, respectively, by 10C6 and 5C2; 6B7, 1E3, and 5F8; and 5A3 MAbs. One could hypothesize that the

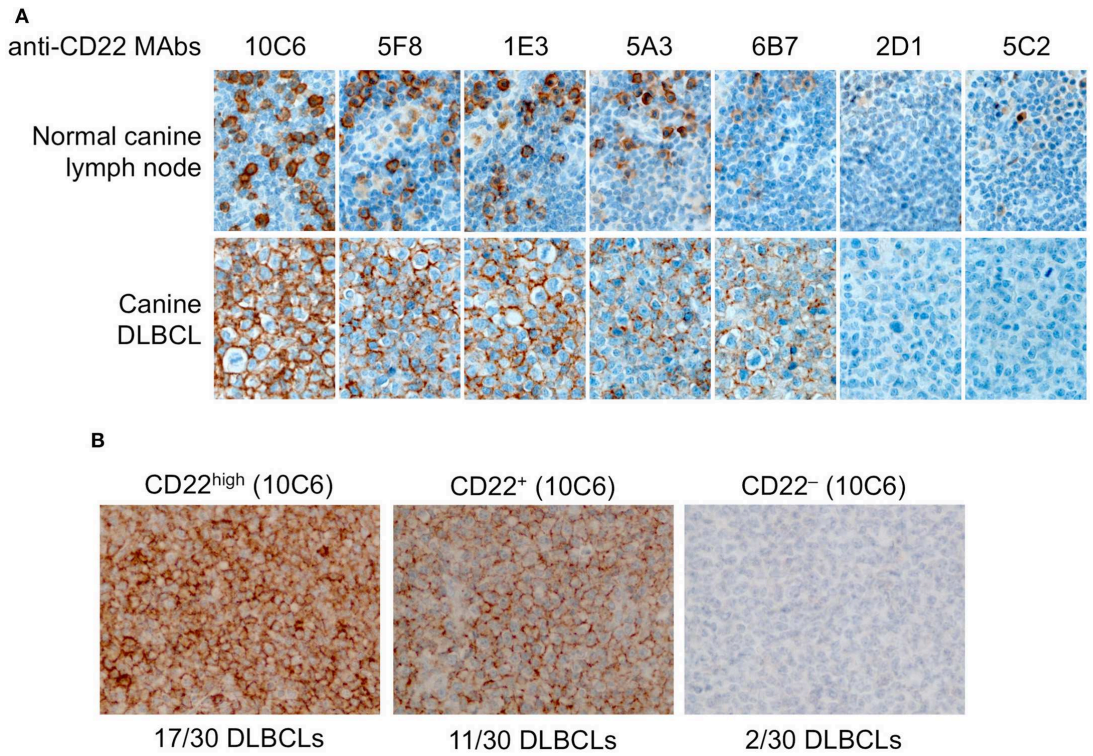

FIGURE 4 | Immunohistochemistry to canine CD22 in a normal lymph node and in 30 canine diffuse large B-cell lymphomas. **(A)** In the normal canine lymph node (upper row), the 10C6, 5F8, and 1E3 MAbs labeled large B cells in germinal centers. CD22 was expressed at the membrane of most but not all B cells. The 5A3 and 6B7 MAbs had poor sensitivity and the 2D1 and 5C2 MAbs yielded no specific signal and were considered improper for IHC. In a CD22-positive canine DLBCL (lower row), the best IHC signal was obtained with the 10C6 clone. **(B)** In a series of 30 canine DLBCLs, 17 cases were strongly CD22-positive, 11 were moderately CD22-positive, and two were CD22-negative.

topology of MAb binding to CD22 affects the efficiency of the internalization process.

Finally, we evaluated the internalization property on human lymphoma cell line of the anti-Human CD22 hLL-2 MAb, already used in phase I/II clinical trials for DLBCL treatment in humans, to obtain an element of comparison with the internalization property of the anti-CD22c MAbs. The internalization profile of hLL-2 MAb at different concentrations was similar to the profile of 6B7 or 1E3 MAbs. As for the 6B7 and 1E3 MAbs, membrane stabilization of CD22 was observed for concentrations corresponding to 0.1- and 1-fold the dissociation constant of the antibody. This indicates that our antibodies against CD22c have similar properties as compared to the anti-CD22h hLL-2, and thus may be suitable to perform preclinical trials in dogs with spontaneous DLBCL for new imaging and therapeutic protocol testing.

Biodistribution of Anti-CD22c in Mice Xenografted With CLBL-1

Because of the different internalizing behaviors of the anti-cCD22 antibodies, we wondered which one would be the most appropriate MAb for imaging and radioimmunotherapy. We chose to compare 10C6, 5C2, 6B7, and 1E3, which displayed distinct internalization patterns and high affinities, in a biodistribution assay. The 2D1 and 5A3 MAbs were excluded from this assay because of the IgG2b isotype of 2D1 and the low affinity of 5A3. Eight-week-old NMRI-nu mice were subcutaneously engrafted in the flank with five million CLBL-1 cells. Fourteen days after engraftment, MAbs 10C6, 5C2, 6B7, and 1E3 radiolabeled with ^{125}I were injected in the tail vein. Mice were sacrificed at 1, 4, and 16 h after injection and the organs were weighed and counted in a gamma counter. The results of biodistribution are shown in **Figure 6**. No significant differences of accumulated activity in tumors and healthy organs could be objectified between the four antibodies. The cumulated activity in the tumor 16 h after injection reached around 4.5% IA/g with the four antibodies tested. Although the activity to the tumor was quite low, the increase over time of the cumulated activity confirmed the specificity of canine CD22 targeting in this mouse model. For imaging and radioimmunotherapy applications, high-affinity antibodies were favored; 5C2 and 10C6 MAbs were the anti-CD22c clones with the highest affinities in our antibody panel, but 10C6 proved to be usable for diagnosis of spontaneous canine DLBCL, contrary to 5C2, which was inefficient for IHC (**Figure 4A**). We therefore pursued our investigations with the 10C6 antibody to validate its value for further applications in veterinary medicine.

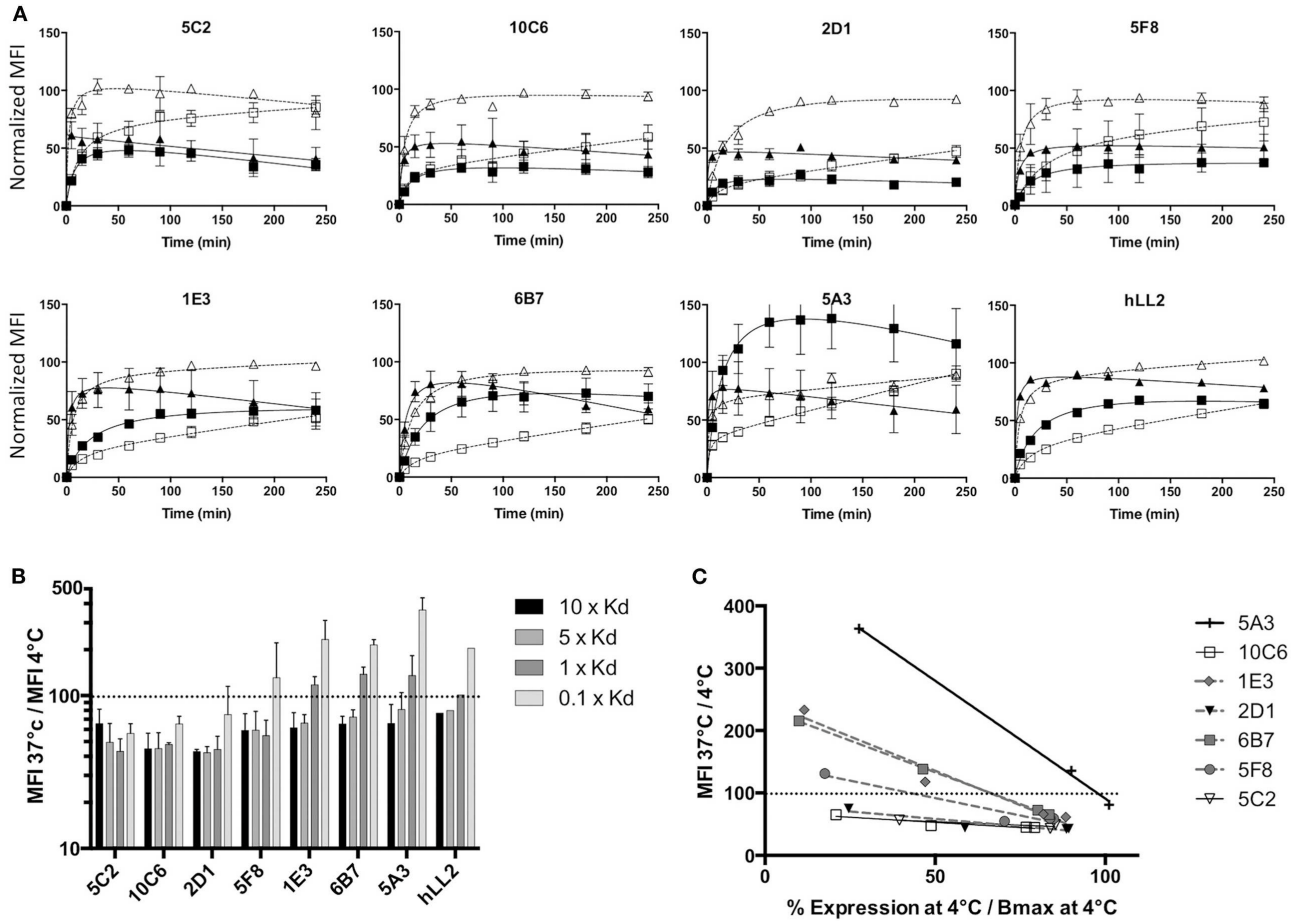

FIGURE 5 | Internalization of anti-CD22c MAbs. The CLBL-1 cell line was incubated with each of the seven anti-CD22c MAbs at concentrations corresponding to 10-, 5-, 1-, and 0.1-fold their own dissociation constant at 4 and 37°C to evaluate MAb internalization at comparable levels of CLBL-1 CD22 saturation. **(A)** Kinetic follow-up of membrane CD22c expression at 4 and 37°C: at each kinetic time point, the cells were placed at 4°C, fixed with paraformaldehyde, labeled with an antimouse Ig Mab, and the MFI was measured by FACS. Open triangle, dashed line: 4°C, 10 × Kd; close triangle, solid line: 37°C, 10 × Kd; open square, dashed line: 4°C, 1 × Kd; closed square, solid line: 37°C, 1 × Kd. For comparison, the antihuman hLL2 antibody internalization was evaluated in the same conditions on the human Burkitt lymphoma cell line Daudi. Here are shown the mean results ± standard deviation of three independent assays. **(B)** Ratio of membrane CD22c expression at 37 vs. 4°C at 240 min for each concentration of anti-CD22c MAbs: the dashed line in this histogram corresponds to equal CD22 expression at 4 and 37°C. Whereas, clear internalization is observed for all antibodies at saturating concentrations of 10 × Kd and 5 × Kd (MFI 37°C/ MFI4°C < 100), non-saturating amounts of antibody (1 × Kd and 0.1 × Kd) induced an over-expression of CD22 at the cell membrane when incubated with 1E3, 6B7, and 5A3 MAbs, and 5F8 to a lesser extent. **(C)** Ratio of CD22c expression at 37°C vs. 4°C as a function of the level of saturation of CD22c at 4°C for each MAb concentration: the dashed line corresponds to an equivalent CD22c expression at 37 and 4°C. Three groups of MAbs can be distinguished: highly internalizing antibodies 5C2, 10C6, and 2D1; intermediary internalizing antibodies 5F8, 1E3, and 6B7; and weakly internalizing antibody 5A3.

PET Imaging in Mice Xenografted With CLBL-1

Our primary goal, isolating anti-CD22c MAbs, was to undertake imaging and radioimmunotherapy assays in dogs with spontaneous DLBCL. We wished to perform SPECT-CT with indium-111 radiolabeled antibody and radioimmunotherapy with yttrium-90. This requires the coupling of a chelating agent, enabling radiolabeling with these isotopes. We sought to ensure that the modification of the 10C6 antibody by the chelating agent DOTA-NCS did not affect its ability to bind to the CD22 antigen. The 10C6 MAb was coupled to DOTA using p-SCN-Bn-DOTA precursors able to covalently link to the lysine side chain on the antibody. The mean number of DOTA chelators on the antibody was estimated by determining the radiolabeling yield of the 10C6 MAb radiolabeled with increasing amounts of copper-64 using thin-layer chromatography. A mean number of 2.78 DOTA per antibody was calculated, which is adapted for nuclear medicine applications. ^{64}Cu-10C6 was then used in PET-CT imaging of nude mice 14 days after engraftment with the CLBL-1 cell line. PET-CT images were acquired 16 h after injection of 10 MBq of ^{64}Cu-10C6 (**Figure 6B**). Mice were then sacrificed and the biodistribution of ^{64}Cu-10C6 was evaluated on tumor and healthy organs (**Figure 6A**). PET imaging provides clear visualization of the subcutaneous CLBL-1 xenograft in the right flank. The intense staining of the liver and the lungs with ^{64}Cu-10C6 MAb is based on the large volume of these organs

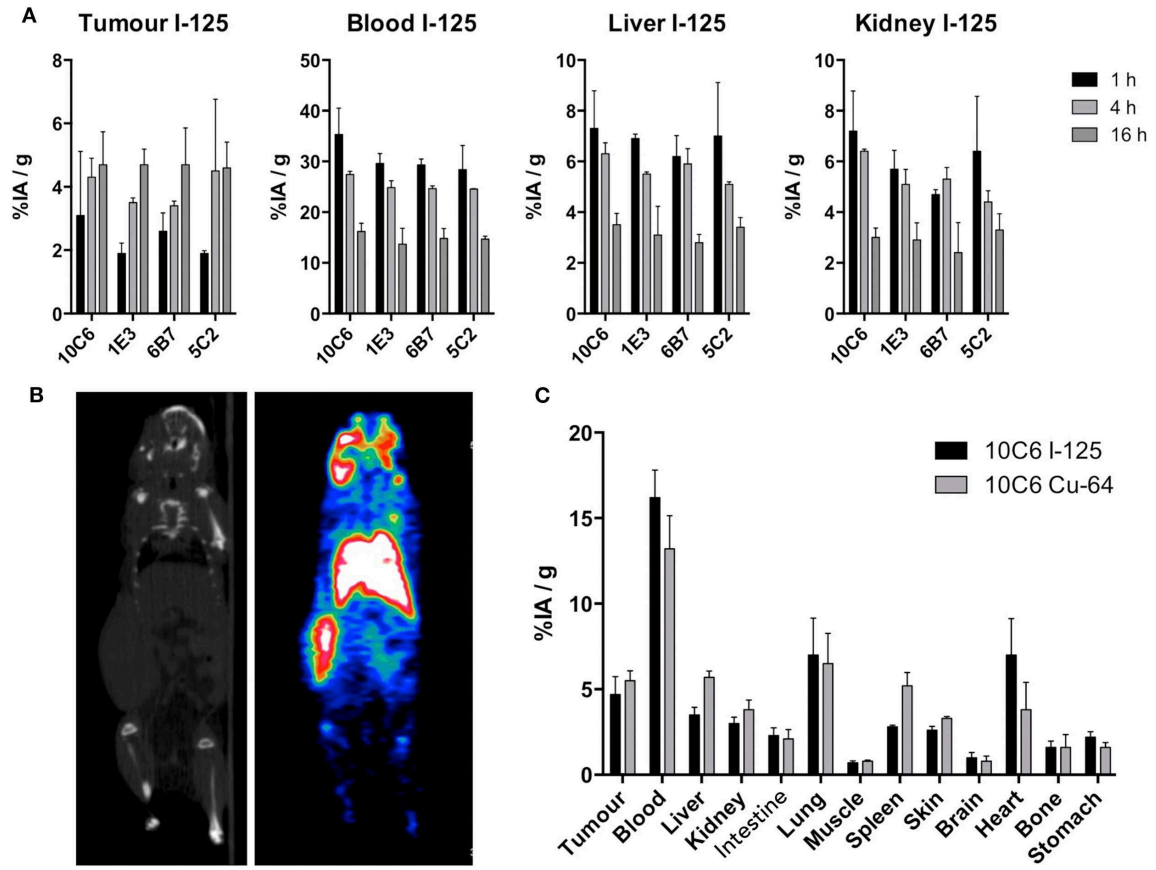

FIGURE 6 | Biodistribution of anti-CD22 antibodies and PET imaging of CLBL-1 xenografts in nude mice. **(A)** Biodistribution to tumors, blood, liver, and kidney 1, 4, and 16 h after injection of 6.10^{-6} g of 10C6, 1E3, 5C2, and 6B7 radiolabeled with ^{125}I. Here are shown the mean results ± standard deviation obtained on three mice. **(B)** PET-CT imaging 16 h after injection of ^{64}Cu-10C6. The CLBL-1 cell line was engrafted in the left flank of nude mice. Left panel: CT scan of the imaged mouse. Right panel: PET imaging showing the radiolabeled tumor in the left flank of the nude mouse. **(C)** Comparison between the biodistribution of 10C6 radiolabeled with ^{125}I and ^{64}Cu. Immediately after imaging at 16 h post-injection of the ^{64}Cu-radiolabeled antibody, the mouse was sacrificed and the biodistribution in the different organs of interest was evaluated and compared to the biodistribution of ^{125}I-10C6 at the same time point.

and their high blood contents. Although copper catabolism implies liver and biliary excretion, we only detected a slight increase in the cumulated activity of ^{64}Cu-10C6 MAb compared to ^{125}I-10C6 to the liver (5.46 ± 0.35 vs. 3.55 ± 0.44% IA/g, respectively). This is consistent with the higher activity to the blood for ^{125}I-10C6 compared to ^{64}Cu-10C6. After cellular catabolism of the antibody, iodine is released as an iodo-tyrosine in the interstitial space. In contrast, chelated metallic isotopes display residualizing properties leading to their sequestration within the cell compartment. This residualizing property may explain in part the higher activity measured to the spleen with ^{64}Cu-10C6 as compared to ^{125}I-10C6 (5.24 ± 0.35 vs. 2.83 ± 0.1%IA/g for ^{125}I-10C6), and the cumulated activity uptake to in the tumor that was also slightly higher with ^{64}Cu-10C6 MAb as compared to ^{125}I-10C6 (5.45 ± 0.57 vs. 4.70 ± 1.04%IA/g, respectively). These results indicate that 10C6 can be efficiently radiolabeled with satisfactory stability, either by iodination or with a metallic isotope using the 10C6-DOTA MAb. The capacity of 10C6 antibody to specifically label canine DLBCL *in vivo* in mouse xenograft models validates its usefulness for future clinical assays in dogs with spontaneous DLBCL for diagnosis, imaging, and radioimmunotherapy.

SPECT-CT Imaging With ^{111}In-10C6 MAb on Experimental Dogs

Before proceeding to imaging on sick dogs, we wished to evaluate the biodistribution of the ^{111}In-10C6 MAb on experimental dogs. The protocol applied to experimental dogs was the same as that planned for dogs with spontaneous DLBCL. The Mab content of endotoxin was tested and was within the range recommended for humans. Given that we used murine antibodies, the dogs were premedicated with methylprednisolone and promethazine in order to avoid any anaphylactic shock at the time of injection. Fourteen dogs were imaged with this protocol without adverse effect, thus validating the safety of this radiolabeled Mab. The objectives of repeating images on several dogs at different time points were to obtain a set of images allowing the implementation

of a population pharmacokinetics and to estimate the doses at healthy organs using quantitative imaging. We also took advantage of this possibility to take images on experimental dogs to test the consequences on the biodistribution and pharmacokinetics of cold antibody co-injection with ^{111}In-10C6 MAb since no specific study has addressed this issue in humans (manuscript in preparation). More generally, this set of images was useful in illustrating the particularity of Mab distribution in dogs compared to humans to facilitate the interpretation of images at diagnosis on sick dogs. Images of the SPECT signal detected on an experimental dog are shown in **Figure 7A**. The best contrast images were obtained at 2 days after injection. The more salient differences with humans were a stronger signal on the dog's nose and liver. Although we cannot exclude a specific binding of the antibody on these sites, this enhanced uptake in dogs compared to the corresponding area in human anatomy may also result from a higher vascularization in dogs. This specific feature in dogs will most particularly lead to higher dose deposition on the liver. However, preliminary evaluation of the dose deposition on the liver of dogs indicates that it remains under the toxic threshold for injected activity within the range of the therapeutic dose evaluated in humans (manuscript in preparation). We therefore proceed to the imaging of dogs with spontaneous DLBCL.

SPECT-CT Imaging With ^{111}In-10C6 MAb on Dogs With Spontaneous DLBCL

Three dogs diagnosed at a veterinary hospital for DLBCL were enrolled for SPECT-CT imaging. ^{111}In-10C6 MAb was injected according to the protocol applied for experimental dogs with no adverse effect. In each of the three cases, we clearly observed tumor sites already detected at initial diagnose and an additional tumor that was undetectable with classical diagnostic methods.

Figure 7B provides an example of a SPECT-CT image performed on a dog with spontaneous DLBCL. The enrolled dog was a 4-year-old female Flat-coated Retriever with stage V multicentric lymphoma. The physical examination revealed apathy, weight loss (weight at diagnosis, 25 kg), dysorexia, hyperthermia, generalized lymphadenopathy (peripheral, thoracic, and abdominal), and abdominal ultrasound showed splenic infiltration. A myelogram on red marrow demonstrated the presence of a contingent of atypical cells, medium to large in size, with a high nucleocytoplasmic ratio. Their morphology was similar to that of cells invading lymph nodes and that of circulating atypical lymphoid cells. The 10C6 Mab was used for immunohistochemistry (IHC) performed on a biopsy of the left prescapular lymph node. The lymph node is invaded by cells with strong membrane labeling. Based on this IHC and histologic feature, it was possible to establish a diagnosis of DLBCL with CD22 overexpression as shown. SPECT-CT acquisition was performed 45 h after radiopharmaceutical injection (0.75 mg ^{111}In-10C6; specific activity 113.9 MBq.mg^{-1}). Radiopharmaceutical injection was well-tolerated. Lymphadenopathy was demonstrated on SPECT-CT images showing tumoral infiltration of the spleen and numerous lymph nodes, as shown for retropharyngeal lymph nodes whose status had remained undetermined until then (**Figure 7B**). In accordance with the results of the myelogram, SPECT-CT confirmed the medullary invasion that was then qualified as severe.

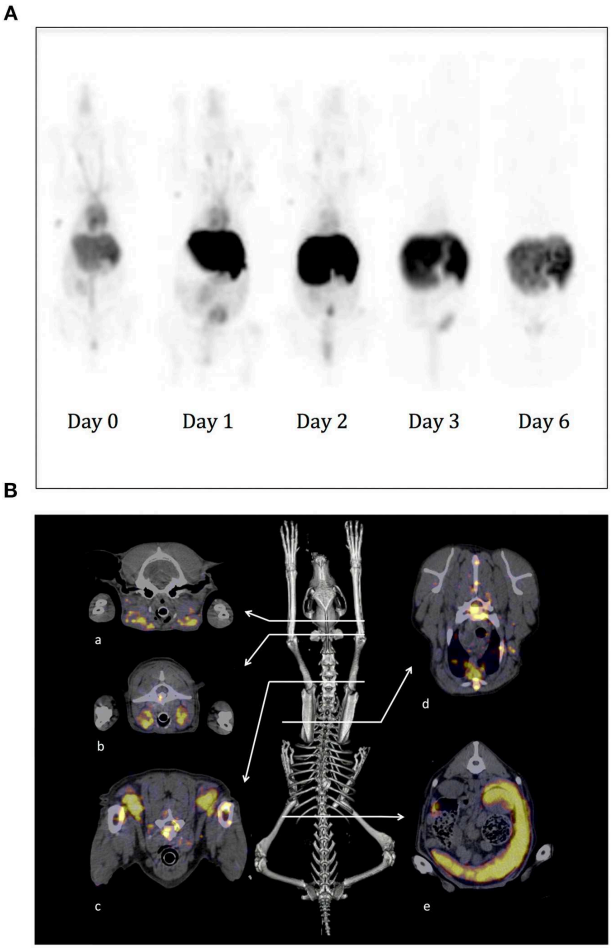

FIGURE 7 | SPECT-CT imaging using ^{111}In-10C6 MAb on experimental and sick dogs. **(A)** A healthy beagle weighing 11.5 kg was injected under anesthesia with ^{111}In-10C6 at a total activity of 3.7 MBq/Kg and a co-injection of 1.5 mg/kg of cold 10C6. Images were acquired 1 h after injection and then at day 1, 2, 3, and 6. Here are shown a planar projection of the whole-body SPECT images. The nose of the dog and the liver, which are highly vascularized in dogs, appear with a strong contrast. The vasculature is visible up to day 2. The signal in the abdomen corresponds to the elimination of radioactivity in the feces after clearance of ^{111}In-10C6 by the hepatobiliary system. In the first three images, 1 ml of blood taken at the beginning of acquisition positioned close to the anterior left leg was imaged in order to obtain a reference of blood activity. **(B)** SPECT-CT images of a dog with spontaneous DLBCL diagnosed at the veterinary hospital. The dog was a 4-year-old female Flat-coated Retriever with stage V multicentric lymphoma. SPECT-CT acquisition was performed 45 h after radiopharmaceutical injection (0.75 mg ^{111}In-10C6; specific activity 113.9 MBq.mg^{-1}; without co-injection of cold 10C6). The skeleton is shown as the anatomic landmark. Here are shown the fusion SPECT and CT images where tumor sites could be easily visualized. a: Mandibular lymph nodes; b: retropharyngeal lymph nodes; c: prescapular lymph nodes; d: body of a thoracic vertebra, substernal lymph node; e: spleen.

DISCUSSION

Here we describe a simple method to generate monoclonal antibodies against all types of membrane proteins with a single transmembrane domain. The possibility of expressing these antigens after stable transfection in CHO cells as a soluble form merged to a tag (β2m herein) enables to easily identify productive CHO clones using an anti-tag antibody in a one step ELISA test. This anti-tag antibody coupled to an affinity chromatography column also enables, after a one-step purification process, to purify sufficient amounts of recombinant protein to immunize mice. This soluble antigen is also useful as a reagent in binding assays to perform immunoreactivity quality controls of the MAbs once radiolabeled. Because we wanted to use this antigen for nuclear medicine applications, we chose to perform hybridoma supernatant screening by flow cytometry analysis in order to discard any antibodies that would recognize epitopes on the unfold antigen in ELISA test. Furthermore, since soluble CD22c was merged to the human β2m, some hybridomas generated against β2m will not recognize CD22-transfected CHO cells. This makes it possible to rapidly perform a first screening of hybridomas producing antibodies recognizing CD22-transfected CHO cells, which obviates the need for a preliminary ELISA with human β2m used as a negative control. This screening method enabled us to screen around 500 hybridoma supernatants and resulted in the isolation of seven monoclonal antibodies reactive against CD22c in its native conformation expressed by the canine DLBCL cell line CLBL-1. The isolation of numerous MAbs with the same antigen specificity gave the opportunity to select the most adapted one for *in vivo* imaging and radioimmunotherapy applications and for diagnosis using immunohistochemistry. At least three distinct epitopes on CD22c antigen were defined in our competition assay with the seven anti-CD22c MAbs. Antibodies 5C2 and 10C6 or 1E3 and 5F8 displayed very similar competition patterns. It is likely that each antibody represents distinct clones owing to their differences in affinity or reactivity by IHC assay: 10C6 gave the best results in IHC, contrary to 5C2, which failed to detect CD22 despite a shared recognition pattern and close dissociation constant values.

A hallmark of CD22 is its clathrin-dependent endocytosis upon antibody binding (29). In the specific context of CD22 targeting in nuclear medicine, the intracellular behavior of the radiopharmaceutical is of primary importance, since it impacts the dose deposition and thus the quality of phenotypic imaging and the efficacy of RIT. Internalized isotopes with a residualizing property like chelated metallic isotopes are trapped within the cell after vector catabolism, enhancing the dose deposition, while iodinated antibody catabolism produces iodo-tyrosine, which is rapidly excreted from the cell (30, 31). This internalization property also determines the efficacy of antibody-drug conjugates (ADC) as it largely determines the efficiency of intracellular release of the drug linked to an antibody. The fate of antibody bound on CD22 once internalized has been largely investigated but remains controversial, some authors favoring its routing in a recycling pathway back to the cell surface via recycling endosome while others arguing for a routing to degradation in lysosome (32, 33). Most often, the CD22 internalization process was evaluated with one antibody on several B-cell lymphomas, underlining the variable internalization capabilities of cell lines of different origins.

Here we sought to take advantage of our panel of antibodies to investigate the variability of the internalization process depending on the antibodies. Internalization was evaluated by measuring antibody binding at 4 and 37°C using the CLBL-1 cell line at different antibody concentrations corresponding to comparable CD22 antigen saturation levels for all antibodies. It clearly appears that at saturating concentration [10-fold the dissociation constant (Kd) of the MAb], internalization was observed for all antibodies with differences in kinetics and intensity. However, at a non-saturating concentration, salient differences appear between antibodies. Some of them, such as 5C2, 10C6, and 2D1, retain their ability to internalize, while other MAbs such as 1E3, 5F8, and 6B7 and above all 5C3 are stabilized at the cell surface, resulting in a higher membrane expression at 37°C than at 4°C. This would indicate that internalization not only depends on antibody binding on its target but also on the density of bound antibody at the cell surface. A threshold of antigen occupation, which is characteristic of each antibody, needs to be surpassed for internalization to take place during the 6 h of the assay. Interestingly, these differences in internalization properties segregated quite well with the epitope recognized on the CD22c antigen. However, the 2D1 antibody is an exception and recognizes an epitope overlapping with 5F8, 1E3, and 6B7 antibodies but displays a very different internalization profile.

The different abilities of monovalent and divalent antibody fragment or native antibody to induce internalization of the transferrin receptor (TfR)—usually taken as a paradigm of clathrin-dependent internalization and recycling to the membrane—has already been investigated. Saturation of transferrin receptor with the monovalent F(ab)′ fragment had no effect on TfR internalization, contrary to F(ab)′2 and IgG (34). We hypothesize that the ability of each antibody to crosslink two CD22c antigens can be either energetically favorable or unfavorable depending on the topology of the antibody–antigen (epitope–paratope) interaction. In the case of 10C6 and 5C2 antibodies, the binding of the first valence of the antibody to CD22c might promote the binding of the second valence, allowing for crosslinking of surface CD22c and internalization at a non-saturating antibody concentration. Conversely, in the case of 1E3, 5F8, 6B7, and 5C3 MAbs, a high antibody burden would be required to offset the energetically unfavorable crosslinking of CD22c in order it occurs at a frequency and/or for a sufficient time course required for initiation of the CD22 internalization. The objective of this article was not to dissect in detail the mechanism and the regulation of CD22 internalization. However, because we were able to distinguish high, intermediate and low internalizing anti-CD22c MAbs, we wondered if this property could modify the dose deposition to cancer cells within a RIT assay.

To address this question, biodistributions were performed with 5C2 and 10C6 on the one hand and 1E3 and 6B7 MAbs on the other hand, which display high and medium internalization abilities, respectively. For this purpose, nude mice were engrafted subcutaneously with CLBL-1 cells and injected 2 weeks after

engraftment with each of the four MAbs radiolabeled with ^{125}I. Even if the activity to the tumor remains rather low, these results are consistent with what is described in the literature after injection of anti-CD22 MAb hLL2 in nude mice bearing human lymphoma xenografts (28). No significant differences were observed regarding the biodistribution of the different MAbs tested in healthy organs. Kidney and liver activities could be explained by the blood kinetics and appeared consistent with an absence of antibody binding in these organs, as expected with mouse IgG_1 specific for a xenogeneic antigen. The tumor uptake of the radiolabeled MAb is also similar for the four MAbs tested. The only notable but non-significant difference is a trend for 10C6 and 5C2 antibodies to accumulate more rapidly in the tumor. As an example, 4 h post-injection the activity into the tumor for the 10C6 antibody was close to what was observed at 16 h (4.3 ± 0.6 and 4.7 ± 1.0%IA/g, respectively), contrary to 6B7 (3.4 ± 0.2 and 4.7 ± 1.2%IA/g, respectively). Since 10C6 is the MAb with highest affinity and the best ability to stain CD22c by immunohistochemistry for spontaneous canine DLBCL diagnosis, we wished to further evaluate it as a potent radiopharmaceutical to perform phenotypic imaging and RIT. These applications require using the 10C6 MAb radiolabeled with metallic isotopes, as ^{111}In for SPECT-CT imaging, ^{64}Cu for PET-CT imaging, and ^{90}Y or ^{177}Lu for RIT. NCS-DOTA could be used as a bifunctional chelator to label immunoconjugates with these three different isotopes. It was thus necessary to check that the coupling of the chelating agent did not affect antibody affinity. The covalent linking of the bi-functional chelating agent NCS-DOTA on the side chains of lysine could in some instances be detrimental to the reactivity of the antibody due to steric hindrance when lysine participates in the recognition site of the antibody or when lysine is close to the recognition site. Modifying an antibody with a bi-functional chelating agent can also modify its pharmacokinetics depending on the mean number of chelating agents coupled to the antibody. These immune-reactivity and pharmacokinetic parameters should be tested for each monoclonal antibody since each of them displays a unique sequence with variable numbers of lysine in their variable regions.

To this end, the 10C6 MAb was coupled to DOTA and radiolabeled with the positron emitter ^{64}Cu in order to perform positron emission tomography (PET-CT) imaging. Despite the low level of antibody accumulation using this tumor model, we were able to clearly detect subcutaneous CLBL-1 tumor 16 h after ^{64}Cu-10C6 injections, validating that the 10C6 antibody affinity is preserved after coupling with DOTA. Mice were sacrificed after imaging and the biodistribution of ^{64}Cu-10C6 was evaluated. The activity to the tumor was comparable to what was observed with the iodinated MAb. The highest activity to the heart observed with the iodinated antibody was consistent with a higher activity in the blood compared to ^{64}Cu-10C6. In addition, the highest activity within the liver was expected due to liver elimination of copper. We used ^{64}Cu in this assay because of the availability of a micro PET-CT device for imaging on mice. We are aware, however, that DOTA is not the best chelating agent for copper (35). Although the ^{64}Cu-10C6 was purified from free ^{64}Cu after radiolabeling, free copper can still be released into the blood flow and accumulate in the organs responsible for copper clearance and elimination. This may explain the high liver uptake noted 16 h after injection, the faster decay in blood and the poor increase in tumor uptake that would be expected with a residualizing metallic isotope compared to ^{125}I-10C6. For future applications in dogs, we plan to use the DOTA chelating agent to radiolabel 10C6 MAb with ^{111}In for SPECT-CT imaging and with ^{90}Y for RIT. These isotopes are more stably chelated with DOTA than copper. This may enable a higher dose deposition to the tumor, as shown by Sharkey et al. comparing iodinate and indium-labeled antibody biodistribution targeting CD22 on nude mice bearing the human B-cell NHL RL cell-line (36).

At the end of this *in vitro* and *in vivo* evaluation we selected 10C6 Mab for IHC and SPECT-CT imaging. First of all, we used the experimental dog to validate the imaging protocol and determine the binding property of ^{111}In-10C6 on healthy organs. We observed a strong antibody accretion on the liver compared to humans. Several explanations could account for this high liver content. The recycling of mouse IgG via dog FcRn binding may be inefficient, as mentioned by Bergson et al. (37), entailing a rapid degradation of antibody after endocytosis and clearance via the hepatobiliary route. Anatomical differences between humans and dogs could also explain differential antibody accretion. The high vascularization of the dog nose compared to humans also results in a stronger signal in the former species. This is also true for liver, which is proportionally larger in dogs than in humans and therefore mobilizes a higher proportion of the total blood content. This needs to be taken into account for toxicity concerns in the course of the RIT planned, especially for the highest dose plan to be evaluated in a dose escalation. However, a preliminary evaluation indicates that the doses to liver remain at a level allowing injection of activity within the range of the therapeutic window determined in humans (manuscript in preparation).

These results prompt us to use ^{111}In-10C6 on dogs with spontaneous DLBCL in order to validate the ability of this antibody to target tumor sites. Three sick dogs were imaged. We were able to visualize the tumor site diagnosed by classical examination using SPECT-CT imaging. In addition, SPECT-CT made it possible to clearly visualize the tumor site not detected by current examination techniques, such as the bone marrow invasion in the example provided in this article. Although myelogram analysis indicated the presence of tumor cells in the marrow, the extent of the tumor invasion could not be assessed. The exclusion criterion of 20% of bone marrow invasion that we retain for future RIT assays could only be assessed with imaging. SPECT-CT could therefore be useful for the staging of the pathology, although ^{18}FDG could be used to this end. Another input of SPECT-CT imaging not provided by ^{18}FDG is that it can provide quantitative imaging and dosimetry, making it possible to extrapolate the actual dose to healthy organs and tumor sites in the course of RIT treatment. The next step of our project will be to perform the dosimetry analysis on experimental dogs in order to determine a population pharmacokinetic model that can be used in the clinical context to evaluate, on a limited number of images of sick dogs, whether they conform to the general pharmacokinetic model or if discrepancies would require

adjusting the injected activity to avoid toxicity or to reach a therapeutic dose to tumor cells. We plan to use this antibody to treat dogs with spontaneous DLBCL based on the encouraging results previously obtained on human DLBCL in a phase I/II assay. This clinical trial in dogs with a preclinical value for human patients could ensure more accurate evaluation of the relevance of CD22 targeting for DLBCL management. It also ensures the transfer of new methods in quantitative imaging and new therapeutic approaches, which are difficult to evaluate in humans, to the clinic.

DATA AVAILABILITY STATEMENT

All datasets generated for this study are included in the article/supplementary material.

ETHICS STATEMENT

The animal study was reviewed and approved by Ethics Committee of Pays de la Loire. Written informed consent was obtained from the owners for the participation of their animals in this study.

AUTHOR CONTRIBUTIONS

FD participated in hybridoma production, antibody radiolabeling, biodistribution, and imaging studies. He was the major contributor in writing the manuscript. MBe, KB, and MD isolated and produced naked and radiolabeled antibodies. FN determined their ability to be used in immunohistochemistry and performed IHC on dog biopsy. JA provided the canine tumor tissue bank and contributed to the development of the project. FE characterized MAb internalization property, performed epitope mapping, and participated to biodistribution on mouse model. She supervised the logistics for dog inclusion in the assay and the clinical assistance at the Veterinary Teaching Hospital. VG-G participated to the assays of MAb internalization. CM supervised and executed experiments on rodents. CI participated in dog imaging. AV radiolabeled 10C6 Mab with Indium-111. MBo radiolabeled 10C6 MAb with copper-64. NC performed SPECT-CT acquisitions. CB-M interpreted SPECT-CT images. All authors read and approved the final manuscript. In addition to the actual implementation of automated radiolabeling in the annex of the hospital pharmacy, AV provided all the necessary information for the writing of this manuscript and participated in the preliminary discussion concerning the process and organization of the radiolabeling of 10C6 antibody for the clinical trial on dogs with spontaneous DLBCL.

FUNDING

This work was supported by the Institut Thématique Multi-Organismes (ITMO) Cancer of the Alliance pour les sciences de la vie et de la santé (AVIESAN) jointly with the Institut National du Cancer (INCA) under one grant entitled: Spontaneous tumor models in animals for translational research in oncology no. A11196NS (CANIMAB). Financial support was also provided by a Physics, Mathematics and Engineering sciences applied to the Cancer Research grant (DogPPK project) awarded by INSERM and INCa.

ACKNOWLEDGMENTS

The authors would like to thank Barbara Rütgen for supplying the CLBL-1 cell line; the Laboratory of Animal Histopathology (Oniris, Nantes, France) for supplying paraffin blocks of canine diffuse large B-cell lymphomas; Florence Lezin and Bernard Fernandez for technical assistance; Gildas Vaillant (STAR, Oniris) and Gwenola Touzot-Jourde (CRIP, Oniris) for dog anesthesia; Marie Roussel and Sonia Becavin for the nursing of the dogs.

REFERENCES

1. Casadei B, Pellegrini C, Pulsoni A, Annechini G, De Renzo A, Stefoni V, et al. 90-yttrium-ibritumomab tiuxetan consolidation of fludarabine, mitoxantrone, rituximab in intermediate/high-risk follicular lymphoma: updated long-term results after a median follow-up of 7 years. *Cancer Med*. (2016) 5:1093–7. doi: 10.1002/cam4.684
2. Morschhauser F, Radford J, Van Hoof A, Vitolo U, Soubeyran P, Tilly H, et al. Phase III trial of consolidation therapy with yttrium-90-ibritumomab tiuxetan compared with no additional therapy after first remission in advanced follicular lymphoma. *J Clin Oncol*. (2008) 26:5156–64. doi: 10.1200/JCO.2008.17.2015
3. Rizzieri D. Zevalin((R)) (ibritumomab tiuxetan): after more than a decade of treatment experience, what have we learned? *Crit Rev Oncol Hematol*. (2016) 105:5–17. doi: 10.1016/j.critrevonc.2016.07.008
4. Tomblyn M. Radioimmunotherapy for B-cell non-hodgkin lymphomas. *Cancer Control*. (2012) 19:196–203. doi: 10.1177/107327481201900304
5. Kaminski MS, Zelenetz AD, Press OW, Saleh M, Leonard J, Fehrenbacher L, et al. Pivotal study of iodine I 131 tositumomab for chemotherapy-refractory low-grade or transformed low-grade B-cell non-Hodgkin's lymphomas. *J Clin Oncol*. (2001) 19:3918–28. doi: 10.1200/JCO.2001.19.19.3918
6. Scholz CW, Pinto A, Linkesch W, Linden O, Viardot A, Keller U, et al. (90)Yttrium-ibritumomab-tiuxetan as first-line treatment for follicular lymphoma: 30 months of follow-up data from an international multicenter phase II clinical trial. *J Clin Oncol*. (2013) 31:308–13. doi: 10.1200/JCO.2011.41.1553
7. Ferrucci PF, Vanazzi A, Grana CM, Cremonesi M, Bartolomei M, Chinol M, et al. High activity 90Y-ibritumomab tiuxetan (Zevalin) with peripheral blood progenitor cells support in patients with refractory/resistant B-cell non-Hodgkin lymphomas. *Br J Haematol*. (2007) 139:590–9. doi: 10.1111/j.1365-2141.2007.06869.x
8. Gopal AK, Rajendran JG, Gooley TA, Pagel JM, Fisher DR, Petersdorf SH, et al. High-dose [131I]tositumomab (anti-CD20) radioimmunotherapy and autologous hematopoietic stem-cell transplantation for adults > or = 60 years old with relapsed or refractory B-cell lymphoma. *J Clin Oncol*. (2007) 25:1396–402. doi: 10.1200/JCO.2006.09.1215
9. Illidge TM, Bayne M, Brown NS, Chilton S, Cragg MS, Glennie MJ, et al. Phase 1/2 study of fractionated (131)I-rituximab in low-grade B-cell lymphoma: the effect of prior rituximab dosing and tumor burden on subsequent radioimmunotherapy. *Blood*. (2009) 113:1412–21. doi: 10.1182/blood-2008-08-175653

10. Illidge TM, Mayes S, Pettengell R, Bates AT, Bayne M, Radford JA, et al. Fractionated (90)Y-ibritumomab tiuxetan radioimmunotherapy as an initial therapy of follicular lymphoma: an international phase II study in patients requiring treatment according to GELF/BNLI criteria. *J Clin Oncol*. (2014) 32:212–8. doi: 10.1200/JCO.2013.50.3110
11. Hoelzer D. Novel antibody-based therapies for acute lymphoblastic leukemia. *Hematology Am Soc Hematol Educ Program*. (2011) 2011:243–9. doi: 10.1182/asheducation-2011.1.243
12. Juweid ME. Radioimmunotherapy of B-cell non-Hodgkin's lymphoma: from clinical trials to clinical practice. *J Nucl Med*. (2002) 43:1507–29.
13. Chevallier P, Eugene T, Robillard N, Isnard F, Nicolini F, Escoffre-Barbe M, et al. (90)Y-labelled anti-CD22 epratuzumab tetraxetan in adults with refractory or relapsed CD22-positive B-cell acute lymphoblastic leukaemia: a phase 1 dose-escalation study. *Lancet Haematol*. (2015) 2:e108–17. doi: 10.1016/S2352-3026(15)00020-4
14. Kraeber-Bodere F, Pallardy A, Maisonneuve H, Campion L, Moreau A, Soubeyran I, et al. Consolidation anti-CD22 fractionated radioimmunotherapy with (90)Y-epratuzumab tetraxetan following R-CHOP in elderly patients with diffuse large B-cell lymphoma: a prospective, single group, phase 2 trial. *Lancet Haematol*. (2017) 4:e45. doi: 10.1016/S2352-3026(16)30168-5
15. Macor P, Secco E, Zorzet S, Tripodo C, Celeghini C, Tedesco F. An update on the xenograft and mouse models suitable for investigating new therapeutic compounds for the treatment of B-cell malignancies. *Curr Pharm Des*. (2008) 14:2023–39. doi: 10.2174/138161208785294591
16. Zullo K, Amengual JE, O'Connor OA, Scotto L. Murine models in mantle cell lymphoma. *Best Pract Res Clin Haematol*. (2012) 25:153–63. doi: 10.1016/j.beha.2012.04.009
17. Zandvliet M. Canine lymphoma: a review. *Vet Q*. (2016) 36:76–104. doi: 10.1080/01652176.2016.1152633
18. LeBlanc AK, Mazcko CN, Khanna C. Defining the value of a comparative approach to cancer drug development. *Clin Cancer Res*. (2016) 22:2133–8. doi: 10.1158/1078-0432.CCR-15-2347
19. Saba C, Paoloni M, Mazcko C, Kisseberth W, Burton JH, Smith A, et al. A comparative oncology study of iniparib defines its pharmacokinetic profile and biological activity in a naturally-occurring canine cancer model. *PLoS ONE*. (2016) 11:e0149194. doi: 10.1371/journal.pone.0149194
20. Kletting P, Maass C, Reske S, Beer AJ, Glatting G. Physiologically based pharmacokinetic modeling is essential in 90Y-labeled anti-CD66 radioimmunotherapy. *PLoS ONE*. (2015) 10:e0127934. doi: 10.1371/journal.pone.0127934
21. Maass C, Kletting P, Bunjes D, Mahren B, Beer AJ, Glatting G. Population-based modeling improves treatment planning before (90)Y-labeled anti-CD66 antibody radioimmunotherapy. *Cancer Biother Radiopharm*. (2015) 30:285–90. doi: 10.1089/cbr.2015.1878
22. Rutgen BC, Hammer SE, Gerner W, Christian M, de Arespacochaga AG, Willmann M, et al. Establishment and characterization of a novel canine B-cell line derived from a spontaneously occurring diffuse large cell lymphoma. *Leuk Res*. (2010) 34:932–8. doi: 10.1016/j.leukres.2010.01.021
23. Diab M, Nguyen F, Berthaud M, Maurel C, Gaschet J, Verger E, et al. Production and characterization of monoclonal antibodies specific for canine CD138 (syndecan-1) for nuclear medicine preclinical trials on spontaneous tumours. *Vet Comp Oncol*. (2017) 15:932–51. doi: 10.1111/vco.12233
24. Matrisian LM, Bowden GT, Krieg P, Furstenberger G, Briand JP, Leroy P, et al. The mRNA coding for the secreted protease transin is expressed more abundantly in malignant than in benign tumors. *Proc Natl Acad Sci USA*. (1986) 83:9413–7. doi: 10.1073/pnas.83.24.9413
25. Fraker PJ, Speck JC Jr. Protein and cell membrane iodinations with a sparingly soluble chloroamide, 1,3,4,6-tetrachloro-3a,6a-diphrenylglycoluril. *Biochem Biophys Res Commun*. (1978) 80:849–57. doi: 10.1016/0006-291X(78)91322-0
26. Nikula TK, Curcio MJ, Brechbiel MW, Gansow OA, Finn RD, Scheinberg DA. A rapid, single vessel method for preparation of clinical grade ligand conjugated monoclonal antibodies. *Nucl Med Biol*. (1995) 22:387–90. doi: 10.1016/0969-8051(94)00126-5
27. Tembhare PR, Marti G, Wiestner A, Degheidy H, Farooqui M, Kreitman RJ, et al. Quantification of expression of antigens targeted by antibody-based therapy in chronic lymphocytic leukemia. *Am J Clin Pathol*. (2013) 140:813–8. doi: 10.1309/AJCPYFQ4XMGJD6TI
28. Mattes MJ, Shih LB, Govindan SV, Sharkey RM, Ong GL, Xuan H, et al. The advantage of residualizing radiolabels for targeting B-cell lymphomas with a radiolabeled anti-CD22 monoclonal antibody. *Int J Cancer*. (1997) 71:429–35. doi: 10.1002/(sici)1097-0215(19970502)71:3<429::aid-ijc21>3.0.co;2-9
29. John B, Herrin BR, Raman C, Wang YN, Bobbitt KR, Brody BA, et al. The B cell coreceptor CD22 associates with AP50, a clathrin-coated pit adapter protein, via tyrosine-dependent interaction. *J Immunol*. (2003) 170:3534–43. doi: 10.4049/jimmunol.170.7.3534
30. Geissler F, Anderson SK, Venkatesan P, Press O. Intracellular catabolism of radiolabeled anti-mu antibodies by malignant B-cells. *Cancer Res*. (1992) 52:2907–15.
31. Naruki Y, Carrasquillo JA, Reynolds JC, Maloney PJ, Frincke JM, Neumann RD, et al. Differential cellular catabolism of 111In, 90Y and 125I radiolabeled T101 anti-CD5 monoclonal antibody. *Int J Rad Appl Instrum B*. (1990) 17:201–7. doi: 10.1016/0883-2897(90)90148-T
32. O'Reilly MK, Tian H, Paulson JC. CD22 is a recycling receptor that can shuttle cargo between the cell surface and endosomal compartments of B cells. *J Immunol*. (2011) 186:1554–63. doi: 10.4049/jimmunol.1003005
33. Shan D, Press OW. Constitutive endocytosis and degradation of CD22 by human B cells. *J Immunol*. (1995) 154:4466–75.
34. Lesley J, Schulte R, Woods J. Modulation of transferrin receptor expression and function by anti-transferrin receptor antibodies and antibody fragments. *Exp Cell Res*. (1989) 182:215–33. doi: 10.1016/0014-4827(89)90293-0
35. Rylova SN, Stoykow C, Del Pozzo L, Abiraj K, Tamma ML, Kiefer Y, et al. The somatostatin receptor 2 antagonist 64Cu-NODAGA-JR11 outperforms 64Cu-DOTA-TATE in a mouse xenograft model. *PLoS ONE*. (2018) 13:e0195802. doi: 10.1371/journal.pone.0195802
36. Sharkey RM, Behr TM, Mattes MJ, Stein R, Griffiths GL, Shih LB, et al. Advantage of residualizing radiolabels for an internalizing antibody against the B-cell lymphoma antigen, CD22. *Cancer Immunol Immunother*. (1997) 44:179–88. doi: 10.1007/s002620050371
37. Bergeron LM, McCandless EE, Dunham S, Dunkle B, Zhu Y, Shelly J, et al. Comparative functional characterization of canine IgG subclasses. *Vet Immunol Immunopathol*. (2014) 157:31–41. doi: 10.1016/j.vetimm.2013.10.018

Conflict of Interest: The authors declare that the research was conducted in the absence of any commercial or financial relationships that could be construed as a potential conflict of interest.

Copyright © 2020 Etienne, Berthaud, Nguyen, Bernardeau, Maurel, Bodet-Milin, Diab, Abadie, Gouilleux-Gruart, Vidal, Bourgeois, Chouin, Ibisch and Davodeau. This is an open-access article distributed under the terms of the Creative Commons Attribution License (CC BY). The use, distribution or reproduction in other forums is permitted, provided the original author(s) and the copyright owner(s) are credited and that the original publication in this journal is cited, in accordance with accepted academic practice. No use, distribution or reproduction is permitted which does not comply with these terms.

frontiers in Oncology

ORIGINAL RESEARCH
published: 11 February 2020
doi: 10.3389/fonc.2020.00117

From the Clinic to the Bench and Back Again in One Dog Year: How a Cross-Species Pipeline to Identify New Treatments for Sarcoma Illuminates the Path Forward in Precision Medicine

Sneha R. Rao[1†], Jason A. Somarelli[2,3†], Erdem Altunel[2], Laura E. Selmic[4], Mark Byrum[4], Maya U. Sheth[5], Serene Cheng[2], Kathryn E. Ware[2], So Young Kim[6], Joseph A. Prinz[7], Nicolas Devos[7], David L. Corcoran[7], Arthur Moseley[7], Erik Soderblom[7], S. David Hsu[2,3] and William C. Eward[1,3*]*

[1] Department of Orthopaedic Surgery, Duke University Medical Center, Durham, NC, United States, [2] Department of Medicine, Duke University Medical Center, Durham, NC, United States, [3] Duke University Medical Center, Duke Cancer Institute, Durham, NC, United States, [4] Department of Veterinary Clinical Sciences, College of Veterinary Medicine, The Ohio State University, Columbus, OH, United States, [5] Pratt School of Engineering, Duke University, Durham, NC, United States, [6] Department of Molecular Genetics and Microbiology, Duke University, Durham, NC, United States, [7] Duke Center for Genomic and Computational Biology, Duke University, Durham, NC, United States

Cancer drug discovery is an inefficient process, with more than 90% of newly-discovered therapies failing to gain regulatory approval. Patient-derived models of cancer offer a promising new approach to identify new treatments; however, for rare cancers, such as sarcomas, access to patient samples is limited, which precludes development of patient-derived models. To address the limited access to patient samples, we have turned to pet dogs with naturally-occurring sarcomas. Although sarcomas make up <1% of all human cancers, sarcomas represent 15% of cancers in dogs. Because dogs have similar immune systems, an accelerated pace of cancer progression, and a shared environment with humans, studying pet dogs with cancer is ideal for bridging gaps between mouse models and human cancers. Here, we present our cross-species personalized medicine pipeline to identify new therapies for sarcomas. We explore this process through the focused study of a pet dog, Teddy, who presented with six synchronous leiomyosarcomas. Using our pipeline we identified proteasome inhibitors as a potential therapy for Teddy. Teddy was treated with bortezomib and showed a varied response across tumors. Whole exome sequencing revealed substantial genetic heterogeneity across Teddy's recurrent tumors and metastases, suggesting that intra-patient heterogeneity and tumoral adaptation were responsible for the heterogeneous clinical response. Ubiquitin proteomics coupled with exome sequencing revealed multiple candidate driver mutations in proteins related to the proteasome pathway. Together, our results demonstrate how the comparative study of canine sarcomas offers important insights into the development of personalized medicine approaches that can lead to new treatments for sarcomas in both humans and canines.

Keywords: precision medicine, tumor evolution, tumor heterogeneity, cancer therapy, comparative oncology

OPEN ACCESS

Edited by:
Rodney L. Page, Colorado State University, United States

Reviewed by:
Seth Pollack, Fred Hutchinson Cancer Research Center, United States
Heather M. Wilson-Robles, Texas A&M University, United States

***Correspondence:**
S. David Hsu
shiaowen.hsu@duke.edu
William C. Eward
william.eward@duke.edu

[†]These authors have contributed equally to this work

Specialty section:
This article was submitted to Cancer Molecular Targets and Therapeutics, a section of the journal Frontiers in Oncology

Received: *05 September 2019*
Accepted: *22 January 2020*
Published: *11 February 2020*

Citation:
Rao SR, Somarelli JA, Altunel E, Selmic LE, Byrum M, Sheth MU, Cheng S, Ware KE, Kim SY, Prinz JA, Devos N, Corcoran DL, Moseley A, Soderblom E, Hsu SD and Eward WC (2020) From the Clinic to the Bench and Back Again in One Dog Year: How a Cross-Species Pipeline to Identify New Treatments for Sarcoma Illuminates the Path Forward in Precision Medicine. Front. Oncol. 10:117. doi: 10.3389/fonc.2020.00117

INTRODUCTION

Despite spending billions of dollars on the preclinical development of new anti-cancer drugs, fewer than 1 in 10 new therapies make it from the bench to the bedside and gain FDA approval (1). These sobering statistics clearly demonstrate that the preclinical models and paradigms currently being used to discover new cancer treatments require improvement. This need for improvement is exemplified by the slow progress in finding new therapies for sarcoma. Though sarcomas are rare, they are highly aggressive cancers that are prevalent in children and young adults. While sarcomas make up <1% of adult solid tumors, they account for nearly 15% of pediatric solid tumors (2). For patients who present with metastatic disease, the 5-years survival is just 16% (3). While chemotherapy has a well-defined role in the treatment of most sarcomas of bone, the same is not true for soft tissue sarcomas (STS). Few new therapies have emerged in recent decades, underscoring the need for creative new approaches in drug discovery.

One approach that has increasingly become a part of the discovery pipeline is the use of patient-derived models of cancer, including low-passage cell lines and patient-derived xenografts (PDXs). To create these patient-derived models, individual patient tumors are grown directly in culture or in immunocompromised mice. Each type of patient-derived model has unique advantages: For example, patient-derived cell lines enable large-scale drug screens to take place quickly and at low cost. On the other hand, the use of PDXs reduces the selective bottleneck of cell line generation and maintains the stromal components of the original tumor, which are increasingly recognized as critical components of a tumor's relative therapeutic sensitivity (4, 5). These patient-derived models are also being used to develop personalized treatments and guide development of novel targeted agents (6, 7). One study in colorectal cancers showed a correlation between transplanted xenograft tumors and clinical response to cytotoxic therapy (8). Another pilot clinical trial of patients with advanced solid tumors received systemic cytotoxic therapies based on *in vivo* validation in PDXs (9). This study showed that 11 out of 17 treatment regimens identified in PDX were clinically efficacious (10). Drug screening in this study was done *in vivo* rather than *in vitro* and used over 200 treatment regimens, including both targeted and non-targeted agents (10). A similar study in advanced sarcoma patients with a variety of histologic subtypes also yielded concordant results between PDX and patient responses, with 13 out of 16 patients showing a correlation between efficacy of the top drug identified through PDX drug trials and clinical outcomes (11). Yet despite these exciting results, there remains a disconnect between drug testing in mice and performance in human patients.

Another approach for cancer drug discovery that is rapidly gaining attention is the study of pet dogs with spontaneously-occurring sarcomas and the inclusion of these patients in therapeutic trials. Canine sarcomas are far more prevalent than their human counterparts, representing ∼15% of all canine malignancies (12) and rendering them an underutilized "model" of human disease (13, 14). Unlike mouse models—which often fail to recapitulate key conditions of spontaneous human disease—dogs share an environment with humans, have an intact immune system, and have nearly identical treatment options. While there are some differences in the histopathologic grading of soft tissue sarcomas between humans and dogs, a study using canine soft tissue sarcomas to compare pathologic diagnoses between veterinary and medical pathologists showed that the majority of canine tumors were given diagnoses congruent with the human counterpart (15). Coupled with patient-derived models and precision medicine strategies, a cross-species approach could illuminate new therapeutic options for sarcoma patients with greater fidelity than the traditional "cells, then mice, then humans" pathway. Most importantly, because the lifespan of dogs is much shorter than that of humans, discoveries in canine clinical trials can be made more quickly in canine patients given the rapid progression of their lives relative to humans. This latter aspect addresses a key pitfall in precision medicine approaches to treat human cancers—the effect of a selected therapy may not be clear for many years.

In the present work, we report the development and testing of a cross-species personalized medicine pipeline that combines patient-derived models, personalized genomics, and drug screening strategies to identify new potential therapies for sarcoma. This pipeline is agnostic to species of origin; we collect and evaluate sarcomas from both canine and human patients at the time of initial presentation. One such patient was a young dog who presented with seven synchronous, spontaneous high grade leiomyosarcomas. This patient was an ideal candidate for the implementation of this pipeline due to the high likelihood of disease recurrence, aggressive presentation of disease, and lack of pre-existing medical conditions that might confound his clinical response. More importantly, this patient initially presented to a general practice veterinary clinic and was subsequently treated by a veterinary surgical oncologist, this closely mimics the presentation and treatment of human sarcoma. Using the pipeline, we first developed an early passaged cell line and then PDX for our patient. Using high throughput drug screen on the cell line, we identified proteasome inhibitors as a candidate therapy for this patient, then validated the tumor response to proteasome inhibition *in vivo* using the patient's PDX, and finally treated the patient's recurrent disease in the clinic with the proteasome inhibitor, bortezomib. Our work provides a generalizable framework for personalized medicine strategies and highlights key challenges in the development of such approaches.

MATERIALS AND METHODS

Generation of Patient-Derived Xenograft Models

Tumor samples were collected from a 3-year-old male golden retriever following surgical resection of the tumors at University of Illinois at Urbana-Champaign, College of Veterinary Medicine (Urbana, IL, USA) with the informed consent of the owner. PDX models of the patient's sarcoma were generated as described previously, and all *in vivo* mouse experiments were performed in accordance with the animal guidelines and with the approval

of the Institutional Animal Care and Use committee (IACUC) at the Duke University Medical Center (16). To develop PDXs, the tumor sample was washed in phosphate buffered saline (PBS), dissected into small pieces (<2 mm), and injected into the flanks of 8–10-week-old JAX NOD.CB17-PrkdcSCID-J mice obtained from the Duke University Rodent Genetic and Breeding Core. Tumors were passaged into successive mice once the tumor size reached between 500 and 1,500 mm^3. Resected PDX tumors were homogenized in a PBS suspension and 150 μl of PDX tissue-PBS suspensions at 150 mg/ml concentration were injected subcutaneously into the right flanks of the 8 weeks old JAX NOD.CB17- PrkdcSCID-J mice. To maintain integrity of the PDX tumor, passages were limited to the 3rd generation.

Low-Passage Cell Line Generation and Characterization

Low passage cell lines were generated from the patient's PDX during passage one of the PDX as follows. PDX tumor was surgically removed with a sterile blade, washed in PBS, and small pieces (<2 mm) of tumor tissue were mechanically homogenized and then suspended in cell growth media and cultured in 12-well plates with DMEM + 10% FBS + 1% Penicillin/Streptomycin. To isolate tumor cells, growing colonies of cells were isolated by trypsinization using O rings and cultured in fresh 12-well plates. This process was repeated until a colony of cells was established that resembled pure tumor cells in morphology. Contamination of the PDX cell line with mouse fibroblasts was detected by polymerase chain reaction (PCR) using canine-specific and mouse-specific primers. The following primers were used: canine reverse (5′-GTA AAG GCT GCC TGA GGA TAA G-3′), canine forward (5′-GGT CCA GGG AAG ATC AGA AAT G-3′), mouse reverse (5′-AGG TGT CAC CAG GAC AAA TG-3′), and mouse forward (5′-CTG CTT CGA GCC ATA GAA CTA A-3′) (17).

High-Throughput Drug Screening

Canine leiomyosarcoma low-passage cell line was cultured in DMEM + 10% FBS + 1% Penicillin/Streptomycin. Automated systems were used for a 119- and 2,100- compound high-throughput drug screens. The 119-drug screen library (Approved Oncology Set VI) was provided by the NCI Developmental Therapeutics Program (https://dtp.cancer.gov/). Automated liquid handling was provided by the Echo Acoustic Dispenser (Labcyte) for drug addition or Well mate (Thermo Fisher) for cell plating, and asays were performed using a Clarioscan plate reader (BMG Labtech). The BioActive compound library includes 2,100 small molecules that are annotated for pathway and drug target (Selleckchem) and was screened in triplicate. Compounds were stamped into 384 well plates for a final concentration of 1 μM using an Echo Acoustic Dispenser (Labcyte). Cells were then plated at a density of 2,000 cells/well using a WellMate (ThermoFisher) and incubated in the presence of drug for 72 h. After 72 h of incubation, Cell Titer Glo was added to each well and luminescence was measured using a Clariostar Plate Reader (BMG Labtech). Percent killing was quantified using the formula $100*[1-(\text{average CellTiterGlo}^{drug}/\text{average CellTiterGlo}^{DMSO})]$ where the value average $\text{CellTiterGlo}^{DMSO}$ was the average DMSO CellTiterGlo value across each plate.

Validation of Top Drug Candidates *In vivo*

To validate top candidates from the *in vitro* drug screens 150 μl of homogenized PDX tissue-PBS suspensions were injected at a concentration of 150 mg/ml of tumor tissue subcutaneously into the right flanks of the 8–10 weeks old JAX NOD.CB17-PrkdcSCID-J mice. Top drug targets identified by the high-throughput drug screens for *in vivo* validation, bortezomib (PS-341) and 17-DMAG (alvespimycin) HCl were purchased from Selleck Chemicals (Houston, TX). Drug were first solubilized in DMSO and then diluted in PBS for intraperitoneal injections. When the tumor volumes reached 100–150 mm^3, mice were randomized ($n = 5$ mice for each treatment group) and 1 mg/kg bortezomib and 25 mg/kg alvespimycin intraperitoneal injections were initiated three times a week (18, 19). Control tumors were treated with 100 μl of 5% DMSO diluted in PBS. Tumor volumes were measured three times a week using calipers, and (length $\times$ $(\text{width})^2$)/2 was used to calculate the tumor size. Mice were sacrificed on day 18 or if the tumor volume reached 1,500 mm^3.

Whole Exome Sequencing

Genomic DNA from seven primary tumors, one recurrent tumor, a patient-derived xenograft, and the cell line were isolated using the QIAGEN DNeasy Blood and Tissue kit. DNA quality analysis, exome capture, and sequencing were performed at the Duke University Sequencing and Genomics Technologies Shared Resource. Genomic DNA samples were quantified using fluorometric quantitation on the Qubit 2.0 (ThermoFisher Scientific). For each sample, 1 μg of DNA was sheared using a Covaris to generate DNA fragments of about 300 bp in length. Sequencing libraries were prepared using the Roche Kapa HyperPrep Library prep Kit. During adapter ligation, unique indexes were added to each sample. Resulting libraries were cleaned using SPRI beads and quantified on the Qubit 2.0. Size distributions were checked on an Agilent Bioanalyzer. Libraries were pooled into equimolar concentration (8 libraries per pool) and library pools were finally enriched using the Roche SeqCap® EZ Dog Exome panel (design 1000003560). Each pool of enriched libraries was sequenced on one lane of a HiSeq 4000 flow cell at 150 bp PE, generating about 41 Million clusters per sample or ∼12 Gb of data. Sequence data was demultiplexed and Fastq files generated using Bcl2Fastq2 conversion software provided by Illumina.

Initial data analysis and variant calling were performed by the Duke University Genomic Analysis and Bioinformatics Resource. Exome sequencing data was processed using the TrimGalore toolkit (20), which employs Cutadapt (21) to trim low-quality bases and Illumina sequencing adapters from the 3' end of the reads. Reads were aligned to the CanFam3.1 version of the dog genome with the BWA algorithm (22, 23). PCR duplicates were flagged using the PICARD Tools software suite (24). Alignment processing and variant calling were performed using the MuTect2 (25) algorithm that is part of the GATK (22) following the Broad Institute's Best Practices Workflow for identifying somatic variants (22). Variants for each sample

were called relative to the normal sample. Variant call files for each sample were filtered for single nucleotide polymorphisms using the Genome Analysis Toolkit and converted to PHYLIP format using the vcf2phylip package (26). Phylogenetic trees were generated using PHYLIP with 1,000 bootstrap replicates per tree (27) and visualized using the ape package in R (28). The number of shared mutations was calculated pairwise between the matched tumor-normal variants of each sample using VCFtools (29). Genes with deleterious mutations in each sample were identified using Ensembl's Variant Effect Predictor tool (29). These results were analyzed and visualized using BioVenn and the UpSetR package in R (30, 31).

Ubiquitin-Tagged Proteomics Analysis of PDX Tumors Treated With Bortezomib

Sample Preparation

Flash frozen vehicle- and bortezomib-treated PDX tumors ($n = 3$ per treatment) were provided to The Duke Proteomics and Metabolomics Shared Resource for processing and analysis. Samples were normalized to 3.3 μL of 8 M urea per mg of wet weight and homogenized using a bead beater at 10,000 rpm. Protein concentration was determined via Bradford assay and was normalized to 5,000 μg of protein in 1.6 M of urea using 50 mM ammonium bicarbonate. Samples were then reduced with 10 mM dithiothreitol for 45 min at 32°C and alkylated with 25 mM iodoacetamide for 45 min at room temperature. Trypsin was added to a 1:25 ratio (enzyme to total protein) and allowed to proceed for 18 h at 37°C. After digestion, peptides were acidified to pH 2.5 with trifluoroacetic acid (TFA) and subjected to C18 SPE cleanup (Sep-Pak, 50 mg bed).

For ubiquitin antibody enrichment, samples were resuspended in 750 uL 1X IAP Buffer (50 mM MOPS pH 7.2, 10 mM sodium phosphate, 50 mM NaCl from Cell Signaling Technology) using vortex and brief bath sonication. Pre-aliquoted PTMScan® Pilot Ubiquitin Remant Motif (K-ε-GG) beads (Cell Signaling Technology) were thawed for each sample, storage buffer was removed following slow centrifugation, and beads were pre-washed with 4 × 1 mL of 1X PBS buffer. Resuspended peptides were then transferred in IAP buffer directly onto beads. Immunoprecipitation was performed for 2 h at 4C using end-over-end mixing. After spinning gently to settle the beads (VWR microfuge) the supernatants were removed. The IAP resins containing the enriched ubiquitinated peptides were then washed with 1 mL of IAP buffer three times, and one time with 0.1 × IAP buffer. After removing the supernatants, the antibody-bound ubiquitinated peptides were eluted with a 50 μl aliquot of 0.15% TFA in water for ∼10 m at room temperature, tapping gently on the bottom of the tube a few times during elution to ensure mixing. Beads were eluted a second time with 45 μL of 0.15% TFA in water and added to the first elution. Combined eluents were lyophilized to dryness.

Samples were resuspended in 35 μL 0.1% formic acid for a final cleanup on a C18 Stage Tip. All samples were then lyophilized to dryness and resuspended in 12 μL 1%TFA/2% acetonitrile containing 12.5 fmol/μL yeast alcohol dehydrogenase. From each sample, 3 μL was removed to create a QC Pool sample that was run periodically throughout the acquisition period.

Quantitative LC/MS/MS was performed on 4 μL of each sample, using a nanoAcquity UPLC system (Waters Corp) coupled to a Thermo QExactive HF-X high resolution accurate mass tandem mass spectrometer (Thermo) via a nanoelectrospray ionization source. Briefly, the sample was first trapped on a Symmetry C18 20 mm × 180 μm trapping column (5 μl/min at 99.9/0.1 v/v water/acetonitrile), after which the analytical separation was performed using a 1.8 μm Acquity HSS T3 C18 75 μm × 250 mm column (Waters Corp.) with a 90-min linear gradient of 5 to 30% acetonitrile with 0.1% formic acid at a flow rate of 400 nanoliters/min (nL/min) with a column temperature of 55°C. Data collection on the QExactive HF mass spectrometer was performed in a data-dependent acquisition (DDA) mode of acquisition with a $r = 120{,}000$ (@ m/z 200) full MS scan from m/z 375−1,600 with a target AGC value of 3e6 ions followed by 30 MS/MS scans at $r = 15{,}000$ (@ m/z 200) at a target AGC value of 5×10^4 ions and 45 ms. A 20 second dynamic exclusion was employed to increase depth of coverage. The total analysis cycle time for each sample injection was ∼2 h.

Data was imported into Proteome Discoverer 2.2 (Thermo Scientific Inc.), and analyses were aligned based on the accurate mass and retention time of detected ions using Minora Feature Detector algorithm in Proteome Discoverer. Relative peptide abundance was calculated based on area-under-the-curve of the selected ion chromatograms of the aligned features across all runs. The MS/MS data was searched against the TrEMBL *C. familiaris* database (downloaded in Nov 2017) with additional proteins, including yeast ADH1, bovine serum albumin, as well as an equal number of reversed-sequence "decoys") false discovery rate determination. Mascot Distiller and Mascot Server (v 2.5, Matrix Sciences) were utilized to produce fragment ion spectra and to perform the database searches. Database search parameters included fixed modification on Cys (carbamidomethyl) and variable modifications on Lysine (Gly-Gly), and Meth (oxidation). Peptide Validator and Protein FDR Validator nodes in Proteome Discoverer were used to annotate the data at a maximum 1% protein false discovery rate.

Data Analysis and Statistics

JMP from SAS software (Cary, NC, USA) was used for the high-throughput drug screen data analysis. Hierarchical clustering of data was used to identify the top drug candidates from the 119-compound drug screen and the 2,100-compound screen. Tumor volumes were recorded in GraphPad Prism 6 software (La Jolla, CA, USA). Two-way ANOVA analysis was used to compare differences in tumor volumes between the control and treatment groups.

RESULTS

Applying a Personalized Medicine Pipeline to an Unusual Case of Leiomyosarcoma

We enrolled a 3-year-old Golden Retriever (Teddy) for this study who presented to a veterinary primary care hospital with six synchronous leiomyosarcomas that underwent excisional

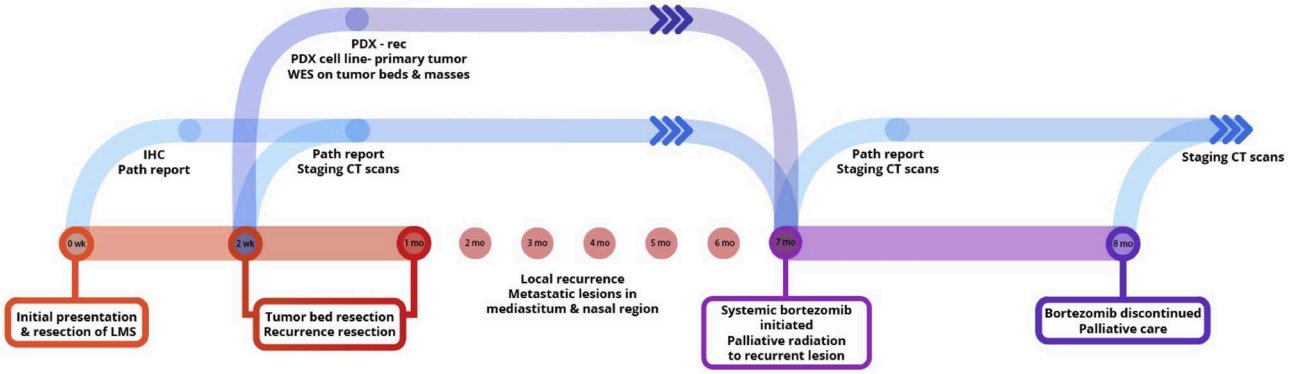

FIGURE 1 | An integrated preclinical drug discovery and validation pipeline. A 3 years old canine patient with synchronous leiomyosarcomas (LMS) was identified and recruited based on high risk of disease recurrence. Using both *in vitro* and *in vivo* patient-derived models, we identified proteasome inhibitors as candidates for validation in clinic. Clinicians applied the information from this preclinical pipeline for the treatment of the patient's recurrent and metastatic disease.

biopsy (**Figure 1**). Teddy was then referred to the Small Animal Oncology team at the University of Illinois at Urbana-Champaign for evaluation of his known leiomyosarcoma and treatment of an additional mass near the stifle. This tumor was excised and scars of the resected tumors were excised. During clipping and preparation for these surgeries, the treating surgeon noted two new masses in addition to previous surgical scars that were also resected and also determined to be high grade leiomyosarcoma (**Figure 1**). Pathology reports from the time of tumor excision noted an "ulcerated, inflamed, highly cellular, invasive mass composed of neoplastic spindyloid cells arranged in short interlacing streams and bundles with many neutrophils throughout the neoplasm with clusters of lymphocytes and plasma cells at the periphery," which was consistent with high grade leiomyosarcoma. Following surgery, Teddy was started on empirical treatment with toceranib, a multi-receptor tyrosine kinase inhibitor and the only FDA-approved targeted cancer therapeutic for dogs, given the high risk for recurrent disease.

Generation of Patient-Derived Models of LMS-D48X

Using one of the excised recurrent tumors from this patient, we applied a personalized medicine pipeline to identify new potential therapies in the event that Teddy's disease would eventually recur (**Figure 2A**). The pipeline included successful development of a matching PDX (designated "LMS-D48X") and low-passage cell line, a high throughput drug screen on the cell line, genomic profiling of mutations in the original tumors, PDX, and cell line, and *in vivo* validation of top drug candidates (**Figure 2A**). Hematoxylin and eosin staining of the canine PDX revealed sheets of highly proliferative, spindle-like cells (**Figure 2B**). Similarly, the matched cell line was also highly proliferative, with an estimated doubling time of 26–36 h and the presence of spindle-shaped, mesenchymal-like cells (**Figure 2C**). PCR using canine- and mouse-specific primers demonstrated that the LMS-D48X cell line is made up of purely canine tumor cells (**Figure 2D**).

High-Throughput Drug Screens Identify Proteasome Inhibitors as a Potential Candidate Therapy

To identify potential candidate therapies to treat Teddy, we performed two high-throughput drug screens. First, we used a panel of 119 FDA-approved anti-cancer drugs. Importantly, this screen identified multiple standard-of-care therapies for soft tissue sarcomas, such as doxorubicin and danurubicin (**Figure 2E**). Interestingly, however, in addition to standard-of-care therapies, the drug screen also identified several novel candidate drugs, such as proteasome inhibitors, HDAC inhibitors (i.e., romidepsin), and MEK inhibitors, as candidate agents (**Figure 2E**). Analysis of drug hits grouped by pathway revealed sensitivity to protein and nucleic acid synthesis pathways, autophagy, topoisomerases, HDACs, and c-kit/BCR/ABL (**Figure 2F**).

To further identify and validate additional novel therapeutic targets, we next performed a second-high throughput drug screen, this time using a larger panel of 2,100 bioactive compounds. The BioActives compound library (Selleckchem) contains a mixture of FDA-approved and non-FDA approved small molecules with confirmed bioactivity against known protein or pathway targets. The Bioactives collection is structurally diverse and is designed to target many key pathways regulating cellular processes including proliferation, apoptosis and signal transduction. Using the targeted pathway annotation for each compound, we were able to select targets and pathways for which multiple drugs had significant inhibitory effects. We hypothesized that this strategy would increase the likelihood of identifying the candidate targets/pathways for which a given tumor is most vulnerable. Our initial analysis of the screen revealed that a large portion (>90%) of compounds had little to no inhibitory effect, with only 6.6% of compounds showing >50% inhibition and 4.2% of drugs showing >75% inhibition (**Figure 3A**). Analysis of top hits by cellular target demonstrated vulnerability for this cell line to some targets already identified from the 119-drug screen, such as proteasome inhibitors and MEK inhibitors, as well as novel drug classes, such as HSP,

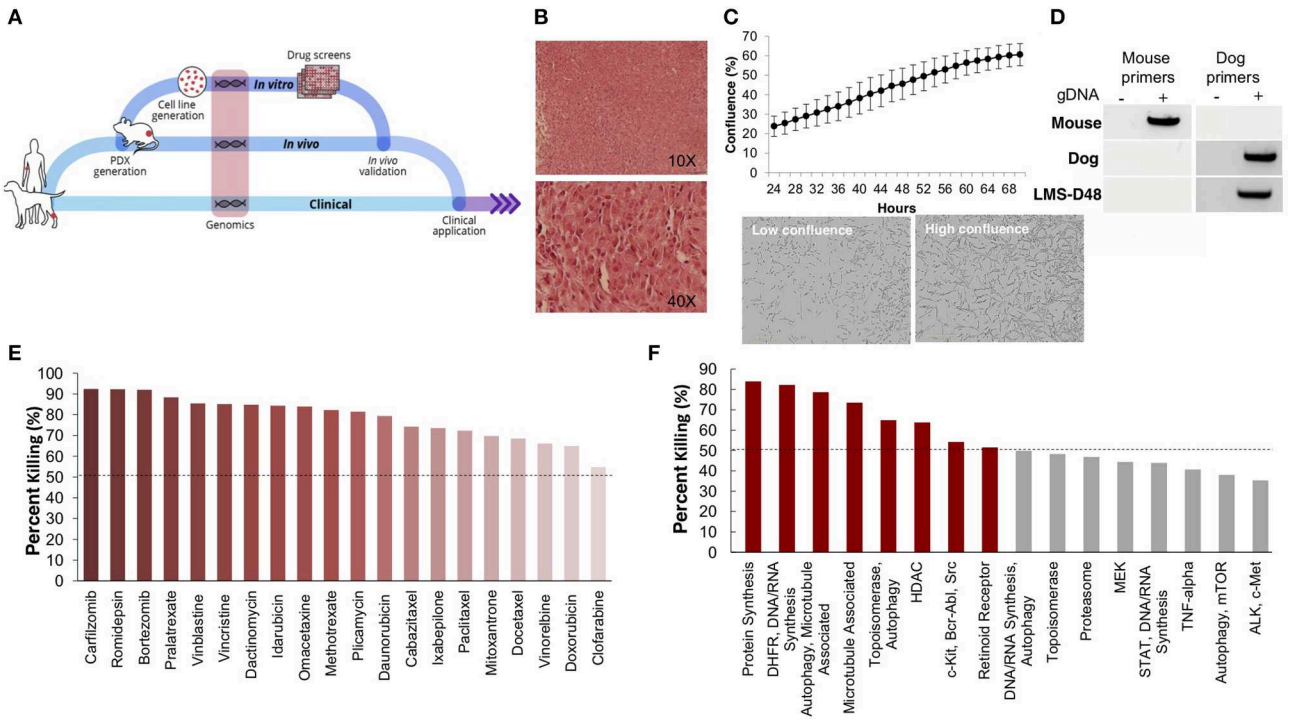

FIGURE 2 | Patient-derived models of cancer enable seamless integration of high throughput drug screening with *in vivo* validations. **(A)** Schematic of the personalized medicine pipeline integrating *in vitro* and *in vivo* drug discovery and validation. **(B)** Hematoxylin and eosin stain of the patient derived xenograft model of the canine patient (LMS-D48) showing highly proliferative spindle-like cells. **(C)** The patient-derived cell line also displays a high proliferation rate, with an estimated doubling time of 26–36 h, and spindle-like mesenchymal morphology. **(D)** A species-specific PCR using mouse- and canine-specific primers confirms that the patient-derived cell line is of canine origin. **(E)** A preliminary drug screen of 119 FDA-approved compounds in the LMS-D48 cell line identified single standard-of-care agents and novel drug candidates. **(F)** Analysis of drug screen data at the pathway level showed sensitivity to protein synthesis, DNA/RNA synthesis, autophagy, and HDAC inhibitors. Novel agents, including HDAC inhibitors and proteasome inhibitors were identified as top candidates for validation.

PLK, CRM1, NAMPT, Kinesin, and p53 inhibitors (**Figure 3B**). Analysis of the top inhibitors by pathway revealed enrichment in drugs targeting cytoskeletal signaling, the proteasome, apoptosis, cell cycle, and NF-κB (**Figure 3C**).

We further explored the potential therapeutic efficacy of top pathways by analyzing the number of inhibitors for each pathway that had >50% cell growth inhibition. Notably, both the HSP and proteasome pathways had multiple drugs with >50% inhibition (15/19 and 5/11, respectively) (**Figures 3D,E**). In the proteasome inhibitor class, 4/11 drugs conferred >90% cell growth inhibition. Likewise, in the HSP inhibitor drug class, 13 out of 19 drugs caused >90% cell growth inhibition (**Figures 3D,E**). From these two drug classes, we selected alvespimycin (HSP inhibitor) and bortezomib (proteasome inhibitor) for further study. Both of these drugs have known toxicity profiles, with bortezomib being FDA approved for the treatment of multiple myeloma. *In vitro* validation of alvespimycin and bortezomib showed sub-micromolar IC_{50} values of 345 and 6 nM, respectively (**Figures 3D,E**).

In vivo Validation of Alvespimycin and Bortezomib in PDX Models of LMS-D48X

We next used the LMS-D48X PDX to assess whether the top candidate therapies we identified *in vitro* would be therapeutically active in the patient's matched PDX *in vivo*. Interestingly, while alvespimycin showed >95% growth inhibition *in vitro*, the PDX was unresponsive to this HSP inhibitor, with no difference in growth rate between vehicle-treated and alvespimycin-treated tumors (**Figure 4A**). On the other hand, tumors treated with bortezomib showed significant tumor growth inhibition, consistent with the *in vitro* drug screen (**Figures 4B,C**). Animal weights in LMS-D48 PDX mice did not change significantly from the vehicle-treated tumors in either of the drug treatment groups (**Figure 4D**).

From Bench to Bedside: Applying Preclinical Modeling to Clinical Practice

For any personalized medicine approach to be clinically useful, it must provide insight into the patient's disease within the time scale of clinical decision making. With an aggressive disease course and high likelihood for recurrence, Teddy presented a unique opportunity to assess the ability of our personalized medicine pipeline to meet the clinical demand for rapidly providing data on potential therapies to treating clinicians. Teddy presented at a 6 months follow up visit with lesions in the mediastinal and right iliac lymph nodes, nasal mucosa, and local recurrence in the right pelvic limb (**Figure 1**; **Supplementary Figure 1**). Using the *in vitro* screening and

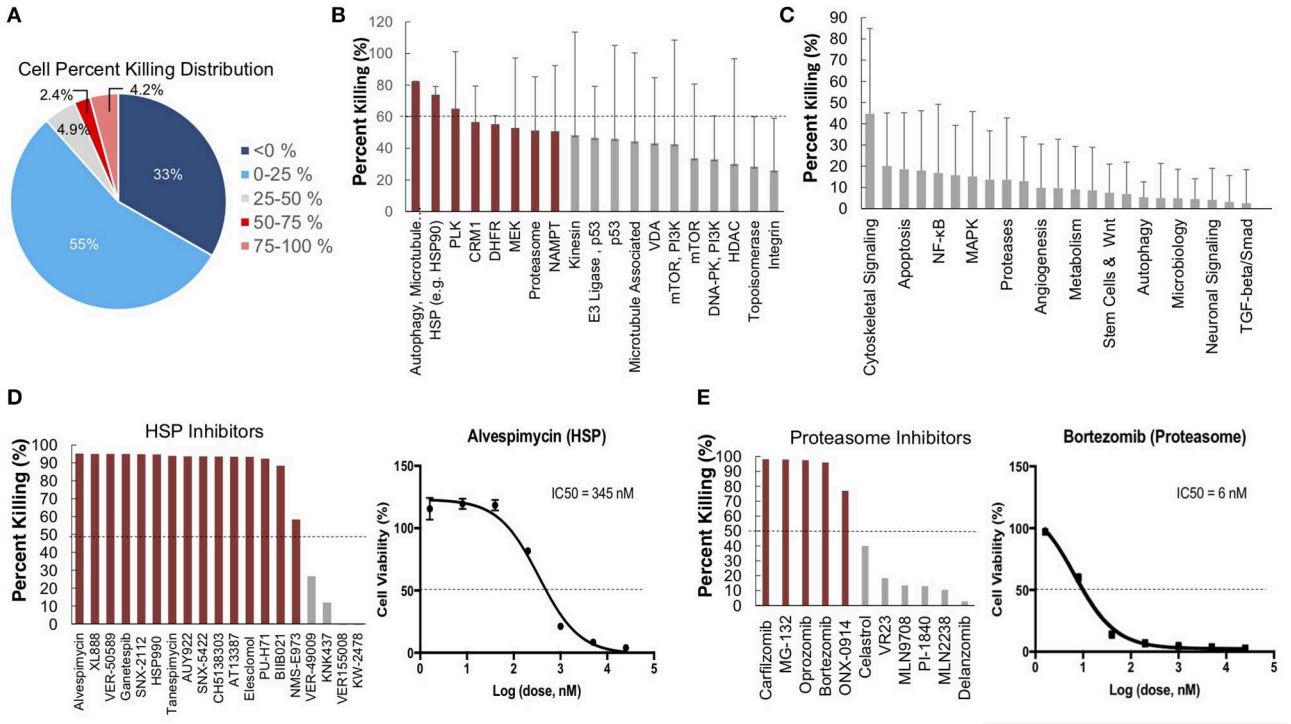

FIGURE 3 | High-throughput drug screens identify HSP inhibitors and proteasome inhibitors as promising therapies for personalized treatment. **(A)** LMS-D48 cells were plated at a density of 2,000 cells/well on plates prestamped with 2,100 drug compounds and DMSO. Cell titer glow assays were performed 72 h after cell plating to determine cell percent killing based on luminosity values. **(B)** Analysis of drug targets from the 2,100 screen with multiple drugs shows HSP inhibitors and proteasome inhibitors among the top pathways for which this cell line displays significant sensitivity. **(C)** Analysis of cellular pathways targeted by all drugs in the 2,100 drug screen shows that the cytoskeletal signaling pathway has the highest cell percent killing. **(D)** LMS-D48 cells were sensitive to 15 out of 19 HSP inhibitors. Among these, alvespimycin was the top candidate, with an estimated IC_{50} of 345 nM. **(E)** Bortezomib was among the top drugs in the proteasome inhibitor class that killed LMS-D48 cells, with an estimated IC_{50} value of 6 nM.

in vivo validations data from our pipeline, a decision was made to treat the patient with systemic bortezomib. The patient was treated with intravenous bortezomib infusions at 1.3 mg/m^2 twice weekly for 4 weeks and also received local palliative radiation therapy to the right pelvic limb to alleviate pain associated with the limb lesion. Measurements of the right pelvic limb lesion showed an initial decrease in tumor size during the first 3 weeks of treatment. Unfortunately, tumor growth resumed by the sixth week of treatment (**Figure 5A**). Metastatic lesions in other locations also increased in size on CT imaging at the conclusion of bortezomib treatment (**Figure 5B**). Representative images of the tumors before and after bortezomib demonstrated the increase in tumor size and aggressiveness, especially in the infiltrative nature of the nasal mucosal lesion eroding into the maxilla (**Supplementary Figure 1**).

Whole Exome Sequencing Reveals Extensive Inter-tumoral Heterogeneity

Our analysis of patient-derived models of cancer identified bortezomib as a promising treatment for Teddy. Consistent with these preclinical observations, Teddy showed an initial response to bortezomib in the first 3 weeks of treatment. However, this response was short lived and tumor growth resumed. By week six of treatment, Teddy also developed rapid resistance to systemic bortezomib (**Figure 5A**). Given the substantial differences in response between tumor sites, we sought to better understand the underlying genetic landscape of the patient's tumors and the relationship between these tumors and our patient-derived models. To do this, we performed whole exome sequencing and phylogenetic reconstructions on 11 samples from Teddy, including seven primary tumors, one recurrent tumor, one PDX and matched cell line, and normal tissue. Phylogenetic analysis of the tumors and patient-derived models grouped the PDX and cell line with the recurrent tumor with strong bootstrap support (**Figure 6A**; **Supplementary Figure 2**). With the exception of the distance trees, the grouping of the PDX and cell line with the recurrent tumor was consistent for all other methods of phylogenetic inference, including DNA compatibility, maximum parsimony, and maximum likelihood (**Figure 6B**). We also counted the number of shared somatic mutations across all samples and found the greatest similarity between the PDX, cell line, the recurrent tumor, and tumor 1 (**Figure 6C**). Together, these results suggest that the PDX and cell line most closely resemble the recurrent tumor. All other tumor samples shared little genetic overlap (3–16%). Tumor 7 was particularly distinct from the other tumors, sharing just 3.5% of somatic mutations with all other tumors (**Figure 6C**). Analysis of unique and shared somatic mutations revealed

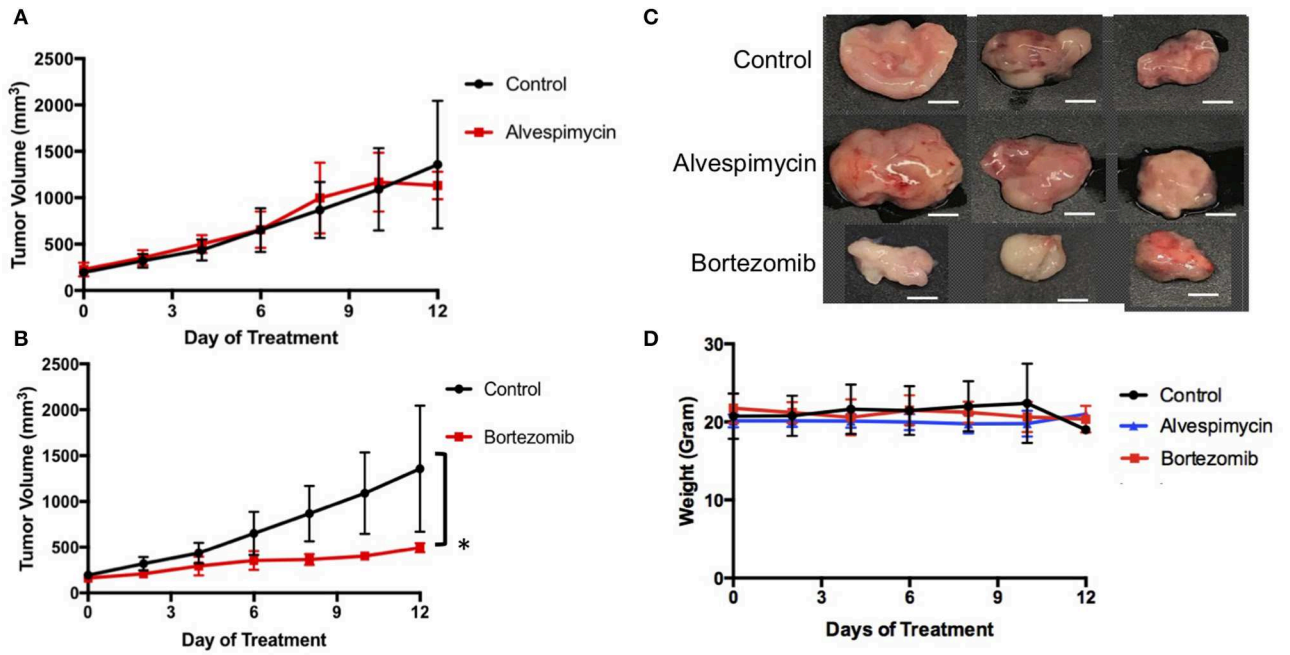

FIGURE 4 | *In vivo* validation of top drug candidates reveals sensitivity of the LMS-D48 PDX to proteasome inhibition. **(A)** Alvespimycin (25 mg/kg) was administered intraperitoneally (i.p.) *in vivo* to SCID beige mice harboring LMS-D48 PDX tumors ($n = 5$ mice per treatment group) each in control and treatment groups. There was no statistical difference between control and treatment groups as measured by analysis of variance. **(B)** Bortezomib (1 mg/kg) was administered i.p. as described for alvespimycin above. Bortezomib significantly inhibited tumor growth of the PDX ($p < 0.0001$). **(C)** Representative images of resected tumors at treatment endpoint from the treatment and control groups show that control tumors are approximately twice the size of bortezomib-treated tumors (scale bar = 0.5 cm). **(D)** Animal weights were not significantly changed during treatment with either alvespimycin or bortezomib during the treatment course.

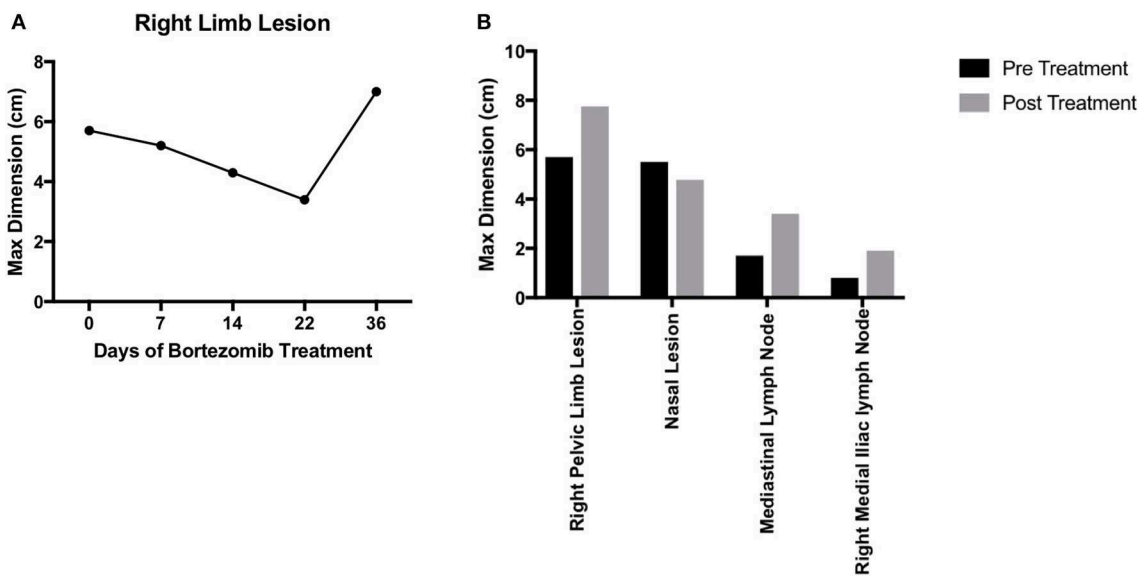

FIGURE 5 | Translation of bortezomib into clinic. **(A)** At the time of metastatic spread of disease, the patient had lesions in the mediastinal and right iliac lymph nodes, the nasal mucosa, and local recurrence at the right pelvic limb. The patient was started on systemic bortezomib therapy at a dose of 1.3 mg/m^2 twice weekly and palliative radiation therapy of 8 Gy by four fractions, once weekly, for pain from the right pelvic limb lesion. Measurement of the pelvic limb lesion during therapy showed decrease in maximal tumor dimension throughout 3 weeks of radiation therapy and systemic bortezomib; though, there was an increase in size 2 weeks after both therapies were stopped. **(B)** CT staging studies and physical exam demonstrated an interval increase in tumor size at all sites of disease and after discontinuation of bortezomib therapy. The canine patient was then transitioned to palliative care.

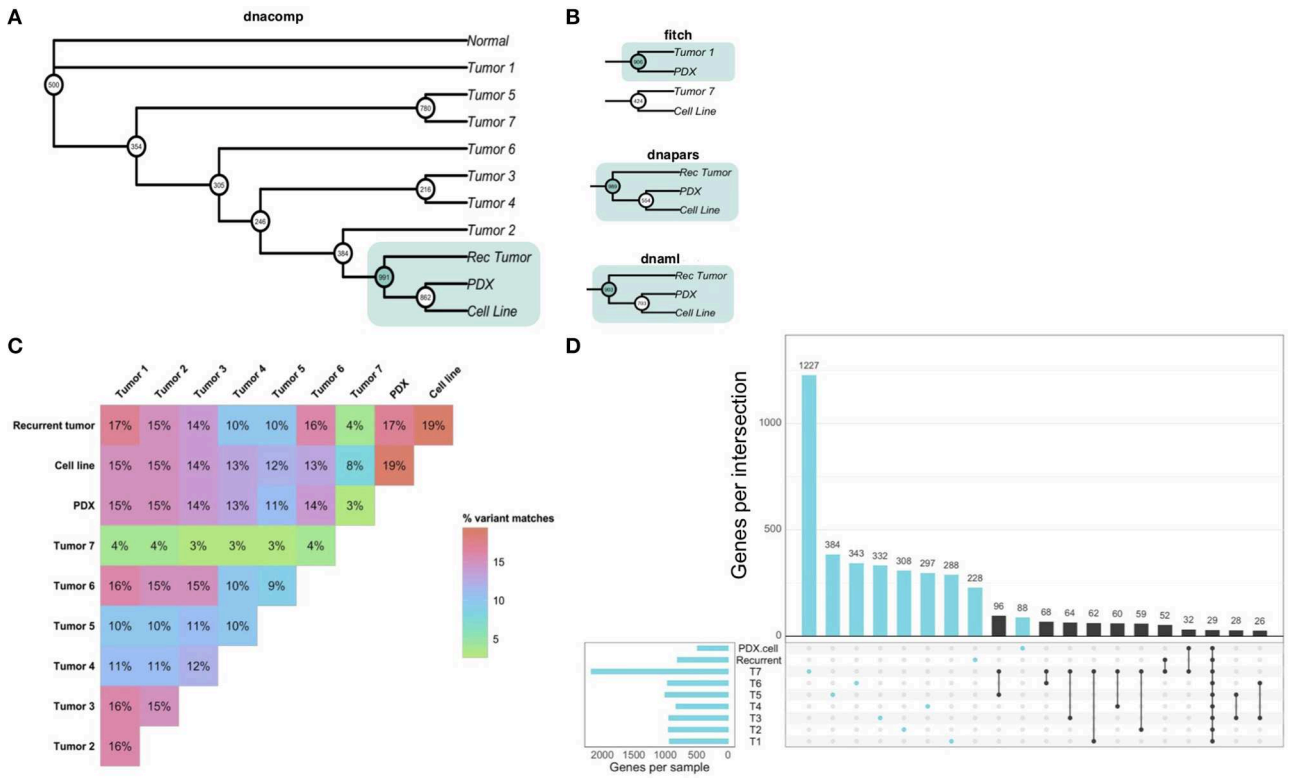

FIGURE 6 | Whole exome sequencing reveals inter-tumoral heterogeneity across the patient's tumors. **(A)** Phylogenetic reconstruction using the DNA compatibility algorithm supports a clade that includes the PDX, cell line, and the recurrent tumor with bootstrap support >900/1,000. **(B)** With the exception of the distance tree (Fitch), trees based on maximum parsimony and maximum likelihood also grouped the cancer models with the recurrent tumor. **(C)** A similarity matrix comparing all somatic variants from each sample shows the percentage of shared mutations across all samples. **(D)** Individual samples had higher numbers of mutated genes that were unique to each sample. Common shared mutations were relatively rare, reflecting the heterogeneity of the samples.

that unique mutations dominate the genetic landscape of each tumor (**Figure 6D**).

Integration of Whole Exome Sequencing and Ubiquitin Proteomics Identifies Potential Mechanisms of Action of Bortezomib

To further understand the underlying molecular mechanisms of sensitivity and resistance to bortezomib for this patient, we performed mass spectrometry proteomics analysis of ubiquitin-tagged proteins in PDX tumors treated with vehicle or bortezomib. Since bortezomib is a proteasome inhibitor, we analyzed proteins that were differentially ubiquitinated in the PDX treated with bortezomib as compared to vehicle-treated tumors. We identified a total of 290 differentially ubiquitinated proteins in vehicle- vs. bortezomib-treated PDX tumors (adjusted $p < 0.05$), 160 of which showed increased ubiquitination and 130 of which showed decreased ubiquitination (**Figure 7A**). Analysis of differentially ubiquitinated targets revealed enrichment for myosins and HSPs as the proteins with the greatest increase in ubiquitination in bortezomib-treated tumors as compared to vehicle-treated tumors (**Figure 7A**; **Supplementary File 1**). It is worth noting that the top hits were unique to this PDX, as additional proteomics analysis of bortezomib-treated osteosarcoma PDXs yielded a different suite of ubiquitinated proteins (32). Pathway analysis of proteins with increased ubiquitination revealed enrichments in pathways related to actin, contractile filament movement, and the proteasome (**Figure 7B**) and pathways related to proteins with decreased ubiquitination were enriched for adherens junctions, focal adhesions, and extracellular vesicles (**Figure 7C**).

We next cross-referenced the proteomics analysis with our whole exome sequencing data to better understand the varied clinical response and rapid progression on bortezomib. We identified 10 proteins that contained identical somatic mutations across multiple samples predicted to alter protein function that were also differentially-ubiquitinated in the PDX and cell-line (**Figure 7D**). Interestingly, two of these 10 proteins are involved in pathways relevant to proteasome inhibition and HSPs, respectively (**Figure 7E**). Defective In Cullin Neddylation 1 Domain Containing 1 (DCUN1D1) is part of an E3 ubiquitin ligase complex for neddylation, and heat shock protein 70 kDa member 8 (HSPA8) is integral to the HSP70 pathway and cellular protein quality control systems (33, 34). Notably, the DCUN1D1 mutation was unique to the PDX and cell line

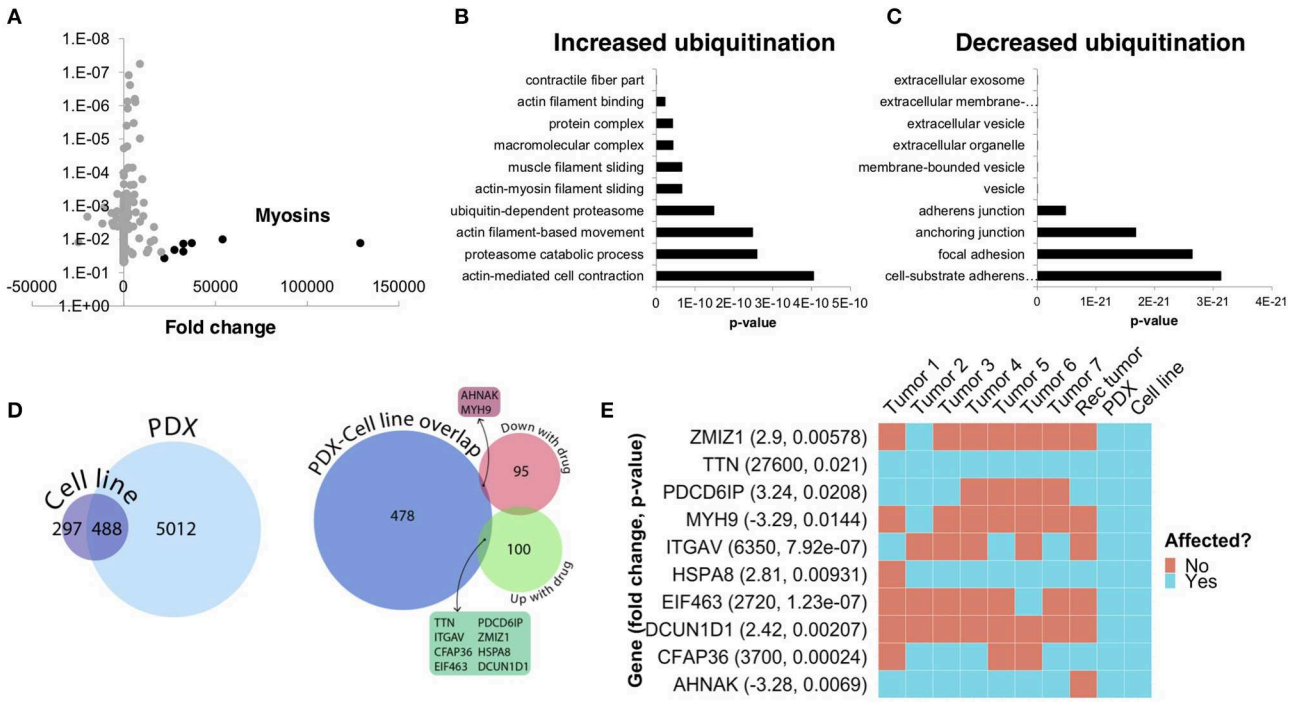

FIGURE 7 | Ubiquitin proteomics of PDX tumors treated with bortezomib show differential ubiquitination in key pathways related to cytoskeletal dynamics and the proteasome. **(A)** Mass spectroscopy proteomics of ubiquitin tagged proteins identified increased ubiquitination of 160 proteins and decreased ubiquitination of 130 proteins. Multiple myosins displayed increased ubiquitination in bortezomib-treated tumors. **(B)** Pathway analysis of proteins with increased ubiquitination showed enrichment in pathways related to actin and proteasome subunits. **(C)** Pathway analysis of proteins with decreased ubiquitination showed enrichment in pathways related to adherens junctions, focal adhesions, and extracellular vesicles. **(D)** Genes affected by deleterious mutations in each sample were determined by analyzing the whole exome sequencing data with the Ensembl Variant Effect Predictor. Affected genes in the PDX were filtered by those in the cell line to eliminate potential contamination by mouse tissue (left). Comparison of this subset of genes with the proteins identified by proteomics analysis with increased or decreased ubiquitination in the PDXs treated with bortezomib identified an overlap of only 10 affected proteins. **(E)** The 10 proteins identified in **(D)** are shown and were affected in the tumors with high variability.

(**Figure 7E**), suggesting the tumor from which this PDX was derived may have harbored unique genetics that could contribute to increased bortezomib sensitivity. Overall, the presence of somatic mutations affecting genes related to the proteasome and the heat shock protein pathway may explain the sensitivity to small molecule inhibitors targeting these pathways. The extensive heterogeneity in somatic mutations across multiple tumors and the patient-derived models may also help explain the rapid progression of the patient treated with the proteasome inhibitor, bortezomib.

DISCUSSION

A Comparative Oncology Approach Enables Rapid Testing of a Drug Discovery Pipeline in the Clinic

This patient—a canine leiomyosarcoma patient—provided an invaluable opportunity to test, in real time, a personalized approach to cancer therapy. To do this, we generated patient-derived cancer models, both *in vitro* and *in vivo*, that helped identify novel therapeutic options, including proteasome inhibitors and HSP inhibitors. After identifying bortezomib as a potential drug for clinical application, we provided the preclinical data to the veterinary oncology team who initiated personalized therapy with bortezomib for local recurrence and metastatic disease. Though there was initial response to bortezomib in the setting of adjuvant palliative radiation therapy for the local recurrence, additional metastatic sites showed either stable disease or progression on bortezomib. While the outcome for this patient was only a slight delay in disease progression, the entire process of evaluating a personalized therapy—from presentation to death—was able to be carried out in ∼1 year, something that would be unlikely in most human patients. This experience illustrates the gaps that will need to be bridged if precision medicine is to be utilized in the treatment of soft tissue sarcoma and other challenging solid tumors.

The Impact of Genetic Heterogeneity on Treatment Response

There are a number of possibilities to explain the disease progression for this patient after initiating therapy with bortezomib. One possible cause is the potential genetic drift that could be associated with generation and passage of the PDX and cell line. Indeed, recent studies have shown that PDXs are subject

to mouse-specific selective pressures beyond a few passages (9). While we strive to keep our passage numbers low for this reason, it is possible that even the first implantation of a tumor into mice leads to selection of a specific sub-clone that has different properties from the original tumor. Interestingly, phylogenetic reconstruction of all seven tumors, a recurrent tumor and the PDX/cell line supports the grouping of the PDX/cell line with the recurrent tumor in a distinct clade. Consistent with this grouping, a recurrent tumor, like the PDX and cell line, had an initial response to bortezomib (**Figure 5**).

One additional possibility for the rapid clinical progression on bortezomib could be that there is not an established dosage or dosing schedule for treating canine cancer with bortezomib. Bortezomib has been used in veterinary medicine as a therapy for golden retriever muscular dystrophy and our therapeutic regimen was extrapolated from this (35). However, it is possible our dosing regimen was incorrect in the context of leiomyosarcoma treatment.

A third possibility—and perhaps the most intriguing possibility—is that the recurrent and metastatic lesions acquired unique mutations in key cellular pathways that conferred bortezomib resistance. Tumors are heterogeneous on the individual level and within the population, greatly contributing to the challenge of discovering novel universal drugs (36–39). Numerous studies across multiple cancer types have revealed significant genotypic variability even within a single tumor (40–44). This is the case for metastatic progression as well. For example, Wu et al. have shown that genetic signatures of metastatic lesions are similar to each other, but distinct from primary tumors, suggesting key genomic differences that could impact therapeutic response (45). Precision medicine approaches often begin with genomic analysis of tumor obtained from the primary tumor. This initiates an immediate disconnect: For lethal solid tumors in most anatomic locations, the cause of death is unrelated to the primary tumor. Rather it is related to metastatic spread to other organs. This scenario is not characterized by clones of the primary tumor thriving in different locations. Rather, it represents populations of tumor thriving in different locations after a cascade of biological changes in the tumor that permit metastasis in the first place. This, then, confounds any approach which bases treatment decisions upon the biology of the primary tumor.

Driven by selective pressure from the tumor microenvironment, the inter-tumoral heterogeneity exhibited by these tumors could explain the difference between the *in vivo* response to bortezomib and the lack of response in the recurrent and metastatic lesions (46, 47). Consistent with this hypothesis, our analysis of whole exome sequencing data revealed substantial tumor heterogeneity across the multiple tumors from this patient, as well as between the group of samples including the recurrent tumor, PDX, and cell line.

It is possible that heterogeneity-mediated differences in response to therapy could be addressed with combination targeted therapy or with therapies that target multiple oncogenic pathways simultaneously (38, 48, 49). Multiple studies in mouse models of EGFR mutant lung cancer have shown the utility of combination therapies in overcoming treatment resistance (50–52). Our 2,100-compound drug screen identified multiple candidate drugs with both single cellular targets and those that target multiple pathways. In future iterations of this personalized pipeline, using combination therapy of top drugs identified from the drug screen could yield promising results.

A Multi-Omics Analysis Identifies Mechanisms of Sensitivity and Resistance to Bortezomib

Using whole exome sequencing we were able to characterize the genomic differences between the tumor used for preclinical modeling and the recurrent tumors treated with bortezomib. In the context of multiple myeloma, for which bortezomib is a standard therapy, multiple cellular pathways have been associated with bortezomib resistance, including mutations in genes regulating the active site for bortezomib (53–56). Our proteomics analysis identified pathways related to actin-myosin filaments, HSPs, and the proteasome as downregulated by bortezomib (**Figure 7**; **Supplementary File 1**). The downregulation of skeletal myosins (MYH1, MYH2, MYH4) by bortezomib is not easily explained, since skeletal myosins are typically markers of rhabdomyosarcoma rather than leiomyosarcoma (57). However, inhibition of pathways related to HSPs and the proteasome further validates the target specificity and mechanism of action for bortezomib. Our integrated comparison of the ubiquitin proteomics data with the exome sequencing data identified 10 key genes that were both differentially ubiquitinated and mutated. Remarkably, two of these genes are members of the HSP and proteasome pathways. This integrated multi-omics analysis suggests that mutations within these two genes may explain, in part, the response to bortezomib. Likewise, the lack of mutation in these two genes within other tumors in this patient may also explain the differential response to bortezomib in different metastatic lesions of this patient.

CONCLUSIONS

We have developed a translational drug discovery pipeline that integrates patient-derived models of cancer, drug screening, genomics, and proteomics to provide a comprehensive view of how to integrate translational preclinical research in the clinic. The unique biology of Teddy, with multiple, synchronous leiomyosarcoma tumors and an aggressive clinical course, enabled us to study the relationships between the molecular/genomic landscape and *in vitro, in vivo,* and clinical response to therapy. This provided both the patient and the clinician with unique information about tumor biology and response to novel therapeutics occurring in a very short period of time. This suggests that utilizing pet dogs with cancer to model personalized medicine approaches can facilitate rapid investigations of therapeutic successes and failures.

DATA AVAILABILITY STATEMENT

The datasets generated for this study can be found in the National Center for Biotechnology Information (NCBI) (https://dataview.ncbi.nlm.nih.gov/), (PRJNA597042).

ETHICS STATEMENT

The animal study was reviewed and approved by The animal study was reviewed and approved by Duke IACUC. Written informed consent was obtained from the owners for the participation of their animals in this study. Written informed consent was obtained from the owners for the participation of their animals in this study.

AUTHOR CONTRIBUTIONS

All authors listed have made a substantial, direct and intellectual contribution to the work, and approved it for publication.

FUNDING

This work was supported by Hyundai Hope on Wheels Foundation Award Duke Health Scholars Award.

ACKNOWLEDGMENTS

JS acknowledges support from Meg and Bill Lindenberger, the Paul and Shirley Friedland Fund, the Triangle Center for Evolutionary Medicine, and funds raised in memory of Muriel E. Rudershausen (riding4research.org). We would like to thank Teddy and his family for their participation in this study and the veterinary team at the University of Illinois at Urbana–Champaign for contributing to Teddy's clinical care. We acknowledge Wayne Glover for contributing to *in vivo* PDX tumor propagation, the Duke Functional Genomics Shared Resource, the Duke Proteomics and Metabolomics Shared Resource, the Duke Sequencing and Genomics Shared Resource, and the Duke Genomic Analysis and Bioinformatics Core Facility. WE acknowledges the generous support of the Hyundai Hope on Wheels Foundation as well as the Duke Health Scholars Program.

SUPPLEMENTARY MATERIAL

The Supplementary Material for this article can be found online at: https://www.frontiersin.org/articles/10.3389/fonc.2020.00117/full#supplementary-material

REFERENCES

1. DiMasi JA, Hansen RW, Grabowski HG. The price of innovation: new estimates of drug development costs. *J Health Econ*. (2003) 22:151–85. doi: 10.1016/S0167-6296(02)00126-1
2. Mirabello L, Troisi RJ, Savage SA. Osteosarcoma incidence and survival rates from 1973 to 2004: data from the surveillance, epidemiology, and end results program. *Cancer*. (2009) 115:1531–43. doi: 10.1002/cncr.24121
3. Howlader N, Noone AM, Krapcho M, Miller D, Brest A, Yu M, editors. *SEER Cancer Statistics Review, 1975-2016*. Bethesda, MD: National Cancer Institute (2019). Available online at: https://seer.cancer.gov/csr/1975_2016/
4. Quail DF, Joyce JA. Microenvironmental regulation of tumor progression and metastasis. *Nat Med*. (2013) 19:1423–37. doi: 10.1038/nm.3394
5. Blomme A, Van Simaeys G, Doumont G, Costanza B, Bellier J, Otaka Y, et al. Murine stroma adopts a human-like metabolic phenotype in the PDX model of colorectal cancer and liver metastases. *Oncogene*. (2018) 37:1237–50. doi: 10.1038/s41388-017-0018-x
6. Tentler JJ, Tan AC, Weekes CD, Jimeno A, Leong S, Pitts TM, et al. Patient-derived tumour xenografts as models for oncology drug development. *Nat Rev Clin Oncol*. (2012) 9:338–50. doi: 10.1038/nrclinonc.2012.61
7. Chen Z, Cheng K, Walton Z, Wang Y, Ebi H, Shimamura T, et al. A murine lung cancer co-clinical trial identifies genetic modifiers of therapeutic response. *Nature*. (2012) 483:613–7. doi: 10.1038/nature10937
8. Fichtner I, Slisow W, Gill J, Becker M, Elbe B, Hillebrand T, et al. Anticancer drug response and expression of molecular markers in early-passage xenotransplanted colon carcinomas. *Eur J Cancer*. (2004) 40:298–307. doi: 10.1016/j.ejca.2003.10.011
9. Hidalgo M, Amant F, Biankin AV, Budinská E, Byrne AT, Caldas C, et al. Patient-derived xenograft models: an emerging platform for translational cancer research. *Cancer Discov*. (2014) 4:998. doi: 10.1158/2159-8290.CD-14-0001
10. Hidalgo M, Bruckheimer E, Rajeshkumar NV, Garrido-Laguna I, De Oliveira E, Rubio-Viqueira B, et al. A pilot clinical study of treatment guided by personalized tumorgrafts in patients with advanced cancer. *Mol Cancer Ther*. (2011) 10:1311–6. doi: 10.1158/1535-7163.MCT-11-0233
11. Stebbing J, Paz K, Schwartz GK, Wexler LH, Maki R, Pollock RE, et al. Patient-derived xenografts for individualized care in advanced sarcoma. *Cancer*. (2014) 120:2006–15. doi: 10.1002/cncr.28696
12. Ehrhart N. Soft-tissue sarcomas in dogs: a review. *J Am Anim Hosp Assoc*. (2005) 41:241–6. doi: 10.5326/0410241
13. Stiller CA, Trama A, Serraino D, Rossi S, Navarro C, Chirlaque MD, et al. Descriptive epidemiology of sarcomas in Europe: report from the RARECARE project. *Eur J Cancer*. (2013) 49:684–95. doi: 10.1016/j.ejca.2012.09.011
14. Dobson JM, Samuel S, Milstein H, Rogers K, Wood JL. Canine neoplasia in the UK: estimates of incidence rates from a population of insured dogs. *J Small Anim Pract*. (2002) 43:240–6. doi: 10.1111/j.1748-5827.2002.tb00066.x
15. Milovancev M, Hauck M, Keller C, Stranahan LW, Mansoor A, Malarkey DE. Comparative pathology of canine soft tissue sarcomas: possible models of human non-rhabdomyosarcoma soft tissue sarcomas. *J Comp Pathol*. (2015) 152:22–7. doi: 10.1016/j.jcpa.2014.09.005
16. Uronis JM, Osada T, McCall S, Yang XY, Mantyh C, Morse MA, et al. Histological and molecular evaluation of patient-derived colorectal cancer explants. *PLoS ONE*. (2012) 7:e38422. doi: 10.1371/journal.pone.0038422
17. Cooper JK, Sykes G, King S, Cottrill K, Ivanova NV, Hanner R, et al. Species identification in cell culture: a two-pronged molecular approach. *In vitro Cell Dev Biol Anim*. (2007) 43:344–51. doi: 10.1007/s11626-007-9060-2
18. Long T, Liu Z, Shang J, Zhou X, Yu S, Tian H, et al. Proteasome inhibition with bortezomib suppresses growth and induces apoptosis in osteosarcoma. *Int J Cancer*. (2010) 127:67–76. doi: 10.1002/ijc.25024
19. Hu Y, Bobb D, He J, Hill DA, Dome JS. The HSP90 inhibitor alvespimycin enhances the potency of telomerase inhibition by imetelstat in human osteosarcoma. *Cancer Biol Ther*. (2015) 16:949–57. doi: 10.1080/15384047.2015.1040964
20. Bioinformatics B. *Trim Galore*. (2018). Available online at: http://www.bioinformatics.babraham.ac.uk/projects/trim_galore/
21. Martin M. Cutadapt removes adapter sequences from high-throughput sequencing reads. *EMBnet J*. (2011) 17:10–11. doi: 10.14806/ej.17.1.200
22. Van der Auwera GA, Carneiro MO, Hartl C, Poplin R, Del Angel G, Levy-Moonshine A, et al. From FastQ data to high confidence variant calls: the genome analysis toolkit best practices pipeline. *Curr Protoc Bioinform*. (2013) 43:11 10 11–33. doi: 10.1002/0471250953.bi1110s43

23. Li H, Durbin R. Fast and accurate short read alignment with burrows-wheeler transform. *Bioinformatics*. (2009) 25:1754–60. doi: 10.1093/bioinformatics/btp324
24. Broad Institute. *Picard toolkit*. Available online at: http://broadinstitute.github.io/picard/
25. Kersey PJ, Staines DM, Lawson D, Kulesha E, Derwent P, Humphrey JC, et al. Ensembl genomes: an integrative resource for genome-scale data from non-vertebrate species. *Nucleic Acids Res.* (2012) 40:D91–7. doi: 10.1093/nar/gkr895
26. Felsenstein J. Using the quantitative genetic threshold model for inferences between and within species. *Philos Trans R Soc Lond B Biol Sci*. (2005) 360:1427–34. doi: 10.1098/rstb.2005.1669
27. Paradis E, Schliep K. Ape 5.0: an environment for modern phylogenetics and evolutionary analyses in R. *Bioinformatics*. (2018) 35:526–8. doi: 10.1093/bioinformatics/bty633
28. Danecek P, Auton A, Abecasis G, Albers CA, Banks E, DePristo MA, et al. The variant call format and VCFtools. *Bioinformatics*. (2011) 27:2156–8. doi: 10.1093/bioinformatics/btr330
29. Zerbino DR, Achuthan P, Akanni W, Amode MR, Barrell D, Bhai J, et al. Ensembl 2018. *Nucleic Acids Res.* (2018) 46:D754–61. doi: 10.1093/nar/gkx1098
30. Hulsen T, de Vlieg J, Alkema W. BioVenn - a web application for the comparison and visualization of biological lists using area-proportional venn diagrams. *BMC Genomics*. (2008) 9:488. doi: 10.1186/1471-2164-9-488
31. Conway JR, Lex A, Gehlenborg N. UpSetR: an R package for the visualization of intersecting sets and their properties. *Bioinformatics*. (2017) 33:2938–40. doi: 10.1093/bioinformatics/btx364
32. Lazarides AL, Somarell J, Altunel E, Rao S, Hoskinson S, Cheng S, et al. *A Cross-Species Personalized Medicine Pipeline Identifies the CRM1 Export Pathway as a Potentially Novel Treatment for Osteosarcoma*. Duke University (2019).
33. Wang F, Bonam SR, Schall N, Kuhn L, Hammann P, Chaloin O, et al. Blocking nuclear export of HSPA8 after heat shock stress severely alters cell survival. *Sci Rep*. (2018) 8:16820. doi: 10.1038/s41598-018-34887-6
34. Scott DC, Hammill JT, Min J, Rhee DY, Connelly M, Sviderskiy VO, et al. Blocking an N-terminal acetylation-dependent protein interaction inhibits an E3 ligase. *Nat Chem Biol*. (2017) 13:850–7. doi: 10.1038/nchembio.2386
35. Araujo KP, Bonuccelli G, Duarte CN, Gaiad TP, Moreira DF, Feder D, et al. Bortezomib (PS-341) treatment decreases inflammation and partially rescues the expression of the dystrophin-glycoprotein complex in GRMD dogs. *PLoS ONE*. (2013) 8:e61367. doi: 10.1371/journal.pone.0061367
36. McGranahan N, Swanton C. Biological and therapeutic impact of intratumor heterogeneity in cancer evolution. *Cancer Cell*. (2015) 27:15–26. doi: 10.1016/j.ccell.2014.12.001
37. Liu J, Dang H, Wang XW. The significance of intertumor and intratumor heterogeneity in liver cancer. *Exp Mol Med*. (2018) 50:e416. doi: 10.1038/emm.2017.165
38. Dagogo-Jack I, Shaw AT. Tumour heterogeneity and resistance to cancer therapies. *Nat Rev Clin Oncol*. (2018) 15:81–94. doi: 10.1038/nrclinonc.2017.166
39. Fisher R, Pusztai L, Swanton C. Cancer heterogeneity: implications for targeted therapeutics. *Br J Cancer*. (2013) 108:479–85. doi: 10.1038/bjc.2012.581
40. Walker BA, Wardell CP, Melchor L, Hulkki S, Potter NE, Johnson DC, et al. Intraclonal heterogeneity and distinct molecular mechanisms characterize the development of t(4;14) and t(11;14) myeloma. *Blood*. (2012) 120:1077–86. doi: 10.1182/blood-2012-03-412981
41. Gerlinger M, Rowan AJ, Horswell S, Math M, Larkin J, Endesfelder D, et al. Intratumor heterogeneity and branched evolution revealed by multiregion sequencing. *N Engl J Med*. (2012) 366:883–92. doi: 10.1056/NEJMoa1113205
42. Sottoriva A, Spiteri I, Piccirillo SG, Touloumis A, Collins VP, Marioni JC, et al. Intratumor heterogeneity in human glioblastoma reflects cancer evolutionary dynamics. *Proc Natl Acad Sci USA*. (2013) 110:4009–14. doi: 10.1073/pnas.1219747110
43. Beà S, Valdés-Mas R, Navarro A, Salaverria I, Martín-Garcia D, Jares P, et al. Landscape of somatic mutations and clonal evolution in mantle cell lymphoma. *Proc Natl Acad Sci USA*. (2013) 110:18250–5. doi: 10.1073/pnas.1314608110
44. Kogita A, Yoshioka Y, Sakai K, Togashi Y, Sogabe S, Nakai T, et al. Inter- and intra-tumor profiling of multi-regional colon cancer and metastasis. *Biochem Biophys Res Commun*. (2015) 458:52–6. doi: 10.1016/j.bbrc.2015.01.064
45. Wu X, Northcott PA, Dubuc A, Dupuy AJ, Shih DJ, Witt H, et al. Clonal selection drives genetic divergence of metastatic medulloblastoma. *Nature*. (2012) 482:529–33. doi: 10.1038/nature10825
46. Junttila MR, de Sauvage FJ. Influence of tumour micro-environment heterogeneity on therapeutic response. *Nature*. (2013) 501:346–54. doi: 10.1038/nature12626
47. Lawrence MS, Stojanov P, Polak P, Kryukov GV, Cibulskis K, Sivachenko A, et al. Mutational heterogeneity in cancer and the search for new cancer-associated genes. *Nature*. (2013) 499:214–8. doi: 10.1038/nature12213.
48. Alizadeh AA, Aranda V, Bardelli A, Blanpain C, Bock C, Borowski C, et al. Toward understanding and exploiting tumor heterogeneity. *Nat Med*. (2015) 21:846–53. doi: 10.1038/nm.3915
49. Liao Z, Nan G, Yan Z, Zeng L, Deng Y, Ye J, et al. The anthelmintic drug niclosamide inhibits the proliferative activity of human osteosarcoma cells by targeting multiple signal pathways. *Curr Cancer Drug Targets*. (2015) 15:726–38. doi: 10.2174/1568009615666150629132157
50. Pirazzoli V, Ayeni D, Meador CB, Sanganahalli BG, Hyder F, de Stanchina E, et al. Afatinib plus cetuximab delays resistance compared to single-agent erlotinib or afatinib in mouse models of TKI-naive EGFR L858R-induced lung adenocarcinoma. *Clin Cancer Res*. (2016) 22:426–35. doi: 10.1158/1078-0432.CCR-15-0620
51. Janjigian YY, Smit EF, Groen HJ, Horn L, Gettinger S, Camidge DR, et al. Dual inhibition of EGFR with afatinib and cetuximab in kinase inhibitor-resistant EGFR-mutant lung cancer with and without T790M mutations. *Cancer Discov*. (2014) 4:1036–45. doi: 10.1158/2159-8290.CD-14-0326
52. Tricker EM, Xu C, Uddin S, Capelletti M, Ercan D, Ogino A, et al. Combined EGFR/MEK inhibition prevents the emergence of resistance in EGFR-mutant lung cancer. *Cancer Discov*. (2015) 5:960–71. doi: 10.1158/2159-8290.CD-15-0063
53. Oerlemans R, Franke NE, Assaraf YG, Cloos J, van Zantwijk I, Berkers CR, et al. Molecular basis of bortezomib resistance: proteasome subunit beta5 (PSMB5) gene mutation and overexpression of PSMB5 protein. *Blood*. (2008) 112:2489–99. doi: 10.1182/blood-2007-08-104950
54. Chauhan D, Li G, Shringarpure R, Podar K, Ohtake Y, Hideshima T, et al. Blockade of Hsp27 overcomes bortezomib/proteasome inhibitor PS-341 resistance in lymphoma cells. *Cancer Res*. (2003) 63:6174–7.
55. Kuhn DJ, Berkova Z, Jones RJ, Woessner R, Bjorklund CC, Ma W, et al. Targeting the insulin-like growth factor-1 receptor to overcome bortezomib resistance in preclinical models of multiple myeloma. *Blood*. (2012) 120:3260–70. doi: 10.1182/blood-2011-10-386789
56. Que W, Chen J, Chuang M, Jiang D. Knockdown of c-Met enhances sensitivity to bortezomib in human multiple myeloma U266 cells via inhibiting Akt/mTOR activity. *APMIS*. (2012) 120:195–203. doi: 10.1111/j.1600-0463.2011.02836.x
57. Saku T, Tsuda N, Anami M, Okabe H. Smooth and skeletal muscle myosins in spindle cell tumors of soft tissue. an immunohistochemical study. *Acta Pathol Jpn*. (1985) 35:125–36. doi: 10.1111/j.1440-1827.1985.tb02211.x

Conflict of Interest: The authors declare that the research was conducted in the absence of any commercial or financial relationships that could be construed as a potential conflict of interest.

Copyright © 2020 Rao, Somarelli, Altunel, Selmic, Byrum, Sheth, Cheng, Ware, Kim, Prinz, Devos, Corcoran, Moseley, Soderblom, Hsu and Eward. This is an open-access article distributed under the terms of the Creative Commons Attribution License (CC BY). The use, distribution or reproduction in other forums is permitted, provided the original author(s) and the copyright owner(s) are credited and that the original publication in this journal is cited, in accordance with accepted academic practice. No use, distribution or reproduction is permitted which does not comply with these terms.

Advantages of publishing in Frontiers

OPEN ACCESS
Articles are free to read for greatest visibility and readership

FAST PUBLICATION
Around 90 days from submission to decision

HIGH QUALITY PEER-REVIEW
Rigorous, collaborative, and constructive peer-review

TRANSPARENT PEER-REVIEW
Editors and reviewers acknowledged by name on published articles

Frontiers
Avenue du Tribunal-Fédéral 34
1005 Lausanne | Switzerland

Visit us: www.frontiersin.org
Contact us: info@frontiersin.org | +41 21 510 17 00

REPRODUCIBILITY OF RESEARCH
Support open data and methods to enhance research reproducibility

DIGITAL PUBLISHING
Articles designed for optimal readership across devices

FOLLOW US
@frontiersin

IMPACT METRICS
Advanced article metrics track visibility across digital media

EXTENSIVE PROMOTION
Marketing and promotion of impactful research

LOOP RESEARCH NETWORK
Our network increases your article's readership